A Comprehensive Study of Prestressing Steel and Concrete Variables Affecting Transfer Length in Pre-Tensioned Concrete Crossties

KSU-21-1

February 2021

Dr. Naga N.B. Bodapati, Civil Engineering, KSU
Dr. Robert J. Peterman, Civil Engineering, KSU
Dr. B. Terry Beck, Mechanical & Nuclear Engineering, KSU
Dr. Chih-Hang Wu, Industrial & Manufacturing Systems Engineering, KSU

Abstract

A comprehensive study was conducted to determine the variation of transfer length in pre-tensioned prestressed concrete railroad ties with varying prestressing steel types and concrete parameters. The in-depth evaluation included eighteen different prestressing reinforcement types that are employed in concrete railroad ties worldwide. The study consisted of two phases: Lab-Phase and Plant-Phase. Throughout the study, transfer lengths were determined from surface strain measurements on pre-tensioned concrete members. During the Lab-Phase, pre-tensioned concrete prisms were fabricated to replicate plant manufactured crossties. A special jacking arrangement was employed to ensure that each of the reinforcements was tensioned to the same force. Later, during the Plant-Phase, pre-tensioned concrete railroad ties were fabricated at a concrete crosstie manufacturing plant using the same reinforcements. In addition, a long-term study was conducted on plant-manufactured crossties to determine the variation of transfer length due to in-track loading.

Corresponding Author: Dr. Robert J. Peterman (bob@ksu.edu)

U.S. Department of Transportation
Federal Railroad Administration

The contents of this report reflect the views of the authors, who are responsible for the facts and accuracy of the information presented herein. This document is disseminated in the interest of information exchange. The report is funded, partially or entirely, by a grant from the U.S. Department of Transportation's University Transportation Centers Program. However, the U.S. Government assumes no liability for the contents or use thereof.

METRIC/ENGLISH CONVERSION FACTORS

ENGLISH TO METRIC

LENGTH (APPROXIMATE)

1 inch (in)	=	2.5 centimeters (cm)
1 foot (ft)	=	30 centimeters (cm)
1 yard (yd)	=	0.9 meter (m)
1 mile (mi)	=	1.6 kilometers (km)

AREA (APPROXIMATE)

1 square inch (sq in, in^2)	=	6.5 square centimeters (cm^2)
1 square foot (sq ft, ft^2)	=	0.09 square meter (m^2)
1 square yard (sq yd, yd^2)	=	0.8 square meter (m^2)
1 square mile (sq mi, mi^2)	=	2.6 square kilometers (km^2)
1 acre = 0.4 hectare (he)	=	4,000 square meters (m^2)

MASS - WEIGHT (APPROXIMATE)

1 ounce (oz)	=	28 grams (gm)
1 pound (lb)	=	0.45 kilogram (kg)
1 short ton = 2,000 pounds (lb)	=	0.9 tonne (t)

VOLUME (APPROXIMATE)

1 teaspoon (tsp)	=	5 milliliters (ml)
1 tablespoon (tbsp)	=	15 milliliters (ml)
1 fluid ounce (fl oz)	=	30 milliliters (ml)
1 cup (c)	=	0.24 liter (l)
1 pint (pt)	=	0.47 liter (l)
1 quart (qt)	=	0.96 liter (l)
1 gallon (gal)	=	3.8 liters (l)
1 cubic foot (cu ft, ft^3)	=	0.03 cubic meter (m^3)
1 cubic yard (cu yd, yd^3)	=	0.76 cubic meter (m^3)

TEMPERATURE (EXACT)

[(x-32)(5/9)] °F = y °C

METRIC TO ENGLISH

LENGTH (APPROXIMATE)

1 millimeter (mm)	=	0.04 inch (in)
1 centimeter (cm)	=	0.4 inch (in)
1 meter (m)	=	3.3 feet (ft)
1 meter (m)	=	1.1 yards (yd)
1 kilometer (km)	=	0.6 mile (mi)

AREA (APPROXIMATE)

1 square centimeter (cm^2)	=	0.16 square inch (sq in, in^2)
1 square meter (m^2)	=	1.2 square yards (sq yd, yd^2)
1 square kilometer (km^2)	=	0.4 square mile (sq mi, mi^2)
10,000 square meters (m^2)	=	1 hectare (ha) = 2.5 acres

MASS - WEIGHT (APPROXIMATE)

1 gram (gm)	=	0.036 ounce (oz)
1 kilogram (kg)	=	2.2 pounds (lb)
1 tonne (t)	=	1,000 kilograms (kg)
	=	1.1 short tons

VOLUME (APPROXIMATE)

1 milliliter (ml)	=	0.03 fluid ounce (fl oz)
1 liter (l)	=	2.1 pints (pt)
1 liter (l)	=	1.06 quarts (qt)
1 liter (l)	=	0.26 gallon (gal)
1 cubic meter (m^3)	=	36 cubic feet (cu ft, ft^3)
1 cubic meter (m^3)	=	1.3 cubic yards (cu yd, yd^3)

TEMPERATURE (EXACT)

[(9/5) y + 32] °C = x °F

QUICK INCH - CENTIMETER LENGTH CONVERSION

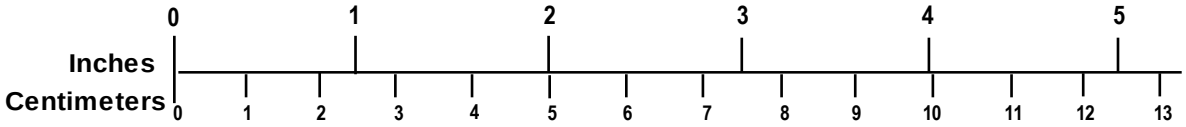

QUICK FAHRENHEIT - CELSIUS TEMPERATURE CONVERSION

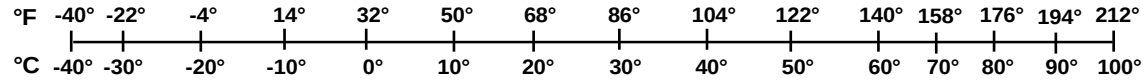

For more exact and or other conversion factors, see NIST Miscellaneous Publication 286, Units of Weights and Measures. Price $2.50 SD Catalog No. C13 10286

Updated 6/17/98

Acknowledgements

The authors would like to thank the Federal Railroad Administration (FRA) for providing the majority of the funding that made this research possible. Additionally, LB Foster/CXT Concrete Ties donated extensive resources, including all of the reinforcements, to make the project a success. The researchers would also like to thank Drs. Hailing Yu and David Jeong at the John A. Volpe National Transportation Systems Center for their valuable suggestions and parallel analysis work. Finally, the authors wish to thank the Precast/Pre-stressed Concrete Institute (PCI) for establishing an industry advisory panel to the project, the Kansas State University's University Transportation Center (K-State UTC) for graduate student tuition support, and the Advanced Manufacturing Institute (AMI) for manufacturing services.

Contents

Acknowledgements ii
Contents iii
Illustrations vii
Tables xviii
Executive Summary i
Chapter 1 Introduction 1
1.1 Background 1
1.2 Objective 2
1.2.1 Lab-Phase Transfer Lengths from Pretensioned Concrete Prisms 2
1.2.2 Plant-Phase Transfer Lengths from Pretensioned Concrete Crossties 3
1.3 Scope 4
1.4 Organization of the Report 4
Chapter 2 Literature Review 6
2.1 First recorded use of concrete railroad ties in the United States 6
2.1.1 Weber (1969) 6
2.2 Advantages of concrete railroad ties over wooden ties 6
2.2.1 (Hanna, 1979) 7
2.2.2 (Crawford, 2009) 7
2.2.3 (Real, et al., 2014) 7
2.3 Previous research recommendations 8
2.3.1 (Hanna, 1979) 8
2.4 Types of concrete railroad ties 9
2.4.1 (Hanna, 1979) 9
2.5 Bonding Mechanisms between concrete and prestressing reinforcement 11
2.5.1 Hoyer & Friedrich (1939) 11
2.6 Effect of diameter of prestressing reinforcement on transfer length results 12
2.6.1 Krishnamurthy (1972) 12
2.7 Effect of reinforcement's surface on transfer length results 14
2.7.1 Kaar & Hanson (1975) 14
2.8 Effect of release strength on transfer length results 16

2.8.1 (Kaar, et al., 1963) 16
2.8.2 Mitchell et. al (1993) 18
Chapter 3 Material storage and operation 20
3.1 Reinforcement 20
3.1.1 Reinforcement surface condition preservation during Lab-Phase 25
3.1.2 Reinforcement employed during Plant-Phase 26
3.2 Concrete Materials and Mix Design 27
3.2.1 Cement 27
3.2.2 Course Aggregates 28
3.2.3 Sand (Fine Aggregate) 28
3.2.4 High-range water-reducing admixture 32
3.2.5 Mix-design during Lab-Phase 32
3.2.6 Mix-design during Plant-Phase 34
Chapter 4 Experimental set-up in Lab-Phase 35
4.1 Prism cross-sections 35
4.2 Experimental set-up 37
4.2.1 Prestressing frame and load cells 37
4.2.2 Prestressing operation and formwork - Bed preparation 41
4.3 Test matrix and casting procedure of prisms during laboratory phase 45
4.3.1 Test matrix 45
4.3.2 Casting procedure of prisms 48
4.3.3 SURE CURE-Mini curing control system 49
4.3.4 Nomenclature for each pour during the Lab-Phase 51
4.4 Transfer Length determination 52
4.4.1 Transfer Length 52
4.4.2 Surface-strain profiles determined through Whittemore gage (Lab-Phase) 52
4.5 Storage of prisms 56
Chapter 5 Lab-Phase results 57
5.1 Effect of Reinforcement type and indent geometry on Transfer length (Group I prisms) 58
5.2 Calculation of percentage increase and percentage decrease (reduction) 69
5.2.1 Calculation of percentage decrease (reduction) in TL 69

5.2.2 Calculation of percentage increase in TL 69
5.3 Effect of Release strength on Transfer length (Group II prisms) 69
5.3.1 Special case study with higher release strength-8300 psi 82
5.4 Effect of concrete consistency on Transfer length (Group III prisms) 85
5.5 Effect of water-to-cementitious (w/c) ratio on transfer length (Group IV prisms)..... 94
5.6 Effect of "Viscosity-Modifying Admixture (VMA) presence" in concrete mix on transfer length (Group V prisms) 98
5.7 Effect of change in source of course aggregate on transfer length (Group VI prisms) .. 102
5.8 Development of model to predict transfer length 107
5.8.1 Bond characteristics of the prestressing reinforcement (Arnold, 2013) 107
5.8.2 Transfer Length Model for Variable Release Strengths 109
Chapter 6 Experimental procedure during Plant-Phase..... 114
6.1 Reinforcement distribution across the tie cross-sections 116
6.1.1 Reinforcement pattern for strands..... 118
6.2 Experimental set-up in Plant-Phase 127
6.2.1 Prestressing bed and adjusting for different reinforcement stiffness..... 127
6.2.2 Prestressing operation for reinforcements with different Modulus of Elasticity (MOE) 127
6.2.3 Concrete Mix 135
6.3 Test matrix and casting procedure during Plant-Phase..... 135
6.3.1 Test Matrix..... 135
6.3.2 Casting procedure 136
6.3.3 Nomenclature for each pour during Plant-Phase 136
6.4 Transfer length measurements during Plant-Phase..... 137
6.4.1 Surface displacement readings using Whittemore gage (Plant-Phase)..... 137
6.4.2 Surface displacement readings using Laser-Speckle Imaging (LSI) device..... 144
Chapter 7 Plant-Phase results, and comparison of Lab-Phase results with Plant-Phase results 154
7.1 Plant-Phase results 154
7.1.1 Transfer length Results 155
7.2 Comparison of Lab-Phase and Plant-Phase results..... 165

7.2.1 Wire reinforcements 165
7.2.2 Strand reinforcements 169
7.2.3 Similarities and differences between Lab-Phase (Group I) and Plant-Phase 170
7.3 Long-term transfer length results from Plant-Phase crossties (Stage I) 172
7.3.1 Transfer length increase in “K”-marked crossties during Stage I 179
7.3.2 Transfer length increase in “T”-marked crossties during Stage I 182
7.3.3 Comparison of transfer lengths at the end of Stage I 185
7.4 Long-term transfer length results from Plant-Phase crossties (Stage II) 185
7.4.1 Change in transfer length for “T”-marked crossties due to 84.46 MGT in-track loading (Stage II) 188
7.4.2 Change in transfer length for “K”-marked crossties during Stage II 190
7.5 Long-term study on plant manufactured ties (Stage III) 193
7.5.1 Transfer length variation in “T”-marked crossties due to additional 151.85 MGT loading in curved track (Stage III) 196
Chapter 8 Conclusions and Recommendations 201
8.1 Conclusions from Lab-Phase 201
8.2 Conclusions from Plant-Phase 203
8.3 Recommendations 206
References 208
APPENDIX – Surface-strain profiles 214
Lab-Phase – Effect of reinforcement type on transfer length 215
Lab-Phase - Effect of release strength on transfer length 234
Lab Phase - Effect of concrete consistency (slump) on transfer length 254
Plant-Phase surface-strain profiles 268

Illustrations

Figure 1 Types of concrete ties (Hanna, 1979) 10
Figure 2 Transfer of prestressing force to the concrete member: Hoyer Effect 12
Figure 3 Strand patterns for different release strengths (Kaar, et al., 1963) 16
Figure 4 Various wire reinforcements employed in the present research (Arnold, 2013) 22
Figure 5 Various strand reinforcements employed in the present research (Arnold, 2013) 22
Figure 6 Close-up view of wire specimens (Arnold, 2013) 23
Figure 7 Close-up view off strand specimens (Arnold, 2013) 24
Figure 8 Preservation of reinforcement at KSU laboratories (Arnold, 2013) 25
Figure 9 Reinforcement storage containers used to preserve the reinforcement surface in the as-received condition 26
Figure 10 CA#1 and CA#2 utilized in the present study (Courtesy Joey Holste) 29
Figure 11 CA#3 utilized in the present study (Courtesy MCM Inc.) 29
Figure 12 FA utilized in the present study (Courtesy Joey Holste) 30
Figure 13 Concrete Mixer used during the Lab-Phase 34
Figure 14 Prism cross-sections utilized during the laboratory phase 36
Figure 15 Prestressing frame jacking assembly fabricated during laboratory phase 38
Figure 16 Four (4) individual load cells mounted at Dead end 39
Figure 17 One individual screw for each reinforcement to adjust the magnitude of the prestressing force 39
Figure 18 Prestressing bed schematic diagram (Lab-Phase) 40
Figure 19 Digital display of Prestressing force measured by load cells 41
Figure 20 Prestressing bed after the completion of pre-tensioning operation 43
Figure 21 Three-piece prism end-forms were installed after the tendons were tensioned 43
Figure 22 Wooden side form equipped with brass inserts before casting 44
Figure 23 Typical prism after the completion of formwork 44
Figure 24 Twelve concrete cylinders under temperature control through SURE CURE mini controlling system 50
Figure 25 Typical Temperature (ºF) plot of Prism and Cylinder specimens 50
Figure 26 Nomenclature for each pour during the Lab-Phase 51
Figure 27 Typical brass insert used to measure surface displacement 53

Figure 28 Steel bars held the brass inserts at a specified locations during casting..... 53
Figure 29 Prism surface with brass points 54
Figure 30 Whittemore gage used for the study 54
Figure 31 Surface distance measurement though Whittemore gage..... 55
Figure 32 Typical surface-strain profile due to prestress transfer 55
Figure 33 Prisms storage (by pour) after the completion of initial strain measurements 56
Figure 34 Transfer length results of wire reinforcements for Group I prisms..... 63
Figure 35 Transfer length results of strand reinforcements for Group I prisms 64
Figure 36 Transfer length results of wire reinforcements from Group I (diameters) 67
Figure 37 Transfer length results of strand reinforcements from Group I (diameters) 68
Figure 38 Transfer length results of wire reinforcements from Group II 73
Figure 39 Transfer length results of wire reinforcements from Group II 74
Figure 40 Average transfer lengths for wire reinforcement at different release strengths, TL in inches 74
Figure 41 Average transfer lengths for wire reinforcement at different release strengths, TL in # of diameters of the reinforcement 75
Figure 42 Average transfer lengths for strand reinforcement at different release strengths, TL in inches 75
Figure 43 Average transfer lengths for strand reinforcement at different release strengths, TL in # diameters of the reinforcement 76
Figure 44 Variation in splitting tensile strength with concrete consistency for Group II prisms . 81
Figure 45 Variation in MOE with release strength for Group II prisms..... 81
Figure 46 TL results for prisms cast with WF reinforcement at different release strengths 83
Figure 47 Average TL results for prisms cast with WF reinforcement at different release strengths 83
Figure 48 Coefficient of determination between average TL and release strength of [WF] 84
Figure 49 Average transfer length values at different release strengths for [WF]..... 84
Figure 50 Transfer length results of wire reinforcements from Group III..... 88
Figure 51 Transfer length results of strand reinforcements from Group III 88
Figure 52 Variation in splitting tensile strength with concrete consistency for Group III prisms 91
Figure 53 Variation in MOE strength with concrete consistency for Group III prisms 91

Figure 54 Average transfer lengths for wire reinforcement at different concrete slumps-TL in inches 92
Figure 55 Average transfer lengths for wire reinforcement at different concrete slumps-TL in # of diameters of the reinforcement 92
Figure 56 Average transfer lengths for strand reinforcement at different concrete slumps-TL in inches 93
Figure 57 Average transfer lengths for strand reinforcement at different concrete slumps-TL in # of diameters of the reinforcement 93
Figure 58 Individual transfer length results for Group IV prisms 96
Figure 59 Average transfer lengths for wire reinforcement at different w/c ratios (TL in inches) 97
Figure 60 Average transfer lengths for wire reinforcement at different w/c ratios (TL in # of diameters of the reinforcement) 97
Figure 61 Transfer length results for Group V prisms 100
Figure 62 Average transfer lengths for companion prisms with and without VMA (in inches) 101
Figure 63 Average transfer lengths for companion prisms with and without VMA (in # of reinforcement diameters) 101
Figure 64 Severe longitudinal splitting occurred along the [WH] wires in prisms cast with Mix-Design #2 103
Figure 65 Transfer length results for Group VI prisms 105
Figure 66 Average transfer lengths for mixtures with different coarse aggregates (in inches) .. 105
Figure 67 Average transfer lengths for mixtures with different coarse aggregates (TL in # of reinforcement diameters) 106
Figure 68 Best fit lines drawn through three data sets 110
Figure 69 Transfer length prediction model for different release strengths 111
Figure 70 Comparison of actual and predicted transfer lengths 113
Figure 71 Different views of a typical CXT concrete railroad tie: (a) Isometric view, (b) Bottom view, (c) Top View, (d) Side View 115
Figure 72 Reinforcement design pattern and nominal position of 5.32-mm-diameter wires (cross-section shown at the end of crosstie) 117
Figure 73 Custom wire chairs to maintain the reinforcement design pattern 118

Figure 74 Offset distance between wire seat location and the reinforcement surface 119
Figure 75 Strand centroid offset from wire centroid 120
Figure 76 Strand pattern for 5/16-in. diameter 3 wire strand 120
Figure 77 Strand pattern for 3/8-in. diameter 7 wire strand 120
Figure 78 Wire "chair" supporting 5.32-mm. diameter wires 121
Figure 79 Wire chair used to support..... 121
Figure 80 5/16-in. diameter strand pattern and reinforcement eccentricities (cross-section shown at the end of crosstie) 124
Figure 81 3/8-in. diameter strand pattern and reinforcement eccentricities (cross-section shown at the end of crosstie) 125
Figure 82 Different reinforcement patterns and tendon anchorages used (cross-sections are at end of crosstie)..... 126
Figure 83 Typical Prestressing bed with four (4) cavities during the Plant-Phase 127
Figure 84 Shim plates used with wire reinforcements..... 130
Figure 85 Shim plates used with strand reinforcements 131
Figure 86 Special jacking plate with four 1-inch diameter 14 TPI bolts 131
Figure 87 Shim plates installed at dead end to compensate for a lower MOE of project wires . 133
Figure 88 Standard bulkhead at dead end of the prestressing bed 133
Figure 89 A center-hole load cell was installed on one of the tendons at the live end to verify the correct prestressing force was achieved with the special jacking plate apparatus..... 134
Figure 90 Nomenclature during Plant-Phase 136
Figure 91 Layout showing the adapted strain measuring system 138
Figure 92 Steel bars with brass points 139
Figure 93 Cross-section for steel bar (for mounting brass inserts)..... 140
Figure 94 Steel bars used to hold brass inserts at proper spacing in the concrete crossties 140
Figure 95 (a) steel bar removal process before taking prior Whittemore gage readings (b) concrete tie surface with brass points 142
Figure 96 Typical strain profile along the length of the concrete tie during Plant-Phase 143
Figure 97 Typical speckle produced due to coherent light from LSI device..... 144
Figure 98 Grooves were cut into the concrete surface to ensure a reference plane..... 145
Figure 99 Preparing the surface for the LSI measurements..... 146

Figure 100 Recording laser speckle images during Plant-Phase 147
Figure 101 Separation of in-track loading ties (“T”) and KSU ties (“K”) during Plant-Phase .. 148
Figure 102 Bottom surface preparation for “T” crossties subjected to in-track loading (a) protecting displacement-measuring inserts with cloth tape; (b) positioning the steel cover plate in place; (c) installation of steel cover plate with brass screws; (d) steel cover plates installation with silicone caulking over brass screws 150
Figure 103 Timeline for long-term study of plant manufactured ties..... 153
Figure 104 Comparison of average transfer length results from Whittemore gage and LSI..... 158
Figure 105 Average TL (by tie number) for the entire Plant-Phase 158
Figure 106 Comparison of transfer lengths (Live End vs Dead End)..... 162
Figure 107 Transfer length results during Plant-Phase (TL in inches)..... 163
Figure 108 Transfer length results during Plant-Phase (TL in # of diameters) 164
Figure 109 Comparison of experimental and predicted TL values during Plant-Phase 167
Figure 110 Comparison of Plant-Phase TL with Lab-Phase Group I prisms TL 168
Figure 111 Average increase in transfer length during Stage I (wire reinforcements)..... 175
Figure 112 Average increase in transfer length during Stage I (strand reinforcements) 176
Figure 113 Percentage growth in TL during Stage I (wire reinforcements)..... 177
Figure 114 Percentage growth in TL during Stage I (strand reinforcements) 178
Figure 115 Typical surface-strain profile for a “K”-marked crosstie at the end of Stage I..... 180
Figure 116 TL increase for “K”-marked crossties at the end of Stage I (wire reinforcements) . 181
Figure 117 TL increase for “K”-marked crossties at the end of Stage I (strand reinforcements) 181
Figure 118 Typical surface-strain profile for a “T”-marked crosstie at the end of Stage I 183
Figure 119 TL increase for “T”-marked crossties at the end of Stage I (wire reinforcements) . 184
Figure 120 TL increase for “T”-marked crossties at the end of Stage I (strand reinforcements)184
Figure 121 Typical surface-strain profile for a “T”-marked tie at the end of Stage II 189
Figure 122 TL variation for “T”-marked ties at the end of Stage II (wire reinforcements) 189
Figure 123 TL variation for “T”-marked ties at the end of Stage II (strand reinforcements)..... 190
Figure 124 Typical surface-strain profile for a “K”-marked tie at the end of Stage II..... 191
Figure 125 TL variation for “K”-marked ties at the end of Stage II (wire reinforcements)..... 192
Figure 126 TL variation for “K”-marked ties at the end of Stage II (strand reinforcements) 192

Figure 127 “T”-marked crossties installed in curved track during Stage III 194
Figure 128 Typical surface-strain profiles for a “T”-marked crosstie at the end of Stage III 197
Figure 129 TL variation for “T”-marked crossties at the end of Stage III (wire reinforcements) 198
Figure 130 TL increase at the end of Stage III – wire reinforcements 199
Figure 131 Percentage increase in TL at the end of Stage III – wire reinforcements..... 200
Figure 132 Surface-strain profiles for [WA]- [0.32]- [4.5]- [6]-[#1] 215
Figure 133 Surface-strain profiles for [WB]-[0.32]-[4.5]-[6]-[#1]..... 216
Figure 134 Surface-strain profiles for [WC]-[0.32]-[4.5]-[6]-[#1]..... 217
Figure 135 Surface-strain profiles for [WD]-[0.32]-[4.5]-[6]-[#1] 218
Figure 136 Surface-strain profiles for [WE]-[0.32]-[4.5]-[6]-[#1]..... 219
Figure 137 Surface-strain profiles for [WF]-[0.32]-[4.5]-[6]-[#1] 220
Figure 138 Surface-strain profiles for [WG]-[0.32]-[4.5]-[6]-[#1] 221
Figure 139 Surface-strain profiles for [WH]-[0.32]-[4.5]-[6]-[#1] 222
Figure 140 Surface-strain profiles for [WI]-[0.32]-[4.5]-[6]-[#1] 223
Figure 141 Surface-strain profiles for [WJ]-[0.32]-[4.5]-[6]-[#1]..... 224
Figure 142 Surface-strain profiles for [WK]-[0.32]-[4.5]-[6]-[#1] 225
Figure 143 Surface-strain profiles for [WL]-[0.32]-[4.5]-[6]-[#1]..... 226
Figure 144 Surface-strain profiles for [WM]-[0.32]-[4.5]-[6]-[#1]..... 227
Figure 145 Surface-strain profiles for [SA]-[0.32]-[4.5]-[6]-[#1] 228
Figure 146 Surface-strain profiles for [SB]-[0.32]-[4.5]-[6]-[#1] 229
Figure 147 Surface-strain profiles for [SC]-[0.32]-[4.5]-[6]-[#1] 230
Figure 148 Surface-strain profiles for [SD]-[0.32]-[4.5]-[6]-[#1] 231
Figure 149 Surface-strain profiles for [SE]-[0.32]-[4.5]-[6]-[#1] 232
Figure 150 Surface-strain profiles for [SF]-[0.32]-[4.5]-[6]-[#1]..... 233
Figure 151 Surface-strain profiles for [WA]-[0.32]-[3.5]-[6]-[#1] 234
Figure 152 Surface-strain profiles for [WE]-[0.32]-[3.5]-[6]-[#1]..... 235
Figure 153 Surface-strain profiles for [WG]-[0.32]-[3.5]-[6]-[#1] 236
Figure 154 Surface-strain profiles for [WH]-[0.32]-[3.5]-[6]-[#1] 237
Figure 155 Surface-strain profiles for [WK]-[0.32]-[3.5]-[6]-[#1] 238
Figure 156 Surface-strain profiles for [SA]-[0.32]-[3.5]-[6]-[#1] 239

Figure 157 Surface-strain profiles for [SC]-[0.32]-[3.5]-[6]-[#1] 240
Figure 158 Surface-strain profiles for [SD]-[0.32]-[3.5]-[6]-[#1] 241
Figure 159 Surface-strain profiles for [SE]-[0.32]-[3.5]-[6]-[#1] 242
Figure 160 Surface-strain profiles for [SF]-[0.32]-[3.5]-[6]-[#1] 243
Figure 161 Surface-strain profiles for [WA]-[0.32]-[6.0]-[6]-[#1] 244
Figure 162 Surface-strain profiles for [WE]-[0.32]-[6.0]-[6]-[#1] 245
Figure 163 Surface-strain profiles for [WG]-[0.32]-[6.0]-[6]-[#1] 246
Figure 164 Surface-strain profiles for [WH]-[0.32]-[6.0]-[6]-[#1] 247
Figure 165 Surface-strain profiles for [WK]-[0.32]-[6.0]-[6]-[#1] 248
Figure 166 Surface-strain profiles for [SA]-[0.32]-[6.0]-[6]-[#1] 249
Figure 167 Surface-strain profiles for [SC]-[0.32]-[6.0]-[6]-[#1] 250
Figure 168 Surface-strain profiles for [SD]-[0.32]-[6.0]-[6]-[#1] 251
Figure 169 Surface-strain profiles for [SE]-[0.32]-[6.0]-[6]-[#1] 252
Figure 170 Surface-strain profiles for [SF]-[0.32]-[6.0]-[6]-[#1] 253
Figure 171 Surface-strain profiles for [WA]-[0.32]-[4.5]-[3]-[#1] 254
Figure 172 Surface-strain profiles for [WE]-[0.32]-[4.5]-[3]-[#1] 255
Figure 173 Surface-strain profiles for [WG]-[0.32]-[4.5]-[3]-[#1] 256
Figure 174 Surface-strain profiles for [WH]-[0.32]-[4.5]-[3]-[#1] 257
Figure 175 Surface-strain profiles for [WK]-[0.32]-[4.5]-[3]-[#1] 258
Figure 176 Surface-strain profiles for [SD]-[0.32]-[4.5]-[3]-[#1] 259
Figure 177 Surface-strain profiles for [SE]-[0.32]-[4.5]-[3]-[#1] 260
Figure 178 Surface-strain profiles for [WA]-[0.32]-[4.5]-[9]-[#1] 261
Figure 179 Surface-strain profiles for [WE]-[0.32]-[4.5]-[9]-[#1] 262
Figure 180 Surface-strain profiles for [WG]-[0.32]-[4.5]-[9]-[#1] 263
Figure 181 Surface-strain profiles for [WH]-[0.32]-[4.5]-[9]-[#1] 264
Figure 182 Surface-strain profiles for [WK]-[0.32]-[4.5]-[9]-[#1] 265
Figure 183 Surface-strain profiles for [SD]-[0.32]-[4.5]-[9]-[#1] 266
Figure 184 Surface-strain profiles for [SE]-[0.32]-[4.5]-[9]-[#1] 267
Figure 185 Surface-strain profiles for [WA]-[09]-[L] (Whittemore gage) 268
Figure 186 Surface-strain profiles for [WA]-[09]-[D] (Whittemore gage) 269
Figure 187 Surface-strain profiles for [WA]-[37]-[L] (Whittemore gage) 270

Figure 188 Surface-strain profiles for [WA]-[37]-[D] (Whittemore gage) 271
Figure 189 Surface-strain profiles for [WB]-[09]-[L] (Whittemore gage) 272
Figure 190 Surface-strain profiles for [WB]-[09]-[D] (Whittemore gage) 273
Figure 191 Surface-strain profiles for [WB]-[37]-[L] (Whittemore gage) 274
Figure 192 Surface-strain profiles for [WB]-[37]-[D] (Whittemore gage) 275
Figure 193 Surface-strain profiles for [WC]-[09]-[L] (Whittemore gage) 276
Figure 194 Surface-strain profiles for [WC]-[09]-[D] (Whittemore gage) 277
Figure 195 Surface-strain profiles for [WC]-[37]-[L] (Whittemore gage) 278
Figure 196 Surface-strain profiles for [WC]-[37]-[D] (Whittemore gage) 279
Figure 197 Surface-strain profiles for [WD]-[09]-[L] (Whittemore gage) 280
Figure 198 Surface-strain profiles for [WD]-[09]-[D] (Whittemore gage) 281
Figure 199 Surface-strain profiles for [WD]-[37]-[L] (Whittemore gage) 282
Figure 200 Surface-strain profiles for [WD]-[37]-[D] (Whittemore gage) 283
Figure 201 Surface-strain profiles for [WE]-[09]-[L] (Whittemore gage) 284
Figure 202 Surface-strain profiles for [WE]-[09]-[D] (Whittemore gage) 285
Figure 203 Surface-strain profiles for [WE]-[37]-[L] (Whittemore gage) 286
Figure 204 Surface-strain profiles for [WE]-[37]-[D] (Whittemore gage) 287
Figure 205 Surface-strain profiles for [WF]-[09]-[L] (Whittemore gage) 288
Figure 206 Surface-strain profiles for [WF]-[09]-[D] (Whittemore gage) 289
Figure 207 Surface-strain profiles for [WF]-[37]-[L] (Whittemore gage) 290
Figure 208 Surface-strain profiles for [WF]-[37]-[D] (Whittemore gage) 291
Figure 209 Surface-strain profiles for [WG]-[09]-[L] (Whittemore gage) 292
Figure 210 Surface-strain profiles for [WG]-[09]-[D] (Whittemore gage) 293
Figure 211 Surface-strain profiles for [WG]-[37]-[L] (Whittemore gage) 294
Figure 212 Surface-strain profiles for [WG]-[37]-[D] (Whittemore gage) 295
Figure 213 Surface-strain profiles for [WH]-[09]-[L] (Whittemore gage) 296
Figure 214 Surface-strain profiles for [WH]-[09]-[D] (Whittemore gage) 297
Figure 215 Surface-strain profiles for [WH]-[37]-[L] (Whittemore gage) 298
Figure 216 Surface-strain profiles for [WH]-[37]-[D] (Whittemore gage) 299
Figure 217 Surface-strain profiles for [WI]-[09]-[L] (Whittemore gage) 300
Figure 218 Surface-strain profiles for [WI]-[09]-[D] (Whittemore gage) 301

Figure 219 Surface-strain profiles for [WI]-[37]-[L] (Whittemore gage) 302
Figure 220 Surface-strain profiles for [WI]-[37]-[D] (Whittemore gage)..... 303
Figure 221 Surface-strain profiles for [WJ]-[09]-[L] (Whittemore gage) 304
Figure 222 Surface-strain profiles for [WJ]-[09]-[D] (Whittemore gage)..... 305
Figure 223 Surface-strain profiles for [WJ]-[37]-[L] (Whittemore gage) 306
Figure 224 Surface-strain profiles for [WJ]-[37]-[D] (Whittemore gage)..... 307
Figure 225 Surface-strain profiles for [WL]-[09]-[L] (Whittemore gage) 308
Figure 226 Surface-strain profiles for [WL]-[09]-[D] (Whittemore gage)..... 309
Figure 227 Surface-strain profiles for [WL]-[37]-[L] (Whittemore gage) 310
Figure 228 Surface-strain profiles for [WL]-[37]-[D] (Whittemore gage)..... 311
Figure 229 Surface-strain profiles for [WM]-[09]-[L] (Whittemore gage) 312
Figure 230 Surface-strain profiles for [WM]-[09]-[D] (Whittemore gage)..... 313
Figure 231 Surface-strain profiles for [WM]-[36]-[L] (Whittemore gage) 314
Figure 232 Surface-strain profiles for [WM]-[36]-[D] (Whittemore gage)..... 315
Figure 233 Surface-strain profiles for [SA]-[09]-[L] (Whittemore gage) 316
Figure 234 Surface-strain profiles for [SA]-[09]-[D] (Whittemore gage)..... 317
Figure 235 Surface-strain profiles for [SA]-[37]-[L] (Whittemore gage) 318
Figure 236 Surface-strain profiles for [SA]-[37]-[D] (Whittemore gage)..... 319
Figure 237 Surface-strain profiles for [SB]-[09]-[L] (Whittemore gage) 320
Figure 238 Surface-strain profiles for [SB]-[09]-[D] (Whittemore gage) 321
Figure 239 Surface-strain profiles for [SB]-[37]-[L] (Whittemore gage) 322
Figure 240 Surface-strain profiles for [SB]-[37]-[D] (Whittemore gage) 323
Figure 241 Surface-strain profiles for [SC]-[09]-[L] (Whittemore gage) 324
Figure 242 Surface-strain profiles for [SC]-[09]-[D] (Whittemore gage) 325
Figure 243 Surface-strain profiles for [SC]-[37]-[L] (Whittemore gage) 326
Figure 244 Surface-strain profiles for [SC]-[37]-[D] (Whittemore gage) 327
Figure 245 Surface-strain profiles for [WA]-[10]-[L] (Whittemore gage)..... 328
Figure 246 Surface-strain profiles for [WA]-[10]-[D] (Whittemore gage) 329
Figure 247 Surface-strain profiles for [WA]-[36]-[L] (Whittemore gage)..... 330
Figure 248 Surface-strain profiles for [WA]-[36]-[D] (Whittemore gage) 331
Figure 249 Surface-strain profiles for [WB]-[10]-[L] (Whittemore gage)..... 332

Figure 250 Surface-strain profiles for [WB]-[10]-[D] (Whittemore gage) 333
Figure 251 Surface-strain profiles for [WB]-[36]-[L] (Whittemore gage)..... 334
Figure 252 Surface-strain profiles for [WB]-[36]-[D] (Whittemore gage) 335
Figure 253 Surface-strain profiles for [WC]-[10]-[L] (Whittemore gage)..... 336
Figure 254 Surface-strain profiles for [WC]-[10]-[D] (Whittemore gage) 337
Figure 255 Surface-strain profiles for [WC]-[36]-[L] (Whittemore gage)..... 338
Figure 256 Surface-strain profiles for [WC]-[36]-[D] (Whittemore gage) 339
Figure 257 Surface-strain profiles for [WD]-[10]-[L] (Whittemore gage)..... 340
Figure 258 Surface-strain profiles for [WD]-[10]-[D] (Whittemore gage) 341
Figure 259 Surface-strain profiles for [WD]-[36]-[L] (Whittemore gage)..... 342
Figure 260 Surface-strain profiles for [WD]-[36]-[D] (Whittemore gage) 343
Figure 261 Surface-strain profiles for [WE]-[10]-[L] (Whittemore gage) 344
Figure 262 Surface-strain profiles for [WE]-[10]-[D] (Whittemore gage)..... 345
Figure 263 Surface-strain profiles for [WE]-[36]-[L] (Whittemore gage) 346
Figure 264 Surface-strain profiles for [WE]-[36]-[D] (Whittemore gage)..... 347
Figure 265 Surface-strain profiles for [WF]-[10]-[L] (Whittemore gage) 348
Figure 266 Surface-strain profiles for [WF]-[10]-[D] (Whittemore gage)..... 349
Figure 267 Surface-strain profiles for [WF]-[36] (Whittemore gage)..... 350
Figure 268 Surface-strain profiles for [WG]-[10]-[L] (Whittemore gage)..... 351
Figure 269 Surface-strain profiles for [WG]-[10]-[D] (Whittemore gage) 352
Figure 270 Surface-strain profiles for [WG]-[36] (Whittemore gage) 353
Figure 271 Surface-strain profiles for [WH]-[10]-[L] (Whittemore gage)..... 354
Figure 272 Surface-strain profiles for [WH]-[10]-[D] (Whittemore gage) 355
Figure 273 Surface-strain profiles for [WH]-[36]-[L] (Whittemore gage)..... 356
Figure 274 Surface-strain profiles for [WH]-[36]-[D] (Whittemore gage) 357
Figure 275 Surface-strain profiles for [WI]-[10]-[L] (Whittemore gage) 358
Figure 276 Surface-strain profiles for [WI]-[10]-[D] (Whittemore gage)..... 359
Figure 277 Surface-strain profiles for [WI]-[36]-[L] (Whittemore gage) 360
Figure 278 Surface-strain profiles for [WI]-[36]-[D] (Whittemore gage)..... 361
Figure 279 Surface-strain profiles for [WJ]-[10]-[L] (Whittemore gage) 362
Figure 280 Surface-strain profiles for [WJ]-[10]-[D] (Whittemore gage)..... 363

Figure 281 Surface-strain profiles for [WJ]-[36]-[L] (Whittemore gage) 364
Figure 282 Surface-strain profiles for [WJ]-[36]-[D] (Whittemore gage)..... 365
Figure 283 Surface-strain profiles for [WL]-[10]-[L] (Whittemore gage) 366
Figure 284 Surface-strain profiles for [WL]-[10]-[D] (Whittemore gage)..... 367
Figure 285 Surface-strain profiles for [WL]-[36]-[L] (Whittemore gage) 368
Figure 286 Surface-strain profiles for [WL]-[36]-[D] (Whittemore gage)..... 369
Figure 287 Surface-strain profiles for [WM]-[10]-[L] (Whittemore gage) 370
Figure 288 Surface-strain profiles for [WM]-[10]-[D] (Whittemore gage)..... 371
Figure 289 Surface-strain profiles for [WM]-[37] (Whittemore gage) 372
Figure 290 Surface-strain profiles for [SA]-[10]-[L] (Whittemore gage) 373
Figure 291 Surface-strain profiles for [SA]-[10]-[D] (Whittemore gage)..... 374
Figure 292 Surface-strain profiles for [SA]-[36] (Whittemore gage)..... 375
Figure 293 Surface-strain profiles for [SB]-[10]-[L] (Whittemore gage) 376
Figure 294 Surface-strain profiles for [SB]-[10]-[D] (Whittemore gage) 377
Figure 295 Surface-strain profiles for [SB]-[36] (Whittemore gage)..... 378
Figure 296 Surface-strain profiles for [SC]-[10]-[L] (Whittemore gage) 379
Figure 297 Surface-strain profiles for [SC]-[10]-[D] (Whittemore gage)..... 380
Figure 298 Surface-strain profiles for [SC]-[36] (Whittemore gage)..... 381

Tables

Table 1 Variables considered during the experimental program 14
Table 2 Transfer length results for different strand conditions when a sudden prestress method was adapted for Type III cement produced concrete 15
Table 3 Transfer length results for different prestress release methods when specimens are fabricated with smooth strand and Type III cement produced concrete. 15
Table 4 Transfer length results with different cement types for specimens fabricated with smooth strand and sudden prestress release method adapted. 15
Table 5 Cross-sectional dimensions of test specimens (Kaar, et al., 1963) 17
Table 6 – Test Parameters 18
Table 7 Material properties of prestressing reinforcement utilized for the present study 21
Table 8 Type III cement composition and potential compounds in % (Holste, 2014) 27
Table 9 Size distribution for CA#1 31
Table 10 Size distribution for CA#2 31
Table 11 Size distribution for CA#3 31
Table 12 Size distribution for FA 31
Table 13 Concrete mix proportions for Mix-Design #1 during Lab-Phase 33
Table 14 Concrete mix proportions for Mix-Design #2 during Lab-Phase 33
Table 15 Prisms test matrix during Lab-Phase 46
Table 16 Transfer Length prism test matrix by group (Lab-Phase) 48
Table 17 Nomenclature for prisms utilized in Group I 59
Table 18 Summary of transfer length results for wire reinforcements (Group I prisms) 60
Table 19 Summary of transfer length results for strand reinforcements (Group I prisms) 61
Table 20 Concrete properties at the release strength for wire and strand reinforcements (Group I prisms) 62
Table 21 Average transfer-length values by wire/strand type 65
Table 22 Nomenclature for prisms utilized in Group II 71
Table 23 Transfer length results from Group II prisms (effect of release strength) 72
Table 24 Percentage reduction in transfer length of wires due to variation in release strength ... 78
Table 25 Percentage reduction in transfer length of strands due to variation in release strength. 78
Table 26 TL ratio for different release strengths (wire reinforcements) 79

Table 27 TL ratio for different release strengths (strand reinforcements) 79
Table 28 Concrete properties at different release strength for Group II prisms 80
Table 29 TL results for prisms cast with WF at different release strengths 82
Table 30 Nomenclature for prisms utilized in Group III 85
Table 31 Transfer length results from Group III testing (effect of concrete slump) 87
Table 32 Percentage increase in avg. TL for both wire and strand reinforcements due to change in consistency (slump) 89
Table 33 Concrete properties at different concrete slumps for Group III prisms 90
Table 34 Nomenclature for prisms utilized in Group IV 94
Table 35 Transfer length results from Group IV testing (effect of w/c ratio) 95
Table 36 Percentage variation in avg. TL due to change in w/c ratio of concrete mixture 96
Table 37 Nomenclature for prisms utilized in Group V 98
Table 38 Results from Group V testing (effect of VMA presence in concrete mixture)..... 99
Table 39 Percentage variation in avg. TL due to presence of VMA in concrete mix 100
Table 40 Nomenclature for prisms utilized in Group VI 102
Table 41 Transfer length results from Group VI testing (effect course aggregate type) 104
Table 42 Percentage variation in average TL due to changes in course aggregate 104
Table 43 Avg. maximum pullout force at end slip ≤ 0.10 in. (reprinted Table 4.7) [after (Arnold, 2013)] 108
Table 44 Data sets used to create transfer length prediction model 109
Table 45 Comparison of average transfer length and predicted transfer length 112
Table 46 Prestressing steel centroid for existing 5.32 mm diameter wires 122
Table 47 Prestressing steel centroid for proposed 5/16 in. diameter 3-wire strand 123
Table 48 Prestressing steel centroid for proposed 3/8 in. diameter 7-wire strands 123
Table 49 Elongation calculations for standard reinforcement (top) and each project reinforcements during Plant-Phase 129
Table 50 Number of transfer lengths determined with each tendon type during Plant-Phase.... 135
Table 51 Description of the terminology utilized for long-term TL results 152
Table 52 Concrete parameters at the time of prestress transfer during Plant-Phase..... 154
Table 53 Transfer length results through Whittemore gage (Plant-Phase)..... 156
Table 54 Transfer length results through LSI devices (Plant-Phase) 156

Table 55 Combined (LSI and Whittemore) transfer length results (Plant-Phase) 160
Table 56 Live-end and dead-end transfer length results (Plant-Phase) 161
Table 57 Prediction of Plant-Phase TL values based on developed TL model 166
Table 58 TL length results immediately after de-tensioning and after Stage I..... 173
Table 59 Transfer length increases during Stage I (in percentages) 174
Table 60 Transfer length results at detensioning, after Stage I, and after Stage II 186
Table 61 Transfer length increases through Stage II in percentages: 187
Table 62 TL length results for “T”-marked ties in all stages..... 195
Table 63 Percentage increase in TL for “T”-marked ties during Stage III 197

Executive Summary

This report summarizes work that is part of a larger project funded by the FRA titled "Quantifying the Effect of Prestressing Steel and Concrete Variables on the Transfer Length in Pretensioned Concrete Crossties." The project has the following Major Research Tasks:

Laboratory Phase

1) Pre-tensioned Concrete Prism Tests
2) Un-Tensioned Pullout Tests with Mortar
3) Tensioned Pullout Tests with Concrete
4) Precise Measurements of the Reinforcement and Indent Geometry
5) Performing Load Tests On The Pre-Tensioned Concrete Prisms

Plant Phase

6) Automated Device for Transfer Length Measurement
7) Measuring Transfer Lengths of Concrete Crossties at the Plant
8) Un-Tensioned Pullout Tests with Concrete

Joint Research Activities

9) Evaluation of Ties Installed in Track

The work presented herein specifically covers task (1) "Pre-tensioned Concrete Prism Tests" and task (7) Measuring Transfer Lengths of Concrete Crossties at the Plant.

Summary from Lab-Phase

During the Lab-Phase of this study, which measured transfer lengths of prisms cast with nineteen (19) different reinforcements, the following conclusions can be drawn.

- The transfer length is highly-dependent on both the reinforcing type (wire or strand) and the indentation pattern.
- Thirteen (13) different 5.32-mm-diameter wires were tested in Group I of Lab-Phase had average transfer lengths that varied between 7.4 and 18.7 inches, with the lowest transfer length corresponding to the spiral wire "[WE]" and the highest transfer length corresponds to the 2-dot wire "[WL]". The average transfer length for the smooth wire in the first phase was 16.3 inch.
- For the 5.32-mm-diameter wires, wires with chevron indentations, diamond indentations, and spirals bonded better than the smooth wire and wires with dot-shaped indentations. The fact that the 2-dot wire did not bond as well as the smooth wire revealed that the

actual surface characteristics can have a significant effect on the bond of wires with minimal indentations.

- Among the stranded reinforcements, higher transfer lengths were observed in the case of 7-wire strands when compared to 3-wire strands.
- The smooth 7-wire 3/8”-diameter ([SA]) had slightly better bond characteristics than the indented 7-wire 3/8”-diameter strands [SB], which was from the same supplier. The general finding related to indented stands is that although indentations serve to improve bonding of the strands, the indentations of the strands evaluated were not sufficiently deep and/or “crisp” enough to provide better bond than smooth strands with very light surface rusting.
- The concrete compression strength at the time of prestress transfer (release strength) is a primary factor influencing the transfer length in pretensioned concrete members utilizing both wires and strands. A consistent decrease in the transfer length was observed for both wires and strands when the release strength was increase from 3500 psi to 4500 psi. This decrease in transfer length averaged 23.0% for wires and 21,9% for strands. Additionally, the increase in release strength from 4500 to 6000 psi resulted in further reduction in transfer length. This average reduction was 12.4% for wires and 21.0% for strands. Limited tests that were conducted with wire [WF] indicate that increasing release strength beyond 6000 psi will result in still further reductions in transfer length.
- A simplified expression was developed, based on the results from Lab-Phase prisms and ASTM A1096 pullout test results, that can be used to predict the transfer length in members utilizing 5.32-mm-diameter wires. This expression, presented below, had a coefficient of determination, R^2, of 0.954 when compared to all transfer length data from Lab-Phase prism tests with 5.32-mm-diameter wires. The expression is:

$$TL = 34.2 - \frac{f'_{ci}}{300} - \frac{(A1096\ value)}{\left[1250 - f'_{ci}\left(0.4 - \frac{f'_{ci}}{16{,}000}\right)\right]} \quad \text{where}$$

TL = Transfer length in inches

f'_{ci} = Concrete compressive strength at de-tensioning in psi

A1096 value = ASTM A1096 pullout value (6-specimen average) in pounds

Thus, a desired transfer length may be achieved by selecting the appropriate combination of reinforcing type and release strength.

- Prism tests conducted at different concrete slumps during group III of the Lab-Phase revealed that the consistency of the concrete mix do not have a statistically-significant effect on the transfer length when the w/c ratio was held constant at 0.32.
- No significant difference in transfer length was observed with the variation of w/c ratio. The selected w/c ratios in the present study were 0.27, 0.32, and 0.42.
- Similarly, the presence of a viscosity-modifying admixture (VMA) in the concrete mixture did not result in a significant variation in transfer length.

- Prisms cast with Mix-Design #2 and wire [WH] resulted in severe cracking (longitudinal splitting along the wires) upon detensioning. However, prisms cast with Mix-Design #1 and wire [WH] had splitting on only a few occasions. From these results, it is evident that both the wire indentation type and concrete coarse aggregate source may play a large role in the splitting propensity of pretensioned concrete railroad ties.

Summary from Plant-Phase

- The two fabricated LSI devices allowed concrete surface-displacement measurements to be made at a much faster rate and eliminated the human errors associated with the traditional Whittemore gage method. The LSI method of measurement allowed for the determination of transfer lengths at many locations along the prestressing bed with minimal interruptions to the production cycle. Hence, this same system could be utilized in quality control programs at concrete crosstie plants.
- Transfer lengths tests performed during Lab-Phase (Group I prisms) had excellent correlation with Plant-Phase transfer lengths. A coefficient of determination of R2=0.858 was observed between the equation developed from Lab-Phase data and Plant-Phase results when all 12 wire reinforcements are considered.
- The laboratory prisms, when cast with a similar concrete mixture, were able to accurately represent the behavior of the prestressing tendons when utilized to manufacture pretensioned concrete crossties. Therefore, in the future, the bond performance of a new reinforcement in pretensioned concrete railroad ties could be determined by measuring transfer lengths on similar prisms using a representative concrete mix.
- Additionally, these small-scale laboratory prisms would also provide an economical option for the tie manufacturing industry to select the proper combination of prestressing tendons and release strength to achieve the desired transfer lengths. Essential information obtained through laboratory tests can also be utilized by reinforcement manufacturers to establish the factors (such as indent type, drawing lubricants, etc.) that effect the bonding performance.

Summary from Long-Term Study of Plant-Manufactured Concrete Ties

- In the present study, the largest transfer length increase was observed during Stage I, which was the time after fabrication and installation in Track. This initial higher TL growth is observed without any loading. Transfer length increases were minimal at the later stages, even for “T”-marked ties subjected to in-track loading. Hence, it can be concluded that the majority of transfer length increase occurs during the first year after fabrication and is primarily time-dependent and climate-dependent rather than load-dependent.

Recommendations

- It is highly recommended to perform laboratory prism tests to evaluate the bond performance of the prestressing reinforcement that is selected for pretensioned concrete tie production. These prism tests should be conducted with the same concrete mixture and de-tensioning strength that is going to be used for the concrete tie production.

- Frequent prisms tests are recommended to evaluate the influence of any changes occurring in the manufacturing process (such as changes in concrete materials, prestressing tendons, etc.).
- Transfer length measurements, without interrupting the production process, can be made using the LSI device and would enhance the quality assurance of concrete tie production.

Chapter 1 Introduction

Prestressed concrete railroad ties are becoming more popular as a suitable alternative to wooden ties in the United States. This preference to prestressed concrete ties is given due to various factors like durability in severe weather conditions, efficiency to carry heavy railroad cars, longer service life, lower maintenance costs and environment friendly product. Identifying the parameters that influence the performance of these concrete railroad ties is important to analyze the behavior throughout their service life. One such parameter is transferring prestressing force to concrete member. Poor or improper bond transfer can result in premature failure of a prestressed concrete tie.

1.1 Background

In a pretensioned concrete member, the length required to transfer the effective prestressing force into the concrete member is defined as "Transfer Length" (TL) (Kaar, et al., 1963). For prestressed concrete ties to have maximum flexural and shear capacity at the rail-seat location, the prestressing force must be fully transferred to the concrete at a location that is closer to the end of the tie than the distance to the rail seat. Typically, 21-in is the distance from the end of the tie to the rail load. Thus, it is essential that the transfer length is significantly shorter than 21-in for the ties to have their full capacity at the rail-seat location.

To ensure these transfer lengths, it is crucial to have good bond between the prestressing reinforcement and the surrounding concrete. For pretensioned concrete ties produced in the United States, indented 5.32-mm-diameter, low-relaxation steel wires have become the industry norm (but are not the case for all concrete tie manufacturers). It is generally understood that these wires achieve shorter transfer lengths due to the presence of indentations; however 3-wire and 7-wire strand have also been successfully used with nominal diameter less than 3/8-in. (Hanna, 1979). Further, tensile stresses can be avoided during the prestressing transfer by using smaller diameter strands/wires (Kaar, et al., 1975).

While it is generally accepted that indentations in the wires improve the bond between the steel and concrete, there is currently not a standardized indentation pattern (shape, size, depth of indent, etc.) that is utilized by all wire manufacturers. Thus, the corresponding bond behavior of these different wires when placed in various concrete mixtures, in terms of average transfer lengths and typical variations, was essentially unknown at the beginning of this research.

An in-depth research program was conducted to evaluate the variation in bond transfer length with prestressing steel and concrete variables. These factors include but not limited to; reinforcement indentations, concrete consistency (slump), compressive strength at the time of prestress transfer (release strength), the water-to-cementitious (w/c) ratio, aggregate type, and the presence of viscosity-modifying admixture (VMA).

Further, information about the transfer length variation with concrete variables is essential; since individual tie manufacturers utilize different concrete materials. Understanding the effect of these variables on transfer length can lead to a better "engineered-product" (concrete tie) that ensures safety at an economical cost.

Results from comprehensive experimental work that was conducted at both the Kansas State University laboratories and at a Precast/Prestressed Concrete Institute (PCI) certified Tie manufacturing plant are presented in this report. Transfer length results from laboratory prism tests are compared to transfer length results in actual concrete ties that were manufactured at a PCI certified plant. Correlation between laboratory transfer length results and Plant-Phase transfer length results demonstrate the efficacy of the small scale experimental tests.

1.2 Objective

The objective of the present research is to quantify the effect of prestressing steel and concrete variables on the transfer length in pretensioned concrete railroad ties. A systematic investigation of the factors affecting this bond performance is essential to understand the transfer length variations. This work was conducted in two phases: a laboratory phase and a Plant-Phase.

1.2.1 Lab-Phase Transfer Lengths from Pretensioned Concrete Prisms

Pretensioned concrete prisms were cast in a controlled environment at Kansas State University (KSU) laboratories to evaluate the variation of transfer length with different parameters; reinforcement indentations, concrete consistency, concrete release strength, w/c ratio, aggregate type, and the presence of viscosity-modifying admixture (VMA). These prisms were designed to have a prestressing steel spacing and overall concrete-to-steel ratio that is representative of pretensioned concrete railroad ties. The intension was to evaluate and quantify the influence of each individual variable on transfer length.

The effect of reinforcement indentation was studied by evaluating transfer length results of prisms cast with different reinforcement types utilizing the uniform concrete mix proportions.

A consistent concrete mix was produced with water-to-cement ratio of 0.32 for this group of prisms. Transfer lengths were measured on prisms cast with nineteen (19) different reinforcement types that are employed in concrete railroad ties worldwide. These reinforcements were obtained from seven (7) different manufacturers with different indentation types. This allowed the researcherss to quantify the various types of reinforcement indentation geometries on transfer length. Additional Lab-Phase details are discussed in Section 5.1.

Variation of transfer length with concrete variables was evaluated by conducting tests on prisms cast with altered concrete variables. Ten (10) out of nineteen (19) reinforcements were employed to accomplish this detailed investigation. Each group of prisms were cast by altering the selected concrete variable and keeping all other variables constant.

1.2.2 Plant-Phase Transfer Lengths from Pretensioned Concrete Crossties

A research group from KSU traveled to a PCI certified concrete tie manufacturing plant to determine transfer lengths in non-prismatic prestressed concrete railroad ties. A subset of fifteen (15) different reinforcement types that were employed in Lab-Phase were chosen to fabricate pretensioned concrete ties over a three-week period. Fifty (50) different transfer-lengths (occurring at both ends of 25 ties) were determined with each reinforcement type, for a combined total of 750 transfer lengths.

As such, this was the most transfer-lengths ever determined for concrete railroad ties in production. The primary variable in this portion of study was prestressing reinforcement type. In-plant concrete surface strains were determined by utilizing both a mechanical gage and two automated laser-speckle imaging devices. Later, long term study was conducted on plant manufactured crossties which were cast exclusively to utilize the mechanical strain gage system.

For the long-term study, four concrete ties were cast with each reinforcement type for a total of 60 concrete ties. Thus, a total of 120 transfer lengths were determined using this method, 8 for each of the 15 different reinforcements. Among the four ties for each reinforcement type, two ties were installed in track and subjected to a cumulative in-track loading of 263.3 million gross tons (MGT). Before being subjected to this in-track loading, special covers were installed to protect the brass inserts (that were cast into the bottom surface of the ties) from surface abrasion. The other two ties, which are companion ties for each reinforcement type, were not

subjected to any loading. Additional information regarding the experimental procedures utilized during the Plant-Phase are presented in Chapter 6.

Transfer lengths for concrete ties manufactured at the plant were used to determine the possible correlation of the results obtained during the laboratory phase and to evaluate the validity of laboratory prisms tests in predicting the transfer lengths that would occur in actual concrete ties. Finally, the possible increase in transfer length due to repeated in-track loading was investigated.

1.3 Scope

A detailed investigation about the possible influential parameters that characterize the transfer length of a pretensioned concrete tie was carried out. The specific parameters investigated in this study included the reinforcement indentations, concrete consistency, release strength, water-to-cementitious (w/c) ratio, aggregate type, and the presence of viscosity-modifying admixture (VMA). Quantifying the effect of each individual parameter on transfer length was achieved by a systematic variation of the mix design and reinforcement type.

Further, experimental investigation conducted in Lab-Phase was compared with Plant-Phase investigation to find out the efficacy of the laboratory tests in predicting actual transfer lengths in pretensioned concrete ties. Additionally, the long-term transfer length increase of concrete ties with different reinforcement types due to in-track loading was determined.

1.4 Organization of the Report

Chapter 2 presents the previous related research pertaining to transfer length determination in pretensioned concrete railroad ties or closely related fields. This review helped the researchers to predict the parameters that may influence the transfer length. This review about the previous research enhances the researchers's knowledge about approaching the research problem statement in a chronological sequence.

Chapter 3 presents the different materials used in this research program (concrete materials and reinforcement) along with their acquisition, storage in the laboratory, and naming conventions used. Additionally, it discusses the established concrete mix-designs during Lab-Phase. It also emphasizes the similarities between actual plant mix design and lab mix design.

Chapter 4 describes the experimental set-up utilized to cast the laboratory prisms, various prism cross-sections employed for different reinforcement sizes to represent the real concrete tie,

different equipment utilized during the testing procedure, prisms casting procedure and the approach used to analyze the results.

Chapter 5 discusses the results obtained from the extensive tests conducted at KSU laboratories or simply “Lab-Phase”.

Chapter 6 presents the experimental setup employed at PCI certified concrete tie manufacturing plant, and various testing procedures adapted to be able to quickly and accurately determine transfer lengths. The chapter explains how the surface-strain measurements were determined from both an 8-inch mechanical gage (Whittemore gage) and from a non-contact laser-speckle imaging (LSI) device. Finally, this chapter provides the details about special surface preparations employed for the concrete crossties installed in the track.

Chapter 7 discusses results obtained from measurements at the tie manufacturing plant and compares these results with the Lab-Phase results. This chapter also includes the long-term study of plant-manufactured crossties.

Chapter 8 concludes the findings from the present comprehensive research which provide vital information about bond transfer length. Further recommendations in the related research are also provided in this chapter.

Chapter 2 Literature Review

This chapter presents the previous related research pertaining to transfer length determination in pretensioned concrete railroad ties or closely related fields. This review helped the researchers to predict the parameters that may influence the transfer length. This review about the previous research enhances the researchers's knowledge about approaching the research problem statement in a chronological sequence.

2.1 First recorded use of concrete railroad ties in the United States

2.1.1 Weber (1969)

Usage of concrete railroad ties in the United States were first recorded in 1893. During this year, 200 ties were installed in Germantown, PA. Around 150 reinforced concrete crosstie design types were proposed and patented between 1893 and 1930. During this period, 60 concrete design types were experimentally tested. These crossties could not gain much attention due to: 1) design failures, 2) improper rail fastening system, 3) incompatibility with changes occurred in track, 4) expensive compared to wooden crossties. Availability of sufficient quantities of appropriate timber and the advancement in wooden pressure treatment caused minimal development in concrete crosstie industry during 1930 through 1957.

Major portion of the early concrete crosstie work in the United States was carried out with the involvement of the Association of American Railroads (AAR). Research staff at AAR initiated the research on prestressed concrete ties in 1957. Three concrete tie designs were initially developed and load tests were conducted. Design requirements for the concrete ties were considered based on the existed wooden tie design requirements. Upon completion of tests on ties with three design criteria, two additional designs were developed followed by the tests. Static and repeated load tests were conducted on the test specimens.

2.2 Advantages of concrete railroad ties over wooden ties

This section discusses the various advantages of concrete railroad ties when compared to its counter parts, wooden railroad ties.

2.2.1 (Hanna, 1979)

Hanna (1979) investigated the advantages of concrete railroad ties over wooden ties. According to Hanna, concrete ties are becoming more popular in most parts of the world due to various advantages. These advantages with concrete railroad ties include: 1) Consistent product with improved quality, 2) Economical product of higher service life along with improved structural performance.

2.2.2 (Crawford, 2009)

Concrete and wood are two predominant materials to produce railway sleepers. Analysis of greenhouse gas emissions for these two predominant materials are compared in this study. This study is important as the production of railway sleepers (crossties) involves remarkable environmental impact. Two materials studied by the authorss are as follows:

- River Red Gum (Eucalyptus Camaldulensis), untreated
- Reinforced concrete
- Eight scenarios were studied for both concrete and wooden sleepers. Greenhouse gas emissions were determined in terms of carbon dioxide equivalent (CO_2-e). This study presents the emission data for 100-year life cycle for more than one-kilometer length of track. The authors found that the utilization of wooden sleepers can result in higher emissions (than concrete sleepers) for up to two to six times.
- Few ways to lower these emissions are: usage of alternative material and thereby reducing the quantity, (example: fly ash to in the place of cement), utilization of recycled materials, improved design to reduce materials required to produce sleepers, utilization of removed timber sleepers to produce thermal energy.

2.2.3 (Real, et al., 2014)

Vibrations developed due to rail loads in concrete and wooden sleepers are investigated and compared. Vibrations were measured on sleepers installed both on straight track and curved track. Four different comparisons were studied are follows:

- Sleeper Concrete Curve/ Straight
- Sleeper Wood curve/Straight
- Sleeper Concrete/Wood Straight

- Sleeper Concrete/Wood curve

During the study measurements were taken using accelerometers based on MEMS technology. A total of 8 sensors were installed for the study. These sensors were installed both on sleepers and on rails. Sensors were installed at the end in the case of sleepers. For rails, these sensors were installed in the web portion.

In the case of concrete sensors located on straight and curve sections, similar accelerations around 10 m/s2 were registered. And the peak accelerations were between 15 and 20 m/s2. Wooden sleepers installed in curve section recorded accelerations around 30 m/s2 which is greater than straight section wooden sleepers' acceleration values 10-15 m/s2. Peak accelerations values for curve section wooden sleepers were 50-60% higher than straight section wooden sleepers. A general trend of higher accelerations is observed in the case of curve section sleepers compared to their counterpart straight section sleepers.

Similar results were observed for both concrete and wooden sleepers installed in straight section. Slight higher values were observed in wooden sleepers installed in straight section. However, the difference in behavior was observed between wooden and concrete sleepers. Due to stability of concrete sleepers, loading in concrete sleepers were more defined than wooden sleepers. Whereas, in the curve section, concrete sleepers registered much lower accelerations compared to wooden sleepers. Concrete sleepers in curve section had 33% of wooden sleeper accelerations. Lower accelerations in concrete sleepers in all cases was due to stability achieved by the weight, isotropic behavior of concrete.

However, accelerations in rails are different. Rails placed on top of wooden sleepers registered lower accelerations than rails placed on concrete sleepers. This difference is higher in curved section and lower in straight section (between rails placed on wooden and concrete sleepers). This is due different damping behaviors of the pads installed above concrete and wooden sleepers.

2.3 Previous research recommendations

2.3.1 (Hanna, 1979)

Along with the stated advantages, Hanna (1979) also suggested some recommendations in order to produce a better pretensioned concrete tie. High early concrete compressive strength allows the prestress transfer at early ages which reduces prestress losses, improves flexural

strength which leads to higher crack resistance. Therefore, high early strength concrete is recommended for pretensioned concrete ties. Previous research stated that the satisfactory compressive strength of the concrete at the time of prestress transfer is 4000 psi (Hanna, 1979). Following guidelines are given to produce satisfactory concrete strengths with freez-thaw durability

- Course aggregate size is limited to ¾-in.
- Concrete mix with 650 lb./cu yd cement or more
- Limit water-cement ratio to the maximum of 0.40 with air-entraining admixtures and achieve proper consolidation during casting.
- Modified curing techniques to increase the strength gaining rate

High strength prestressing reinforcement with indentations can accomplish better bond between reinforcement and concrete and thereby improving the load carrying capacity of the member. It is also recommended to limit the maximum size of the reinforcement to 3/8-in diameter. Prestressed reinforcement should be chosen with proper surface treatment to accomplish the adequate bond between concrete and reinforcement.

Concrete tie dimensions should be chosen in such a way so that the bond between concrete and reinforcement is achieved prior to the rail seat location and to keep lower ballast pressures. During the application of rail car loads, tensile stresses will develop on top fibers at the center of a Tie. Therefore, it is essential to keep the prestressing force near to the tension zone. This can be achieved by reducing the sectional depth where top tensile stresses are produced.

2.4 Types of concrete railroad ties

2.4.1 (Hanna, 1979)

Various types of concrete ties have been utilized since the development of concrete ties. Prestressed monoblock, prestressed two-block, reinforced two-block, and longitudinal concrete ties were few types among the concrete ties. Typical two-block and monoblock concrete ties are shown in Figure 1.

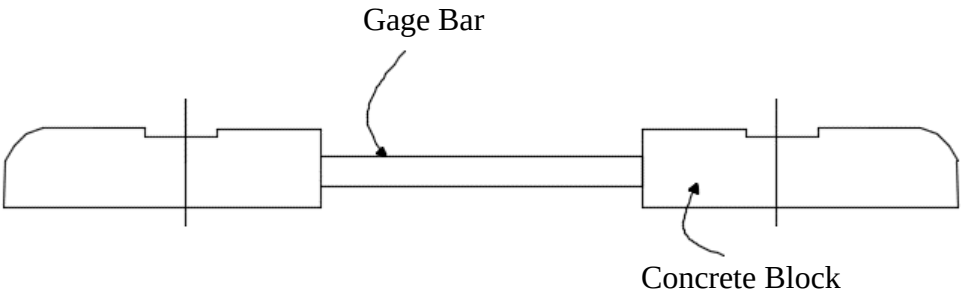

1) Two-Block

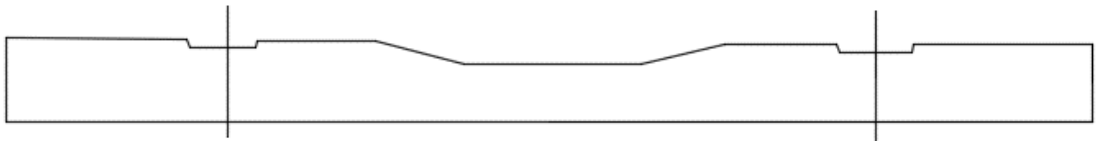

2) Monoblock

Figure 1 Types of concrete ties (Hanna, 1979)

2.4.1.1 Fabrication methods

Prestresed concrete crossties are fabricated either by post-tensioning or by pre-tensioning. In the case of pre-tensioned concrete ties, reinforcing tendons are tensioned prior to the concrete being cast. Later, after concrete has sufficiently cured to the specified compressive strength, the prestressing force is transferred through bond to the member. Whereas, in post-tensioning members, the tendon tensioning operation is carried out after the concrete reached the specified compressive strength and the prestressing force is transferred through end-bearing.

Majority of the prestressed concrete ties produced in North America are pre-tensioned members. Pre-tensioned crossties can be by the following three methods:

1) **Long-Line method:** Long prestressing beds are used in this method to cast multiple crossties end-to-end. Common pre-tensioning operation is carried out for the all the concrete members on one single prestressing bed. Upon the completion of pre-tensioning operation, concrete is placed on the forms. Prestressing force is transferred once the concrete reaches the desired strength.

2) **Stress-Bench Method:** Structural steel mobile benches are used in this method. Mechanical operation of these benches provides the possibility to move in longitudinal and transverse directions. Using this method, crossties manufacturing process can be performed at desired locations.
3) **Individual Form Method:** Each crosstie is pre-tensioned separately in this method. End Forms are utilized to perform the pre-tensioning operation.

2.5 Bonding Mechanisms between concrete and prestressing reinforcement

2.5.1 Hoyer & Friedrich (1939)

Hoyer & Friedrich (1939) explained the theory behind the frictional mechanism between concrete and prestressing reinforcement in pre-tensioned concrete members. This theroy is popuraly known as “Hoyer Effect”.

Upon pretensioning, the diameter of the prestressing reinforcement will reduce due to poisson’s effect. After the completion of pre-tensioning process, concrete is cast and cured to the required strength. Prestress force is then transferred to the hardened concrete member after achieving desired concrete compressive strength. While transferring the prestressing force to the concrete member, diameter of the reinforcement will try to expand to regain its original diameter and also slip in the prestressing reinforcement takes place. However, the concrete surrounding the reinforcement acts to resist this lateral expansion and as a result, radial forces will develop which create a frictional bond between concerete and reinforcement. This bond transfer mechanism in a pre-tensioned member is called “Hoyer Effect”. At the ends of a pre-tensioned concrete member, stress in the reinforcement will be zero and increases over certain length after which it reaches a constant value. During this process, diameter of the reinforcement varies as shown in Figure 2.

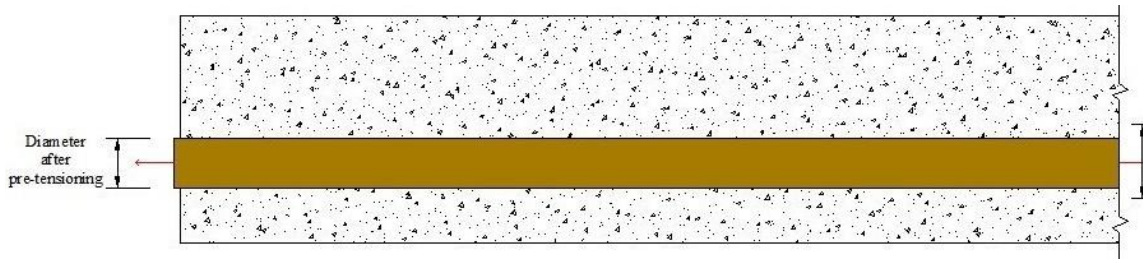

(a) Reinforcement in the concrete before the transfer of prestressing force

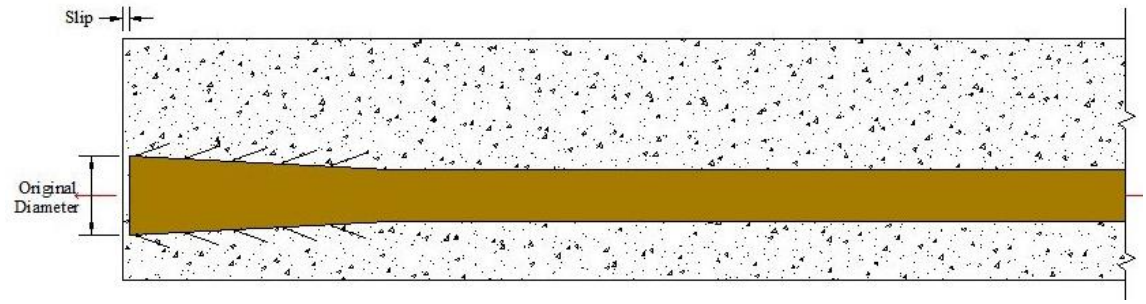

(a) Reinforcement in the concrete after the transfer of prestressing force

Figure 2 Transfer of prestressing force to the concrete member: Hoyer Effect

2.6 Effect of diameter of prestressing reinforcement on transfer length results

Various prestressing tendon diameters are used in the production concrete railroad ties. This section presents information pertaining to previous studies that investigated the use of prestressing tendons with various diameters.

2.6.1 Krishnamurthy (1972)

According to Krishnamurthy (1972), transfer length of pretensioned member is related to the diameter of the prestressing reinforcement. Various tests were conducted by the authors using 5-mm-diamter wire reinforcements. A de-mountable mechanical (DEMEC) strain gage was used to obtain surface-strain profiles along pretensioned specimens. Transfer lengths were then determined from these surface-strain profiels at different release strengths, and by different methods of prestress transfer.

Data from various tests conducted by researcherss were obtained and compared to estlabilsh the relationship between transfer lengths of different diameter prestressing reinforcements. Tests conducted by British Railways with 2 and 5 mm wire reinforcements were carried out at concrete strength varying from 270 to 550 kg/cm^2. Tests conducted at Leeds

university were focused on small dismater wire reinforcements of 2, 5, and 7 mm diameters. Transfer lengths of various German-made reinforcement were measured by Rusch and Rehm at different; concrete strengths varying from 160 to 340 kg/cm^2, prestress levels, reinforcement indent types, pre-stress transfer method, and time factors. Tests were conducted both in the lab and in the factory with different wires.

Five different factories across the United Kingdom were visited during the study, and the mix designs used among the factories were different. Tests were conducted by Arthur and Ganguli on 5 mm wires, a total of 19 tests were conducted at concrete strengths ranging from 158 to 435 kg/cm^2. Concrete specimens were fabricated using Belgian pattern B-type indented wire. All these test data were summarized to establish the relationship between transfer length and diameter. In the case of wire reinforcements the following relationship was obtained as shown in equation 2.1. This relation is valid for two, five, and seven mm diameter wires. Additionally, the relationship shown in Equation 2.1 is valid when the gradual prestress transfer takes place. Where “d” is wire diameter in “mm”.

$$l_t = 100d \tag{2.1}$$

Whereas, in the case of sudden release of prestressing force, transfer length for 5 mm diameter reinforcement is given by equation 2.2.

$$l_t = 120d \tag{2.2}$$

From the summarized test data, transfer length expression for strand of diameters 9.52, 12.70, and 17.80-mm with gradual prestress transfer is given by equation 2.3.

$$l_t = 10d + 1.2d^2 \tag{2.3}$$

2.7 Effect of reinforcement's surface on transfer length results

Various studies have been conducted to evaluate the influence of prestressing tendon's surface condition on bond characteristics. Some of the studies are discussed in this section to provide background information.

2.7.1 Kaar & Hanson (1975)

Kaar & Hanson (1975) conducted a series of experiments on 108 pre-tensioned concrete members and drew important conclusions for concrete railroad ties. In this experimental program, three types of strand surface conditions were used with two different types of prestress release methods. Additionally two different cements were used during the experimental program. Various conditions used during this experimental program are tabulated in Table 1.

Table 1 Variables considered during the experimental program

Variables Evaluated	Conditions
Surface Condition	Smooth
	Lightly rusted
	Sandblasted
Method of Prestress transfer	Sudden release
	Gentle release
Cement type	Type III cement
	Regulated set cement

Tests were performed on beams with cross-sectional dimensions of 3.5 in. x 7 in. and 8.5 ft long. Four test specimens were fabricated during each pour. All specimens were pretensioned with one 7-wire 3/8-inch diameter strand. A minimum compressive strength of 4000 psi was ensured at the time of prestress transfer.

Developed surface-strain profiles due to prestressing force were obtained though prior and after de-tensioning measurements of surface displacement, measured using a 10-in. Whittemore mechanical strain gage. A total of 76 transfer lengths were measured in this study for the different conditions noted in Table 1. Average transfer lengths obtained during this study with different conditions are tabulated in Table 2 through Table 4.

Table 2 Transfer length results for different strand conditions when a sudden prestress method was adapted for Type III cement produced concrete

Strand Surface Condition	**Average Transfer Length, in.**
Smooth Strand	29.4
Lightly Rusted strand	14.2
Sandblasted strand	18.6

Table 3 Transfer length results for different prestress release methods when specimens are fabricated with smooth strand and Type III cement produced concrete.

Prestress release method	**Average Transfer Length, in.**
Gentle release	23.9
Sudden release	29.4

Table 4 Transfer length results with different cement types for specimens fabricated with smooth strand and sudden prestress release method adapted.

Cement Type	**Average Transfer Length, in.**
Type III	29.4
Regulated Set	18.8

From Table 2, transfer lengths can be greatly influenced by surface condition of the strand. Better bond performance was observed, in the case of lightly rusted and sandblasted strand surfaces when compared to smooth surfaced strands where all the remaining conditions were uniformly maintained. Highest bond performance was observed in the case of slightly rusted strand.

From Table 3, gentle prestress transfer method results in better bond performance over the sudden prestress transfer method. From Table 4, concrete produced with regulated-set cement results in significantly-lower transfer lengths over concrete produced with Type III cement.

2.8 Effect of release strength on transfer length results

2.8.1 (Kaar, et al., 1963)

In this study, the authorss investigated the influence of release strength on prestress transfer. Tests were conducted on four different 7-wire strands to investigate the transfer length variation due to concrete compressive strength. The different strands utilized in this study had diameters of 1/4, 3/8, 1/2 and 0.6 in. Rectangular cross-sectional concrete members with different release strengths were cast with these strands. Release strengths investigated in the study were 1660, 2500, 3330, 4170, and 5000 psi. Cross-sectional dimensions for various tests are tabulated in Table 5.

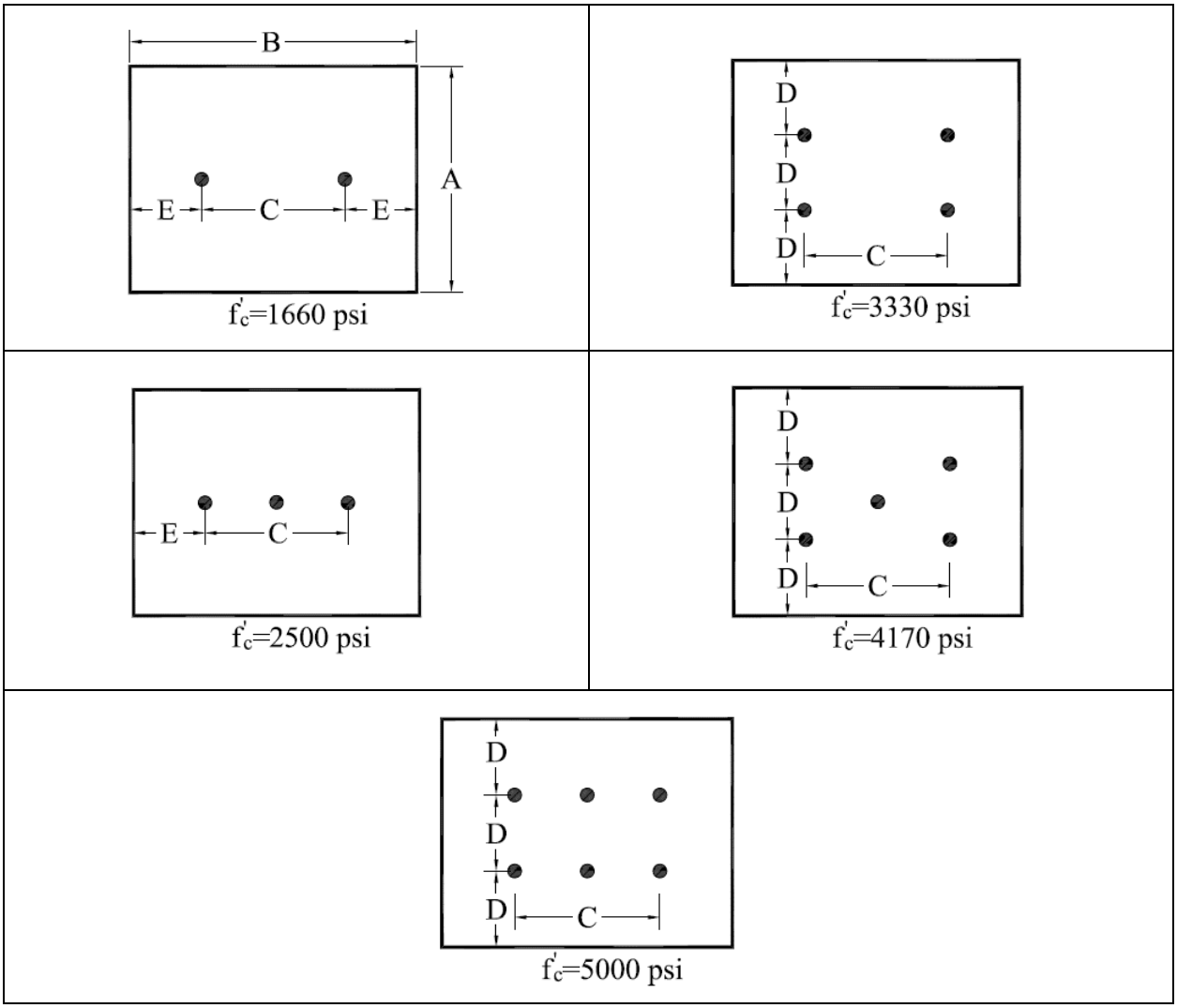

Figure 3 Strand patterns for different release strengths (Kaar, et al., 1963)

Table 5 Cross-sectional dimensions of test specimens (Kaar, et al., 1963)

Strand Size (in.)	Strand Area (sq in.)	All dimensions given in inches					Length of Specimen (ft)
		A	B	C	D	E	
1/4	0.036	3	4 3/16	2 3/16	1	1	8
3/8	0.080	4 1/2	6 9/32	3 9/32	1 1/2	1 1/2	8
1/2	0.144	6	8 3/8	4 3/8	2	2	8
6/10	0.221	7 1/2	10 1/2	5 1/2	2 1/2	2 1/2	10

Strands were pre-tensioned to slightly over the desired stress at the time of prestress transfer. Load cells were arranged to monitor the pre-tensioning force in a strand. Upon the completion of concrete casting, desired release strengths of 1660, 2500, 3300, 4170, and 5000 psi were obtained at average ages of 1, 2, 3, 9, and 22 days respectively.

Brass disks (inserts) were installed to determine the concrete strain values. These brass inserts were installed on both sides of the concrete member at a spacing of 2-in. center to center. A 10-inch Whittemore mechanical strain gage was used to measure the distance between brass disks. Additionally, a steel bracket was installed on each end side to accommodate the support for strain gage when the distance is less than 10-in. Distance between brass disks were measured prior to the prestress transfer, immediately after the prestress transfer, and also at later ages (1, 3, 7, 14, 28, 56, 90, 180, and 365 days). Concrete strains were then determined using reference measurements taken before prestress transfer and at a given age after prestress transfer.

For the 1/4, 3/8, 1/2 and 0.6 in.-diameter strands, there was not a consistent variation in transfer length observed with the increase in concrete release strength. However the 0.6-in diameter strand did show a reduction in transfer length with the increase in release strength at the cut end.

An increase trend in transfer length was observed for cut ends when compared to dead ends. Additionally, it was found that the time-dependent increase in transfer length did not depend on the magnitude of release strength. From the studies conducted, an average of 6% increase in transfer length was observed over one year after prestress transfer.

2.8.2 Mitchell et. al (1993)

Mitchell et.al (1993) conducted tests to evaluate the effect of release strength on transfer and development lengths of members cast with three different strand sizes, 3/8-in, 1/2-in, and 0.6-in. The concrete strength at de-tensioning ranged from 3050 to 7250 psi. Later these concrete specimens were tested, at 28-days, at 4500 to 12900 psi.

Table 6 – Test Parameters

Strand Diameter (in)	Surface condition	Strand Ultimate Tensile Strength (ksi)
3/8	Slightly rusted	263
1/2	Smooth untreated	276
0.62	Smooth untreated	260

Transfer lengths were evaluated through surface displacement measurements at the level of prestress reinforcement. Gradual prestressing method was adapted during this experimental program. For each specimen, surface displacement measurements were recorded three times; prior to de-tension, after to de-tension, and at the time of load testing respectively.

In the case of 3/8-in.-diameter strand, reduction in transfer length was observed from 19.9 in. to 16.3 in. when the concrete compressive strength at prestress transfer was increased from 3000 psi to 7310 psi. Average transfer lengths for lower compressive strengths were observed to be $53d_b$, $55d_b$, and $49d_b$ for the strands 3/8 in., 1/2 in., and 0.62 in. respectively, where, "d_b" is the diameter of the prestressing reinforcement.

Mitchell et.al (1993) also explained that "the concrete with higher compressive strength also associated with higher Modulus of Elasticity, lower creep strains and small shrinkage strains" and due to this reason, long-term loasses will be reduced and further higher percentage of prestressing force can be retained in the member. The researcherss proposed the following equation for transfer length:

$$l_t = 0.33 f_{pi} d_b \sqrt{\frac{3}{f'_{ci}}} \tag{2.1}$$

where

$l_t = Transfer\ length, in.$

$f_{pi} = Prestress\ at\ the\ time\ of\ transfer, ksi$

$d_b = diameter\ of\ the\ strand, in.$

$f_{ci}' = compressive\ strength\ at\ the\ time\ of\ prestress\ transfer, ksi$

Chapter 3 Material storage and operation

3.1 Reinforcement

The present study included nineteen (19) different prestressing reinforcement types, from seven different steel manufacturers, that are used in the manufacture of pretensioned concrete railroad ties worldwide. The reinforcements were obtained and donated to Kansas State University (KSU) by LB Foster/CXT Concrete Ties (CXT). Among these nineteen different reinforcements, thirteen (13) of them were 5.32-mm-diameter wires and the remaining six (6) were strands. All wires were labeled from [WA] through [WM], sequentially, based on their date of arrival at the KSU laboratory. Similarly, strands are labeled from [SA] through [SF]. The seven different steel manufacturers that produced the reinforcements were also labeled from "A" though "G". This generic labeling for the reinforcement was adapted (instead of providing manufacturing information), to avoid any misusage of the data.

All of the reinforcements were low-relaxation type, Grade 270 ksi steel. One of the thirteen wires was smooth (i.e. no indents) and the remaining twelve wires were indented. All thirteen wire reinforcements types are shown in Figure 4 (Arnold, 2013). Strands are further divided into 3-wire strands having diameters of 5/16-in. and 3/8-in., and 7-wire strands having a diameter of 3/8-in. Different strand samples employed in the research are shown in Figure 5. Material properties of each reinforcement type, as provided by the manufacturer, are tabulated in Table 7

Table 7 Material properties of prestressing reinforcement utilized for the present study

	Reinforcement Manufacturer	Reinforcement Label	Indentation Type, Diameter	Ultimate Tensile Force (lb.)	Ultimate Tensile Strength (ksi)	Cross-Sectional Area (in2)	Modulus of Elasticity, E (ksi)
Wires	A	[WA]	Smooth, 5.32-mm	10,184	293.5	0.0347	29,700
	A	[WB]	Chevron, 5.32-mm	9,712	281.7	0.0345	30,510
	A	[WC]	Spiral, 5.32-mm	9,892	290.3	0.0341	28,400
	B	[WD]	Chevron, 5.32-mm	9,696	275.5	0.0352	30,120
	B	[WE]	Spiral, 5.32-mm	9,258	268.6	0.0345	28,570
	B	[WF]	Diamond, 5.32-mm	9,280	269.2	0.0345	29,000
	C	[WG]	Chevron, 5.32-mm	9,376	271	0.0346	30,300
	D	[WH]	Chevron, 5.32-mm	9,438	271.2	0.0348	29,870
	E	[WI]	Chevron, 5.32-mm	9,389	279.5	0.0336	29,000
	E	[WJ]	Chevron, 5.32-mm	9,702	276.9	0.0350	28,600
	F	[WK]	4-Dot, 5.32-mm	9,839	284.6	0.0346	29,430
	F	[WL]	2-Dot, 5.32-mm	9,711	280.9	0.0346	29,480
Strands	E	[SA]	Smooth, 3/8-inch, 7-wire	23,661	278.4	0.0850	29,000
	E	[SB]	Indented, 3/8-inch, 7-wire	23,793	279.9	0.0850	29,000
	E	[SC]	Smooth, 5/16-inch, 3-wire	15,871	272.7	0.0582	29,000
	F	[SD]	Indented, 3/8-inch, 7-wire	24,630	288.1	0.0855	29,090
	G	[SE]	Indented, 3/8-inch, 7-wire	23,069	272.4	0.0847	28,100
	B	[SF]	Indented, 3/8-inch, 3-wire	18,550	285.4	0.0650	28,560

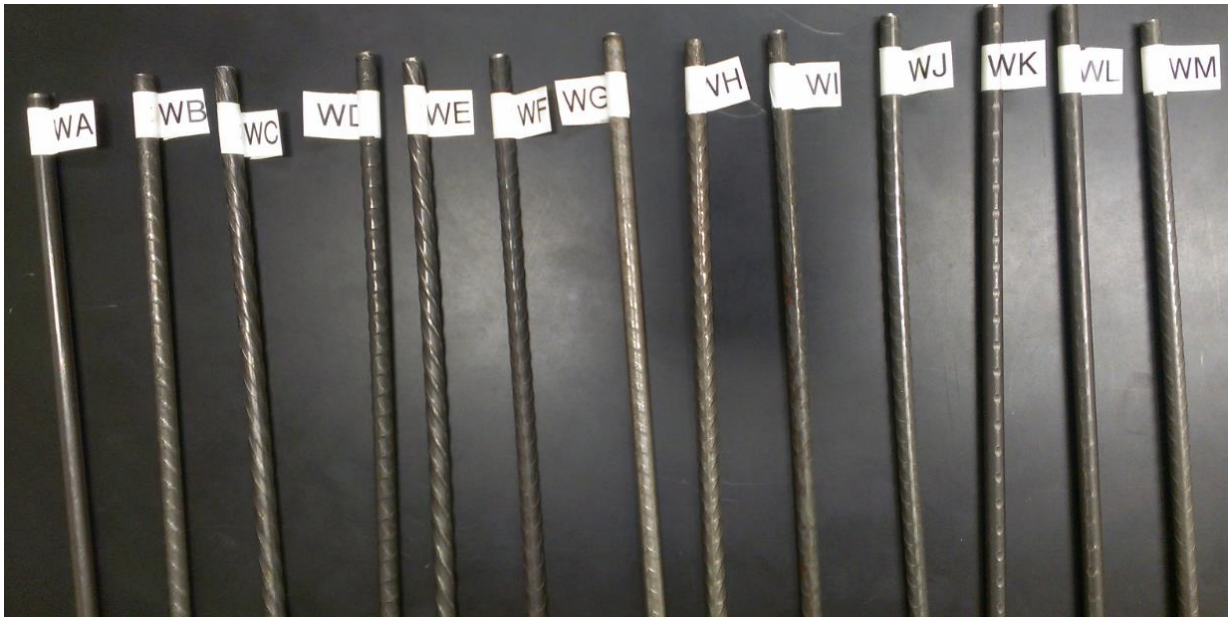

Figure 4 Various wire reinforcements employed in the present research (Arnold, 2013)

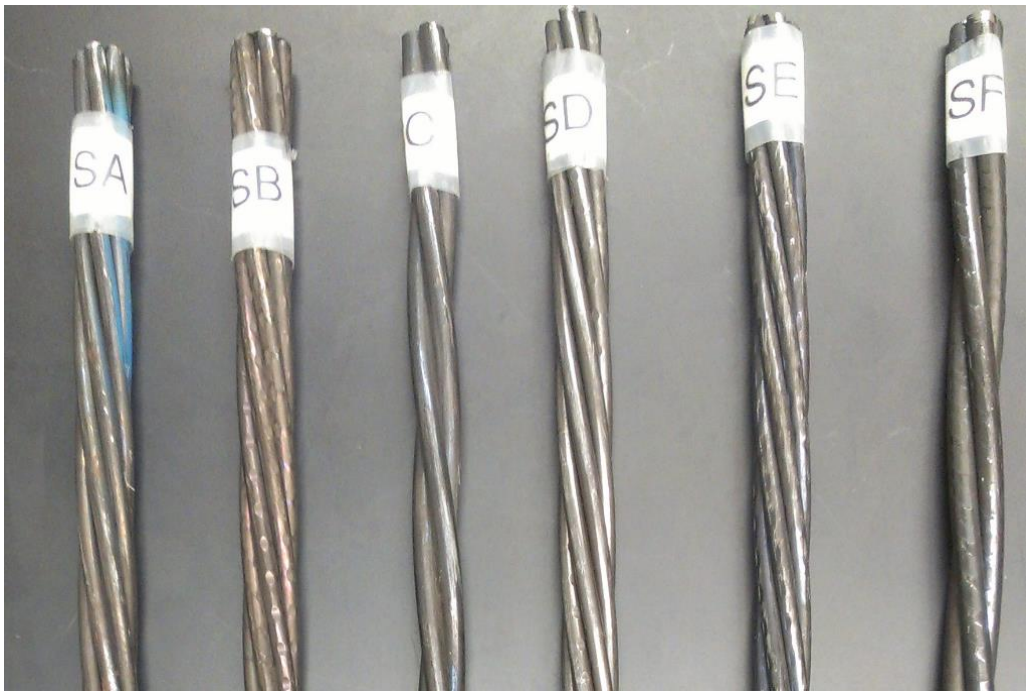

Figure 5 Various strand reinforcements employed in the present research (Arnold, 2013)

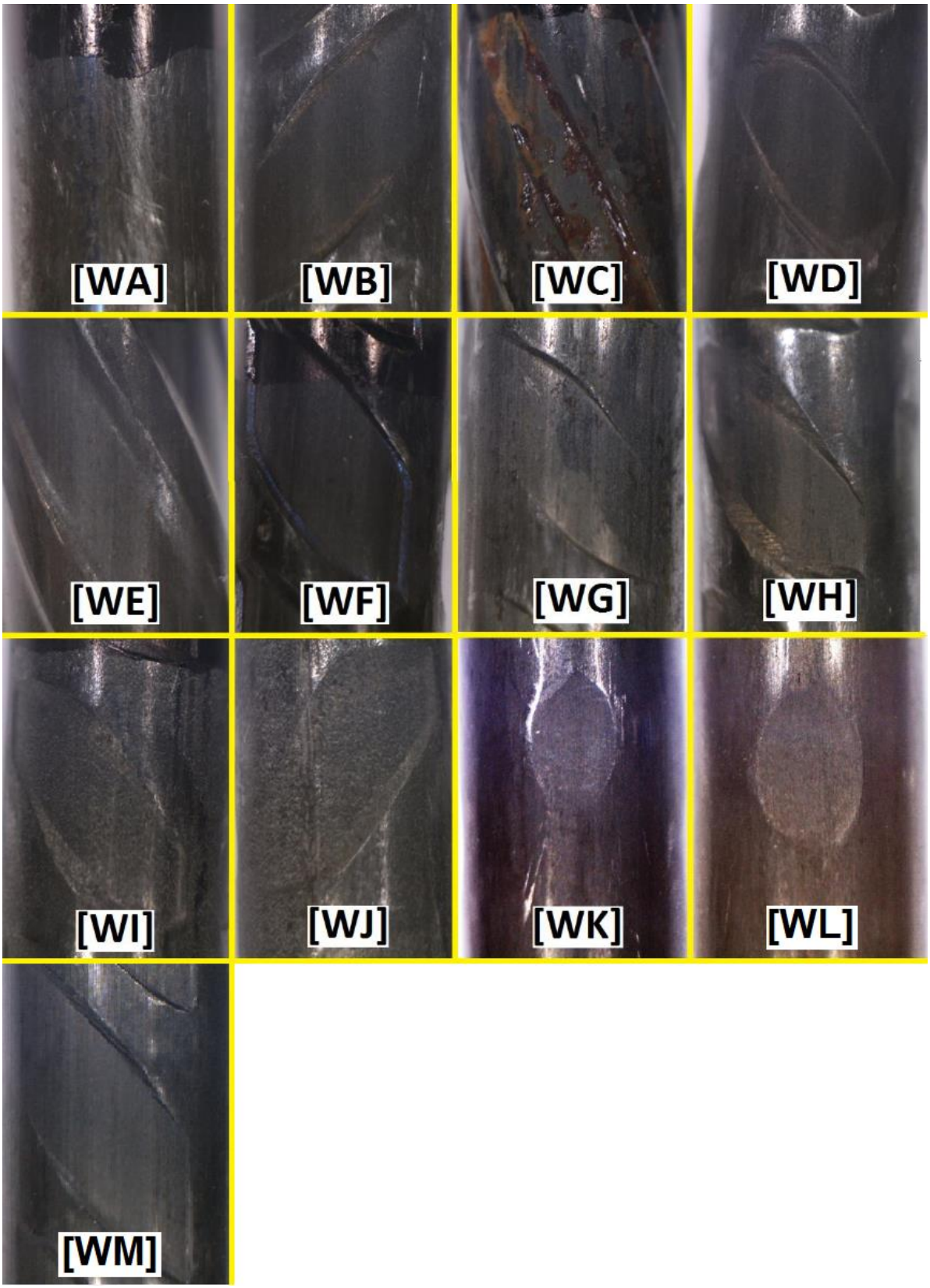

Figure 6 Close-up view of wire specimens (Arnold, 2013)

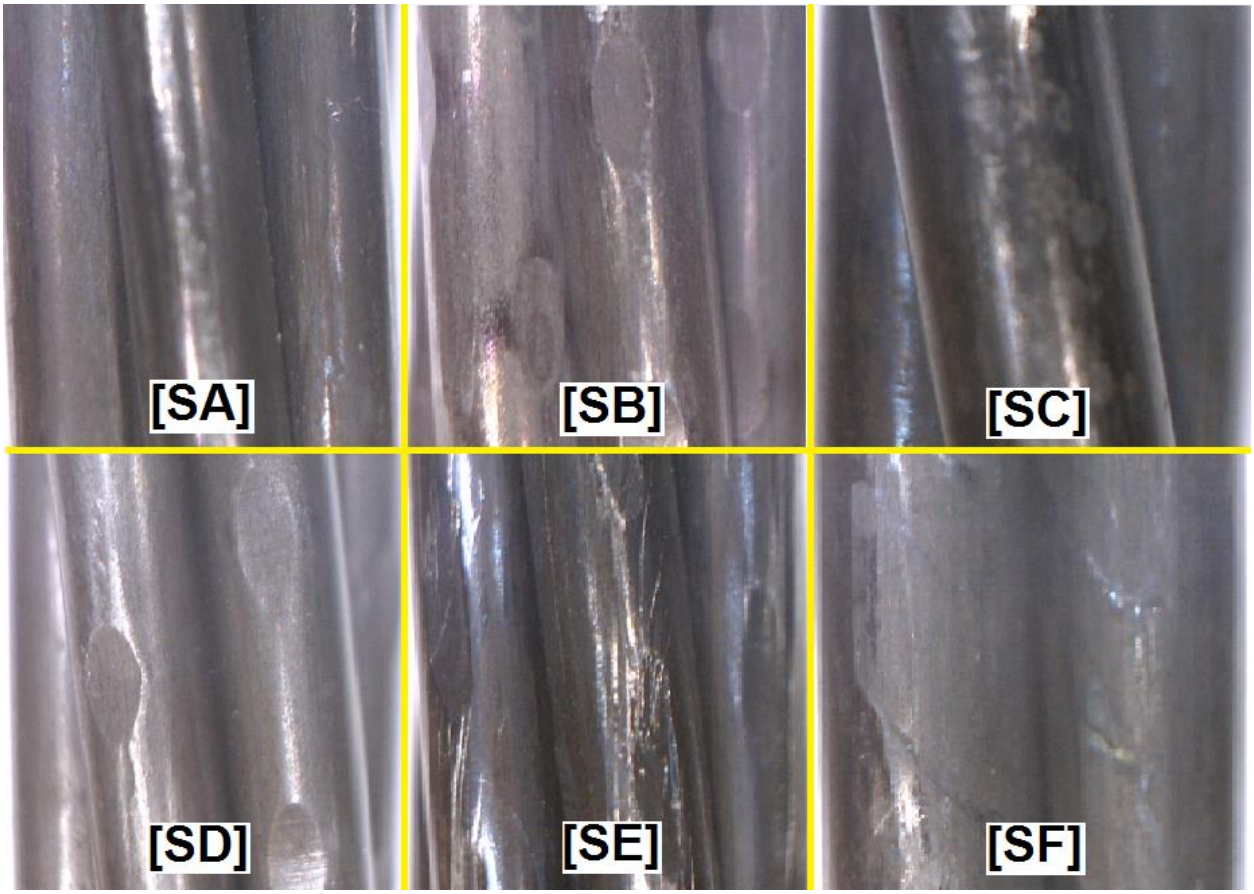

Figure 7 Close-up view off strand specimens (Arnold, 2013)

3.1.1 Reinforcement surface condition preservation during Lab-Phase

All reinforcements were received in coils and were further cut into approximately 25-foot-long samples that were subsequently stored in polyvinyl chloride (PVC) tubes. To ensure the reinforcement would remain in the as- received condition, a sufficient number of silica-based desiccant packets were placed in these PVC tubes.

The number of silica-based desiccant packets per tube varied since the reinforcement was stored in 3-in. and 4-in. diameter tubes for wires and strands, respectively. The approximate length of 25-foot was selected in order to manufacture pre-tensioned concrete prisms in the KSU laboratories. Reinforcements were removed from these PVC tubes just before usage in the prestressing operation. Figure 8 shows the reinforcement storage at the KSU laboratory.

Figure 8 Preservation of reinforcement at KSU laboratories (Arnold, 2013)

3.1.2 Reinforcement employed during Plant-Phase

Prestressing reinforcement employed during plant and Lab-Phases were obtained from the same source (master coil). The master coils were first shipped to the CXT Concrete tie manufacturing facility in Tucson, AZ and stored in special storage containers. Figure 9 shows the reinforcement storage containers used to store the master coils. Large desiccant bags were hung inside these storage containers to provide the low-humidity storage environment. Prior to storing the coils, approximately 1000-ft-long pieces of each reinforcement type (wire or strand) were removed and shipped to the KSU laboratories (in smaller-diameter coils). These smaller coils were later cut to 25-ft-long pieces by KSU personnel and stored in PCV tubes (Figure 8).

Figure 9 Reinforcement storage containers used to preserve the reinforcement surface in the as-received condition

3.2 Concrete Materials and Mix Design

This section discusses the concrete materials that were used in the present study. Throughout the Lab-Phase, proper measures were taken to maintain uniformity of the concrete mixture. Uniformity of the concrete mixture was necessary to separate out the effect caused by each selected variable on transfer length.

3.2.1 Cement

Type III cement was used in this study and stored inside the laboratory (temperature controlled) before its usage for casting. Early strengths were achieved by employing Type III cement, since it is common practice for concrete tie manufacturers to utilize rapid strength gaining cement for the crosstie production. All of the Type III cement was sourced from the same mill throughout the entire study. Table 8 lists the representative properties (from a mill certificate) of the Type III cement used.

Table 8 Type III cement composition and potential compounds in % (Holste, 2014)

Silicon dioxide	21.8
Ferric oxide	3.4
Aluminum oxide	4.27
Calcium oxide	63.2
Magnesium oxide	1.95
Sulphur trioxide	3.18
Loss on ignition (%)	2.64
Free lime	0.99
Sodium oxide	0.21
Potassium oxide	0.52
Alkalies (equiv.)	0.55
Blaine Surface Area (cm^2/g)	5590
Tricalcium silicate (C_3S)	49.2
Dicalcium silicate (C_2S)	25.3
Tricalcium aluminate (C_3A)	5.6
Tetracalcium aluminoferrite (C_4AF)	10.3

3.2.2 Course Aggregates

Three different types of course aggregates were employed in the present study. These were given the names CA#1 through CA#3 as explained below.

CA#1 = a No. 57 crushed gravel from Tucson, AZ (78.1% retained on ¾" sieve)

CA#2 = a crushed gravel from Tucson, AZ with 100% passing the 3/8" sieve

CA#3 = a local pea gravel with ½" max-sized aggregate

All aggregates were oven-dried prior to using, to ensure uniformity of the concrete mixtures. In the sub-sequent parts of this report, "CA#1" and "CA#2" will be used to represent #57 and 3/8-inch course aggregates respectively. Local pea Gravel is represented by "CA#3" from hereafter. At the time of this study, CA#1 and CA#2 were utilized by the CXT plant in Tucson AZ and were typically blended together in the same mixture. Representative photos of these two aggregates are shown in Figure 10. A representative photo of CA#3 is shown in Figure 11. Gradations for course aggregates; CA#1, CA#2, CA#3 are tabulated in Table 9, Table 10, and Table 11 respectively.

3.2.3 Sand (Fine Aggregate)

A locally-available natural silica sand was employed for the research. This was similar to the fine aggregate utilized at the crosstie manufacturing plant. Oven-dried room-temperature sand was used throughout the Lab-Phase to maintain the consistency. "FA" will be used to represent fine aggregate in the rest of this report. Figure 12 shows a representative photo of the FA utilized in during Lab-Phase, and Table 12 lists the FA gradation.

(a) CA#1 (b) CA#2

Figure 10 CA#1 and CA#2 utilized in the present study (Courtesy Joey Holste)

Figure 11 CA#3 utilized in the present study (Courtesy MCM Inc.)

Figure 12 FA utilized in the present study (Courtesy Joey Holste)

Table 9 Size distribution for CA#1

	Sieve	Opening (mm)	% Passing
CA#1 (Holste, 2014)	1-in.	25.4	100
	3/4-in.	19	78.1
	1/2-in.	12.7	31.3
	3/8-in.	9.51	9.2
	#4	4.75	0

Table 10 Size distribution for CA#2

	Sieve	Opening (mm)	% Passing
CA#2 (Holste, 2014)	3/8-in.	9.51	100
	#4	4.75	25.6
	#8	2.38	0.5
	#16	0.599	0
	#50	0.297	0

Table 11 Size distribution for CA#3

	Sieve	Opening (mm)	% Passing
CA#3 (courtesy Jan Vosahlik)	4	4.75	80
	8	2.38	20
	16	1.2	3
	30	0.599	1
	50	0.297	1
	100	0.152	1

Table 12 Size distribution for FA

	Sieve #	Opening (mm)	% Passing
FA (Arnold, 2013)	4	4.75	95
	8	2.38	80
	16	1.2	50
	30	0.599	25
	50	0.297	12
	100	0.152	2

3.2.4 High-range water-reducing admixture

In order to achieve the desired concrete consistencies (slump) with low water-to-cementitious (w/c) ratios, researchers employed high-range water-reducing (HRWR) admixtures in the study. ADVA CAST 530 was used for the present study. This HRWR is a polycarboxylate-based superplasticizer. Further, ADVA CAST 530 complies with ASTM C494 Type A and Type F (W. R. Grace & Co.–Conn., 2007).

3.2.5 Mix-design during Lab-Phase

A controlled mix proportioning was ensured to maintain uniformity of the concrete mixture throughout the Lab-Phase portion of this study. Concrete for pre-tensioned concrete prisms was batched using the concrete mixer shown Figure 13. Predominantly two mix proportions were employed to cast concrete prisms during Lab-Phase; Mix-Design #1 and Mix-Design #2.

Mix-Design #1 was similar to a mixture used at the CXT concrete tie plant in Tucson, AZ. Mix Design #2 was selected to investigate the changes in bond performance (transfer length) due to variations in course aggregate type. The primary variable between Mix-Design #1 and Mix-Design #2 was the source of course aggregate.

Mix-Design #1 consisted of CA#1, CA#2, FA, Type III cement, water, and ADVA CAST 530 admixture. Whereas in Mix-Design #2, constituent materials are; CA#3, FA, Type III cement, water, and ADVA CAST 530 admixture. Water content in Mix-Design #1 varied depending on the desired w/c ratio. The majority of the study was conducted with Mix-Design #1 having 0.32 w/c ratio. However, other w/c ratios were employed for the fabrication of a few concrete prisms. This assisted the researchers to quantify the attributed variation of transfer length due to change w/c ratio.

The uniformity of the concrete mix was achieved though the utilization of same source of aggregates (both course and fine), cement, and admixture. Mix proportions for Mix-Design #1 and Mix-Design #2 are tabulated in Table 13 and Table 14 respectively. Admixture quantity for the mix design varied based on the consistency (slump) requirement.

Table 13 Concrete mix proportions for Mix-Design #1 during Lab-Phase

Material type	Quantities per 1.0 ft^3		Quantities per 1.0 Yd^3	
CA#1	40.00	lbs.	1080.00	lbs.
CA#2	24.00	lbs.	648.00	lbs.
FA	48.00	lbs.	1296.00	lbs.
Cement	36.00	lbs.	972.00	lbs.
Water	(varies)	lbs.	(varies)	lbs.
W/C	0.27, 0.32, 0.42		0.27, 0.32, 0.42	
HRWR	varies (6 to 15)	fl oz	(162 to 405)	fl oz

Table 14 Concrete mix proportions for Mix-Design #2 during Lab-Phase

Material type	Quantities per 1.0 ft^3		Quantities per 1.0 Yd^3	
CA#3	52.19	lbs.	1409.13	lbs.
FA	52.19	lbs.	1409.13	lbs.
Cement	28.89	lbs.	780.03	lbs.
Water	9.24	lbs.	249.48	lbs.
W/C	0.32		0.32	
HRWR	varies (9-12)	fl oz	varies (243-324)	fl oz

Figure 13 Concrete Mixer used during the Lab-Phase

3.2.6 Mix-design during Plant-Phase

Mix-Design #1 (which was employed during Lab-Phase) was similar to the mixture used to fabricate concrete ties during the Plant-Phase. The main difference in mix designs between the Lab-Phase and Plant-Phase was use of air-entraining admixture for the Plant-Phase concrete mixture, and also the source of the Type III cement used.

The Lab-Phase experiments enabled very tight control of the concrete mixture properties and the compressive strength at de-tensioning, which allowed differences in the prestressing reinforcement properties to be thoroughly investigated. The Plant-Phase crossties were used to investigate the bond behavior of the various reinforcements when subjected to in-track rail loads.

Chapter 4 Experimental set-up in Lab-Phase

This chapter explains the experimental set-up used to cast pretensioned concrete prisms during Lab-Phase, and the various prism cross-sections utilized with different reinforcement sizes to represent the behavior in actual concrete crossties. It also details the different equipment used during the testing procedure, the mix proportions adapted for each part of the study, and the prisms casting procedure and approach established to analyze the results.

4.1 Prism cross-sections

During this laboratory phase, pretensioned concrete prisms were designed to have a prestressing steel spacing and overall concrete-to-steel ratio that is representative of currently-produced pretensioned concrete railroad ties. The prism cross-sections each contained four wires or strands, and the dimensions were chosen to maintain the same approximate tendon spacing and reinforcement-to-concrete proportions as typical pre-tensioned concrete railroad ties. This required that the overall cross-sections be changed with varying tendon sizes. The three prism cross-sections that were utilized for different reinforcement sizes during the laboratory phase are shown in Figure 14. All prisms had a 69-inch overall length.

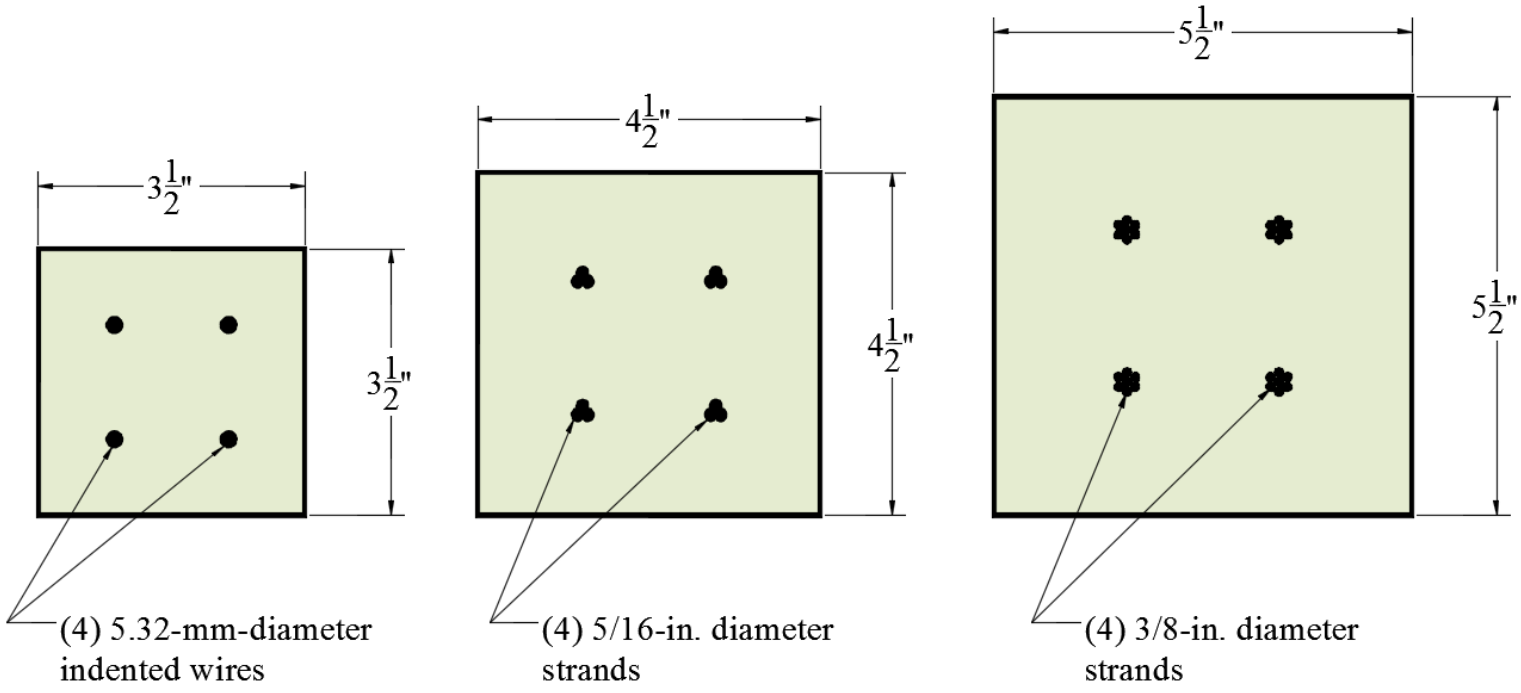

Figure 14 Prism cross-sections utilized during the laboratory phase

4.2 Experimental set-up

4.2.1 Prestressing frame and load cells

A steel jacking assembly was designed and fabricated at KSU laboratories to perform the prestressing operations during the Lab-Phase. A mechanical gear jack was attached to this steel frame to enable the prestressing and gradual release operations. Figure 15 shows the steel frame jacking assembly along with the mechanical gear jack. Tensioning of the steel prestressing tendons took place at this end of the steel frame end and is called “Live End”, whereas the other end is called “Dead End”. The jacking frame was attached to the existing prestressing bed.

Additionally, for explanation purpose, left side of bed, when viewing from the live end towards the dead end, is denoted “Side A” and the right side is denoted “Side B”. During the prestressing operation, it was vital to measure the amount of prestressing force of each individual wire/strand and to verify this prestressing force at both ends (Live and Dead ends) to ensure the stress in the prestressing tendons was within the allowable limit. A single 200,000-pound-capacity calibrated load cell was used to measure the total prestressing force (total of 4 wires/strand) at the Live End (refer to Figure 15).

At the Dead end of the frame, four smaller (20,000-pound-capacity) calibrated load cells were used to measure the prestressing force in each individual wire/strand. Figure 16 shows the four load cells installed at the Dead end. Note, due to the staggered arrangement of the load cells at the dead end, only three of the four load cells are not visible in Figure 16. A procedure was established to apply the initial tension to each individual tendon (wire/strand) and the same procedure was utilized to ensure and maintain nearly equal initial force each tendon. An initial tension of approximately 400-500 pounds was first applied to each tendon using this procedure, and then the tendons were tensioned as a group to the desired final level using the mechanical gear jack with electrical controls.

Figure 17 shows the arrangement used during the Lab-Phase to adjust the initial force in each individual tendon (wire/strand) at the live end. This arrangement consisted of a hollow screw (that had been drilled on a lathe) installed under each chuck at the live-end of each tendon. These screws were then manually adjusted while monitoring the load cell at the opposite end of the tendon to ensure the precise initial prestressing force. It was most important to ensure that all tendons had the same initial force (±20 pounds) rather than the exact value. Therefore, the initial

tensioned was typically between 400-500 pounds, but with each tendon at the same value (±20 pounds) before tensioning with the mechanical gear jack.

Figure 18 shows a schematic diagram of prestressing bed used during Lab-Phase. During the tensioning operation, a slight rotation and corresponding lateral shifting occurs at live end. Unless accounted for, this rotation could cause unequal tension in prestressing reinforcement during group tensioning. In order to avoid this, a pin was used to secure the load-cell assembly to the dead end of the steel frame as shown in Figure 18. This pin ensured equal tension in the prestressing reinforcement during the group tensioning operation.

The force measured through each load cell was output to the same digital display as shown in Figure 19. In Figure 19 Cell#1 through Cell#4 represent the prestressing force in each individual wire/strand measured at the dead end of the bed, and the algebraic sum of these individual forces is displayed as “Total” in Figure 19. Cell#5 is the load cell at the live end of the bed that measures the total jacking force.

(a) View from Live end (b) View from Dead end

Figure 15 Prestressing frame jacking assembly fabricated during laboratory phase

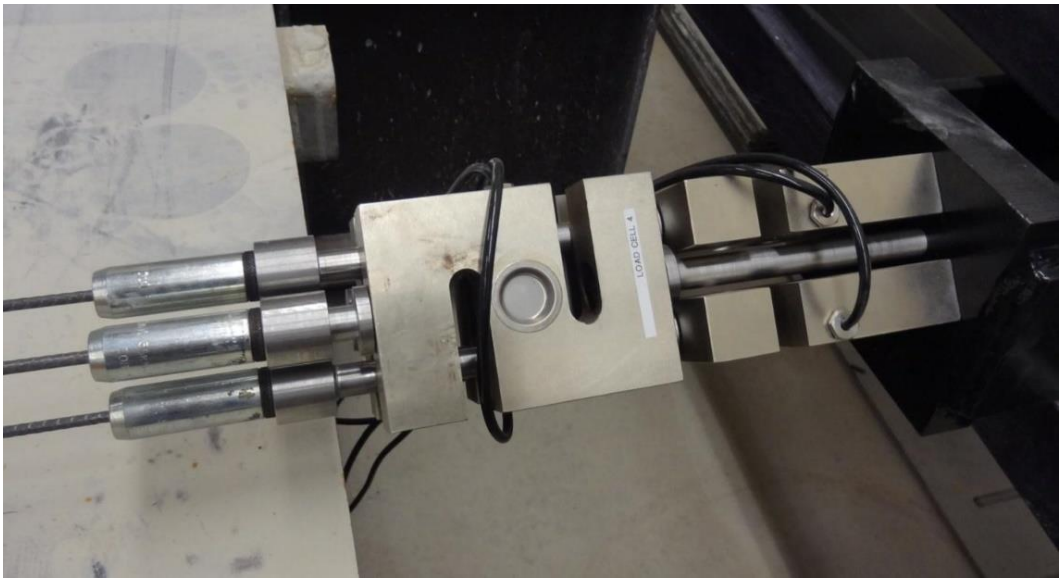

Figure 16 Four (4) individual load cells mounted at Dead end

Figure 17 One individual screw for each reinforcement to adjust the magnitude of the prestressing force

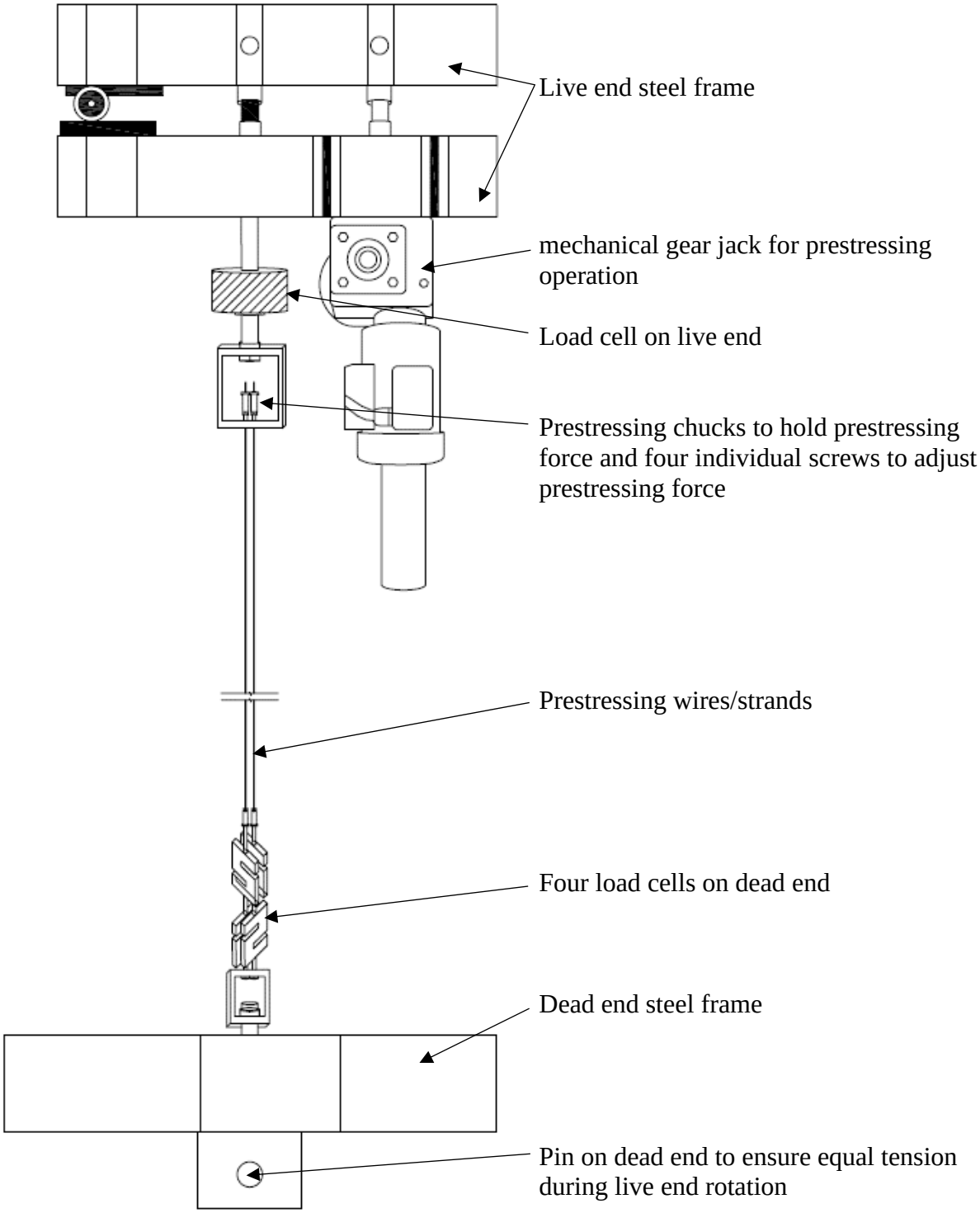

Figure 18 Prestressing bed schematic diagram (Lab-Phase)

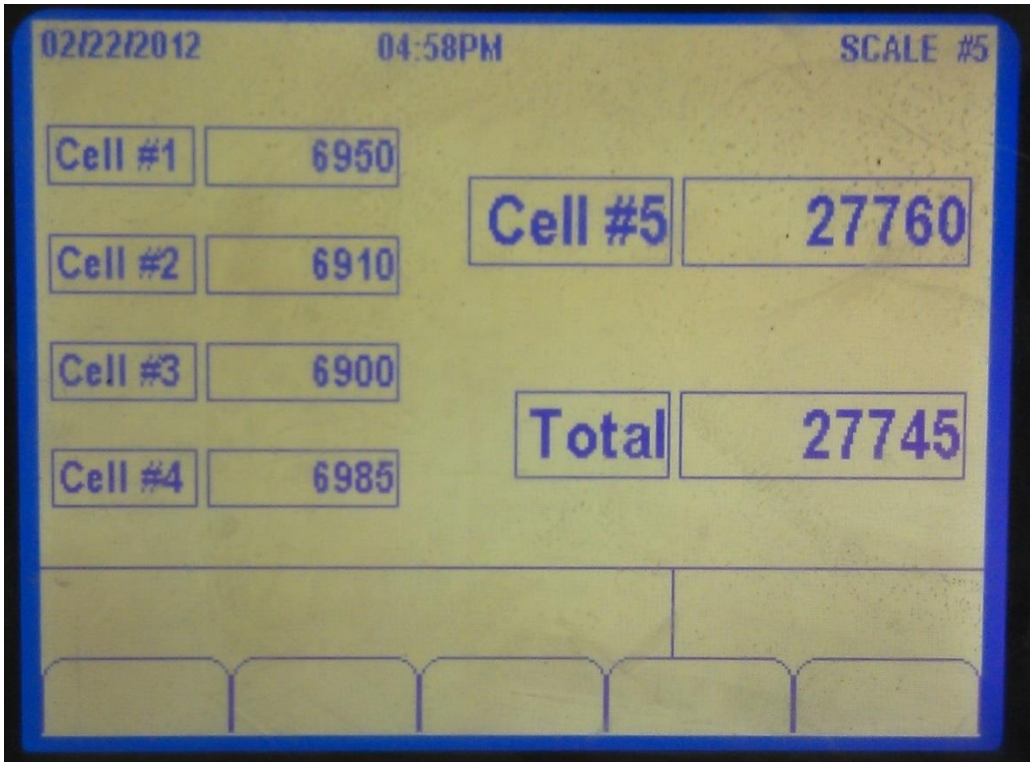

Figure 19 Digital display of Prestressing force measured by load cells

4.2.2 Prestressing operation and formwork - Bed preparation

Sequential prestressing operation details for different types of reinforcements are discussed in this section. This discussion will be followed by the formwork preparation prior to concrete pour.

4.2.2.1 Prestressing operation

A 20-foot-long prestressed bed at KSU laboratories was utilized for the prestressing operations and to cast three (3) prisms during each pour. It is vital to adapt proper sequential steps to achieve safe prestressing operation. The following steps were followed prior to each pour:

1. Ensure proper condition of prestressing chucks and spray the inside of the chuck barrel with a dry film graphite lubricant at least 15 minutes prior the usage.
2. Make sure the indicated values for each load cell were at zero prior to starting.

3. Four reinforcement tendons were removed from the PVC storage tubes and placed on the cleaned prestressing bed. The chucks at both ends (live and dead end) were secured for tensioning.
4. Prestressing tendons were initially tensioned to 500 lbs. each and at this stage, any differences in the forces were adjusted using the bolts in Figure 17 to ensure each wire/strand had nearly equal pretensioning force.
5. Using the same mechanical jacking system, all prestressing tendons were tensioned to the desired calculated force. Care was taken to avoid the presence of personnel in laboratory during the process of tendon tensioning.

   Prestressing bed after completion of pre-tensioning operation is shown in Figure 20.

4.2.2.2 Formwork

Throughout the study, wooden formwork was utilized for the prism sides and bottom. However, prism end-forms were manufactured with steel which enabled the forms to be used for many pours. The 3-piece end-form design (Figure 21) allowed the forms to be installed after the individual tendons were tensioned.

Provision was made to equip the wooden side-forms with brass inserts as shown in Figure 22, which later were utilized to measure concrete surface displacements to obtain strain profiles. Detailed procedure and discussion about surface displacement measurements will be presented in section 4.4.2. For each concrete pour, three (3) prisms were cast and formwork was arranged in a line for all these prisms. A typical finished formwork for one prism is shown in Figure 23. Upon the completion of the formwork, poly tarp sheets were placed on both sides (of the formwork) to keep the prestressing bed free from concrete residue during the casting process.

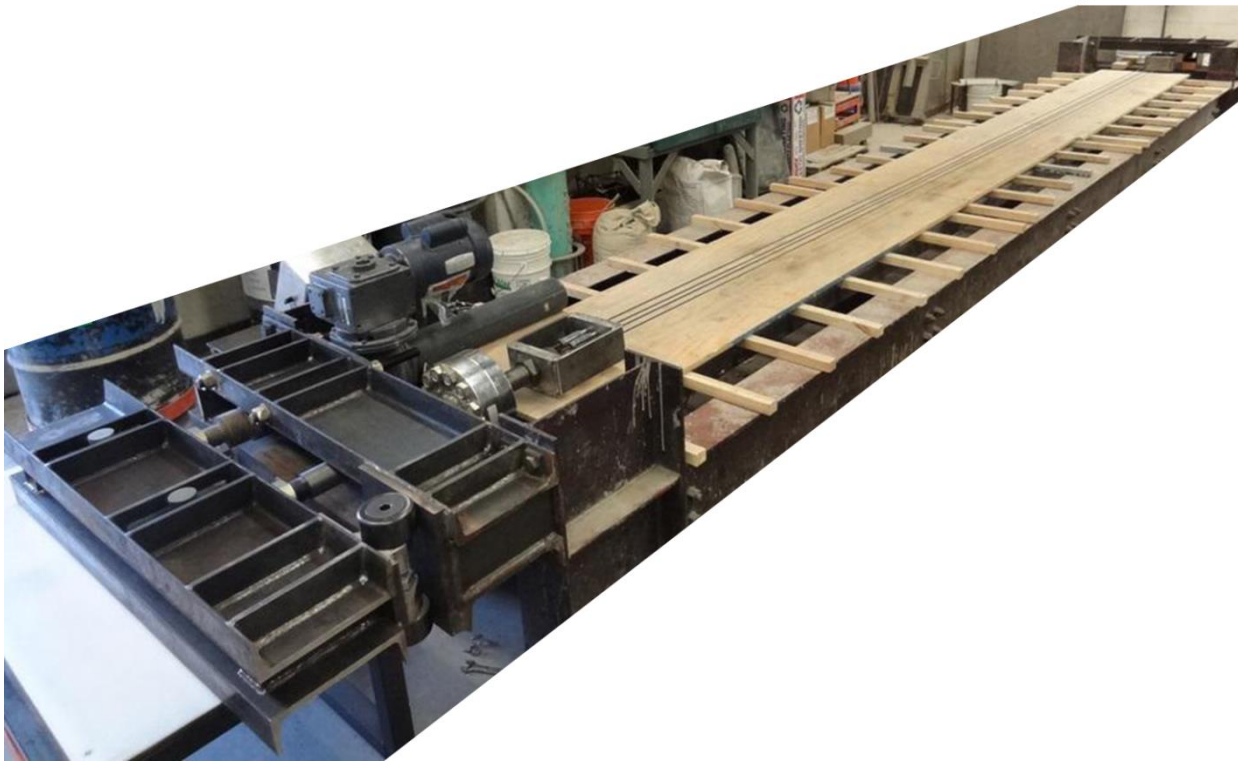

Figure 20 Prestressing bed after the completion of pre-tensioning operation

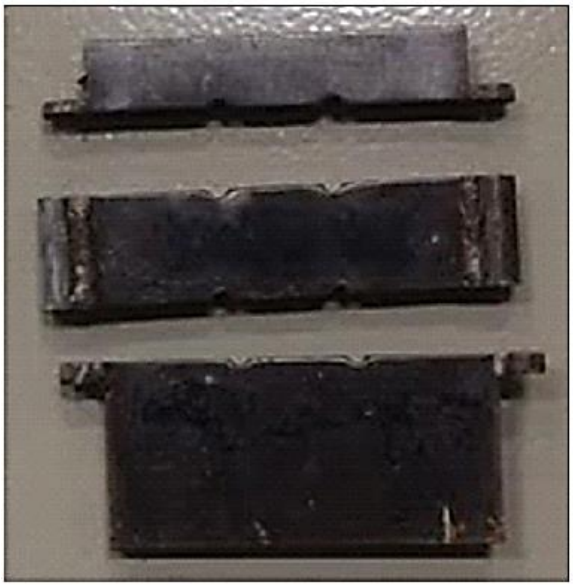

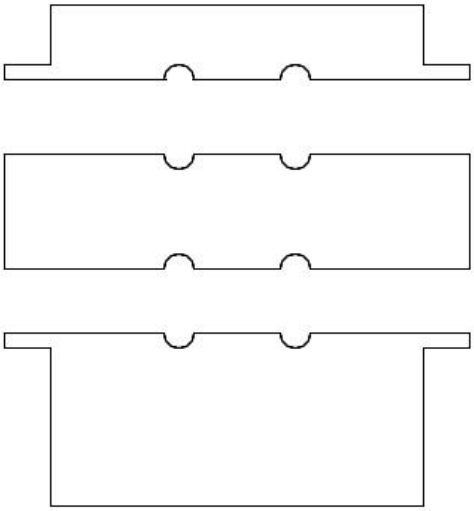

Figure 21 Three-piece prism end-forms were installed after the tendons were tensioned

Figure 22 Wooden side form equipped with brass inserts before casting

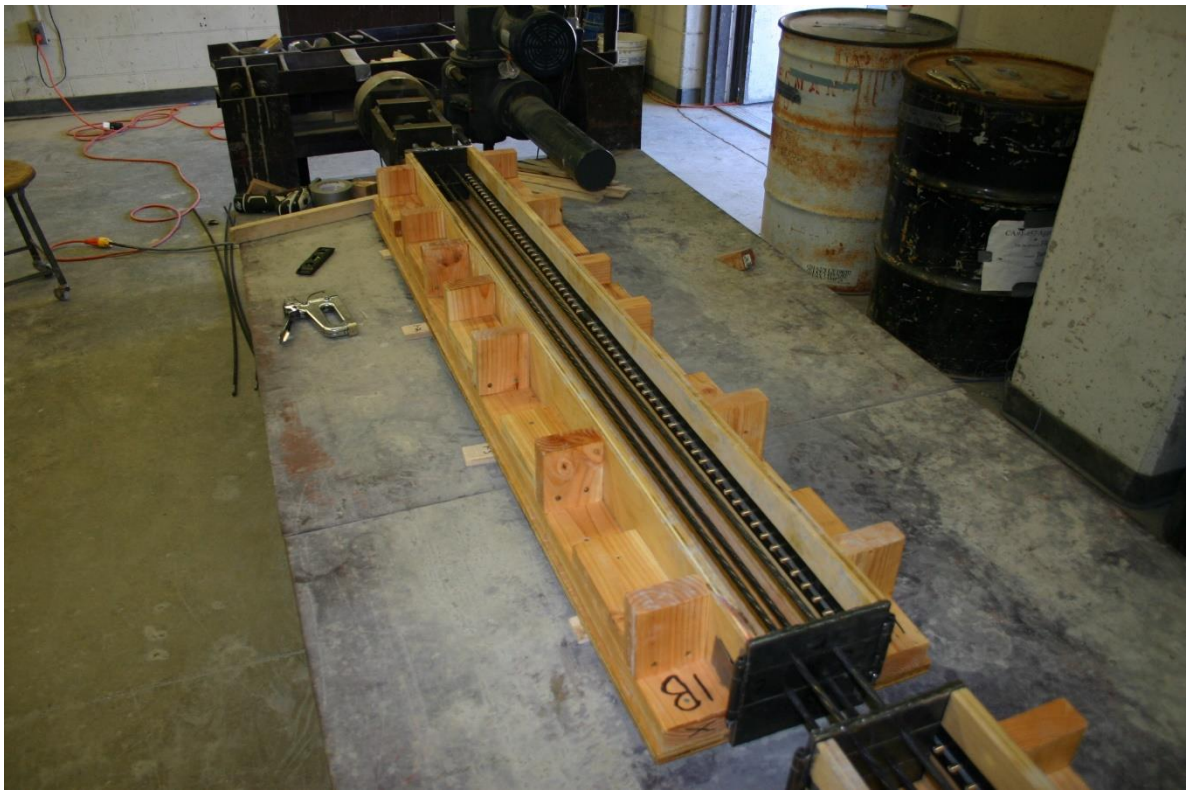

Figure 23 Typical prism after the completion of formwork

4.3 Test matrix and casting procedure of prisms during laboratory phase

4.3.1 Test matrix

During the laboratory phase, 195 prisms were cast to quantify the parameters that characterize the transfer length in pretensioned concrete prisms. Table 15 shows the experimental program test matrix. Entire Lab-Phase is divided into different groups for the explanation purposes and each group, with the corresponding objective, are tabulated in Table 16. Each group was selected to investigate the influence of prestressing and concrete variables on transfer length variation. The intent was to evaluate the influence of individual parameters. Several of the experimental tests were repeated in different groups in order to confirm the individual prestressing and concrete variables' influence on transfer length variation.

Table 15 Prisms test matrix during Lab-Phase

Prestressing Tendons Utilized	W/C ratio	Release Strength (psi)	Slump (inches)	Mix design Type	Presence of VMA?	# of Prisms Per Each Reinforcement Type	Total # of Prisms per test type
All 19 reinforcement types	0.32	4500	6	#1	No	3	57
10 reinforcement types	0.32	6000	6	#1	No	3	30
10 reinforcement types	0.32	3500	6	#1	No	3	30
7 reinforcement types	0.32	4500	3	#1	No	3	21
7 reinforcement types	0.32	4500	9	#1	No	3	21
2 reinforcement types	0.27	4500	6	#1	No	3	6
2 reinforcement types	0.42	4500	6	#1	No	3	6
2 reinforcement types	0.27	4500	6	#1	Yes	3	6
2 reinforcement types	0.42	4500	6	#1	Yes	3	6
2 reinforcement types	0.27	4500	6	#2	No	3	6
2 reinforcement types	0.42	4500	6	#2	No	3	6
						Total	195

4.3.1.1 Influence of reinforcement type and indent geometry on transfer length

Influence of reinforcement type and indent geometry on transfer length was investigated by casting prisms with 19 different reinforcements while maintaining uniformity in all other variables.

4.3.1.2 Influence of concrete release strength and concrete consistency on transfer length

Prisms were cast with a selected group of 10 reinforcements at different release strengths (3500 psi, 4500 psi, and 6000 psi) and at different concrete slumps (3-inch, 6-inch, and 9-inch) to find the effect of release strength and concrete consistency on transfer length variation.

4.3.1.3 Influence of w/c ratio on transfer length

Tests were conducted on prisms cast with different w/c ratios. Proper care was taken to maintain the uniformity in other variables during this evaluation. Different w/c ratios utilized during the Lab-Phase were; 0.27, 0.32, and 0.42. The same slump at the time of casting was achieved by use of different dosages of the polycarboxylate-based HRWR admixture. Transfer length results obtained from this set or group of prisms were specifically used to investigate the variation in bond performance due to w/c ratio of concrete mixture.

4.3.1.4 Influence of "VMA presence" in concrete mixture on transfer length.

Some known advantages of using a viscosity-modifying admixture (VMA) in concrete mixtures include reduction in segregation and minimizing concrete bleeding. A few prisms were cast with a concrete mixture that contained a highly-potent VMA to determine if there would be a notable variation in transfer length. All remaining parameters were kept constant and the VMA was simply an addition to the existing mixture.

4.3.1.5 Influence of course aggregate type on transfer length.

Two different mix designs with different sources of course aggregates were utilized in this study. These were Mix-Design #1 and Mix-Design #2 as previously presented (Table 13 and Table 14).

Table 16 Transfer Length prism test matrix by group (Lab-Phase)

Group or set	Objective of the group
Group I	Influence of reinforcement type and indent geometry on transfer length
Group II	Influence of concrete release strength on transfer length
Group III	Influence of concrete consistency on transfer length
Group IV	Influence of water-to-cementitious ratio on transfer length
Group V	Influence of "VMA presence" in concrete mix on transfer length
Group VI	Influence of course aggregate type in concrete mix on transfer length

4.3.2 Casting procedure of prisms

A consistent casting procedure was followed during the fabrication of all prisms during the laboratory phase. Concrete production quantities were varied based on the required quantity but following the same concrete mix-design (i.e. large-sized prisms cast with strands required more concrete quantity than prisms cast with wires). Casting procedure followed during the Lab-Phase of the present study is explained in the following steps:

1. Required (oven-dry) concrete materials for desired concrete quantity were weighed out and mixed in a horizontal-shaft electric concrete mixer (Figure 13).
2. Desired concrete slump was assured by adjusting the dosage of high-range water reducing (HRWR) admixture. Concrete slump was measured just prior to the casting process.
3. Concrete placed in all three prisms' formwork and consolidated properly using a flexible-shaft internal vibrator with a 1-inch-diameter head. Twelve (12) 4-in. x 8-in. concrete cylinders were cast during each pour to track the compressive strength of concrete and to ensure transferring of prestressing force precisely at the desired strength. Later, remaining cylinders were used to test the Modulus of Elasticity (MOE) and splitting-tensile strength of the concrete. All cylinders were match cured

with prism specimens using “SURE CURE” match curing system (see Section 4.3.3 for more information) to ensure same temperature and thereby the same strength. Concrete strength parameter tests; compressive strength, MOE, splitting tensile strength are carried out according to the specifications (ASTM C39 / C39M-12a, 2012), (ASTM C469/C469M-10, 2010), (ASTM C496 / C496M - 11, 2011).

4. After casting, the finished pre-tensioned concrete specimens were covered with a poly tarp to contain the internally-generated heat and increase the strength-gaining rate of the concrete similar to a concrete tie manufacturing plant.

4.3.3 SURE CURE-Mini curing control system

For each concrete pour, Twelve (12) 4-in. x 8-in. concrete cylinders were cast along with the three (3) pretensioned prism specimens. These concrete cylinders were later used to determine the compressive strength of prisms, so that prestressing force could be transferred precisely at the desired concrete strength. Later, remaining cylinders were used to determine Modulus of Elasticity (MOE) and splitting-tensile strength of the concrete. In all cases throughout this study, the desired compressive strength at detensioning was achieved within ±220psi of the targeted values (3500 psi, 4500 psi, and 6000 psi).

A Type-T thermocouple wire was inserted in the middle prism specimen during each pour. The pre-installed “SURE CURE” match curing computer software was programmed to maintain the temperature of all cylinder molds the same as the prism specimen’s temperature. Figure 24 illustrates shows all twelve match-cured cylinder molds under the process of temperature control through the SURE CURE mini curing control system.

A typical temperature vs time plot for a prism is shown in Figure 25. In Figure 25 the blue line represents the temperature of the concrete prism and remaining colors represent temperature in cylindrical molds. It can be observed in Figure 25, that the temperature in cylinder molds closely followed the concrete prism temperature. For the particular pour represented by the graph in Figure 25, concrete cylinders were cast around 8.15 AM on May-30-2012 and prestress was transferred around 1.20 PM on May-30-2012.

Figure 24 Twelve concrete cylinders under temperature control through SURE CURE mini controlling system

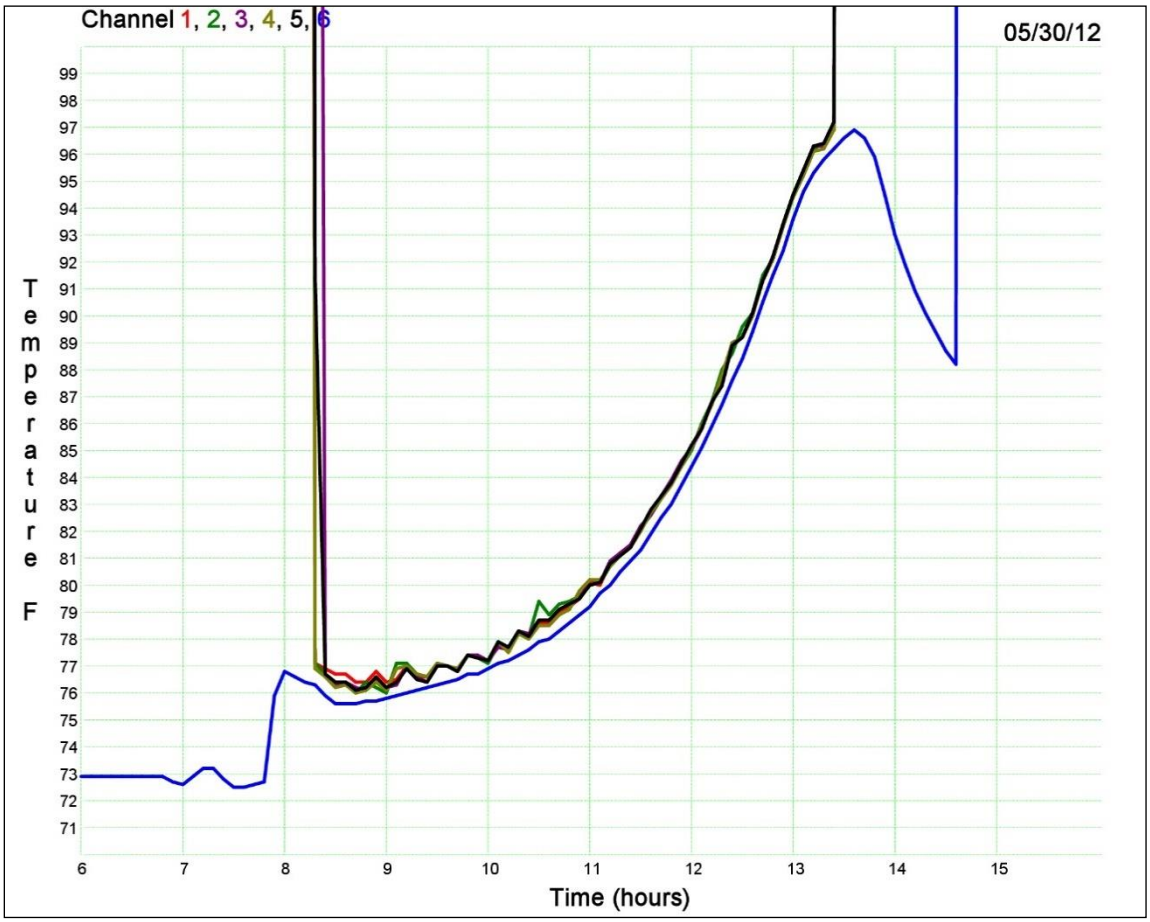

Figure 25 Typical Temperature (ºF) plot of Prism and Cylinder specimens

4.3.4 Nomenclature for each pour during the Lab-Phase

In order to best describe the transfer lengths results corresponding to different combination of the concrete variables and types of reinforcements, a suitable nomenclature was chosen and is shown in Figure 26. Through this nomenclature, selected variables (four concrete parameters and one reinforcement type) can be described. Reinforcement type, w/c, release strength (in ksi), concrete slump (in inches), and type of concrete mix are represented respectively from left to right in the nomenclature shown in Figure 26.

For the example shown in Figure 26, the particular prisms would be cast using [WG] wire reinforcement and Mix-Design #1 with a 0.32 w/c ratio and 6-inch slump at placement, and detensioned when the concrete was 4500 psi. During the Lab-Phase, few prisms were cast with VMA and the results for these prisms will be marked with an additional term “with VMA”.

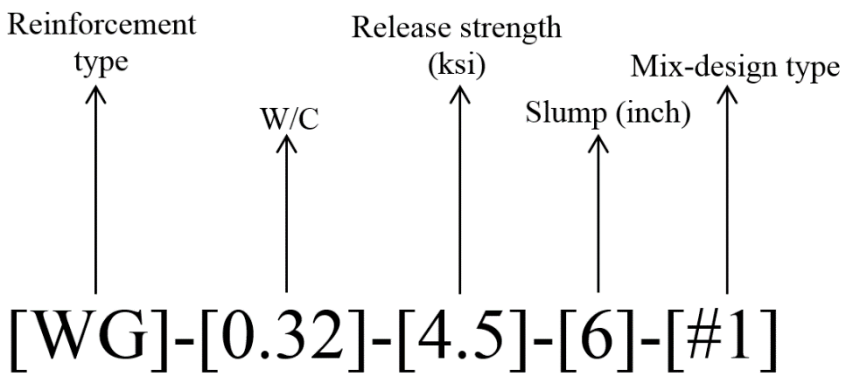

Figure 26 Nomenclature for each pour during the Lab-Phase

4.4 Transfer Length determination

In this section, researchers discuss the transfer length determination and surface-displacement measurement techniques utilized in this study. An accurate evaluation of transfer length is required, as it is the primary focus of this study since the transfer length can affect the load-carrying capacity of pretensioned concrete rail-road ties.

4.4.1 Transfer Length

Upon prestress transfer, the pretensioned-concrete member will be subjected to axial stress and therefore axial strain. The developed strain will be zero at the end of the member and then reach a theoretical maximum and constant value (for members with constant cross-section) at some distance from the end of the member. The length required to develop the maximum strain from the end of the member is the transfer length. Hence, transfer length can be evaluated though determination of concrete surface strains which developed due to the prestressing force.

Two different techniques were adapted to measure concrete surface displacements and to establish the surface-strain profile of the concrete members in this study; through mechanical Whittemore gage and optical laser-speckle imaging (LSI) device. During the laboratory part of the study Whittemore gage was exclusively used to determine concrete surface-strain profiles. The Plant-Phase included strain profiles determined through both Whittemore gage and though LSI device.

4.4.2 Surface-strain profiles determined through Whittemore gage (Lab-Phase)

A mechanical (Whittemore) gage with an eight-inch gage length was used to measure in-plane concrete surface displacements. The instrument was fitted with a Mitutoyo digital indicator with a precision of 0.0001 in. (Figure 30). At the time of casting, brass inserts (Figure 27.) with a small center hole were cast into the prisms at mid-height on both sides and at both ends.

The inserts were first attached to a steel bar (with #4-40 screws) that had been precisely drilled at a one-inch center-to-center spacing as shown in Figure 28. The center-to-center spacing of the indents extended for a distance of 34” longitudinally from each prism end. Provision was made in the formwork to accommodate the steel bars with brass inserts and still allow the surface to be nearly flat. These steel bars were inserted in such a way that the first brass point was located precisely at 0.5” from the end of the prism.

Figure 27 Typical brass insert used to measure surface displacement

Figure 28 Steel bars held the brass inserts at a specified locations during casting

The special formwork used in this study allowed the wooden side forms to be removed and thereby allow access to the steel bars. Next, the #4-40 screws that secured the brass inserts to the steel bar were removed, and then the steel bar was then pulled from the surface of the concrete thereby leaving the brass inserts embedded in the prism. Figure 29 shows a concrete prism side-surface with installed brass points. The distance between these brass points was precisely measured to within 0.0001 in. prior to prestress transfer and immediately after de-tensioning by utilizing the Whittemore gage (Figure 31).

The corresponding surface-strain at each location was then determined by dividing the difference in displacement readings by the gage length of 8 inches. These values were then plotted at the mid-point location of the gage, and a typical resulting smoothed surface-strain profile along a prism is shown in Figure 32.

This surface-strain data was then used to determine the corresponding transfer length value. A statistically-based method (ZL Method) that incorporated a least-squares algorithm (Zhao, Beck, Peterman, Wu, Murphy, & Lee, 2013) was employed to determine the transfer length from the surface-strain data in this study. It is to be noted that at each end of a prism (live

and dead end), the surface-strain profile used to determine transfer length was obtained by averaging the data from both sides of the prism (Side A and Side B) on that end. This methodology consistently resulted in high-quality surface-strain profiles (Figure 32).

Figure 29 Prism surface with brass points

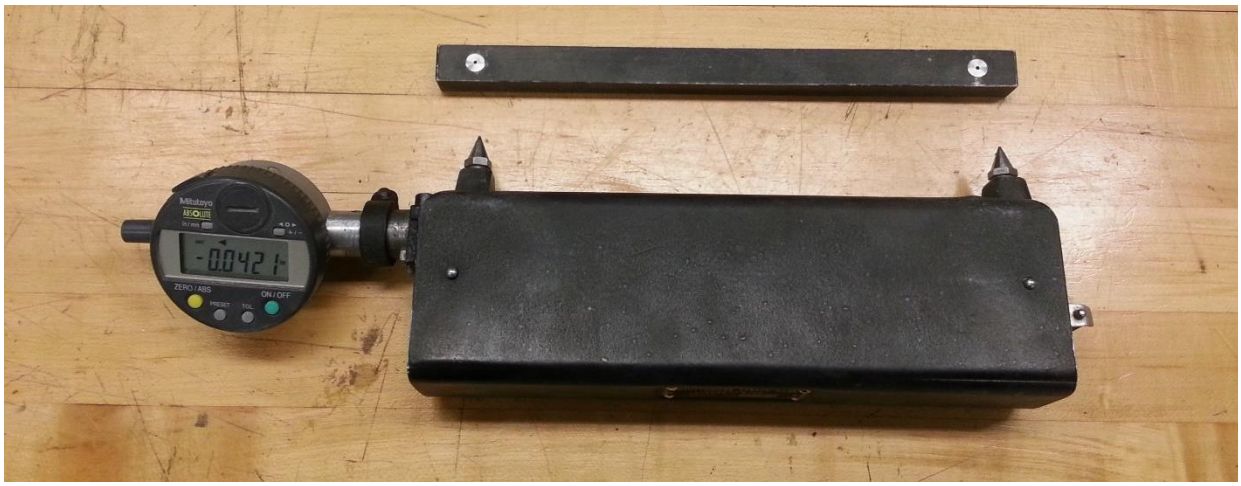

Figure 30 Whittemore gage used for the study

Figure 31 Surface distance measurement though Whittemore gage

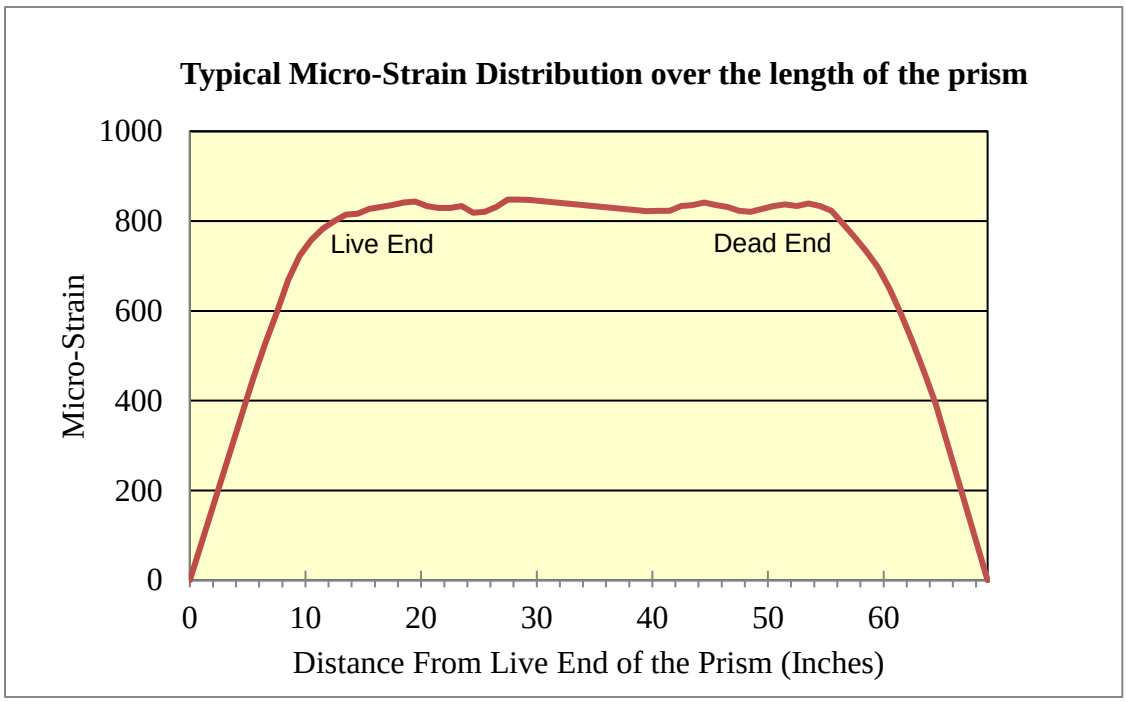

Figure 32 Typical surface-strain profile due to prestress transfer

4.5 Storage of prisms

All prisms were stored in a temperature-controlled laboratory area upon the completion of initial strain measurements. Figure 33 shows the storage area with three prisms corresponding to the same pour stacked together.

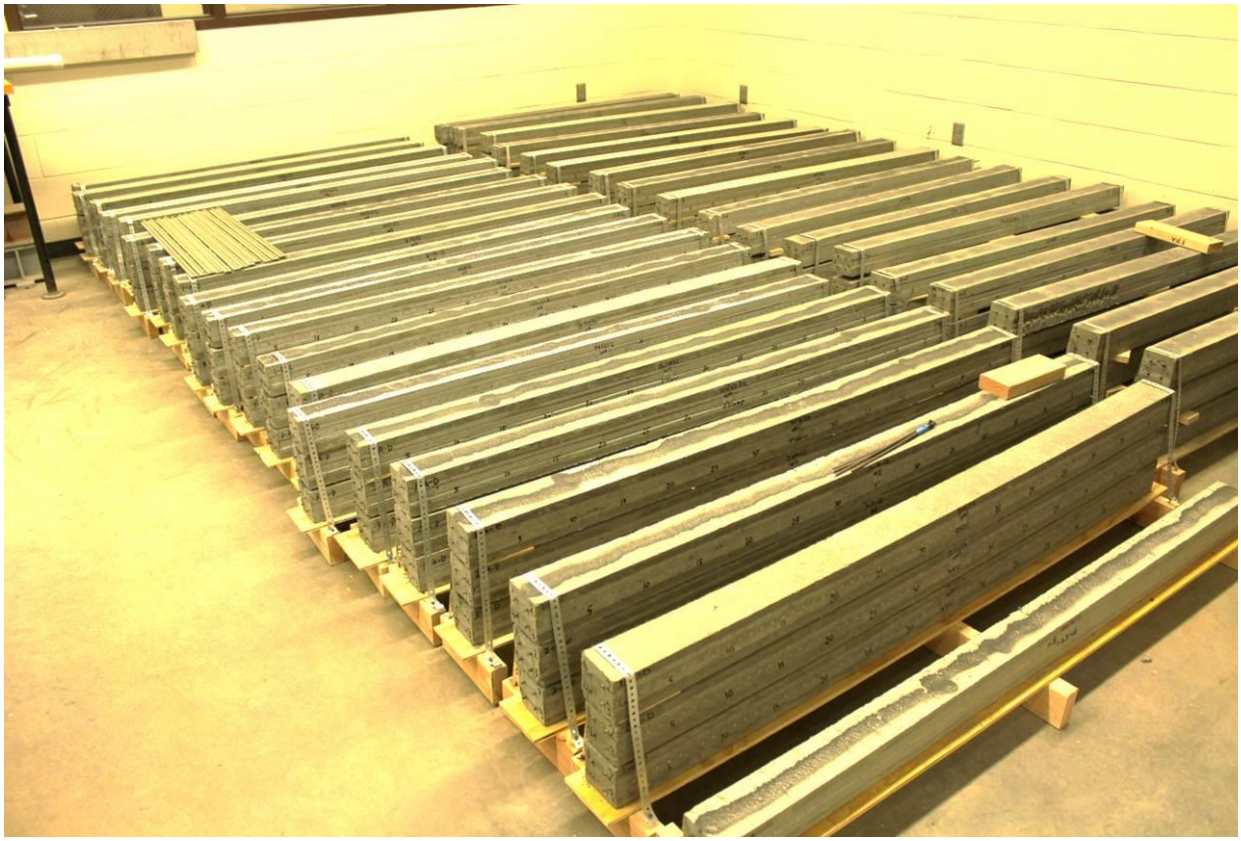

Figure 33 Prisms storage (by pour) after the completion of initial strain measurements

Chapter 5 Lab-Phase results

Chapter 5 discusses the results obtained from the extensive laboratory tests conducted at KSU. A methodological approach allows the authors to find out each parameters' influence on transfer length.

Pretensioned concrete prisms were cast with all nineteen (19) different reinforcement types to determine the influence of reinforcement type, indent geometry, and concrete parameters on transfer length. A uniform release strength of 4500 ± 220 psi and concrete consistency of 6 ± 1/2 in. was maintained for all prisms.

Ten (10) of the nineteen (19) reinforcement were used specifically to determine the influence of concrete release strength on transfer length. Concrete release strength's attributed influence on transfer length was investigated by casting different prisms and varying the release strength while maintaining uniformity of the remaining parameters.

Similarly, prisms were cast to determine the influence of consistency (slump) at concrete placement on transfer length. This influence is investigated by casting prisms with various concrete consistencies and maintaining uniformity of the remaining parameters. This procedure allowed researchers to separate out the essential attributed influence of concrete consistency on transfer length.

Tests were conducted on prisms cast with different water-to-cementitious (w/c) ratios. Three different w/c ratios were utilized during the Lab-Phase; 0.27, 0.32, and 0.42. Transfer length results obtained from this set of prisms was used to evaluate the variation in bond performance due to w/c ratio.

Variation of transfer length due to different coarse aggregate sources was investigated during the present study. For these tests, prisms were cast with two different concrete mixture designs, each having a different source of course aggregates were utilized in this study. Prisms were fabricated with a concrete mixture that contained a highly-potent viscosity-modifying admixture (VMA) to investigate a possible influence on transfer length.

In the following sections, the entire Lab-Phase is divided into different groups. Each group, along with the corresponding objective, are shown in Table 16. Each group was selected to investigate the influence of prestressing and concrete variables on transfer length.

5.1 Effect of Reinforcement type and indent geometry on Transfer length (Group I prisms)

Group 1 prisms utilized Mix-Design #1 at a 0.32 w/c ratio, 6-inch slump, and a concrete release strength of 4500 psi. The minimum, maximum, and average transfer length values determined for the Group I prisms are tabulated in Table 18 (for wires) and Table 19 (for strands). Each value in these tables represents the average of six individual transfer length values (two ends of three prisms).

It is to be noted that the transfer length on each end of a prism was determined by averaging the two sides (Side A and Side B) surface-strain data. During Group I prisms testing, uniform release strength and uniform concrete consistency were maintained. Exact release strength and concrete consistency for individual reinforcement type are tabulated in Table 20 along with the Modulus of Elasticity and splitting-tensile strength of the concrete at the time of detensioning.

In Table 18 and Table 19, the transfer lengths are shown in units of inches, and also as a function of the tendon diameter (d_b). It is common in the precast pre-tensioned concrete industry to represent the transfer lengths in terms of the number of wire/strand diameters. Expressing the value of transfer lengths in terms of number of tendon diameters allows the bond quality of various reinforcement sizes to be compared.

Individual transfer-length results for Group I prisms cast with thirteen different wire reinforcements are shown in Figure 34, while Figure 35 presents individual transfer-length results for Group I prisms cast with six different strand types. These same results are also shown, in terms of reinforcement diameters, in Figure 36 and Figure 37 for wire reinforcements and strand reinforcements respectively.

Table 17 Nomenclature for prisms utilized in Group I

Nomenclature for the	
Wire Reinforcements	Strand Reinforcements
[WA]-[0.32]-[4.5]-[6]-[#1]	[SA]-[0.32]-[4.5]-[6]-[#1]
[WB]-[0.32]-[4.5]-[6]-[#1]	[SB]-[0.32]-[4.5]-[6]-[#1]
[WC]-[0.32]-[4.5]-[6]-[#1]	[SC]-[0.32]-[4.5]-[6]-[#1]
[WD]-[0.32]-[4.5]-[6]-[#1]	[SD]-[0.32]-[4.5]-[6]-[#1]
[WE]-[0.32]-[4.5]-[6]-[#1]	[SE]-[0.32]-[4.5]-[6]-[#1]
[WF]-[0.32]-[4.5]-[6]-[#1]	[SF]-[0.32]-[4.5]-[6]-[#1]
[WG]-[0.32]-[4.5]-[6]-[#1]	
[WH]-[0.32]-[4.5]-[6]-[#1]	
[WI]-[0.32]-[4.5]-[6]-[#1]	
[WJ]-[0.32]-[4.5]-[6]-[#1]	
[WK]-[0.32]-[4.5]-[6]-[#1]	
[WL]-[0.32]-[4.5]-[6]-[#1]	
[WM]-[0.32]-[4.5]-[6]-[#1]	

Table 18 Summary of transfer length results for wire reinforcements (Group I prisms)

Pour Identity or Nomenclature	Average Transfer Length Values		
	Min., in. [TL/d_b]	Avg., in. [TL/d_b]	Max., in. [TL/d_b]
[WA]-[0.32]-[4.5]-[6]-[#1]	14.40 [69]	16.33 [78]	18.70 [89]
[WB]-[0.32]-[4.5]-[6]-[#1]	10.40 [50]	11.60 [55]	12.80 [61]
[WC]-[0.32]-[4.5]-[6]-[#1]	7.80 [37]	8.85 [42]	10.80 [52]
[WD]-[0.32]-[4.5]-[6]-[#1]	10.30 [49]	11.08 [53]	12.40 [59]
[WE]-[0.32]-[4.5]-[6]-[#1]	6.80 [32]	7.43 [35]	8.00 [38]
[WF]-[0.32]-[4.5]-[6]-[#1]	6.80 [32]	8.45 [40]	9.30 [44]
[WG]-[0.32]-[4.5]-[6]-[#1]	11.60 [55]	11.78 [56]	12.60 [60]
[WH]-[0.32]-[4.5]-[6]-[#1]	6.50 [31]	7.50 [36]	8.30 [40]
[WI]-[0.32]-[4.5]-[6]-[#1]	9.30 [44]	10.10 [48]	11.30 [54]
[WJ]-[0.32]-[4.5]-[6]-[#1]	8.00 [38]	9.02 [43]	11.70 [56]
[WK]-[0.32]-[4.5]-[6]-[#1]	13.50 [64]	14.00 [67]	14.90 [71]
[WL]-[0.32]-[4.5]-[6]-[#1]	17.60 [84]	18.73 [89]	20.30 [97]
[WM]-[0.32]-[4.5]-[6]-[#1]	7.50 [36]	9.83 [47]	11.30 [54]

Note: Three (3) prisms were cast for each pour type that resulted for 6 transfer lengths. Hence the minimum, average, and maximum values correspond to these 6 transfer lengths.

Table 19 Summary of transfer length results for strand reinforcements (Group I prisms)

Pour Identity or Nomenclature	Transfer Lengths		
	Min., in. [TL/d_b]	Avg., in. [TL/d_b]	Max., in. [TL/d_b]
[SA]-[0.32]-[4.5]-[6]-[#1]	15.10 [40]	16.15 [43]	17.90 [48]
[SB]-[0.32]-[4.5]-[6]-[#1]	15.40 [41]	16.25 [43]	17.00 [45]
[SC]-[0.32]-[4.5]-[6]-[#1]	13.10 [42]	13.77 [44]	15.30 [49]
[SD]-[0.32]-[4.5]-[6]-[#1]	14.00 [37]	15.83 [42]	17.50 [47]
[SE]-[0.32]-[4.5]-[6]-[#1]	17.60 [47]	19.02 [51]	21.80 [58]
[SF]-[0.32]-[4.5]-[6]-[#1]	11.90 [32]	12.52 [33]	13.20 [35]

Note: Three (3) prisms were cast for each pour type that resulted for 6 transfer lengths. Hence the minimum, average, and maximum values were among 6 transfer lengths.

Table 20 Concrete properties at the release strength for wire and strand reinforcements (Group I prisms)

Pour Identity or Nomenclature	Concrete Slump (in.)	Release Strength (psi)	Splitting tensile Strength (psi)	Modulus of Elasticity ($x10^6$ psi)
[WA]-[0.32]-[4.5]-[6]-[#1]	6-1/4	4664	418	3.53
[WB]-[0.32]-[4.5]-[6]-[#1]	6-1/2	4453	403	3.46
[WC]-[0.32]-[4.5]-[6]-[#1]	6-1/2	4701	482	3.88
[WD]-[0.32]-[4.5]-[6]-[#1]	5-1/2	4400	476	3.89
[WE]-[0.32]-[4.5]-[6]-[#1]	6-1/4	4650	479	3.46
[WF]-[0.32]-[4.5]-[6]-[#1]	6	4466	466	3.71
[WG]-[0.32]-[4.5]-[6]-[#1]	6-1/4	4697	496	3.55
[WH]-[0.32]-[4.5]-[6]-[#1]	6-1/2	4695	485	3.90
[WI]-[0.32]-[4.5]-[6]-[#1]	6	4547	439	3.73
[WJ]-[0.32]-[4.5]-[6]-[#1]	6-1/2	4521	409	3.63
[WK]-[0.32]-[4.5]-[6]-[#1]	6-1/4	4572	392	3.56
[WL]-[0.32]-[4.5]-[6]-[#1]	6-1/2	4476	328	3.58
[WM]-[0.32]-[4.5]-[6]-[#1]	6-1/4	4506	415	3.55
[SA]-[0.32]-[4.5]-[6]-[#1]	6-1/4	4636	481	3.68
[SB]-[0.32]-[4.5]-[6]-[#1]	6-1/4	4736	419	3.98
[SC]-[0.32]-[4.5]-[6]-[#1]	6-1/2	4449	390	3.70
[SD]-[0.32]-[4.5]-[6]-[#1]	6-1/2	4715	403	3.18
[SE]-[0.32]-[4.5]-[6]-[#1]	6-1/4	4636	483	4.06
[SF]-[0.32]-[4.5]-[6]-[#1]	6-1/2	4635	444	3.57

Note: "Concrete Slump" is a fresh concrete parameter

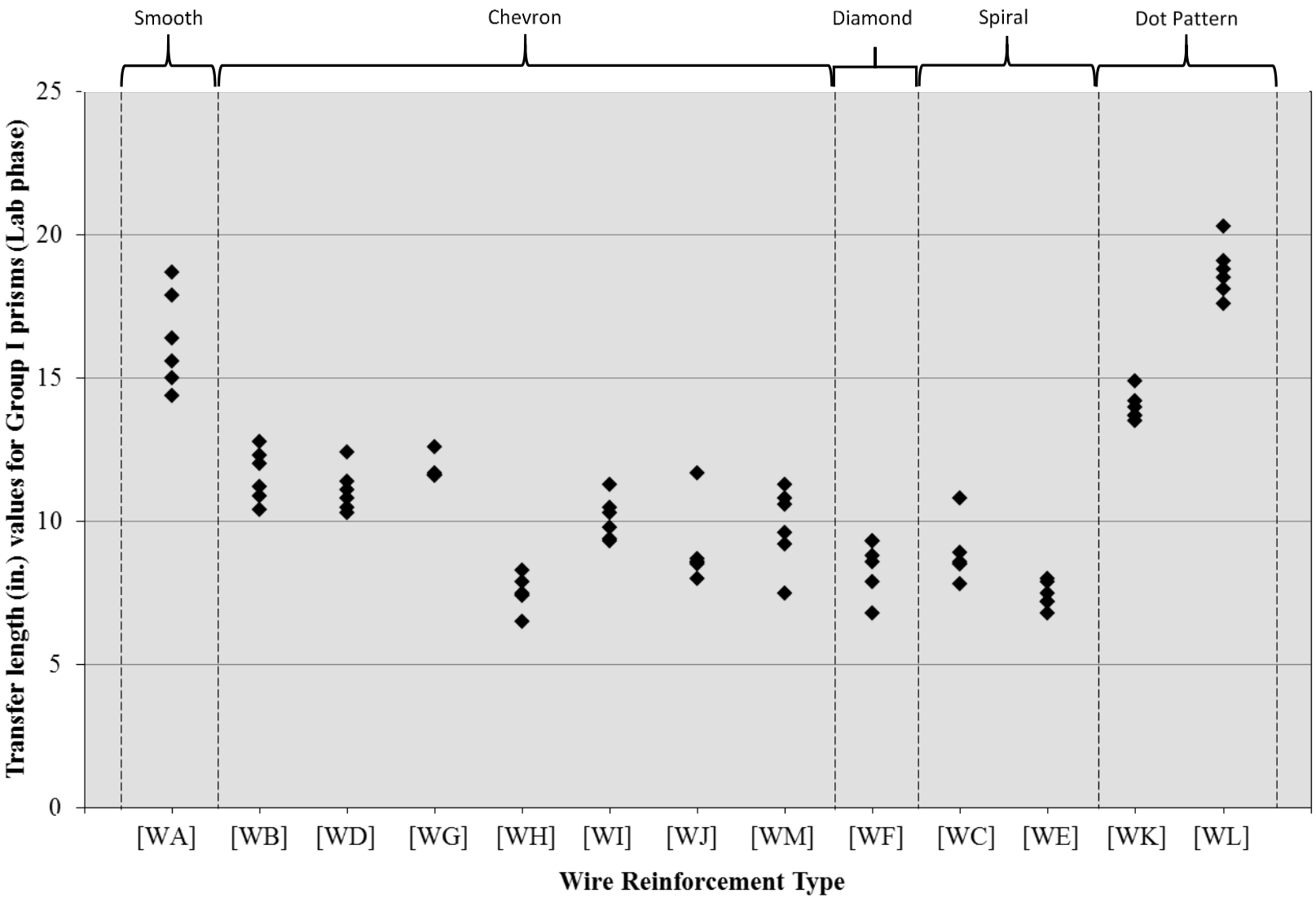

Figure 34 Transfer length results of wire reinforcements for Group I prisms

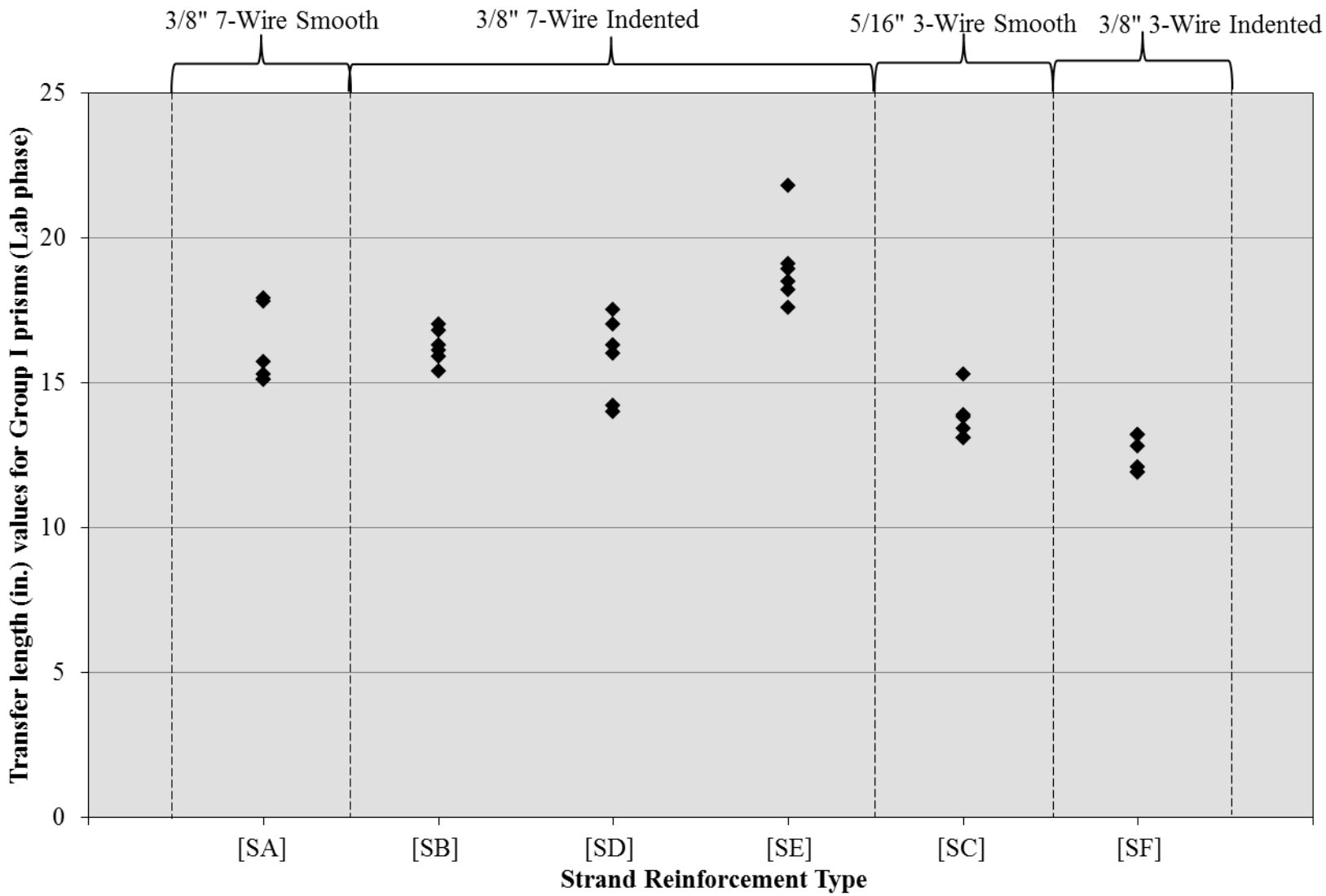

Figure 35 Transfer length results of strand reinforcements for Group I prisms

During Group I experiments, the average transfer length results for thirteen different wire reinforcements (all 5.32-mm diameter) were 53 d_b (11.13-inch). Average results for the five 3/8-inch strand reinforcements (which included one three wire strand), and for one 5/16-inch strand reinforcement were 43 d_b (15.95-inch), and 44 d_b (13.75-inch) respectively. For all wires except smooth ([WA]) and Dot pattern ([WK] & [WL]) wires, average transfer length is 46 d_b (9.56-inch). However, wide variation in transfer lengths were observed for prisms cast even with same size of the reinforcement type, but with different indentation types. In general, lower transfer length values were observed for prisms cast with wire reinforcement compared to prisms cast with strand reinforcement.

Average transfer lengths for smooth (1), chevron (7), diamond (1), spiral (2), dot (2), 3/8-in. strands, and 5/16-in. strand are 78 d_b, 48 d_b, 40 d_b, 39 d_b, 78 d_b, 43 d_b, and 44 d_b respectively with corresponding average transfer length values of 16.33-in., 10.13-in., 8.45-in., 8.14-in., 16.37-in., 15.95-in., and 13.77-in. Table 21 tabulates these average transfer length values.

Table 21 Average transfer-length values by wire/strand type

Wire/Strand type	Individual Tendons	Avg. Transfer Length for the group (in.) [# diameters]
Smooth Wires	[WA]	16.33 [78]
Chevron Wires	[WB], [WD], [WG], [WH], [WI], [WJ], [WM]	10.13 [48]
Diamond Wires	[WF]	8.45 [40]
Spiral Wires	[WC], [WE]	8.14 [39]
Dot Wires	[WK], [WL]	16.37 [78]
3/8-in. strands	[SA], [SB], [SD], [SE], [SF]	15.95 [43]
5/16-in. strands	[SC]	13.77 [44]

Transfer length results from the Group I indicated that, with the exception of wire [WL], all of the indented reinforcements resulted in a lower transfer length than the smooth wire. The smooth wire, [WA], had an average transfer length of 16.3 inches (78 d_b), while the wire with the 2-dot indentation pattern ([WL]) had an average transfer length of 18.7 inches (90 d_b). Note, the 2-dot reinforcement had the fewest amount and smallest size of indentations per length. Additionally, there were residual lubricants present on all wires.

This finding would suggest that the residual lubricants and/or surface condition of the wires do contribute to the bond capacity of the prestressing tendons. This is similar to the findings of Rose and Russell for strand (Rose, et al., 1997). However, when there is a large number of deeper indentations (such as for the chevron, 4-dot, diamond, and spiral wires), these indentations apparently become the dominant feature influencing the bond.

The average transfer length of the 7 chevron-indented wires ranged from 7.5 (36 d_b) to 11.78 in. (56 d_b), while the 2 spiral wires had average transfer lengths of 7.43 (35 d_b) and 8.85 in. (42 d_b). The diamond-indented wire had a transfer length of 8.45 in. (40 d_b) and the 4-dot wire had an average transfer length of 14.0 in. (67 d_b).

Among the strands, lower average transfer length was observed for the prisms cast with [SA] (smooth 3/8-in.-diameter 7-wire smooth strand) when compared to prisms cast with 3/8-in.-diameter 7-wire indented strands [SB], and [SE]. At the time of receipt of [SA] reinforcement, slight surface rusting was observed for [SA]. The better performance of [SA] may be due to the developed roughness (Rose, et al., 1997) with the surface rusting.

The lowest average transfer length among prisms cast with the four different 3/8-in.-diameter 7-wire strand was obtained for prisms cast with [SD]. Average transfer lengths for [SA], [SB], [SD], and [SE] are 16.15-inch (43 d_b), 16.25-inch (43 d_b), 15.83-inch (42 d_b) and 19.02-inch (51 d_b) respectively. It is to be noted two 3-wire strands ([SC], [SF]) are of two different diameters. Average transfer lengths for smooth 5/16-in. diameter 3-wire strand, [SC], was 13.77-inch (44 d_b) and for 3/8-in. diameter 3-wire indented strand, [SF], was 12.52-inch (33 d_b).

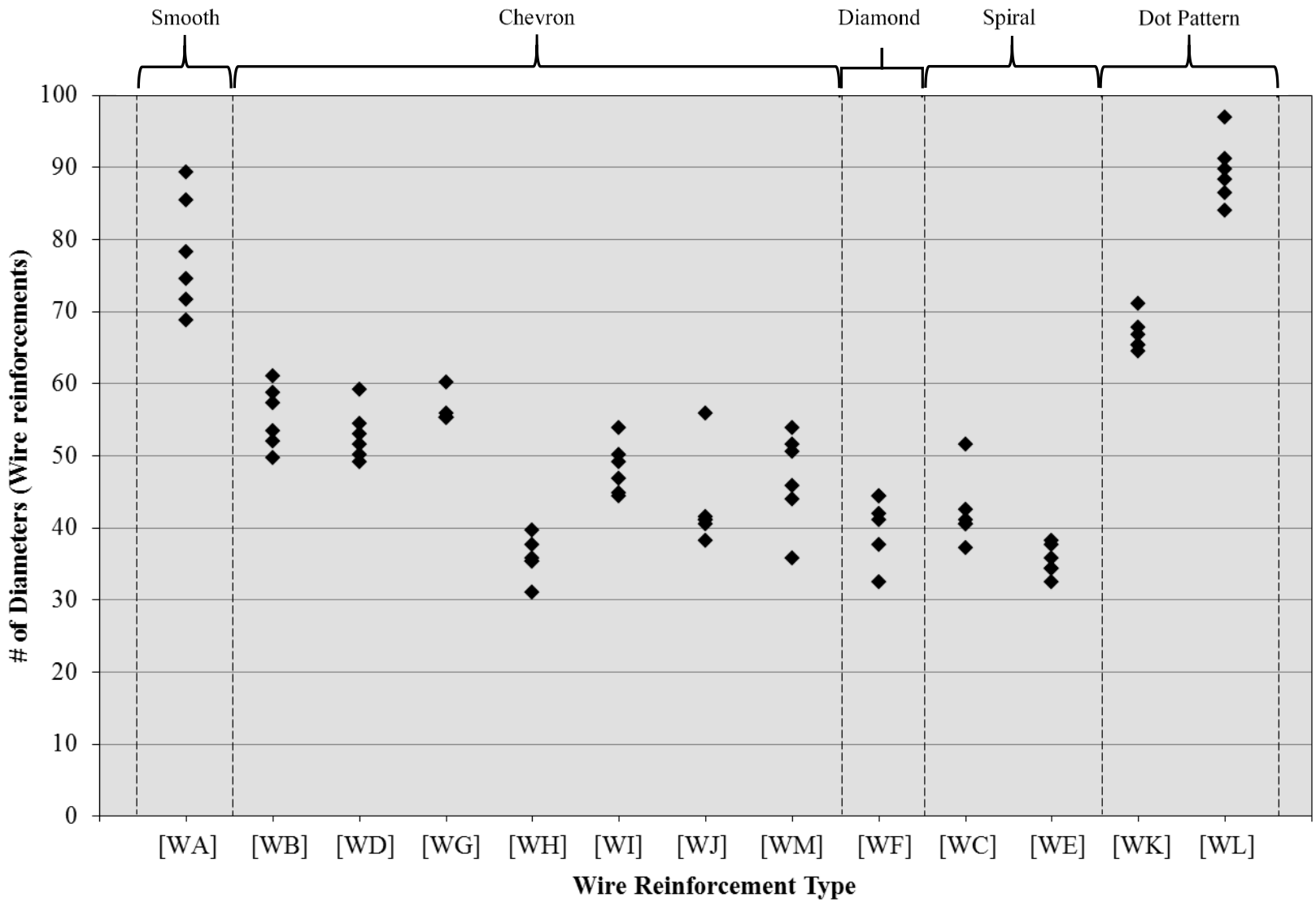

Figure 36 Transfer length results of wire reinforcements from Group I (diameters)

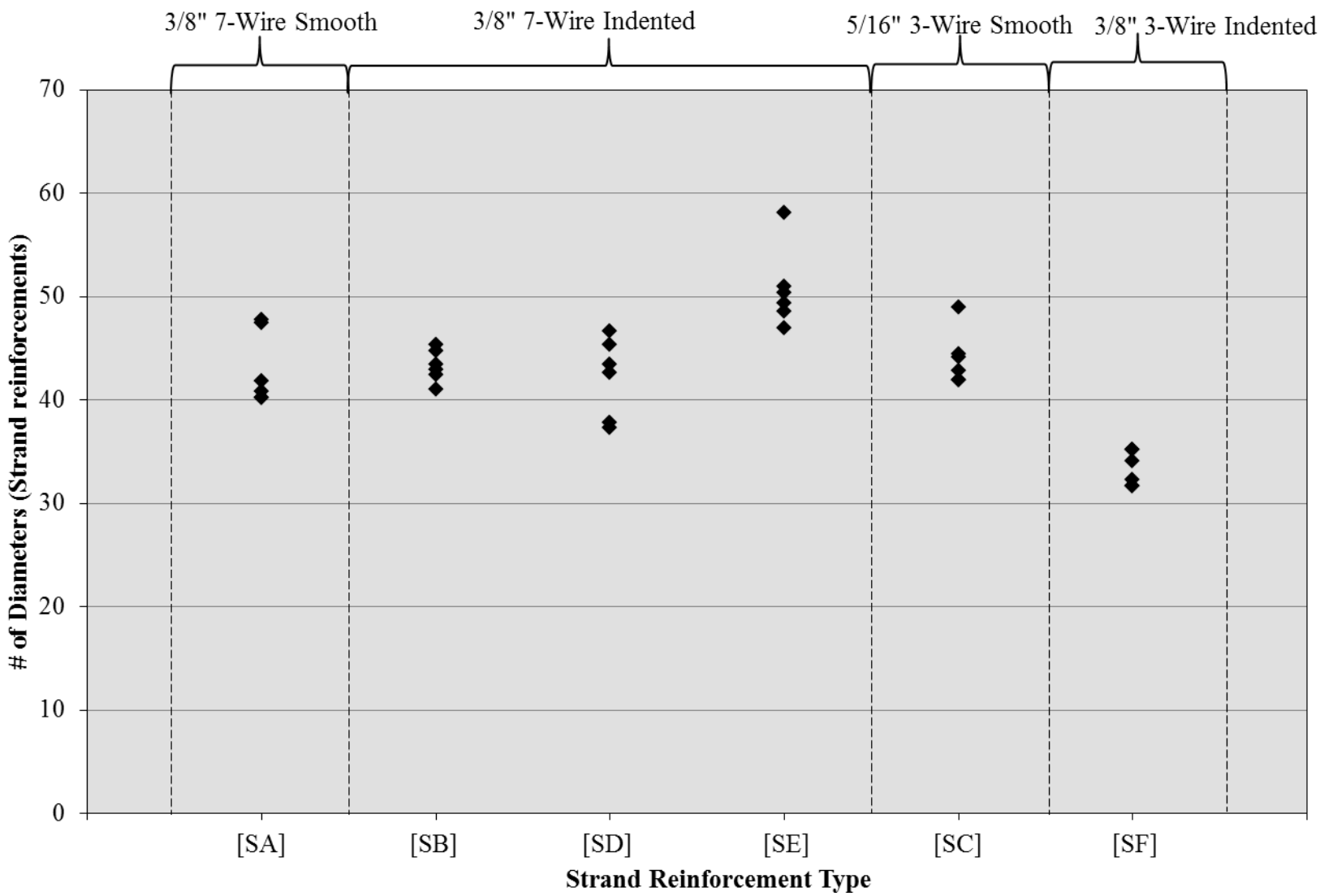

Figure 37 Transfer length results of strand reinforcements from Group I (diameters)

5.2 Calculation of percentage increase and percentage decrease (reduction)

TL results were compared throughout the present work at different stages. Calculations for percentage increase and percentage decrease (reduction) in TL values are explained in this section.

5.2.1 Calculation of percentage decrease (reduction) in TL

Percentage decrease or reduction was determined by the following steps:

1. Reduction or decrease in TL is first calculated by deducting the new TL value from referenced TL value (Decrease in TL (Δ) = referenced TL – new TL).
2. Percentage reduction was then calculated, dividing the decrease in TL (Δ) by referenced TL and then multiplied by 100 (Percentage reduction in TL = $\left(\frac{\text{Decrease in TL } (\Delta)}{\text{referenced TL}}\right) * 100$).

It is to be noted that negative values in these calculations represent percentage increase.

5.2.2 Calculation of percentage increase in TL

Percentage increase was determined by the following steps:

1. Increase in TL is first calculated by deducting the referenced TL value from new TL value (Increase in TL (Δ) = new TL – referenced TL).
2. Percentage increase was calculated, dividing the increase in TL (Δ) by referenced TL and then multiplied by 100 (Percentage increase in TL = $\left(\frac{\text{Increase in TL } (\Delta)}{\text{referenced TL}}\right) * 100$).

It is to be noted that negative values in these calculations represent percentage reduction.

5.3 Effect of Release strength on Transfer length (Group II prisms)

In case of pre-tensioned concrete members, prestressing force is transferred to the concrete member though bond between the concrete and the prestressing reinforcement. One of the previously-noted factors that influences the bond between concrete and prestressing strands is the strength at the time of prestress transfer (Barnes, et al., 2003). As a part of the research program, the effect of release strength (concrete strength at the time of prestress transfer) on transfer length was investigated by casting series of prisms (Group II prisms) with ten (10) different reinforcements at three targeted release strengths (3500 psi, 4500 psi, and 6000 psi).

The reinforcements selected for this study were based on the results from Group I prisms and were the following:

1. Best-bonding 5.32-mm-diameter wire with chevron indent pattern (WH)
2. Worst-bonding 5.32-mm-diameter wire with chevron indent pattern (WG)
3. 5.32-mm-diameter smooth wire (WA)
4. 5.32-mm-diameter spiral wire (WE)
5. 5.32-mm-diameter dot-patterned wire (WK)
6. 3/8”-diameter 7-wire smooth strand (SA)
7. Best-bonding 3/8”-diameter 7-wire indented strand (SD)
8. Worst-bonding 3/8”-diameter 7-wire indented strand (SE)
9. 3/8”-diameter 3-wire indented strand (SF)
10. 5/16”-diameter 3-wire smooth strand (SC)

Nomenclature of the various prisms utilized in this Group II are tabulated in Table 22. In every case, the release strength was within ±220 psi of the desired release strength. Average transfer lengths of prisms cast with the same reinforcement type and different release strengths were compared and analyzed. Transfer length results from Group I prisms were used for the comparison of release strengths at 4500 psi.

Table 23 lists the minimum, average, and maximum transfer length results for the prisms cast with the ten (10) reinforcements and detensioned at the three concrete compressive strengths. In order to accommodate all TL results, in Table 23 results are not represented with corresponding nomenclature. Plots showing all Group II prisms’ transfer length results are presented in Figure 38 and Figure 39, respectively, for wire and strand reinforcements. Transfer length values were obtained from surface-strain profiles as explained in Section 4.4.2. The concrete parameters for each pour are tabulated in Table 28.

Table 22 Nomenclature for prisms utilized in Group II

Nomenclature for the		
Release strength 3500 psi	Release strength 4500 psi	Release strength 6000 psi
[WA]-[0.32]-[3.5]-[6]-[#1]	[WA]-[0.32]-[4.5]-[6]-[#1]	[WA]-[0.32]-[6.0]-[6]-[#1]
[WE]-[0.32]-[3.5]-[6]-[#1]	[WE]-[0.32]-[4.5]-[6]-[#1]	[WE]-[0.32]-[6.0]-[6]-[#1]
[WG]-[0.32]-[3.5]-[6]-[#1]	[WG]-[0.32]-[4.5]-[6]-[#1]	[WG]-[0.32]-[6.0]-[6]-[#1]
[WH]-[0.32]-[3.5]-[6]-[#1]	[WH]-[0.32]-[4.5]-[6]-[#1]	[WH]-[0.32]-[6.0]-[6]-[#1]
[WK]-[0.32]-[3.5]-[6]-[#1]	[WK]-[0.32]-[4.5]-[6]-[#1]	[WK]-[0.32]-[6.0]-[6]-[#1]
[SA]-[0.32]-[3.5]-[6]-[#1]	[SA]-[0.32]-[4.5]-[6]-[#1]	[SA]-[0.32]-[6.0]-[6]-[#1]
[SC]-[0.32]-[3.5]-[6]-[#1]	[SC]-[0.32]-[4.5]-[6]-[#1]	[SC]-[0.32]-[6.0]-[6]-[#1]
[SD]-[0.32]-[3.5]-[6]-[#1]	[SD]-[0.32]-[4.5]-[6]-[#1]	[SD]-[0.32]-[6.0]-[6]-[#1]
[SE]-[0.32]-[3.5]-[6]-[#1]	[SE]-[0.32]-[4.5]-[6]-[#1]	[SE]-[0.32]-[6.0]-[6]-[#1]
[SF]-[0.32]-[3.5]-[6]-[#1]	[SF]-[0.32]-[4.5]-[6]-[#1]	[SF]-[0.32]-[6.0]-[6]-[#1]

Group I prisms

Table 23 Transfer length results from Group II prisms (effect of release strength)

Wire/Strand Type	Release Strength 3500 psi			Release Strength 4500 psi			Release Strength 6000 psi		
	Transfer Lengths			Transfer Lengths			Transfer Lengths		
	Min., in.	Avg., in.	Max., in.	Min., in.	Avg., in.	Max., in.	Min., in.	Avg., in.	Max., in.
[WA]	19.80 [95]	21.40 [102]	23.30 [111]	14.40 [69]	16.33 [78]	18.70 [89]	12.90 [62]	13.50 [64]	14.30 [68]
[WE]	8.60 [41]	10.50 [50]	11.30 [54]	6.80 [32]	7.43 [35]	8.00 [38]	5.10 [24]	7.10 [34]	8.30 [40]
[WG]	12.80 [61]	13.80 [66]	14.40 [69]	11.60 [55]	11.78 [56]	12.60 [60]	8.50 [41]	9.80 [47]	10.90 [52]
[WH]*	9.90 [47]	10.18 [49]	10.40 [50]	6.50 [31]	7.50 [36]	8.30 [40]	6.40 [31]	7.30 [35]	8.40 [40]
[WK]	16.60 [79]	17.70 [85]	19.00 [91]	13.50 [64]	14.00 [67]	14.90 [71]	10.00 [48]	11.10 [53]	13.30 [64]
[SA]	19.00 [51]	20.53 [55]	22.30 [59]	15.10 [40]	16.15 [43]	17.90 [48]	10.70 [29]	11.18 [30]	12.60 [34]
[SC]	17.10 [55]	18.20 [58]	19.50 [62]	13.10 [42]	13.77 [44]	15.30 [49]	8.30 [27]	10.20 [33]	11.60 [37]
[SD]	22.00 [59]	24.28 [65]	27.20 [73]	14.00 [37]	15.83 [42]	17.50 [47]	13.70 [37]	15.25 [41]	17.30 [46]
[SE]	20.50 [55]	21.33 [57]	22.70 [61]	17.60 [47]	19.02 [51]	21.80 [58]	12.40 [33]	13.22 [35]	14.60 [39]
[SF]	14.50 [39]	15.35 [41]	16.80 [45]	11.90 [32]	12.52 [33]	13.20 [35]	9.60 [26]	10.73 [29]	12.40 [33]

*[WH]-[0.32]-[3.5]-[6]-[#1] pour includes only 5 TL values (not 6 TL values), since there was cracking at one end.

Average transfer length results obtained at different release strengths of prisms cast with the five 5.32-mm-diameter wire reinforcements are shown in Figure 40 and Figure 41. In Figure 40, average transfer lengths for each wire type at different release strengths are shown in bar-chart format, with the minimum and maximum TL ranges depicted by the vertical bars. Whereas, Figure 41 represents the same average TL information in terms of "number of diameters (d_b)".

It is to be noted that all prisms in Group II were cast with Mix-Design #1 and with "no VMA". Due to space restrictions, entire nomenclature is not written in the graphs. The variation in experimentally-determined concrete splitting-tensile strength due to change in release strength is illustrated in Figure 44. Figure 45 illustrates the change in experimentally-determined MOE with release strength.

Similarly, average transfer lengths for each of the five strand reinforcements at the three different release strengths are shown in Figure 42 and Figure 43. Average transfer lengths of strands are represented in "inches" and "number of diameters" in Figure 42 and Figure 43, respectively. As with the Group II wire prisms, the Group I strand prisms utilized Mix-Design #1 without VMA.

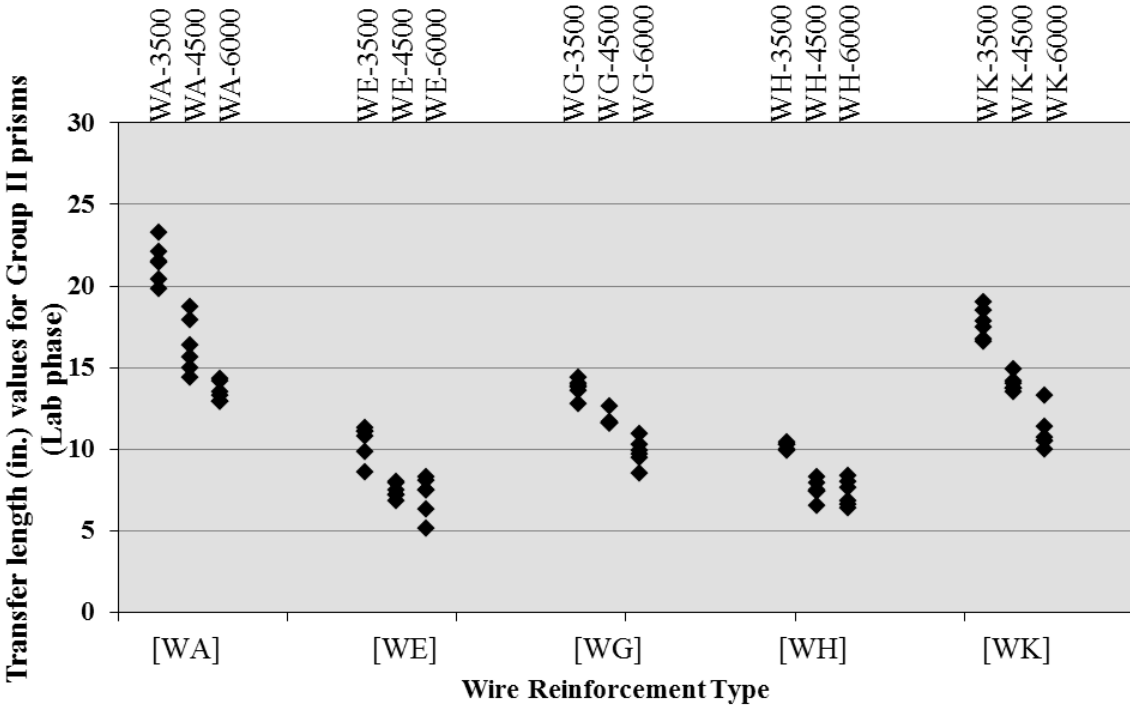

Figure 38 Transfer length results of wire reinforcements from Group II

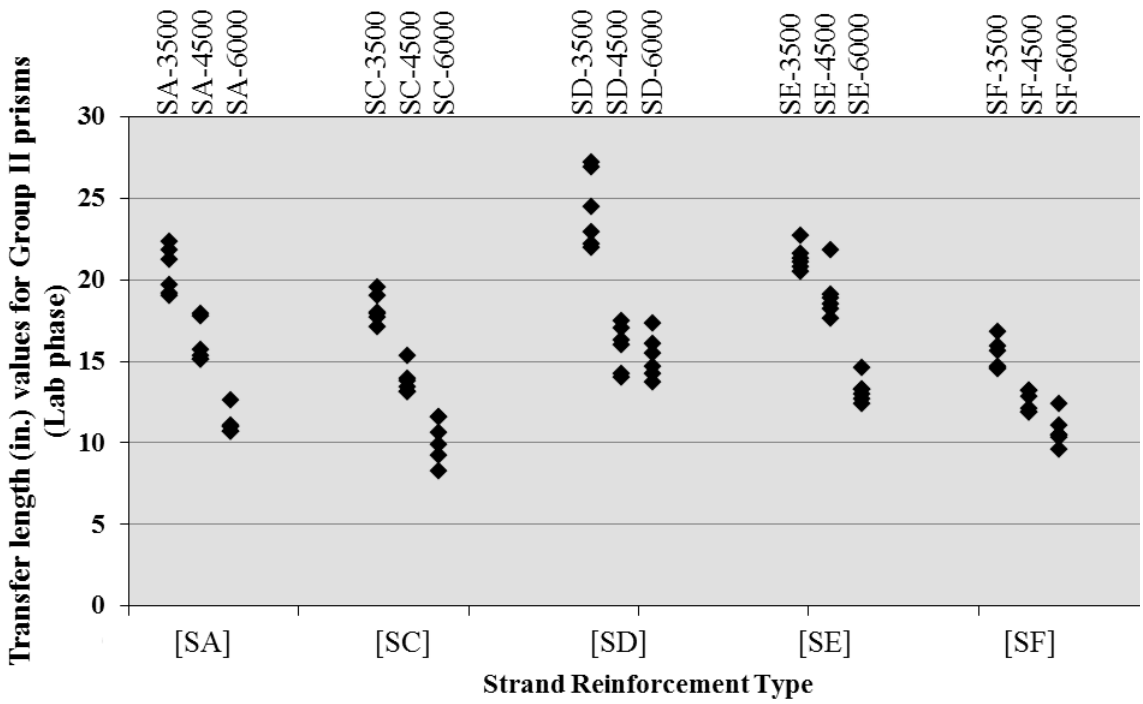

Figure 39 Transfer length results of wire reinforcements from Group II

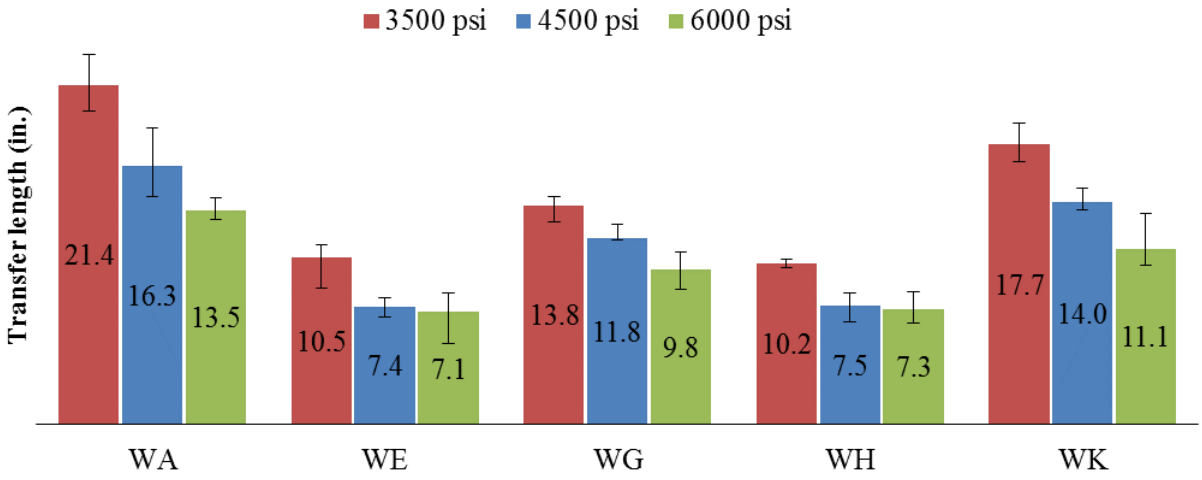

Figure 40 Average transfer lengths for wire reinforcement at different release strengths, TL in inches

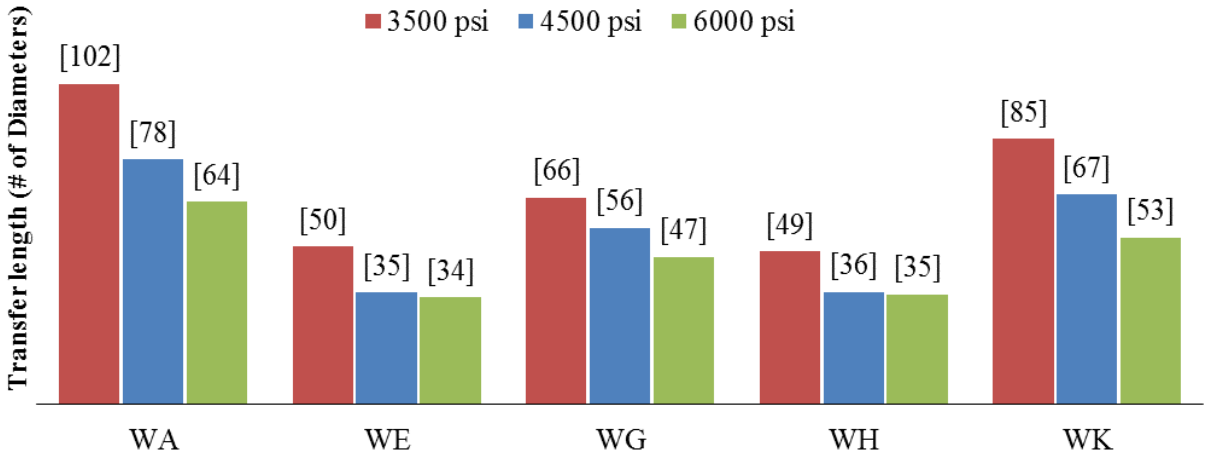

Figure 41 Average transfer lengths for wire reinforcement at different release strengths, TL in # of diameters of the reinforcement

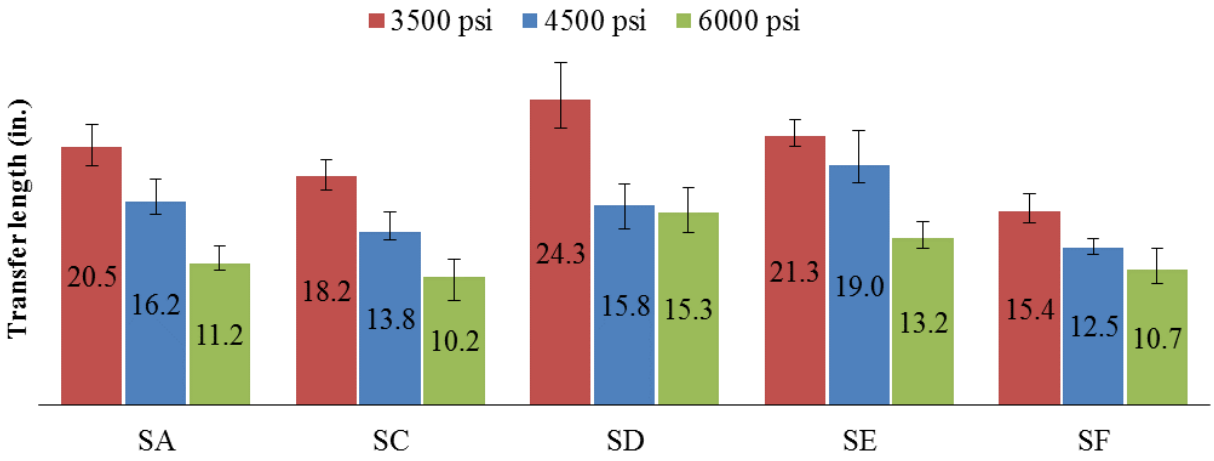

Figure 42 Average transfer lengths for strand reinforcement at different release strengths, TL in inches

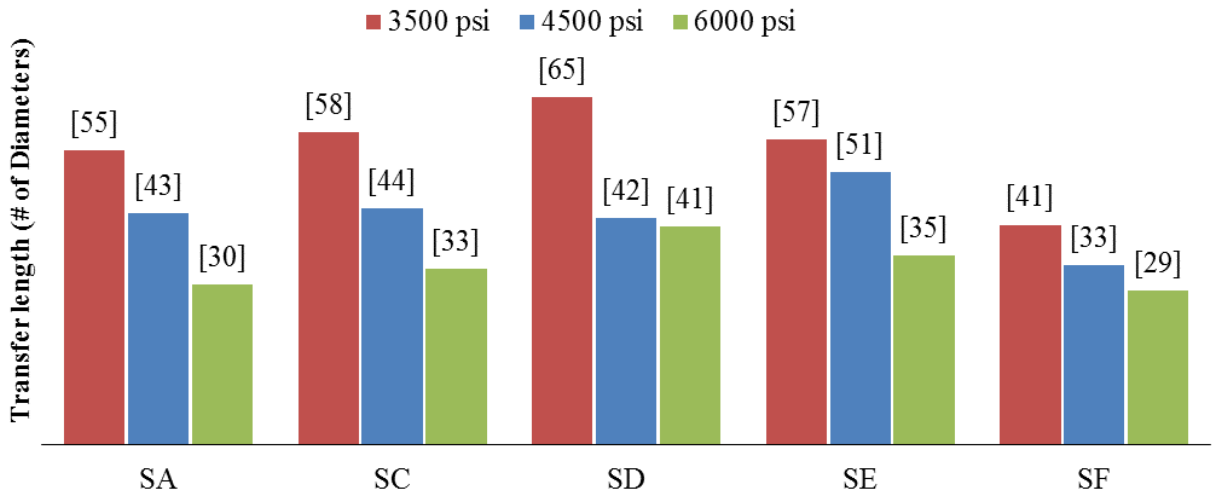

Figure 43 Average transfer lengths for strand reinforcement at different release strengths, TL in # diameters of the reinforcement

Based on the results from Group II prisms, a clear trend of better bond (lower transfer lengths) was observed with the increase in concrete release strength. This was true for both wire and strand reinforcements.

In the case of wire reinforcements, when the release strength was increased from 3500 psi to 6000 psi, percent reduction in average transfer lengths for [WA], [WE], [WG], [WH], and [WK] were 36.9%, 32.4%, 29.0%, 28.3%, and 37.3% respectively. However, the largest reductions are observed in the case of wires with minimal and no indent pattern ([WK], and [WA]) reinforcement. Percentage reductions in average transfer lengths due increase in release strength in the case wire reinforcements are tabulated in Table 24. This table presents the percent reduction in average transfer length due to increase in the release strength from 3500 psi to 4500 psi, and from 4500 psi to 6000 psi. From this table, the average reduction for all five wires was 23.0% when increasing strength from 3500 psi to 4500 psi, but only 12.4% when increasing from 4500 psi to 6000 psi. The average reduction for all five wires when compressive strength is increased from 3500 psi to 6000 psi was 32.8%.

Percentage reduction in average transfer lengths in strand reinforcements due to increase in release strength are tabulated in Table 25. This table presents the percent reduction due to increase in the release strength from 3500 psi to 4500 psi, and from 4500 psi to 6000 psi. From

this table, the average reduction for all five strands was 21.9% when increasing strength from 3500 psi to 4500 psi, and 21.0% when increasing from 4500 psi to 6000 psi. The average reduction for all five strands when compressive strength is increased from 3500 psi to 6000 psi was 39.0%.

When compared to wire reinforcements, higher relative reduction in percentages of avg. transfer lengths were observed in the case of strand reinforcements when the release strength was increased from 3500 psi to 6000 psi In this case, percentage reductions in average transfer lengths for strand reinforcements were observed to be 45.5%, 44.0%, 37.2%, 38.0%, and 30.1% for [SA], [SC], [SD], [SE], and [SF] respectively. Higher reduction in average transfer lengths was noted for both 7-wire ([SA]) and 3-wire ([SC]) smooth strands.

Table 24 Percentage reduction in transfer length of wires due to variation in release strength

Pour Identity	Percentage reduction in Transfer Length		
	from 3500 psi to 4500 psi	from 4500 psi to 6000 psi	from 3500 psi to 6000 psi
[WA]-[0.32]-[variable]-[6]-[#1]	23.7%	17.3%	36.9%
[WE]-[0.32]-[variable]-[6]-[#1]	29.2%	4.4%	32.4%
[WG]-[0.32]-[variable]-[6]-[#1]	14.6%	16.8%	29.0%
[WH]-[0.32]-[variable]-[6]-[#1]	26.3%	2.7%	28.3%
[WK]-[0.32]-[variable]-[6]-[#1]	20.9%	20.7%	37.3%
Average:	**23.0%**	**12.4%**	**32.8%**

Table 25 Percentage reduction in transfer length of strands due to variation in release strength

Pour Identity	Percentage reduction in Transfer Length		
	from 3500 psi to 4500 psi	from 4500 psi to 6000 psi	from 3500 psi to 6000 psi
[SA]-[0.32]-[variable]-[6]-[#1]	21.3%	30.8%	45.5%
[SC]-[0.32]-[variable]-[6]-[#1]	24.3%	25.9%	44.0%
[SD]-[0.32]-[variable]-[6]-[#1]	34.8%	3.7%	37.2%
[SE]-[0.32]-[variable]-[6]-[#1]	10.8%	30.5%	38.0%
[SF]-[0.32]-[variable]-[6]-[#1]	18.4%	14.3%	30.1%
Average:	**21.9%**	**21.0%**	**39.0%**

Transfer length ratios for different release strength were calculated and presented in Table 26 and Table 27 for wire and strand reinforcements respectively. Average TL ratio between 4500 psi and 3500 psi are 0.77 and 0.78 for wire and strand reinforcements respectively. Whereas, average TL ratio between 6000 psi and 3500 psi are 0.67 and 0.61 for wire and strand reinforcements respectively.

Table 26 TL ratio for different release strengths (wire reinforcements)

Wire Designation	$\frac{TL_{4500\ psi}}{TL_{3500\ psi}}$	$\frac{TL_{6000\ psi}}{TL_{4500\ psi}}$	$\frac{TL_{6000\ psi}}{TL_{3500\ psi}}$
[WA]	0.763	0.827	0.631
[WE]	0.708	0.956	0.676
[WG]	0.854	0.832	0.710
[WH]	0.737	0.973	0.717
[WK]	0.791	0.793	0.627
Average:	**0.770**	**0.876**	**0.672**

Table 27 TL ratio for different release strengths (strand reinforcements)

Strand Designation	$\frac{TL_{4500\ psi}}{TL_{3500\ psi}}$	$\frac{TL_{6000\ psi}}{TL_{4500\ psi}}$	$\frac{TL_{6000\ psi}}{TL_{3500\ psi}}$
[SA]	0.787	0.692	0.545
[SC]	0.757	0.741	0.560
[SD]	0.652	0.963	0.628
[SE]	0.892	0.695	0.620
[SF]	0.816	0.857	0.699
Average:	**0.781**	**0.790**	**0.610**

Table 28 Concrete properties at different release strength for Group II prisms

Pour Identity	Concrete Slump (in.)	Release Strength (psi)	Splitting tensile Strength (psi)	Modulus of Elasticity ($x10^6$ psi)
[WA]-[0.32]-[3.5]-[6]	6	3741	427	3.19
[WA]-[0.32]-[4.5]-[6]	6-1/4	4664	418	3.53
[WA]-[0.32]-[6.0]-[6]	6-1/4	6128	513	4.17
[WE]-[0.32]-[3.5]-[6]	6	3486	304	3.36
[WE]-[0.32]-[4.5]-[6]	6-1/4	4650	479	3.46
[WE]-[0.32]-[6.0]-[6]	6-1/2	6020	486	4.27
[WG]-[0.32]-[3.5]-[6]	6-1/4	3561	288	3.18
[WG]-[0.32]-[4.5]-[6]	6-1/4	4697	496	3.55
[WG]-[0.32]-[6.0]-[6]	6-1/4	5825	426	3.89
[WH]-[0.32]-[3.5]-[6]	6-1/2	3614	397	3.05
[WH]-[0.32]-[4.5]-[6]	6-1/2	4695	485	3.9
[WH]-[0.32]-[6.0]-[6]	6-1/4	6059	474	3.84
[WK]-[0.32]-[3.5]-[6]	6-1/2	3528	414	3.51
[WK]-[0.32]-[4.5]-[6]	6-1/4	4572	392	3.56
[WK]-[0.32]-[6.0]-[6]	6-1/2	5857	495	3.96
[SA]-[0.32]-[3.5]-[6]	6-1/4	3626	396	2.89
[SA]-[0.32]-[4.5]-[6]	6-1/4	4636	481	3.68
[SA]-[0.32]-[6.0]-[6]	6-1/4	6134	602	4.28
[SC]-[0.32]-[3.5]-[6]	6-1/4	3512	379	3.46
[SC]-[0.32]-[4.5]-[6]	6-1/2	4449	390	3.7
[SC]-[0.32]-[6.0]-[6]	6-1/2	6015	527	NA*
[SD]-[0.32]-[3.5]-[6]	6-3/4	3711	461	3.57
[SD]-[0.32]-[4.5]-[6]	6-1/2	4715	403	3.18
[SD]-[0.32]-[6.0]-[6]	6-1/4	6073	499	4.08
[SE]-[0.32]-[3.5]-[6]	6-1/2	3719	426	3.5
[SE]-[0.32]-[4.5]-[6]	6-1/4	4636	483	4.06
[SE]-[0.32]-[6.0]-[6]	6-1/4	5856	473	4.1
[SF]-[0.32]-[3.5]-[6]	6-1/4	3622	396	3.62
[SF]-[0.32]-[4.5]-[6]	6-1/2	4635	444	3.57
[SF]-[0.32]-[6.0]-[6]	6-1/2	5985	523	4.02

*data not available

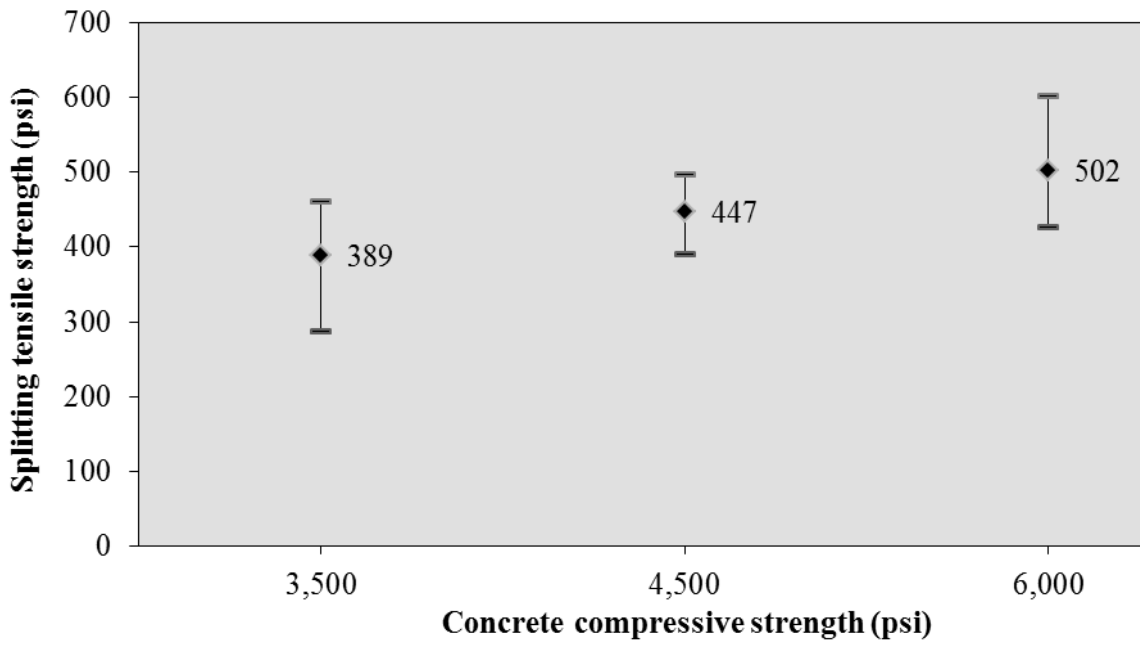

Figure 44 Variation in splitting tensile strength with concrete consistency for Group II prisms

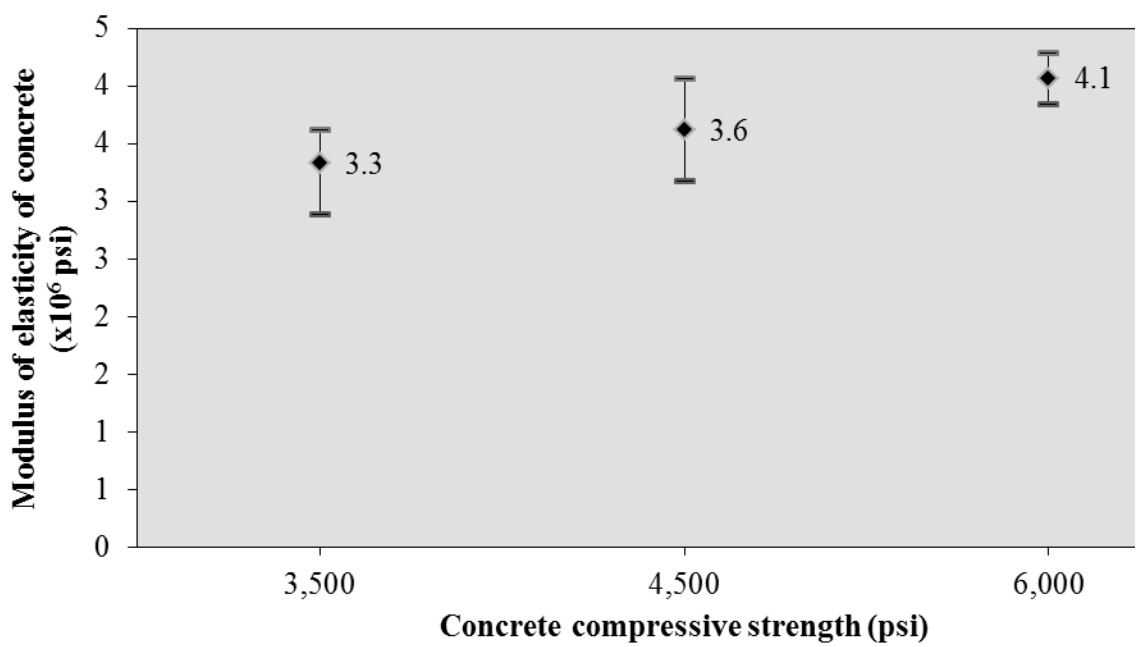

Figure 45 Variation in MOE with release strength for Group II prisms

5.3.1 Special case study with higher release strength-8300 psi

Additional prisms were cast with WF reinforcement, to study the TL variation due to higher release strength (8300 psi). TL values were determined for the prisms cast with WF reinforcement at 3500 psi, 6000 psi, and 8300 psi. Later, these results were compared with TL results determined from [WF]-[0.32]-[4.5]-[3]-[#1]. Table 29 tabulates minimum, average, and maximum TL results for prisms cast with WF reinforcement at different release strengths. Figure 46 shows scatter plot of all TL results determined at four different release strengths.

Figure 47 shows the average TL at each release strength, along with the range of values. Figure 48 shows the coefficient of determination (R^2) between release strength and average TL values for [WF]. This exceptionally-high R^2-value indicates that the relationship between transfer length and release strength is approximately linear for release strengths between 3500 psi and 8300 psi. Figure 49 shows the average data for [WF] in bar-chart format.

Table 29 TL results for prisms cast with WF at different release strengths

Nomenclature	[WF]-[0.32]-[varies]-[6]-[#1]		
Release Strength	Transfer Lengths		
	Min., in. [TL/d_b]	Avg., in. [TL/d_b]	Max., in. [TL/d_b]
3500 psi	9.20 [44]	9.63 [46]	10.40 [50]
4500 psi	6.80 [32]	8.45 [40]	9.30 [44]
6000 psi	6.10 [29]	7.15 [34]	8.20 [39]
8300 psi	4.60 [22]	5.27 [25]	6.60 [32]

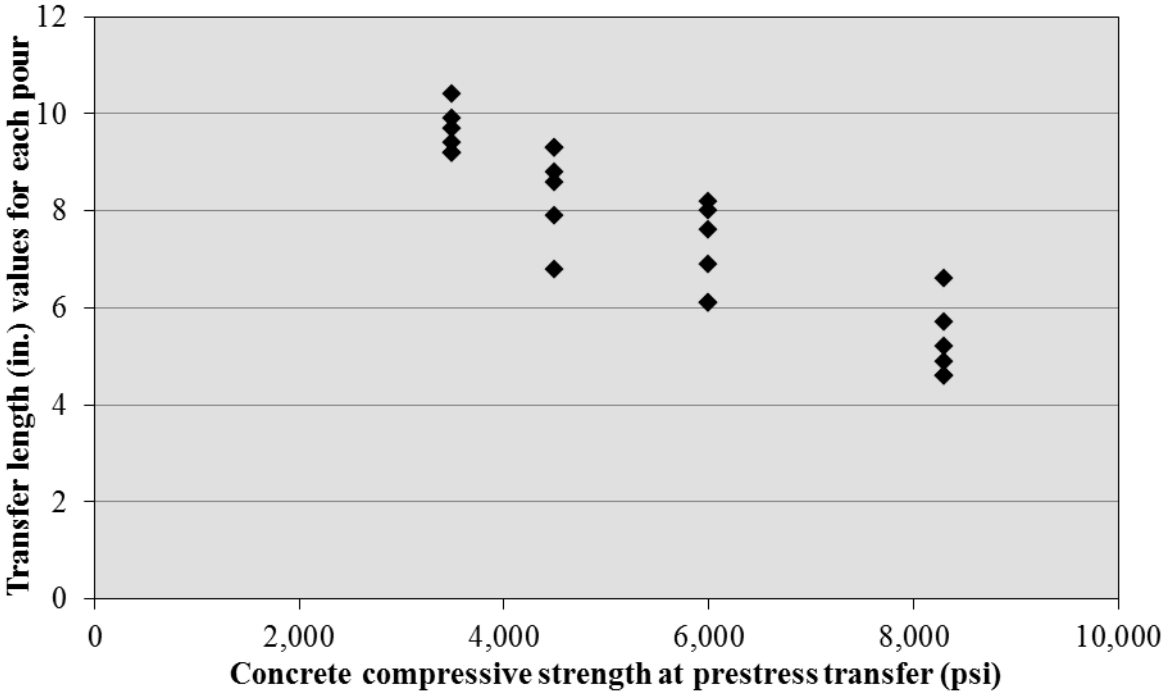

Figure 46 TL results for prisms cast with WF reinforcement at different release strengths

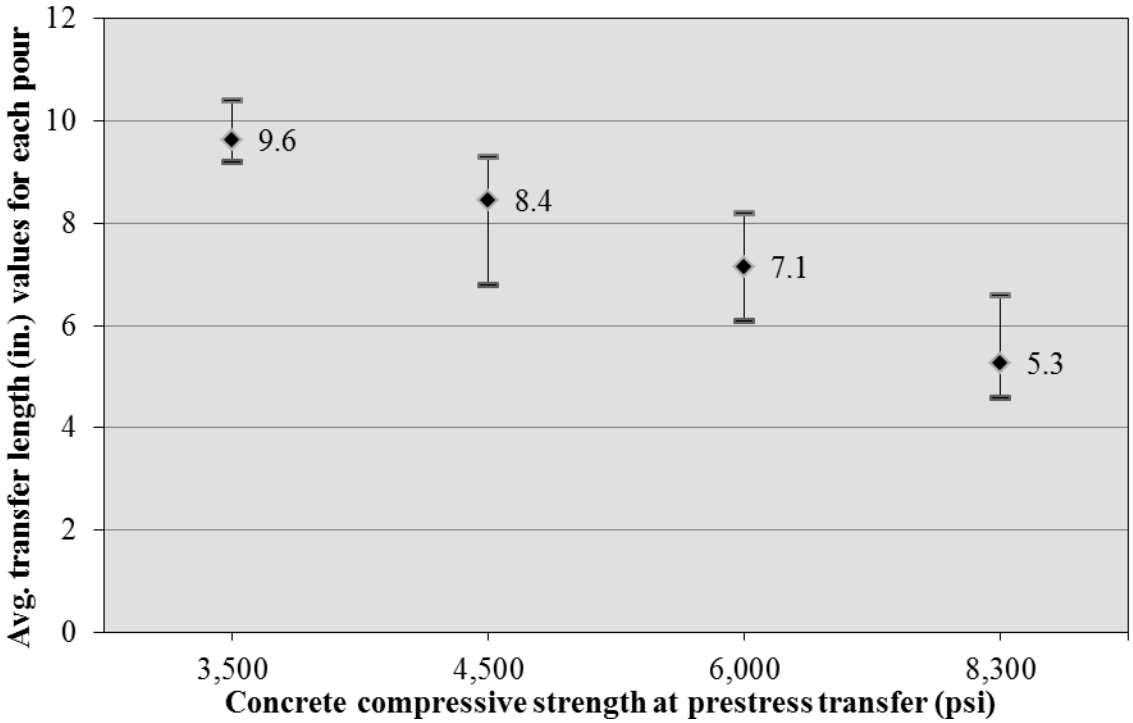

Figure 47 Average TL results for prisms cast with WF reinforcement at different release strengths

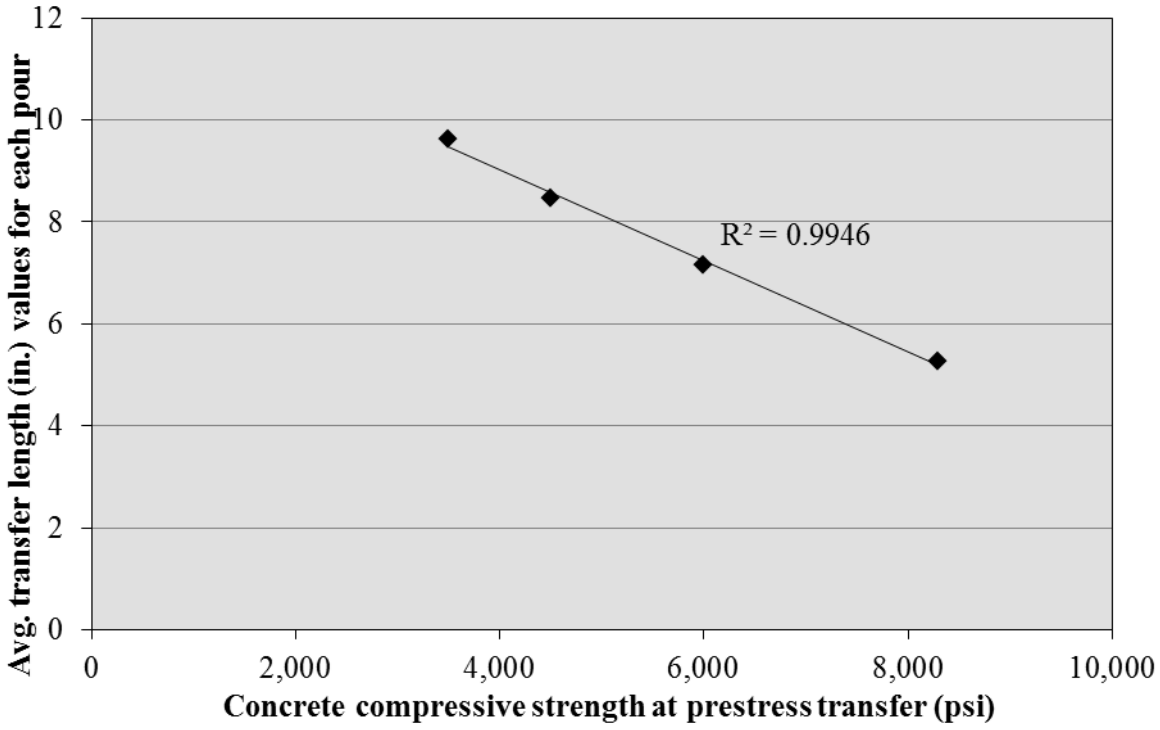

Figure 48 Coefficient of determination between average TL and release strength of [WF]

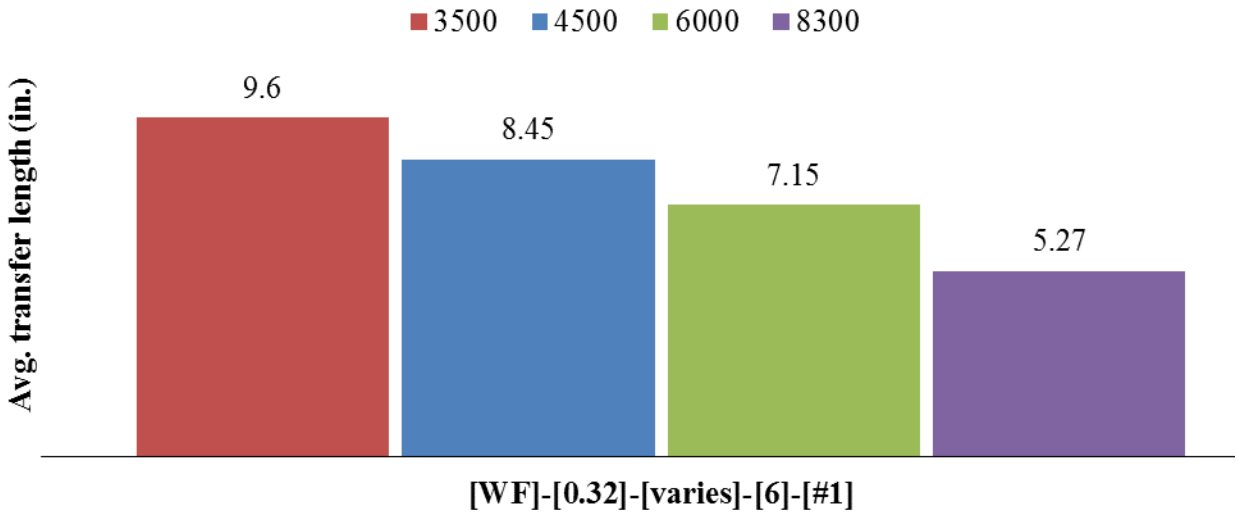

Figure 49 Average transfer length values at different release strengths for [WF]

5.4 Effect of concrete consistency on Transfer length (Group III prisms)

During Group III testing in Lab-Phase, prisms were cast with three (3) different concrete slumps (3-inches, 6-inche, and 9-inches) to evaluate the effect of concrete consistency on transfer length. Concrete slump at the beginning of casting was maintained within the variation of ±0.5 inches from the desired value. All of the prisms had a w/c ratio of 0.32, and the different slump was obtained by varying the HRWR dosage (Section 3.2.4). Average transfer lengths for prisms cast with various concrete slumps at uniform release strength of 4500 psi (±220 psi) are compared and discussed in this section. Nomenclature for various prisms utilized in Group III are tabulated in Table 30.

Table 30 Nomenclature for prisms utilized in Group III

Nomenclature for the Prisms utilized in Group III		
Concrete Consistency 3-in.	Concrete Consistency 6-in.	Concrete Consistency 9-in.
[WA]-[0.32]-[4.5]-[3]-[#1]	[WA]-[0.32]-[4.5]-[6]-[#1]	[WA]-[0.32]-[4.5]-[9]-[#1]
[WE]-[0.32]-[4.5]-[3]-[#1]	[WE]-[0.32]-[4.5]-[6]-[#1]	[WE]-[0.32]-[4.5]-[9]-[#1]
[WG]-[0.32]-[4.5]-[3]-[#1]	[WG]-[0.32]-[4.5]-[6]-[#1]	[WG]-[0.32]-[4.5]-[9]-[#1]
[WH]-[0.32]-[4.5]-[3]-[#1]	[WH]-[0.32]-[4.5]-[6]-[#1]	[WH]-[0.32]-[4.5]-[9]-[#1]
[WK]-[0.32]-[4.5]-[3]-[#1]	[WK]-[0.32]-[4.5]-[6]-[#1]	[WK]-[0.32]-[4.5]-[9]-[#1]
[SD]-[0.32]-[4.5]-[3]-[#1]	[SD]-[0.32]-[4.5]-[6]-[#1]	[SD]-[0.32]-[4.5]-[9]-[#1]
[SE]-[0.32]-[4.5]-[3]-[#1]	[SE]-[0.32]-[4.5]-[6]-[#1]	[SE]-[0.32]-[4.5]-[9]-[#1]

Transfer lengths (minimum, average, maximum) of prisms cast during Group III testing with different concrete slumps are tabulated in Table 31. Plots showing all Group III prisms' TL results are presented in Figure 50 and Figure 51, respectively, for wire and strand reinforcements. All transfer length values were obtained using the procedure in Section 4.4.2. Concrete parameters such as slump, release strength, splitting tensile strength, and Modulus of Elasticity (MOE) for the corresponding prisms are tabulated in Table 33

Table 33 Concrete properties at different concrete slumps for Group III prisms

. Change in splitting tensile strength due to change in slump is illustrated in Figure 52. Figure 53 illustrates the change in MOE with release strength.

Average transfer lengths (in inches) obtained at various concrete slumps for a chosen set of five (5) wire reinforcements are shown in Figure 54, along with the range of values for each group of six measurements. The same average data values, converted to "number of diameters (d_b)" are represented in Figure 55.

Similarly, average transfer lengths for each strand type at different concrete slumps are shown in Figure 56. Average transfer lengths of strands are represented in "inches" and "number of diameters" in Figure 56 and Figure 57, respectively. Concrete properties for prisms cast with different strand reinforcements at different concrete slumps are tabulated in Table 33.

Based on the results from Group III prisms, no consistent trend in transfer length values was observed with the variation of concrete consistency between 3-in. and 9-in. slump. The increase in average transfer length results from Group III prisms cast with different concrete consistencies are tabulated in Table 32. In Table 32, positive number indicate an increase in transfer length while negative number indicate a reduction in transfer length. From this table, the average transfer lengths for all seven reinforcements decreases by 4.1% when the slump was increased from 3-in. to 6-in. However, when the slump was increased from 6-in. to 9-in., the same seven reinforcements had an average transfer length increase of 13.2%.

In the case of wire reinforcements, when the concrete slump was increased from 3-inches to 9-inches, percent increase in average transfer lengths for [WA], [WE], [WG], [WH], and [WK] were 5.0%, 11.9%, 12.9%, 0.2%, and 8.7% respectively. Except in the case of [WH], the transfer lengths of the increased by 5-13% when concrete slumps are increased from 3-inches to 9-inches. From Table 32, the largest increase in average transfer lengths (in the case of wire reinforcements) was observed when slumps increased from 6-inches to 9-inches.

In the case of the two strand reinforcements, no trend was observed in the variation of average transfer lengths with different concrete slumps. When the concrete slump was increased from 3-inches to 9-inches, percentage increase in average transfer lengths for strand reinforcements were observed to be 0.4%, and 10.7% for [SD], and [SE] respectively. Whereas, inconsistent average transfer length variations were observed in prisms (with strand

reinforcement) when concrete slumps are varied from 3-inches to 6-inches and 6-inches to 9-inches.

Table 31 Transfer length results from Group III testing (effect of concrete slump)

Wire/Strand Type	Concrete Slump 3-inches			Concrete Slump 6-inches			Concrete Slump 9-inches		
	Transfer Lengths			Transfer Lengths			Transfer Lengths		
	Min., in. [TL/d_b]	Avg., in. [TL/d_b]	Max., in. [TL/d_b]	Min., in. [TL/d_b]	Avg., in. [TL/d_b]	Max., in. [TL/d_b]	Min., in. [TL/d_b]	Avg., in. [TL/d_b]	Max., in. [TL/d_b]
[WA]	15.10 [72]	16.10 [77]	17.60 [84]	14.40 [69]	16.33 [78]	18.70 [89]	15.80 [75]	16.90 [81]	17.90 [85]
[WE]	6.40 [31]	8.27 [39]	10.10 [48]	6.80 [32]	7.43 [35]	8.00 [38]	7.70 [37]	9.25 [44]	10.60 [51]
[WG]	10.00 [48]	11.78 [56]	12.90 [62]	11.60 [55]	11.78 [56]	12.60 [60]	12.00 [57]	13.30 [64]	14.40 [69]
[WH]*	8.00 [38]	9.20 [44]	10.80 [52]	6.50 [31]	7.50 [36]	8.30 [40]	8.00 [38]	9.22 [44]	10.80 [52]
[WK]	12.50 [60]	14.00 [67]	15.90 [76]	13.50 [64]	14.00 [67]	14.90 [71]	13.40 [64]	15.22 [73]	17.10 [82]
[SD]	18.80 [50]	20.15 [54]	21.10 [56]	14.00 [37]	15.83 [42]	17.50 [47]	19.40 [52]	20.23 [54]	22.80 [61]
[SE]	14.60 [39]	15.85 [42]	17.40 [46]	17.60 [47]	19.02 [51]	21.80 [58]	16.20 [43]	17.55 [47]	19.00 [51]

*[WH]-[0.32]-[4.5]-[3]-[#1] pour includes only 5 TL values (not 6 TL values), since there was cracking at one end.

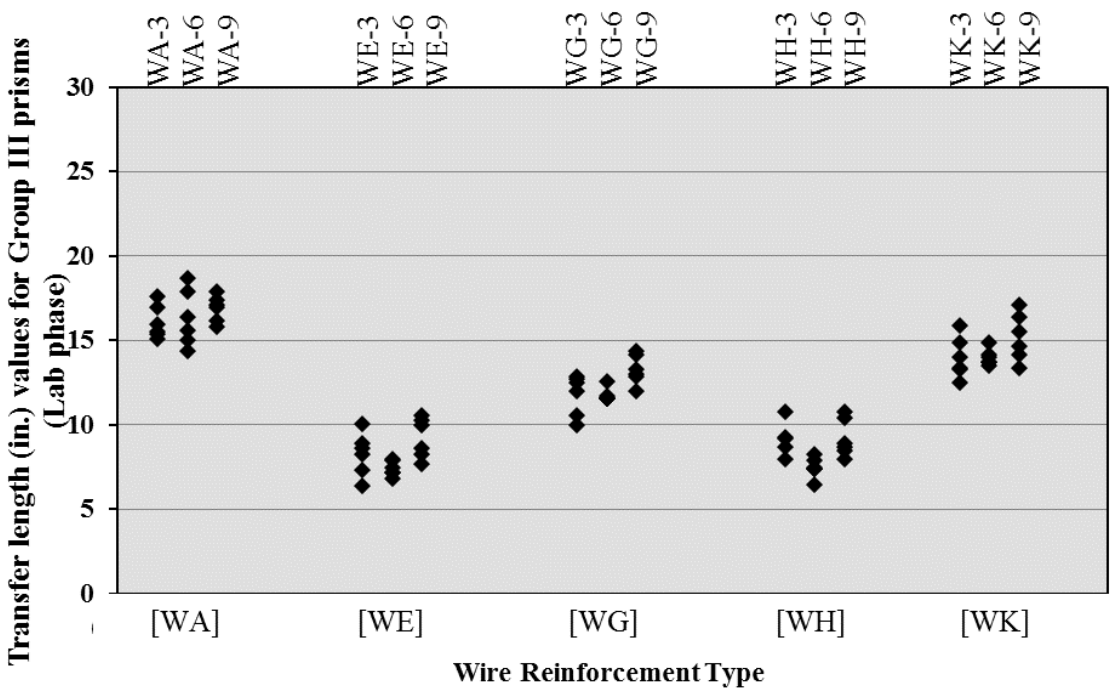

Figure 50 Transfer length results of wire reinforcements from Group III

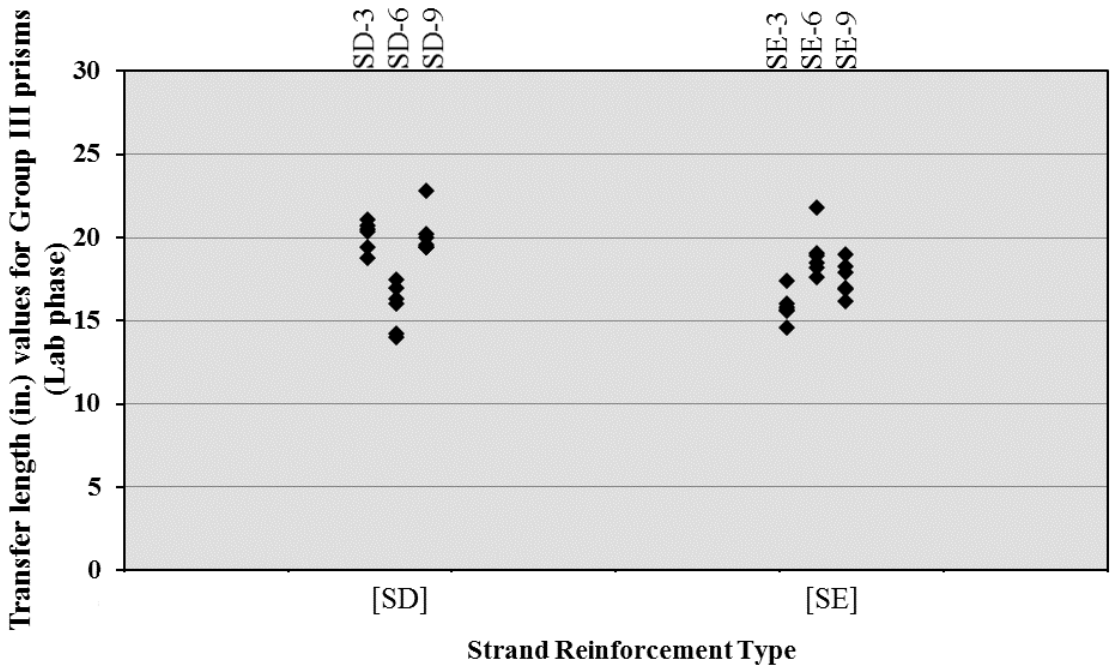

Figure 51 Transfer length results of strand reinforcements from Group III

Table 32 Percentage increase in avg. TL for both wire and strand reinforcements due to change in consistency (slump)

Pour Identity	Percentage increase in Transfer Length		
	from 3 inches to 6 inches	from 6 inches to 9 inches	from 3 inches to 9 inches
[WA]-[0.32]-[4.5]-[variable]-[#1]	1.4%	3.5%	5.0%
[WE]-[0.32]-[4.5]-[variable]-[#1]	-10.2%	24.5%	11.9%
[WG]-[0.32]-[4.5]-[variable]-[#1]	0.0%	12.9%	12.9%
[WH]-[0.32]-[4.5]-[variable]-[#1]	-18.5%	22.9%	0.2%
[WK]-[0.32]-[4.5]-[variable]-[#1]	0.0%	8.7%	8.7%
[SD]-[0.32]-[4.5]-[variable]-[#1]	-21.4%	27.8%	0.4%
[SE]-[0.32]-[4.5]-[variable]-[#1]	20.0%	-7.7%	10.7%
Average:	**-4.1%**	**13.2%**	**7.1%**

Table 33 Concrete properties at different concrete slumps for Group III prisms

Pour Identity	Concrete Slump (inch)	Release Strength (psi)	Splitting tensile Strength (psi)	Modulus of Elasticity ($x10^6$ psi)
[WA]-[0.32]-[4.5]-[3]	3	4442	367	3.43
[WA]-[0.32]-[4.5]-[6]	6-1/4	4664	418	3.53
[WA]-[0.32]-[4.5]-[9]	9-1/4	4645	406	3.29
[WE]-[0.32]-[4.5]-[3]	3-1/2	4461	350	3.64
[WE]-[0.32]-[4.5]-[6]	6-1/4	4650	479	3.46
[WE]-[0.32]-[4.5]-[9]	9-1/2	4649	332	3.39
[WG]-[0.32]-[4.5]-[3]	3-1/4	4669	349	3.79
[WG]-[0.32]-[4.5]-[6]	6-1/4	4697	496	3.55
[WG]-[0.32]-[4.5]-[9]	9-1/4	4592	348	3.59
[WH]-[0.32]-[4.5]-[3]	3-3/4	4622	426	3.61
[WH]-[0.32]-[4.5]-[6]	6-1/2	4695	485	3.9
[WH]-[0.32]-[4.5]-[9]	9-1/2	4482	351	3.27
[WK]-[0.32]-[4.5]-[3]	3-1/4	4633	413	3.37
[WK]-[0.32]-[4.5]-[6]	6-1/4	4572	392	3.56
[WK]-[0.32]-[4.5]-[9]	9-1/4	4450	318	3.52
[SD]-[0.32]-[4.5]-[3]	3-3/4	4455	492	4.01
[SD]-[0.32]-[4.5]-[6]	6-1/2	4715	403	3.18
[SD]-[0.32]-[4.5]-[9]	9-1/4	4604	492	3.92
[SE]-[0.32]-[4.5]-[3]	3-1/2	4461	488	4.07
[SE]-[0.32]-[4.5]-[6]	6-1/2	4635	444	4.06
[SE]-[0.32]-[4.5]-[9]	9-1/4	4485	462	4.02

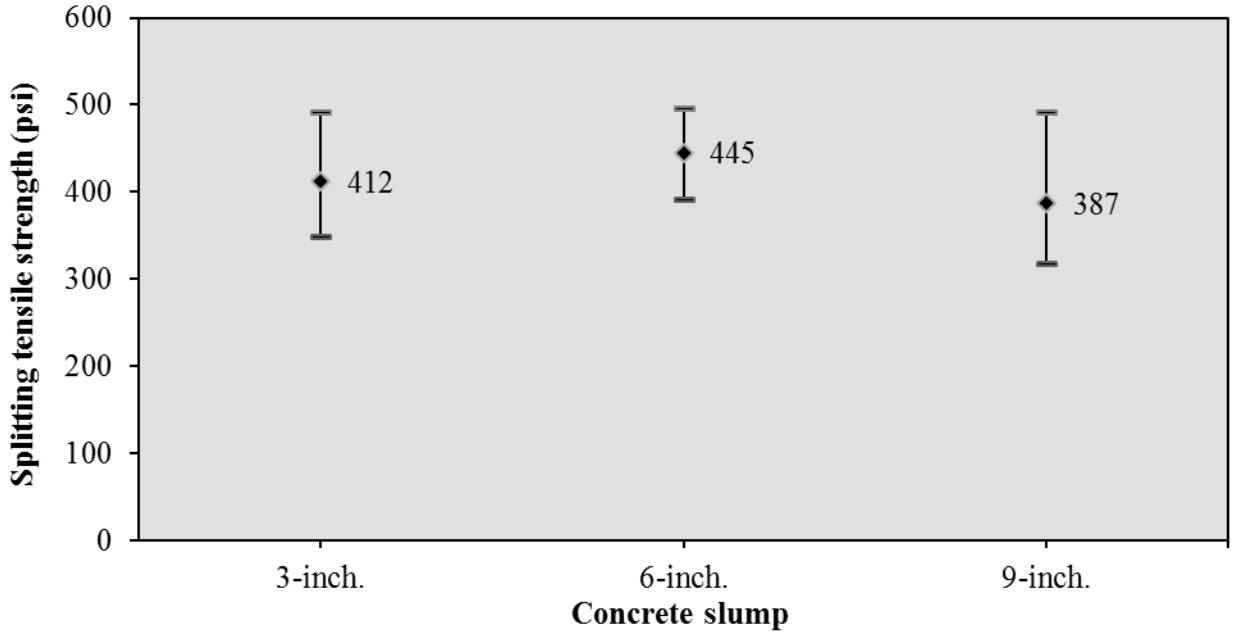

Figure 52 Variation in splitting tensile strength with concrete consistency for Group III prisms

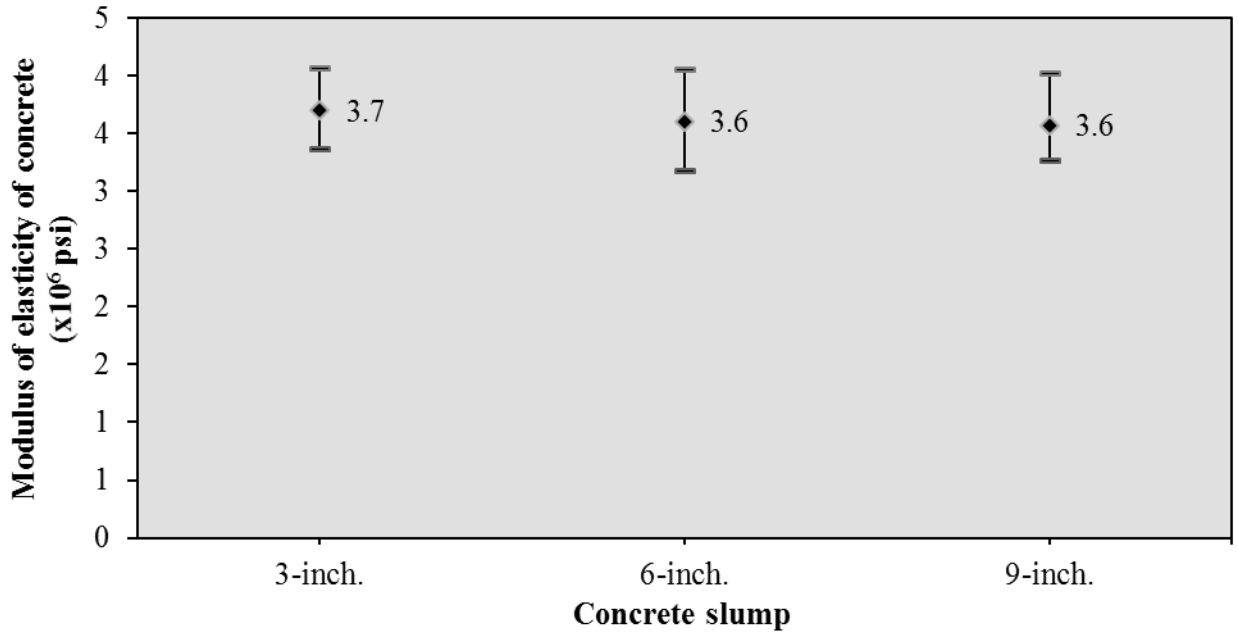

Figure 53 Variation in MOE strength with concrete consistency for Group III prisms

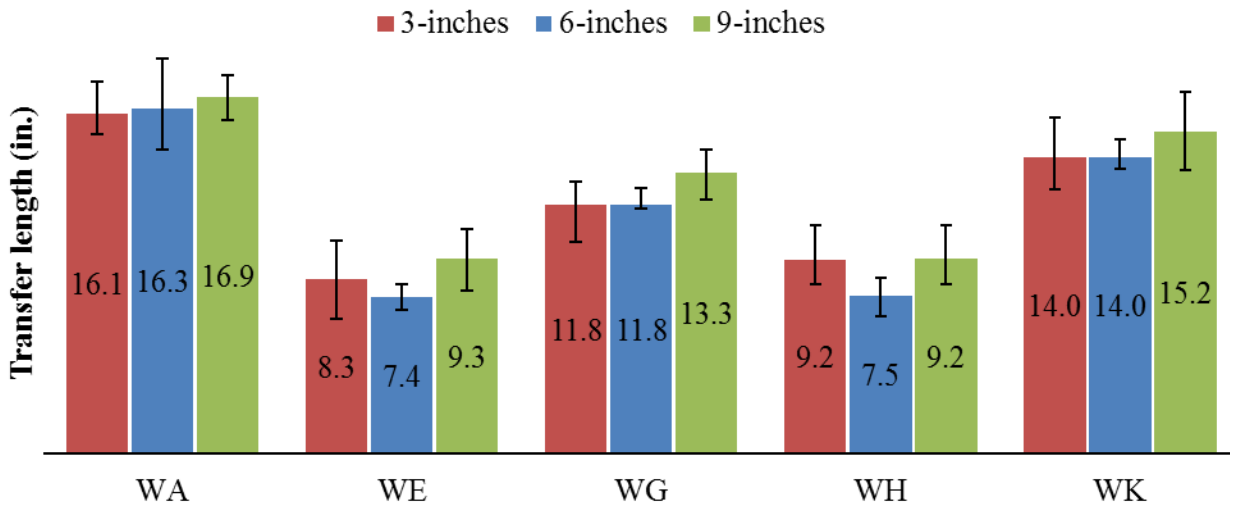

Figure 54 Average transfer lengths for wire reinforcement at different concrete slumps-TL in inches

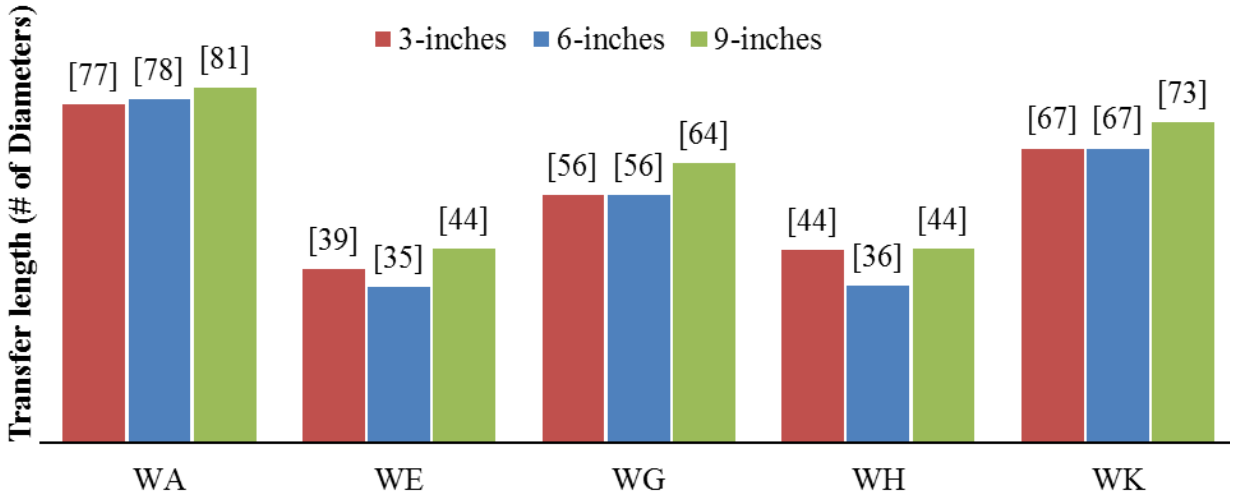

Figure 55 Average transfer lengths for wire reinforcement at different concrete slumps-TL in # of diameters of the reinforcement

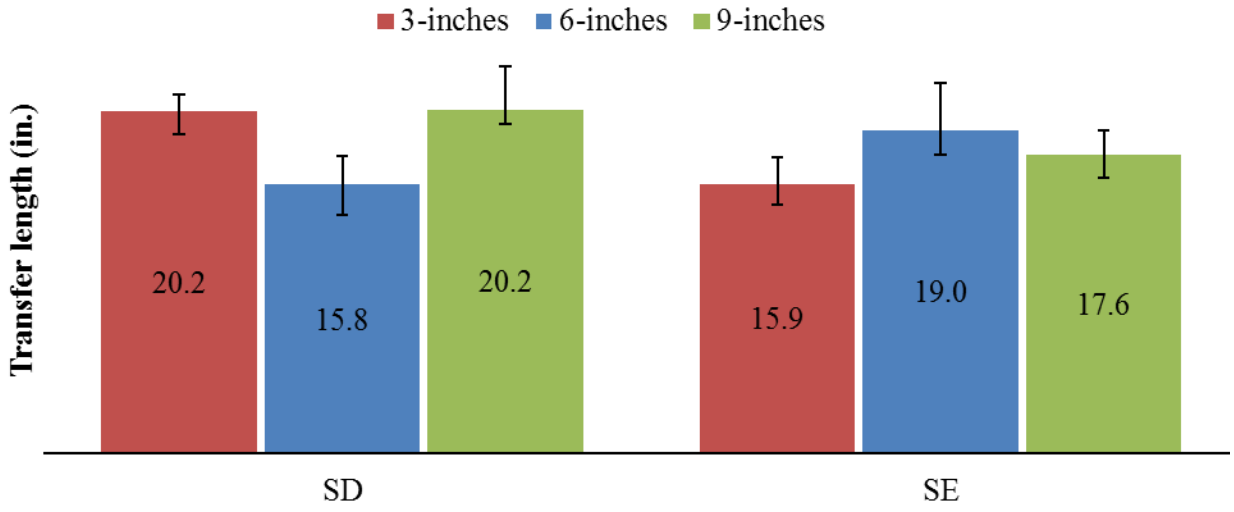

Figure 56 Average transfer lengths for strand reinforcement at different concrete slumps-TL in inches

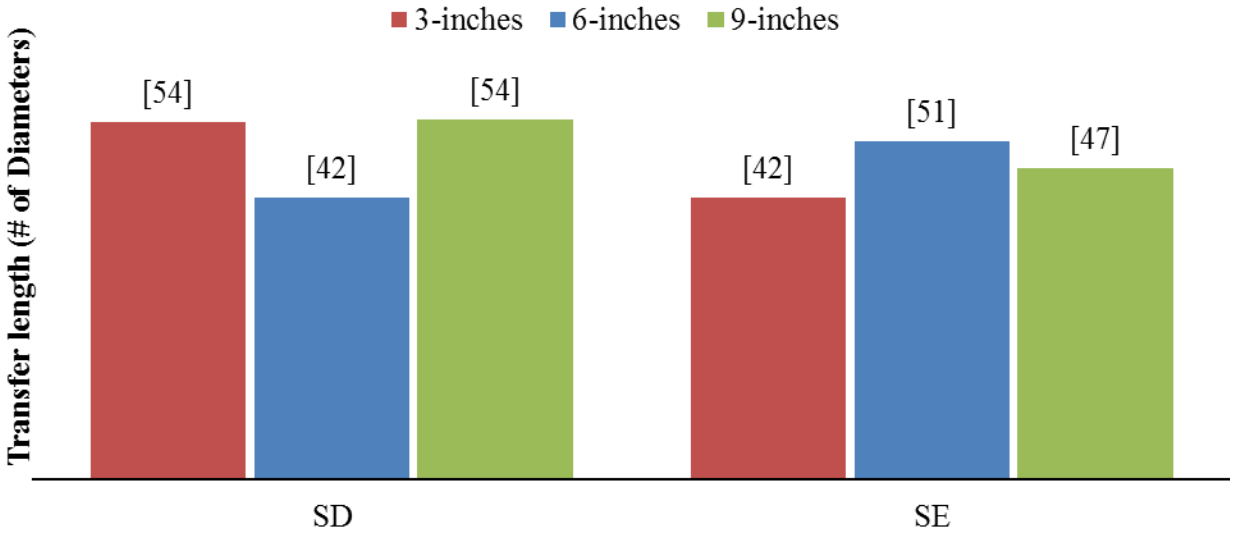

Figure 57 Average transfer lengths for strand reinforcement at different concrete slumps-TL in # of diameters of the reinforcement

5.5 Effect of water-to-cementitious (w/c) ratio on transfer length (Group IV prisms)

In the present study, a few prisms were cast to evaluate the effect of w/c ratio on transfer length. During Group IV testing, three w/c ratios (0.27, 0.32, and 0.42) were used with Mix-Design #1 while maintaining a 6-in. slump. No VMA was used for prisms cast in Group IV. Two reinforcements were selected for use in this limited investigation, [WG] and [WH]. These wires were the worst-bonding and best-bonding chevron-indented wires, respectively, identified from Group I prism tests. Nomenclature for the prisms utilized in Group IV are tabulated in Table 34.

Table 34 Nomenclature for prisms utilized in Group IV

Nomenclature for the Prisms utilized in Group IV		
w/c ratio = 0.27	w/c ratio = 0.32	w/c ratio = 0.42
[WG]-[0.27]-[4.5]-[6]-[#1]	[WG]-[0.32]-[4.5]-[6]-[#1]	[WG]-[0.42]-[4.5]-[6]-[#1]
[WH]-[0.27]-[4.5]-[6]-[#1]	[WH]-[0.32]-[4.5]-[6]-[#1]	[WH]-[0.42]-[4.5]-[6]-[#1]

Transfer lengths (minimum, average, and maximum) of prisms cast during Group IV testing with different concrete w/c ratios are tabulated in Table 35. A plot of all individual Group IV prisms' TL results is presented in Figure 58. All transfer length results were obtained through the procedure explained in Section 4.4.2.

Average transfer lengths for each wire type at the different w/c ratios are shown in bar-chart format, along with the corresponding range of values for each pour, in Figure 59. Figure 60 depicts the same average TL values in terms of number of diameters (d_b) of the reinforcement.

From Figure 59, a consistent change in transfer length was not observed due to variation in w/c ratio. Percent increase in average transfer length results of prisms cast with different w/c ratios are tabulated in Table 36. In this table, positive numbers indicate an increase in transfer length while negative numbers indicate reduction in transfer length.

In the case of prisms cast with [WG] wire reinforcement, when the w/c ratio was increased from 0.27 to 0.42, percent increase in average transfer length was 25.9%. This increase was 7.2% when [WH] was employed. However, from Table 36, inconsistent average transfer length variations were observed when varying w/c from 0.27 and 0.32, and between 0.32 and 0.42.

Table 35 Transfer length results from Group IV testing (effect of w/c ratio)

Pour Identity or Nomenclature	Transfer Lengths		
	Min., in. [TL/d_b]	Avg., in. [TL/d_b]	Max., in. [TL/d_b]
[WG]-[0.27]-[4.5]-[6]-[#1]	7.40	9.15	11.20
	[35]	[44]	[53]
[WH]-[0.27]-[4.5]-[6]-[#1]*	6.30	8.38	10.80
	[30]	[40]	[52]
[WG]-[0.32]-[4.5]-[6]-[#1]	11.60	11.80	12.60
	[55]	[56]	[60]
[WH]-[0.32]-[4.5]-[6]-[#1]	6.50	7.50	8.30
	[31]	[36]	[40]
[WG]-[0.42]-[4.5]-[6]-[#1]	11.00	11.52	12.30
	[53]	[55]	[59]
[WH]-[0.42]-[4.5]-[6]-[#1]	8.40	8.98	11.10
	[40]	[43]	[53]

*[WH]-[0.27]-[4.5]-[6]-[#1] pour includes only 5 TL values (not 6 TL values), since there was cracking at one end.

Table 36 Percentage variation in avg. TL due to change in w/c ratio of concrete mixture

Pour Identity	Percentage increase in Transfer Length		
	from w/c = 0.27 to w/c = 0.32	from w/c = 0.32 to w/c = 0.42	from w/c = 0.27 to w/c = 0.42
[WG]-[variable]-[4.5]-[6]-[#1]	29.0%	-2.4%	25.9%
[WH]-[variable]-[4.5]-[6]-[#1]	-10.5%	19.7%	7.2%
Average:	**9.2%**	**8.7%**	**16.5%**

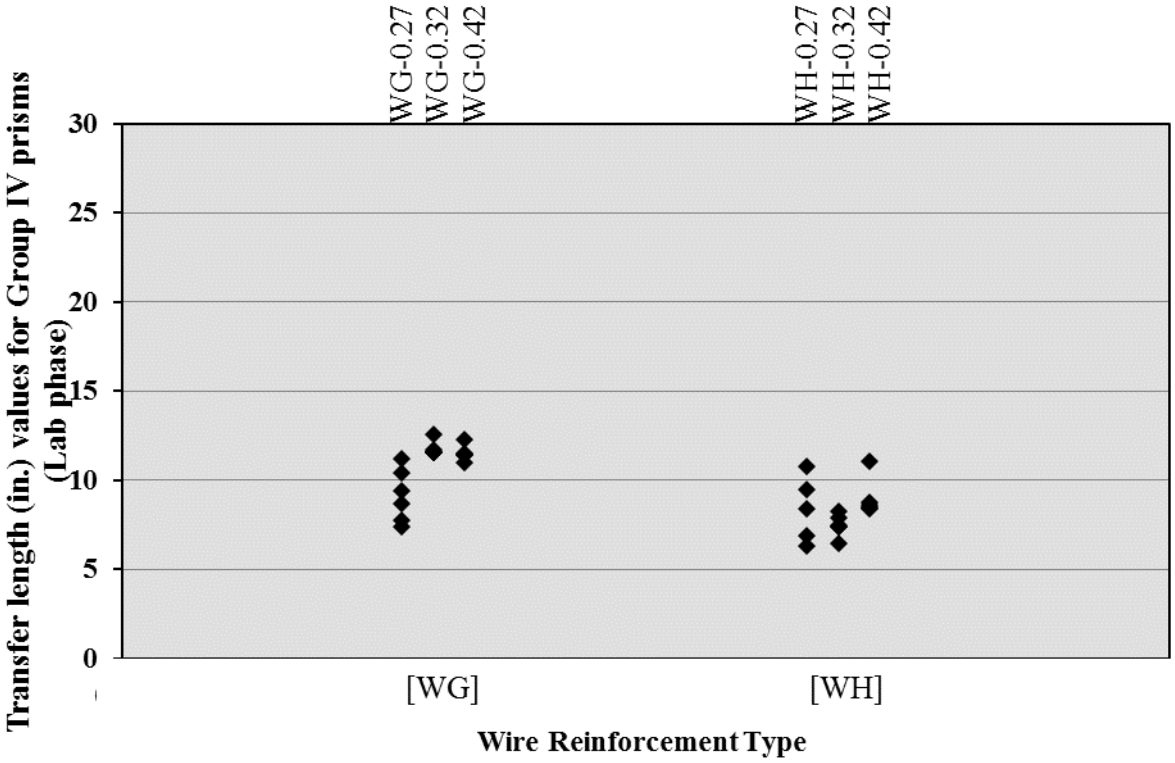

Figure 58 Individual transfer length results for Group IV prisms

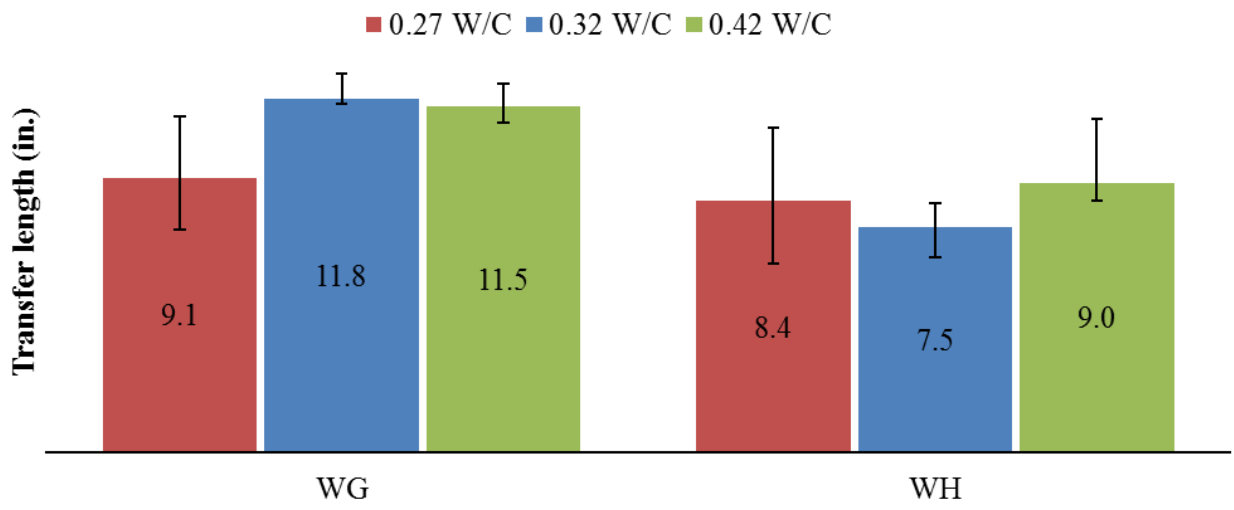

Figure 59 Average transfer lengths for wire reinforcement at different w/c ratios (TL in inches)

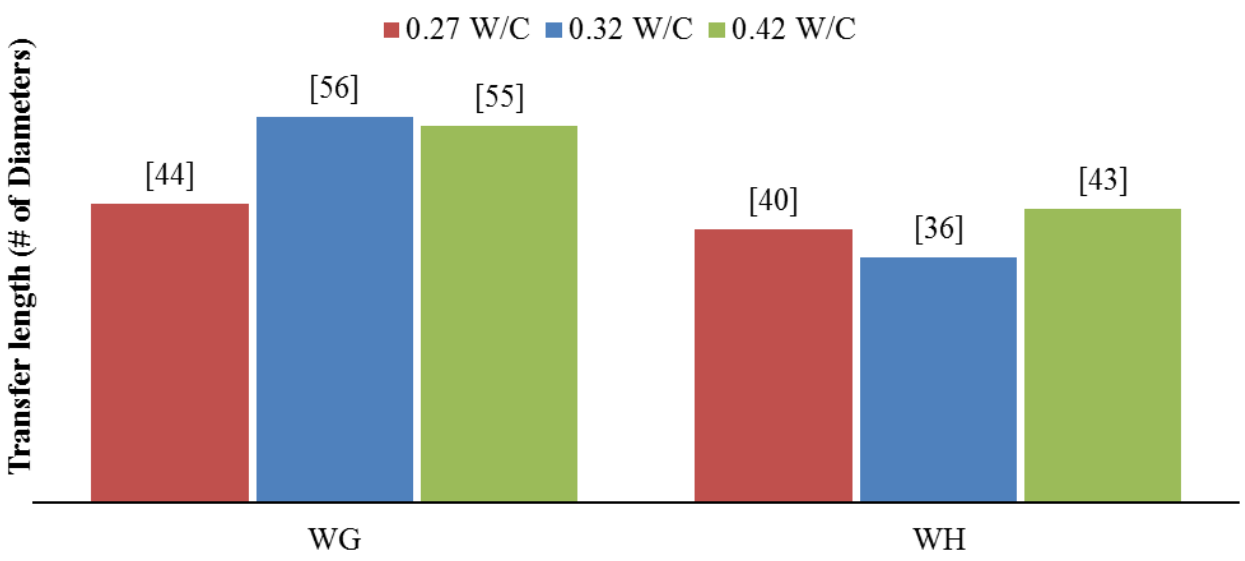

Figure 60 Average transfer lengths for wire reinforcement at different w/c ratios (TL in # of diameters of the reinforcement)

5.6 Effect of "Viscosity-Modifying Admixture (VMA) presence" in concrete mix on transfer length (Group V prisms)

Twelve additional prisms (four pours) were cast to evaluate the effect of presence of VMA in concrete mix on bond transfer length. Prisms were poured with concrete Mix-Design #1 with the addition of VMA and the corresponding transfer lengths determined. These results were then compared with companion (similar prestressing and concrete variables except with no presence of VMA) prism TL results. Average transfer length results for Group V prisms are presented and discussed in this section. Nomenclature for prisms utilized in Group V are tabulated in Table 37.

Table 37 Nomenclature for prisms utilized in Group V

no VMA	with VMA
[WG]-[0.27]-[4.5]-[6]-[#1]	[WG]-[0.27]-[4.5]-[6]-[#1] with VMA
[WH]-[0.27]-[4.5]-[6]-[#1	[WH]-[0.27]-[4.5]-[6]-[#1] with VMA
[WG]-[0.42]-[4.5]-[6]-[#1]	[WG]-[0.42]-[4.5]-[6]-[#1] with VMA
[WH]-[0.42]-[4.5]-[6]-[#1]	[WH]-[0.42]-[4.5]-[6]-[#1] with VMA

The minimum, average, and maximum transfer length values of Group V prisms are tabulated in Table 38. A graph showing the individual Group V prisms results is presented in Figure 61. All transfer length results are obtained using the procedure described in Section 4.4.2.

Average transfer lengths, and corresponding range of values, for companion prisms cast with and without VMA are shown in bar-chart format in Figure 62. Similar results are graphed in terms of "number of diameters (d_b)" in Figure 63.

From these figures, there was no significant change in transfer length when VMA was added to the concrete mixture. Percent reduction in average transfer length results of prisms cast with VMA are tabulated in Table 39. In Table 39, positive number indicates a reduction in transfer length while negative number indicate an increase in transfer length.

Variation in transfer length results for pour identities [WG]-[0.27]-[4.5]-[6]-[#1], [WH]-[0.27]-[4.5]-[6]-[#1], [WG]-[0.42]-[4.5]-[6]-[#1], and [WH]-[0.42]-[4.5]-[6]-[#1] are -14.0%,

13.8%, 0.3%, and -2.1% respectively. Hence, random average transfer length variations were observed due the presence of VMA in concrete mix.

Table 38 Results from Group V testing (effect of VMA presence in concrete mixture)

Pour Identity	Transfer Lengths		
	Min., in. [TL/d_b]	Avg., in. [TL/d_b]	Max., in. [TL/d_b]
[WG]-[0.27]-[4.5]-[6]-[#1]	7.40 [35]	9.15 [44]	11.20 [53]
[WH]-[0.27]-[4.5]-[6]-[#1]*	6.30 [30]	8.38 [40]	10.80 [52]
[WG]-[0.42]-[4.5]-[6]-[#1]	11.00 [53]	11.52 [55]	12.30 [59]
[WH]-[0.42]-[4.5]-[6]-[#1]	8.40 [40]	8.98 [43]	11.10 [53]
[WG]-[0.27]-[4.5]-[6]-[#1] with VMA	9.20 [44]	10.43 [50]	11.50 [55]
[WH]-[0.27]-[4.5]-[6]-[#1] with VMA	6.40 [31]	7.22 [34]	8.40 [40]
[WG]-[0.42]-[4.5]-[6]-[#1] with VMA	9.30 [44]	11.48 [55]	13.10 [63]
[WH]-[0.42]-[4.5]-[6]-[#1] with VMA	7.30 [35]	9.17 [44]	12.50 [60]

*[WH]-[0.27]-[4.5]-[6]-[#1] no VMA pour includes only 5 TL values (not 6 TL values), since there was cracking at one end.

Table 39 Percentage variation in avg. TL due to presence of VMA in concrete mix

Pour Identity	Percentage reduction in Transfer Length from "prisms cast no VMA concrete mix" to "prisms cast with VMA concrete mix"
[WG]-[0.27]-[4.5]-[6]-[#1] [variable]	-14.0%
[WH]-[0.27]-[4.5]-[6]-[#1] [variable]	13.8%
[WG]-[0.42]-[4.5]-[6]-[#1] [variable]	0.3%
[WH]-[0.42]-[4.5]-[6]-[#1] [variable]	-2.1%

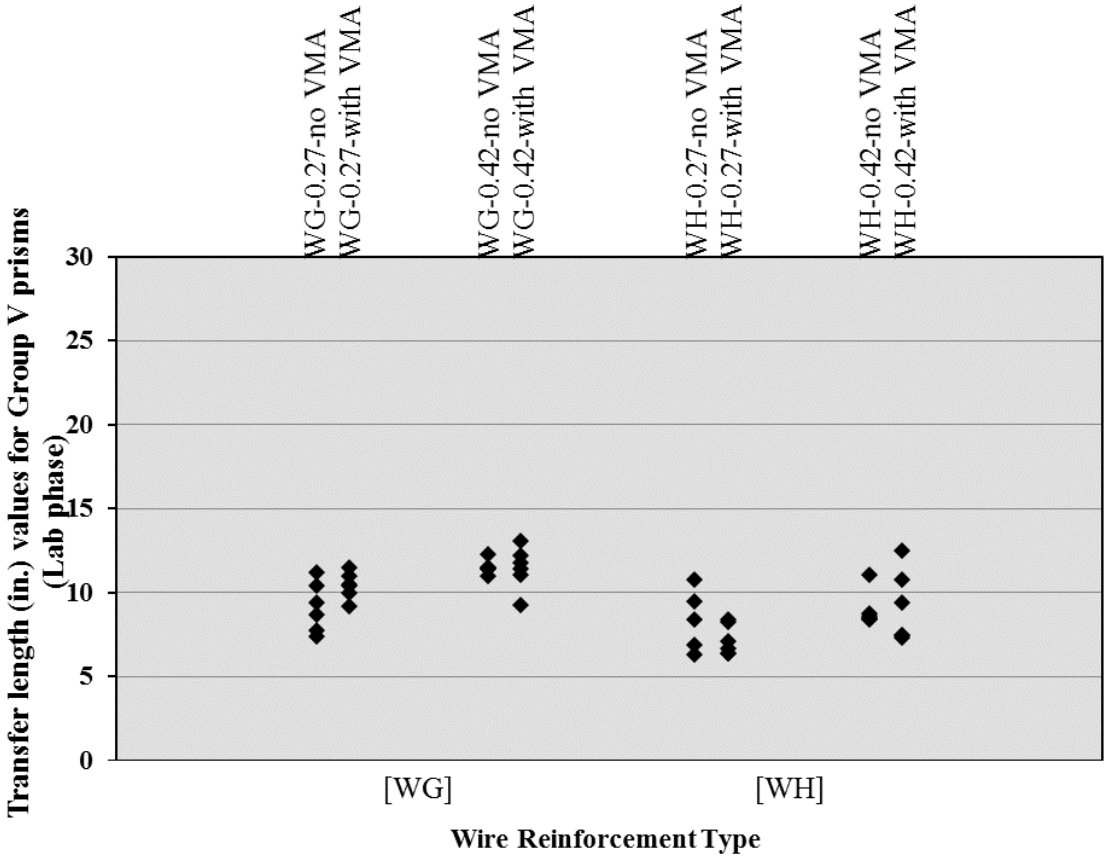

Figure 61 Transfer length results for Group V prisms

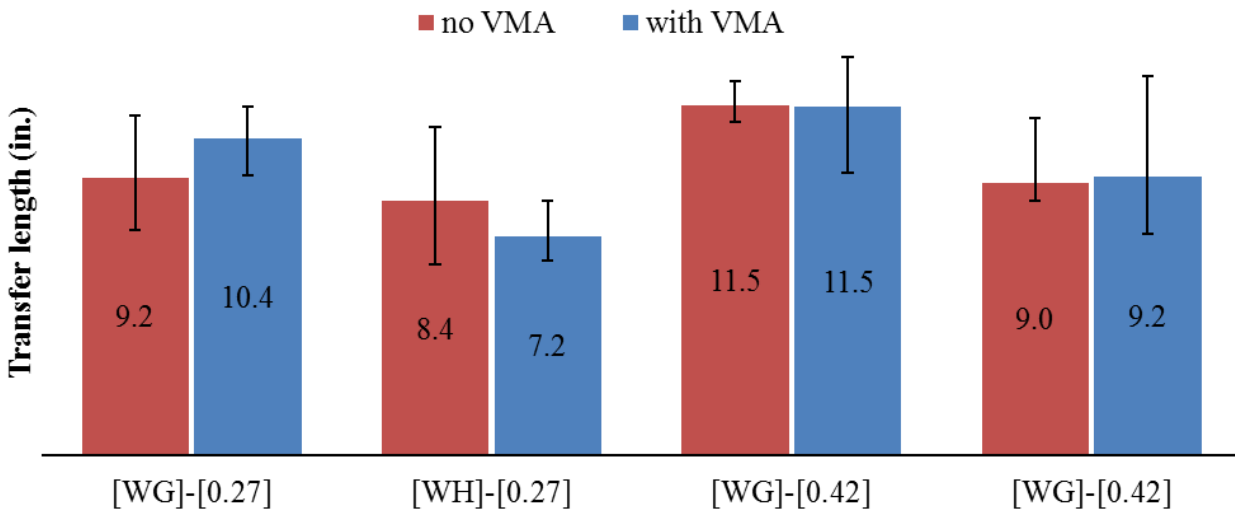

Figure 62 Average transfer lengths for companion prisms with and without VMA (in inches)

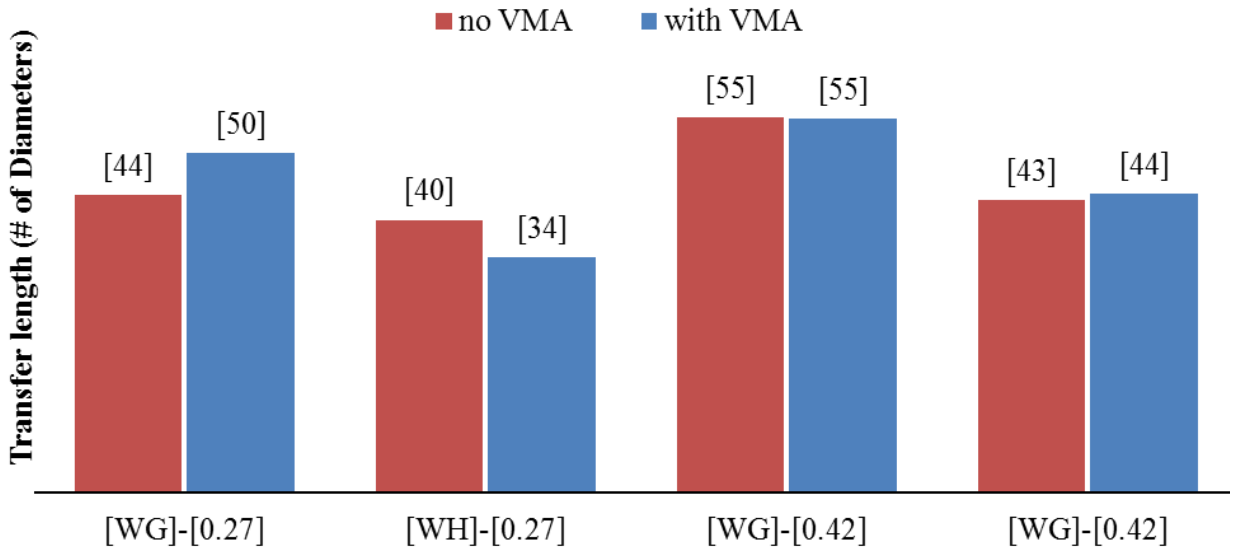

Figure 63 Average transfer lengths for companion prisms with and without VMA (in # of reinforcement diameters)

5.7 Effect of change in source of course aggregate on transfer length (Group VI prisms)

Twelve additional prisms (four pours) were cast to evaluate the effect of changes in course aggregate on transfer length. Prisms were poured with Mix-Design #1 and transfer length results were obtained. Later, these TL results are compared with companion (similar prestressing and concrete variables cast with Mix-Design #2) prism TL results. Average transfer lengths for prisms cast for Group VI testing are presented and discussed in this section. Nomenclature for various prisms utilized in this Group VI are tabulated in Table 40.

Table 40 Nomenclature for prisms utilized in Group VI

Nomenclature for the Prisms utilized in Group VI	
Mix-Design #1	Mix-Design #2
[WG]-[0.27]-[4.5]-[6]-[#1]	[WG]-[0.27]-[4.5]-[6]-[#2]
[WH]-[0.27]-[4.5]-[6]-[#1]	[WH]-[0.27]-[4.5]-[6]-[#2]
[WG]-[0.42]-[4.5]-[6]-[#1]	[WG]-[0.42]-[4.5]-[6]-[#2]
[WH]-[0.42]-[4.5]-[6]-[#1]	[WH]-[0.42]-[4.5]-[6]-[#2]

The minimum, average, and maximum transfer length results for Group VI prisms cast with Mix-Design #1 and Mix-Design #2, respectively, are tabulated in Table 41. A plot showing individual transfer length measurements for all Group VI prisms is presented in Figure 65. All transfer length results were obtained using the procedure described in Section 4.4.2.

These same average transfer lengths values, and corresponding ranges, are shown in bar-chart format in Figure 66. TL results in terms of "number of diameters (d_b)" are represented in Figure 67.

From the Figure 66 (or Figure 67), a significant reduction in TL is observed in the case of prisms cast with [WG] wire reinforcement and Mix-Design #2. However, prisms cast with Mix-Design #2 and [WH] wire resulted in severe longitudinal splitting along the wire lines upon prestress transfer (Figure 64). Hence, TL results could not be obtained for these prisms.

Figure 64 Severe longitudinal splitting occurred along the [WH] wires in prisms cast with Mix-Design #2

From these results, it is evident that short transfer lengths are not the only priority required to produce structurally-sound pre-tensioned concrete ties. Throughout the study, prisms cast with [WH] produced consistently lower TL results compared to prisms cast with [WG]. However, prisms cast with the combination of [WH] wire and Mix-Design #2 resulted in severe splitting in all 6 prisms evaluated (3 with w/c = 0.27 and 3 with w/c = 0.42). Note, prisms cast with [WH] wire and Mix Design #1 had splitting cracks in three other instances during Lab-Phase. Hence, in order for pretensioned concrete tie producers to determine the overall performance associated with a given set of variables (wires and concrete mixture design), prior tests on small-scale pre-tensioned laboratory prisms may provide valuable insight and is recommended.

Percent reduction in average transfer length results of prisms cast with different mix proportions are tabulated in Table 42. In Table 42, positive numbers indicate the reduction in transfer length. Variation in transfer length results for pour identities [WG]-[0.27]-[4.5]-[6] and [WH]-[0.42]-[4.5]-[6] are 18.4% and 29.9% respectively.

Table 41 Transfer length results from Group VI testing (effect course aggregate type)

Pour Identity	Transfer Lengths		
	Min., in. [TL/d_b]	Avg., in. [TL/d_b]	Max., in. [TL/d_b]
[WG]-[0.27]-[4.5]-[6]-[#1]	7.40	9.15	11.20
	[35]	[44]	[53]
[WH]-[0.27]-[4.5]-[6]-[#1]*	6.30	8.38	10.80
	[30]	[40]	[52]
[WG]-[0.42]-[4.5]-[6]-[#1]	11.00	11.52	12.30
	[53]	[55]	[59]
[WH]-[0.42]-[4.5]-[6]-[#1]	8.40	8.98	11.10
	[40]	[43]	[53]
[WG]-[0.27]-[4.5]-[6]-[#2]	6.50	7.47	9.30
	[31]	[36]	[44]
[WH]-[0.27]-[4.5]-[6]-[#2]	Cracked		
[WG]-[0.42]-[4.5]-[6]-[#2]	6.40	8.08	11.20
	[31]	[39]	[53]
[WH]-[0.42]-[4.5]-[6]-[#2]	Cracked		

*[WH]-[0.27]-[4.5]-[6]-[#1] pour includes only 5 TL values (not 6 TL values), since there was cracking at one end.

Table 42 Percentage variation in average TL due to changes in course aggregate

Pour Identities	% Reduction in Transfer Length (from "prisms cast Mix-Design #1" to "prisms cast with Mix-Design #2")
[WG]-[0.27]-[4.5]-[6]	18.4%
[WH]-[0.27]-[4.5]-[6]	NA
[WG]-[0.42]-[4.5]-[6]	29.9%
[WH]-[0.42]-[4.5]-[6]	NA

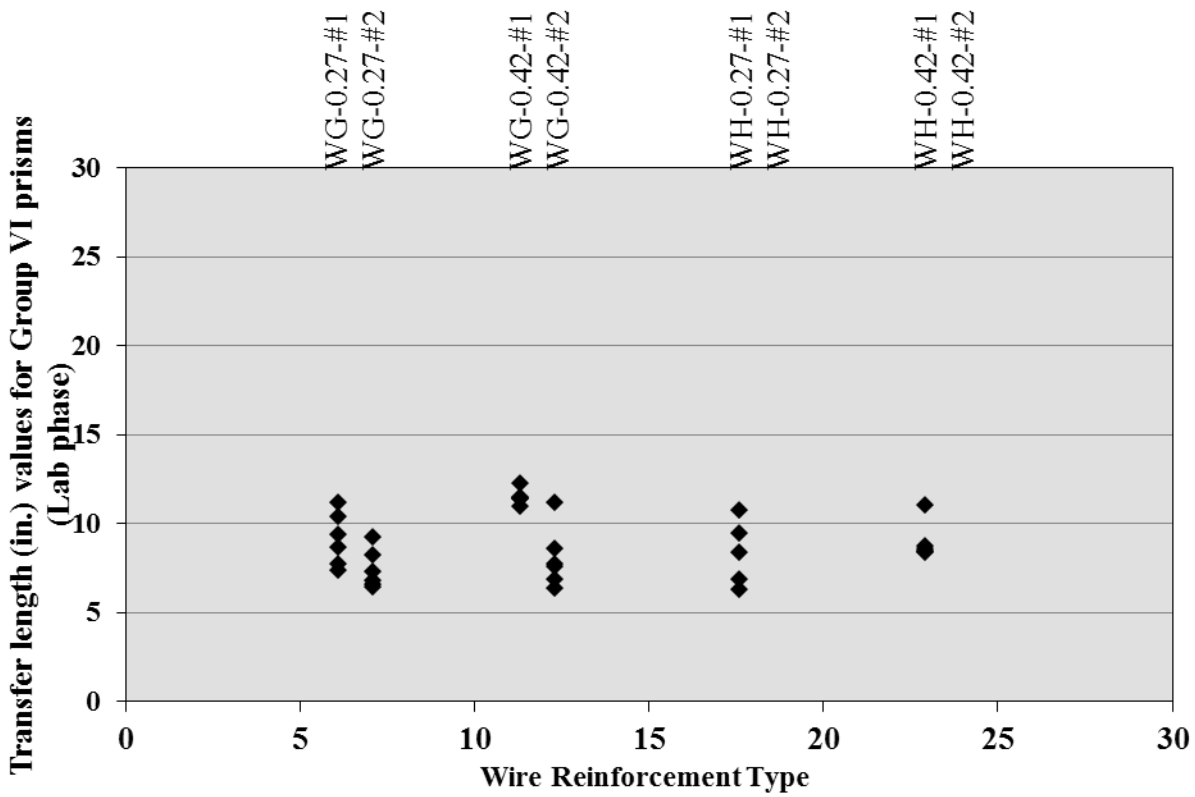

Figure 65 Transfer length results for Group VI prisms

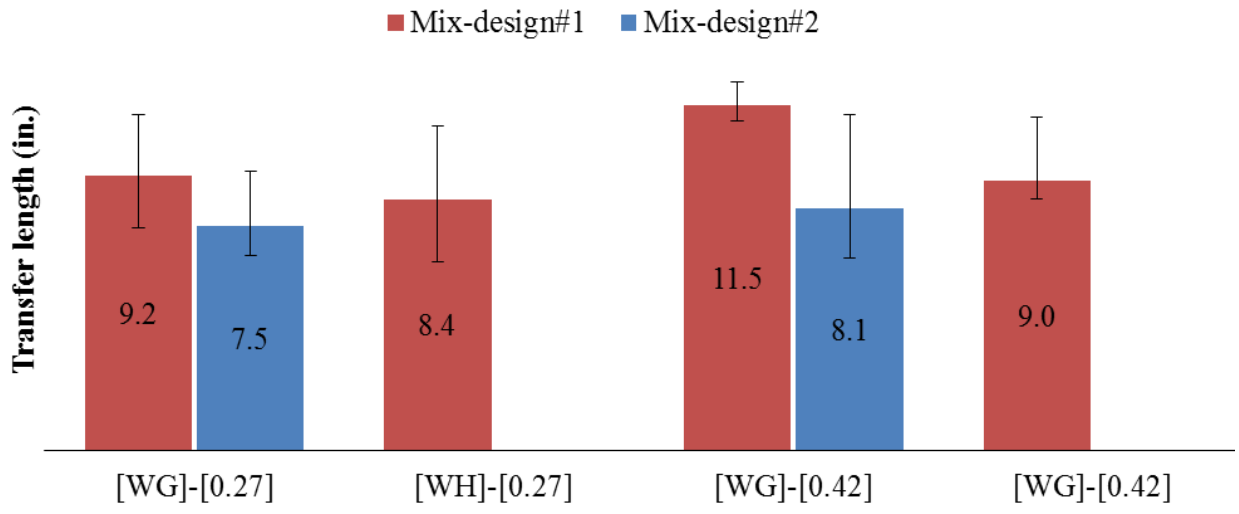

Figure 66 Average transfer lengths for mixtures with different coarse aggregates (in inches)

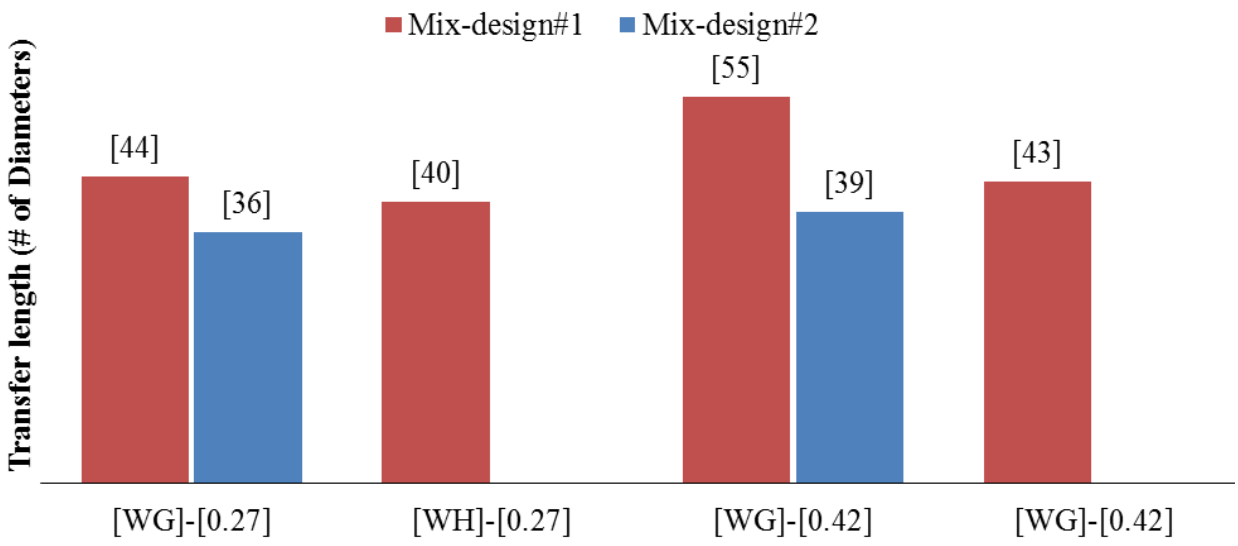

Figure 67 Average transfer lengths for mixtures with different coarse aggregates (TL in # of reinforcement diameters)

5.8 Development of model to predict transfer length

Based on results from Lab-Phase prisms, a transfer length prediction model is developed in this section. During the Lab-Phase, predominant variables affecting transfer length were identifies as the individual wire type (presumably due to indent geometry) and release strength of the concrete.

5.8.1 Bond characteristics of the prestressing reinforcement (Arnold, 2013)

Along with the present research, simultaneous research (Arnold, 2013) was conducted to determine the bond characteristics of the same prestressing reinforcement. Un-tensioned pullout tests were performed during this research. Bond characteristics obtained from this research are utilized here in the development of the predictive model. The authors (Arnold, 2013), conducted both force-controlled and displacement-controlled pullout test methods before finalizing the recommended test method. Similar results obtained in both methods and the Arnold chose force-controlled method to perform the pullout tests.

This same method was subsequently adopted as ASTM A1096 (2015) in 2015. ASTM A1096 section 4.3 states:

> *The maximum pullout force occurring at an end slip less than or equal to 0.10 in. [2.5 mm] is recorded as the "test result." One complete test is comprised of the average of these six specimens.*

These TL results (from the authors of this current report) were statistically correlated with the pullout tests results (Arnold, 2013) and represent the bond characteristics of the same reinforcements. Hence, these maximum pullout force at end slip ≤ 0.10 in. results are incorporated in the present model. In Table 43 (reprinted Table 4.7 from Arnold), average pullout force for WM is not listed. However, the result is available in the same Report and is equal to 6879 lb. (Arnold, 2013).

Table 43 Avg. maximum pullout force at end slip ≤ 0.10 in. (reprinted Table 4.7) [after (Arnold, 2013)]

As-Received Pullout Test Results 4 in. Diameter, 6 in. Bond Length, Ottawa Sand Maximum Pullout Force				
Wire	Avg. Pullout Force (lbf)	Std. Dev. (lbf)	C.V. (%)	Transfer Length (in.)
[WA]	487	42	8.7	16.3
[WB]	6481	570	8.8	11.6
[WC]	7646	967	12.6	8.8
[WD]	5555	357	6.4	11.1
[WE]	7674	526	6.9	7.4
[WF]	8312	459	5.5	8.5
[WG]	5505	385	7.0	11.8
[WH]	7605	497	6.5	7.5
[WI]	6567	522	8.0	10.1
[WJ]	7034	635	9.0	9.0
[WK]	3447	354	10.3	14.0
[WL]	2068	322	15.6	18.7

Note: Sample Size = 6

Arnold performed an initial correlation with transfer-lengths from Group I prisms (Mix-Design #1, w/c = 0.32, 6”-slump, and release strength at 4500 psi) in this current report and developed the predictive relationship:

$$\boldsymbol{TL} = -\mathbf{0.0016}(\boldsymbol{Max\ Force}) + \mathbf{20.9} \qquad \text{Equation 4.1 from Arnold}$$

Where: TL = expected transfer length (in inches) for prisms detensioned at 4500 psi

Max Force = maximum pullout force with an end-slip ≤ 0.10 in.

However, now that the test method has been adopted as ASTM A1096, this same expression may be re-written in terms of the ASTM A1096 pullout value:

$$TL = \left[20.9 - \frac{(A1096\ value)}{625}\right] \quad \text{in inches for 4500 psi release strength}$$

5.8.2 Transfer Length Model for Variable Release Strengths

A model was developed by incorporating the predominant factors affecting the transfer length in the case of prisms cast with wire reinforcements. Variables considered in this model were: wire type (represented by ASTM A1096 pullout value) and concrete release strength. A multiple linear regression process was used to develop the TL prediction model in Microsoft excel 2013. A total of 23 experimental data sets were available, based on the data from Group I and Group II prisms. Table 44 lists the data sets utilized to create the statistical best-fit model.

Table 44 Data sets used to create transfer length prediction model

	Wire Type	Release Strength (f'_{ci}) (psi)	Transfer Length (Inches)	ASTM A1096 Value (pounds)
Nominally 3500 psi	WA	3741	21.4	487
	WE	3486	10.5	7674
	WG	3561	13.8	5505
	WH	3614	10.18	7605
	WK	3528	17.7	3447
Nominally 6000 psi	WA	6128	13.5	487
	WE	6020	7.1	7674
	WG	5825	9.8	5505
	WH	6059	7.3	7605
	WK	5857	11.1	3447
Nominally 4500 psi	WA	4664	16.33	487
	WB	4453	11.6	6481
	WC	4701	8.85	7646
	WD	4400	11.08	5555
	WE	4650	7.43	7674
	WF	4466	8.45	8312
	WG	4697	11.78	5505
	WH	4695	7.5	7605
	WI	4547	10.1	6567
	WJ	4521	9.02	7034
	WK	4572	14	3447
	WL	4476	18.73	2068
	WM	4506	9.83	6879

The data sets in Table 44 were first plotted and best-fit curves were determined for data within each targeted release-strength group (3500 psi, 4500 psi, and 6000 psi). The resulting data and best-fit lines are shown in Figure 68.

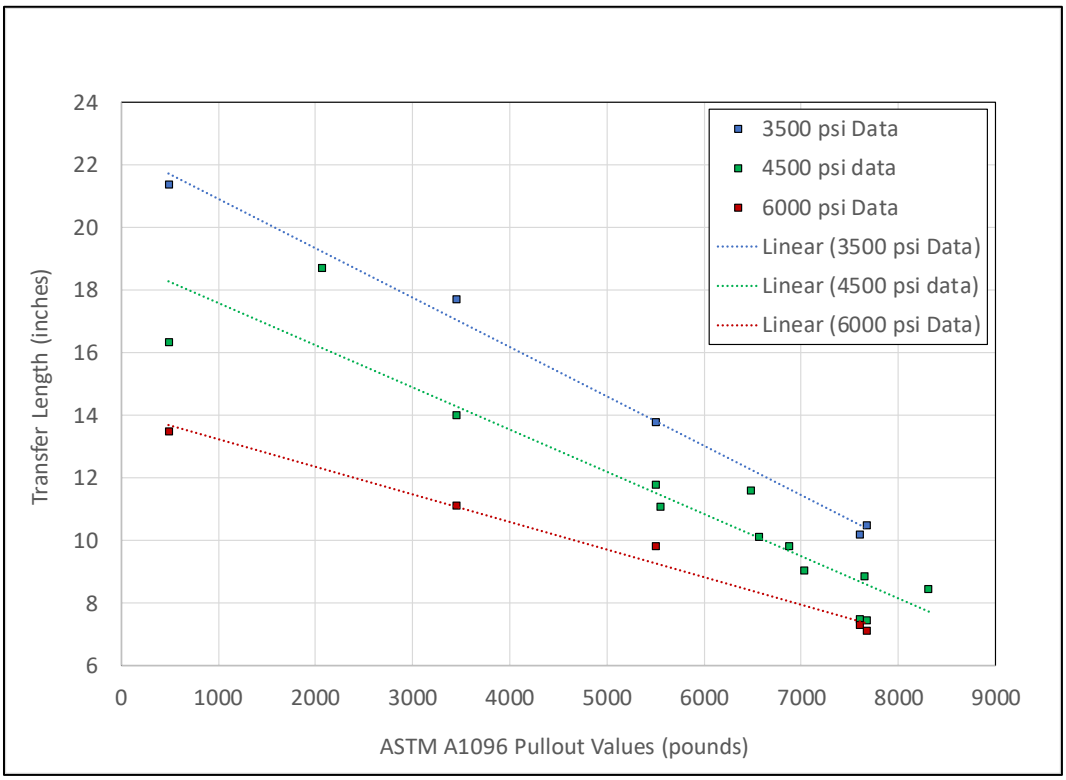

Figure 68 Best fit lines drawn through three data sets

From this figure, both the intercept and slope of the best-fit lines depend on the release strength. Next, the corresponding three intercept-values were plotted versus the release strength, and a best-fit linear expression was developed. Finally, the corresponding three slope-values were plotted versus the release strength, and a best-fit 2nd order expression was developed. The numerical coefficients were then rounded slightly to produce the simplified expression:

$$TL = 34.2 - \frac{f'_{ci}}{300} - \frac{(A1096\ value)}{\left[1250 - f'_{ci}\left(0.4 - \frac{f'_{ci}}{16{,}000}\right)\right]} \quad \text{where}$$

TL = Transfer length in inches

f'_{ci} = Concrete compressive strength at de-tensioning in psi

A1096 value = ASTM A1096 pullout value (6-specimen average) in pounds

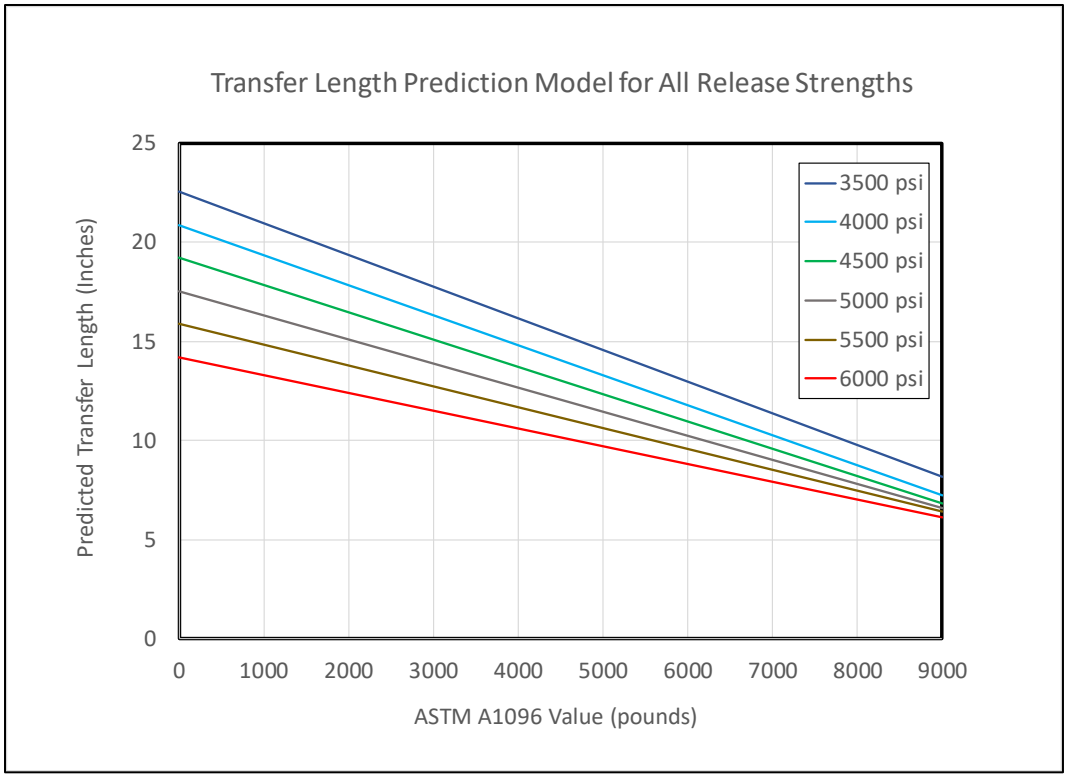

Figure 69 Transfer length prediction model for different release strengths

5.8.2.1 Experimental TL vs predicted TL

Predicted TL results from individual pours were calculated and tabulated in Table 45, along with the absolute difference between experimental TL and predicted TL. In this table, the average absolute difference is 0.60 in., with the maximum absolute difference of 2.36 in. occurring for prisms with wire [WL] and 4500 psi nominal release strength. The comparison of actual and predicted transfer lengths is presented in Figure 70. From this figure, the coefficient of determination, R^2, is 0.954 which indicated excellent correlation between the TL prediction model and experimental results, Note, the data used to develop the model pertained to concrete compressive strength at release that varied between 3486 psi and 6128 psi.

Table 45 Comparison of average transfer length and predicted transfer length

	Wire Type	Release Strength (f'_{ci}) (psi)	Average Transfer Length (Inches)	ASTM A1096 Value (pounds)	Predicted Transfer Length (inches)	Absolute Difference (inches)
Nominally 3500 psi	WA	3741	21.4	487	21.0	0.45
	WE	3486	10.5	7674	10.1	0.40
	WG	3561	13.8	5505	13.4	0.38
	WH	3614	10.18	7605	9.9	0.28
	WK	3528	17.7	3447	16.9	0.85
Nominally 6000 psi	WA	6128	13.5	487	13.3	0.15
	WE	6020	7.1	7674	7.2	0.10
	WG	5825	9.8	5505	9.5	0.31
	WH	6059	7.3	7605	7.2	0.08
	WK	5857	11.1	3447	11.4	0.30
Nominally 4500 psi	WA	4664	16.33	487	18.0	1.67
	WB	4453	11.6	6481	10.2	1.40
	WC	4701	8.85	7646	8.3	0.50
	WD	4400	11.08	5555	11.6	0.52
	WE	4650	7.43	7674	8.3	0.92
	WF	4466	8.45	8312	7.6	0.84
	WG	4697	11.78	5505	11.2	0.58
	WH	4695	7.5	7605	8.4	0.91
	WI	4547	10.1	6567	10.0	0.13
	WJ	4521	9.02	7034	9.3	0.33
	WK	4572	14	3447	14.2	0.22
	WL	4476	18.73	2068	16.4	2.36
	WM	4506	9.83	6879	9.6	0.25

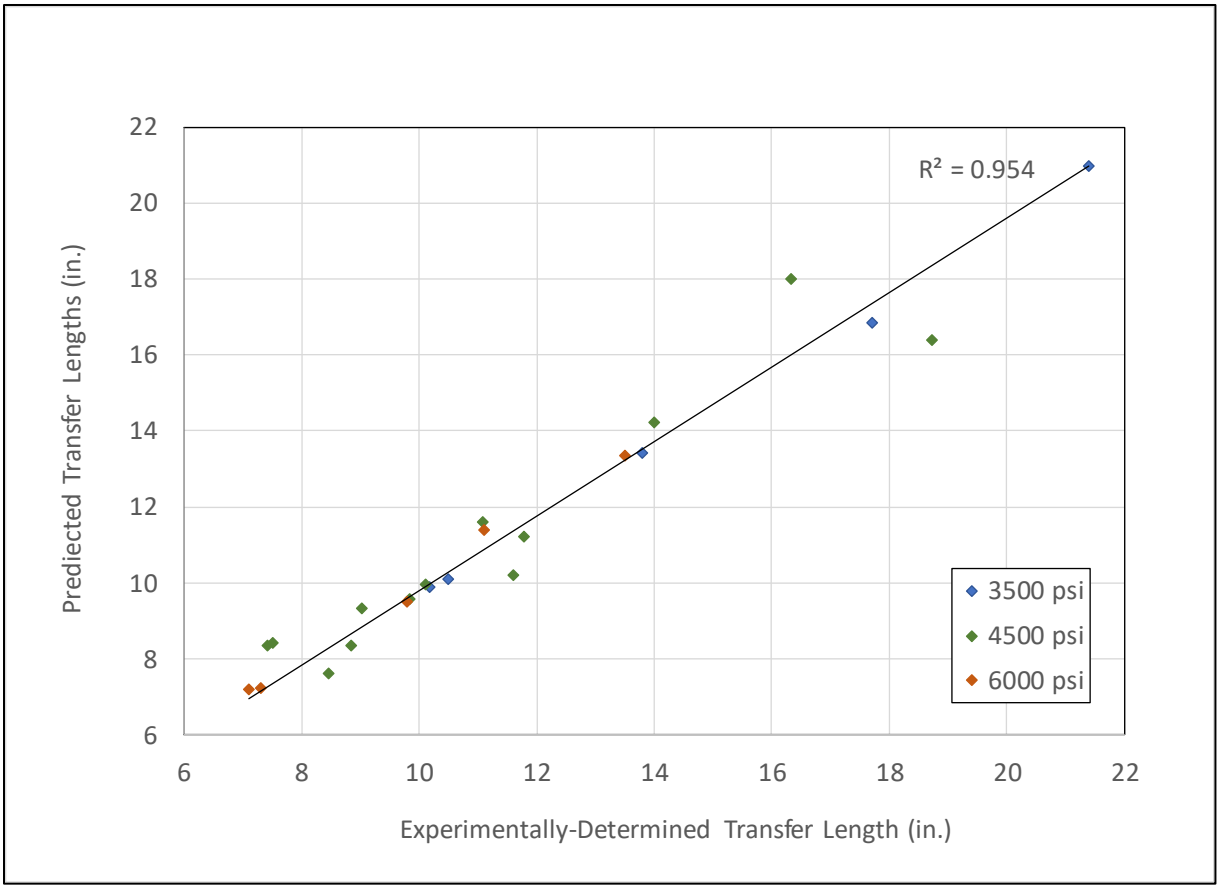

Figure 70 Comparison of actual and predicted transfer lengths

Chapter 6 Experimental procedure during Plant-Phase

This chapter presents the experimental setup employed at the LB Foster/CXT concrete tie manufacturing plant in Tucson, AZ., and two testing procedures used to obtain concrete surface strains for use in the determination of transfer lengths. The onsite work in Tucson, AZ during the Plant-Phase of this project was conducted in January 2013.

During the Plant-Phase of the project, series of tests were conducted on concrete railroad ties manufactured with fifteen (15) different reinforcement types at the PCI-certified concrete tie manufacturing plant. These reinforcements had been stored in a low-humidity environment since the start of the project and were essentially still in the "as-received" condition when the concrete ties were manufactured in January 2013. Figure 9 shows the reinforcement storage containers used to store Plant-Phase reinforcement. Large desiccant bags were hung inside these (Figure 9) storage containers.

All pretensioned concrete ties were fabricated using the same concrete mixture (having a w/c ratio of 0.32), so the primary variable in this portion of the study was the prestressing reinforcement type. Fifty transfer-length measurements were attempted for each reinforcement type, for a combined total of approximately 750 transfer lengths. Later, two of the crossties with each reinforcement type were subjected to in-track loading, while two companion ties (that were not subjected to any loading) were monitored for comparison.

The pretensioned concrete crossties produced at the CXT concrete tie plant had a 102-inch (8'-6") length and were model 505S. These crossties had a variable cross-section with symmetry about the mid-length of the tie. Figure 71 shows various views of the crossties.

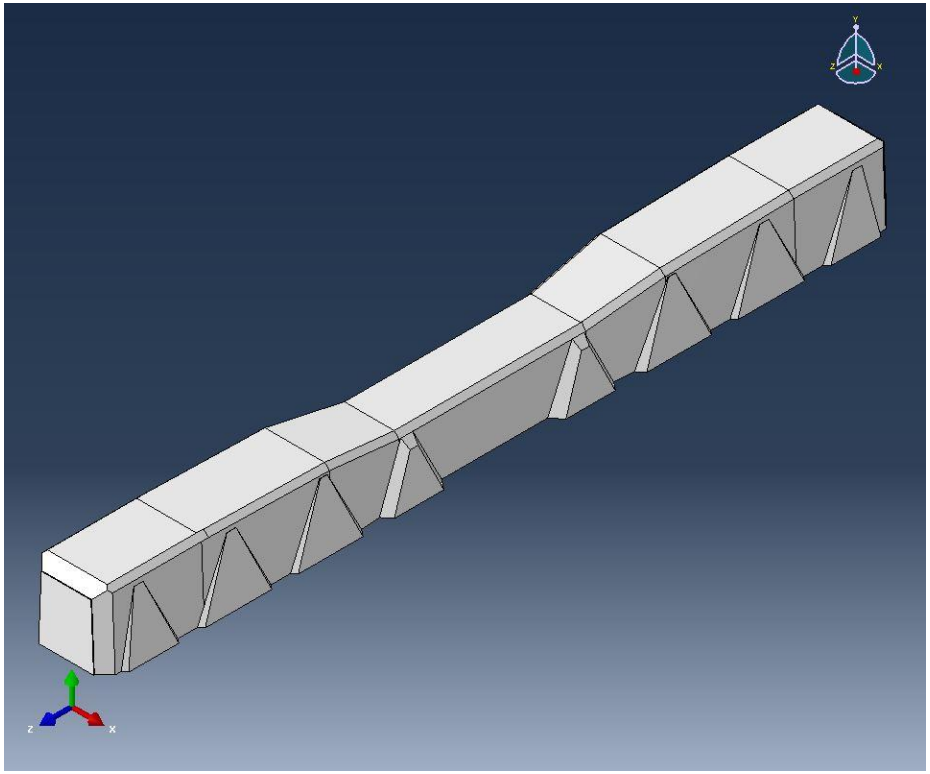

(a)

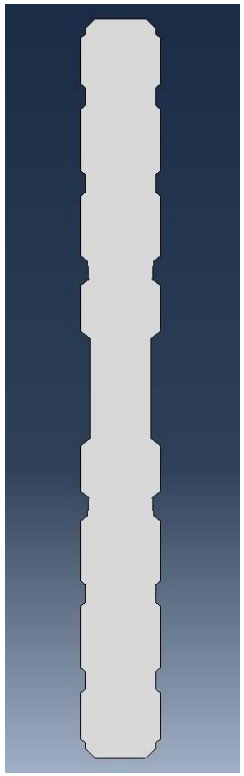

(b)

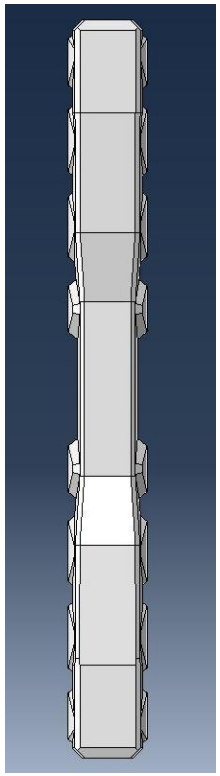

(c)

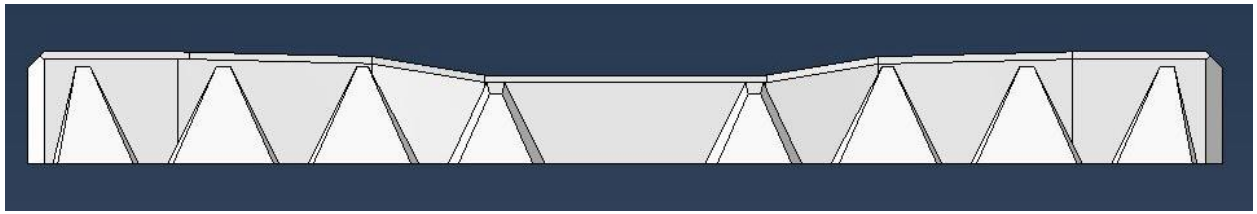

(d)

Figure 71 Different views of a typical CXT concrete railroad tie: (a) Isometric view, (b) Bottom view, (c) Top View, (d) Side View

6.1 Reinforcement distribution across the tie cross-sections

Typical design for concrete crossties manufactured at this plant consisted of twenty (20) 5.32-mm-diameter indented wires. The existing reinforcement pattern for the crossties consisted of twenty (20) 5.32-mm-diameter prestressing wires as shown in Figure 72. Figure 72 shows the reinforcement pattern, along with nominal wire positions, at the end of the crosstie.

Intermediate reinforcement supports (custom wire chairs) were used along the bed to maintain the specified wire pattern (or distribution) as shown in Figure 72. Figure 73 shows a custom "chair" used during the manufacturing process to maintain the specified wire pattern. In Figure 73, numbers (1 through 10) represent the location of 5.32-mm diameter wires on one side of the centerline (about the width of cross-section). Similar number of wire locations are present on the other side of centerline.

However, the selected group of 15 reinforcements includes one (1) 5/16-inch-diameter 3-wire strand [SC] and two (2) 3/8-inch-diameter 7-wire strands ([SA] and [SB]) in addition to twelve (12) 5.32-mm-diameter wires. Note, the same forms and therefore the same cross-section was used for all fifteen (15) types of reinforcements (wires and strands). In order to manufacture concrete ties with reinforcements ([SA], [SB], and [SC]) other than the normal 5.32-mm-diameter wires, the following challenges were incurred and successfully overcome:

1. Need to maintain approximately the same total prestressing steel area and prestress force.
2. Need to maintain approximately the same eccentricity of the prestressing reinforcement for similar moment capacities
3. Need to utilize the existing custom wire chairs to maintain the design pattern of other reinforcements.
4. .Need to ensure a symmetric (side-to-side) pattern of the prestressing reinforcement.

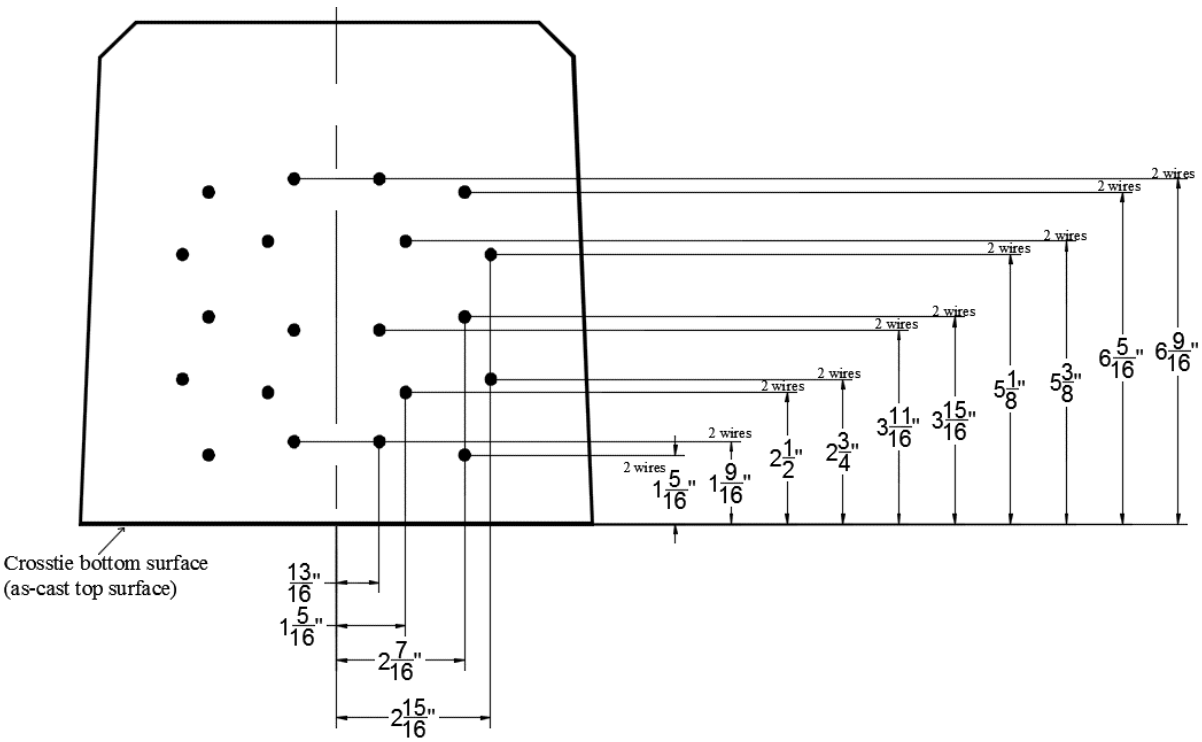

Figure 72 Reinforcement design pattern and nominal position of 5.32-mm-diameter wires (cross-section shown at the end of crosstie)

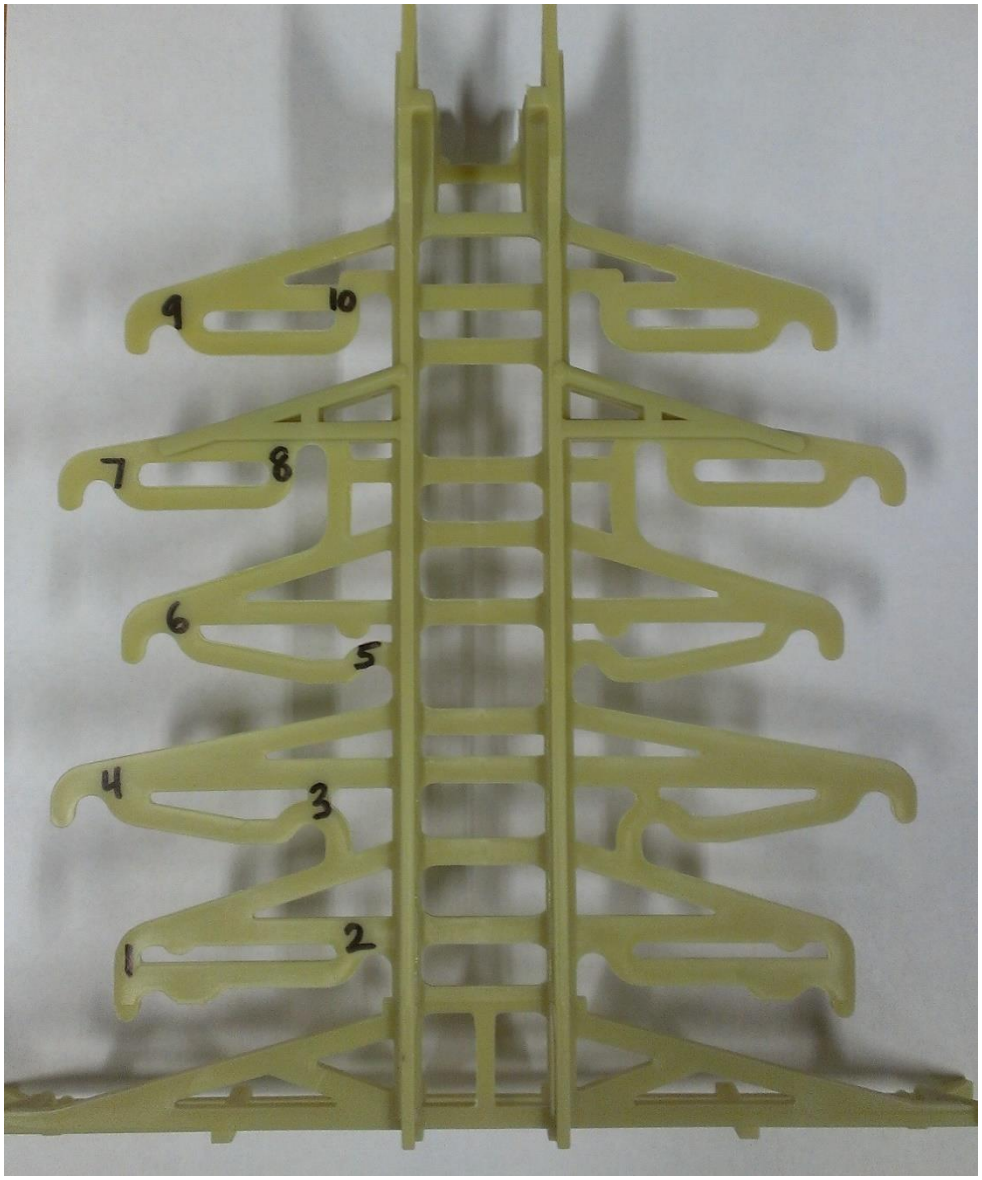

Figure 73 Custom wire chairs to maintain the reinforcement design pattern

6.1.1 Reinforcement pattern for strands

The number of strands used in the manufacture of the crossties was selected so that the total prestressing steel area was approximately equal to the original crosstie designed with twenty (20) 5.32-mm-diameter wires. In the case of 5/16-in.-diameter 3-wire strand [SC], twelve (12) strands were incorporated and for the 3/8-in.-diameter 7-wire strands ([SA] and [SB]), only eight (8) strands per crosstie were used.

Later, the exact patterns for the selected prestressing strands was selected so that the existing custom rebar chairs could be utilized. Additionally, the selected pattern also assured the center of gravity of the prestress force would be approximately equal to the original design.

Since the custom rebar chairs were originally designed for 5.32-mm-diameter wires, larger-diameter strands did not fit properly into the designated areas. Accordingly, a difference in wire centroid at each "chair" position resulted due to the following two factors:

1.) Difference in tendon diameter (wire and strand)

2.) Offset distance between wire seat location and the strand surface (Figure 74).

"Strand centroid offset from wire centroid" values (Figure 75) were calculated to incorporate the above mentioned two variables. It can be observed in Figure 74 that the wire reinforcement theoretically had no offset, whereas the strand reinforcements had offsets between the wire seat location and strand surface. Variable "e" shown in Figure 74 represents the offset distance between wire seat location and the strand surface.

5.32-mm-diameter wire	5/16-in. diameter 3-wire strand	3/8-in. diameter 7-wire strand
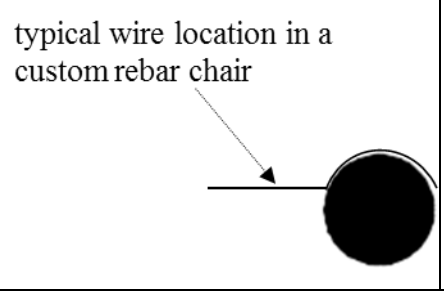	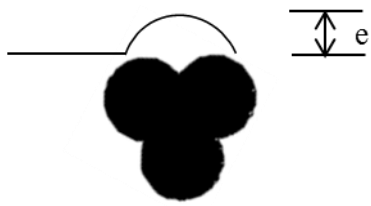	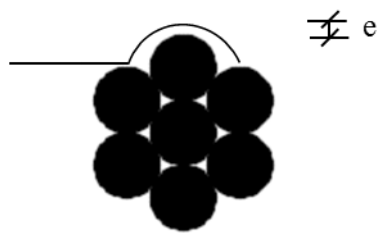
Figure 74 Offset distance between wire seat location and the reinforcement surface		

Prior to casting ties at the Tucson plant, the individual strand centroid at each possible support location on an existing CXT wire "chair" was determined by KSU researcherss. Later, these possible centroid locations were used to determine the nominal locations of the strands so that the same approximate force and centroid would be maintained.

Distance between strand centroid to wire seat	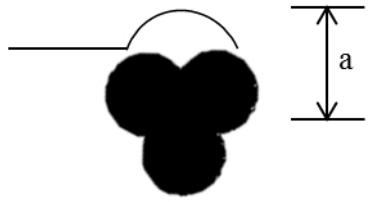	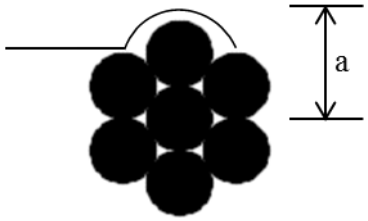
Figure 75 Strand centroid offset from wire centroid		

Figure 76 and Figure 77 show the strand patterns used to fabricate crossties with 5/16-in.-diameter and 3/8-in.-diameter strands, respectively. The strand patterns were selected so that the centroid of strand reinforcement would be approximately the same as the centroid for wire reinforcements. The typical "chair" supporting 5.32-mm-diameter wires is shown in Figure 78. - Figure 79 shows an example of the standard wire chair used with 3/8-in.-diameter 7-wire strands.

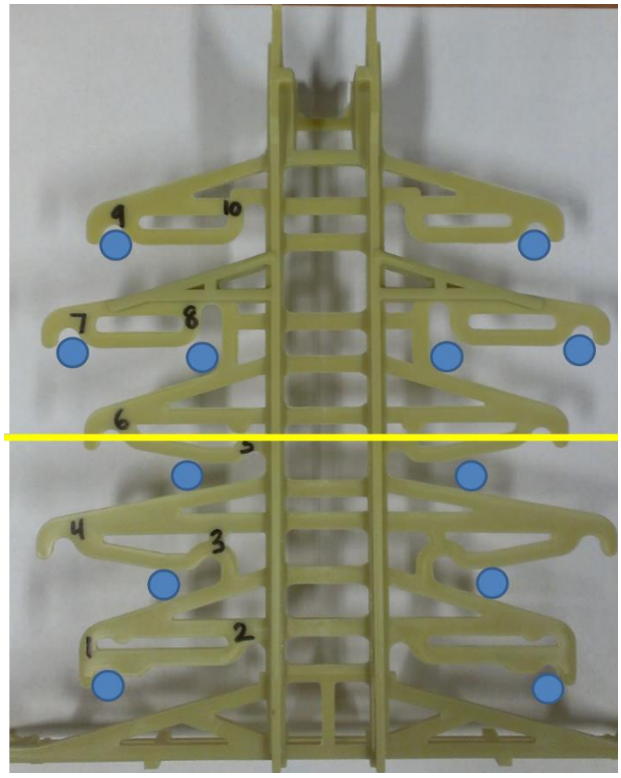

Figure 76 Strand pattern for 5/16-in. diameter 3 wire strand

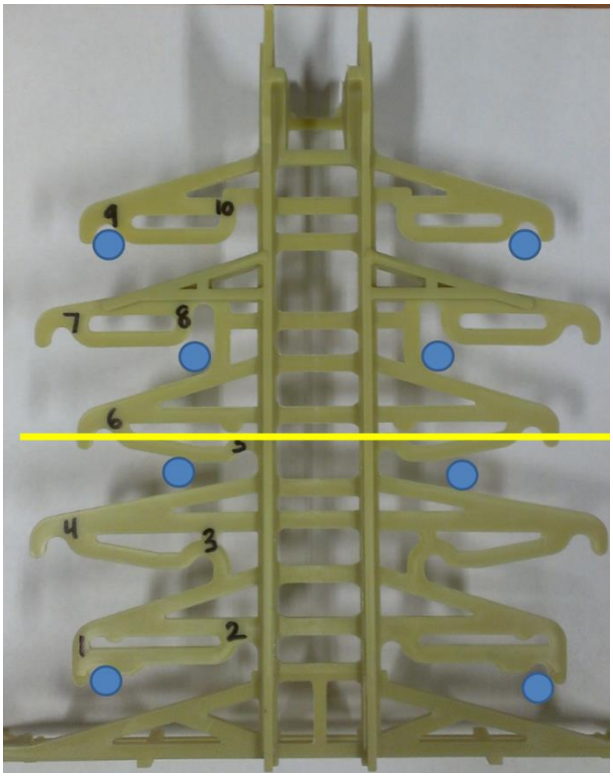

Figure 77 Strand pattern for 3/8-in. diameter 7 wire strand

	
Figure 78 Wire “chair” supporting 5.32-mm. diameter wires	Figure 79 Wire chair used to support 3/8-in.-diameter 7-wire strand

6.1.1.1 Prestressing steel centroids for proposed strand patterns

From Figure 76 and Figure 77, the strand pattern utilized was significantly different from the typical wire pattern. Horizontal line (yellow line) in Figure 76 and Figure 77 represents the calculated prestressing steel centroid. From these two figures, the strand patterns' centroid are approximately the same, and nearly equal to the wire pattern's nominal centroid.

Table 46 lists the calculated individual prestressing steel centroids for wire reinforcements along with total prestressing reinforcement centroid from the bottom surface of crosstie. Whereas, Table 47 and Table 48 presents reinforcement centroid values for 5/16-in. diameter strand pattern and 3/8-in. diameter strand pattern respectively. Figure 80 and Figure 81 shows individual reinforcement eccentricities (rounded to the nearest 1/16-in.) for 5/16-in. diameter strand pattern and 3/8-in. diameter strand pattern respectively. In-plant dead end assembly for various reinforcement patterns are shown in Figure 82 along with theoretical reinforcement pattern.

Table 46 Prestressing steel centroid for existing 5.32 mm diameter wires

n*	Number of wires at each numbered level	d†
10	2	6.5625
9	2	6.3125
8	2	5.3750
7	2	5.1250
6	2	3.9375
5	2	3.6875
4	2	2.7500
3	2	2.5000
2	2	1.5625
1	2	1.3125

*number on custom rebar chair (Figure 73)
†Individual wire centroids from bottom of crosstie (in.) (Figure 72)

Total number of wires = 20
Wire centroid from bottom surface of crosstie ($\overline{y}_{wb}$, in.) = 3.9125 in.

Table 47 Prestressing steel centroid for proposed 5/16 in. diameter 3-wire strand

n*	Strands at each level	a§	c‡	d†
10		0.604	0.499	-
9	2	0.177	0.072	6.240
8	2	0.405	0.300	5.075
7	2	0.189	0.084	5.041
6		0.193	0.088	-
5	2	0.240	0.135	3.552
4		0.212	0.107	-
3	2	0.250	0.145	2.355
2		0.215	0.110	-
1	2	0.174	0.069	1.243

Table 48 Prestressing steel centroid for proposed 3/8 in. diameter 7-wire strands

n*	Strands at each level	a§	c‡	d†
10		0.65	0.55	-
9	2	0.26	0.16	6.157
8	2	0.55	0.45	4.930
7		0.2	0.13	-
6		0.25	0.15	-
5	2	0.29	0.19	3.502
4		0.24	0.14	-
3		0.30	0.20	-
2		0.44	0.34	-
1	2	0.2	0.10	1.217

12	=	Total number of strands	=	8
3.918	=	Strand centroid from bottom surface of crosstie ($\bar{y}_{sb}$, in.)	=	3.952
3.9125	=	Wire centroid from bottom surface of crosstie ($\bar{y}_{wb}$, in.)	=	3.9125
0.0052	=	Difference in centroid location (in.)	=	0.0391
-0.13%	=	Percentage difference	=	-1.00%

*number on custom rebar chair (Figure 73, Figure 76, and Figure 77)

§Distance between strand centroid to wire seat (in.) (Figure 75)

‡Strand centroid offset from wire centroid (c=a-b) (in.) (Figure 75)

†Individual strand centroids from bottom of crosstie at selected pattern locations (in.) (Figure 80, and Figure 81)

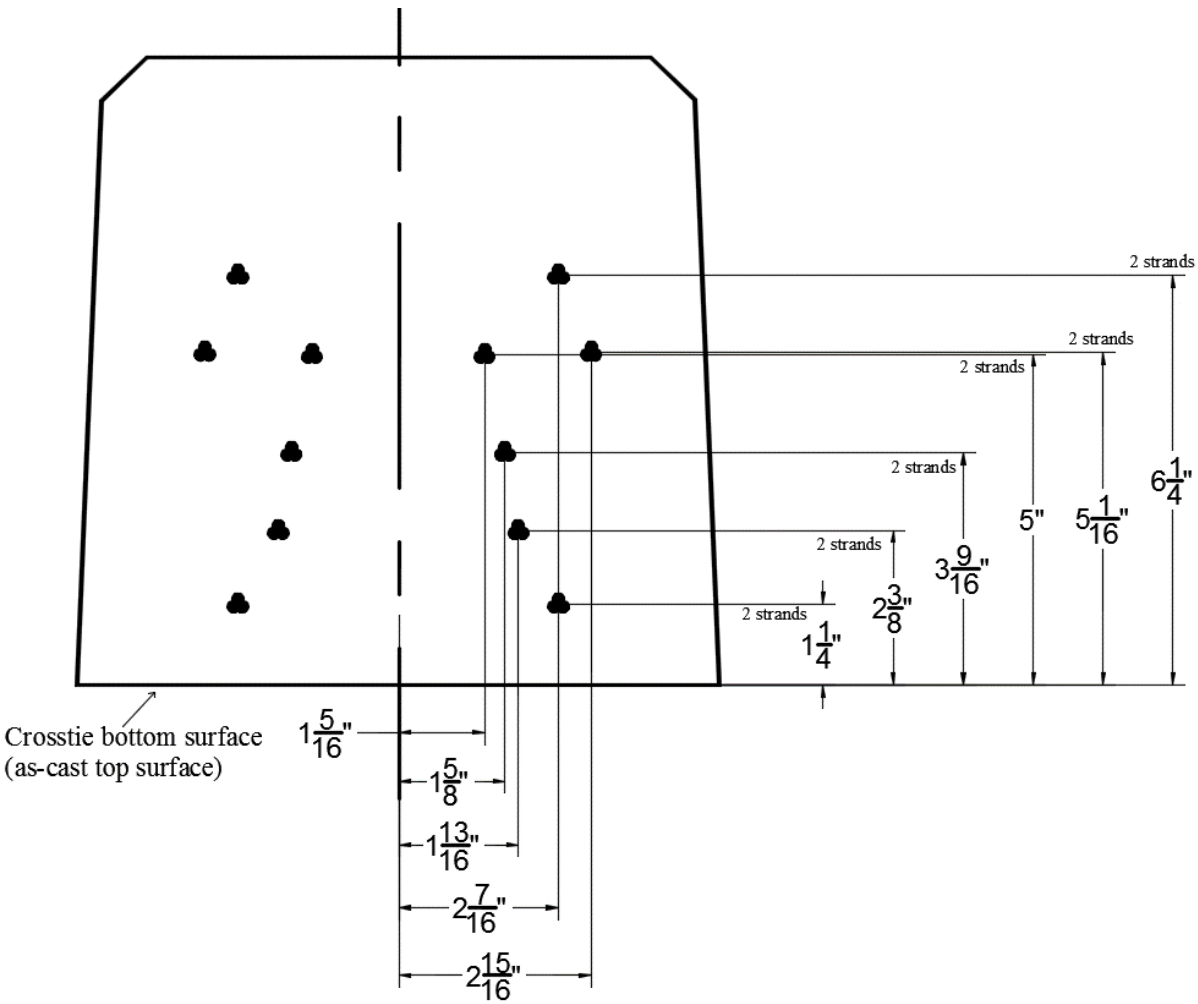

Figure 80 5/16-in. diameter strand pattern and reinforcement eccentricities (cross-section shown at the end of crosstie)

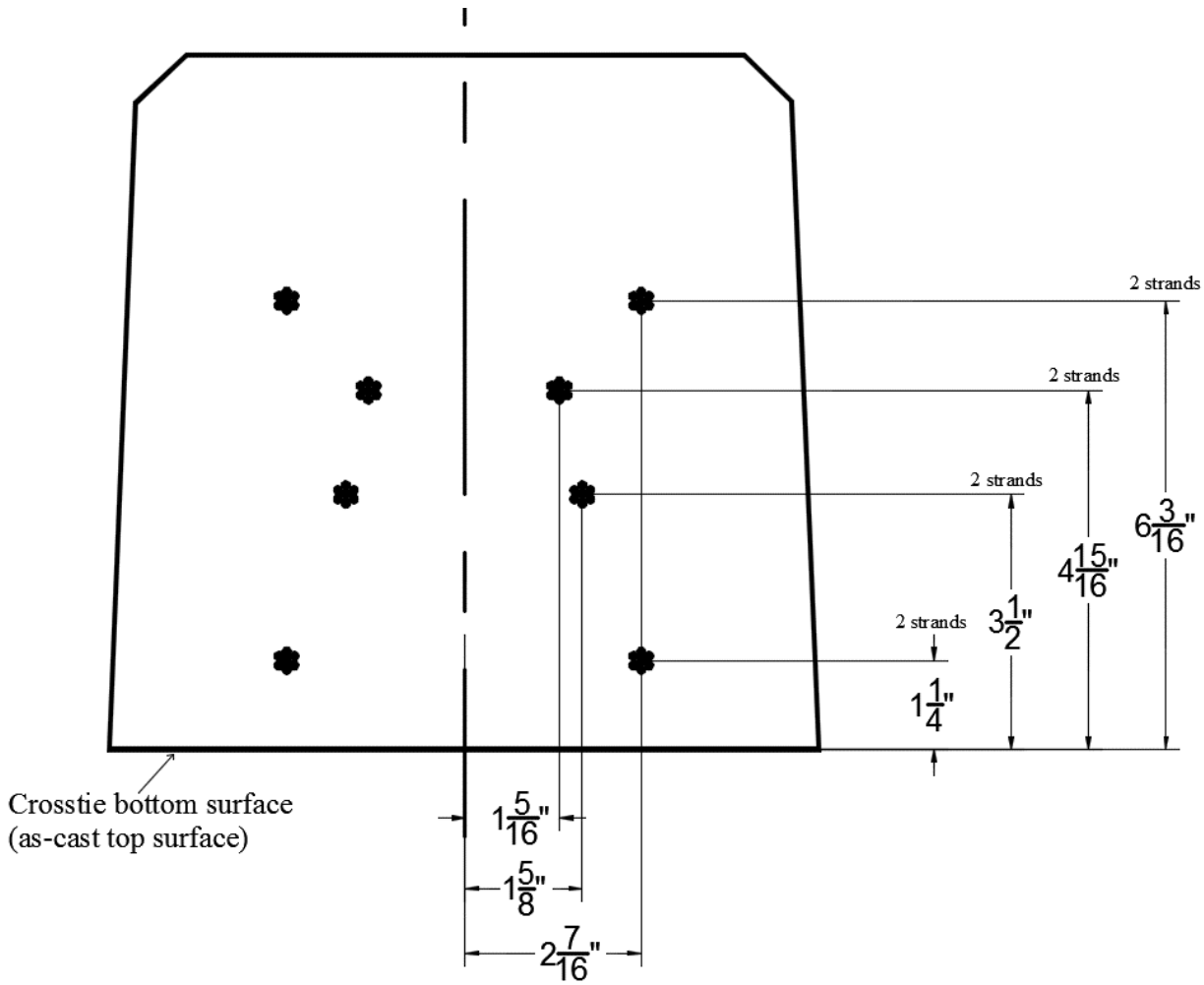

Figure 81 3/8-in. diameter strand pattern and reinforcement eccentricities (cross-section shown at the end of crosstie)

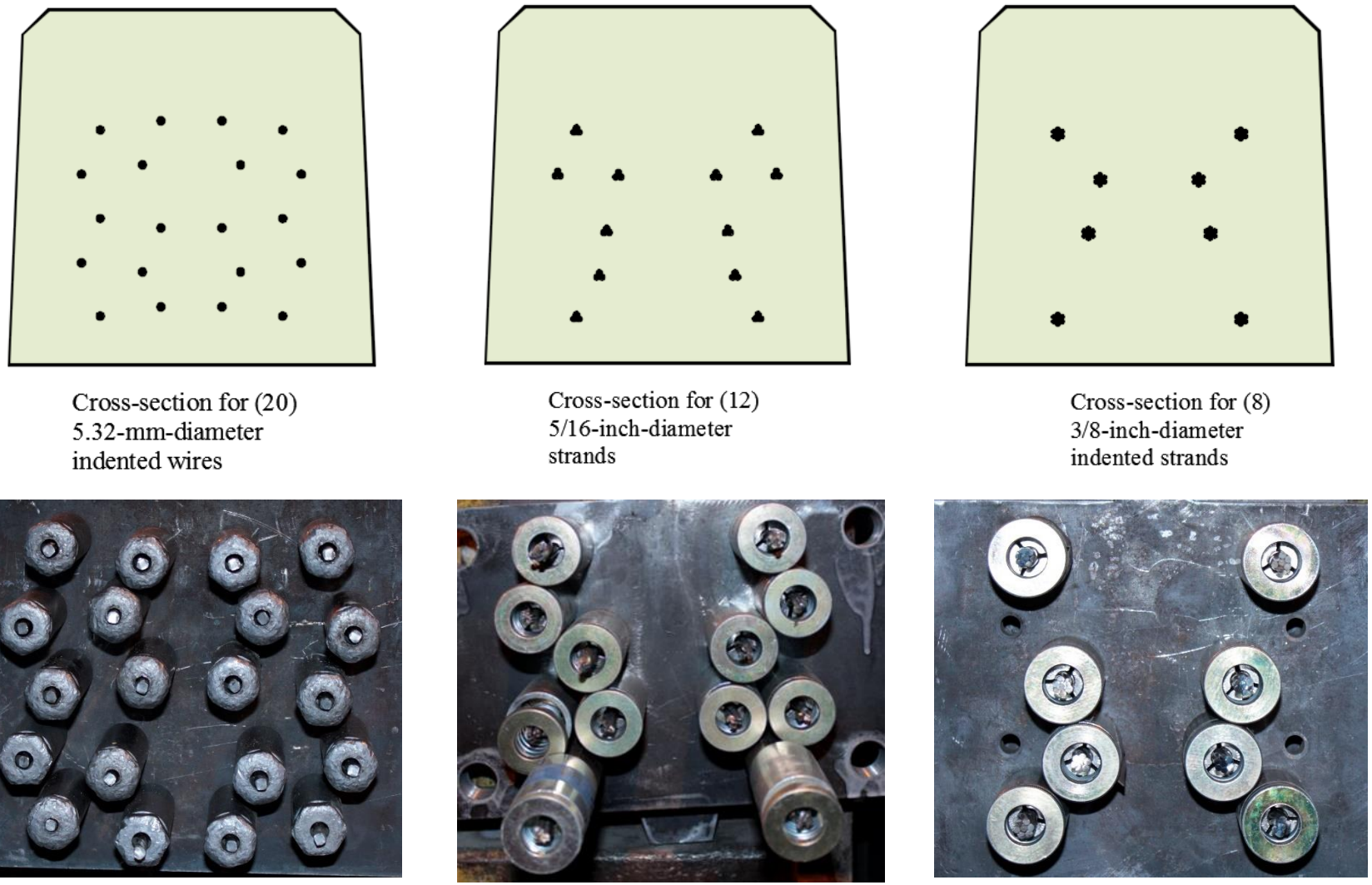

Figure 82 Different reinforcement patterns and tendon anchorages used (cross-sections are at end of crosstie)

6.2 Experimental set-up in Plant-Phase

6.2.1 Prestressing bed and adjusting for different reinforcement stiffness

Pre-tensioned concrete railroad ties with the 15 different reinforcements in this project were fabricated along with ties containing the tie manufacturer's standard indented wires in the same prestressing bed. Each of the prestressing beds at the CXT plant in Tucson, AZ had four cavities and was 385.75 ft. long. Each bed could produce a total of 180 crossties at a time (4 cavities wide x 45 crossties long).

During the Plant-Phase of this project, cavities of a given prestressing bed consisted of both regular crossties which were manufactured with standard 5.32-mm-diameter wires and research crossties that were fabricated with the special project reinforcements. In all cases, the research crossties were fabricated in one or two outer cavities of the prestressing bed. This is illustrated in Figure 83.

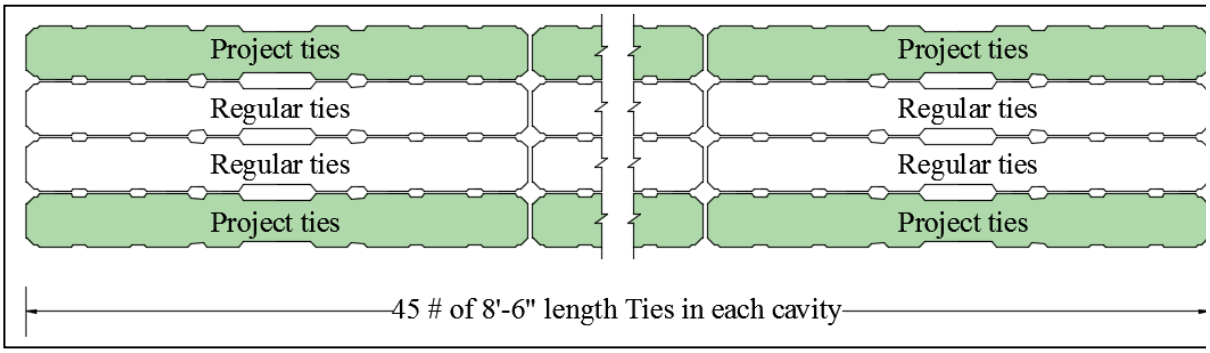

Figure 83 Typical Prestressing bed with four (4) cavities during the Plant-Phase

6.2.2 Prestressing operation for reinforcements with different Modulus of Elasticity (MOE)

One of the key technical challenges during the Plant-Phase was the ability to accommodate prestressing tendons with different elastic stiffness values (MOE-values) in the same prestressing bed, since tensioning of all four cavities was performed with the same hydraulic jacks. The standard jacking procedure at the CXT plant consisted of first systematically removing the slack from all 80 wires (20 wires x 4 cavities) and then group-tensioning all wires simultaneously to the desired pretension force.

The tensioning operation at the CXT plant utilized two hydraulic jacks with equal pressure that were extended (while bearing against a common bulkhead) until the total desired jacking force was achieved. The fact that only two jacks were used to tension four cavities meant that all cavities would have equal elongation, and not necessarily equal force if the wires had different MOE values. The jacking elongation calculations were based on the MOE value of the standard wires being used at the plant (and in the middle two cavities).

This meant that if the special project tendons (wires or strands) had a higher MOE value than the standard CXT wires, the project wires could be over-stressed to an unsafe level while the CXT wires would be under-stressed. Whereas, if the project reinforcements had a lower MOE than the CXT wires, the project strands would be under-tensioned and standard wires could be over-stressed to an unsafe level.

Elongation of prestressing reinforcement during tensioning is a vital factor that is measured in a tie manufacturing company to ensure that proper tensioning has occurred along the prestressing bed length (385.75 ft. in this case). PCI requires the measured elongation to be within 5% of the theoretical computed elongations (MNL-116-99, Fourth edition, 1999).

A strategic approach was adapted to achieve the required elongation of tendons in each cavity and thereby maintain desired stress levels in all reinforcements. Elongation required for each reinforcement type was calculated based on the individual reinforcement's cross-sectional area and MOE value (from manufacturer's data sheets supplied with reinforcements) and shown in Table 49. Note, wire WK was no longer available, so CXT's standard wire [WM] was substituted in this test series. Differences between required elongation for the 15 project reinforcements and the elongation of the standard [WM] wire (31.4-in.) was calculated and is also tabulated in Table 49.

Table 49 Elongation calculations for standard reinforcement (top) and each project reinforcements during Plant-Phase

Targeted jacking force for CXT standard wire [WM], P (lb.) =	7000
number of wires=	20
Total target jacking force (lb.) =	140000
Bed Length, L (in.) =	4629

$$\delta = \frac{PL}{AE} = \frac{(7000\ \text{lbs}) * (4629\ \text{in.})}{(0.0347\ \text{in.}^2) * (29.7 * 10^6\ \text{psi})} = 31.4\ \text{in.}$$

Regular Elongation (in) = 31.4

Reinforcement		Area (in^2)	Modulus of Elasticity, E (x 10^6 psi)	Number of wires/strands used	Elongation, δ (in.)	Difference in Required Elongation	Difference in Required Elongation to Nearest (1/8")
Wire	A	0.0347	29.70	20	31.4	0.0	0
	B	0.0345	30.51	20	30.8	-0.6	- 5/8
	C	0.0341	28.40	20	33.5	2.0	2
	D	0.0352	30.12	20	30.6	-0.9	- 7/8
	E	0.0345	28.57	20	32.9	1.5	1 4/8
	F	0.0345	29.00	20	32.4	1.0	1
	G	0.0346	30.30	20	30.9	-0.5	- 4/8
	H	0.0348	29.87	20	31.2	-0.3	- 2/8
	I	0.0336	29.00	20	33.3	1.8	1 7/8
	J	0.0350	28.60	20	32.3	0.9	7/8
	L	0.0346	29.48	20	31.8	0.4	3/8
Strand	A	0.0850	29.00	8	32.9	1.4	1 3/8
	B	0.0850	29.00	8	32.9	1.4	1 3/8
	C	0.0582	29.00	12	32.0	0.6	4/8

Prior to group-tensioning with the two large hydraulic jacks, the initial slack in each tendon was removed by pulling each wire to approximately 1400 pounds each and then releasing this force. It was during the initial tensioning stage that the elongation differences (Table 49) were compensated with specially-fabricated shim plates. Different shim plate designs were used to accommodate the different reinforcement patterns for the wires and strands. The two different types of shim plates used during the Plant-Phase are shown in Figure 84 and Figure 85. Shim plates like the one shown in Figure 84 were used for wire reinforcements. Whereas, Figure 85 shows the shim plate type that was used for strand reinforcements.

One or multiple shim plates were utilized (depending on the thickness required to ensure correct elongation) in the increments of 1/8-in. Adjustment in elongation was achieved during the initial wire tensioning by using a special jacking plate that had four (4) one-inch-diameter 14 thread-per-inch (TPI) bolts (one in each corner of the end-plate). The jacking plate was located at the dead end of the bed. The shim plates were needed to provide adequate bearing area, since the four (4) screws could not support entire 140,000-pound load. Figure 86 shows these four jacking crews in action.

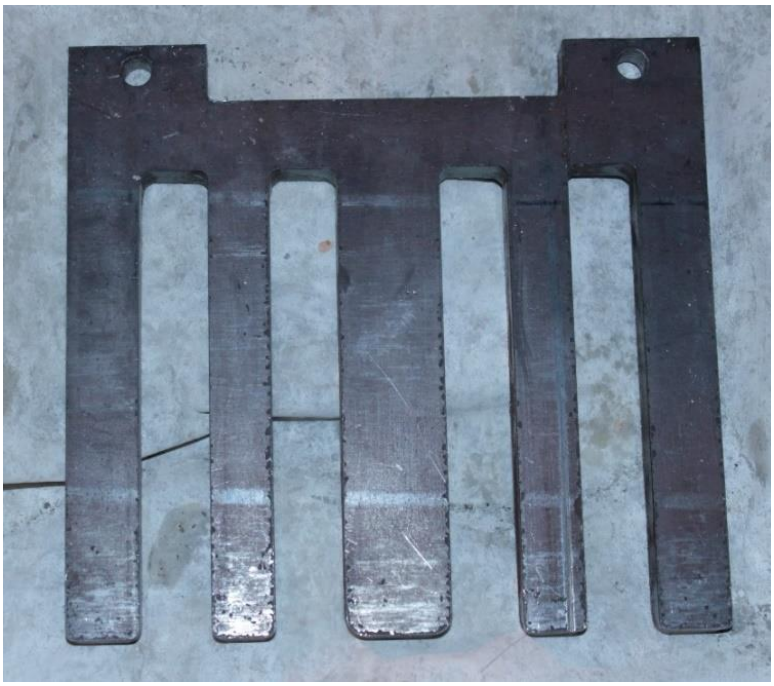

Figure 84 Shim plates used with wire reinforcements

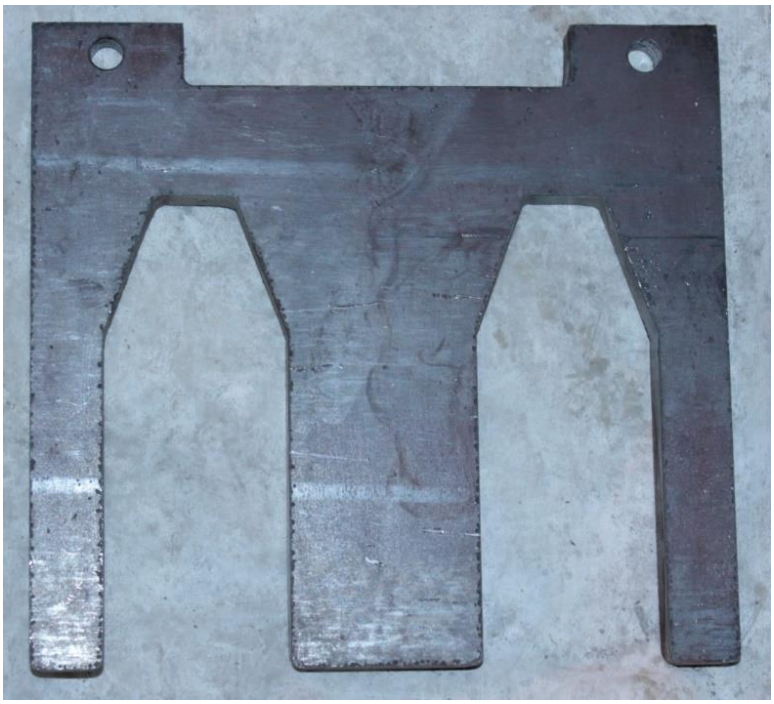

Figure 85 Shim plates used with strand reinforcements

Figure 86 Special jacking plate with four 1-inch diameter 14 TPI bolts

The special jacking plates and shims were used to adjust the total tendon elongation in the cavities with the project reinforcements.

If the required elongation of the project reinforcements was greater than the elongation of the standard CXT wires, then the following procedure was used for that cavity.

1) Remove the slack in all tendons by tensioning the individual tendons (wires or strands) to approximately 1400 pounds and then removing the force
2) Tighten the 4 jacking bolts to produce a uniform gap (between the standard bulkhead and jacking plate) that slightly exceeds the required additional elongation shown in Table 49.
3) Insert stack of shim plates with a total thickness equal to the difference in required elongation shown in Table 49
4) Back off jacking bolts until initial force is bearing solely on shim plates.
5) Group tension the bed with all four cavities to the standard elongation of 31.4 inches.

If the required elongation of the project reinforcements was less than the elongation of the standard CXT wires, then the following procedure was used.

1) Tighten the 4 jacking bolts in order to create a uniform gap between the standard bulkhead and jacking plate that is equal to the difference in required elongation shown in Table 49.
2) Remove the slack in all tendons by tensioning the individual tendons (wires or strands) to approximately 1400 pounds and then releasing the force
3) Loosen all 4 jacking bolts until the jacking plate is fully touching the standard bulkhead
4) Group tension the bed with all four cavities to the standard elongation of 31.4 inches.

Note, the prestressing force in the 15 different project wires/strands was also verified using a center-hole load cell that was installed on one of the tendons at the live end (Figure 89).

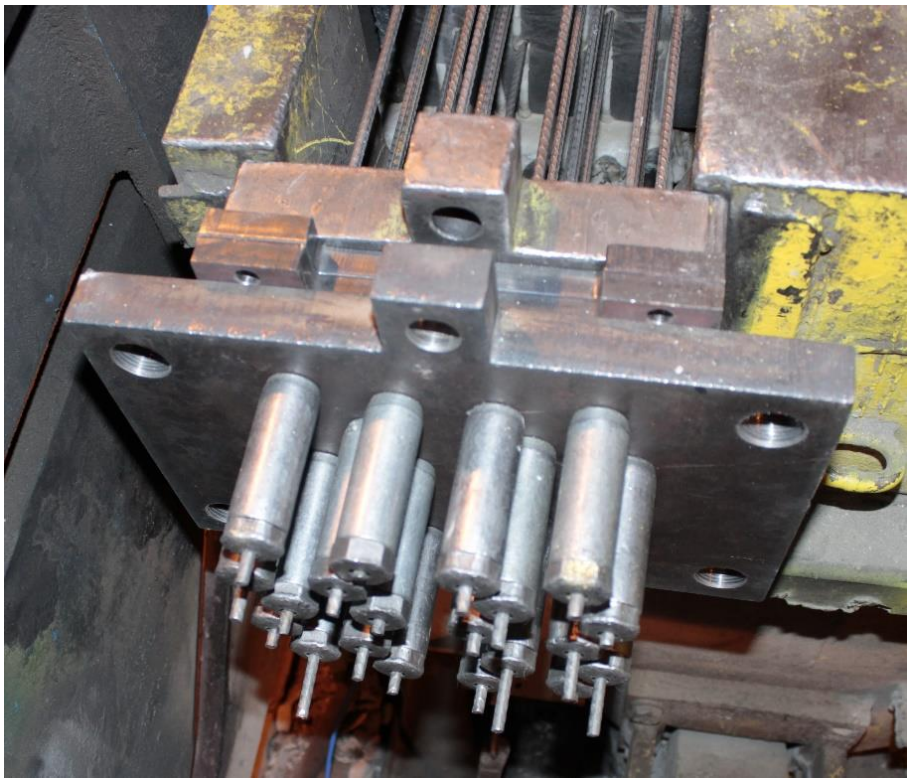

Figure 87 Shim plates installed at dead end to compensate for a lower MOE of project wires

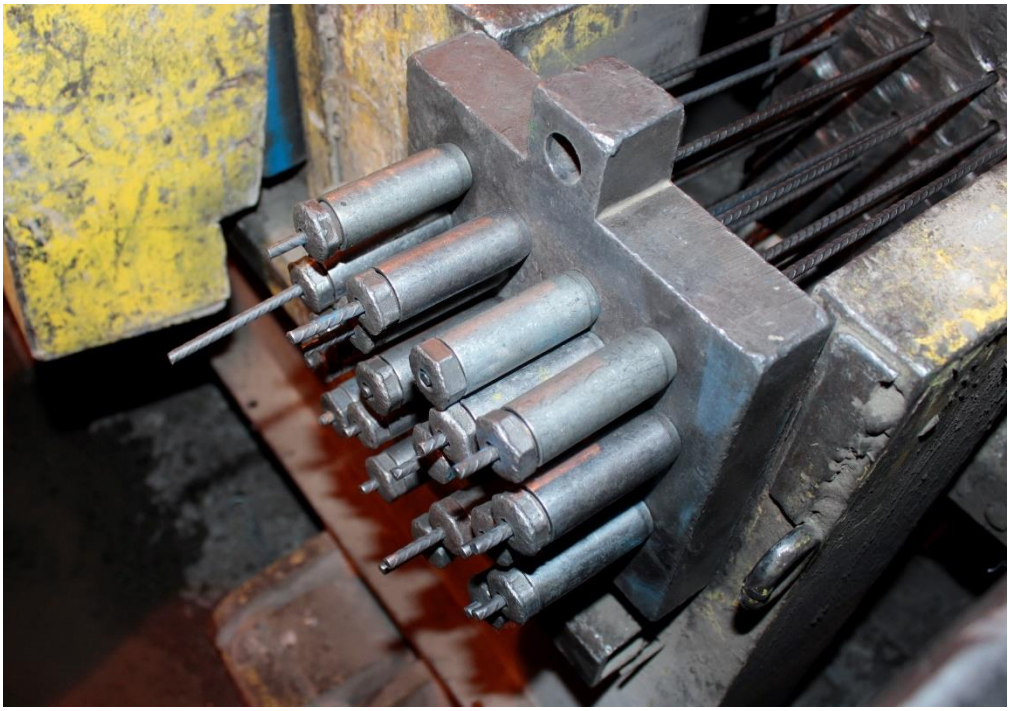

Figure 88 Standard bulkhead at dead end of the prestressing bed

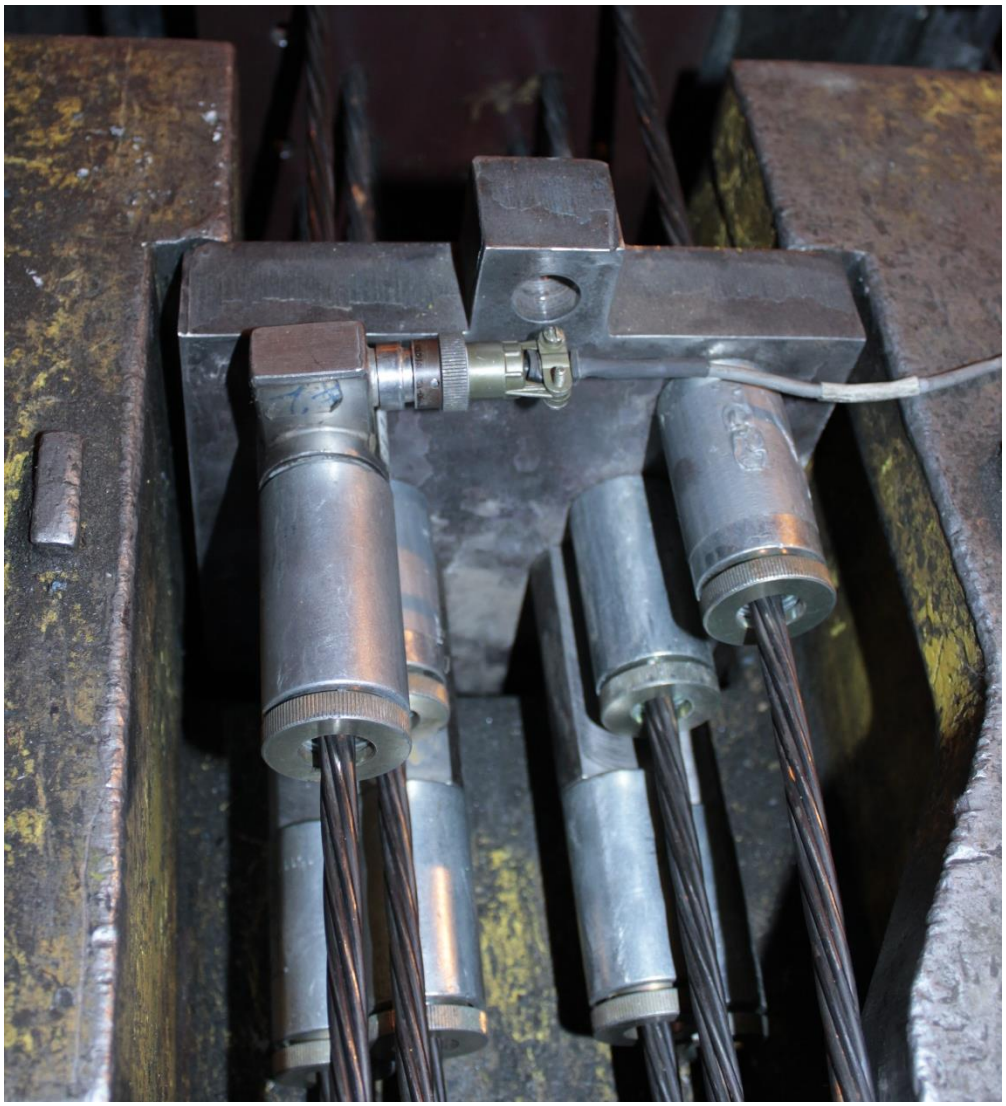

Figure 89 A center-hole load cell was installed on one of the tendons at the live end to verify the correct prestressing force was achieved with the special jacking plate apparatus

6.2.3 Concrete Mix

All crossties produced during the Plant-Phase were fabricated utilizing a similar concrete mixture design as used in the Lab-Phase, so the primary variable in this portion of the study was the prestressing tendon type. The principal differences in the concrete mixture used to fabricate the crossties (compared with Lab-Phase Mix-Design #1) in that the sand source for the crossties was from Tucson, AZ and the crosstie mixture contained an air-entraining admixture.

6.3 Test matrix and casting procedure during Plant-Phase

6.3.1 Test Matrix

During the Plant-Phase, crossties were fabricated with fifteen (15) different prestressing reinforcements and the corresponding transfer lengths were determined. KSU researcherss attempted to obtain fifty (50) transfer length values for each reinforcement type, for a total of 750 transfer lengths. However, due to some difficulties, only 727 successful transfer lengths were obtained. Table 50 lists the number of transfer lengths determined for crossties fabricated with each tendon type.

Table 50 Number of transfer lengths determined with each tendon type during Plant-Phase

	Transfer Lengths attempted to measure	Transfer Lengths measured
[WA]	50	49
[WB]	50	50
[WC]	50	47
[WD]	50	49
[WE]	50	48
[WF]	50	49
[WG]	50	49
[WH]	50	50
[WI]	50	50
[WJ]	50	47
[WL]	50	47
[WM]	50	49
[SA]	50	45
[SB]	50	50
[SC]	50	48
Total	**750**	**727**

6.3.2 Casting procedure

After the prestressing operation was completed as described in section 6.2.2, concrete ties with project reinforcements were cast along with regular concrete crossties using the CXT standard mixture and consolidation was achieved by form vibrators that were installed along the length of the bed. After the cast, concrete ties were covered with heavy tarps and subjected to the standard curing environment. Temperature match-cured concrete cylinders were used to determine the compressive strength of the concrete ties at the time of prestress transfer. A minimum concrete compressive strength of 5000 psi was required at the plant before de-tensioning of the tendons could occur.

6.3.3 Nomenclature for each pour during Plant-Phase

A nomenclature was adopted to identify transfer length results corresponding to a specific crosstie end. This nomenclature identified the specific prestressing tendon type used and the location of the crosstie within the cavity of the prestressing bed (from the live end). Figure 90 shows the nomenclature employed during Plant-Phase. The example shown in Figure 90 describes the live end of the concrete crosstie produced with [WH] reinforcement type and was the 9th tie in the cavity from live end.

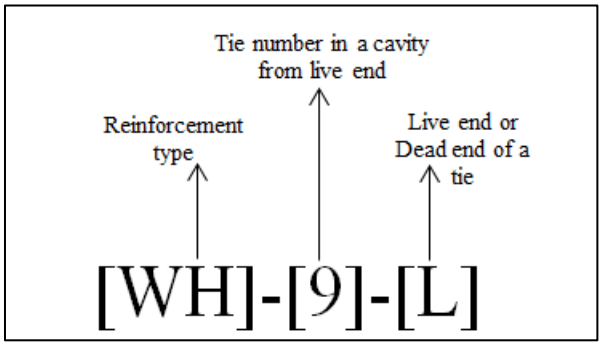

Figure 90 Nomenclature during Plant-Phase

6.4 Transfer length measurements during Plant-Phase

During the Plant-Phase, transfer lengths were determined from surface-strain profiles resulting from the application of prestressing force. These strain profiles were obtained by measuring concrete surface displacements on the bottom of the tie. The surface measured was actually the as-cast top surface, since the crossties were fabricated in the upside-down position.

Two different methods were used to obtain concrete surface-displacement measurements. These were:

1) Whittemore gage

2) Laser-Speckle Imaging (LSI) device.

The surface displacement measurements were then used to determine the corresponding strain profile by dividing by the corresponding gage length (8-in. for Whittemore gage and 6-in. for LSI system). The surface strain data was then used to determine the corresponding transfer length value using the statistically-based ZL Method (refer to 4.4.2).

Figure 91 illustrates the layout of single cavity in a prestressing bed, denoting the ties were surface displacements were measured with the Whittemore gage, and those that were measured using the two LSI devices. For each reinforcement type, 21 ties were evaluated using the LSI device and four (4) ties were evaluated using the Whittemore gage. During the long-term study, only the ties utilized the Whittemore strain measuring system were investigated.

6.4.1 Surface displacement readings using Whittemore gage (Plant-Phase)

This method consisted of casting brass inserts into the as-cast top surface of the tie at 1-inch center-to-center spacing for a total length of 42-inches longitudinally from the tie end. Then, the distance between these brass inserts was measured before and after de-tensioning using a Whittemore gage with an 8-inch gage length in a similar manner as done for the prisms in the Lab-Phase (Section 4.4.2). Four (4) crossties with each reinforcement type were fabricated with brass inserts to measure surface displacements using the Whittemore gage, for a total of 8 transfer lengths. Hence, a total of 120 transfer lengths were determined using this method, 8 for each of the 15 different reinforcements.

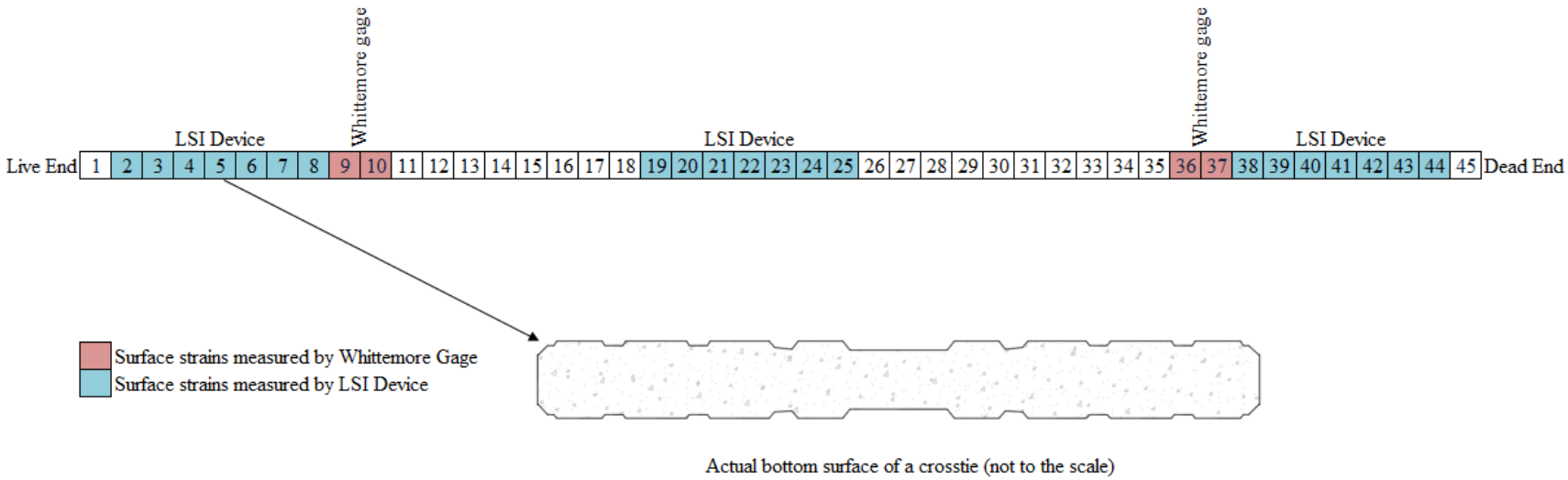

Figure 91 Layout showing the adapted strain measuring system

Figure 92 shows the steel bars with brass inserts used during the Plant-Phase. Cross-section for these steel bars was selected to accommodate the unique arrangement adapted for the crossties that were subjected to in-track loading. This unique arrangement was required to safeguard the brass inserts during in-track loading. Further details about the arrangement will be explained in the section 6.4.2.1. Selected cross-section for steel bar (for mounting brass inserts) is illustrated in Figure 93. During the casting process, these steel bars were placed on the as-cast top surface (actual bottom of the tie) as shown in Figure 94.

Figure 92 Steel bars with brass points

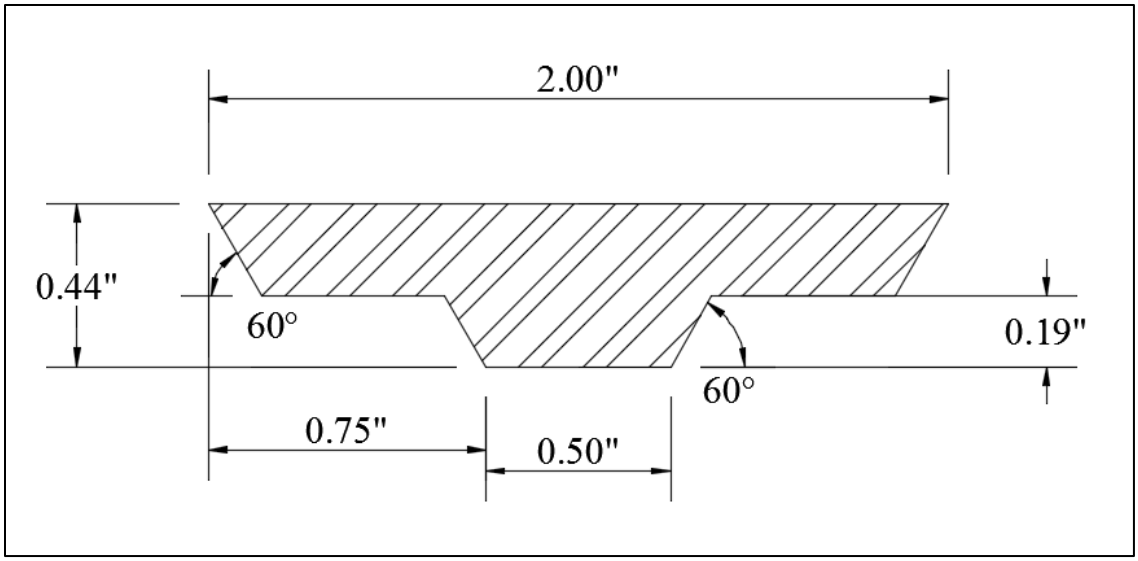

Figure 93 Cross-section for steel bar (for mounting brass inserts)

Figure 94 Steel bars used to hold brass inserts at proper spacing in the concrete crossties

These steel bars were detached from the concrete surface by removing the screws which held the brass inserts, leaving the brass inserts embedded in concrete ties as shown in Figure 95. The distance between these brass points was then measured prior to de-tensioning and immediately after de-tensioning using the Whittemore gage that had a precision of 0.0001 in.

A typical surface-strain profile, measured during the Plant-Phase, is shown in Figure 96. From Figure 96, it is clear that there is not a consistent strain plateau due to the changing area and centroid of the cross-section. This measured surface strain data is then used to obtain the corresponding transfer length value. A statistically-based method that incorporated a least-squares algorithm (Zhao, et al., 2013) was used to determine the transfer length from the surface-strain data.

(a)

(b)

Figure 95 (a) steel bar removal process before taking prior Whittemore gage readings (b) concrete tie surface with brass points

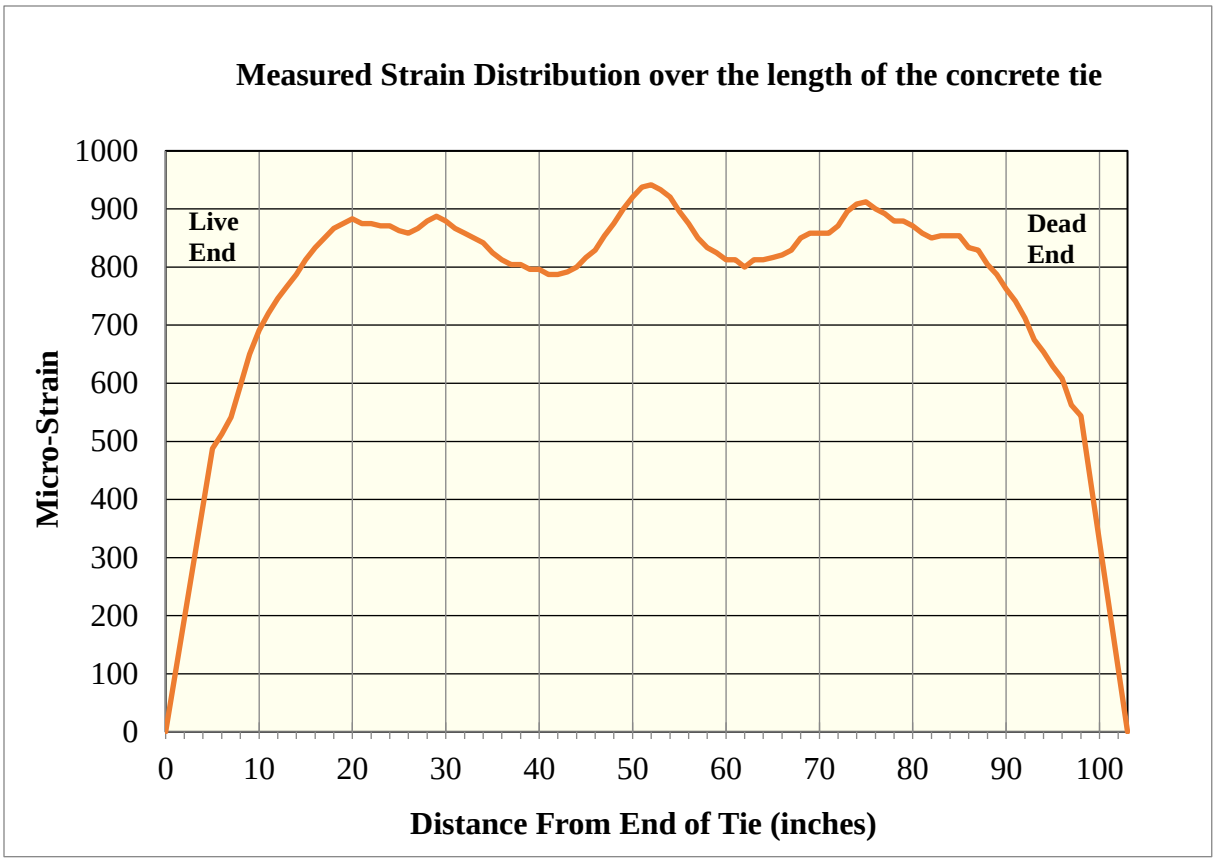

Figure 96 Typical strain profile along the length of the concrete tie during Plant-Phase

6.4.2 Surface displacement readings using Laser-Speckle Imaging (LSI) device

Concrete surface displacements were also determined using two automated laser-speckle imaging (LSI) devices that were fabricated specifically for the Plant-Phase of this project. These devices enabled displacement measurements to be made at a much faster rate and eliminated the human errors associated with the traditional Whittemore method. The application of laser-speckle imaging for strain measurements on prestressed concrete members was pioneered at KSU and is well documented (Zhao, et al., Winter 2012), (Zhao, et al., 2013). The devices used lasers to illuminate a speckled paint that was sprayed onto the concrete surface. By tracking the moment of individual speckles, concrete displacement may be determined to within 0.00012 in.

A typical speckle pattern captured by the LSI device is shown in Figure 97. Speckled images were synchronously captured by two cameras that were located precisely 6-in. apart, coupled by a carbon-fiber member to minimize errors due to thermal changes. The LSI devices were programmed to automatically traverse 32-inches at the end of each crosstie while capturing image pairs at an interval of 0.5-in. A series of paired speckle patterns were recorded before and after de-tensioning. The longitudinal displacement due to the application of prestressing was then determined using advanced digital image processing algorithms that analyzed the speckle patterns (Zhao, et al., Winter 2012). The corresponding strain was then determined by dividing the displacement by the gage length of 6-in.

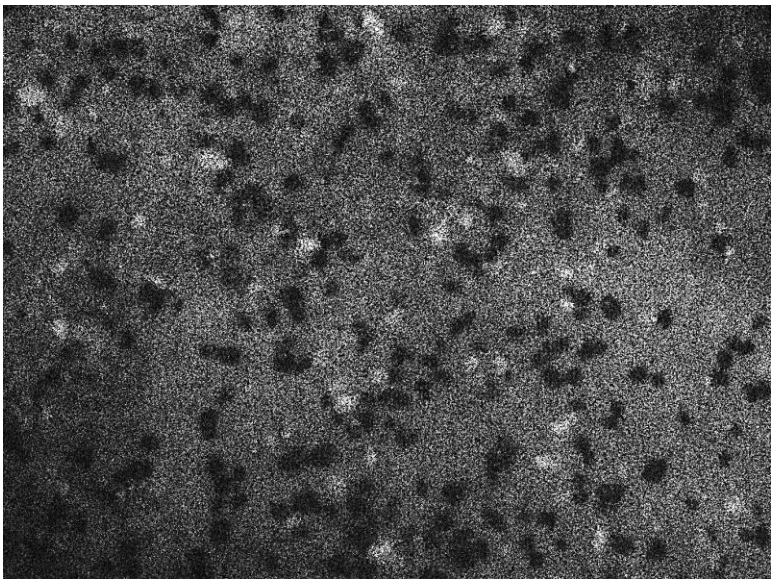

Figure 97 Typical speckle produced due to coherent light from LSI device

Prior to taking initial readings with the automated LSI system, the concrete surface of the crosstie was first prepared by grinding a 1/2-inch-wide x 1/8-inch-deep groove (Figure 98) at the location to be measured. This was necessary since the concrete surface was irregular, and a near-constant measurement plane was required to ensure the speckle pattern would be in focus which maximized the accuracy of the measurement. This groove was then painted with special paint that contained specked particles (Figure 99).

Prior research (Murphy, 2012) found this step necessary to enable accurate image correlation after the wet saw-cutting and vacuum-lifting operations that are part of the plant's de-tensioning and stripping process. In order to ensure consistent placement of the LSI device for all readings, small holes were drilled to a depth of about ½" LSI conical supports to be placed in these holes. The small holes were circled with a market to allow them to be easily found.

A consistent, clean surface was maintained throughout the speckle measurement process, since this was essential for the image correlation process. After de-tensioning by saw-cutting, the painted surface was immediately flushed with water to remove the concrete slurry left by the saw-cutting operation.

(a) Track-mounted saw used to cut groove

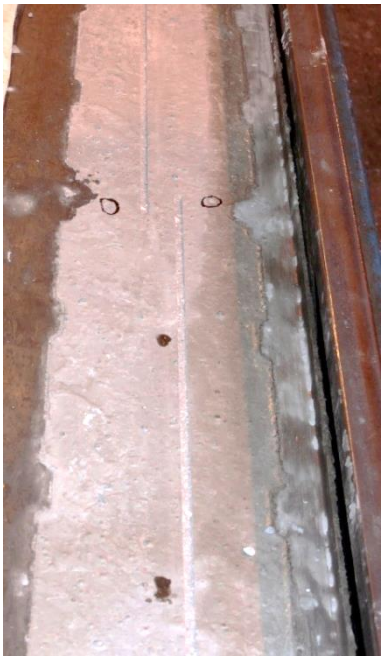

(b) Cut grooves with reference points marked

Figure 98 Grooves were cut into the concrete surface to ensure a reference plane

(a) Applying the speckle paint

(b) After painting the grooves

(c) Marking the reference holes

Figure 99 Preparing the surface for the LSI measurements

Figure 100 (a) shows the two automated LSI devices recording initial images prior to de-tensioning; while Figure 100 (b) shows the subsequent images being taken after the ties were de-tensioned and removed from the casting bed area. A total of 630 transfer lengths (approximately 42 for each of the 15 different reinforcements) were attempted using the automated LSI device and 607 transfer lengths were determined. There were 23 cases out of 630 where the data was not adequate to determine a transfer length value with confidence.

(a) Recording initial images prior to prestress transfer

(b) Recording images after prestress transfer

Figure 100 Recording laser speckle images during Plant-Phase

6.4.2.1 Special bottom surface preparation for in-track installed crossties

Of the 60 crossties manufactured with embedded brass inserts for the Whittemore gage readings (4 with each prestressing tendon type), 30 crossties were subjected to in-track loading while the other 30 were monitored for comparison. Upon the completion of crosstie surface strain measurements immediately after detensioning, separate identification marks applied to the four crossties (per tendon type) with embedded brass inserts. Two of the ties were shipped back to the KSU campus in Manhattan, KS for long-term evaluation. These ties were painted with a red letter “K” on the end of the crossties. The two remaining ties with brass inserts were initially stored at the CXT plant (in Tucson, AZ) and then subsequently shipped to the Transportation Technology Center, Inc. (TTCI) facility in Pueblo, CO where they were subjected to in-track loading.

This process was used to compare long-term transfer length variation due to different environments and due in-track rail loading. The ties that were planned for installation in track were painted with green letter “T” (Figure 101). Hence, at the conclusion of the Plant-Phase, there were 30 ties marked with “T” and thirty ties marked with “K”

Figure 101 Separation of in-track loading ties (“T”) and KSU ties (“K”) during Plant-Phase

The bottom surfaces of the crossties subjected to in-track loading were protected to prevent damage to the brass inserts during the loading. This preparation was vital in order to ensure the inserts were not damaged and thereby to ensure the integrity of long-term readings. Steel cover plates were installed at the bottom surface of the “T”-marked crossties and the plates covered all inserts used to measure displacement. During fabrication, the special cross-section of the insert template plates shown in Figure 93 assured that the inserts would be inset from the cover plate distance, thereby protecting the brass inserts from abrasion. Figure 102 illustrates the step-by-step procedure of the steel plate installation.

Figure 102 (a) shows the brass inserts being covered with a cloth tape. This step was used to prevent intrusion of any dust or debris into the displacement-measuring inserts. Figure 102 (b) illustrates the positioning of the steel cover plate. Whereas Figure 102 (c) illustrates the securing the steel plate to the concrete surface using brass screws. Figure 102 (d) shows “T” concrete crossties after the complete installation of the steel cover plates with additional caulking to protect the brass screws. Note, the “K”-marked crossties were not subjected to in-track loading and hence the bottom cover plates were not needed or installed.

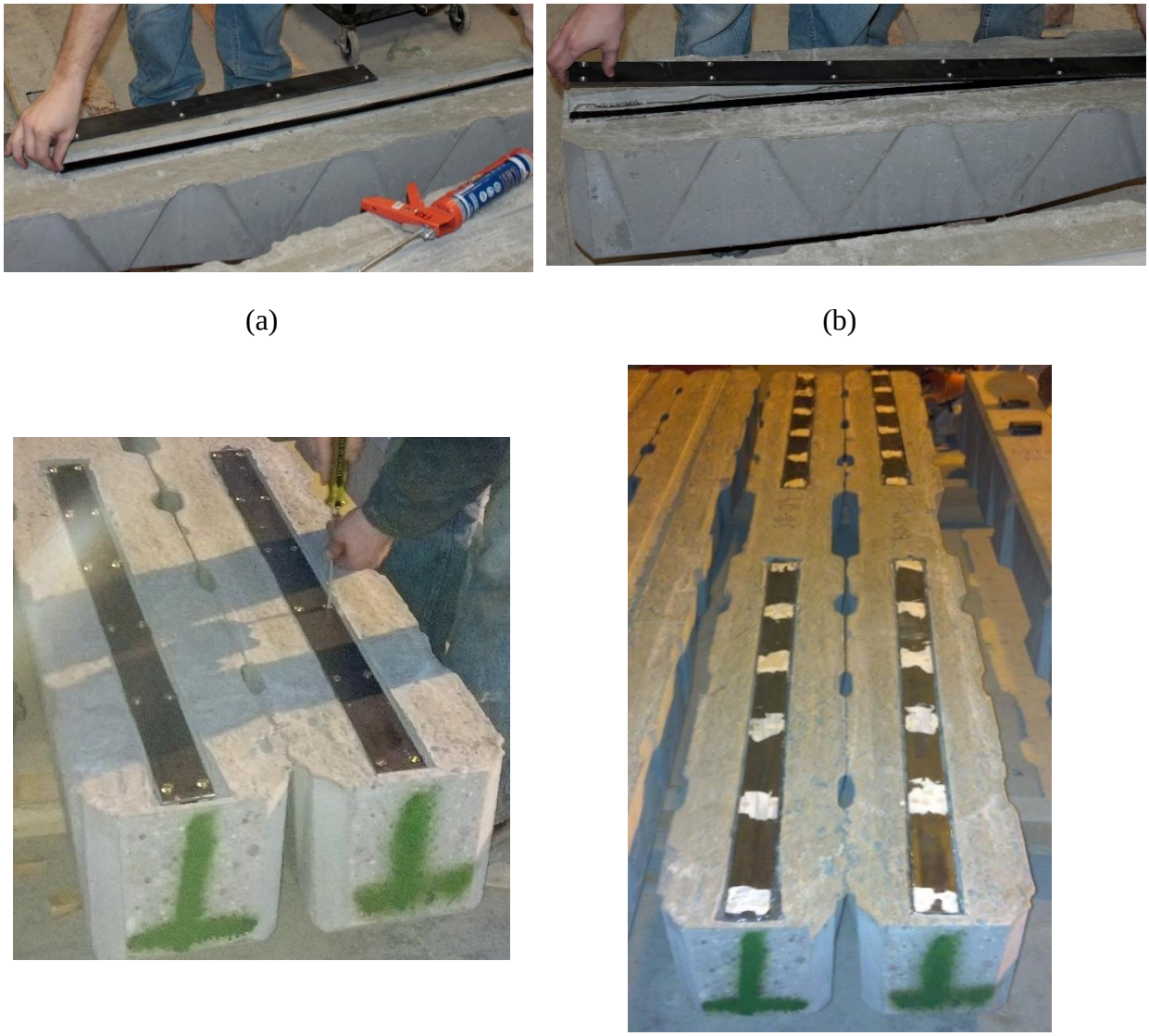

(a) (b)

(c) (d)

Figure 102 Bottom surface preparation for “T” crossties subjected to in-track loading (a) protecting displacement-measuring inserts with cloth tape; (b) positioning the steel cover plate in place; (c) installation of steel cover plate with brass screws; (d) steel cover plates installation with silicone caulking over brass screws

6.4.2.2 Further investigation on plant manufactured crossties

The “K-marked crossties were shipped to KSU in February 2013, within weeks after fabrication, and were not subjected to in-track rail loading. Whereas, “T”-marked crossties were stored at the plant for one year (from Jan 2013 to Jan 2014) and then subsequently shipped to the TTCI facility for in-track loading. For explanation purposes, this initial storage period is depicted as “Stage I”. Therefore, during Stage I, neither the “K”-marked crossties or “T”-marked crossties) were subjected to loading. However, they were stored in two different environments. Hence, Stage I is used to determine the transfer length variation of crossties due to different storage environments. After the “T”-marked crossties were shipped to the TTCI facility in January 2014, KSU researcherss traveled to Pueblo, CO to measure concrete surface displacements (and determine transfer lengths) of the 30 crossties prior to their installation in track.

These same 30 crossties were then installed in tangent track and subjected to a cumulative loading of 84.46 Million Gross Tons (MGT). Later, the ties were removed from track to evaluate the concrete surface displacements (using the embedded brass inserts on the bottom surface) and thereby determine transfer lengths. During this time, the “K”-marked crossties continued to be stored at KSU without any subjection of loading. This timeline is called “Stage II” and is used to compare the transfer length variation due to loading in tangent track. Upon the completion of Stage II, “T”-marked crossties were removed from track and KSU researcherss traveled to the TTCI facility to measure concrete surface displacements (using the embedded brass inserts on the bottom surface) and thereby determine transfer lengths.

Next, all 30 T-marked crossties were installed in 5-degree curved track subjected to an additional 151.85 MGT loading (for a cumulative of 236.31 MGT). This time period is called “Stage III”. During all 3 stages, “K”-marked crossties continued to be stored at KSU without any subjection to loading. For better understanding, the terminology to represent the data is described in Table 51.

Table 51 Description of the terminology utilized for long-term TL results

Terminology	Description
In-Plant TL results for "T"-marked crossties	TL results determined immediately after the prestress transfer at the plant and marked with letter "T”. These were stored in Tucson, AZ for 1-year.
In-Plant TL results for "K"-marked crossties	TL results determined immediately after the prestress transfer at the plant and marked with "K". These were shipped to KSU in Manhattan, KS and stored there.
End of "Stage I" TL results for "T"-marked crossties	TL results determined at the end of "Stage I" after shipment to TTCI in Pueblo, CO
End of "Stage I" TL results for "K"-marked crossties	TL results determined at the end of "Stage I" in Manhattan, KS
End of "Stage II" TL results for "T"-marked crossties	Ties were subjected to **84.46 MGT** of loading in tangent track. TL results determined at TTCI in Pueblo. CO.
End of "Stage II" TL results for "K"-marked crossties	TL results determined in Manhattan, KS.
End of "Stage III" TL results for "T"-marked crossties	Ties were subjected to **151.85 MGT** additional loading in curved track. TL results determined after ties were shipped to Manhattan, KS
End of "Stage III" TL results for "K"-marked crossties	TL results determined in Manhattan, KS.

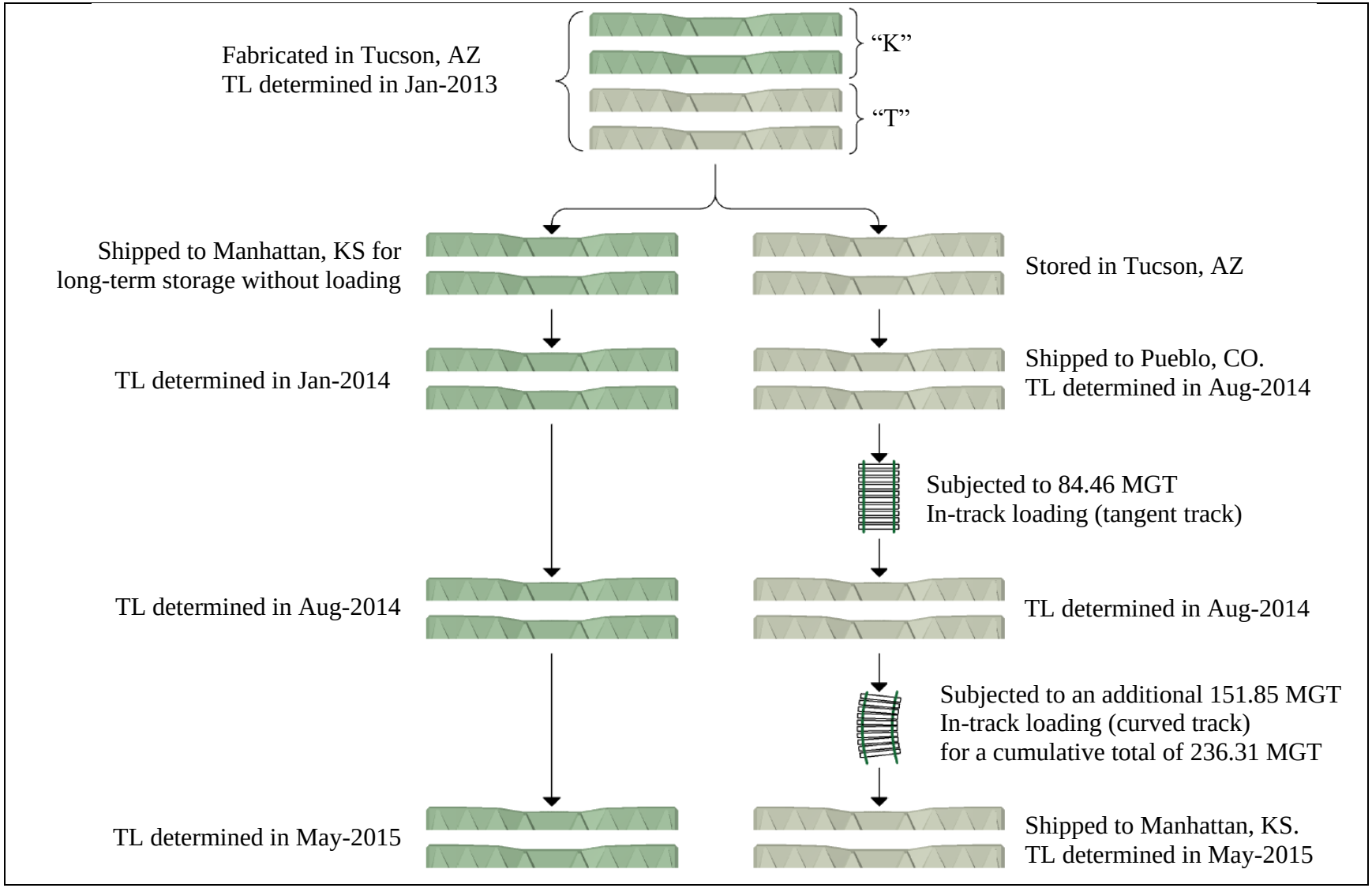

Figure 103 Timeline for long-term study of plant manufactured ties

Chapter 7 Plant-Phase results, and comparison of Lab-Phase results with Plant-Phase results

This chapter discusses the Plant-Phase results and compares these results with the Lab-Phase results. This chapter also includes the long-term study of plant manufactured crossties.

7.1 Plant-Phase results

Concrete ties fabricated during the Plant-Phase were used to quantify the influence of the prestressing tendon type and indentation geometry on transfer lengths in actual crossties. A total of 727 transfer length results were determined during the Plant-Phase for pretensioned crossties that were fabricated with 15 different prestressing tendon types. All concrete crossties were fabricated, and transfer lengths determined, using the procedures described in Chapter 6.

Concrete compressive strengths and splitting tensile strengths for ties produced with each prestressing tendon type were determined from match-cured cylinders at the time of prestress transfer. The measured concrete parameters during the Plant-Phase are tabulated in Table 52.

Table 52 Concrete parameters at the time of prestress transfer during Plant-Phase

Prestressing Tendon Type	Indent Type	Compressive Strength at Release (psi)	Splitting Tensile Strength (psi)
[WA]	Smooth	5365	672
[WB]	Chevron	6450	573
[WC]	Spiral	5617	520
[WD]	Chevron	5440	550
[WE]	Spiral	5277	618
[WF]	Diamond	5063	513
[WG]	Chevron	5440	550
[WH]	Chevron	5063	513
[WI]	Chevron	5217	515
[WJ]	Chevron	5447	598
[WL]	2-Dot	6600	554
[WM]	Chevron	6650	590
[SA]	Smooth	5277	618
[SB]	Indented	6600	554
[SC]	Smooth	5617	520

7.1.1 Transfer length Results

7.1.1.1 Results from measurements with Whittemore gage

Eight (8) transfer lengths (at both ends of four crossties) were determined for each prestressing tendon type for a total of 120 transfer lengths. For each tendon type, crossties produced at the same location within the prestressing bed were evaluated for transfer length. The specific crossties evaluated were the 9th, 10th, 36th, and 37th crossties from the live-end of the prestressing bed (Figure 91). Transfer lengths were determined from measured concrete surface displacements as explained in section 6.4.1. The transfer lengths determined from surface displacements measured by Whittemore gage (both in inches and # diameters of the reinforcement) are tabulated in Table 53.

7.1.1.2 Results from measurements with Laser Speckle Imaging (LSI) devices

Forty-two (42) transfer lengths were attempted for each reinforcement type using the two LSI devices, and a total of 607 transfer lengths were successfully determined by this technique during the Plant-Phase. TL were determined for three (3) groups of seven adjacent crossties along the prestressing bed. These groups include 2nd through 8th, 19th through 25th, and 38th through 44th ties from the live-end (Figure 91). A few transfer lengths could not be accurately determined by this method, primarily due to out-of-focus images obtained from LSI devises. Transfer length values (both in inches and # diameters of the reinforcement) determined though LSI devises are tabulated in Table 54.

Table 53 Transfer length results through Whittemore gage (Plant-Phase)

Prestressing Tendon Type	Min., in. [TL/d_b]	Avg., in. [TL/d_b]	Max., in. [TL/d_b]
[WA]	10.7 [51]	13.3 [64]	15.7 [75]
[WB]	6.1 [29]	7.6 [36]	8.5 [41]
[WC]	5.2 [25]	6.7 [32]	8.5 [41]
[WD]	5.4 [26]	6.7 [32]	8.5 [41]
[WE]	4.5 [21]	5.5 [26]	6.7 [32]
[WF]	4.9 [23]	5.6 [27]	6.8 [32]
[WG]	5.8 [28]	7.5 [36]	8.6 [41]
[WH]	5.1 [24]	5.8 [28]	6.7 [32]
[WI]	6.0 [29]	8.0 [38]	9.8 [47]
[WJ]	5.5 [26]	6.1 [29]	7.2 [34]
[WL]	7.2 [34]	8.9 [43]	11.2 [53]
[WM]	4.1 [20]	5.8 [28]	7.8 [37]
[SA]	7.7 [21]	11.4 [30]	14.4 [38]
[SB]	11.6 [31]	13.9 [37]	15.4 [41]
[SC]	9.0 [29]	11.1 [36]	14.3 [46]

Table 54 Transfer length results through LSI devices (Plant-Phase)

Prestressing Tendon Type	Min., in. [TL/d_b]	Avg., in. [TL/d_b]	Max., in. [TL/d_b]
[WA]	12.1 [58]	14.5 [69]	18.0 [86]
[WB]	6.5 [31]	10.7 [51]	16.0 [76]
[WC]	5.0 [24]	12.2 [58]	22.9 [109]
[WD]	6.6 [32]	10.3 [49]	15.7 [75]
[WE]	6.6 [32]	9.2 [44]	14.5 [69]
[WF]	5.2 [25]	8.2 [39]	13.0 [62]
[WG]	7.6 [36]	11.5 [55]	16.0 [76]
[WH]	6.3 [30]	8.8 [42]	11.5 [55]
[WI]	7.6 [36]	11.3 [54]	14.9 [71]
[WJ]	5.4 [26]	10.1 [48]	14.8 [71]
[WL]	10.1 [48]	14.2 [68]	22.9 [109]
[WM]	6.4 [31]	9.9 [47]	14.2 [68]
[SA]	10.7 [29]	15.1 [40]	20.7 [55]
[SB]	12.6 [34]	15.9 [42]	20.5 [55]
[SC]	12.1 [39]	16.8 [54]	22.9 [73]

7.1.1.3 Comparison between LSI and Whittemore gage transfer lengths

The average transfer length (TL) results from readings obtained by both LSI devices and Whittemore gage are compared and a coefficient of determination, $R^2 = 0.812$, was determined. For this correlation, the average TL values for all 15 reinforcements (tendon types) are plotted as shown in Figure 104. Each data point in this figure corresponds to a single prestressing tendon type. In Figure 104, the vertical-axis value is the average (of 8) TL determined from Whittemore gage readings, while the horizontal-axis value is the average (of approximately 42) TL determined from LSI readings. From this figure, TL results from LSI devices are consistently higher than from Whittemore gage.

However, when average TL values are plotted as a function of the crosstie position along the prestressing bed rather than grouped by reinforcing type (Figure 105), a better understanding of why average LSI values were consistently higher than Whittemore values begins to emerge. In (Figure 105), the four points denoted by red diamonds are the average TL results from Whittemore gage readings, while the blue diamonds are average results from the LSI devices. Note, the Whittemore readings were always taken on the 9th, 10th, 36th, and 37th crossties from the live-end.

From (Figure 105), there are significant trends in the average TL data that occur based on the casting position in the prestressing bed. At the ends of the bed, TL values were consistently the highest. Based on the LSI data only (blue points) these values tend to decrease in an approximately linearly from the two ends of the bed until the last tie in the grouping. The very next two crossties (the 9th and 10th tie from each end of the bed) were ties measured using the Whittemore gage. Based on the near-linear trend of the LSI values near the ends of the bed, it would be expected that the Whittemore TL values would be lower still than the adjacent LSI ties.

The scatter noted in the plant data is apparently due, in part, to the casting position along the prestressing bed. The large TL values near the ends of the bed may be due, in part, to temperature variation between end ties and middle ties caused by the end ties being adjacent to large steel bulkheads that are not covered. Strength gaining rate (maturity) may be significantly different due to difference in temperature. This was the first attempt that the researcherss were aware of where TL values were consistently determined along the length of long (385.75-ft.) prestressing bed. It is also important to note that the entire bed of crossties were cast with about 14 different batches of the same concrete mixture over nearly a 2-hour period.

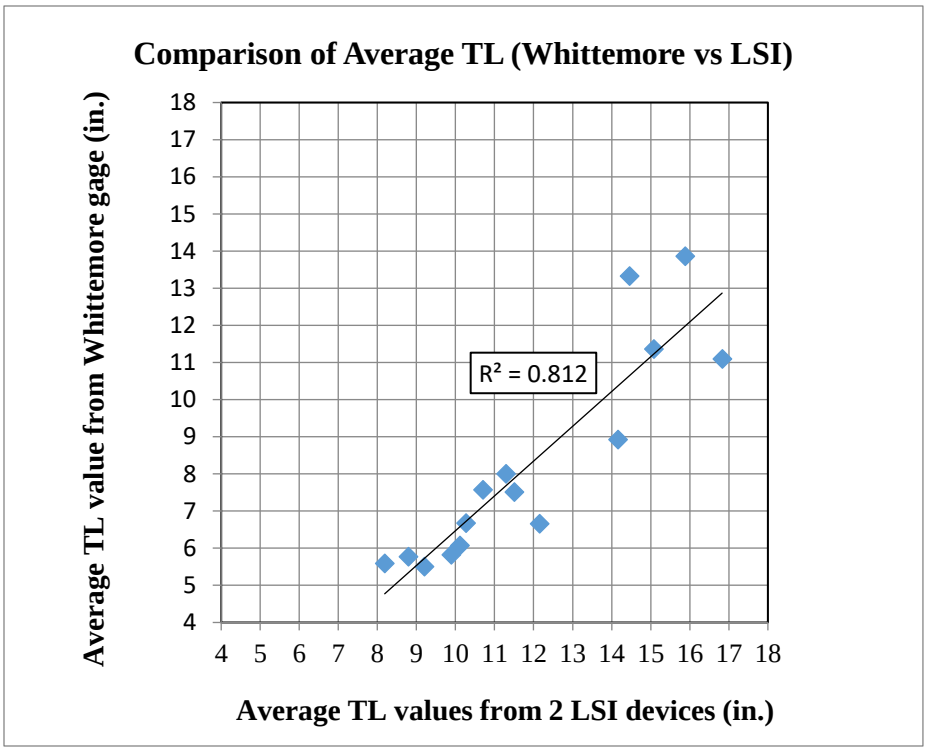

Figure 104 Comparison of average transfer length results from Whittemore gage and LSI

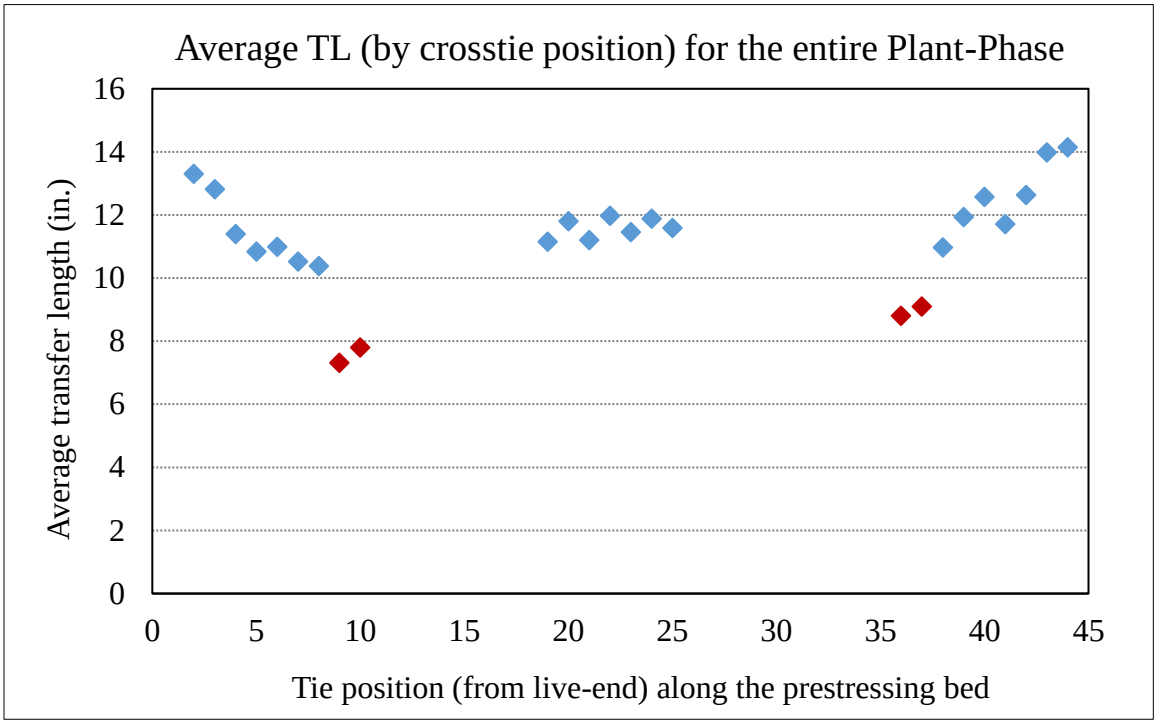

Figure 105 Average TL (by tie number) for the entire Plant-Phase

7.1.1.4 Combined transfer length results during Plant-Phase and comparison between Live end and Dead end

Since a good correlation (R^2 = 0.812) was obtained between LSI devices and Whittemore gage TL measurements, all Plant-Phase results are grouped and tabulated (both in inches and # diameters of the reinforcement) in Table 55. This table includes the minimum, maximum, and average transfer lengths obtained for each tendon type.

During the Plant-Phase, live-end and dead-end transfer length results were compared and no significant differences were observed. Live-end and dead-end transfer length results are tabulated in Table 56, separately. A correlation of R^2 = 0.917 was observed between live-end and dead-end transfer length results. Correlation between live-end and dead-end transfer length results are shown in Figure 106. From Table 56, the difference in average TL results between live-end and dead-end is less than 1.0 in. for 11 reinforcements used during Plant-Phase. Maximum difference in avg. TL among 15 reinforcements is 1.9 in.

Table 55 Combined (LSI and Whittemore) transfer length results (Plant-Phase)

Prestressing Tendon Type	Min., in. [TL/d_b]	Avg., in. [TL/d_b]	Max., in. [TL/d_b]
[WA]	10.7 [51]	14.3 [68]	18.0 [86]
[WB]	6.1 [29]	10.2 [49]	16.0 [76]
[WC]	5.0 [24]	11.2 [54]	22.9 [109]
[WD]	5.4 [26]	9.7 [46]	15.7 [75]
[WE]	4.5 [21]	8.6 [41]	14.5 [69]
[WF]	4.9 [23]	7.8 [37]	13.0 [62]
[WG]	5.8 [28]	10.9 [52]	16.0 [76]
[WH]	5.1 [24]	8.3 [40]	11.5 [55]
[WI]	6.0 [29]	10.8 [51]	14.9 [71]
[WJ]	5.4 [26]	9.4 [45]	14.8 [71]
[WL]	7.2 [34]	13.3 [63]	22.9 [109]
[WM]	4.1 [20]	9.2 [44]	14.2 [68]
[SA]	7.7 [21]	14.4 [38]	20.7 [55]
[SB]	11.6 [31]	15.6 [41]	20.5 [55]
[SC]	9.0 [29]	15.9 [51]	22.9 [73]

Table 56 Live-end and dead-end transfer length results (Plant-Phase)

Wire/strand Type	Live-End (LE)			Dead-End (DE)			Difference in average TL between LE and DE (in.)
	Min., in. [TL/d_b]	Avg., in. [TL/d_b]	Max., in. [TL/d_b]	Min., in. [TL/d_b]	Avg., in. [TL/d_b]	Max., in. [TL/d_b]	
[WA]	11.7	14.1	18.0	10.7	14.4	17.8	0.3
	[56]	[67]	[86]	[51]	[69]	[85]	
[WB]	7.4	10.9	15.5	6.1	9.5	16.0	1.4
	[35]	[52]	[74]	[29]	[45]	[76]	
[WC]	5.0	11.2	19.5	6.1	11.2	22.9	0.1
	[24]	[54]	[93]	[29]	[53]	[109]	
[WD]	5.6	9.3	15.7	5.4	10.1	13.5	0.8
	[27]	[44]	[75]	[26]	[48]	[64]	
[WE]	4.5	8.6	11.9	4.6	8.5	14.5	0.1
	[21]	[41]	[57]	[22]	[41]	[69]	
[WF]	4.9	8.7	13.0	4.9	6.8	11.2	1.9
	[23]	[41]	[62]	[23]	[32]	[53]	
[WG]	5.8	10.8	14.9	7.3	11.0	16.0	0.2
	[28]	[51]	[71]	[35]	[52]	[76]	
[WH]	5.1	7.7	11.0	5.5	8.9	11.5	1.2
	[24]	[37]	[53]	[26]	[43]	[55]	
[WI]	6.2	11.1	14.9	6.0	10.5	14.7	0.6
	[30]	[53]	[71]	[29]	[50]	[70]	
[WJ]	5.9	9.8	14.8	5.4	9.1	13.4	0.7
	[28]	[47]	[71]	[26]	[43]	[64]	
[WL]	7.8	13.2	17.2	7.2	13.3	22.9	0.2
	[37]	[63]	[82]	[34]	[64]	[109]	
[WM]	5.5	10.0	14.2	4.1	8.4	12.3	1.6
	[26]	[48]	[68]	[20]	[40]	[59]	
[SA]	7.7	14.3	19.0	9.0	14.6	20.7	0.3
	[21]	[38]	[51]	[24]	[39]	[55]	
[SB]	11.6	15.4	17.7	13.0	15.8	20.5	0.4
	[31]	[41]	[47]	[35]	[42]	[55]	
[SC]	9.9	15.7	22.9	9.0	16.1	22.0	0.4
	[32]	[50]	[73]	[29]	[51]	[70]	

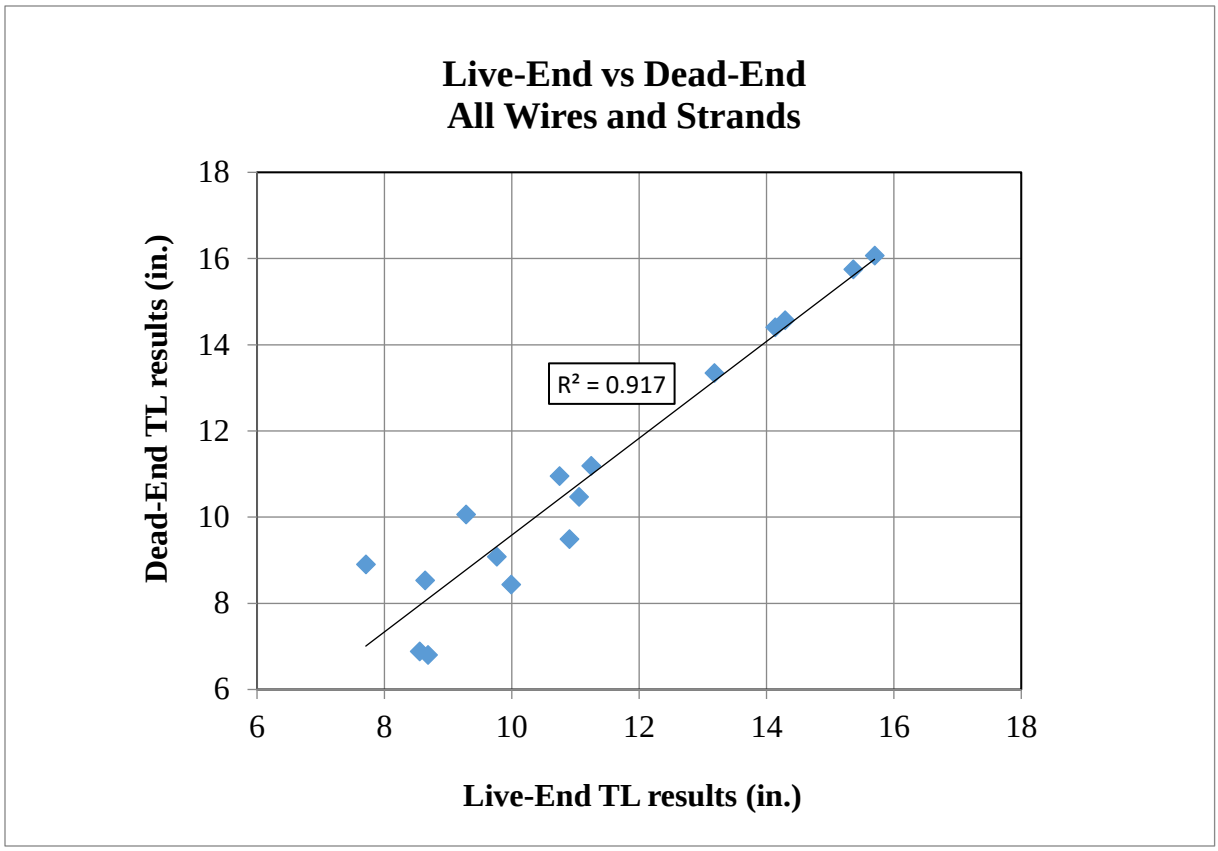

Figure 106 Comparison of transfer lengths (Live End vs Dead End)

All 727 transfer lengths that were determined during the Plant-Phase are shown in Figure 107 (in inches) and Figure 108 (in # diameters). Since these crossties were manufactured in a production environment where many other ties were also being fabricated during the same day, de-tensioning did not occur at precisely the same compressive strength for each prestressing reinforcement type. Rather, the ties were de-tensioned when the compressive strength was at least 5000 psi and when the de-tensioning crew was available. Thus, the compressive strength at de-tensioning varied between 5063 psi and 6650 psi (Table 52) for the ties manufactured with the 15 different reinforcements.

During the Plant-Phase, the average transfer lengths of the 5.32-mm wires ranged from 7.8 in. to 14.3 in. This corresponds to a value of 37 d_b to 68 d_b, where d_b is the diameter of the wire. The average transfer length of the chevron-shaped indented wires ranged from 8.3 in. ([WH]) to 10.9 in. ([WG]), or 40 d_b to 52 d_b. The average transfer length of the spiral-indented

wires ranged from 8.6 in. to 11.2 in., or 41 d_b to 53 d_b. Average transfer lengths for smooth, 2-Dot, and Diamond wires are 14.3-in., 13.3-in., and 7.8-in. respectively or 68 d_b, 63 d_b, and 37 d_b.

The average transfer lengths for the 7-wire 3/8-in. diameter smooth ([SA]) and 7-wire 3/8-in. diameter indented ([SB]) strands were 14.4 in. and 15.6 in. respectively. This corresponds to values of 38 d_b and 42 d_b respectively. Since the reinforcement source was the same for both laboratory and Plant-Phases; Strand [SA] had some very minor surface rusting, whereas strand [SB] did not contain any visible rusting. The 3-wire 5/16-in. diameter smooth strand ([SC]) had an average transfer length of 15.9 in., which corresponds to 51 d_b.

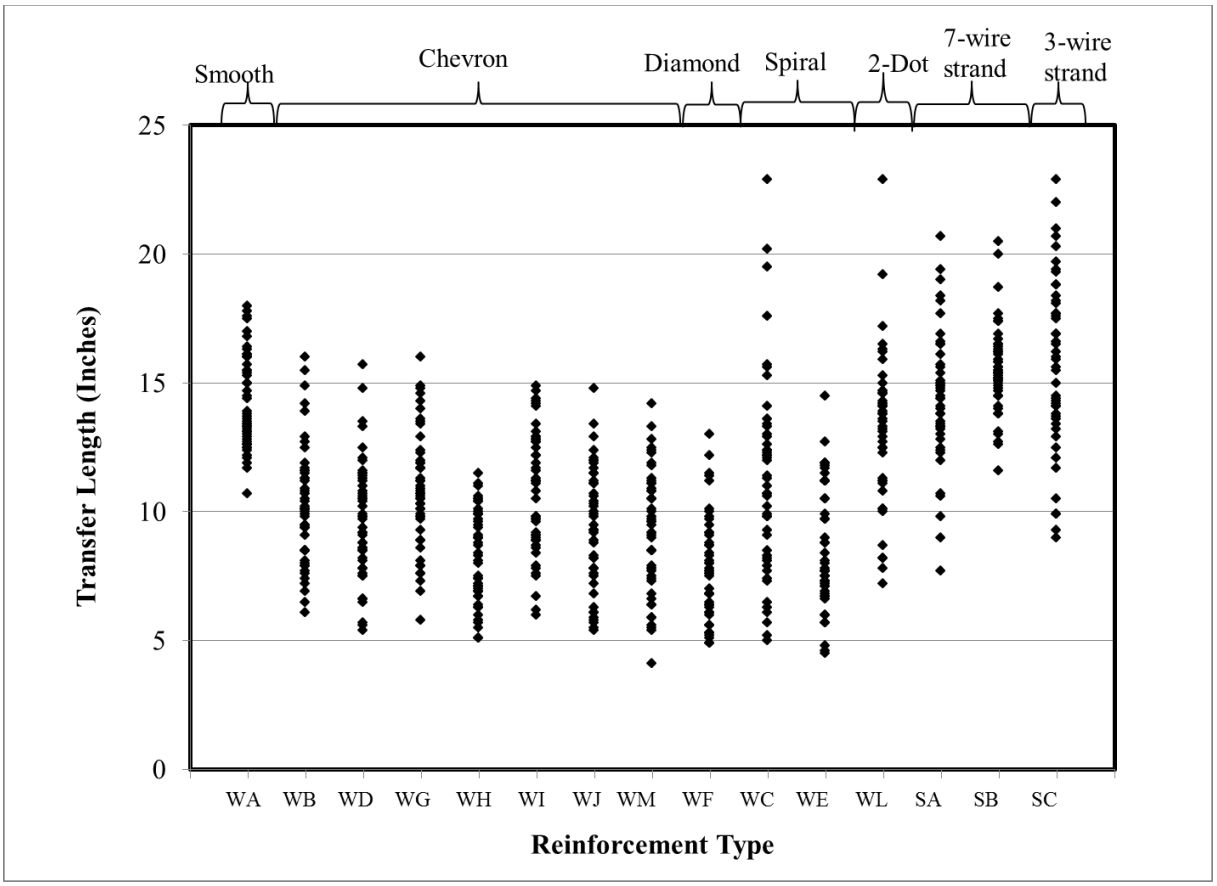

Figure 107 Transfer length results during Plant-Phase (TL in inches)

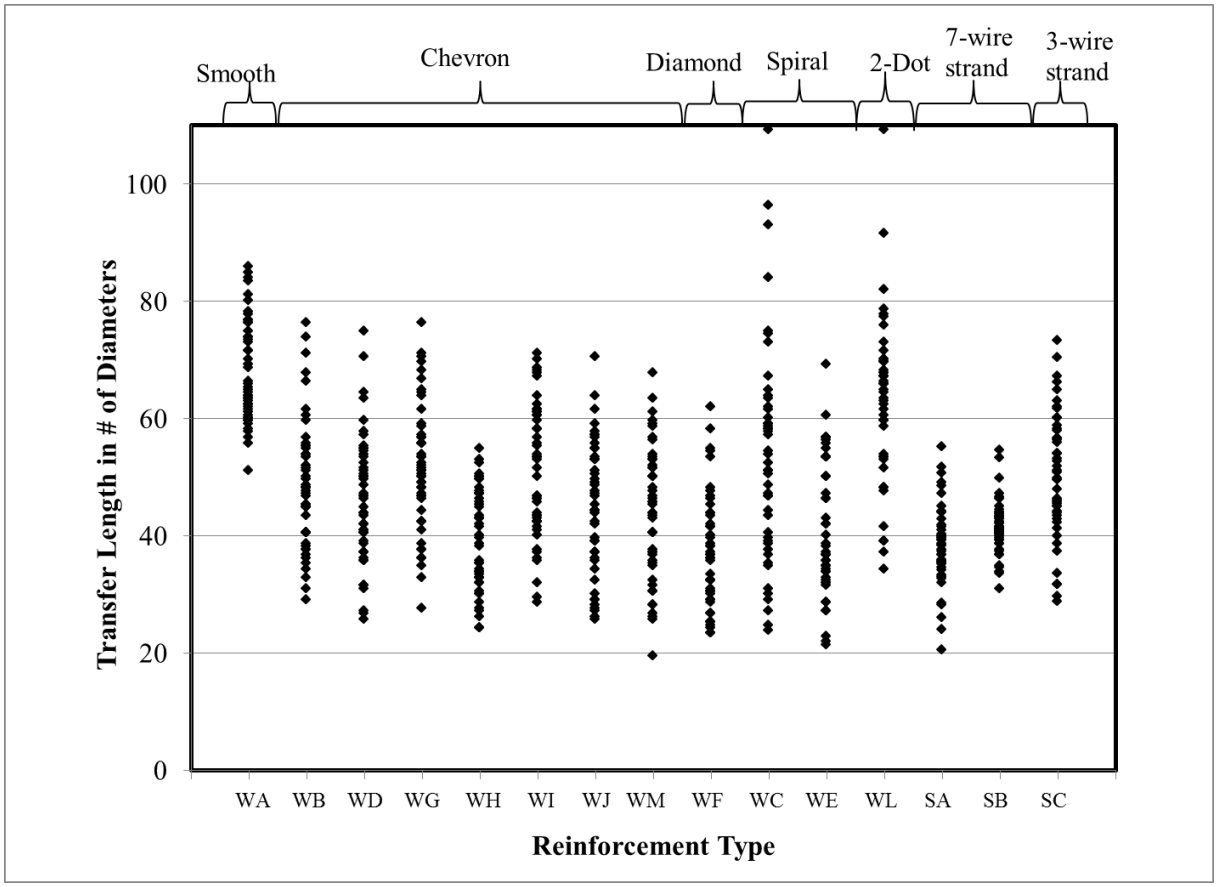

Figure 108 Transfer length results during Plant-Phase (TL in # of diameters)

7.2 Comparison of Lab-Phase and Plant-Phase results

7.2.1 Wire reinforcements

In this section, for wire reinforcements, Lab-Phase results from Group I prims are directly compared with Plant-Phase results. Average transfer lengths in the Lab-Phase ranged from 7.4-in. to 18.7-in., corresponding to 35 d_b and 89 d_b. Whereas, Plant-Phase average transfer lengths ranged from 7.8-in. to 14.3-in., corresponding to 37 d_b and 68 d_b.

During the Lab-Phase, the highest average transfer lengths (for wire reinforcements) were obtained when the smooth wire ([WA]) and 2-dot ([WL]) were used and these values were 16.3 in. (78 d_b) and 18.7 in. (89 d_b), respectively. During the Plant-Phase, as with the laboratory phase, the highest average transfer lengths were obtained when the smooth wire ([WA]) and 2-dot ([WL]) were used and these values were 14.3 in. and 13.3 in., respectively. This corresponds to 68 d_b and 64 d_b, where d_b is the diameter of the wire. Note that, 2-Dot wire had minimal amount of indentations.

In the case of chevron-type wires, transfer lengths ranged from 8.3-in. ([WH]) to 10.9-in. ([WG]), or 40 d_b to 52 d_b during Plant-Phase and 7.5-in. ([WH]) to 11.8-in. ([WG]), or 36 d_b to 56 d_b during Lab-Phase. Other chevron types; [WB], [WD], [WI], [WJ], and [WM], produced 10.2-in. (49 d_b), 9.7-in. (46 d_b), 10.8-in. (51 d_b), 9.4-in. (45 d_b), and 9.2-in. (44 d_b) transfer lengths respectively during the Plant-Phase compared to their respected Lab-Phase results of 11.6-in. (55 d_b), 11.1-in. (53 d_b), 10.1-in. (48 d_b), 9.0-in. (43 d_b), and 9.8-in. (47 d_b).

Spiral wire reinforcements; [WC] and [WE], had average transfer lengths of 11.2-in. (54 d_b) and 8.6-in. (41 d_b) during Plant-Phase and 8.8-in. (42 d_b) and 7.4-in. (35 d_b) during Lab-Phase. In the case of diamond type wire ([WF]) these values were 7.8-in. (37 d_b) and 8.5-in. (41 d_b) during Plant-Phase and Lab-Phase respectively.

From Table 52, it can be observed that compressive strengths during Plant-Phase were clearly higher than Lab-Phase values. Also, from results of Group II Lab-Phase prisms, it was shown that concrete release strengths are significantly influencing TL results. Hence, the consistently-lower average TL results noted for Plant-Phase prisms may likely be due to higher concrete release strengths.

The transfer length prediction model developed during the Lab-Phase is used to predict the TL values at the corresponding release strengths for the Plant-Phase ties measured using the Whittemore gage. Comparison is made only with Whittemore gage Plant-Phase TL results since the Lab-Phase TL results were evaluated using the Whittemore gage. With this comparison, any TL differences associated with the systems and different measurement systems are eliminated. Table 57 lists the predicted and average experimental TL values determined from Whittemore gage readings, along with the absolute difference in these values.

Table 57 Prediction of Plant-Phase TL values based on developed TL model

$$TL = 34.2 - \frac{f'_{ci}}{300} - (A1096\ value)\left[f'_{ci}\left(0.4 - \frac{f'_{ci}}{16{,}000}\right) - 1250\right]$$

Wire type	Release strength during Plant-Phase (psi)	ASTM A1096 value (pounds)	TL predicted by model for Plant-Phase at release strength values (in.)	Experimental Plant-Phase TL (Whittemore) (in.)	Absolute Difference (in.)
WA	5365	487	15.8	13.3	2.4
WB	6450	6481	7.6	7.6	0.0
WC	5617	7646	7.6	6.7	1.0
WD	5440	5555	10.1	6.7	3.4
WE	5277	7674	7.9	5.5	2.4
WF	5063	8312	7.3	5.6	1.7
WG	5440	5505	10.1	7.5	2.6
WH	5063	7605	8.1	5.8	2.3
WI	5217	6567	9.2	8	1.2
WJ	5447	7034	8.4	6.1	2.4
WL	6600	2068	10.6	8.9	1.7
WM	6650	6879	7.0	5.8	1.1

The average experimental TL data and predicted TL values are plotted in Figure 109 for comparison. From this figure, the coefficient of determination, R^2, was 0.858 between Plant-Phase TL results (Whittemore gage) and the value predicted by the equation developed during the Lab-Phase.

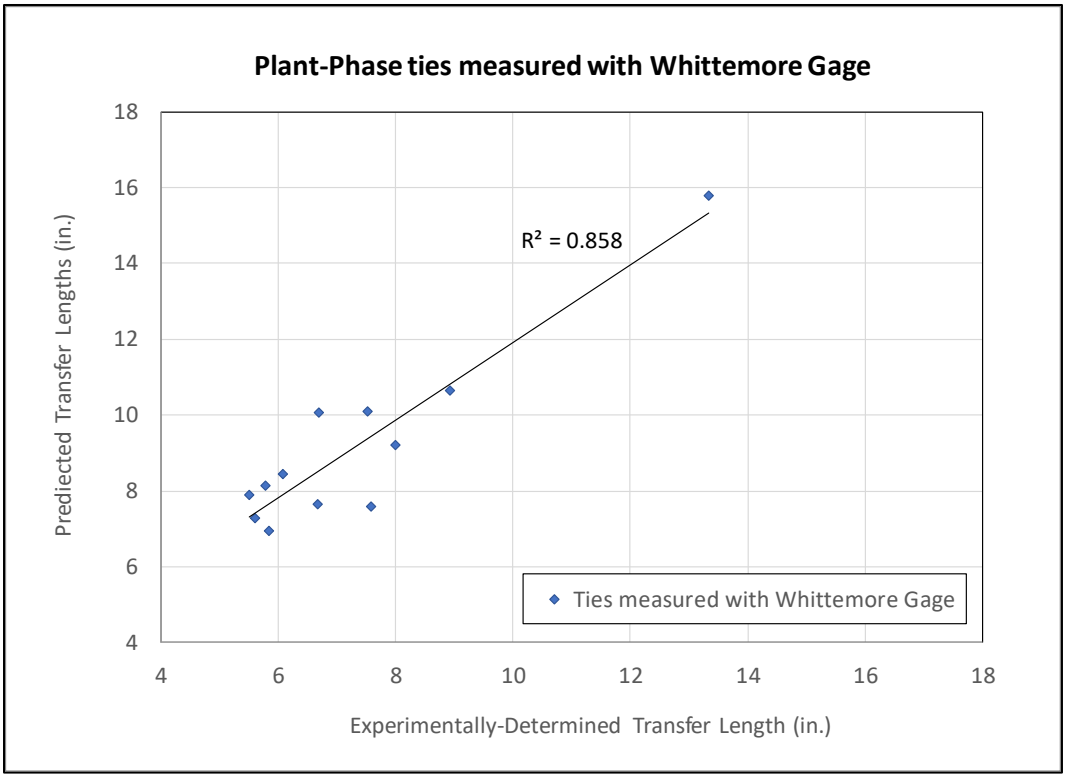

Figure 109 Comparison of experimental and predicted TL values during Plant-Phase

Figure 110 presents the average Plant-Phase TL values for each reinforcement type along with the average TL values from Lab-Phase Group I prisms. The excellent correlation between the Plant-Phase TL data and Lab-Phase TL data indicates that the laboratory prisms, cast with a similar concrete mixture, were able to accurately represent the behavior of the same reinforcement in a concrete railroad tie.

Therefore, in the future, the bond performance of a new reinforcement in concrete railroad ties could be determined by measuring transfer lengths on similar prisms using a representative concrete mix. The small-scale testing of laboratory prisms would provide an economical option for the tie manufacturing industry to select the proper combination of reinforcement type and release strengths to produce the desired transfer length values.

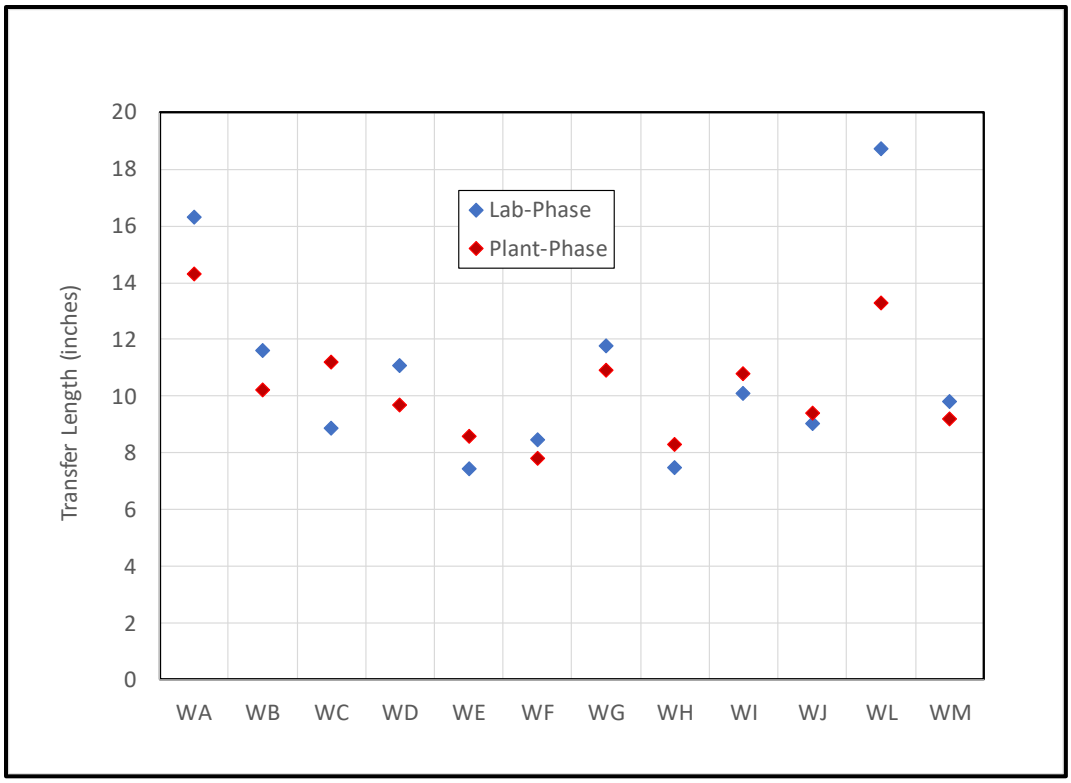

Figure 110 Comparison of Plant-Phase TL with Lab-Phase Group I prisms TL

7.2.2 Strand reinforcements

Strand reinforcement transfer length results obtained Lab-Phase Group I prisms are compared with Plant-Phase results in this section. However, it should be noted that release strengths were significantly different during Lab-Phase and Plant-Phase.

Transfer lengths for strand reinforcements evaluated from Group I prisms during Lab-Phase ranged from 13.8-in. to 16.3-in., corresponding to 44 d_b and 43 d_b, respectively. Whereas, during the Plant-Phase transfer lengths for similar reinforcements ranged from 14.4-in. to 15.9-in. (38 d_b to 51 d_b). The diameters of the three strand reinforcements ([SA], [SB], and [SC]) were 3/8-in., 3/8-in., and 5/16-in. respectively.

During Plant-Phase, the average transfer lengths for the 7-wire 3/8”-diameter smooth ([SA]) and 7-wire 3/8”-diameter indented ([SB]) strands were 14.4-in. and 15.6-in. respectively (38 d_b and 42 d_b). Average transfer lengths during Lab-Phase for [SA], and [SB] were 16.2-in. (43 d_b), and 16.3-in. (43 d_b) respectively. Note, smooth strand [SA] had some very minor surface rusting, whereas indented strand [SB] did not contain any visible rusting. The 3-wire 5/16”-diameter smooth strand ([SC]) had an average transfer length of 15.9-in. (51 d_b) during the Plant-Phase and an average transfer length of 13.8-in. (44 d_b) during Lab-Phase.

7.2.3 Similarities and differences between Lab-Phase (Group I) and Plant-Phase

This section discusses important similarities and differences occurred during the two phases of the study.

Notable Similarities

The same reinforcement samples were used for both Lab-Phase and Plant-Phase of the study and were stored in low-humidity environment (Figure 9). So, these reinforcements were believed to be essentially in the "as-received" condition at the time of casting for both phases.

Similar concrete mixture proportions, having a water-to-cementitious ratio of 0.32, were used during Plant-Phase and for Lab-Phase Group I prisms. However, the source of fine aggregate was different and the Plant-Phase concrete utilized an air-entraining admixture. Approximately same prestressing force was maintained for each reinforcement during Plant-Phase and Lab-Phase. During the Lab-Phase, a special jacking arrangement was fabricated to ensure the tendon pretensioning process was similar to Plant-Phase and the transfer of prestress force into the members was accomplished by a gradual release method that replicating the one used in the Plant-Phase.

During the Lab-Phase; the prism cross-sections each contained four wires or strands, and the dimensions were chosen to replicate the same tendon spacing and reinforcement-to-concrete proportions as typical pre-tensioned concrete crossties produced in a concrete tie manufacturing plant. Whittemore gage was used in both phases to measure the surface displacements due to the introduction of prestressing force.

Notable Differences

There were few notable differences between Lab-Phase (Group I) and Plant-Phase as described below. During the Lab-Phase, the entire casting process of each pour took around 20 minutes and the concrete produced was from a single batch. Later, 6 different transfer length results were recorded from 3 prisms which were cast on a 20-feet length prestressing bed. Whereas, during the Plant-Phase, the entire bed was poured with about 14 different batches of the same concrete mixture over nearly a 2-hour period. Thus, for the Plant-Phase there would naturally be some variations in the fresh concrete properties from mix-to-mix, but there may be also be significant differences in the maturity (compressive strength, tensile strength, and MOE)

of the different mixes at the time of de-tensioning. It is to be noted that 50 transfer length results were recorded on 25 ties that were cast near the beginning, middle, and ends of a 385.75-ft. long prestressing bed. Uniform release strengths (4500 psi ±220 psi) were maintained during Lab-Phase for all the reinforcements. During the Plant-Phase, since the ties were manufactured in a production environment where many other ties were also being fabricated during the same day, de-tensioning did not occur at precisely the same compressive strength for each reinforcement. Rather, the ties were de-tensioned when the compressive strength was at least 5000 psi and when the de-tensioning crew was available. Thus, the compressive strength at de-tensioning varied between 5063 psi and 6650 psi for the ties manufactured with the 15 different reinforcements. This corresponds to a comparative release strength of 5860 psi ±795 psi.

7.3 Long-term transfer length results from Plant-Phase crossties (Stage I)

During the long-term study, only crossties with embedded brass inserts (that utilized the Whittemore gage) for surface-displacement measurements were investigated. Upon the completion of the surface preparation of “T”-marked crossties, all Plant-Phase crossties with brass inserts were separated by markings. The “K”-marked crossties were shipped to KSU for long-term monitoring without being subjected to in-track loading. Whereas, “T”-marked crossties were stored at the CXT plant in Tucson, AZ for one year (from Jan 2013 to Jan 2014) and subsequently shipped to the TTCI facility in Pueblo, CO for in-track loading.

Table 58 summarized the TL results at de-tensioning and after Stage I for "T"-marked and "K"-marked crossties. TL increase during Stage I for wire and strand reinforcements are depicted in Figure 111 and Figure 112, respectively. Similarly, the percentage increase in TL during Stage I is tabulated in Table 59 and shown in Figure 113 and Figure 114.

Table 58 TL length results immediately after de-tensioning and after Stage I

Prestressing tendon type	TL results at de-tensioning for "T"-marked crossties [TL/d_b]	End of "Stage I" TL results for "T" mark crossties [TL/d_b]	TL results at de-tensioning for "K"-marked crossties [TL/d_b]	End of "Stage I" TL results for "K"-marked crossties [TL/d_b]
WA	13.45 [64]	15.55 [74]	13.20 [63]	17.63 [84]
WB	7.93 [38]	8.90 [42]	7.23 [34]	8.93 [43]
WC	6.45 [31]	10.75 [51]	6.88 [33]	12.13 [58]
WD	6.78 [32]	8.10 [39]	6.58 [31]	8.18 [39]
WE	4.90 [23]	7.08 [34]	6.10 [29]	8.33 [40]
WF	5.53 [26]	7.10 [34]	5.65 [27]	7.25 [35]
WG	7.15 [34]	9.35 [45]	7.88 [38]	10.13 [48]
WH	5.78 [28]	7.30 [35]	5.78 [28]	7.23 [34]
WI	7.90 [38]	10.20 [49]	8.10 [39]	9.60 [46]
WJ	6.08 [29]	7.25 [35]	6.08 [29]	7.85 [37]
WL	9.53 [45]	12.20 [58]	8.33 [40]	11.68 [56]
WM	6.15 [29]	7.58 [36]	5.50 [26]	6.60 [32]
SA	11.23 [30]	13.53 [36]	11.50 [31]	17.40 [46]
SB	13.55 [36]	14.80 [39]	14.18 [38]	17.15 [46]
SC	11.23 [36]	12.53 [40]	10.98 [35]	14.35 [46]

Table 59 Transfer length increases during Stage I (in percentages)

Prestressing tendon type	Percentage increase in transfer lengths for “T”-marked ties during "Stage I"	Percentage increase in transfer lengths for “K”-marked ties during "Stage I"
WA	16%	34%
WB	12%	24%
WC	67%	76%
WD	20%	24%
WE	44%	36%
WF	29%	28%
WG	31%	29%
WH	26%	25%
WI	29%	19%
WJ	19%	29%
WL	28%	40%
WM	23%	20%
SA	20%	51%
SB	9%	21%
SC	12%	31%

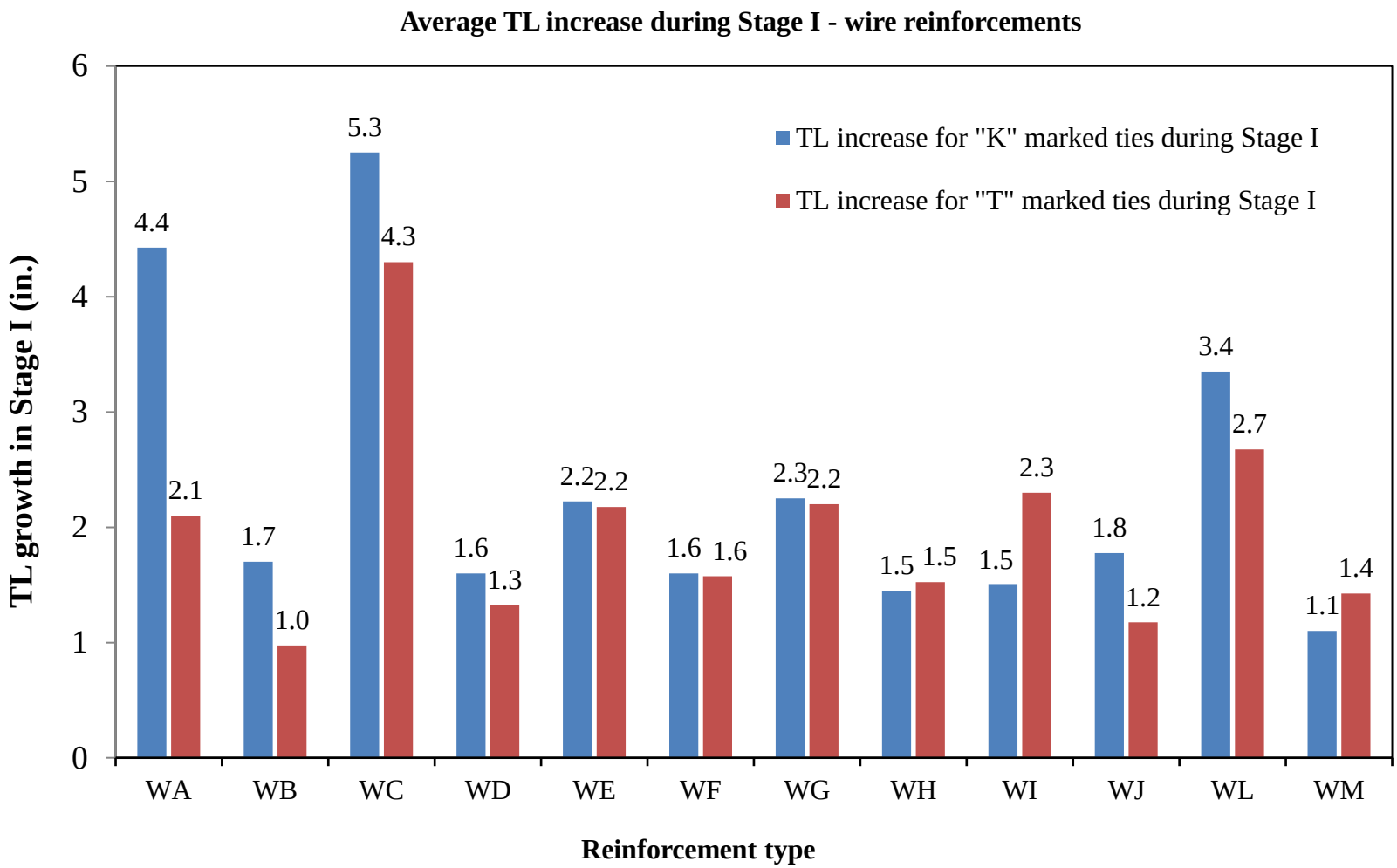

Figure 111 Average increase in transfer length during Stage I (wire reinforcements)

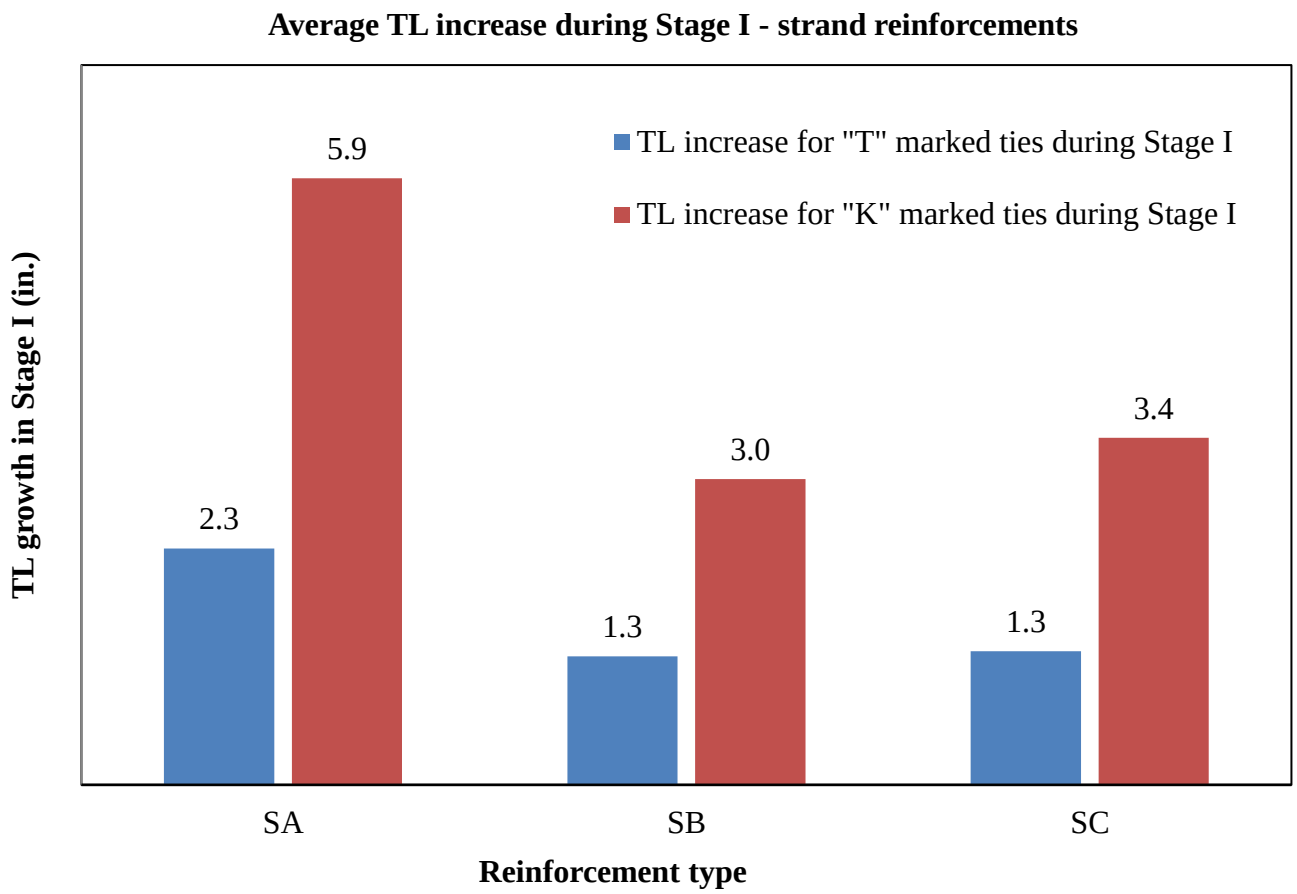

Figure 112 Average increase in transfer length during Stage I (strand reinforcements)

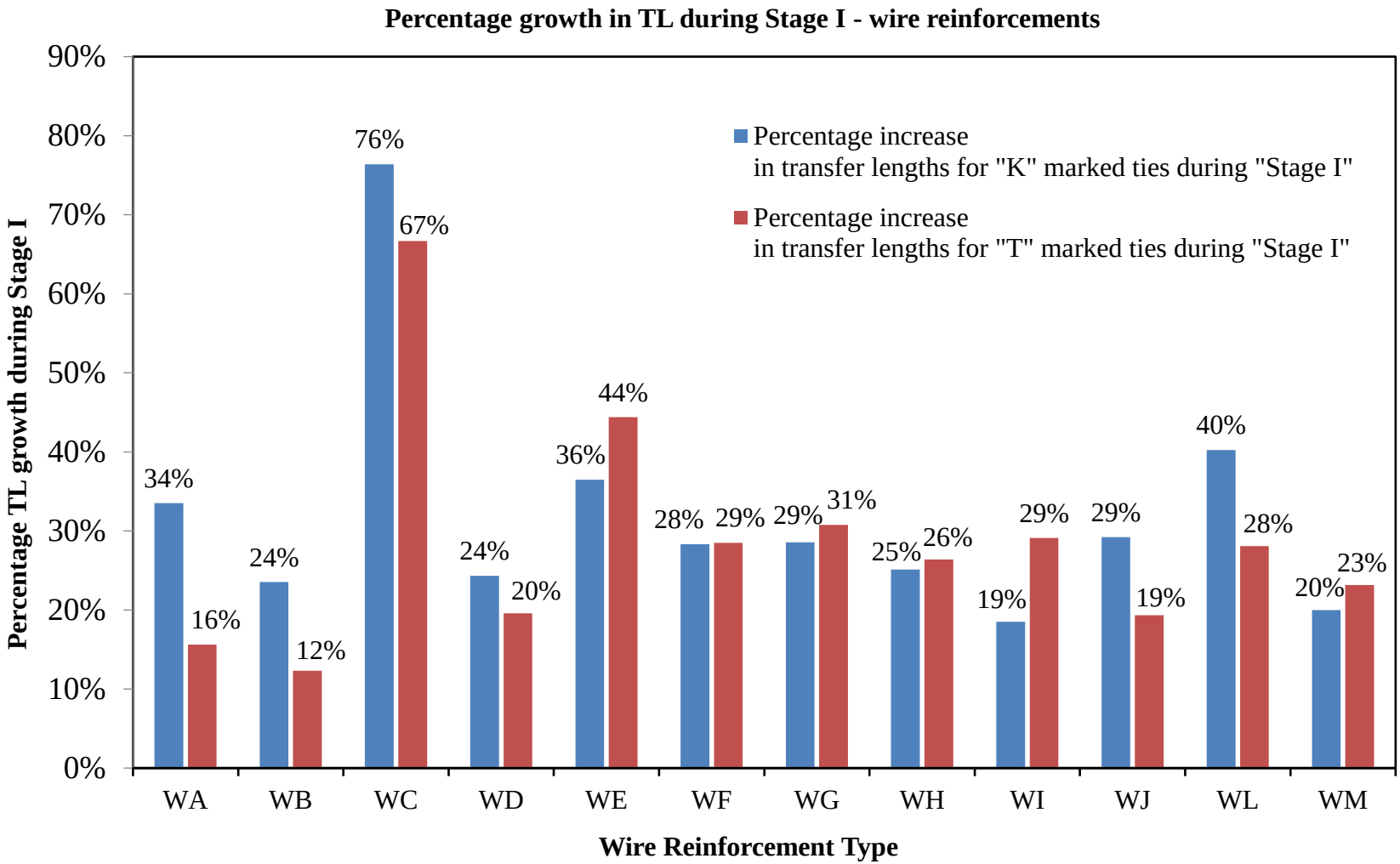

Figure 113 Percentage growth in TL during Stage I (wire reinforcements)

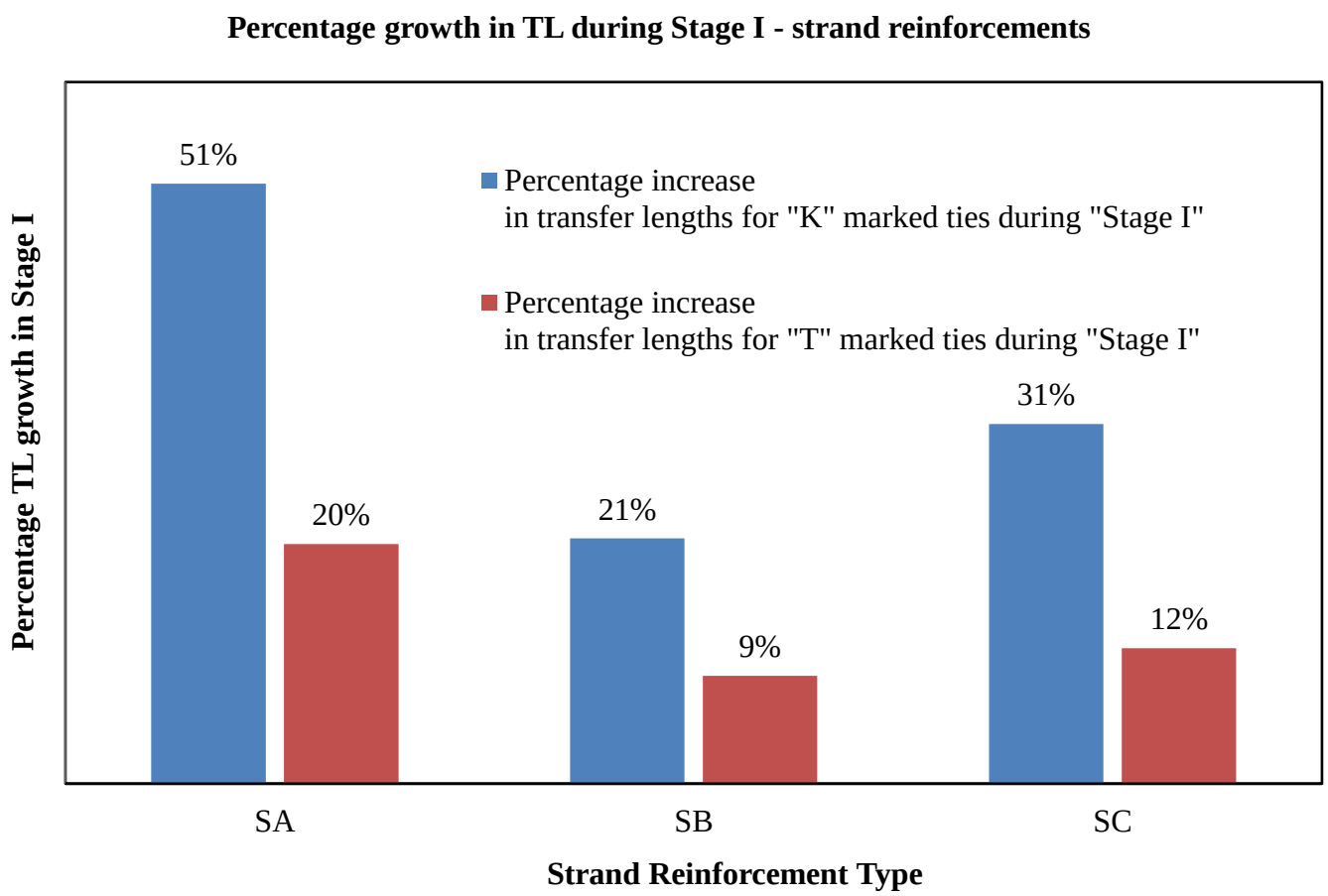

Figure 114 Percentage growth in TL during Stage I (strand reinforcements)

7.3.1 Transfer length increase in “K”-marked crossties during Stage I

From Table 58, the average long-term transfer lengths for the ties stored at KSU and fabricate with 5.32-mm wires ranged from 6.60 in. to 17.63 in. This corresponds to a value of 32 d_b to 84 d_b. Percentage growths in transfer lengths for different reinforcements are tabulated in Table 59 and shown in Figure 113 and Figure 114. Figure 116 and Figure 117 compare the average transfer length at detensioning and after Stage I for the “K”-marked crossties with wire reinforcements and strand reinforcements, respectively. A typical surface-strain profile for a “K”-marked crosstie at the end of Stage I is shown in Figure 115.

The average transfer length increase (“K”-marked crossties) for chevron-shaped indented wires ranged from 19% [WI] to 29% ([WG], [WJ]). The average transfer length increase of the spiral-indented wires were 36% and 76% for [WE] and [WC] respectively. An average transfer length increase of 40% was observed in the case of 2-dot indent pattern (minimal indentation). In the case of diamond pattern [WF], the average transfer length increase was 28%. Transfer length increase for the ties manufactured with [WA] and stored at KSU was 34%.

The average transfer lengths (after Stage I) for the 7-wire 3/8”-diameter smooth [SA] and 7-wire 3/8”-diameter indented [SB] strands were 17.40 in. and 17.15 in. respectively (transfer length increases of 51% and 21%). This corresponds to values of 46 d_b and 46 d_b respectively. The 3-wire 5/16”-diameter smooth strand [SC] had an average transfer length (after Stage I) of 14.35 in., which corresponds to 46 d_b (for a transfer length increase of 31%).

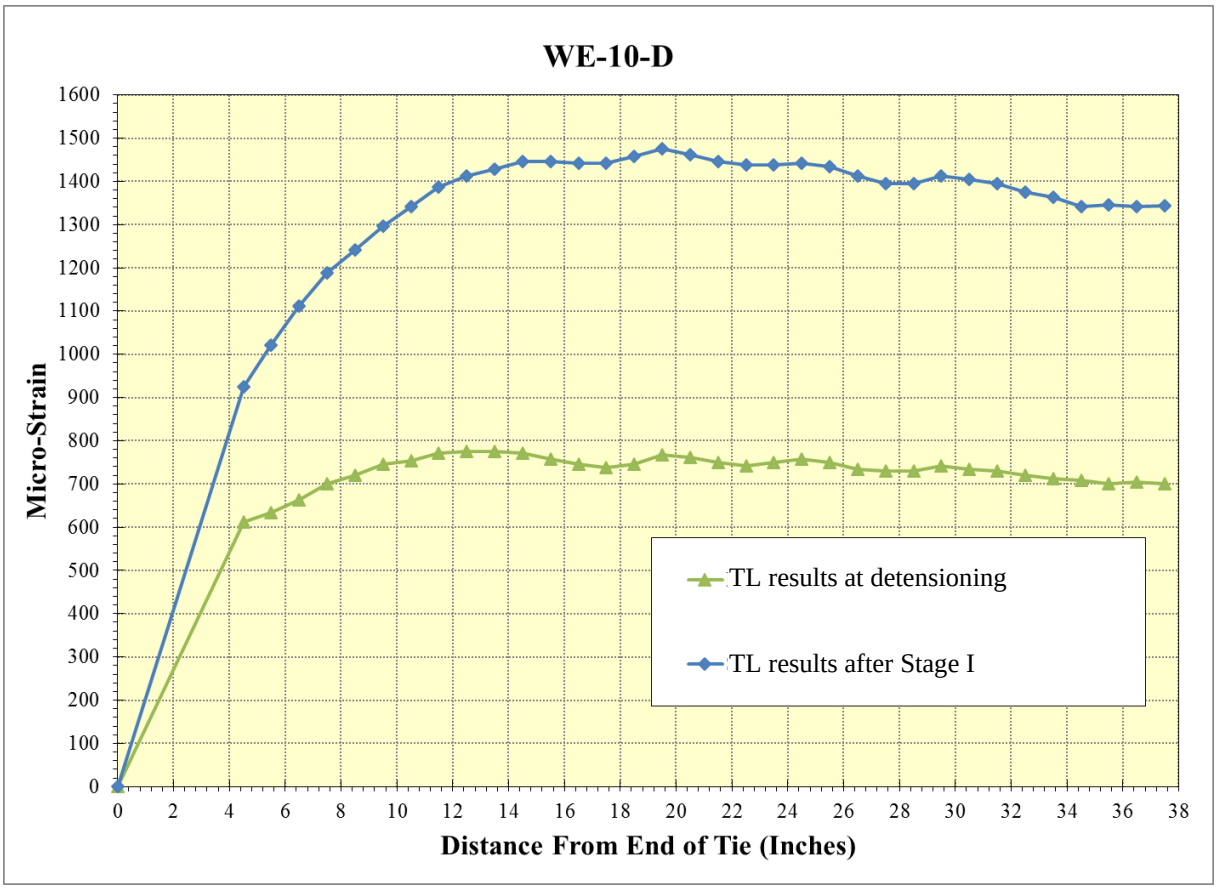

Figure 115 Typical surface-strain profile for a “K”-marked crosstie at the end of Stage I

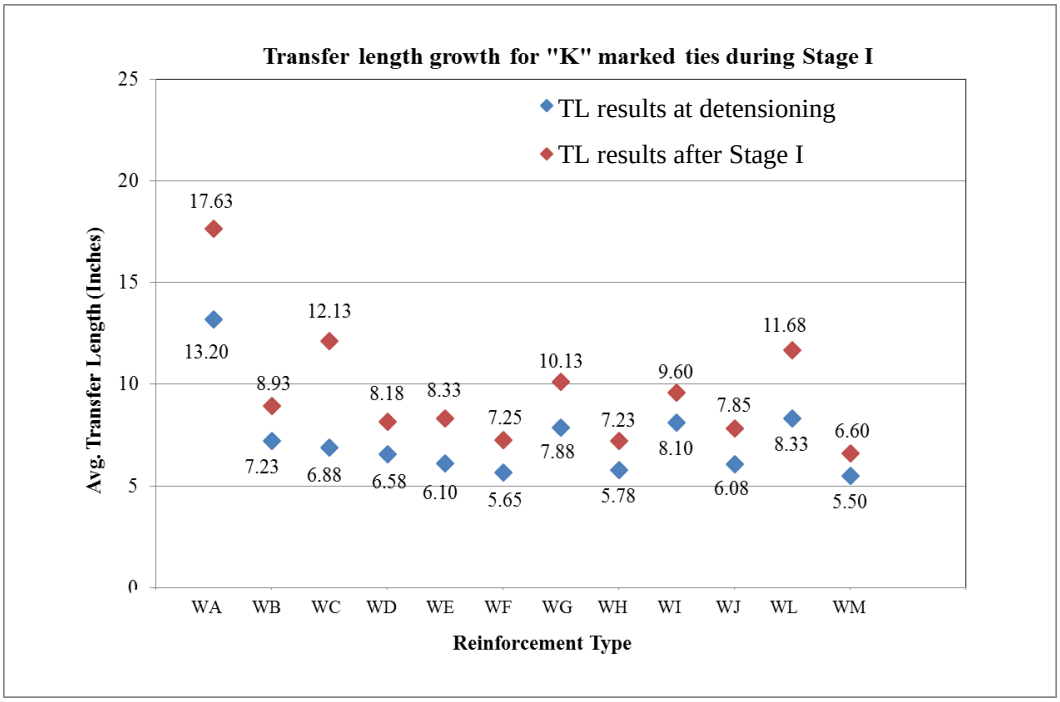

Figure 116 TL increase for “K”-marked crossties at the end of Stage I (wire reinforcements)

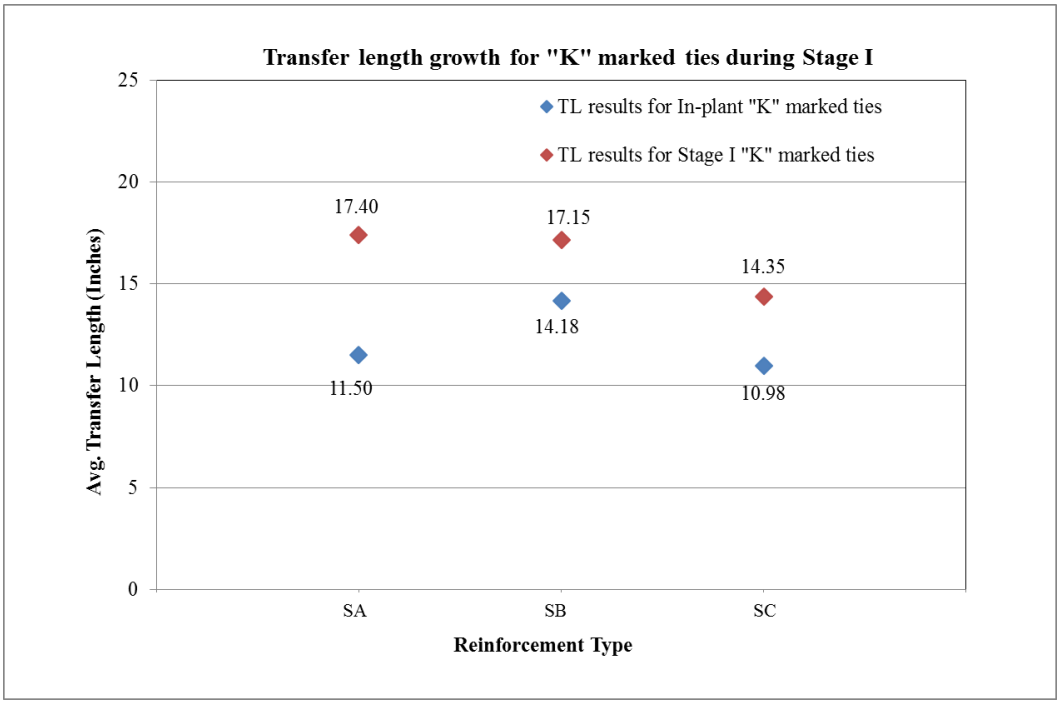

Figure 117 TL increase for “K”-marked crossties at the end of Stage I (strand reinforcements)

7.3.2 Transfer length increase in “T”-marked crossties during Stage I

From Table 58, the average long-term transfer lengths for the crossties stored at the Tucson, AZ plant and fabricated with 5.32-mm wires ranged from 7.08 in. to 15.55 in. This corresponds to values of 34 d_b to 74 d_b. Percentage growths in transfer lengths for the different wire reinforcements are tabulated in Table 59 and shown in Figure 113 and Figure 114. Figure 119 and Figure 120 compares the average transfer lengths at detensioning and after Stage I for “T”-marked crossties with wire reinforcements and strand reinforcements respectively. A typical surface-strain profile for a “T”-marked crosstie at the end of Stage I is shown in Figure 118.

The average transfer length increase (“T”-marked crossties) for chevron-shaped indented wires ranged from 12% [WB] to 31% [WG]. The average transfer length increase of the spiral-indented wires were 44% and 67% for [WE] and [WC] respectively. An average transfer length increase of 28% was observed in the case of 2-dot indent pattern (minimal indentation). In the case of diamond pattern [WF], the average transfer length increase was 29%. The transfer length increase for the manufactured with [WA] 16%.

The average transfer lengths (“T”-marked ties) for the 7-wire 3/8”-diameter smooth [SA] and 7-wire 3/8”-diameter indented [SB] strands were 13.53 in. and 14.80 in. respectively (for a transfer length increase of 20% and 9%). This corresponds to values of 36 d_b and 39 d_b respectively. The 3-wire 5/16”-diameter smooth strand [SC] had an average transfer length of 12.53 in., which corresponds to 40 d_b (for a transfer length increase of 12%).

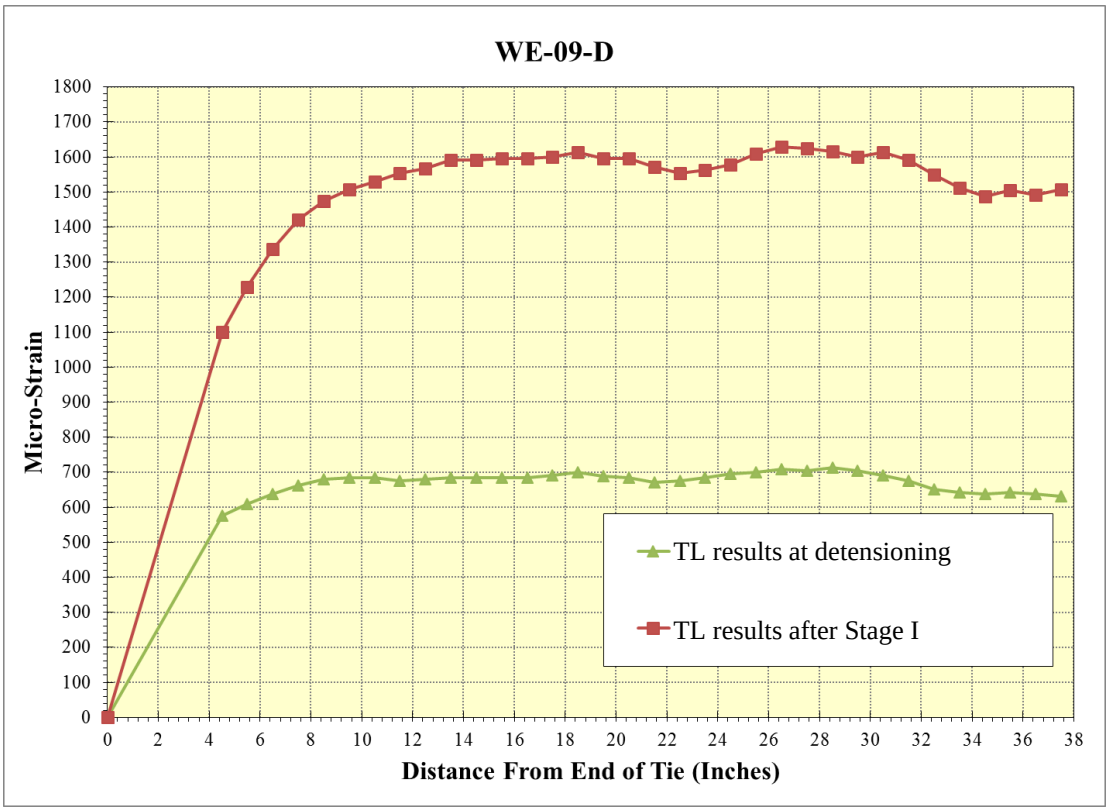

Figure 118 Typical surface-strain profile for a “T”-marked crosstie at the end of Stage I

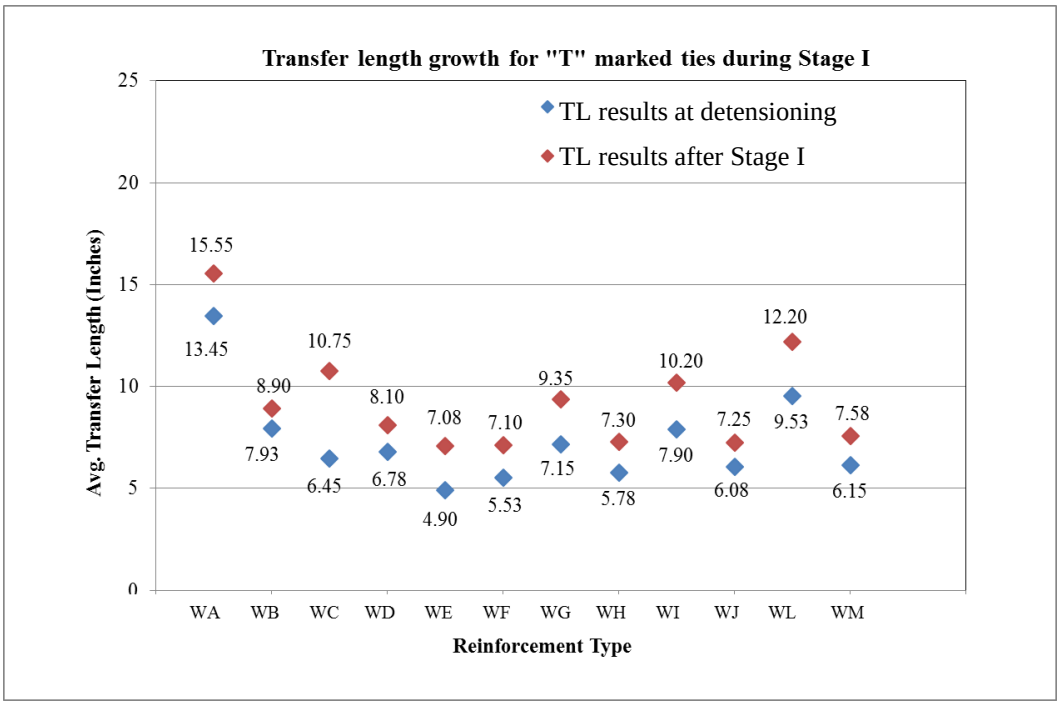

Figure 119 TL increase for “T”-marked crossties at the end of Stage I (wire reinforcements)

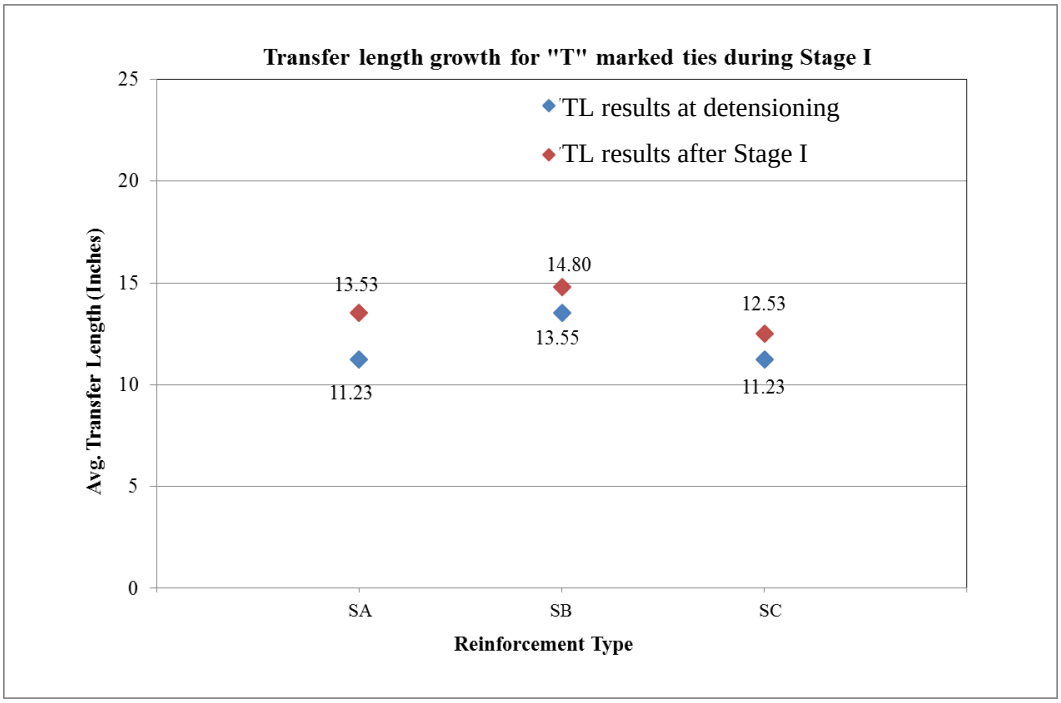

Figure 120 TL increase for “T”-marked crossties at the end of Stage I (strand reinforcements)

7.3.3 Comparison of transfer lengths at the end of Stage I

Figure 113 and Figure 114 compares the percentage growth in transfer length at the end of Stage I for “K”-marked ties and “T”-marked ties. From these figures, the transfer length percentage growth is observed to be somewhat inconsistent for the different reinforcing tendon types. However, higher percentage increase in transfer lengths were generally observed for the ties stored at KSU (“K”-marked crossties) compared to ties stored in Tucson, AZ (“T”-marked crossties). From Table 61, the average increase for “K”-marked crossties through Stage 1 was 33% while for “T”-marked crossties the average was only 27%.

It is to be noted that any differences in the transfer length trends during State I are believed to be primarily due to different climatic conditions (Manhattan, KS vs Tucson, AZ), since during Stage I both “T”-marked crossties and “K”-marked crossties were not subjected to any loading. However, crossties were stored at two very different climatic conditions.

Among all the reinforcements, highest transfer growth was observed for the ties manufactured with [WC]. These highest transfer length increases were 67% and 76% for the ties stored at plant and KSU, respectively.

For the “T”-marked crossties stored in Tucson, AZ, the lowest transfer length increase was 9% in the case of [SB], whereas for the ties stored at KSU, the lowest transfer length increase was observed in the case of [WI] which was 19%.

7.4 Long-term transfer length results from Plant-Phase crossties (Stage II)

After the completion of Stage I, “T”-marked crossties were shipped to the TTCI facility in Pueblo, CO for in-track loading. These ties were subjected to a cumulative in-track loading of 84.46 Million Gross Tons (MGT) in straight (tangent) track. This is referred to as “Stage II”. Later, these ties were removed from track to measure the concrete surface displacements using the embedded brass inserts and the Whittemore gage. The corresponding surface-strain profile was then used to determine the long-term transfer lengths.

During this same period, the “K”-marked crossties continued to be stored at KSU without any loading. Transfer length results of both “K”-marked and “T”-marked crossties through the end of “Stage II” are tabulated in Table 60. Percentage growths in transfer lengths for different reinforcements are tabulated in Table 61.

Table 60 Transfer length results at detensioning, after Stage I, and after Stage II

	"T"-marked Crossties			"K"-marked Crossties		
Tendon type	TL results at detensioning inches [TL/d_b]	TL results at End of "Stage I" inches [TL/d_b]	TL results at End of "Stage II" inches [TL/d_b]	TL results at detensioning inches [TL/d_b]	TL results at End of "Stage I" inches [TL/d_b]	TL results at End of "Stage II" inches [TL/d_b]
WA	13.45 [64]	15.55 [74]	17.95 [86]	13.20 [63]	17.63 [84]	15.75 [75]
WB	7.93 [38]	8.90 [42]	9.48 [45]	7.23 [34]	8.93 [43]	8.73 [42]
WC	6.45 [31]	10.75 [51]	11.70 [56]	6.88 [33]	12.13 [58]	11.48 [55]
WD	6.78 [32]	8.10 [39]	8.58 [41]	6.58 [31]	8.18 [39]	7.53 [36]
WE	4.90 [23]	7.08 [34]	7.40 [35]	6.10 [29]	8.33 [40]	8.43 [40]
WF	5.53 [26]	7.10 [34]	7.48 [36]	5.65 [27]	7.25 [35]	7.30 [35]
WG	7.15 [34]	9.35 [45]	10.08 [48]	7.88 [38]	10.13 [48]	9.55 [46]
WH	5.78 [28]	7.30 [35]	7.90 [38]	5.78 [28]	7.23 [34]	7.13 [34]
WI	7.90 [38]	10.20 [49]	10.43 [50]	8.10 [39]	9.60 [46]	9.63 [46]
WJ	6.08 [29]	7.25 [35]	8.15 [39]	6.08 [29]	7.85 [37]	7.43 [35]
WL	9.53 [45]	12.20 [58]	13.60 [65]	8.33 [40]	11.68 [56]	11.75 [56]
WM	6.15 [29]	7.58 [36]	8.05 [38]	5.50 [26]	6.60 [32]	7.33 [35]
SA	11.23 [30]	13.53 [36]	14.98 [40]	11.50 [31]	17.40 [46]	16.30 [43]
SB	13.55 [36]	14.80 [39]	17.18 [46]	14.18 [38]	17.15 [46]	17.33 [46]
SC	11.23 [36]	12.53 [40]	13.85 [44]	10.98 [35]	14.35 [46]	13.88 [44]

Table 61 Transfer length increases through Stage II in percentages:

	"T"-marked Crossties			"K"-marked Crossties		
Prestressing Tendon type	% increase in LT from prestress transfer to end of Stage I"	% increase in LT from prestress transfer to end of Stage II"	% increase during Stage II"	% increase in LT from prestress transfer to end of Stage I"	% increase in LT from prestress transfer to end of Stage II"	% increase during Stage II"
WA	16%	33%	15%	34%	19%	-11%
WB	12%	20%	6%	24%	21%	-2%
WC	67%	81%	9%	76%	67%	-5%
WD	20%	27%	6%	24%	14%	-8%
WE	44%	51%	5%	36%	38%	1%
WF	29%	35%	5%	28%	29%	1%
WG	31%	41%	8%	29%	21%	-6%
WH	26%	37%	8%	25%	23%	-1%
WI	29%	32%	2%	19%	19%	0%
WJ	19%	34%	12%	29%	22%	-5%
WL	28%	43%	11%	40%	41%	1%
WM	23%	31%	6%	20%	33%	11%
SA	20%	33%	11%	51%	42%	-6%
SB	9%	27%	16%	21%	22%	1%
SC	12%	23%	11%	31%	26%	-3%
Averages	**27%**	**38%**	**9%**	**33%**	**29%**	**-2%**

7.4.1 Change in transfer length for "T"-marked crossties due to 84.46 MGT in-track loading (Stage II)

From Table 60, the average transfer lengths at the end of Stage II for "T"-marked crossties ranged from 7.40 in. to 17.95 in. This corresponds to a range of 35 d_b to 86 d_b. Surface-strain profiles for a "T"-marked tie through the end of Stage II are shown in Figure 121.Figure 122 and Figure 123 compares the average TLs at the end of Stage II for "T"-marked crossties with wires and strands, respectively.

The average transfer length increase from Stage I to Stage II ("T"-marked ties) for chevron-shaped indented wires ranged from 2% [WI] to 12% [WJ]. The average transfer length increase (from Stage I to Stage II) of the spiral-indented wires were 5% and 9% for [WE] and [WC] respectively. An average transfer length increase of 11% was observed in the case of 2-dot indent pattern [WL] having minimal indentations. In the case of diamond pattern [WF], the average transfer length increase was only 5%. Transfer length increase for the ties manufactured with WA was 15%. Therefore, upon the application of 84.46 MGT in-track loading, TL increase was not nearly as substantial as the increase occurring during Stage I (without any loading).

Also, TL results for ties cast with smooth wire [WA] displayed highest increase in TL during Stage II. This suggests that the indentation of wire reinforcements may serve to resist additional slippage of the prestressing reinforcements when subjected to loading (and minimize the long-term increase in transfer length).

From Table 60 and Table 61, the average transfer lengths (Stage II "T"-marked ties) for the 7-wire 3/8"-diameter smooth [SA] and 7-wire 3/8"-diameter indented [SB] strands were 14.98 in. and 17.18 in. respectively (for a transfer length increase of 11% and 16% during Stage II). This corresponds to values of 40 d_b and 46 d_b respectively. The 3-wire 5/16"-diameter smooth strand [SC] had an average transfer length of 13.85 in., which corresponds to 44 d_b (for a transfer length increase of 11%).

Percentage increase in transfer length for the different reinforcements are tabulated in Table 61. Under the Stage II loading conditions, ties manufactured with indented wire reinforcements typically had lower percentage increase in TL compared to the ties manufactured with strand reinforcements. From this, it can be said that, crossties manufactured with indented wire reinforcements generally tend to have less TL increase under in-track loading conditions.

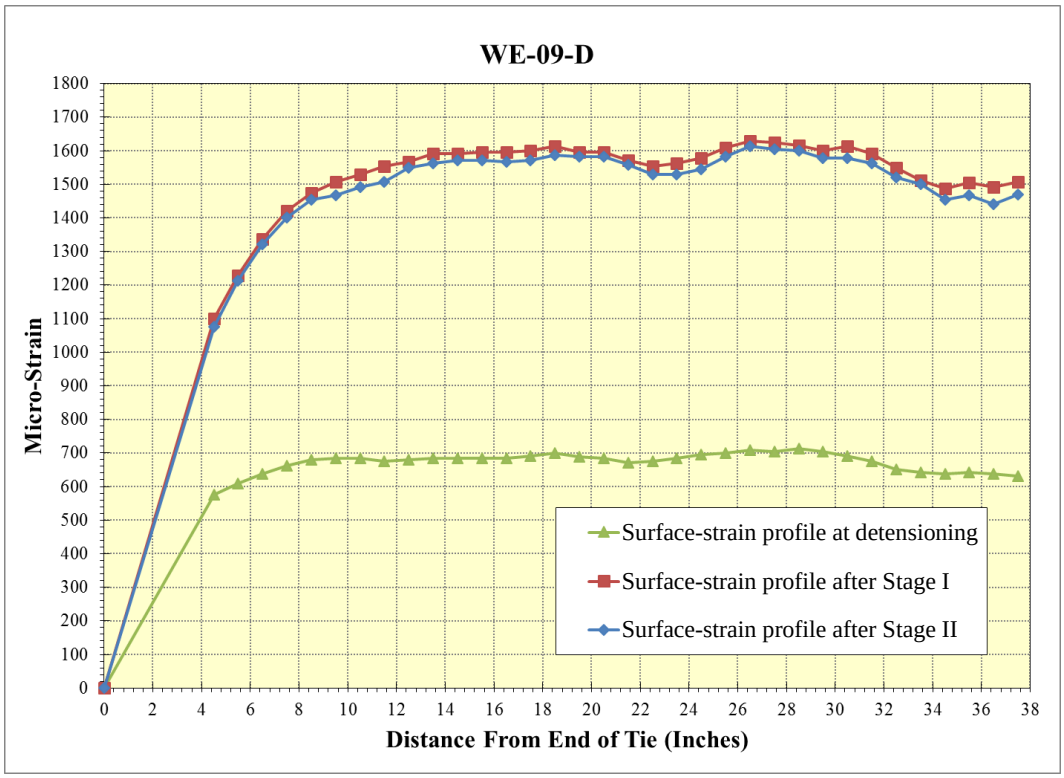

Figure 121 Typical surface-strain profile for a “T”-marked tie at the end of Stage II

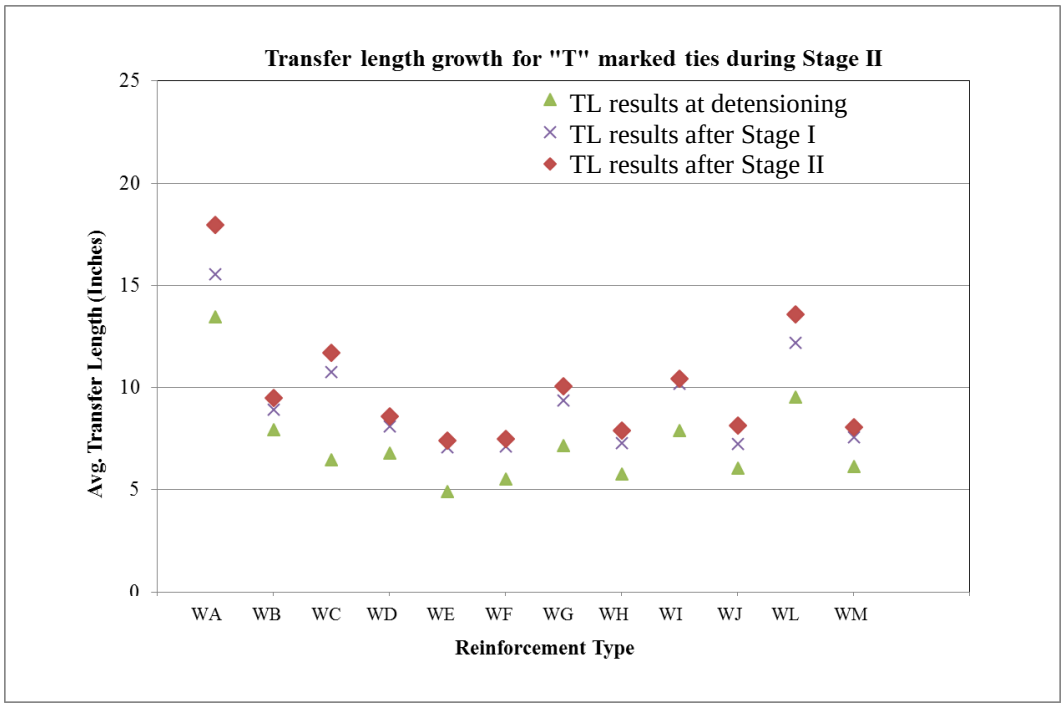

Figure 122 TL variation for “T”-marked ties at the end of Stage II (wire reinforcements)

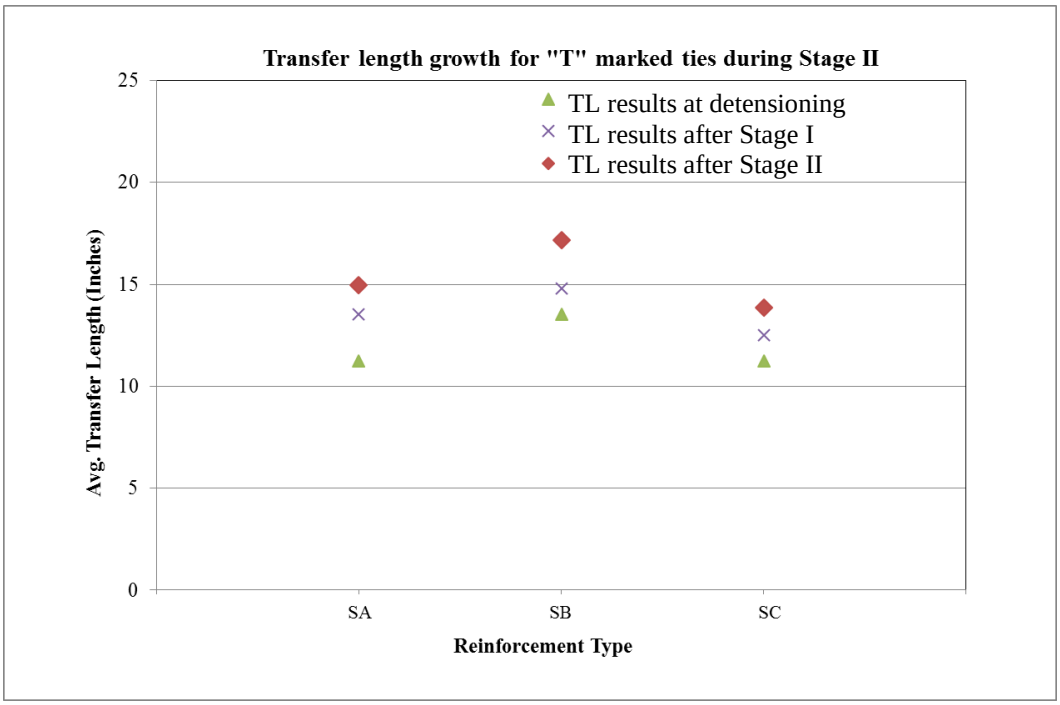

Figure 123 TL variation for “T”-marked ties at the end of Stage II (strand reinforcements)

7.4.2 Change in transfer length for “K”-marked crossties during Stage II

Transfer length results for “K”-marked ties at the end of Stage II are also tabulated in Table 60 and Table 61. The average transfer lengths at the end of Stage II for crossties fabricated with 5.32-mm wires and stored at KSU ranged from 7.13 in. to 15.75 in. This corresponds to values of 34 d_b to 75 d_b. A surface-strain profiles for a “K”-marked tie through the end of Stage II are shown in Figure 124. Figure 125 and Figure 126 compare the average TLs at the end of Stage II for “K”-marked crossties with wires and strands, respectively.

From Table 61, the average indicated change in transfer length during Stage II for “K”-marked ties was -2%, which means that the overall average transfer lengths did not increase during this stage. Note, the indicated average change of -2% is believed to be in the margin of error for the measurements, and that no consistent change actually occurred. For the “K”-marked crossties, 9 of the 15 reinforcements indicated a negative percentage change, while 6 of 15 had a positive percentage change.

This behavior is in contrast with Stage II results for “T”-marked ties, in which every reinforcing type exhibited a transfer length increase with an average increase of 9% for all reinforcements.

It should also be noted that, at the time of initial data analysis of Plant-Phase crossties, the processing algorithm for use with non-prismatic cross-sections (Zhao, et al., 2013) had not been developed. Therefore, the original ZL processing algorithm based on a prismatic cross-section was used for the determination of all initial transfer lengths from the Plant-Phase. Hence, in order to provide a consistent methodology, the same algorithm was use for the processing of all long-term data of “T”-marked and “K”-marked crossties.

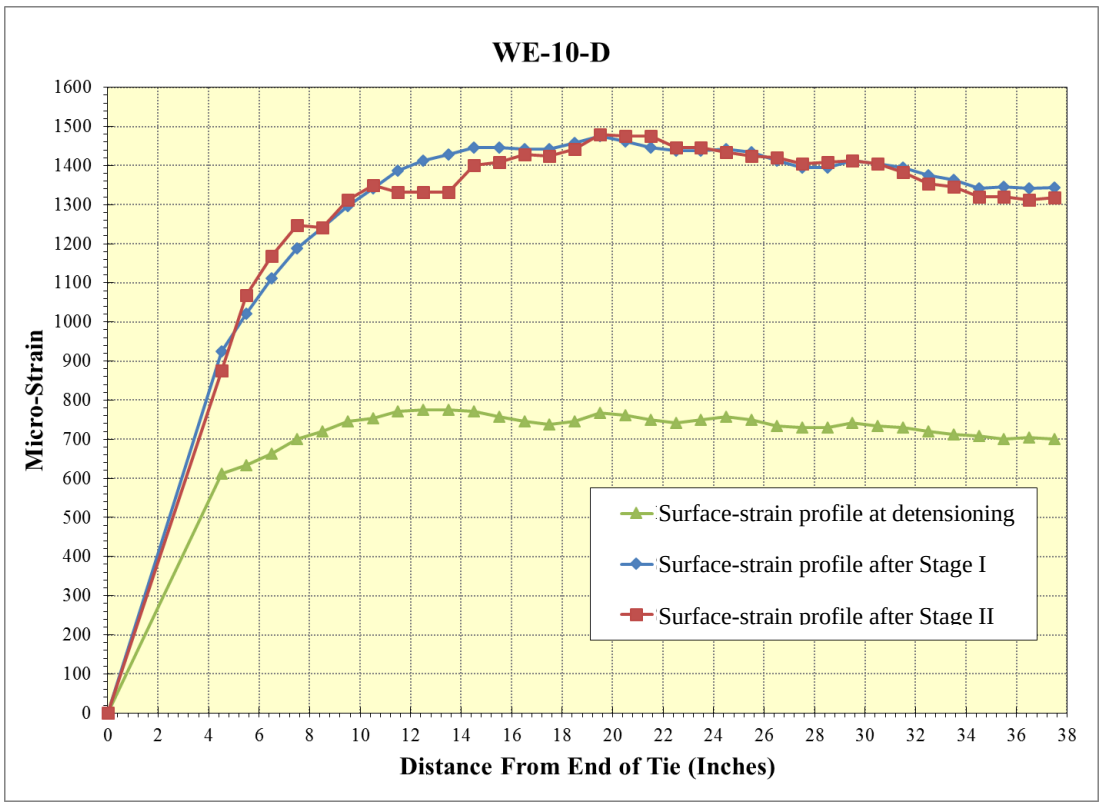

Figure 124 Typical surface-strain profile for a “K”-marked tie at the end of Stage II

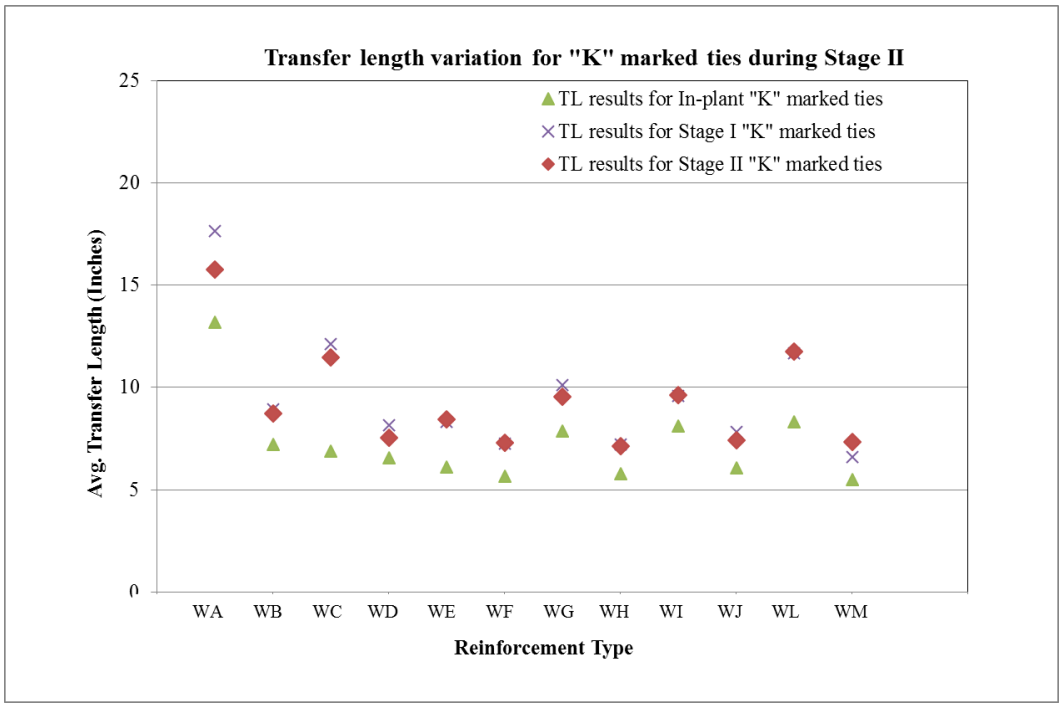

Figure 125 TL variation for “K”-marked ties at the end of Stage II (wire reinforcements)

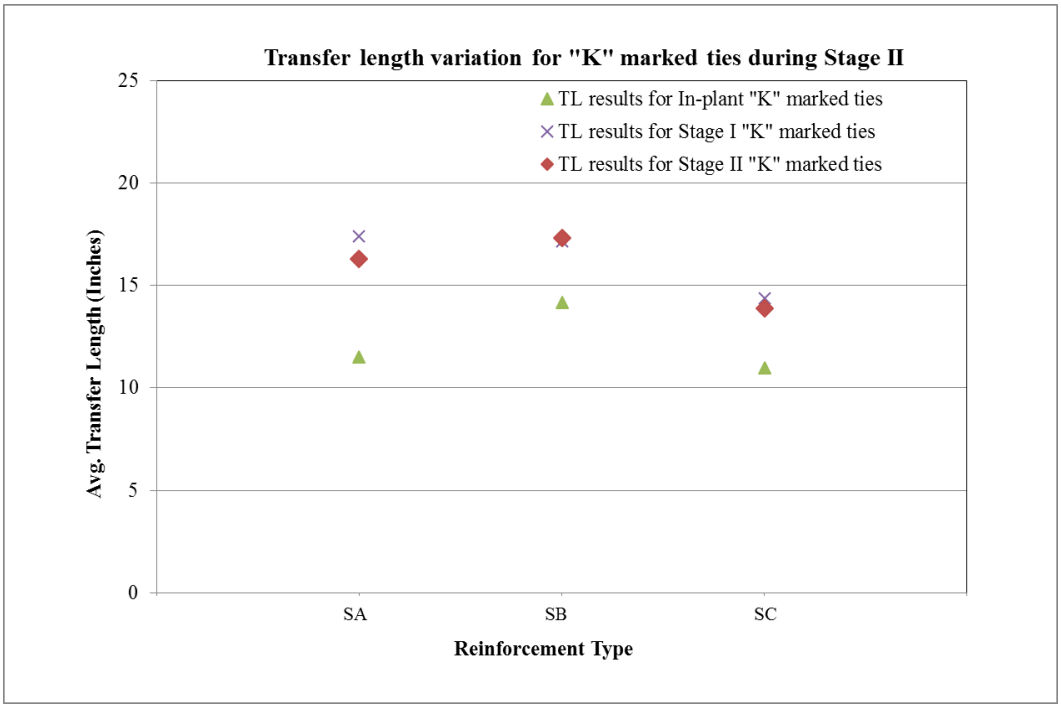

Figure 126 TL variation for “K”-marked ties at the end of Stage II (strand reinforcements)

7.5 Long-term study on plant manufactured ties (Stage III)

Upon the completion of Stage II, “T”-marked crossties were again installed in track at TTCI and subjected to additional loading. During Stage III, these ties were subjected to an additional 151.85 MGT loading in curved track, for a cumulative (including Stage II) in-track loading of 236.31 MGT. During Stage III, the “K”-marked crossties continued to be stored at KSU without any loading.

After the application of Stage III loading in curved track, the “T”-marked crossties were once again removed from track to measure the concrete surface displacements using the Whittemore gage, and thereby determine transfer lengths from the corresponding strain profiles. Prior to removing the protective bottom plates for the Whittemore readings, the crossties were shipped to Manhattan, KS where they remained until the end of the project. Transfer length changes for “T”-marked crossties during Stage III, along with all other stages, are tabulated in Table 62. In this section, results for “T”-marked crossties cast with the 12 wire reinforcements are presented.

Figure 127 “T”-marked crossties installed in curved track during Stage III

Table 62 TL length results for “T”-marked ties in all stages

Reinforcement type	In-Plant TL results for "T" mark crossties [TL/d_b]	End of "Stage I" TL results for "T" mark crossties [TL/d_b]	End of "Stage II" TL results for "T" mark crossties [TL/d_b]	End of "Stage III" TL results for "T" mark crossties [TL/d_b]
WA	13.45 [64]	15.55 [74]	17.95 [86]	18.38 [88]
WB	7.93 [38]	8.90 [42]	9.48 [45]	9.66 [46]
WC	6.45 [31]	10.75 [51]	11.70 [56]	12.23 [58]
WD	6.78 [32]	8.10 [39]	8.58 [41]	8.80 [42]
WE	4.90 [23]	7.08 [34]	7.40 [35]	7.72 [37]
WF	5.53 [26]	7.10 [34]	7.48 [36]	7.52 [36]
WG	7.15 [34]	9.35 [45]	10.08 [48]	10.61 [51]
WH	5.78 [28]	7.30 [35]	7.90 [38]	8.07 [39]
WI	7.90 [38]	10.20 [49]	10.43 [50]	10.59 [51]
WJ	6.08 [29]	7.25 [35]	8.15 [39]	8.04 [38]
WL	9.53 [45]	12.20 [58]	13.60 [65]	14.47 [69]
WM	6.15 [29]	7.58 [36]	8.05 [38]	8.47 [40]

7.5.1 Transfer length variation in "T"-marked crossties due to additional 151.85 MGT loading in curved track (Stage III)

From Table 62, the average transfer lengths for "T"-marked crossties fabricated with 5.32-mm wires at the end of Stage III ranged from 7.52 in. [WF] to 18.38 in. [WA]. This corresponds to values of 36 d_b to 88 d_b. Surface-strain profiles for a typical "T"-marked crosstie through the end of Stage III are shown in Figure 128. Figure 129 compares the average TLs at the end of Stage III for "T"-marked crossties with wire reinforcements.

Percentage increases in transfer lengths for the different wire reinforcements through the end of Stage III are tabulated in Table 63 and shown in Figure 131. TL increase for different wire reinforcements at the end of Stage III are shown in Figure 130. From this figure, all "T"-marked crossties with wire reinforcements exhibited a small increase in transfer length during Stage III.

From Figure 130, the average transfer length increase from Stage II to Stage III was less than one inch for all wire reinforcements. The uniform trend for all "T"-marked ties was that the largest increase in transfer length occurred during Stage I (no loading), with smaller increases occurring for Stage II and Stage III, with Stage II increase larger than the Stage III increase.

Hence, the increase in transfer length seems to be more affected by the amount of elapsed time since detensioning and by storage location, rather than the subjection to in-track transverse loading. As previously noted, transfer length changes in "T"-marked crossties were minimal during Stage III, while being subjected to an additional 151.85 MGT of loading in curved track.

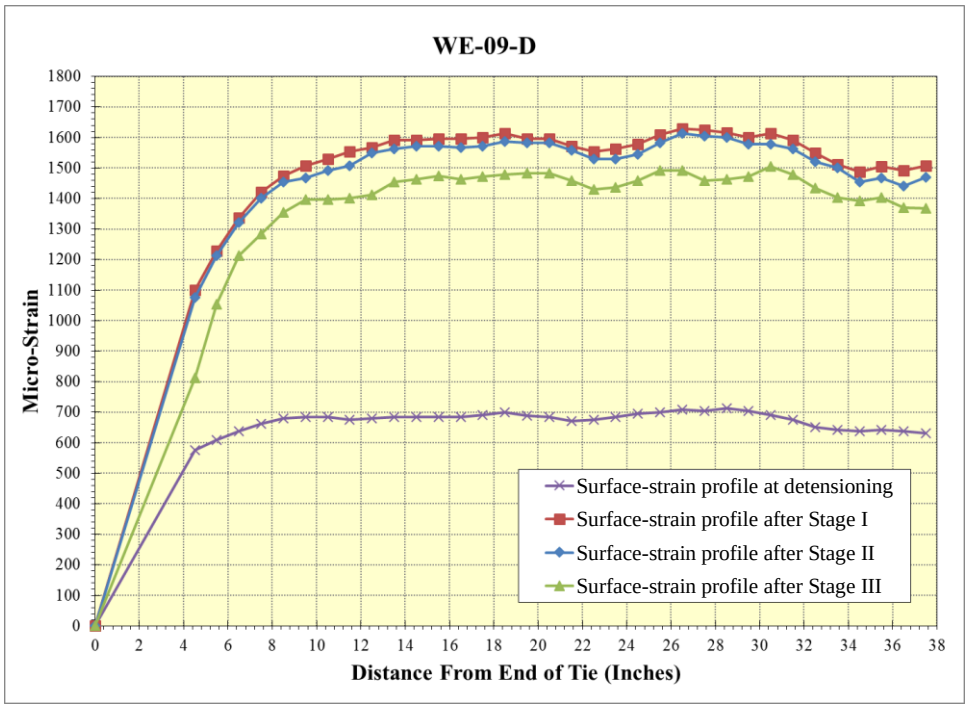

Figure 128 Typical surface-strain profiles for a “T”-marked crosstie at the end of Stage III

Table 63 Percentage increase in TL for “T”-marked ties during Stage III

Wire/Strand Type	% increase in LT from prestress transfer to end of Stage III”	% increase in LT from End of Stage I to end of Stage III"	% increase in LT from End of Stage II to end of Stage III"
WA	37%	18%	2%
WB	22%	8%	2%
WC	90%	14%	5%
WD	30%	9%	3%
WE	58%	9%	4%
WF	36%	6%	1%
WG	48%	14%	5%
WH	40%	11%	2%
WI	34%	4%	2%
WJ	32%	11%	-1%
WL	52%	19%	6%
WM	38%	12%	5%

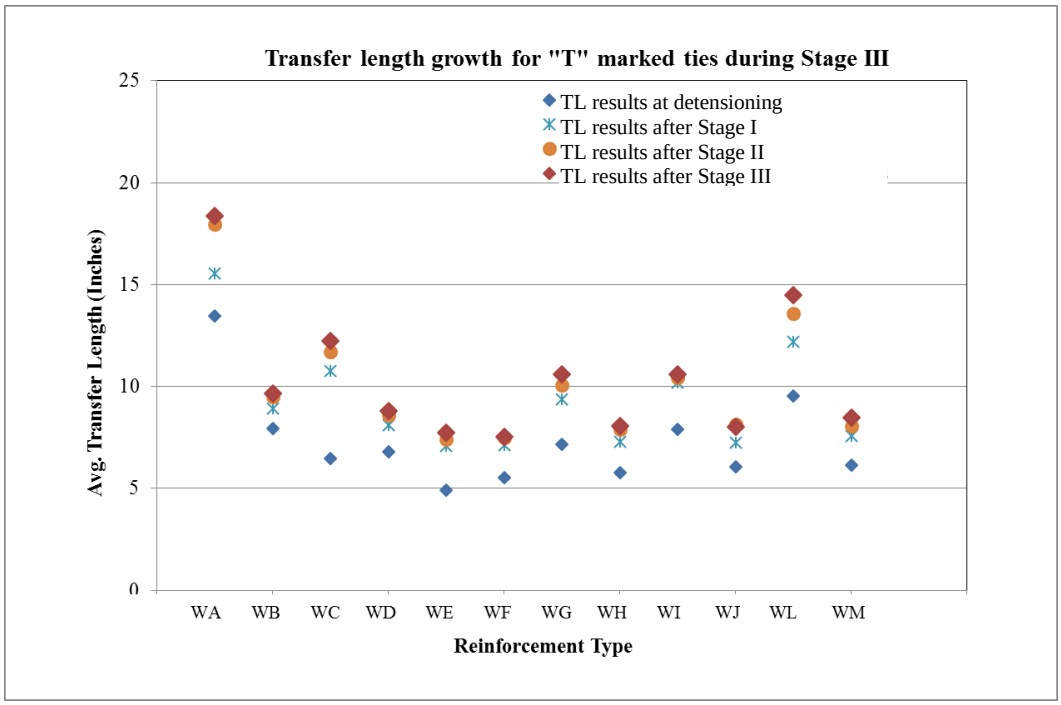

Figure 129 TL variation for “T”-marked crossties at the end of Stage III (wire reinforcements)

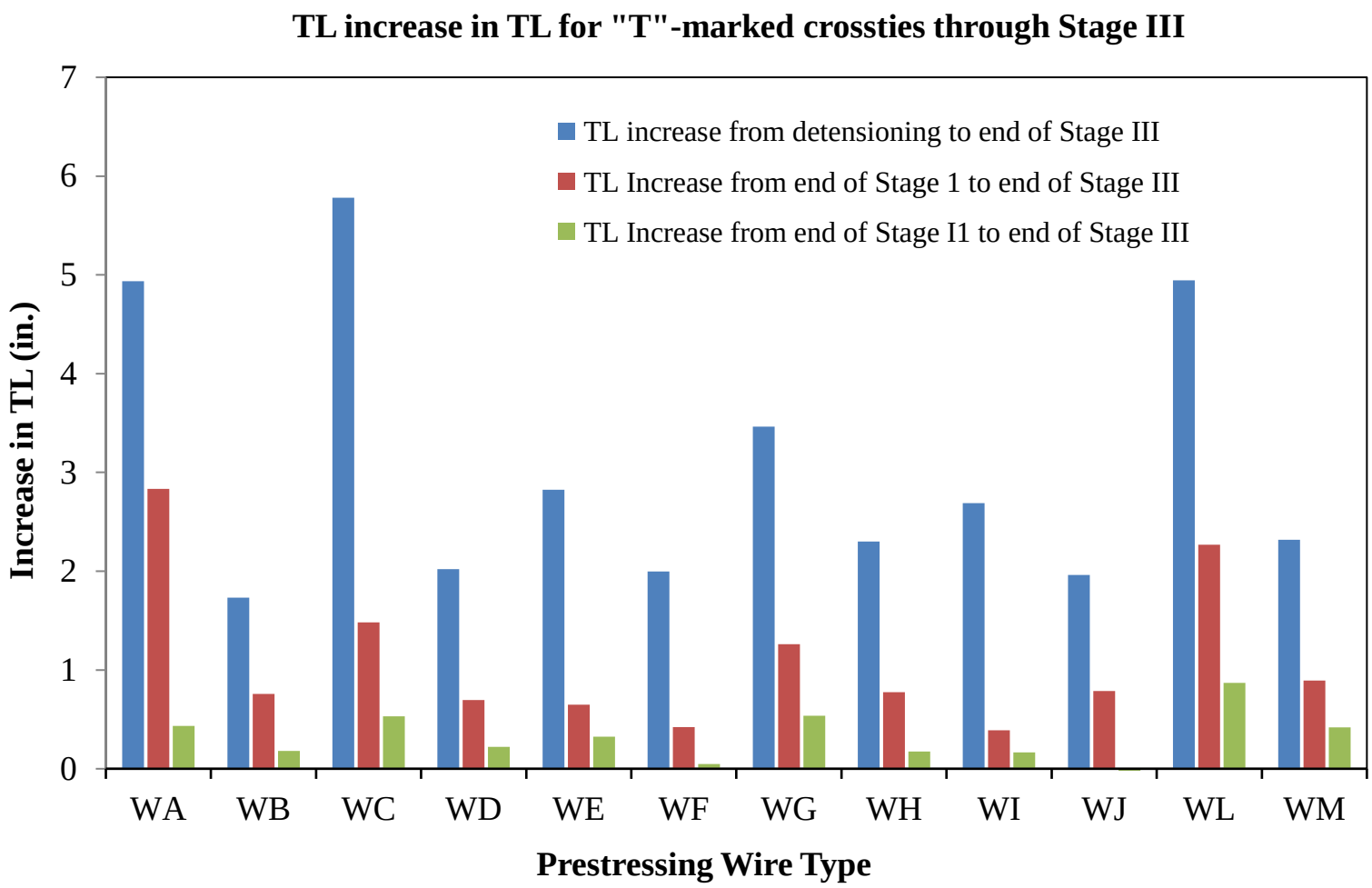

Figure 130 TL increase at the end of Stage III – wire reinforcements

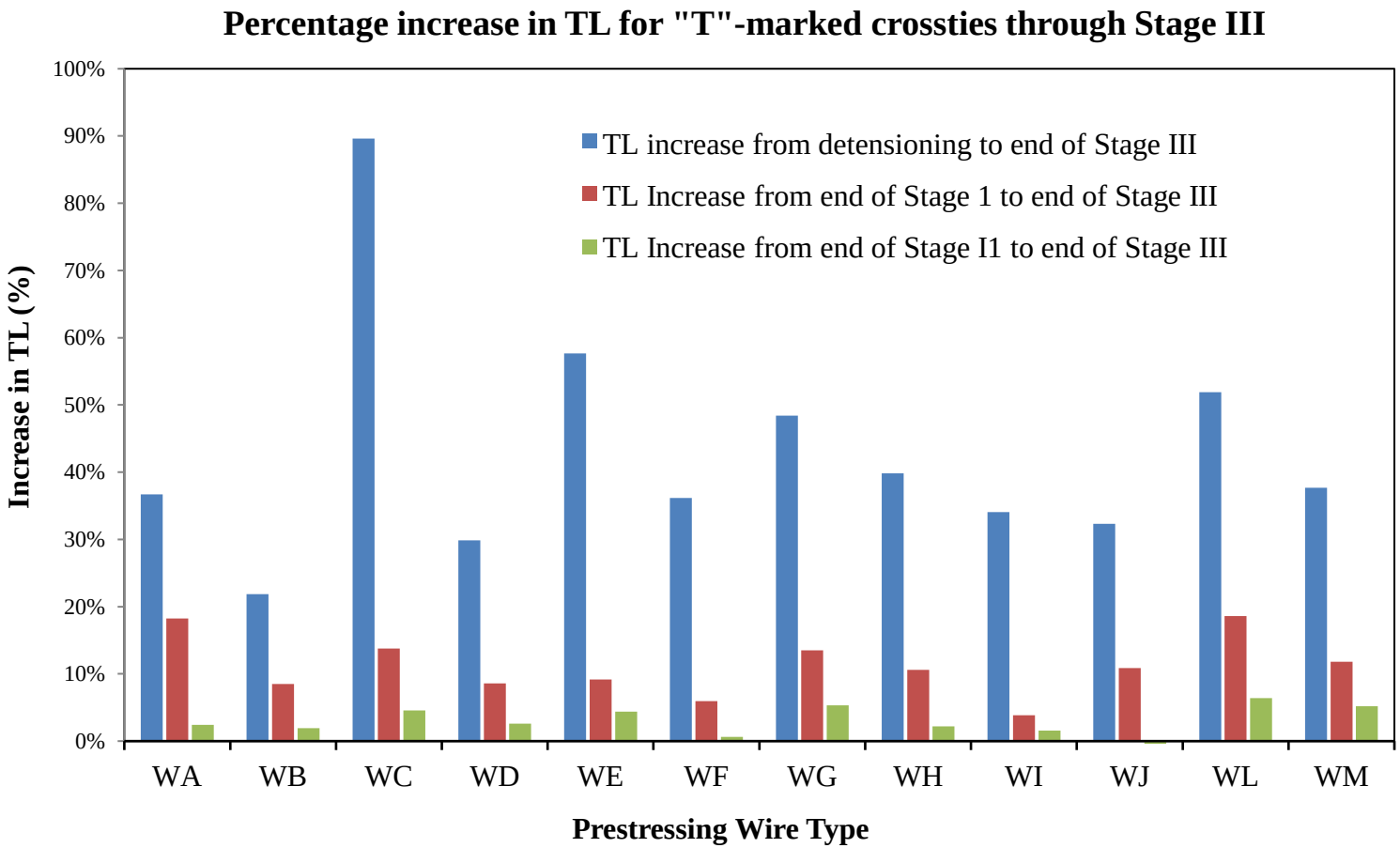

Figure 131 Percentage increase in TL at the end of Stage III – wire reinforcements

Chapter 8 Conclusions and Recommendations

8.1 Conclusions from Lab-Phase

From the Group I testing during the Lab-Phase, which measured transfer lengths of prisms cast with nineteen (19) different reinforcements, the following conclusions can be drawn.

1. The transfer length is highly-dependent on the reinforcing type and indentation pattern.
2. The thirteen (13) wires tested in Group I of Lab-Phase had average transfer lengths that varied between 7.4 and 18.7 inches, with the lowest transfer length corresponding to the spiral wire "[WE]" and the highest transfer length corresponds to the 2-dot wire "[WL]". The average transfer length for the smooth wire in the first phase was 16.3 inch. Detailed results for individual wire reinforcements were presented in section 5.1.
3. For the 5.32-mm-diameter wires, wires with chevron indentations, diamond indentations, and spirals bonded better than the smooth wire and wires with dot-shaped indentations. The fact that the 2-dot wire did not bond as well as the smooth wire revealed that the actual surface characteristics can have a significant effect on the bond of wires with minimal indentations.
4. Among the strand reinforcements (Group I Lab-Phase), higher transfer lengths were observed in the case of 7-wire strands when compared to 3-wire strands. The smooth 7-wire 3/8"-diameter ([SA]) had slightly better bond characteristics than the indented 7-wire 3/8"-diameter strands [SB], which was from the same supplier. Lower transfer lengths in the case of [SA] may be due to the presence of very light surface rusting on [SA], whereas remaining 7-wire 3/8"-diameter strands did not contain any visible rusting. However, lowest average transfer length during Lab-Phase for 7-wire 3/8"-diameter strand was observed for strand [SD]. Transfer length ranges for individual strand reinforcements including the average values are presented in section 5.1.
5. Lower average transfer lengths were obtained for two 3-wire strands with different diameters [SC], [SF] and are 13.77 inches and 12.52 inches respectively. It is also observed that [SF], 3-wire 3/8"-diameter, has lower average transfer length when compared to 7-wire 3/8"-diameter strands [SA], [SB], [SD], and [SE].

During the Group II and Group III prisms evaluated during the Lab-Phase, which were used to determine the effect of different release strengths and different concrete slumps, the following conclusions are drawn.

6. The concrete compression strength at the time of prestress transfer (release strength) is a primary factor influencing the transfer length in pretensioned concrete members utilizing both wires and strands. A consistent decrease in the transfer length was observed for both wires and strands when the release strength was increase from 3500 psi to 4500 psi. This decrease in transfer length averaged 23.0% for wires and 21,9% for strands. Additionally, the increase in release strength from 4500 to 6000 psi resulted in further reduction in transfer length. This average reduction was 12.4% for wires and 21.0% for strands. The average reduction in transfer length when concrete compressive strength increased from 3500 psi to 6000 psi was 32.8% for wires and 39.0% for strands (refer to Table 24 and Table 25). Limited tests that were conducted with wire {WF} indicate that increasing release strength beyond 6000 psi will result in still further reductions in transfer length.
7. A simplified expression was developed, based on the results from Lab-Phase prisms and ASTM A1096 pullout test results, that can be used to predict the transfer length in members utilizing 5.32-mm-diameter wires. This expression, presented below, had a coefficient of determination, R^2, of 0.954 when compared to all transfer length data from Lab-Phase prism tests with 5.32-mm-diameter wires. The expression is:

$$TL = 34.2 - \frac{f'_{ci}}{300} - \frac{(A1096\ value)}{\left[1250 - f'_{ci}\left(0.4 - \frac{f'_{ci}}{16{,}000}\right)\right]} \quad \text{where}$$

TL = Transfer length in inches

f'_{ci} = Concrete compressive strength at de-tensioning in psi

A1096 value = ASTM A1096 pullout value (6-specimen average) in pounds

8. Thus, a desired transfer length may be achieved by selecting the appropriate combination of reinforcing type and release strength.
9. Prism tests conducted at different concrete slumps during group III of the Lab-Phase revealed that the consistency of the concrete mix do not have a statistically-significant effect on the transfer length when the w/c ratio was held constant at 0.32.
10. During Group IV prism tests in the Lab-Phase, no significant difference in transfer length was observed with the variation of w/c ratio. The selected w/c ratios in the present study were 0.27, 0.32, and 0.42.

11. Similarly, during Group V testing, the presence of VMA in the concrete mixture did not result in a significant variation in transfer length. No correlation was observed when comparing transfer length results from companion prisms cast with and without VMA.
12. During group VI testing, reduction in TL was observed in the case of prisms cast with [WG] wire reinforcement and Mix-Design #2. However, prisms cast with Mix-Design #2 and [WH] resulted in severe cracking (longitudinal splitting along the wires) upon detensioning. From these results, it is evident that lower transfer results are not the only priority to produce structurally-sound pre-tensioned concrete ties.

8.2 Conclusions from Plant-Phase

Relevant conclusions for crossties cast during the Plant-Phase of the current research program are discussed below:

1. The two fabricated LSI devices allowed concrete surface-displacement measurements to be made at a much faster rate and eliminated the human errors associated with the traditional Whittemore gage method. The LSI method of measurement allowed for the determination of transfer lengths at many locations along the prestressing bed with minimal interruptions to the production cycle. Hence, this same system could be utilized in quality control programs at concrete crosstie plants.
2. Transfer lengths obtained through LSI devices were directly compared with results from Whittemore gage measurements for each reinforcing type, and a coefficient of determination of R^2=0.812 was noted. The likely reason for the lower-than-expected correlation is due to the noted variations in transfer length along the casting bed, since both reading methods were not utilized at the same bed location.
3. During Plant-Phase, the average transfer lengths of the 5.32-mm wires ranged from 7.8 in. to 14.3 in. Highest average transfer lengths were obtained when the smooth wire [WA] and 2-dot wire [WL] were used, and these values were 14.3 in. and 13.3 in., respectively. The average transfer length of the chevron-shaped indented wires ranged from 8.3 in. [WH] to 10.9 in. [WG]. The average transfer length of the Spiral-indented wires ranged from 8.6 in. [WE] to 11.2 in. [WC] Transfer length ranges for individual wire reinforcements, including the average values, were presented section 7.1.1.

4. The average transfer lengths for the 7-wire 3/8”-diameter smooth strand [SA] and 7-wire 3/8”-diameter indented strand [SB] were 14.4 in. and 15.6 in., respectively. This corresponds to values of 38 d_b and 42 d_b respectively, which are significantly less than the assumption of 60 d_b in current code equations. Strand [SA] had some very minor surface rusting, whereas strand [SB] did not contain any visible rusting. The 3-wire 5/16”-diameter smooth strand [SC] had an average transfer length of 15.9 in. Detailed strand transfer length results were presented in section 7.1.1.

Results from Lab-Phase (Group I prisms) and Plant-Phase crossties were compared to determine the efficiency of the laboratory prisms in predicting the actual concrete tie transfer length. Related conclusions are drawn and presented below:

1. Transfer lengths tests performed during Lab-Phase (Group I prisms) had excellent correlation with Plant-Phase transfer lengths. A coefficient of determination of R^2=0.858 was observed between the equation developed from Lab-Phase data and Plant-Phase results when all 12 wire reinforcements are considered (refer to Section 7.2.1).
2. The laboratory prisms, when cast with a similar concrete mixture, were able to accurately represent the behavior of the prestressing tendons when utilized to manufacture pretensioned concrete crossties. Therefore, in the future, the bond performance of a new reinforcement in pretensioned concrete railroad ties could be determined by measuring transfer lengths on similar prisms using a representative concrete mix.
3. Additionally, these small-scale laboratory prisms would also provide an economical option for the tie manufacturing industry to select the proper combination of prestressing tendons and release strength to achieve the desired transfer lengths. Essential information obtained through laboratory tests can also be utilized by reinforcement manufacturers to establish the factors (such as indent type, drawing lubricants, etc.) that effect the bonding performance.
4. The largest discrepancy between the Lab-Phase prisms and Plant-Phases occurred for wire [WL], with the laboratory-obtained transfer lengths being significantly longer than the plant-obtained transfer lengths by 5.4 in. (18.7 in. compared to 13.3 in.). However, this may be largely due to the following two observations. First, the concrete de-tensioning strength at the plant for the [WL] pour was 6600 psi, which was significantly higher than the laboratory release strength of 4476 psi for the same reinforcement.

Second, the concrete mixture used to fabricate the [WL] prisms had the lowest tensile strength of all the laboratory mixes (328 psi).

Major conclusions drawn from the long-term study on plant manufactured concrete ties are as follows.

1. The average transfer length increase (Stage I "K"-marked ties) for chevron-shaped indented wires ranged from 19% (WI) to 29% (WG, WJ). The average transfer length increases of the spiral-indented wires were 36% and 76% for WE and WC respectively. An average transfer length increase of 40% was observed in the case of 2-dot indent pattern (minimal indentation). In the case of diamond pattern (WF), the average transfer length increase was 28%. Transfer length increase for the ties manufactured with WA and stored at KSU was 34%. At the end of Stage I ("K"-marked ties), the average transfer length increases were 51%, 21%, and 31% for SA, SB, and SC respectively.
2. The average transfer length increases (Stage I "T"-marked ties) for chevron-shaped indented wires ranged from 12% (WB) to 31% (WG). The average transfer length increase of the spiral-indented wires were 44% and 67% for WE and WC respectively. An average transfer length increase of 28% was observed in the case of 2-dot indent pattern (minimal indentation). In the case of diamond pattern (WF), the average transfer length increase is observed as 29%. Transfer length increase for the ties manufactured with wire WA was 16%. At the end of Stage I ("T"-marked ties), the average transfer length increases were 30%, 9%, and 12% for SA, SB, and SC respectively.
3. For the ties manufactured with WE, WI, and WM; higher transfer lengths were observed for the ties stored at plant. Transfer length increase for the ties stored both at KSU and plant were approximately the same in the case of WF, WG, and WH. For the ties manufactured with the remaining reinforcements (6 reinforcements), higher transfer length increases were observed in the ties stored at KSU.
4. Upon the application of 84.46 MGT in-track loading, TL increase was not substantial (in "T"-marked ties) as compared to Stage I (without any loading). Also, TL results for ties cast with smooth wire (WA) displayed highest increase in TL from Stage I to Stage II (for the crossties cast with wire reinforcements). This suggests that the indentation of wire reinforcements likely assisted to improve the long-term bond performance (and thereby minimize the increase in transfer length).

5. TL results of “K”-marked ties did not have any significant variation in TL during Stage II.
6. The average transfer length increase, when the crossties were subjected to cumulative in-track loading of 236.31 MGT, from Stage II to Stage III was minimal (“T”-marked ties).
7. In the present study, the largest transfer length increase was observed during Stage I. This initial higher TL growth is observed without any loading. Transfer length increases were minimal at the later stages, even for “T”-marked ties subjected to in-track loading. Hence, it can be concluded that the majority of transfer length increase occurs during the first year after fabrication and is primarily time-dependent and climate-dependent rather than load-dependent.

8.3 Recommendations

The following recommendations are made based on the current research results:

1. It is highly recommended to perform laboratory prism tests to evaluate the bond performance of the prestressing reinforcement that is selected for pretensioned concrete tie production. These prism tests should be conducted with the same concrete mixture and de-tensioning strength that is going to be used for the concrete tie production.
2. Frequent prisms tests are recommended to evaluate the influence of any changes occurring in the manufacturing process (such as changes in concrete materials, prestressing tendons, etc.).
3. Transfer length measurements, without interrupting the production process, can be made using the LSI device and would enhance the quality assurance of concrete tie production.

Suggested areas for additional research include the following:

1. Conducting load tests on the “T”-marked ties and “K”-marked ties will provide further insight on the bond quality of the plant manufactured ties.
2. For the majority of the present study, Mix-Design #1 was employed. Whereas, concrete ties are produced at different locations and with different concrete mixtures though the world. Hence, it is recommended to conduct similar research with different concrete materials (coarse and fine aggregates, cements, and supplementary cementitious materials) to determine the effect of these different concrete materials on transfer length.

3. Bond quality of crossties installed and subjected to in-track loading at different environments is unknown. Further research on crossties loaded at different environments will provide the knowledge about variation in bond quality due to adverse conditions.

References

Influence of Concrete Strength on Strand Transfer Length [Journal] / auth. Kaar P H, La Fraugh R W and Mass M A // PCI. - October 1963. - 5 : Vol. 8. - pp. 47-67.

A Direct Comparison of the Traditional Method and A New Approach in Determining 220 Transfer Lengths in Prestressed Concrete Railroad Ties [Conference] / auth. Zhao Weixin [et al.] // Joint Rail Conference . - Knoxville, TN : [s.n.], 2013.

A New Development Length Equation for Pretensioned Strands in Bridge Beams and Piles [Report] / auth. Lane Susan N / Federal Highway Administration ; Structures Division. - McLean, VA : [s.n.], 1998.

A Non-Contact Inspection Method to Determine the Transfer Length in Pre-tensioned Concrete Railroad Ties [Journal] / auth. Zhao Weixin [et al.] // ASCE Journal of Engineering Mechanics. - March 2013. - 3 : Vol. 139. - pp. 256-263.

A Review of Strand Development Length for Pretensioned Concrete Members [Journal] / auth. Buckner C Dale // PCI Journal. - 1995. - 2 : Vol. 40. - pp. 84-105.

Acceptance Criteria for Bond Quality of Strand for Pretensioned Prestressed Concrete Applications [Journal] / auth. Logan Donald R // PCI Journal. - March-April 1997. - 2 : Vol. 42. - pp. 52-90.

ADVA Cast 530 Data Sheet [Online] / auth. W. R. Grace & Co.–Conn. // GCP applied technologies (GRACE CONSTRUCTION & PACKING). - 2007. - https://gcpat.com/construction/en-us/Documents/DCAC-31D_ADVA_Cast_530_11_15_07.pdf.

ASTM A1096 Standard Test Method for Evaluating Bond of Individual Steel Wire, Indented or Plain, for Concrete Reinforcement [Report]. - West Conshohocken, PA : ASTM International, 2015.

Bond fatigue tests of beams simulating pretensioned concrete crossties [Journal] / auth. Kaar Paul H and Hanson Norman W // PCI Journal. - September-October 1975. - 5 : Vol. 20. - pp. 65-80.

Building Code Requirements for Structural Concrete [Report] / auth. ACI 318-11. - [s.l.] : American Concrete Institute, 2011.

Capacity optimization of a prestressed concrete railroad tie [Report] : Master's Report / auth. Lutch Russell H / Department of Civil and Environmental Engineering ; Michigan Technological University. - 2009.

Comparison of the effect of different sleeper typologies and track layout on railway vibrations [Journal] / auth. Real J [et al.] // Latin American Journal of Solids and Structures. - 2014. - 12 : Vol. 11. - pp. 2241-2254.

Concrete Crossties in the United States [Journal] / auth. Weber J W // PCI JOURNAL. - February 1969. - 1 : Vol. 14. - pp. 46-61.

Design guidelines for transfer, development and debonding of large diameter seven wire strands in pretensioned concrete girders [Report] : Final Report: TX-93+1210-5F / auth. Russell Bruce W and Burns Ned H / Texas Department of Transportation. - January 1993.

Determining the transfer length in prestressed concrete railroad ties produced in the United States [Report] : Master's Report / auth. Murphy Robert Lawrence / Department of Civil Engineering ; Kansas State University. - 2012.

Determining Transfer Length In Pre-Tensioned Concrete Railroad Ties: Is Anew Evaluation Method Needed? [Conference] / auth. Zhao Weixin [et al.] // ASME Rail Transportation Division Fall Technical Conference. - Altoona, PA : [s.n.], 2013.

Development Length and Lateral Spacing Requirements of Prestressing Strand for Prestressed Concrete Bridge Girders [Journal] / auth. Deatherage J Harold, Burdette Edwin G and Chew Chong Key // PCI Journal. - 1994. - 1 : Vol. 39. - pp. 70-83.

Development Length of Prestressing Strands [Journal] / auth. Zia Paul and Mostafa Talat // PCI Journal. - 1977. - 5 : Vol. 22. - pp. 54-63.

Development of A Laster Speckle Imaging Device to Determine the Transfer Length in Pretensioned Concrete Members [Journal] / auth. Zhao Weixin [et al.] // PCI. - Winter 2012. - pp. 135-143.

Development of a Portable Optical Strain Sensor with Applications to Diagnostic Testing of Prestressed Concrete [Report] / auth. Zhao Weixin. - Manhattan, KS : Kansas State University, 2011.

Development of a Standard Bond Test for Indented Prestressing Wires [Conference] / auth. Arnold Matthew L [et al.] // 2013 Joint Rail Conference. - Knoxville, Tennessee, USA : [s.n.], April 15–18, 2013. - pp. JRC2013-2461.

Development of Presressing Strand in Pretensioned Memebers [Journal] / auth. Marin Leslie D and Scott Norman L // ACI Journal. - 1976. - 8 : Vol. 73. - pp. 453-456.

Effect of load pattern and history on performance of reinforced concrete columns [Report] / auth. Shirmohammadi F / Doctoral report. - [s.l.] : Kansas State University, 2015.

Effect of Strand Blanketing on Performance of Pretensioned Girders [Journal] / auth. Kaar Paul H and Magura Donald D // PCI Journal. - December 1965. - 6 : Vol. 10. - pp. 20-34.

Effect of Surface-Strain Sampling Interval On The Reliability of Pretensioned Concrete Railroad Tie Transfer Length Measurements [Conference] / auth. Beck Terry B [et al.] // PCI Convention and National Bridge Conference. - Gaylord National Resort in Washington, D.C. : [s.n.], 2014.

Effects of concrete composition on transmission length of prestressing strands [Journal] / auth. Marti-Vargas J R [et al.] // Construction and Building Materials. - February 2012. - 1 : Vol. 27. - pp. 350-356.

Evaluation of As-Cast Strand-Depth on transfer and Development Length in Concrete Mixes with Different Fludity [Report] : Draft Final Report submitted to PCI / auth. Peterman Robert J / RJ Peterman & Associates, Inc. . - January 2012.

Experimental Assessment of Factors Affecting Transfer Length [Journal] / auth. Barnes Robert W, Grove J W and Burns N H // ACI Structural Journal. - Nov-Dec 2003. - Vol. 100. - pp. 740-748.

Experimental Determination of Prestressing Wire Bond and Splitting Propensity Characteristics through Tensioned Pullout Tests [Report] / auth. Holste Joseph Robert / Department of Civil Engineering. - Manhattan, KS : Kansas State University, 2014.

Flexural Bond Tests of Pretensioned Prestressed Beams [Journal] / auth. Hanson Norman W and Kaar Paul H // ACI Journal. - 1959. - 1 : Vol. 55. - pp. 783-802.

Formulation of New Development Length Equation for 0.6 in. Prestressing Strand [Journal] / auth. Kose Mehmet M and Burkett William R // PCI Journal. - 2005. - 5 : Vol. 50. - pp. 96-105.

Grade 300 Prestressing Strand and the Effect of Vertical Casting Position [Report] : Final Contract Report VTRC 10-CR2 / auth. Roberts-Wollmann Carin, Cousins Tommy and Carroll Chris. - [s.l.] : Virginia Transportation Research Council, September 2009.

Greenhouse Gas Emissions Embodied in Reinforced Concrete and Timber Railway Sleepers [Journal] / auth. Crawford Robert H // Environmental Science & Technology. - [s.l.] : American Chemical Society, April 17, 2009. - 10 : Vol. 43. - pp. 3885-3890.

Influence of Flexure-Shear Cracking on Strand Development Length in Prestressed Concrete Members [Journal] / auth. Peterman Robert J, Ramirez Julio A and Olek Jan // PCI Journal. - September-October 2000. - 5 : Vol. 45. - pp. 76-94.

Influence of High Strength Concrete on Transfer and Development Length of Pretensioning Strand [Journal] / auth. Mitchell Denis [et al.] // PCI Journal. - 1993. - 3 : Vol. 38. - pp. 52-66.

In-Plant Testing of a New Multi-Camera Transfer Length Measurement System for Monitoring Quality Control of Railroad Crosstie Production [Conference] / auth. Beck Terry B [et al.] // Proceedings of the 2015 Joint Rail Conference. - San Jose, CA : [s.n.], 2015. - p. presentation.

Investigation of Standardized Tests to Measure the Bond Performance of Prestressing Strand [Journal] / auth. Rose Dallas R and Russell Brice W // PCI Journal Paper. - July-August 1997. - 4 : Vol. 42. - pp. 56-80.

LRFD Bridge Design Specifications [Book] / auth. AASHTO. - Washington, DC : American Association of State Highway and Transportation Officials, 2014.

Manual for quality control for plants and production of structural precast concrete products [Report] / auth. MNL-116-99, Fourth edition. - [s.l.] : PCI, 1999.

Measurement of Transfer Lengths on pretensioned Concrete Elements [Journal] / auth. Russell Bruce W and Burns Ned H // Journal of Structural Engineering. - May 1997. - pp. 541-549.

Optimization of a Prestressed Concrete Railroad Crosstie for Heavy-Haul Applications [Journal] / auth. Harris D [et al.] // Journal of Transportation Engineering. - November 2011. - 11 : Vol. 137. - pp. 815-822.

PCI Design Handbook [Book] / auth. Precast/Prestressed Concrete Institute. - Chicago, IL : [s.n.], 2010.

Performance and Capacity Assessment of Reinforced Concrete Bridge Piers Considering the Current Load and Resistance Factor Design Provisions and Plastic Hinge Length in Kansas. [Report] / auth. Esmaeily A and Shirmohammadi F / Kansas Department of Transportation. - Topeka, Kansas : Report No. KSU-11-5, 2014.

Performance of Reinforced Concrete Columns under Bi-Axial Lateral Force/Displacement and Axial Load [Journal] / auth. Shirmohammadi F and Esmaeily A // Engineering Structures. - 2015. - Vol. 99. - pp. 63-77.

Preliminary Specifications for Standard Concrete Ties and Fastenings for Transit Track [Report] / auth. Hanna Amir N / U. S. Department of Transportation. - [s.l.] : Report No. UMTA-MA-06-0100-79-3, 1979. - UMTA-MA-06-0100-79-3.

Prestressed Concrete Ties for North American Railroads [Journal] / auth. Hanna Amir N // PCI. - Sept.-Oct. 1979. - pp. 32-61.

Realistic Evaluation of Transfer Lengths in Pretensioned, Prestressed Concrete Members [Journal] / auth. Oh Byung Hwan and Kim Eui Sung // ACI Structural Journal. - November 2000. - 6 : Vol. 97. - pp. 821-830.

Reliable Transfer Length Assessment For Real-Time Monitoring Of Railroad Cross-Tie Production [Conference] / auth. Zhao Weixin [et al.] // Joint Rail Conference . - Colorado Spring, CO : [s.n.], 2014.

Software for biaxial cyclic analysis of reinforced concrete columns [Journal] / auth. Shirmohammadi F and Esmaeily A // Computers and Concrete. - 2016. - Vol. 17(3). - pp. 353-386.

Standard Test Method for Compressive Strength of Cylindrical Concrete Specimens [Journal] / auth. ASTM C39 / C39M-12a // ASTM International. - West Conshohocken, PA : [s.n.], 2012.

Standard Test Method for Splitting Tensile Strength of Cylindrical Concrete Specimens [Journal] / auth. ASTM C496 / C496M - 11 // ASTM International. - West Conshohocken, PA : [s.n.], 2011.

Standard Test Method for Static Modulus of Elasticity and Poisson's Ratio of Concrete in Compression [Journal] / auth. ASTM C469/C469M-10 // ASTM International. - West Conshohocken, PA : [s.n.], 2010.

Strand Transfer Lengths in Full Scale AASHTO Prestressed Concrete Girders [Journal] / auth. Shahawy Mohsen A, Issa Moussa and Batchelor Barrington deV // PCI Journal. - 1992. - 3 : Vol. 37. - pp. 84-96.

Stress-Strain Model for Circular Concrete Column Confined by FRP and Conventional Lateral Steel [Journal] / auth. Shirmohammadi F, Esmaeily A and Kiaeipour Z // Engineering Structures. - 2015. - Vol. 84. - pp. 395-405.

Tensioned Pullout Test Used to Investigate Wire Splitting Propensity in Concrete Railroad Ties [Conference] / auth. Holste Joseph R [et al.] // 2014 Joint Rail Conference. - Colorado Springs, Colorado, USA : [s.n.], April 2–4, 2014. - pp. JRC2014-3833.

The Effects of As-Cast Depth and Concrete Fluidity on Strand Bond [Journal] / auth. Peterman Robert J // PCI Journal. - May-June 2007. - 3 : Vol. 52. - pp. 72-101.

Top strand effect and evaluation of effective prestress in prestressed concrete beams [Report] : Master of Science Report / auth. Hodges Hunter T / Department of Civil and Environmental Engineering ; Virginia Polytechnic Institute and State University. - 2006.

Transfer and development length of 15.2mm(0.6 in.) diameter prestressing strand in high performance concrete: results of the Hobitzell-Buckner beam tests [Report] / auth. Gross Shawn P and Burns Ned H / Center for Transportation Research, The University of Texas at Austin. - [s.l.] : Research report: FHWA/TX-97/580-2, June 1995.

Transfer and Development Length of Epoxy Coated and Uncoated Prestressing Strand [Journal] / auth. Cousins Thomas E, Johnston David W and Zia Paul // PCI Journal. - 1990. - 4 : Vol. 35. - pp. 92-103.

Transfer Bond Test Used to Predict Transfer Length of Concrete Railroad Ties [Conference] / auth. Holste Joseph R [et al.] // ASME 2013 Rail Transportation Division Fall Technical Conference. - Altoona, Pennsylvania, USA : ASME, October 15–17, 2013. - pp. RTDF2013-4726.

Transfer Length Measurements in Pretensioned Concrete Railroad Ties Under Rail Loads [Conference] / auth. Beck Terry B [et al.] // Proceedings of the 2015 Joint Rail Conference. - San Jose, CA : [s.n.], 2015. - pp. JRC2015-5690.

Un-tensioned Pull-Out Tests to Predict the Bond Quality of Different Prestressing Reinforcements Used in Concrete Railroad Ties [Report] / auth. Arnold Matthew

Lukas / Department of Civil Engineering. - Manhattan, KS : Kansas State University, 2013.

APPENDIX – Surface-strain profiles

Lab-Phase – Effect of reinforcement type on transfer length

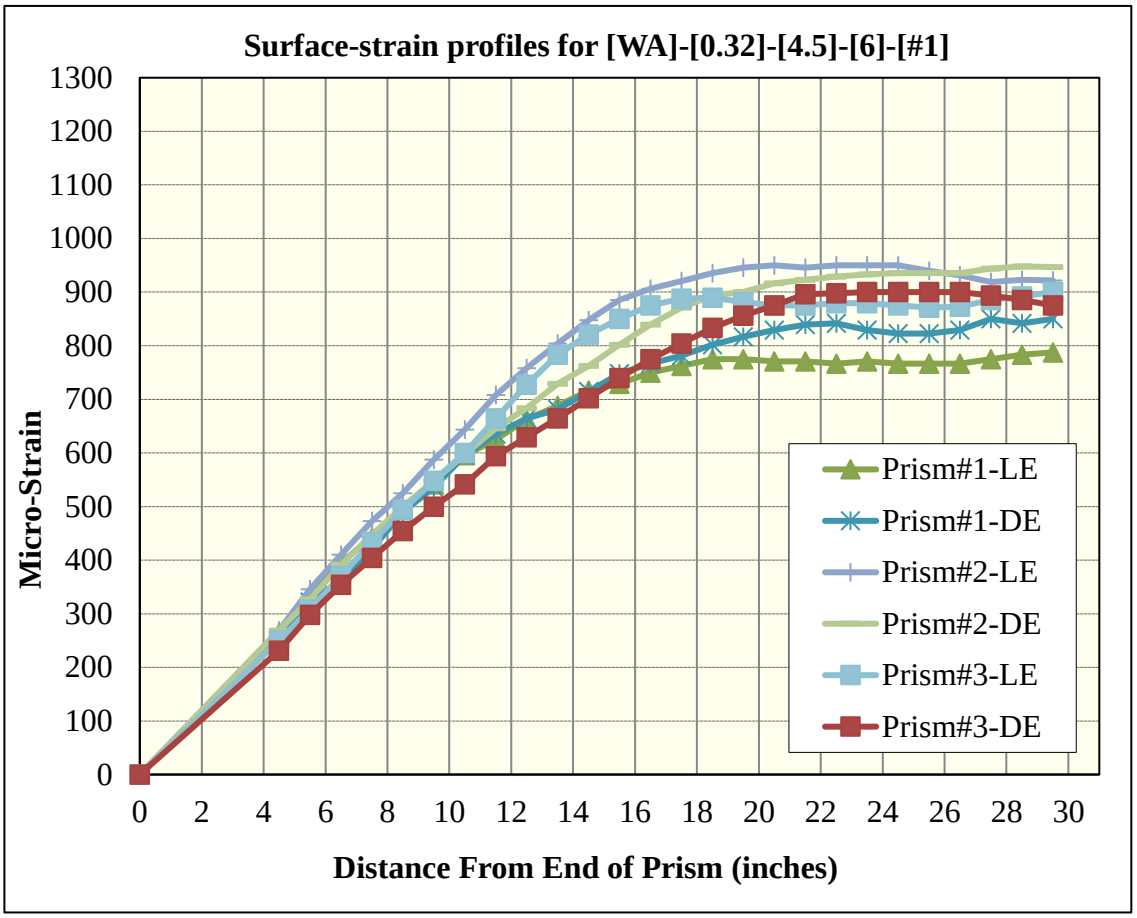

Figure 132 Surface-strain profiles for [WA]- [0.32]- [4.5]- [6]-[#1]

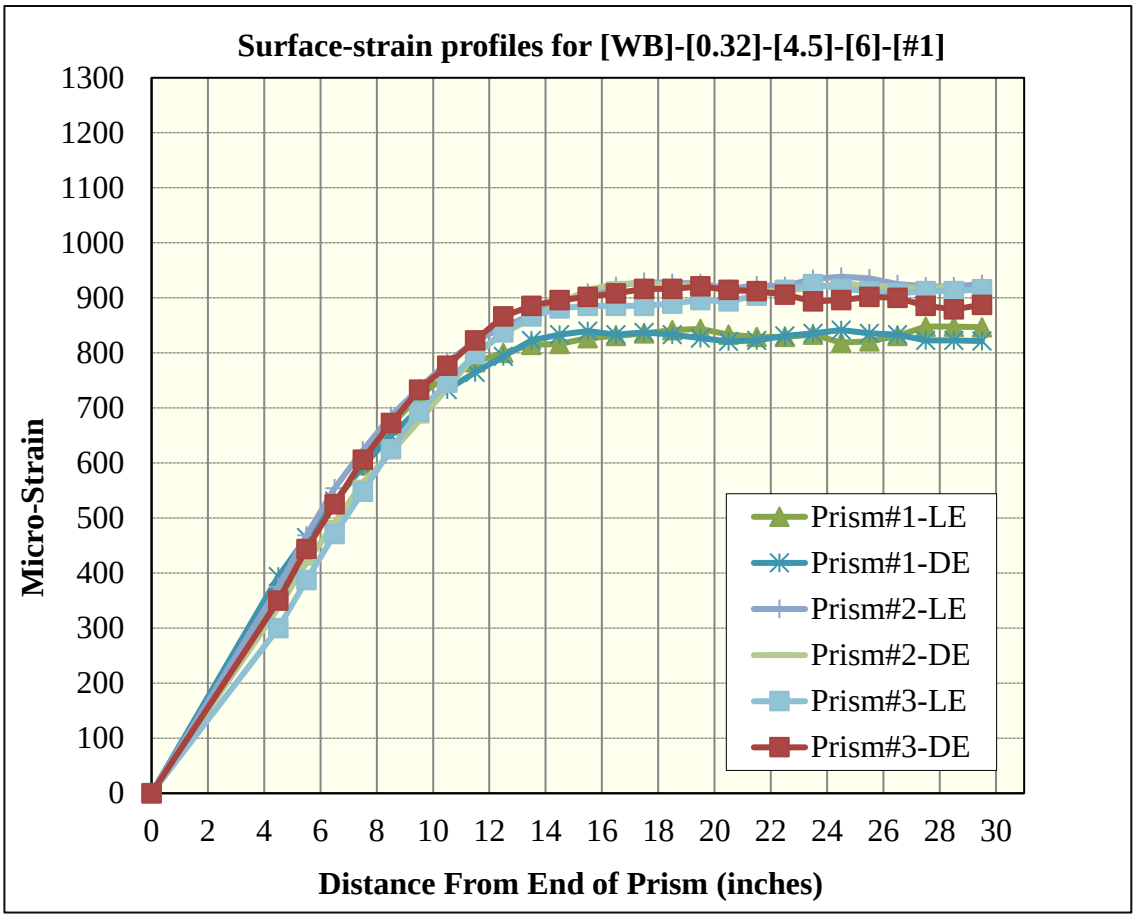

Figure 133 Surface-strain profiles for [WB]-[0.32]-[4.5]-[6]-[#1]

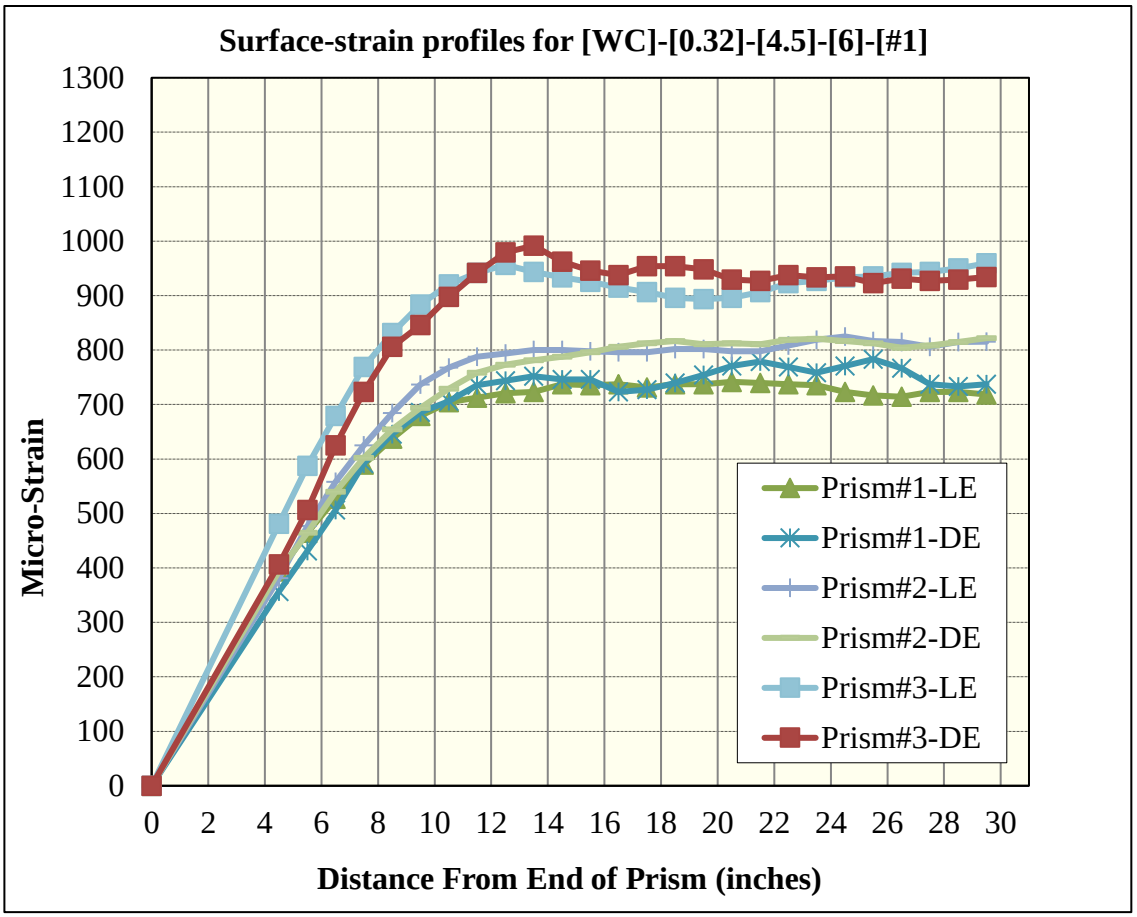

Figure 134 Surface-strain profiles for [WC]-[0.32]-[4.5]-[6]-[#1]

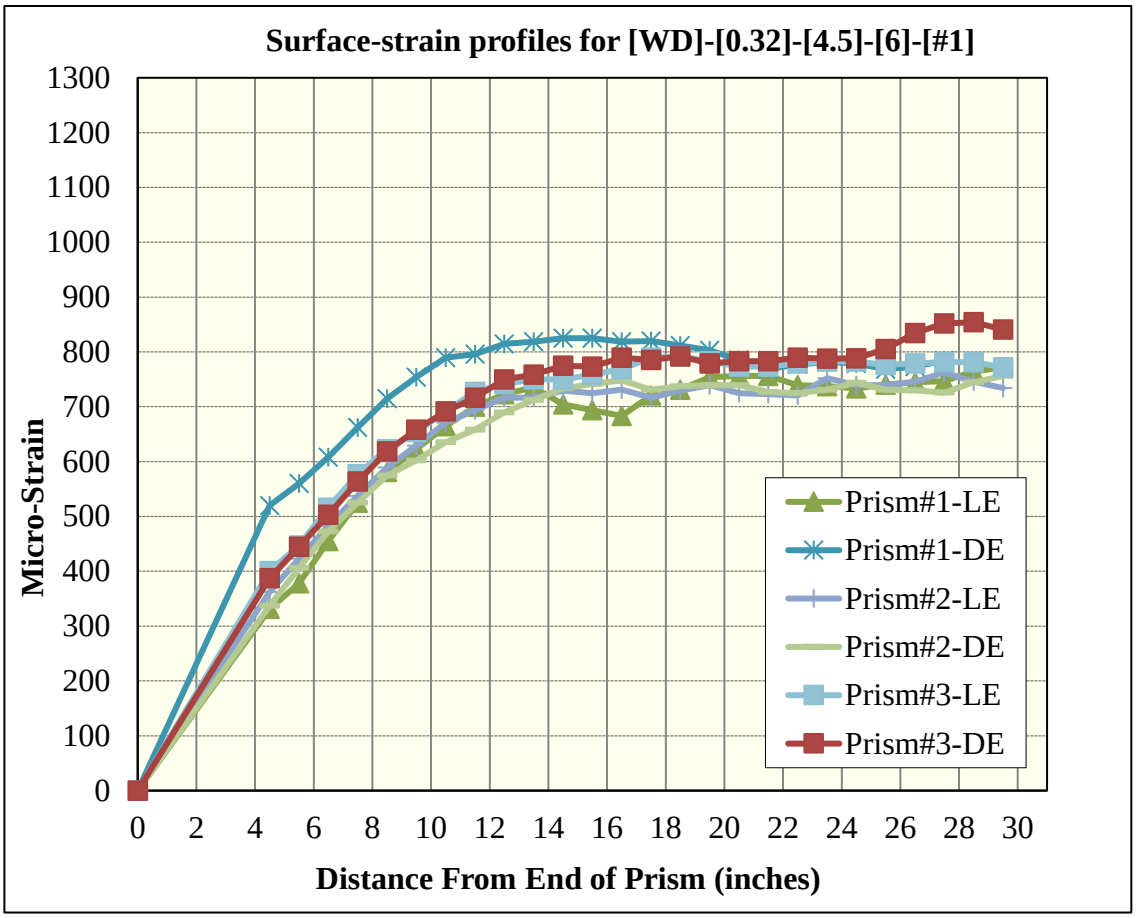

Figure 135 Surface-strain profiles for [WD]-[0.32]-[4.5]-[6]-[#1]

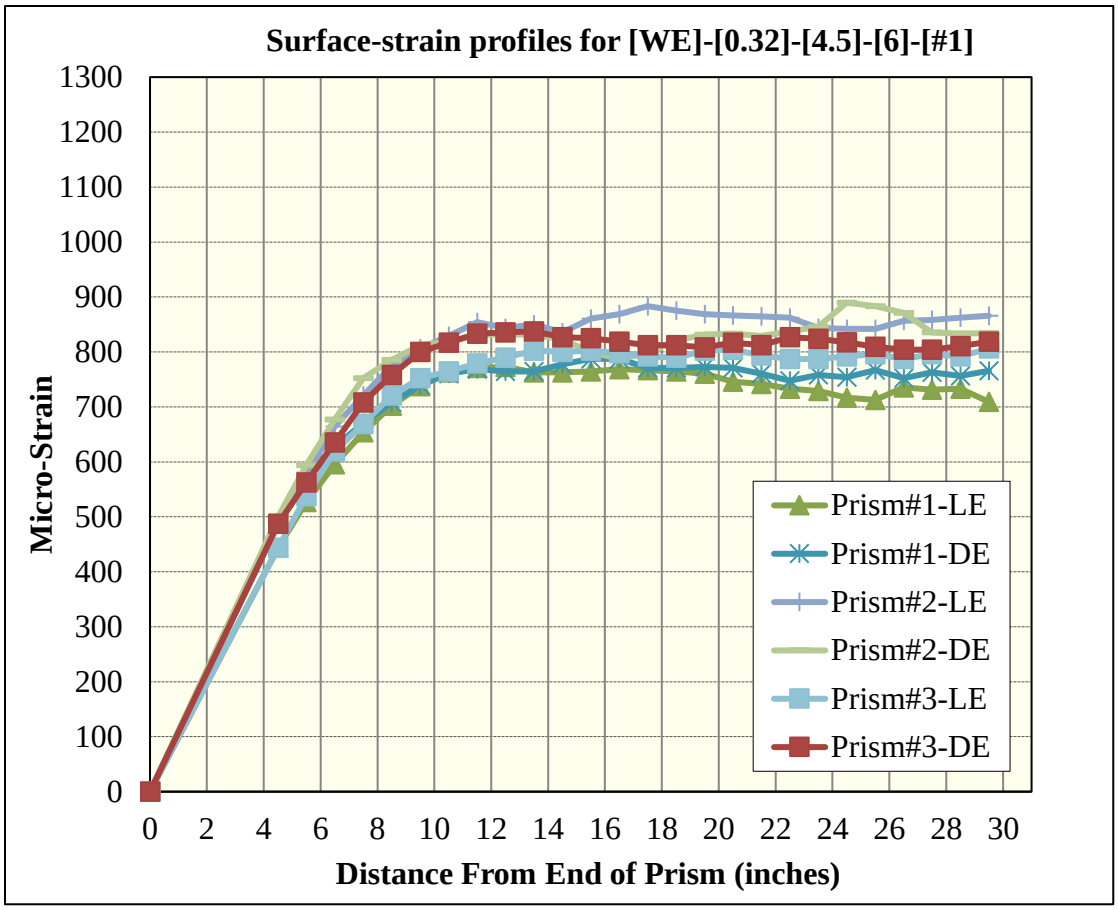

Figure 136 Surface-strain profiles for [WE]-[0.32]-[4.5]-[6]-[#1]

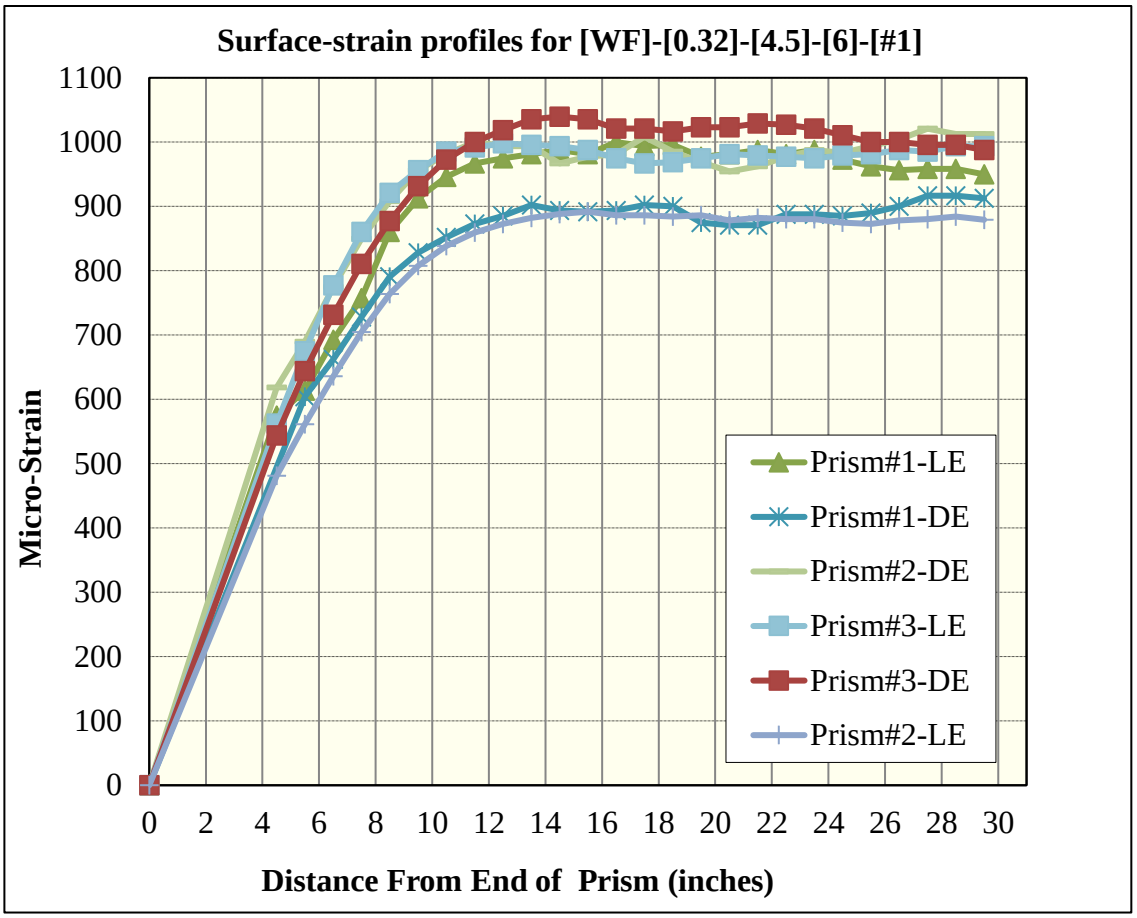

Figure 137 Surface-strain profiles for [WF]-[0.32]-[4.5]-[6]-[#1]

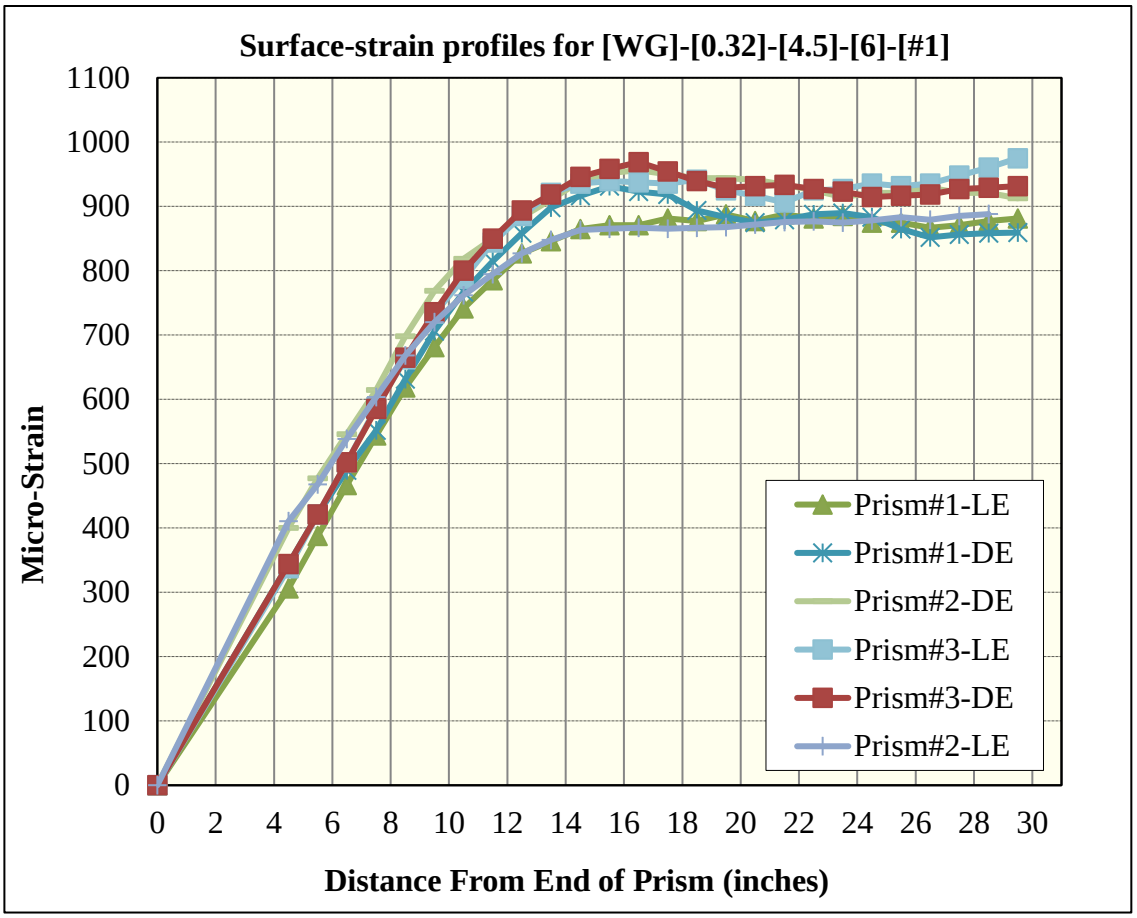

Figure 138 Surface-strain profiles for [WG]-[0.32]-[4.5]-[6]-[#1]

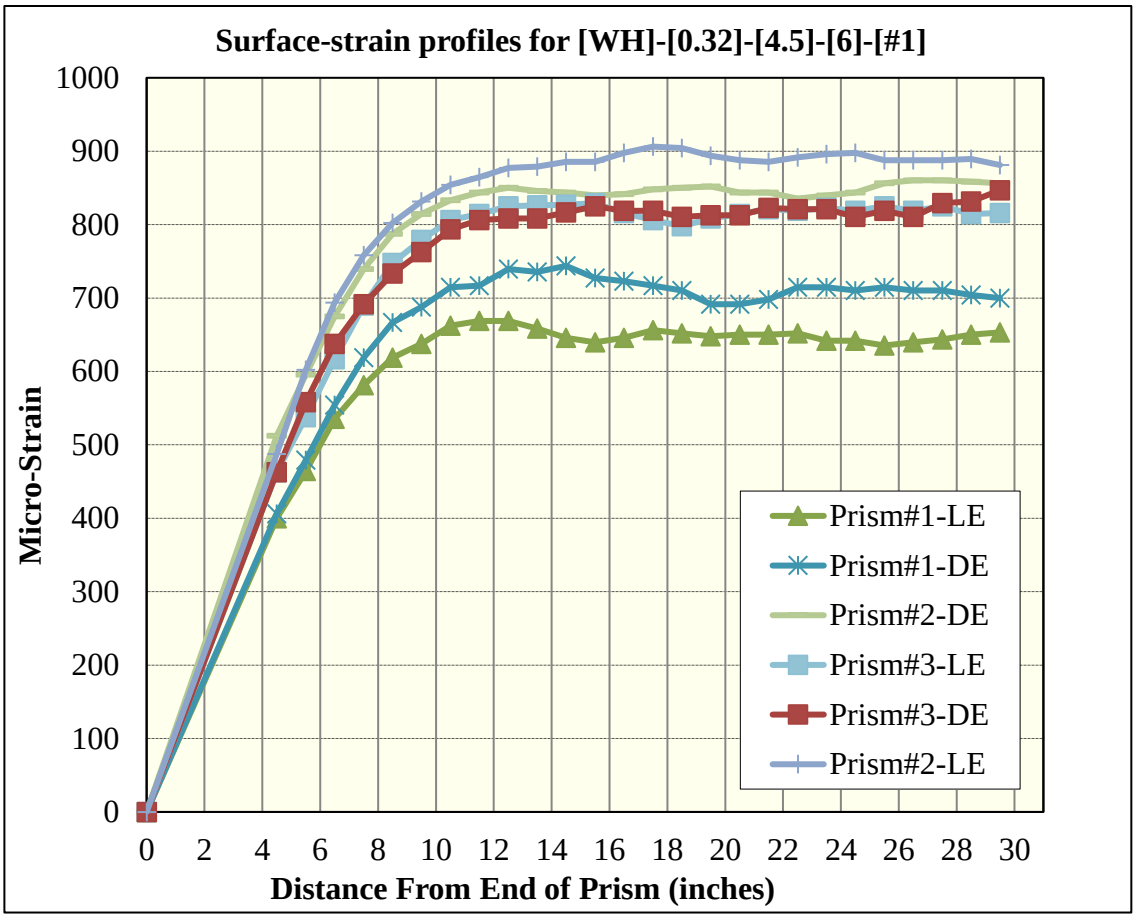

Figure 139 Surface-strain profiles for [WH]-[0.32]-[4.5]-[6]-[#1]

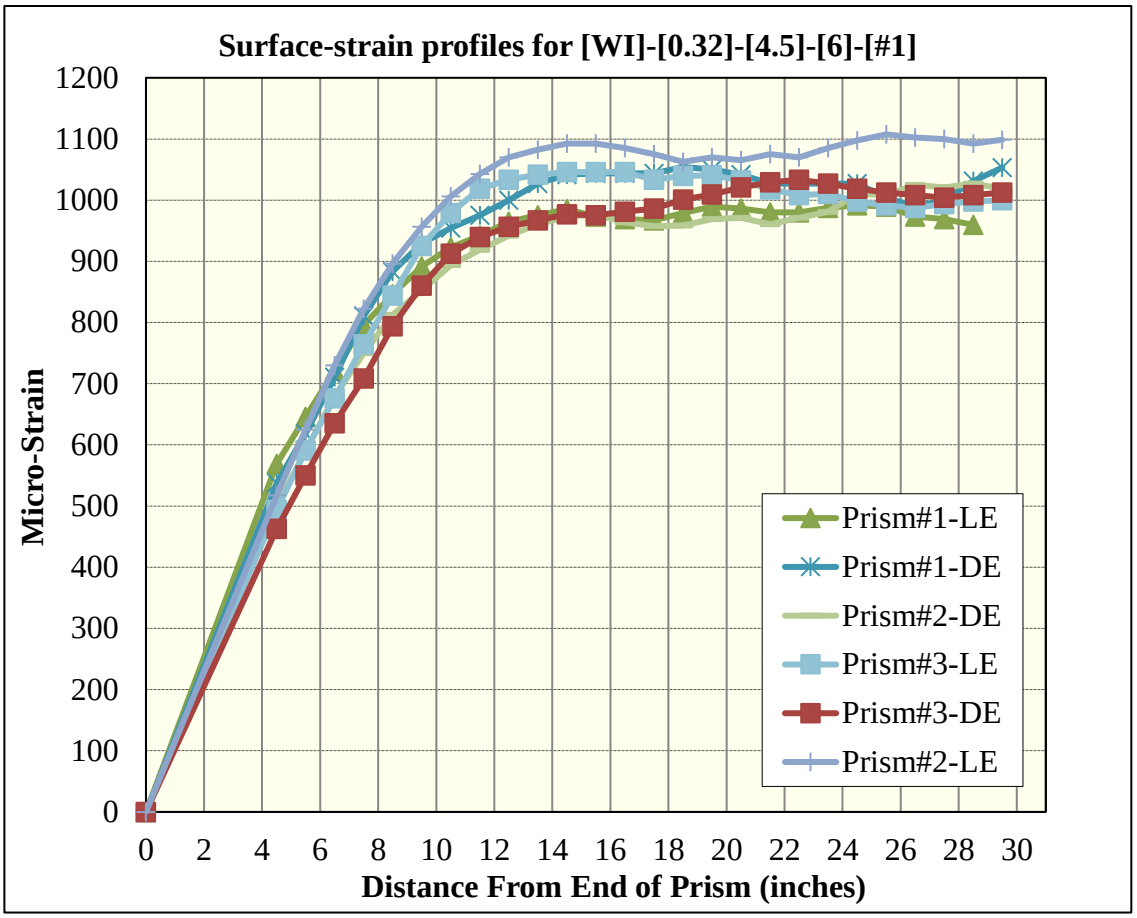

Figure 140 Surface-strain profiles for [WI]-[0.32]-[4.5]-[6]-[#1]

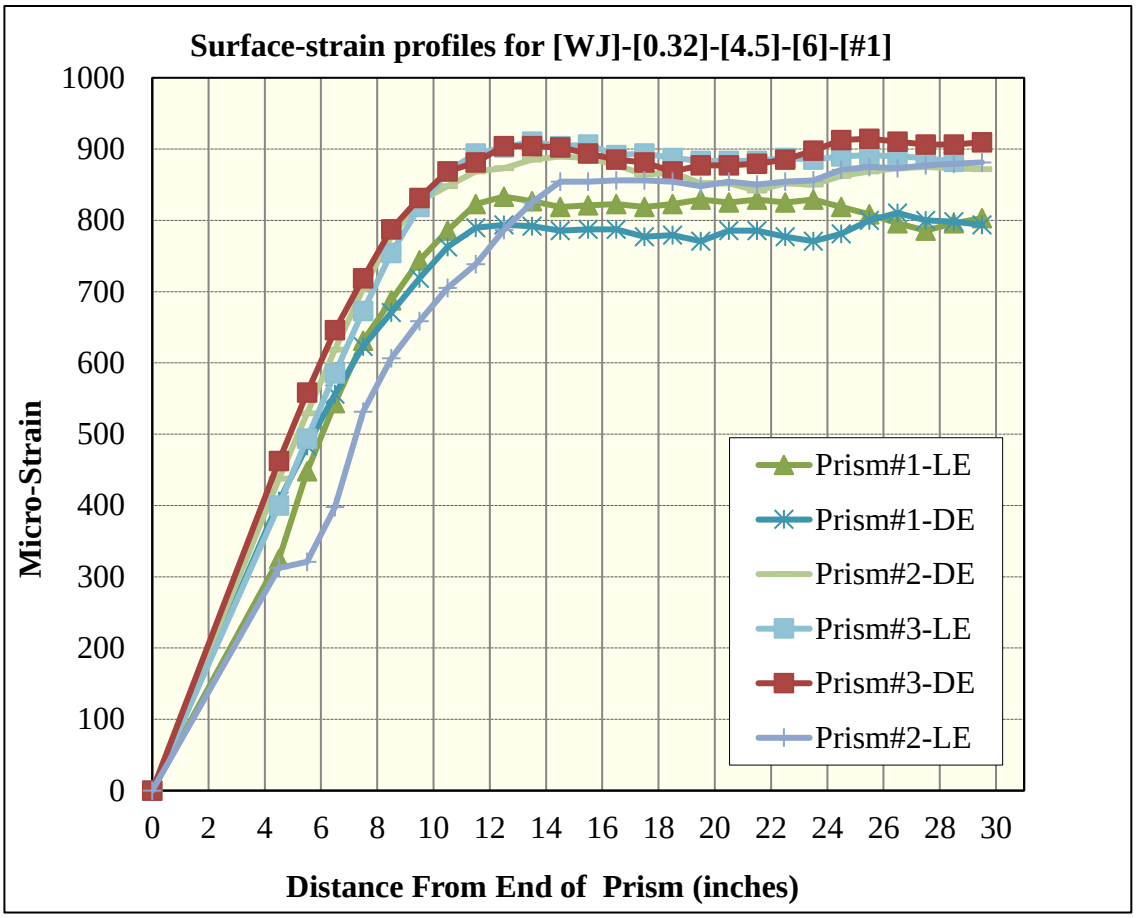

Figure 141 Surface-strain profiles for [WJ]-[0.32]-[4.5]-[6]-[#1]

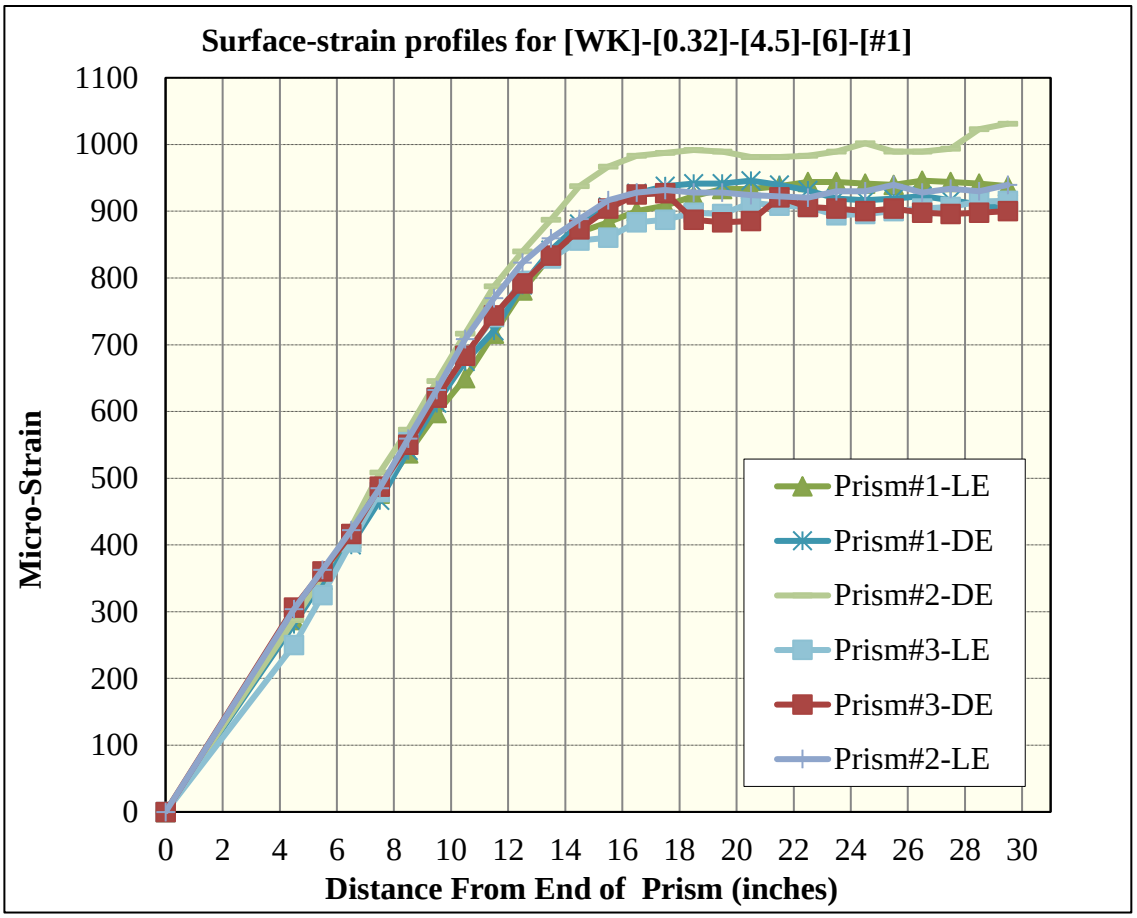

Figure 142 Surface-strain profiles for [WK]-[0.32]-[4.5]-[6]-[#1]

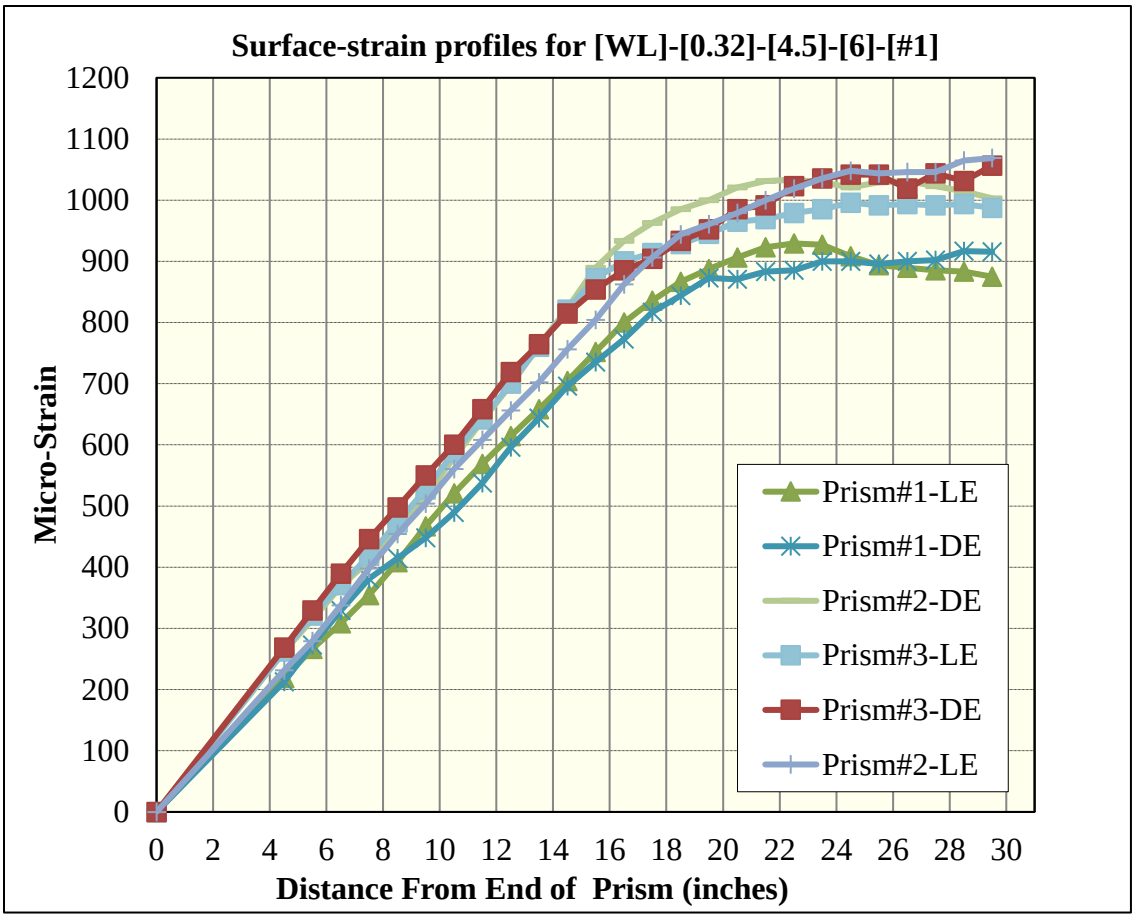

Figure 143 Surface-strain profiles for [WL]-[0.32]-[4.5]-[6]-[#1]

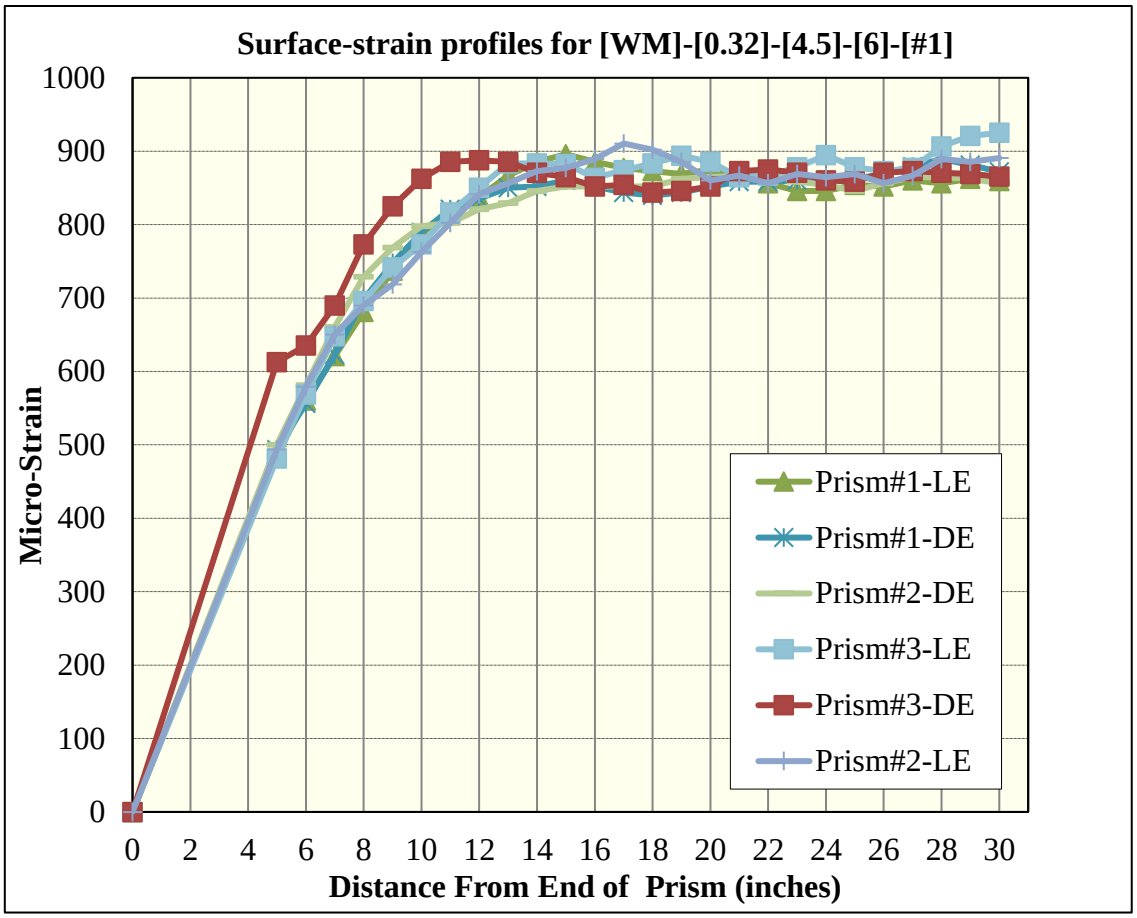

Figure 144 Surface-strain profiles for [WM]-[0.32]-[4.5]-[6]-[#1]

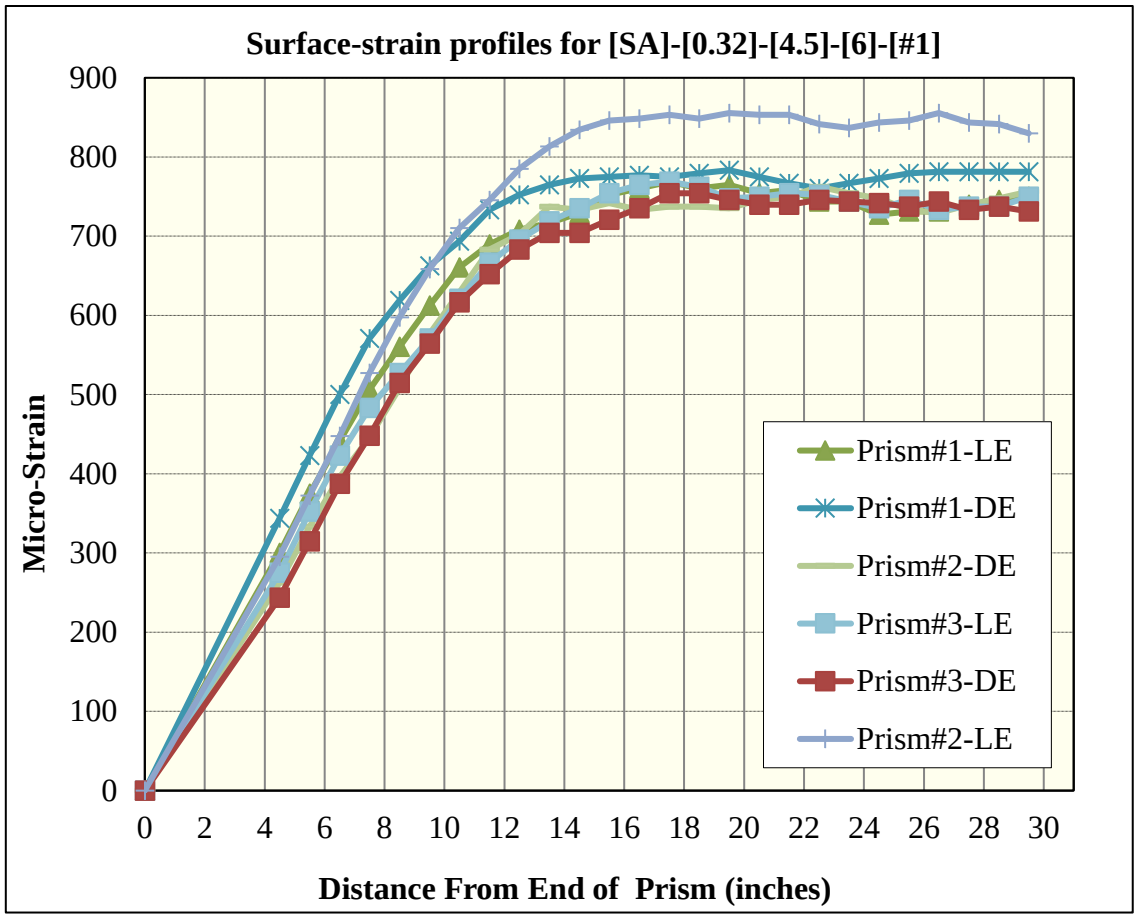

Figure 145 Surface-strain profiles for [SA]-[0.32]-[4.5]-[6]-[#1]

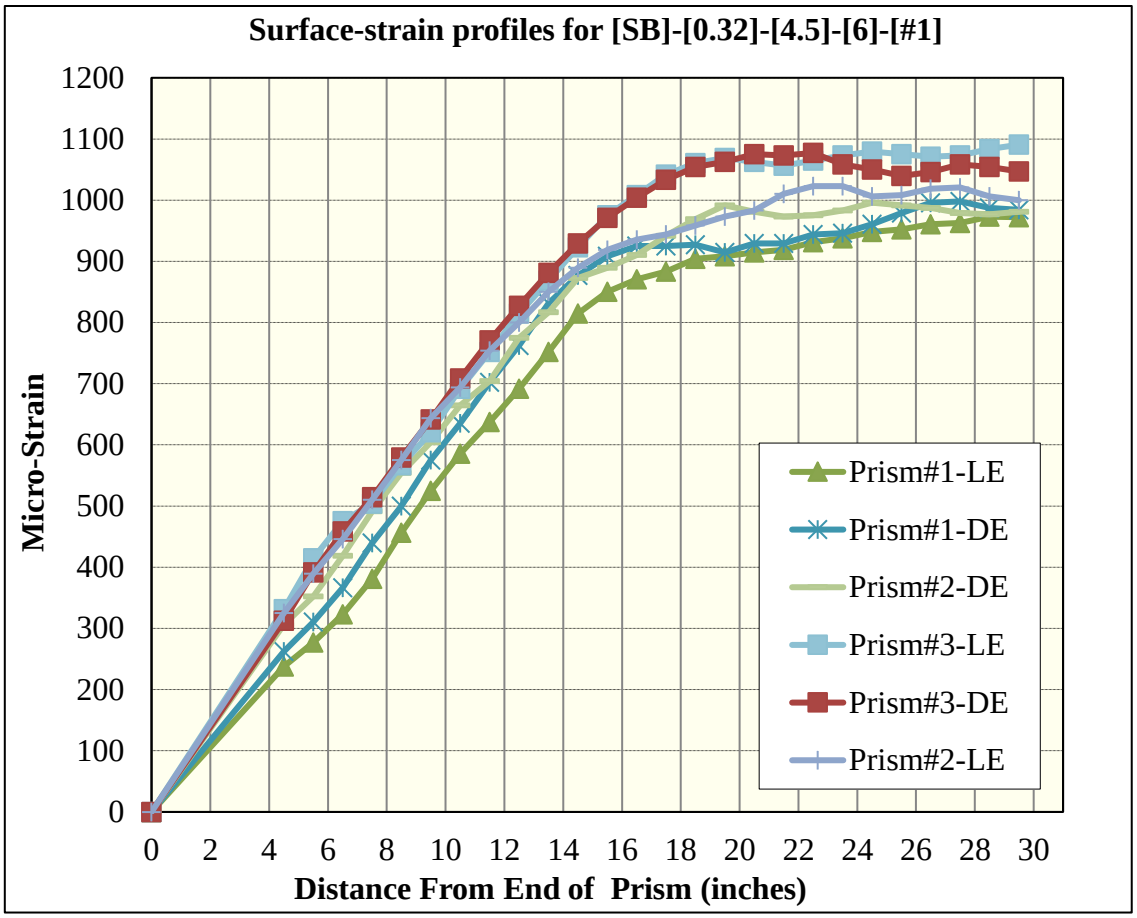

Figure 146 Surface-strain profiles for [SB]-[0.32]-[4.5]-[6]-[#1]

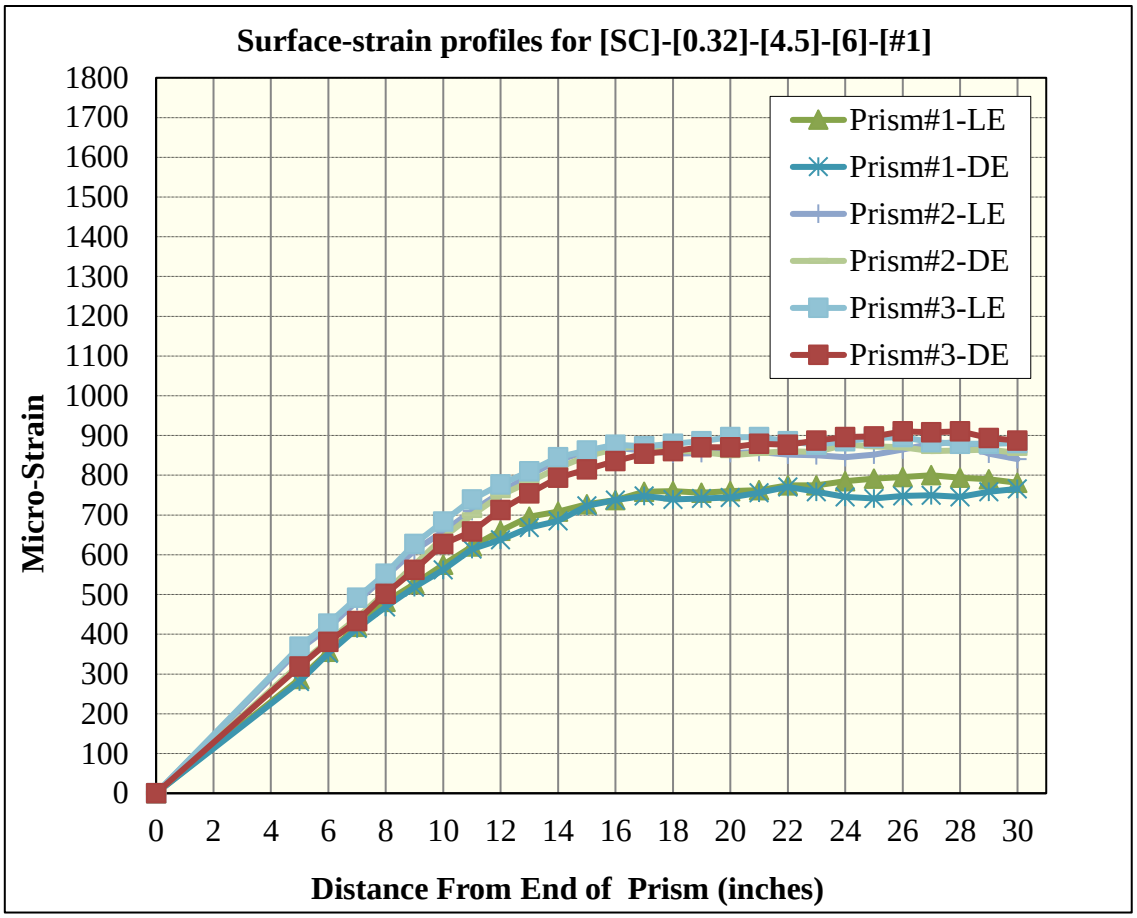

Figure 147 Surface-strain profiles for [SC]-[0.32]-[4.5]-[6]-[#1]

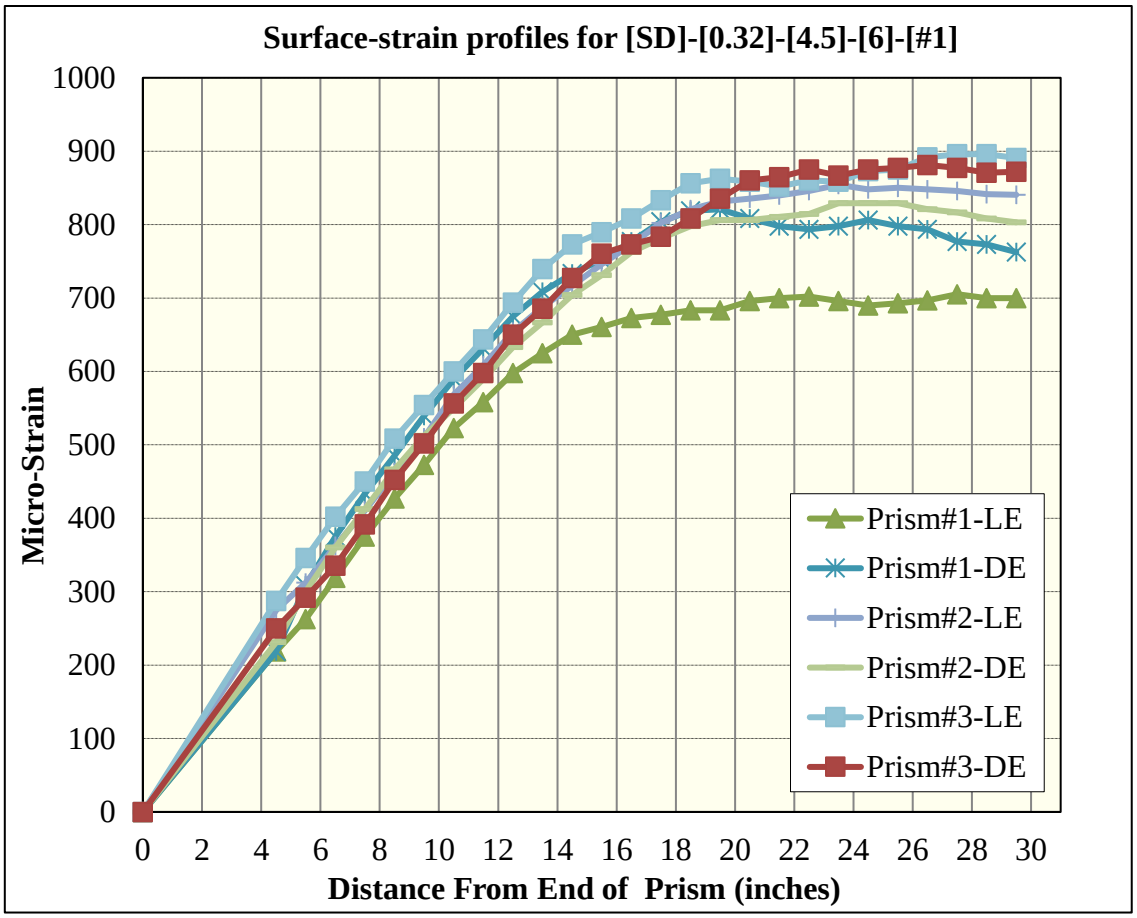

Figure 148 Surface-strain profiles for [SD]-[0.32]-[4.5]-[6]-[#1]

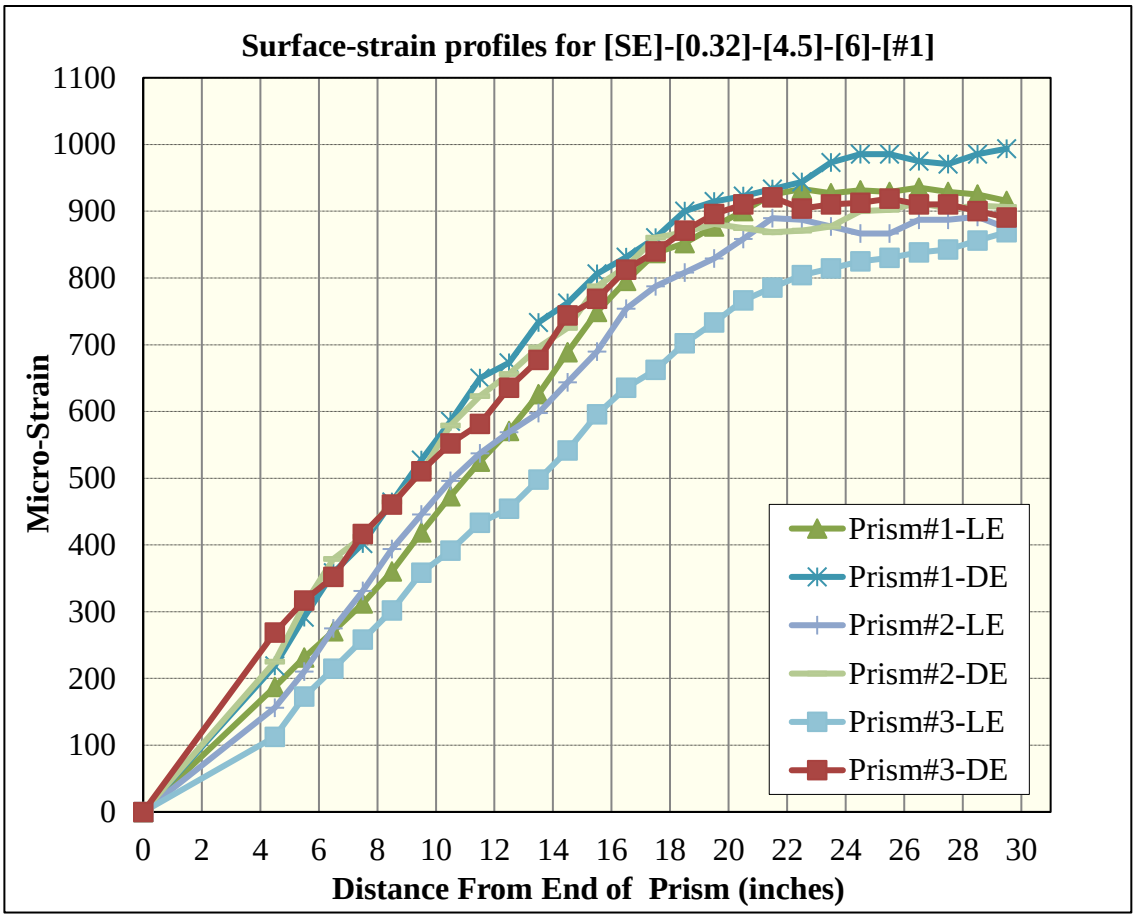

Figure 149 Surface-strain profiles for [SE]-[0.32]-[4.5]-[6]-[#1]

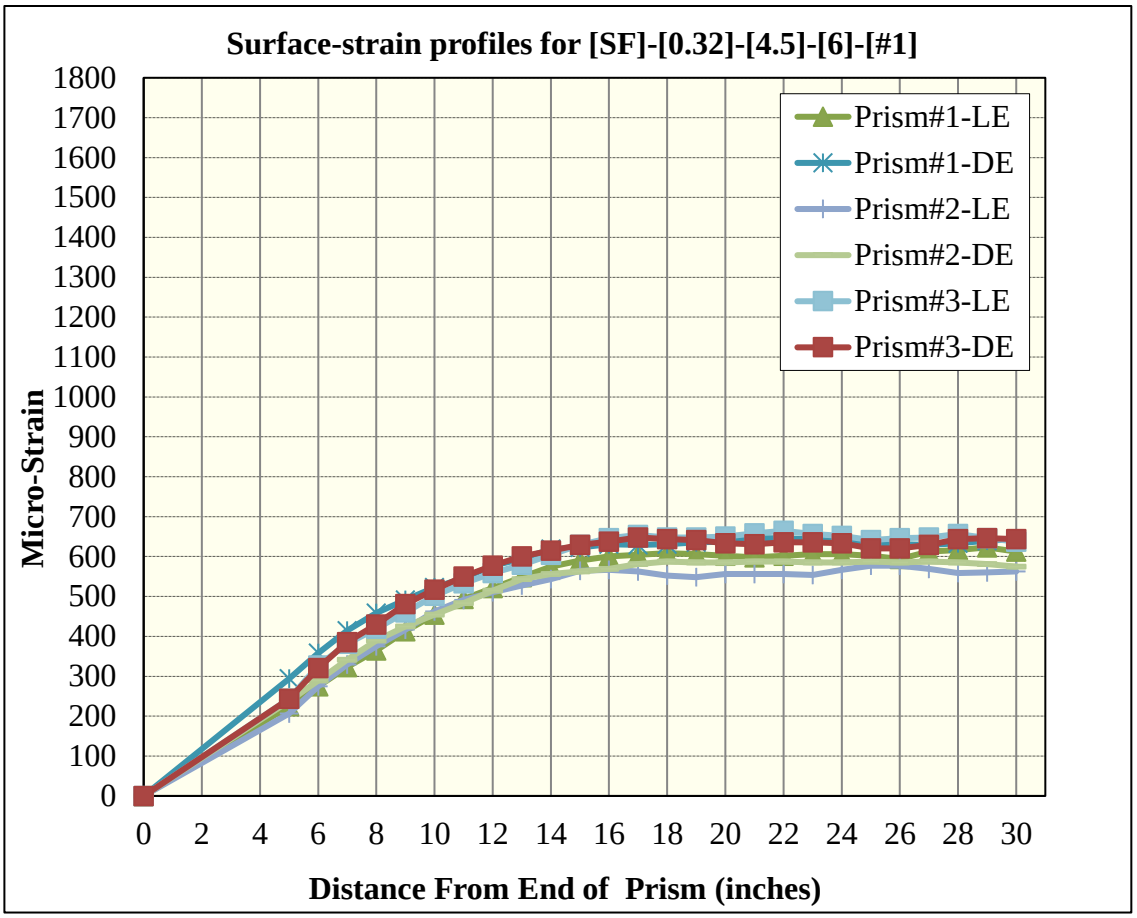

Figure 150 Surface-strain profiles for [SF]-[0.32]-[4.5]-[6]-[#1]

Lab-Phase - Effect of release strength on transfer length

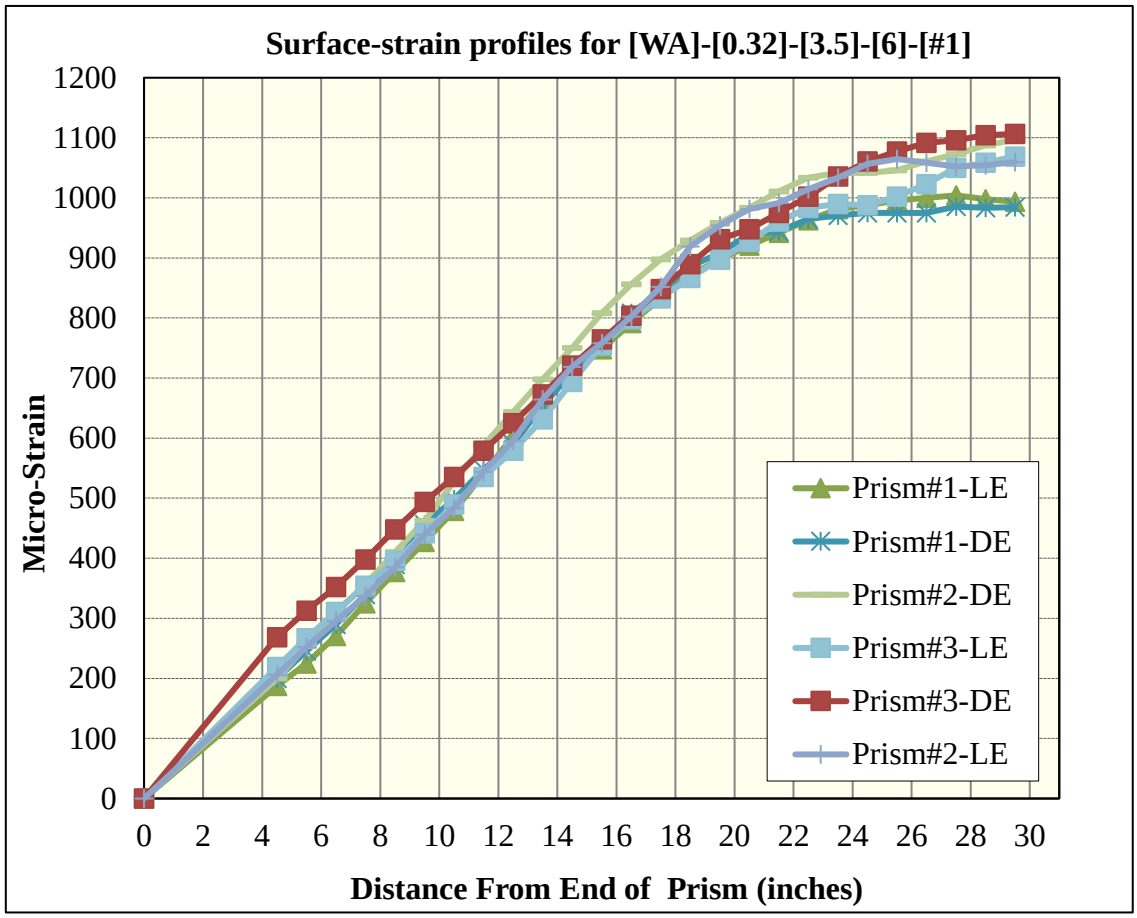

Figure 151 Surface-strain profiles for [WA]-[0.32]-[3.5]-[6]-[#1]

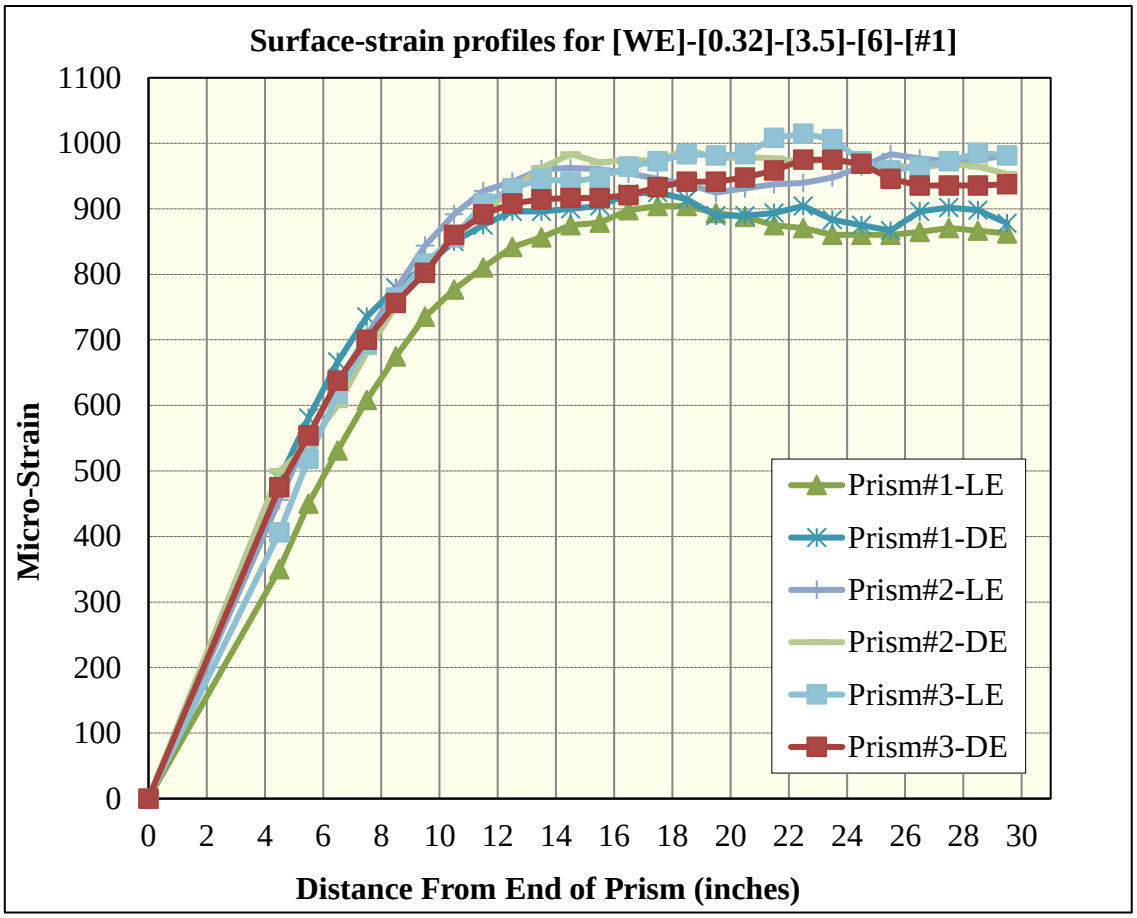

Figure 152 Surface-strain profiles for [WE]-[0.32]-[3.5]-[6]-[#1]

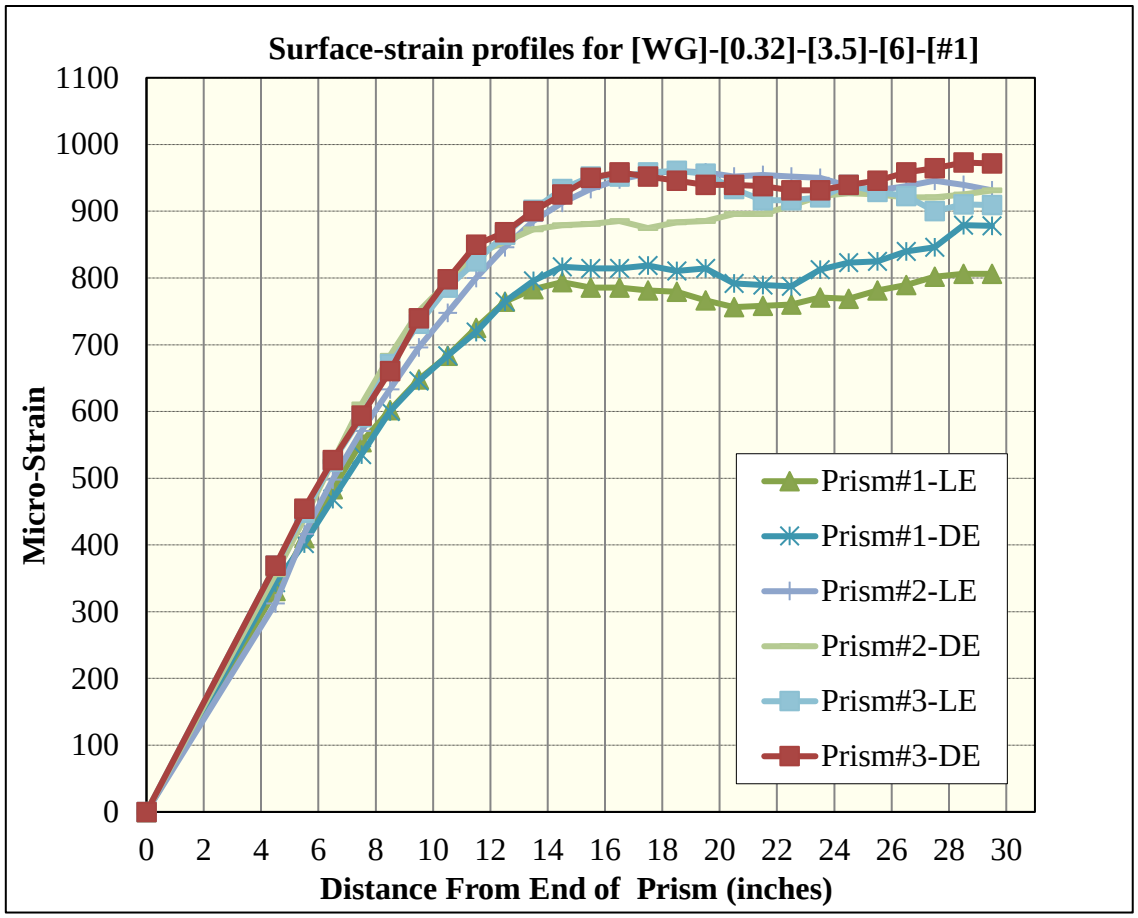

Figure 153 Surface-strain profiles for [WG]-[0.32]-[3.5]-[6]-[#1]

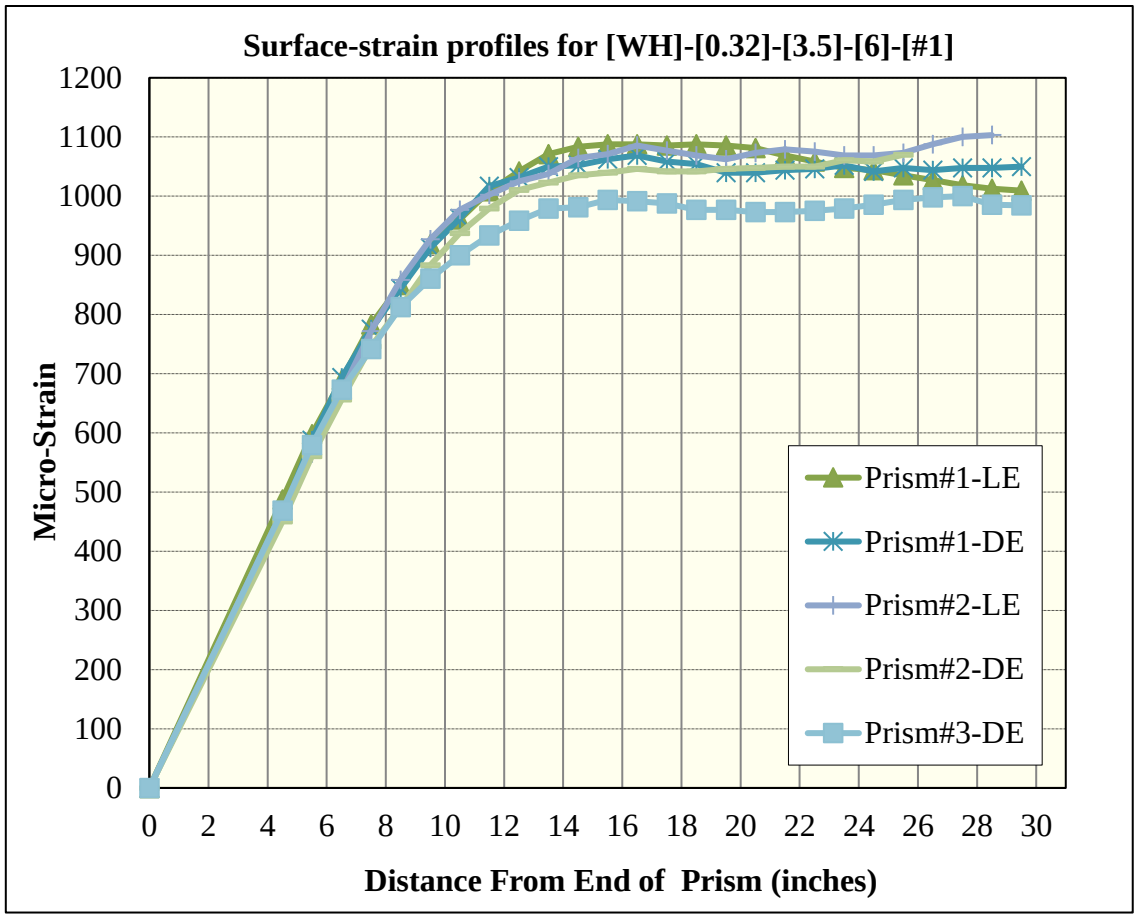

Figure 154 Surface-strain profiles for [WH]-[0.32]-[3.5]-[6]-[#1]

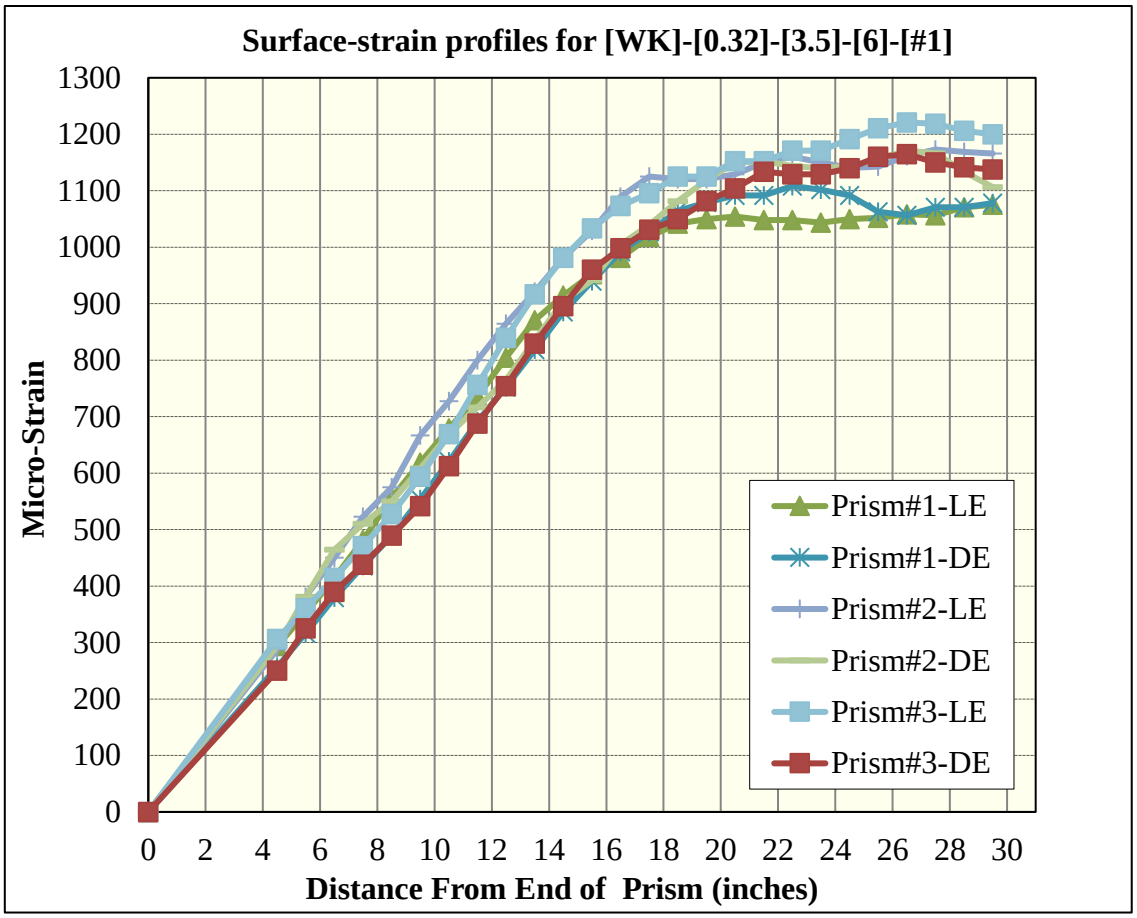

Figure 155 Surface-strain profiles for [WK]-[0.32]-[3.5]-[6]-[#1]

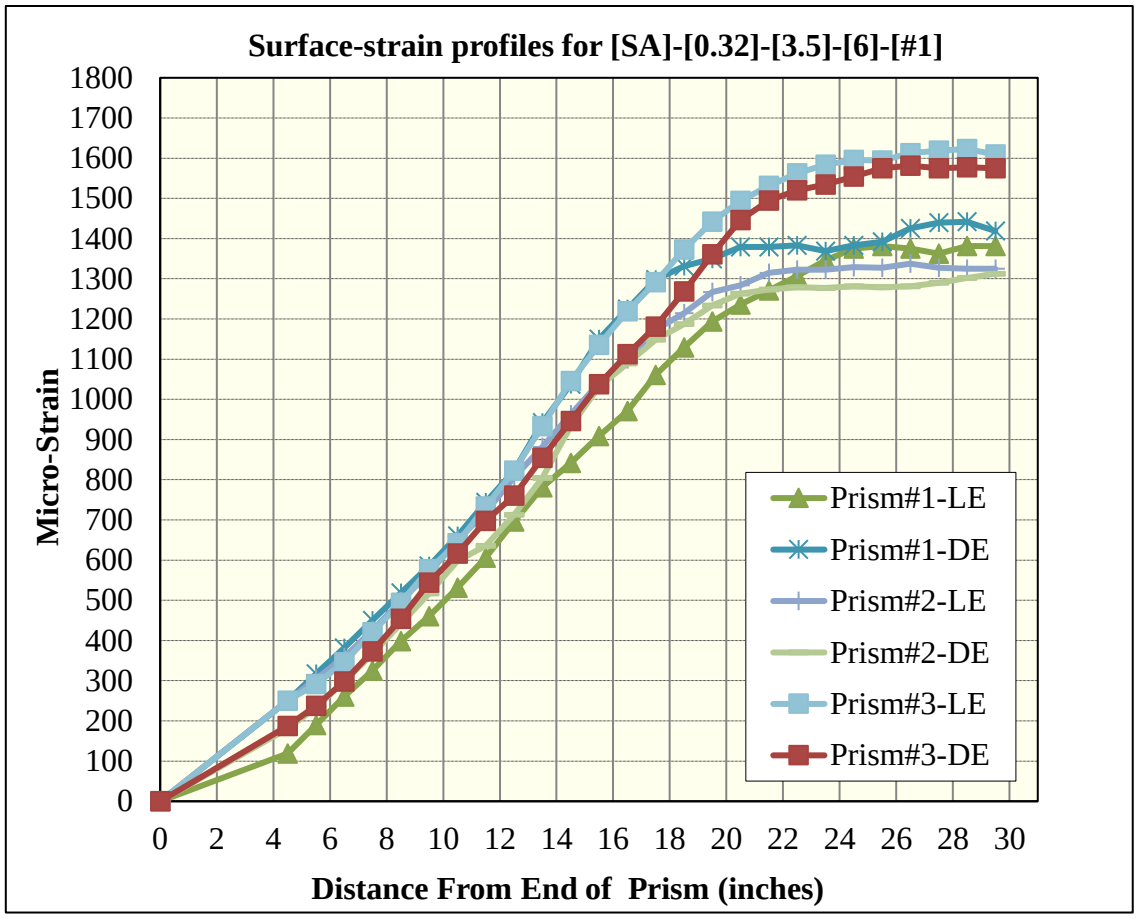

Figure 156 Surface-strain profiles for [SA]-[0.32]-[3.5]-[6]-[#1]

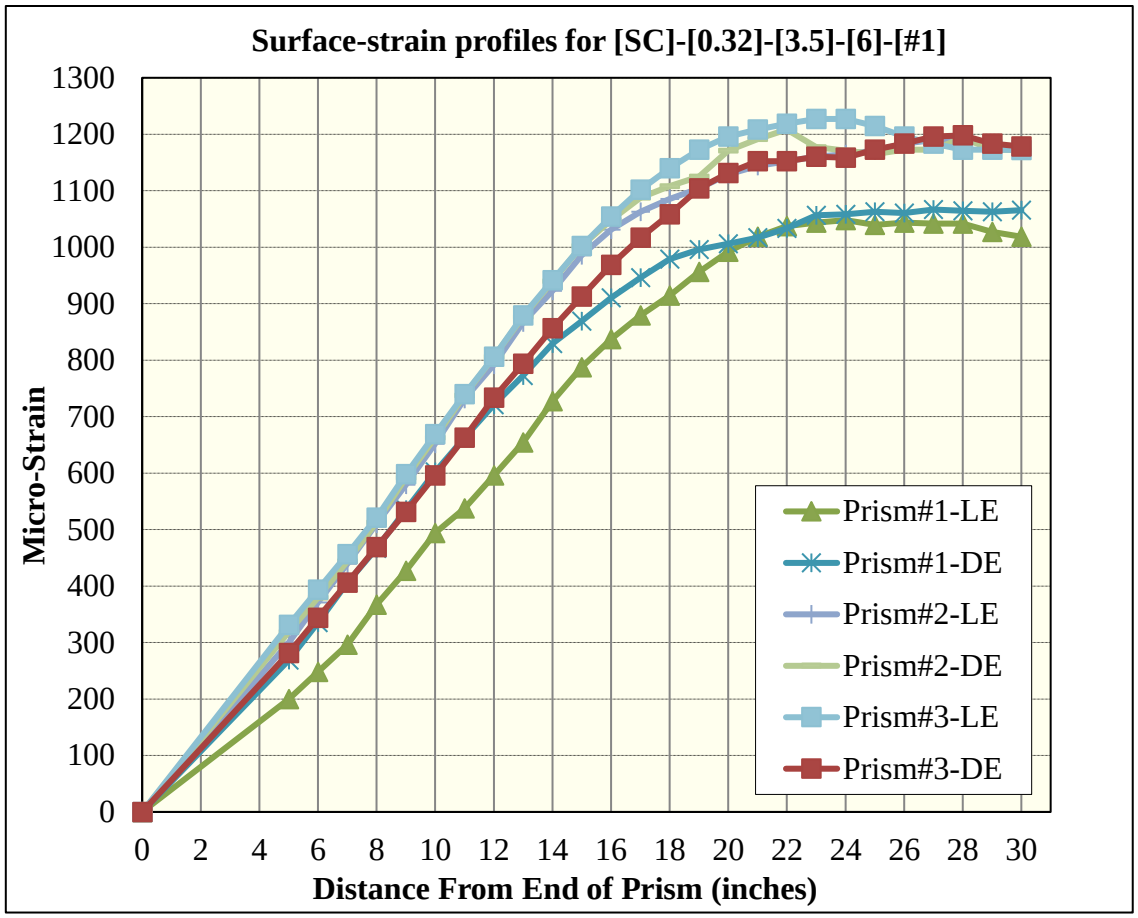

Figure 157 Surface-strain profiles for [SC]-[0.32]-[3.5]-[6]-[#1]

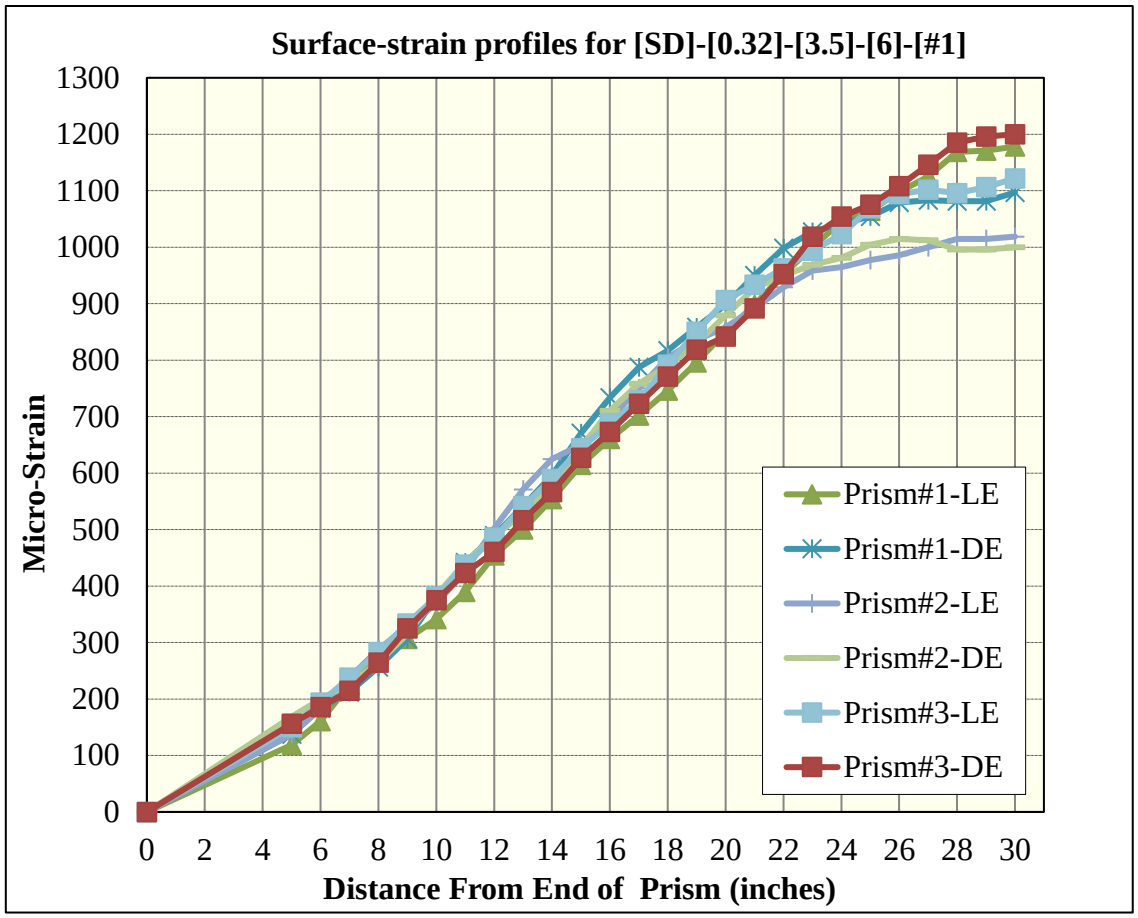

Figure 158 Surface-strain profiles for [SD]-[0.32]-[3.5]-[6]-[#1]

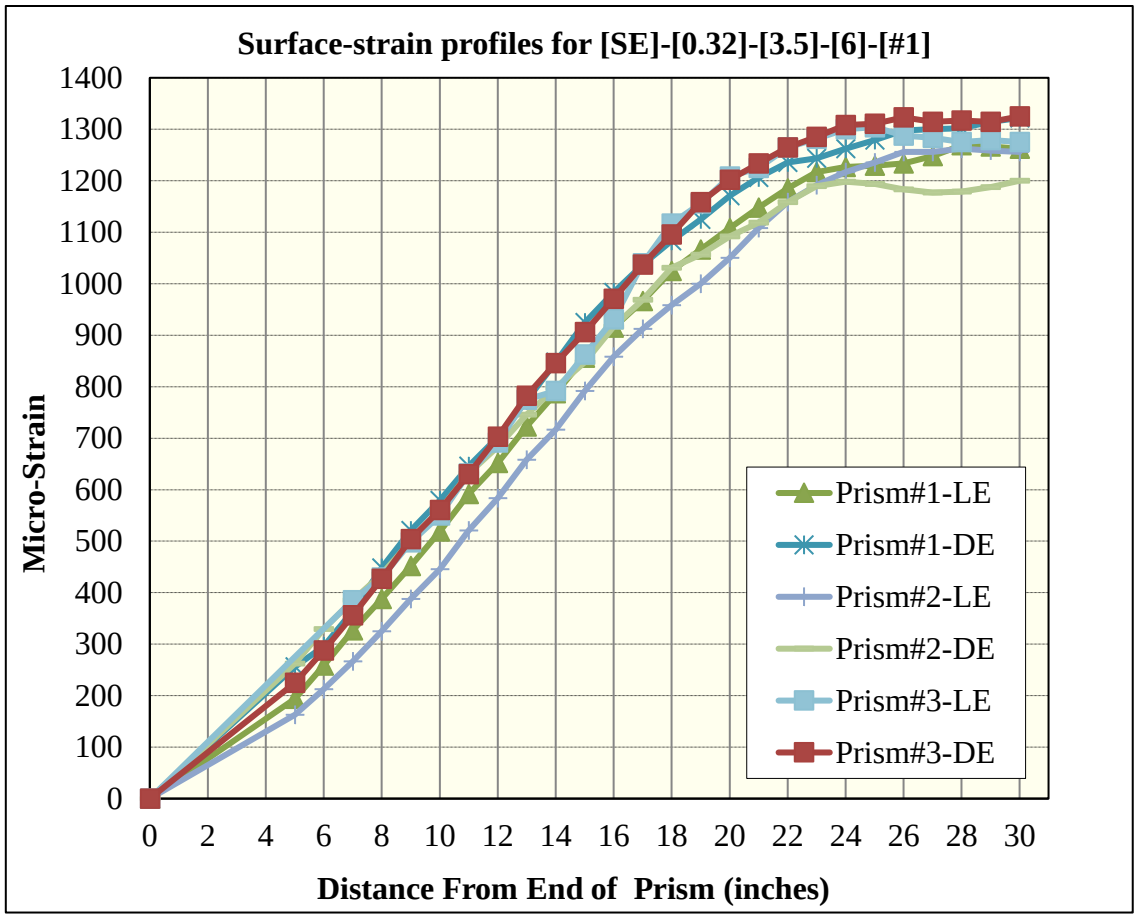

Figure 159 Surface-strain profiles for [SE]-[0.32]-[3.5]-[6]-[#1]

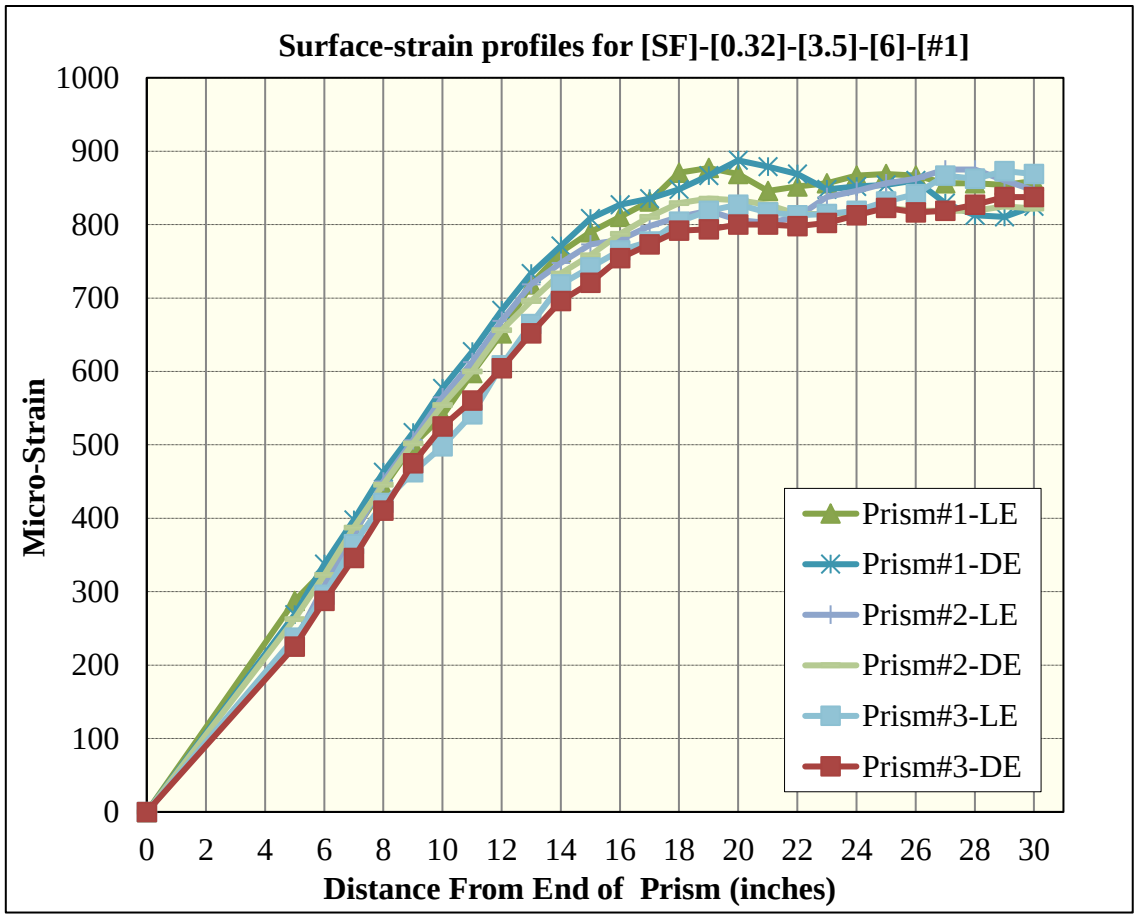

Figure 160 Surface-strain profiles for [SF]-[0.32]-[3.5]-[6]-[#1]

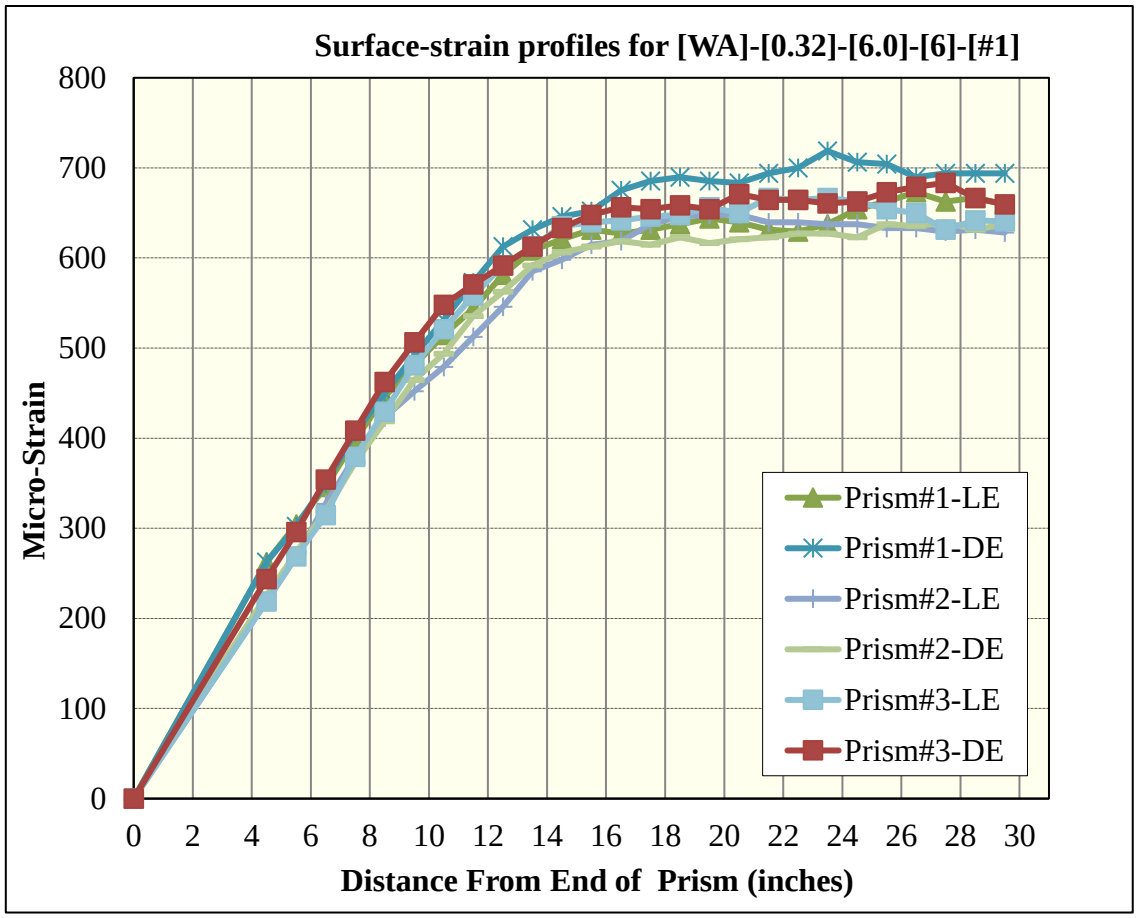

Figure 161 Surface-strain profiles for [WA]-[0.32]-[6.0]-[6]-[#1]

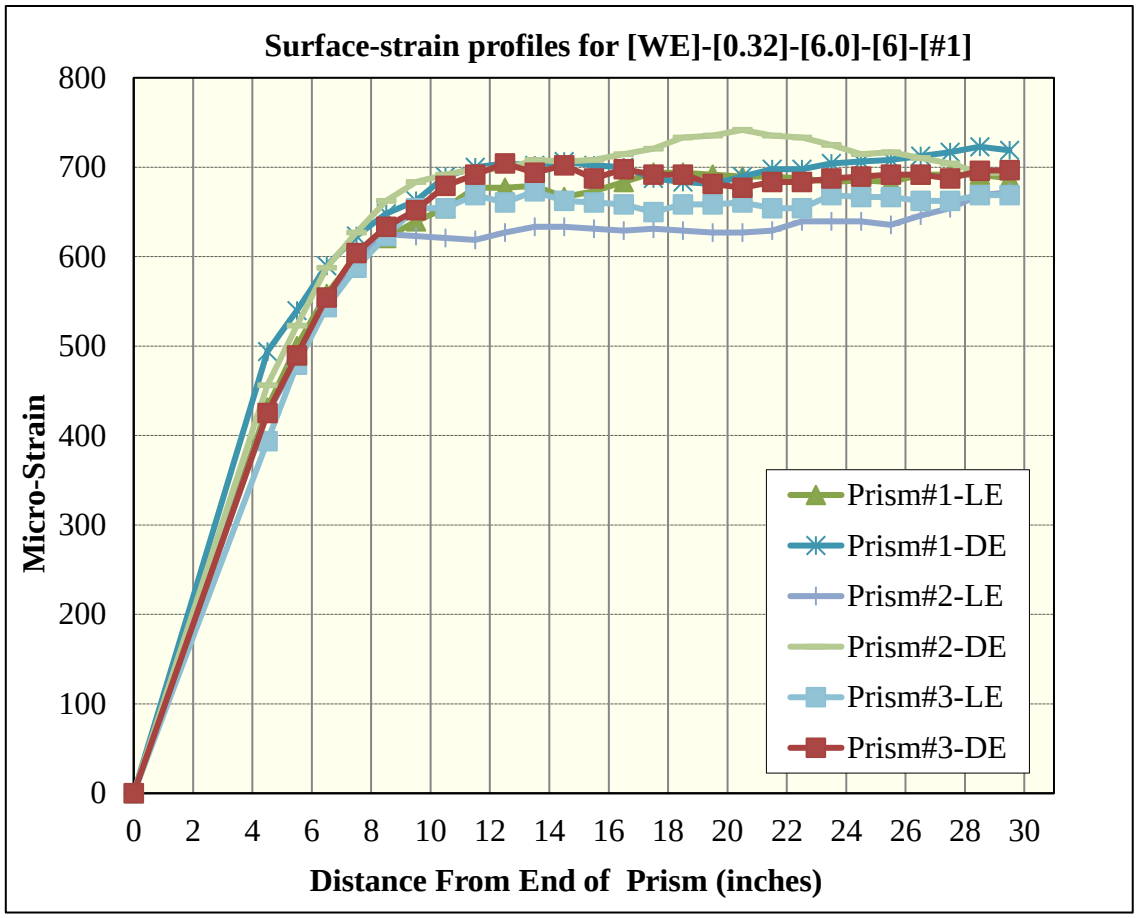

Figure 162 Surface-strain profiles for [WE]-[0.32]-[6.0]-[6]-[#1]

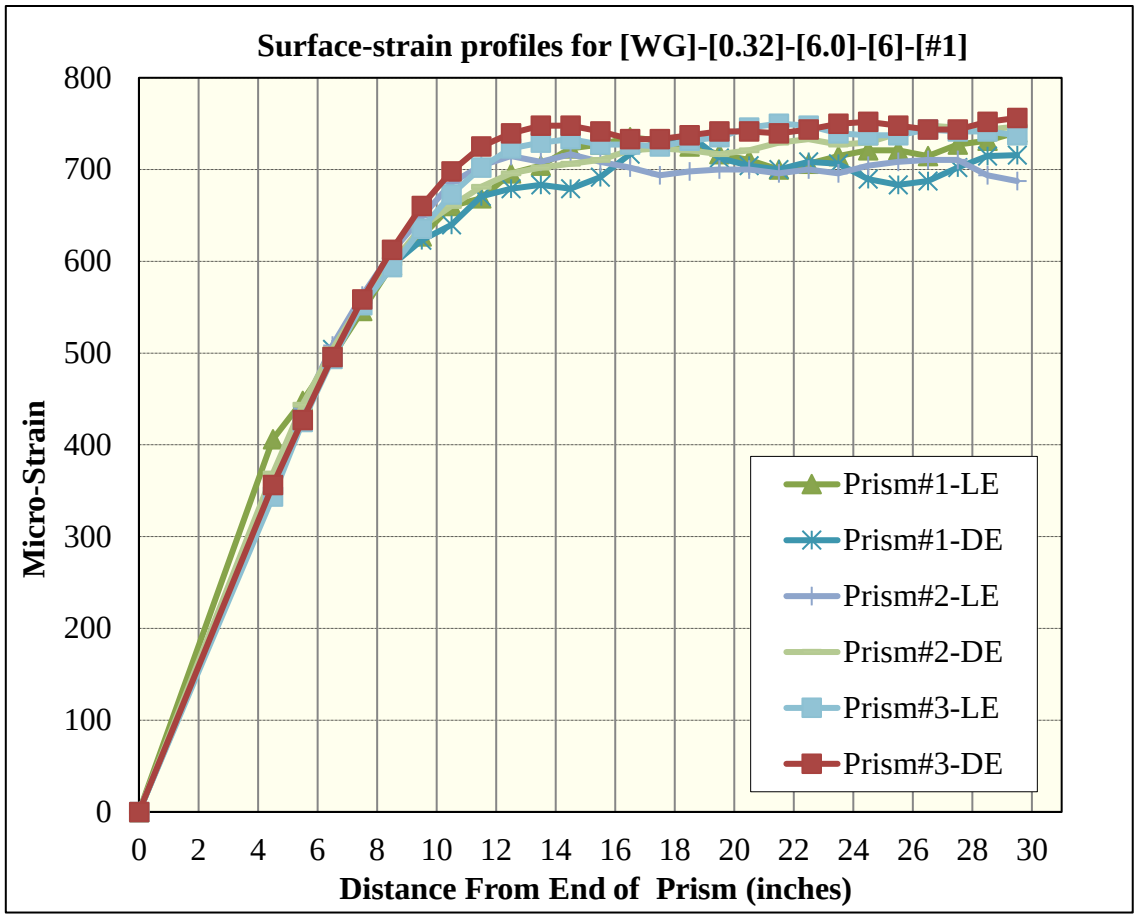

Figure 163 Surface-strain profiles for [WG]-[0.32]-[6.0]-[6]-[#1]

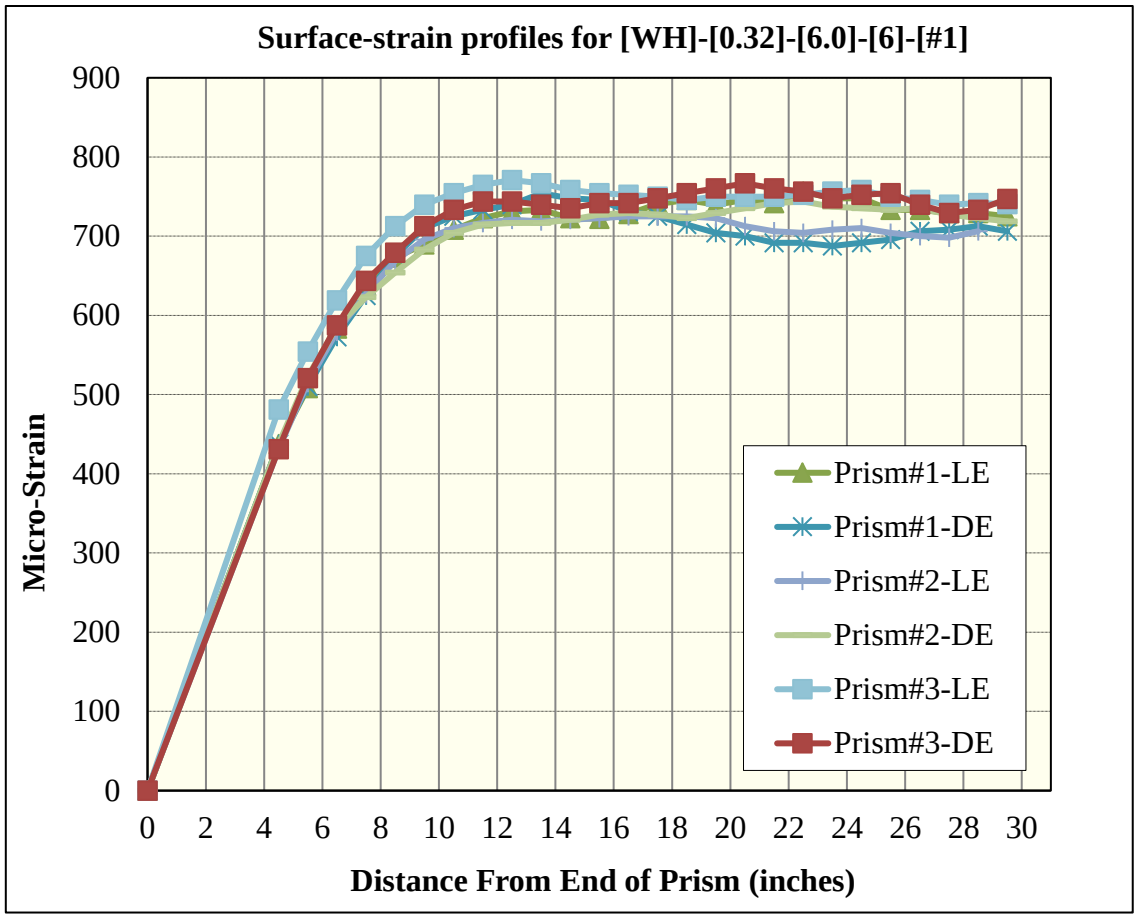

Figure 164 Surface-strain profiles for [WH]-[0.32]-[6.0]-[6]-[#1]

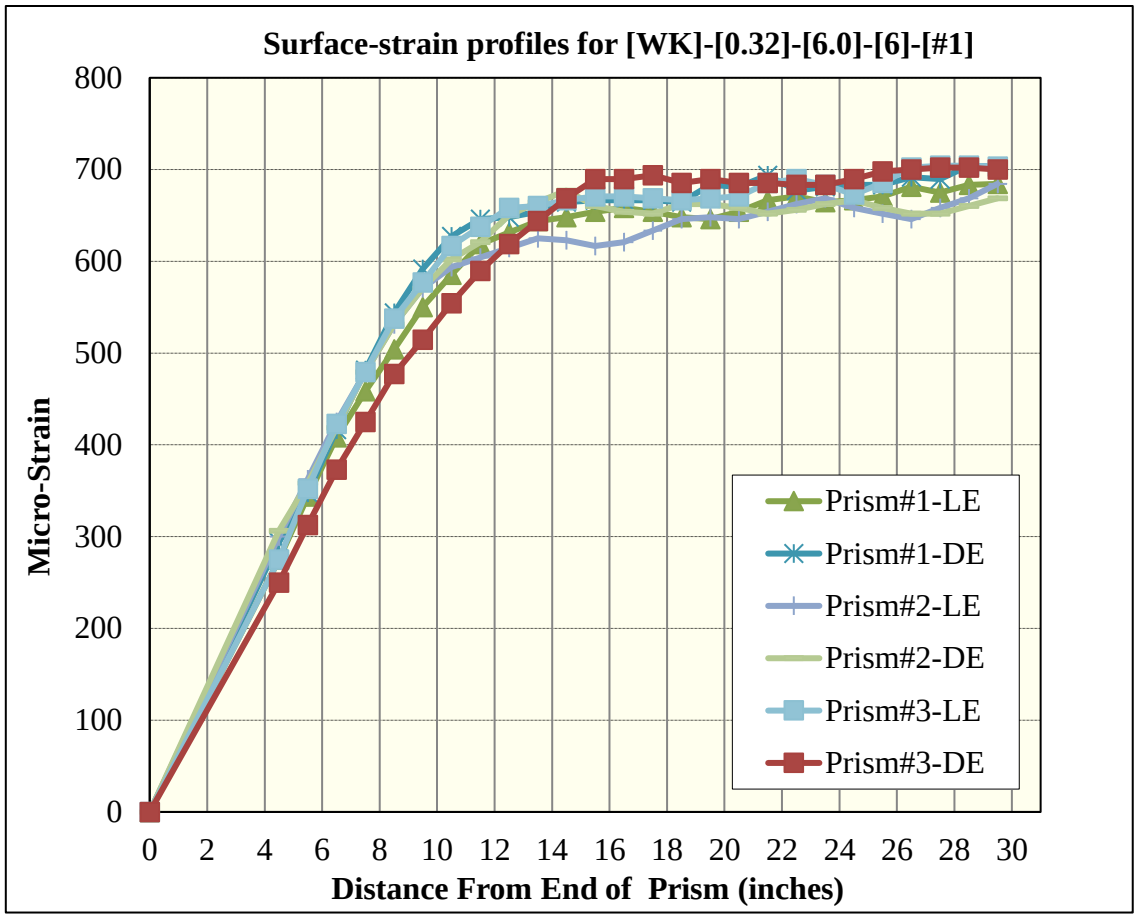

Figure 165 Surface-strain profiles for [WK]-[0.32]-[6.0]-[6]-[#1]

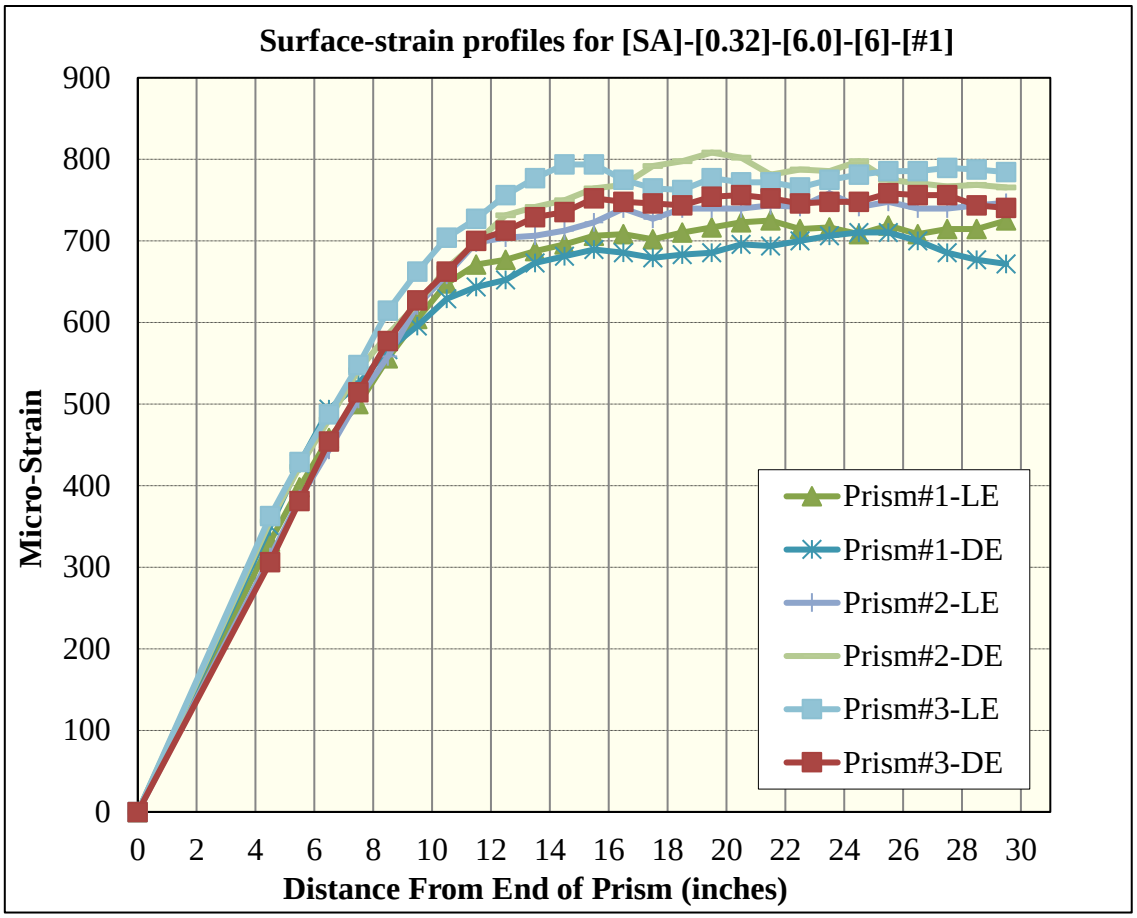

Figure 166 Surface-strain profiles for [SA]-[0.32]-[6.0]-[6]-[#1]

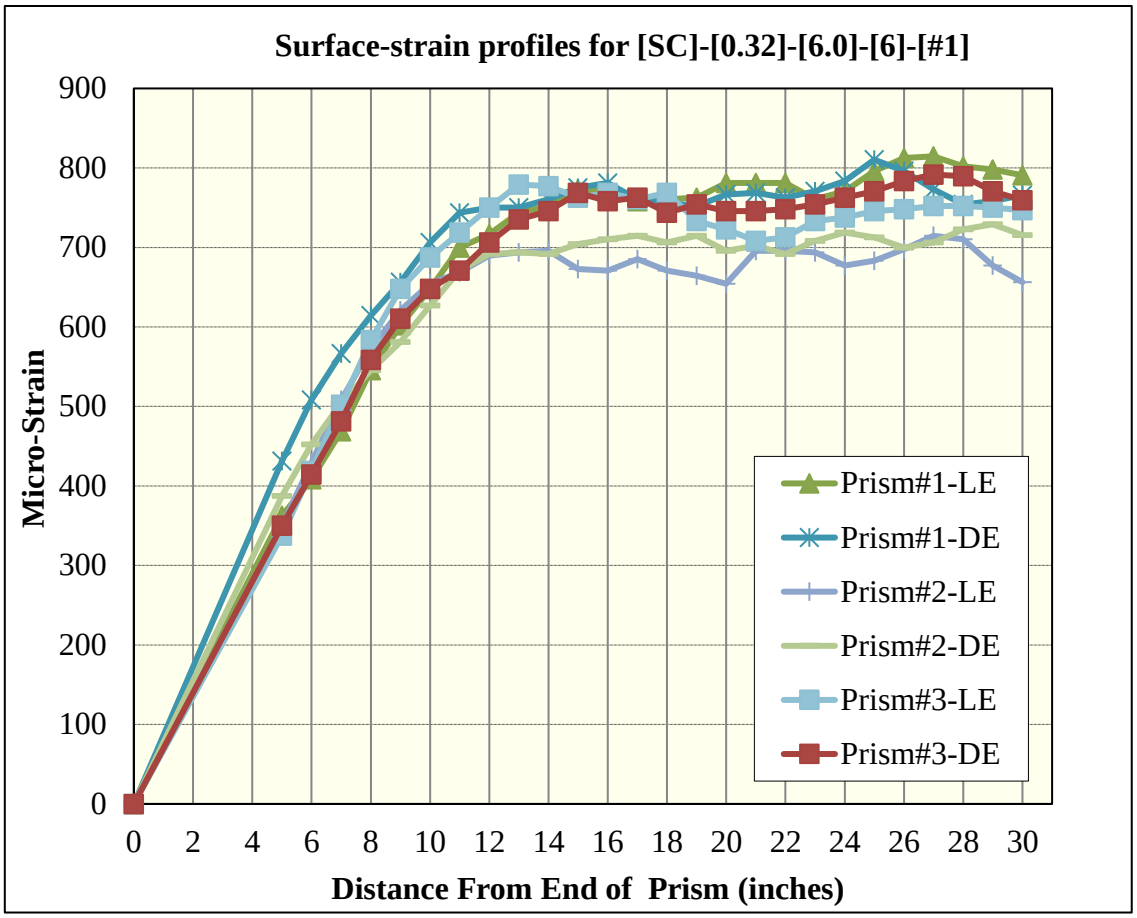

Figure 167 Surface-strain profiles for [SC]-[0.32]-[6.0]-[6]-[#1]

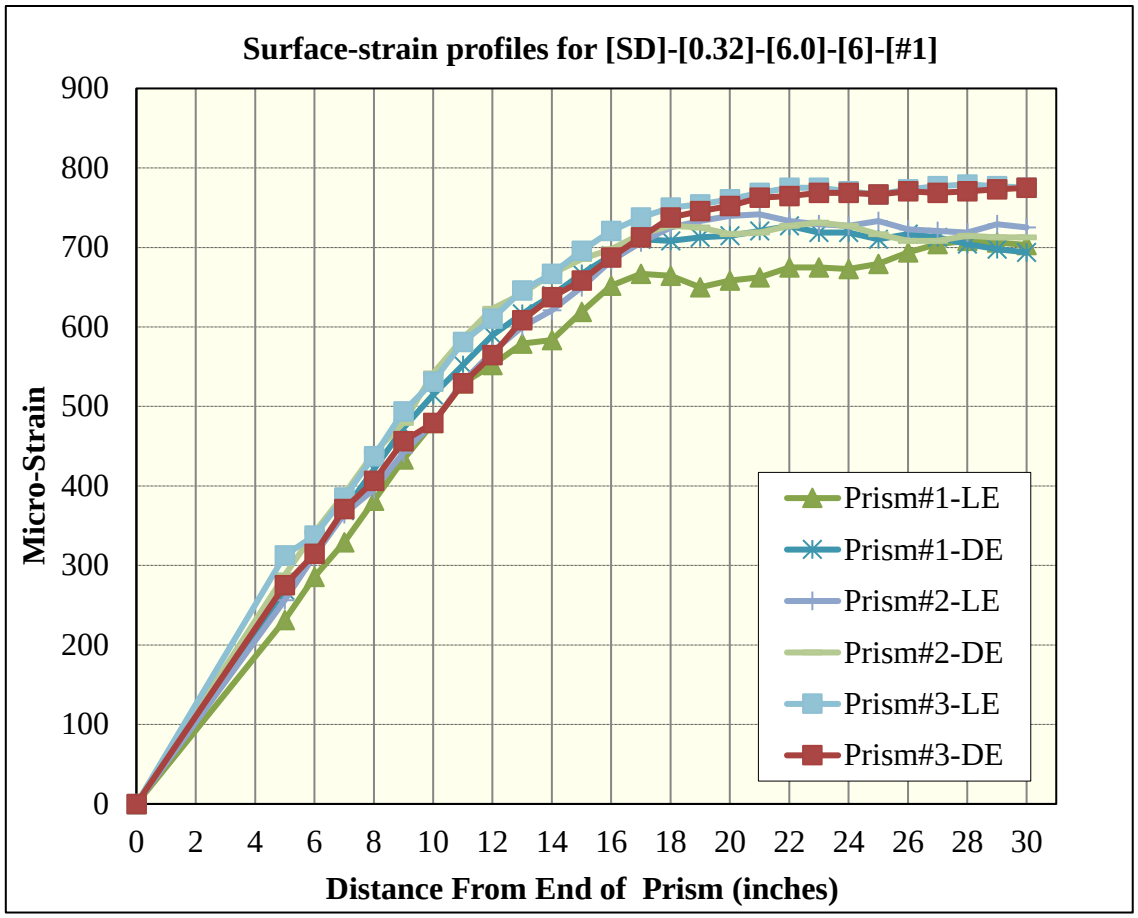

Figure 168 Surface-strain profiles for [SD]-[0.32]-[6.0]-[6]-[#1]

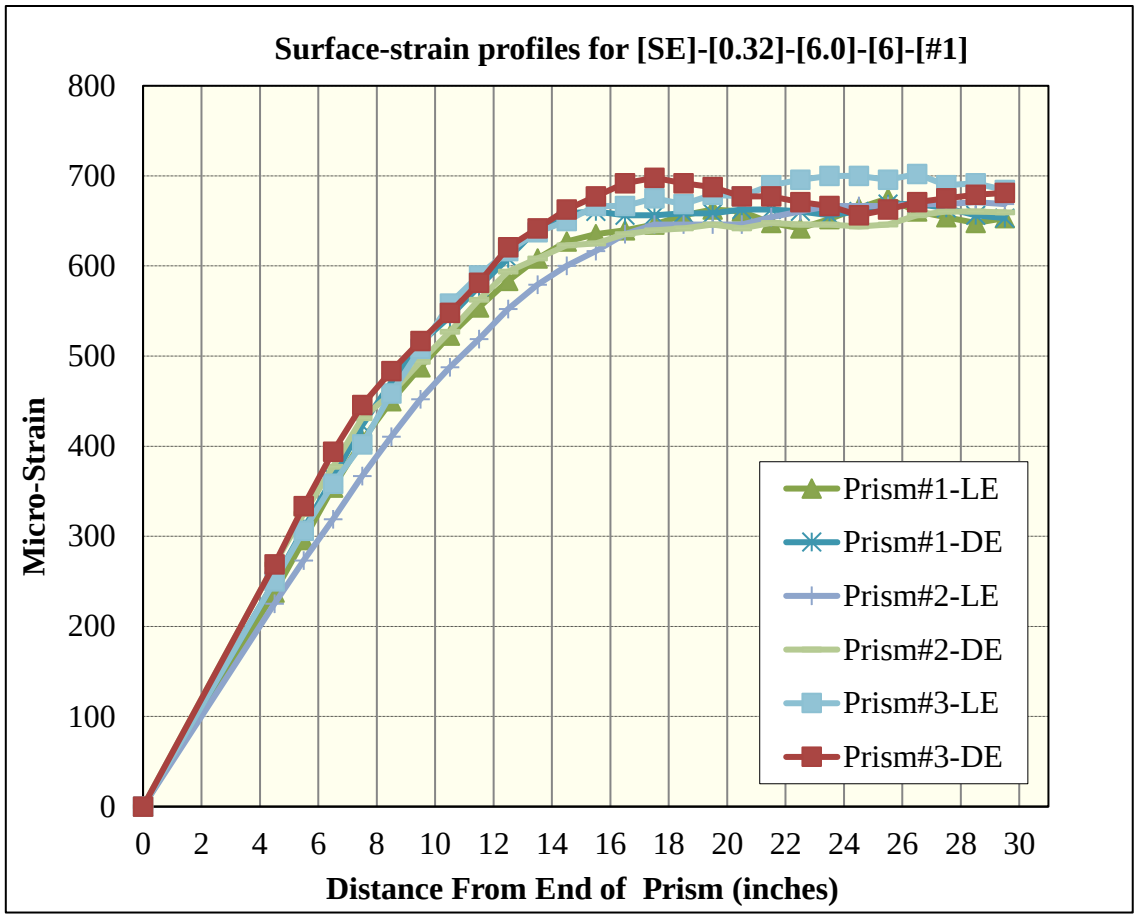

Figure 169 Surface-strain profiles for [SE]-[0.32]-[6.0]-[6]-[#1]

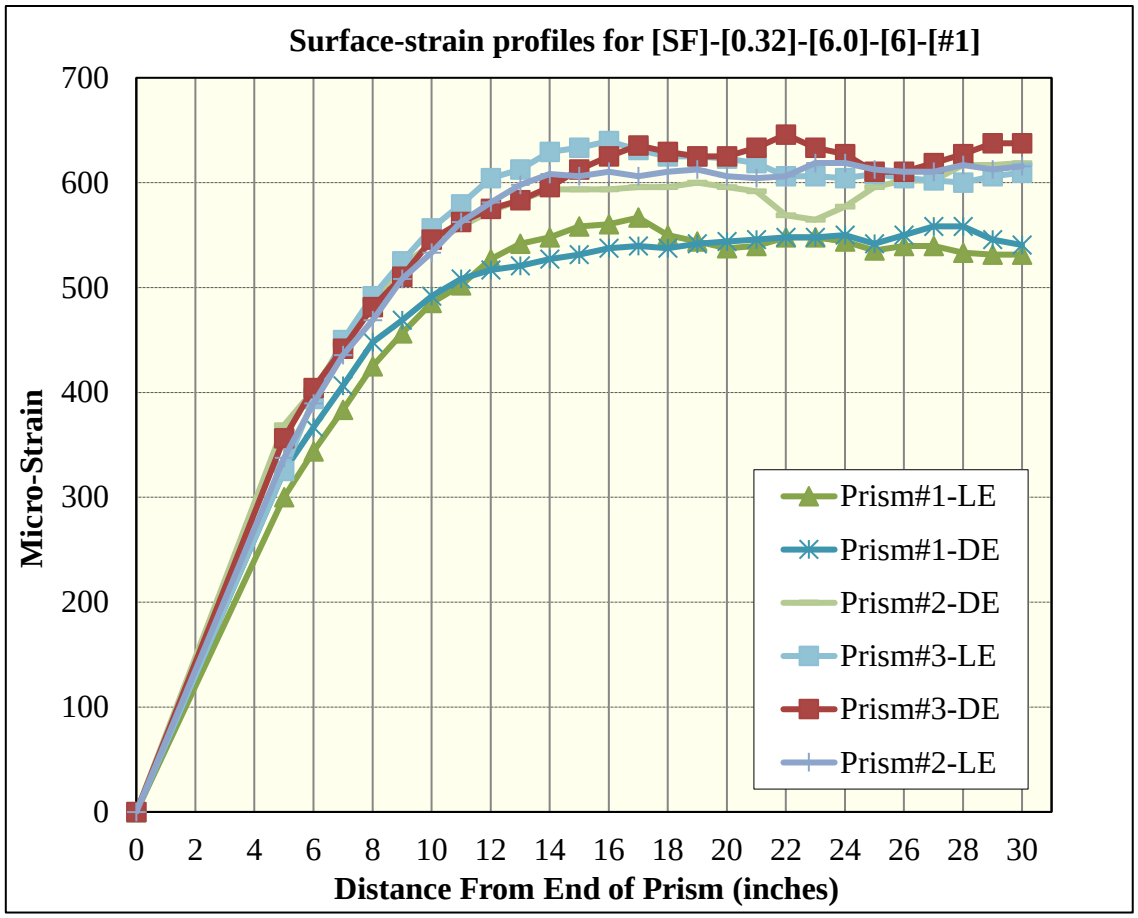

Figure 170 Surface-strain profiles for [SF]-[0.32]-[6.0]-[6]-[#1]

Lab Phase - Effect of concrete consistency (slump) on transfer length

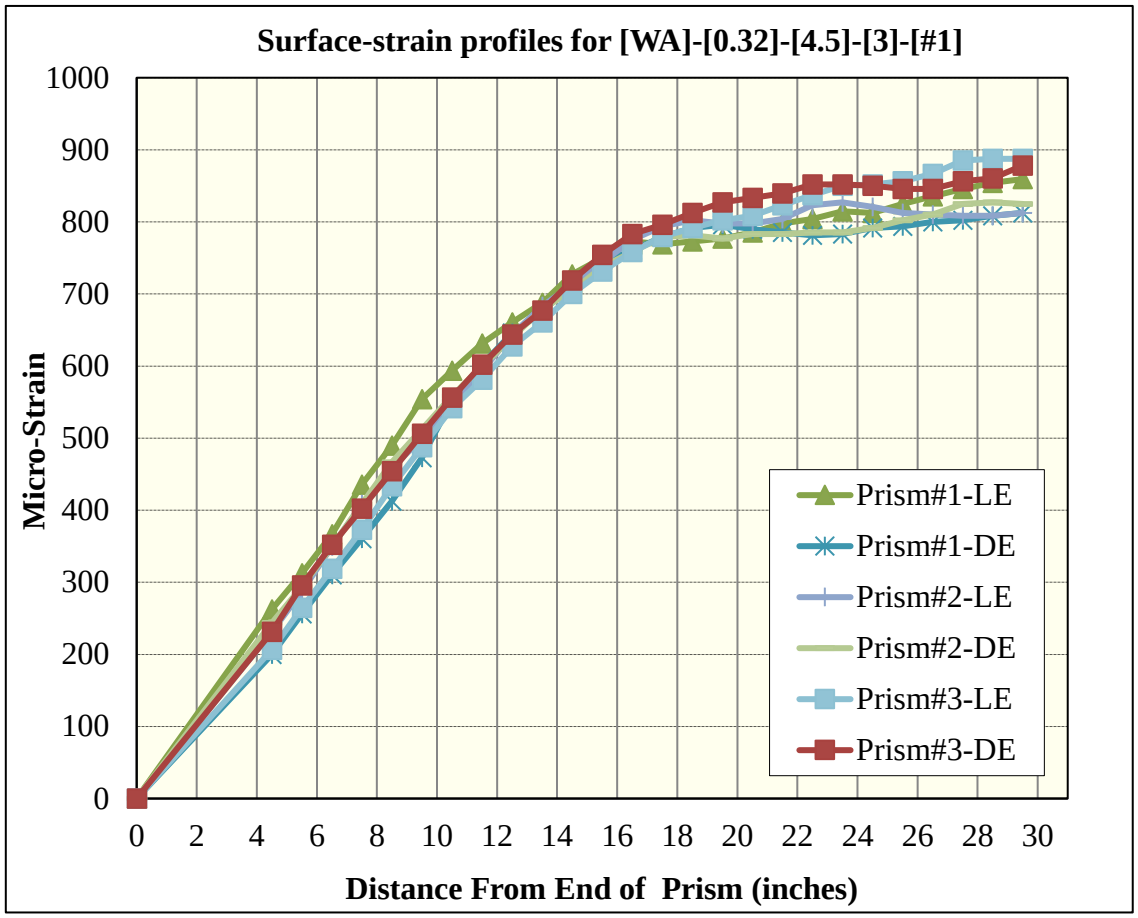

Figure 171 Surface-strain profiles for [WA]-[0.32]-[4.5]-[3]-[#1]

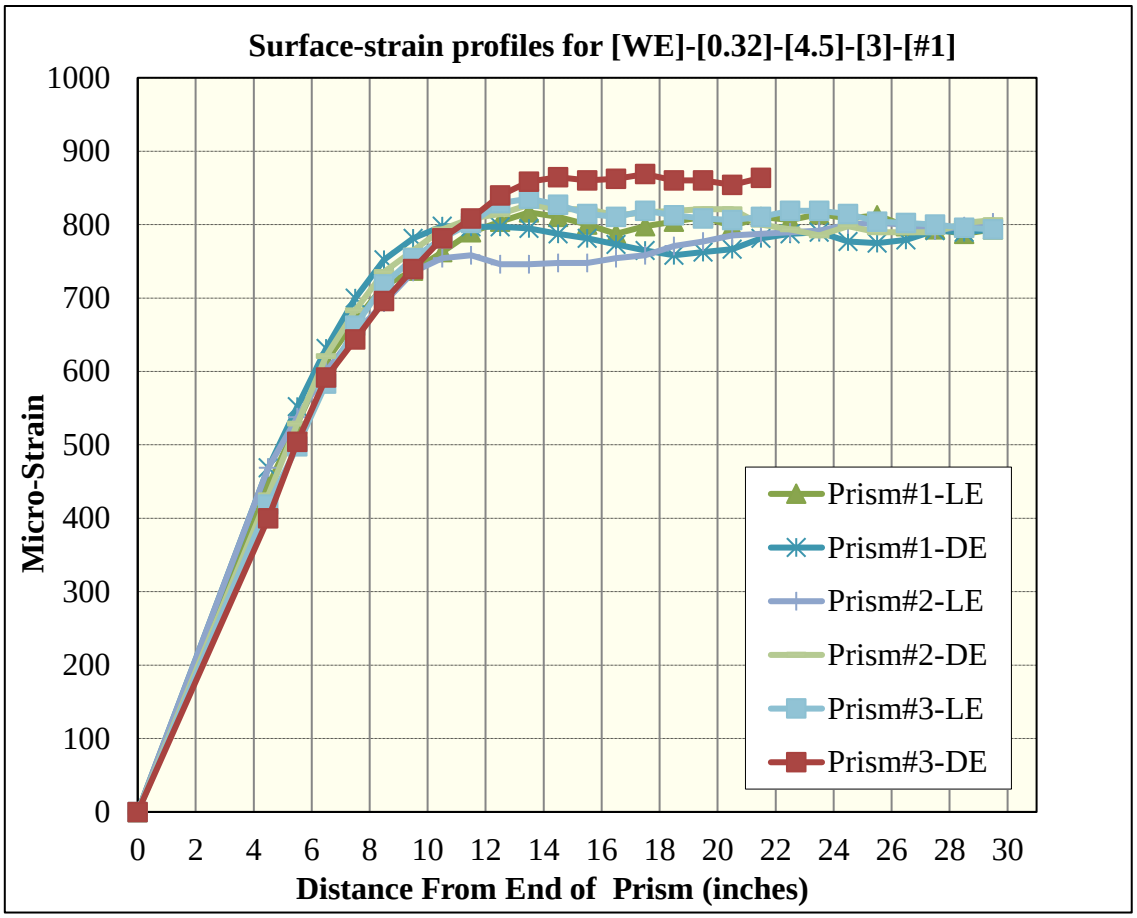

Figure 172 Surface-strain profiles for [WE]-[0.32]-[4.5]-[3]-[#1]

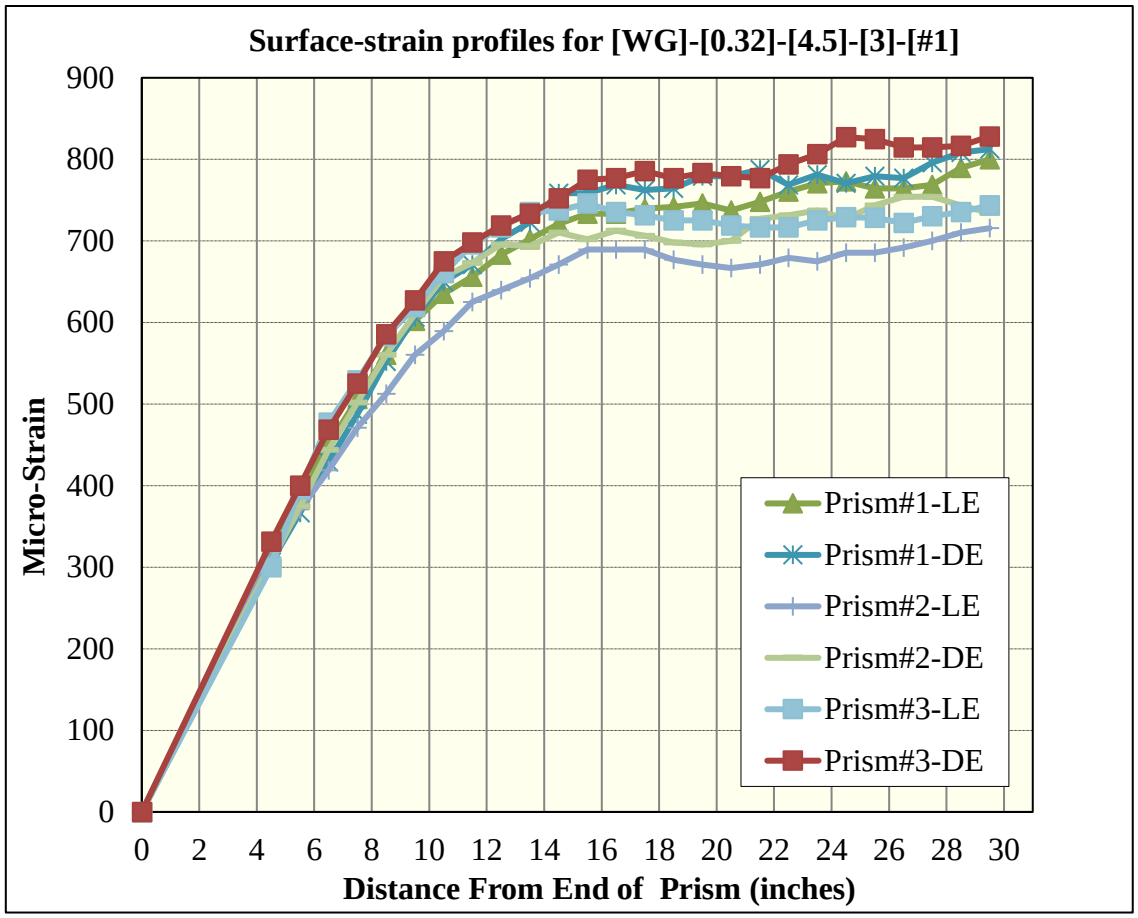

Figure 173 Surface-strain profiles for [WG]-[0.32]-[4.5]-[3]-[#1]

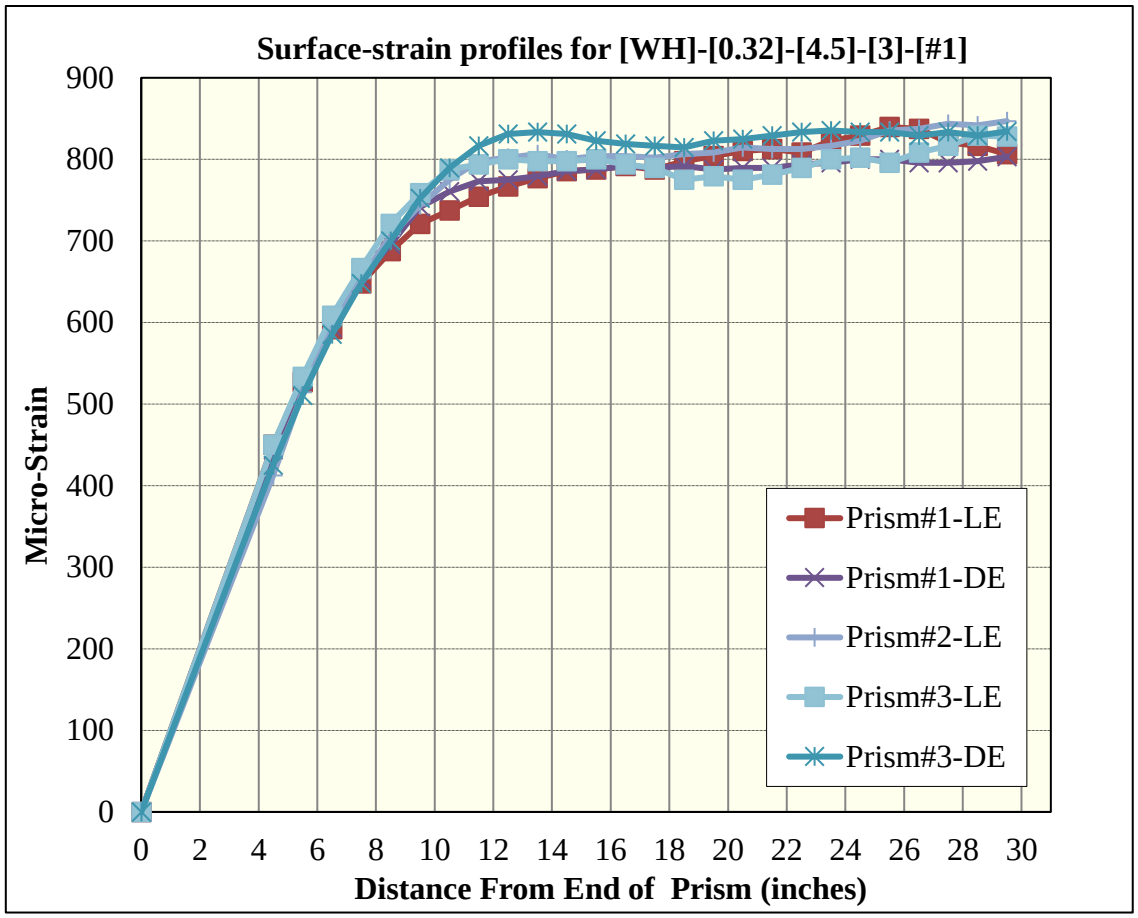

Figure 174 Surface-strain profiles for [WH]-[0.32]-[4.5]-[3]-[#1]

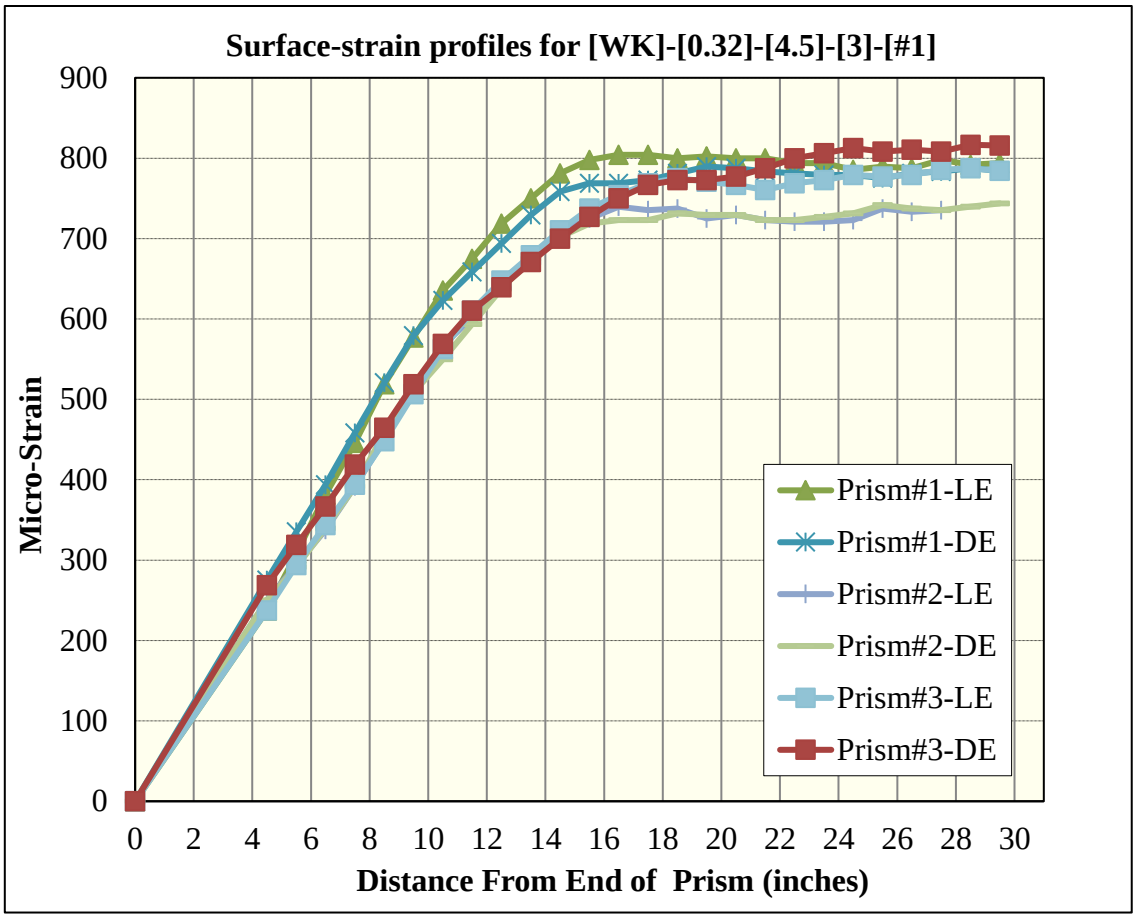

Figure 175 Surface-strain profiles for [WK]-[0.32]-[4.5]-[3]-[#1]

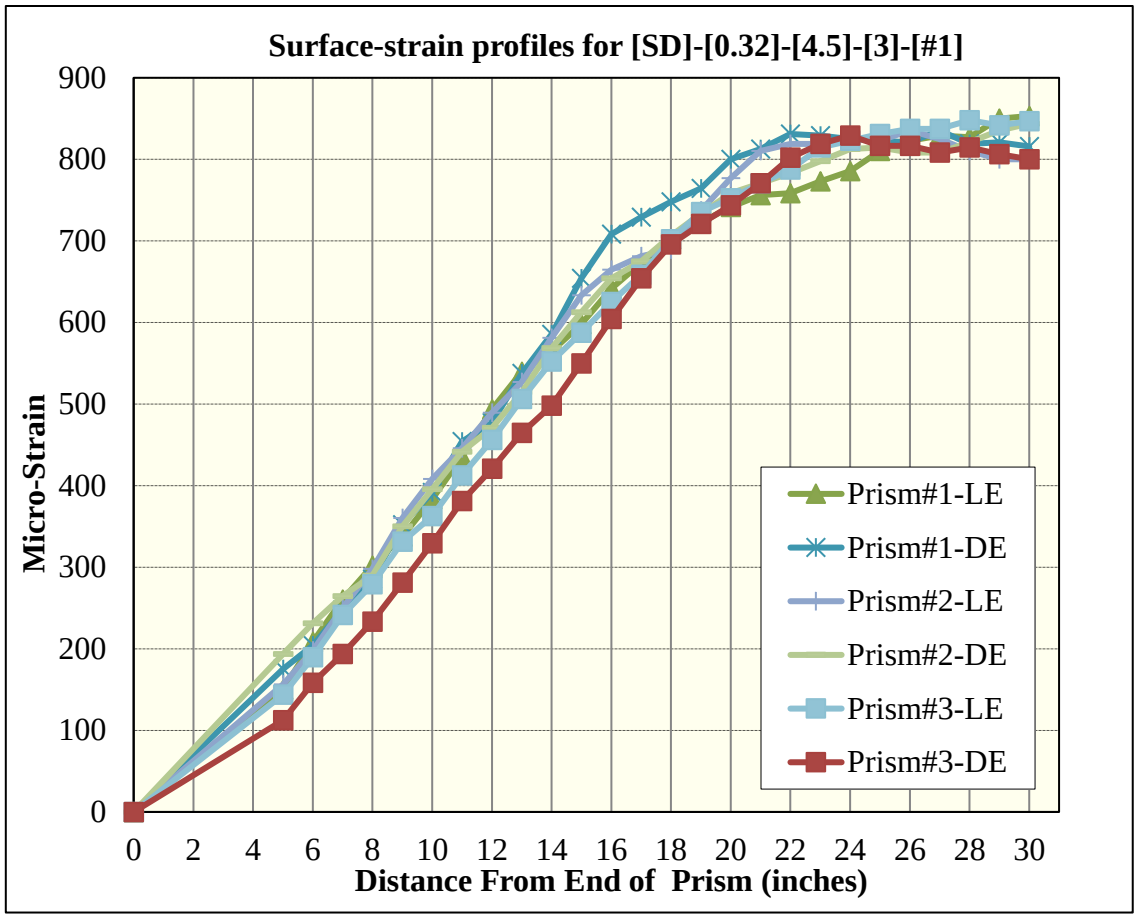

Figure 176 Surface-strain profiles for [SD]-[0.32]-[4.5]-[3]-[#1]

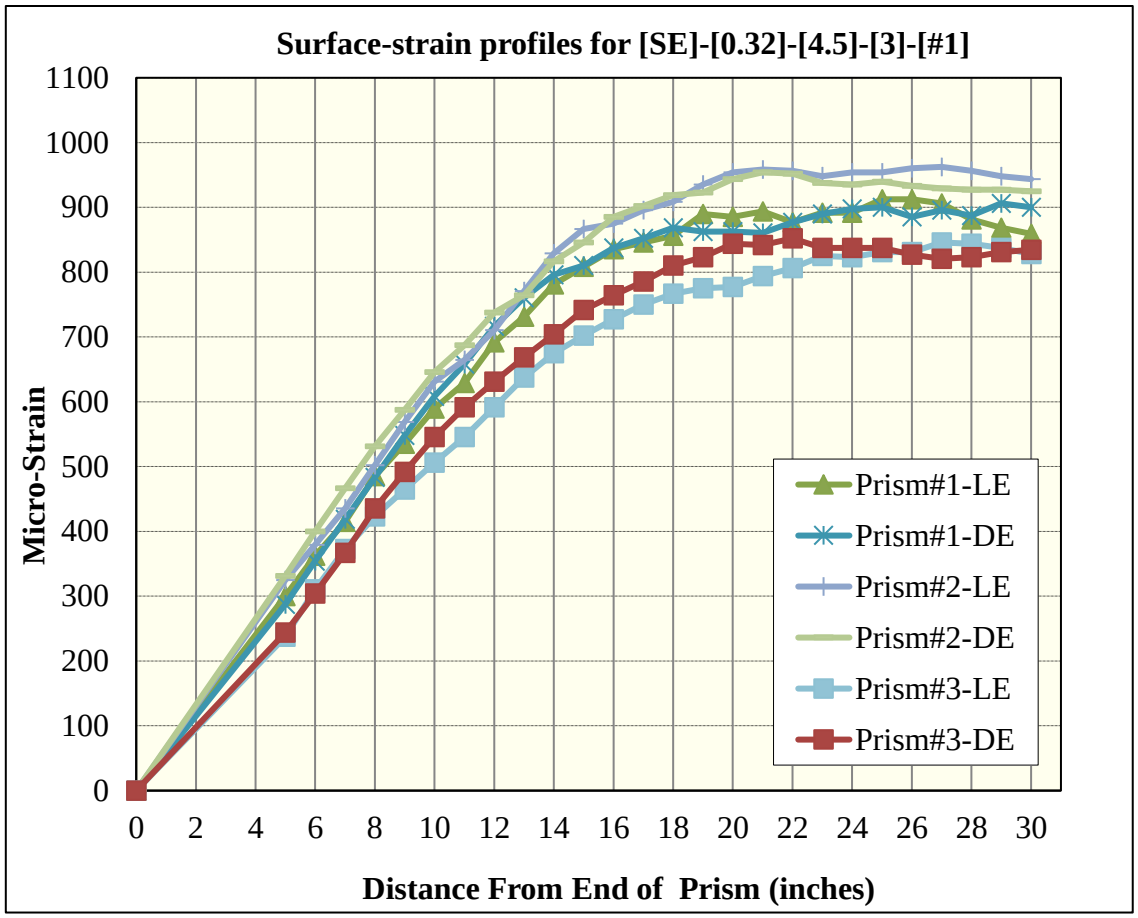

Figure 177 Surface-strain profiles for [SE]-[0.32]-[4.5]-[3]-[#1]

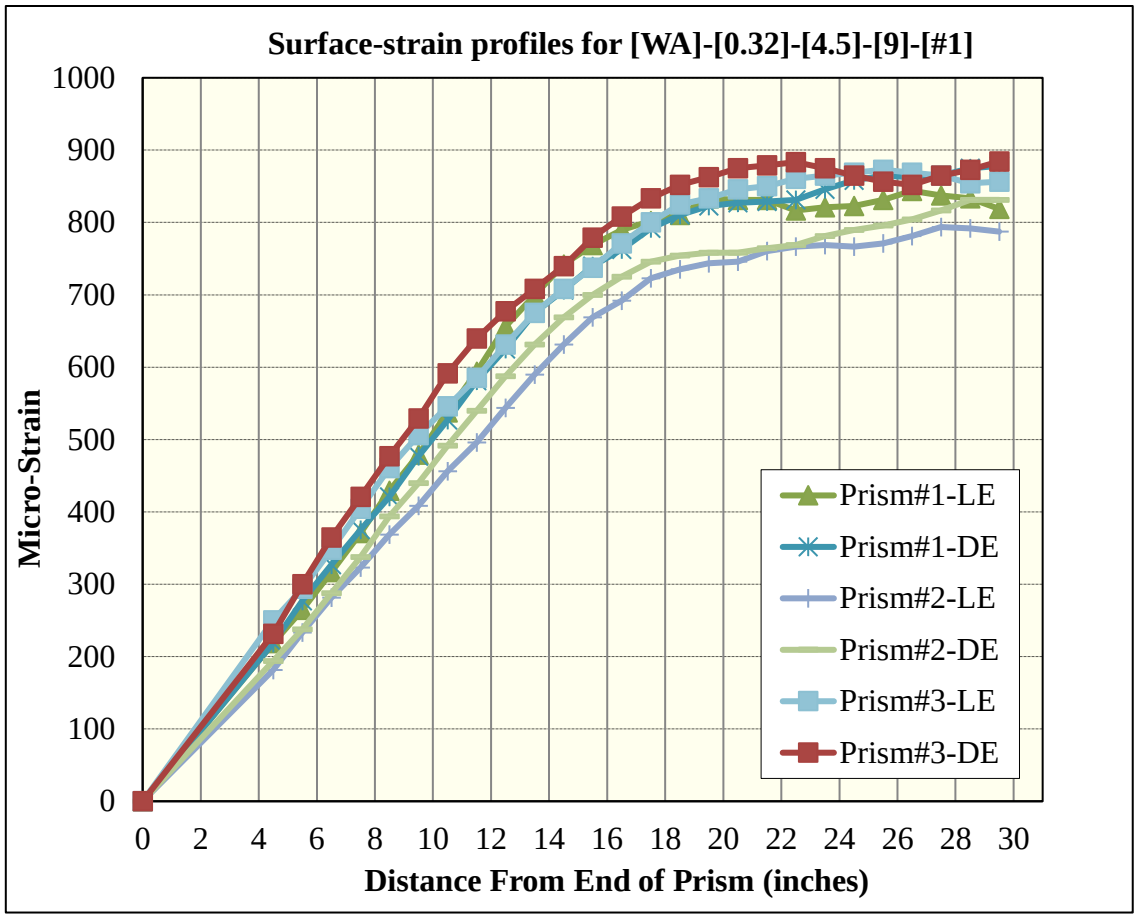

Figure 178 Surface-strain profiles for [WA]-[0.32]-[4.5]-[9]-[#1]

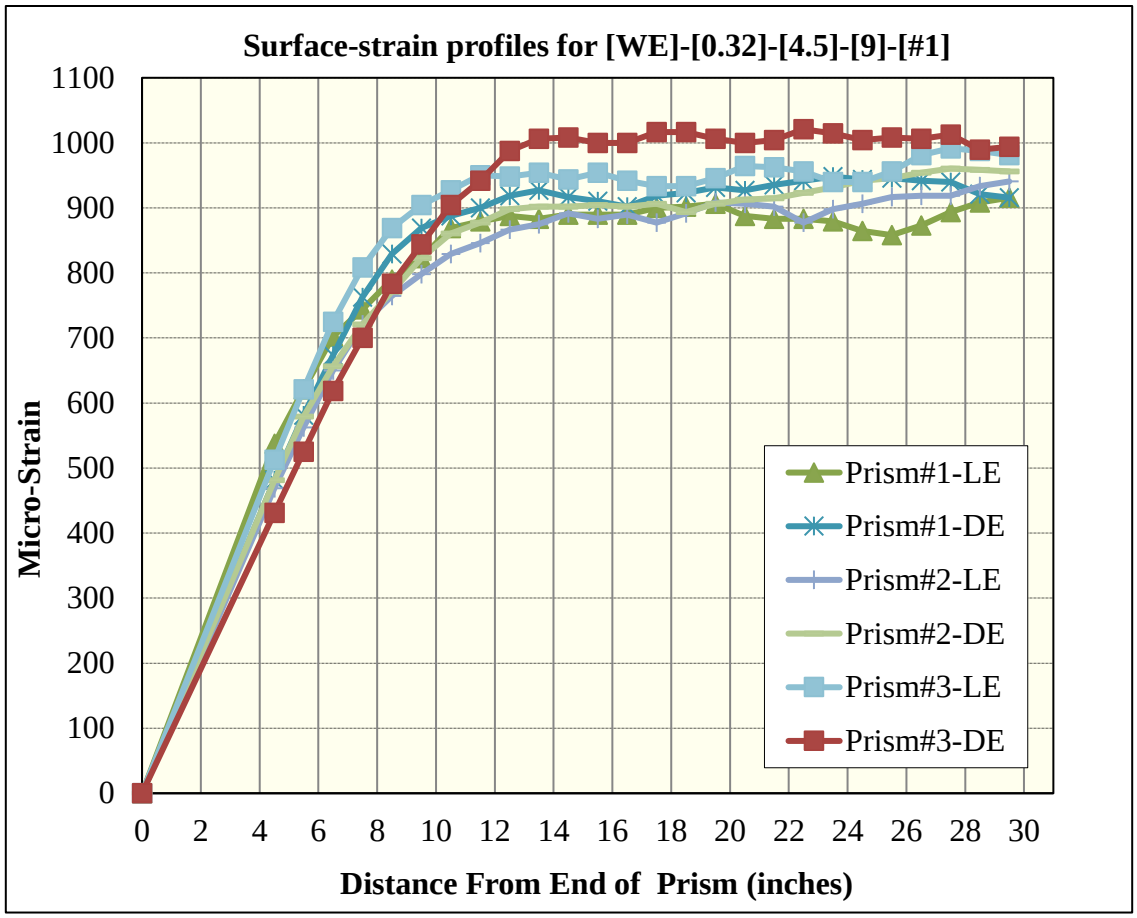

Figure 179 Surface-strain profiles for [WE]-[0.32]-[4.5]-[9]-[#1]

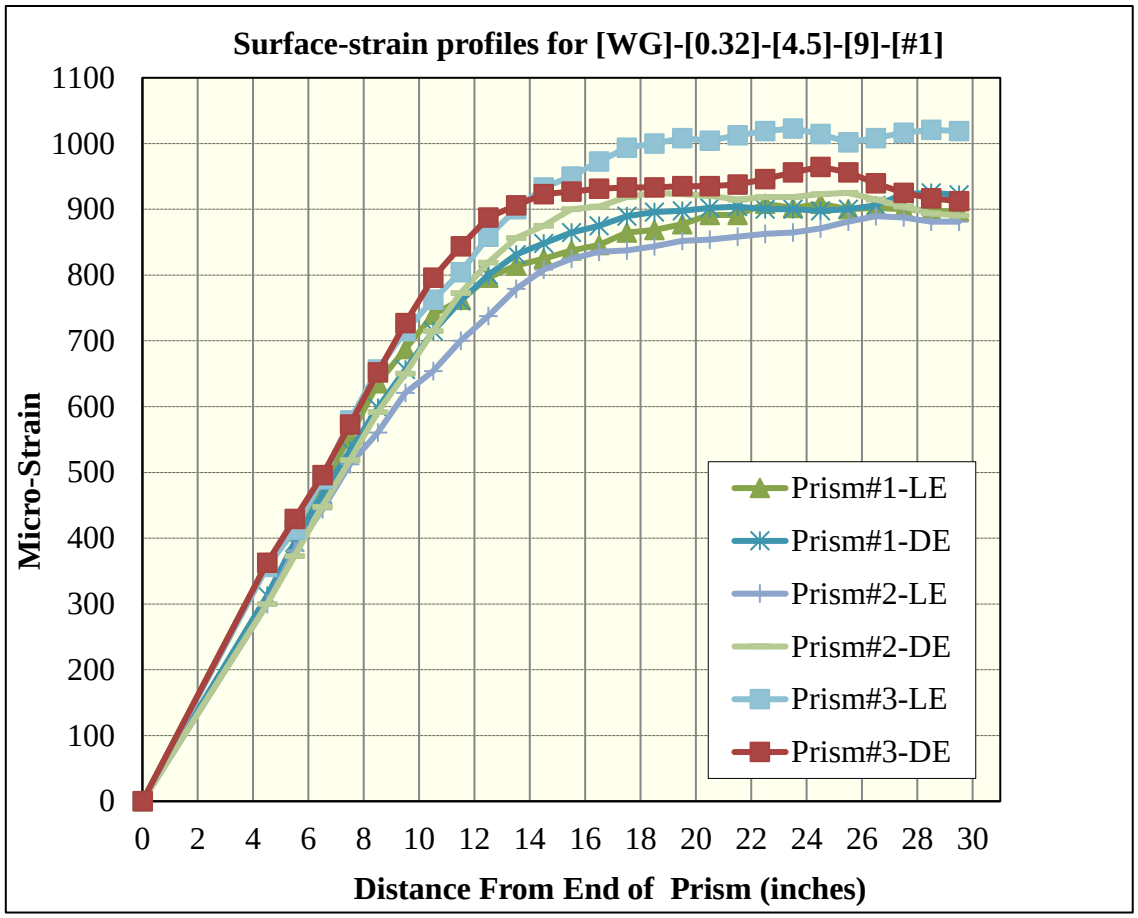

Figure 180 Surface-strain profiles for [WG]-[0.32]-[4.5]-[9]-[#1]

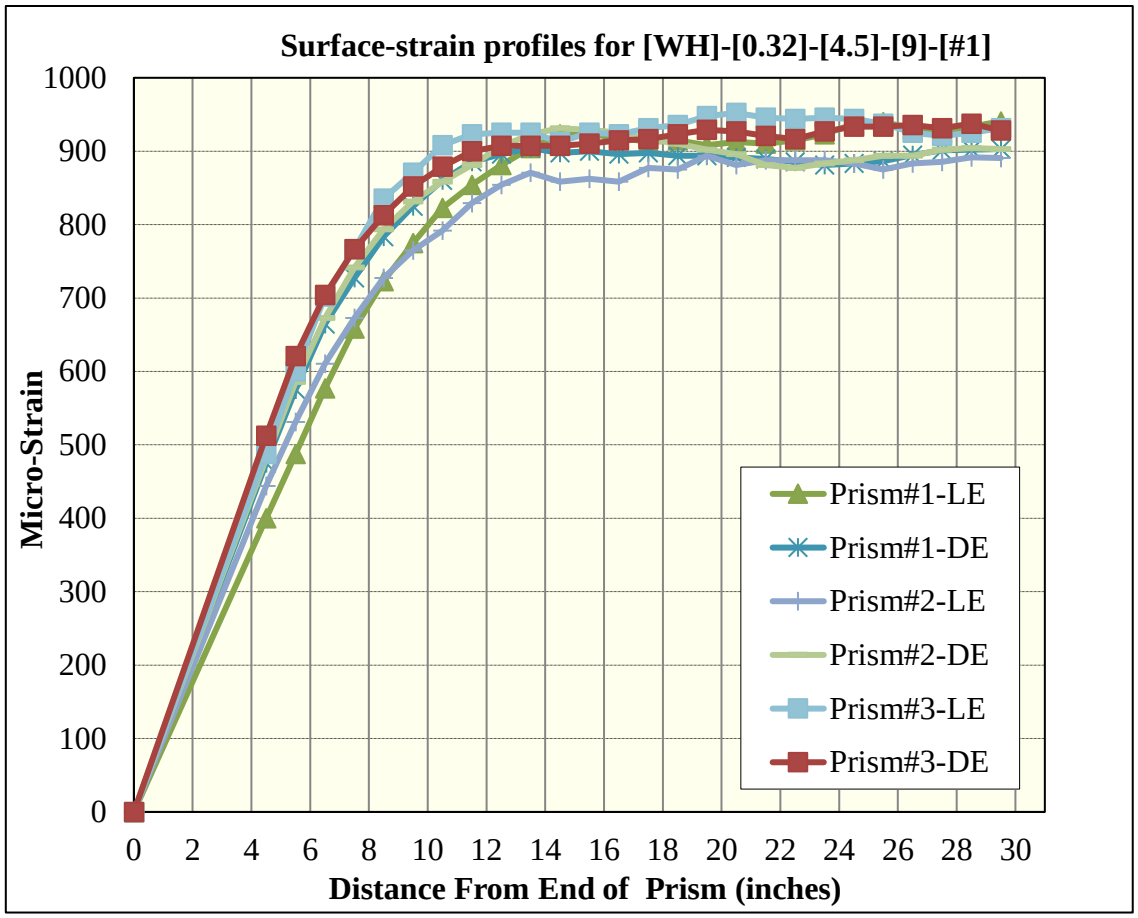

Figure 181 Surface-strain profiles for [WH]-[0.32]-[4.5]-[9]-[#1]

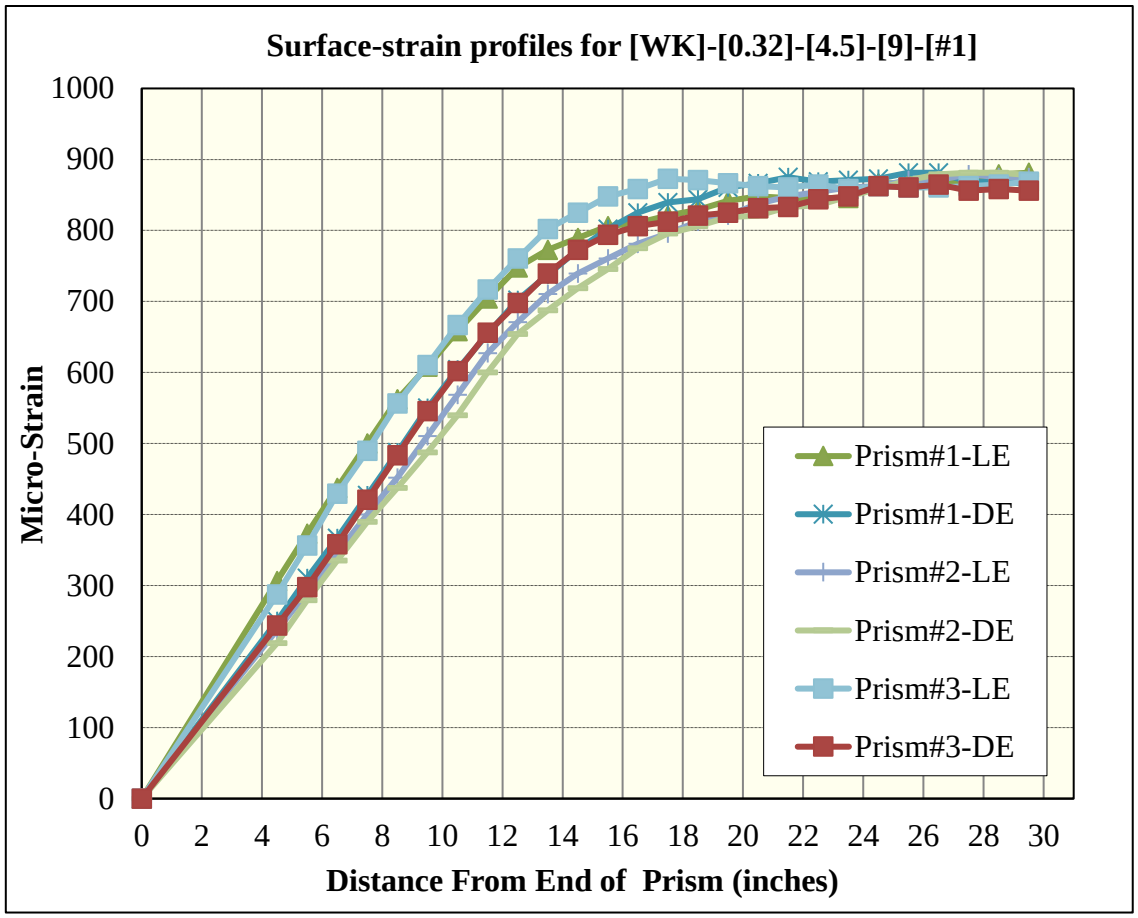

Figure 182 Surface-strain profiles for [WK]-[0.32]-[4.5]-[9]-[#1]

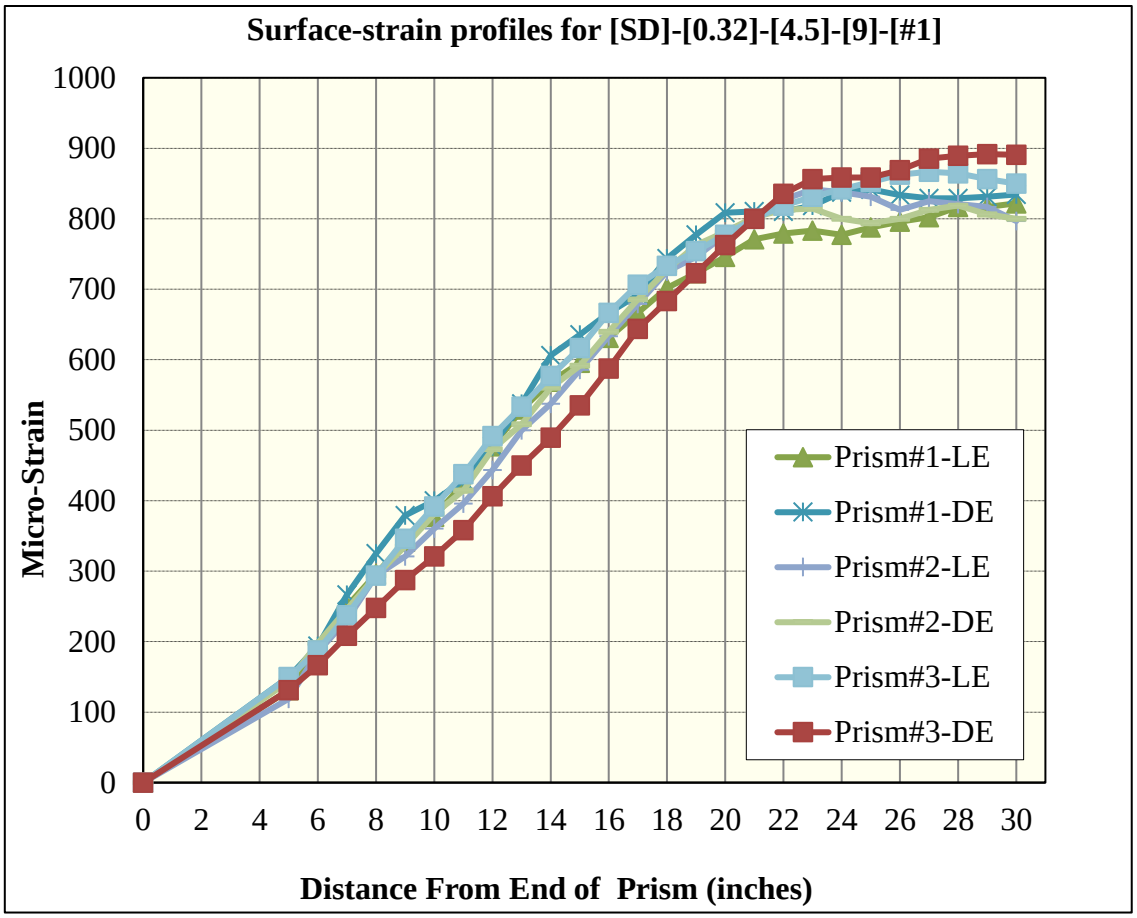

Figure 183 Surface-strain profiles for [SD]-[0.32]-[4.5]-[9]-[#1]

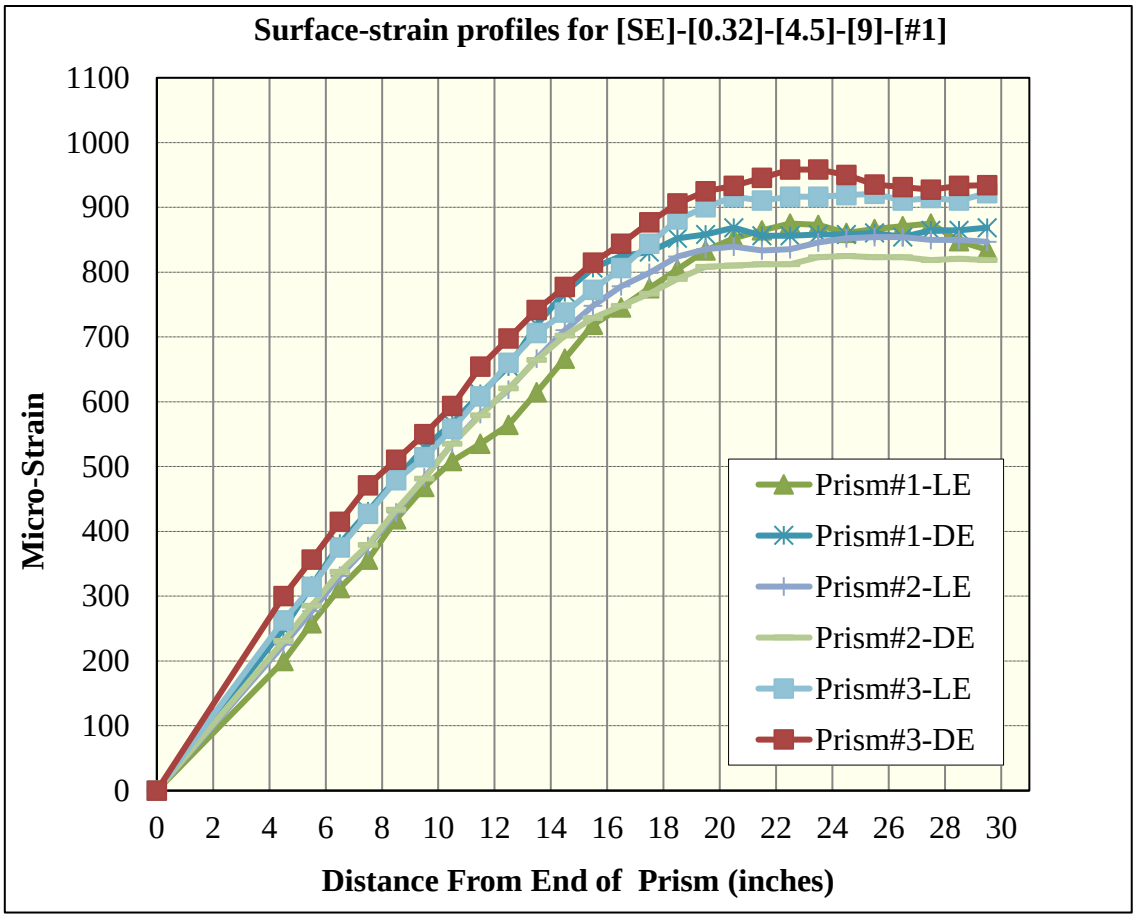

Figure 184 Surface-strain profiles for [SE]-[0.32]-[4.5]-[9]-[#1]

Plant-Phase surface-strain profiles

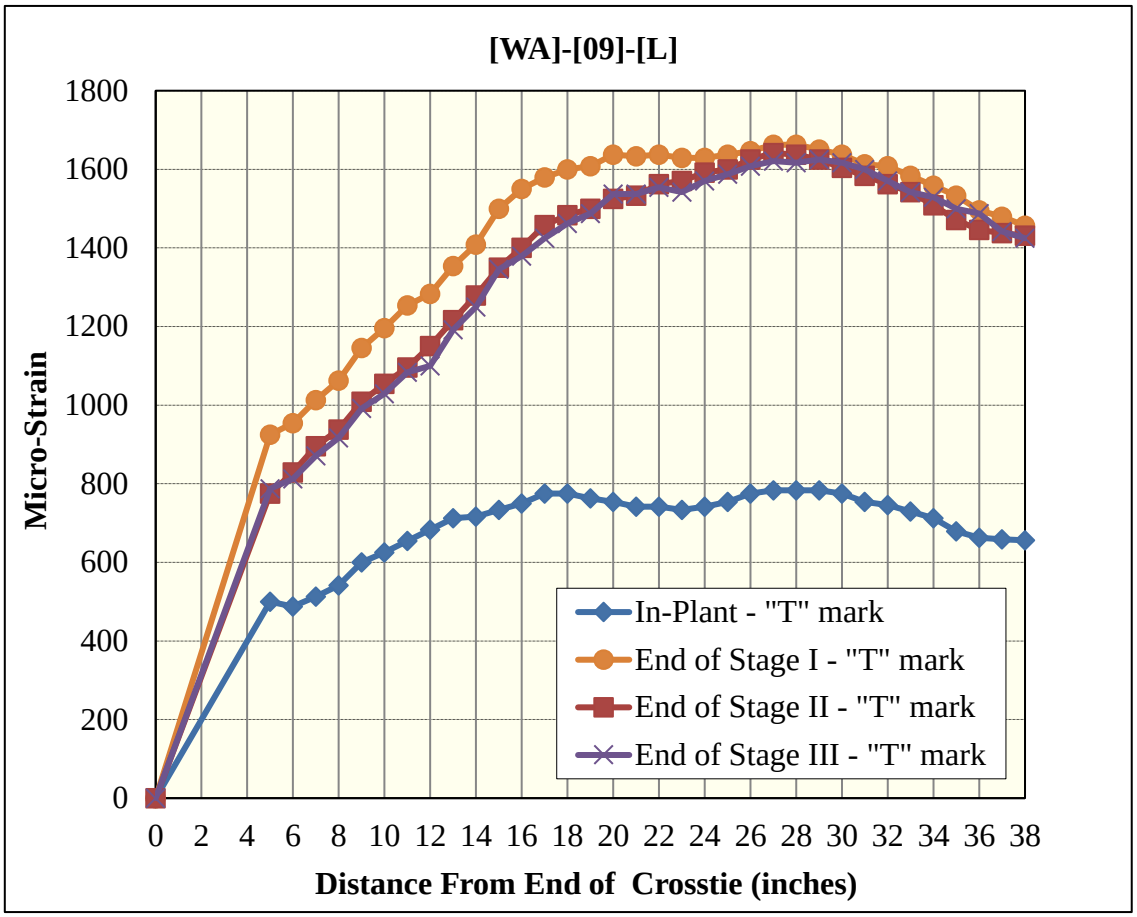

Figure 185 Surface-strain profiles for [WA]-[09]-[L] (Whittemore gage)

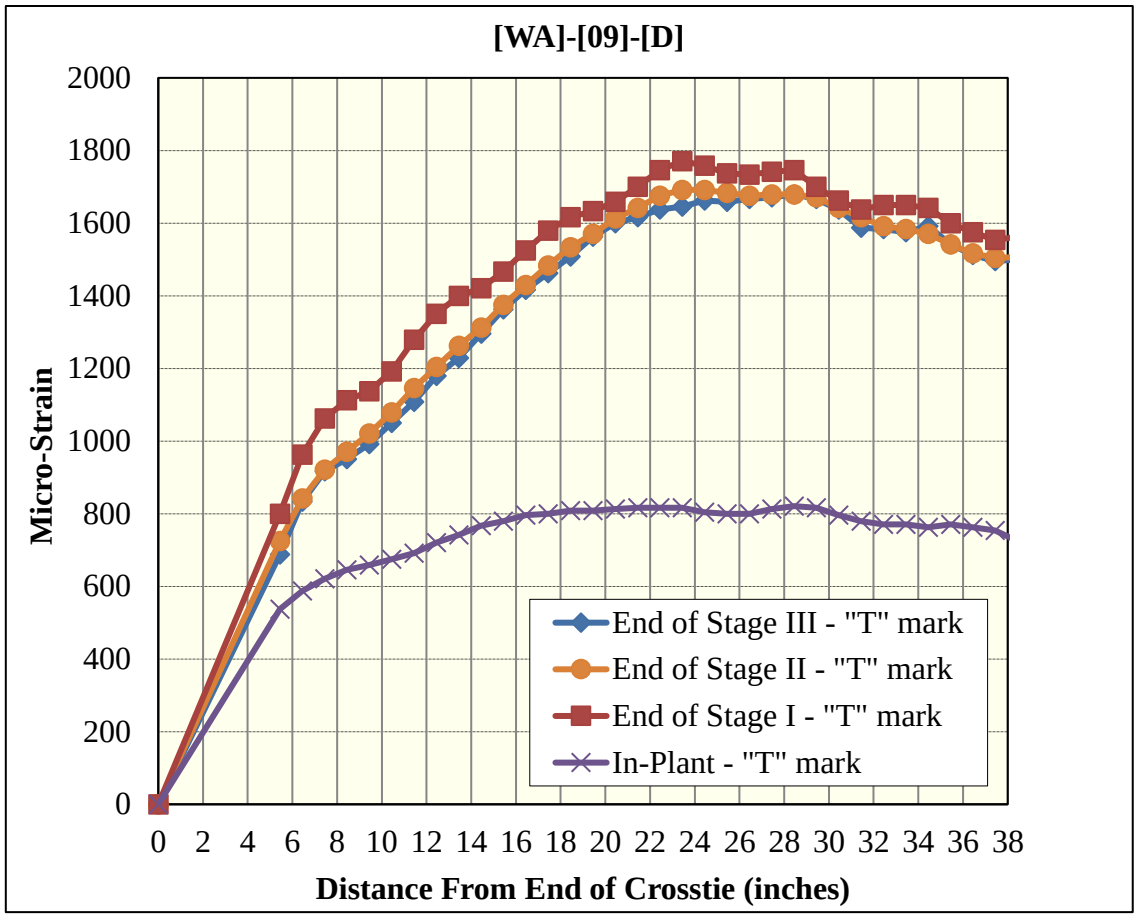

Figure 186 Surface-strain profiles for [WA]-[09]-[D] (Whittemore gage)

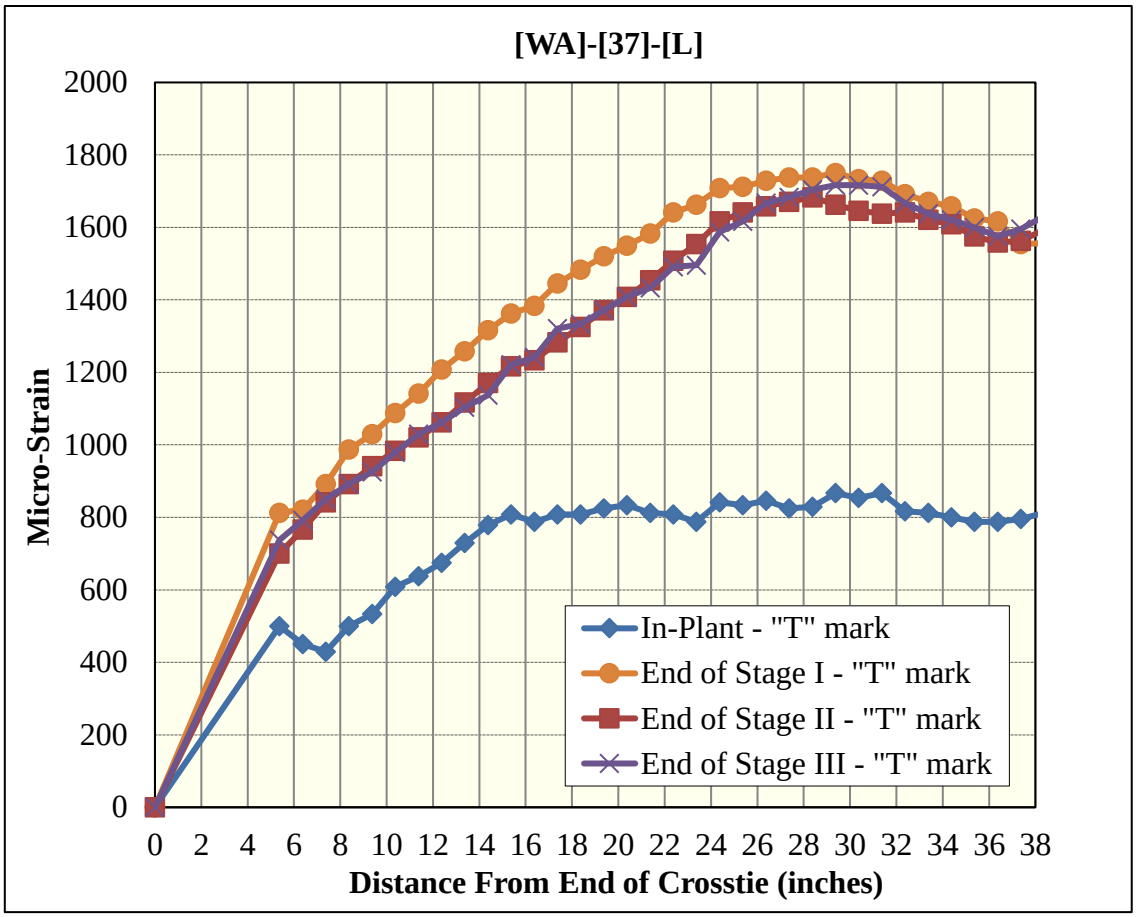

Figure 187 Surface-strain profiles for [WA]-[37]-[L] (Whittemore gage)

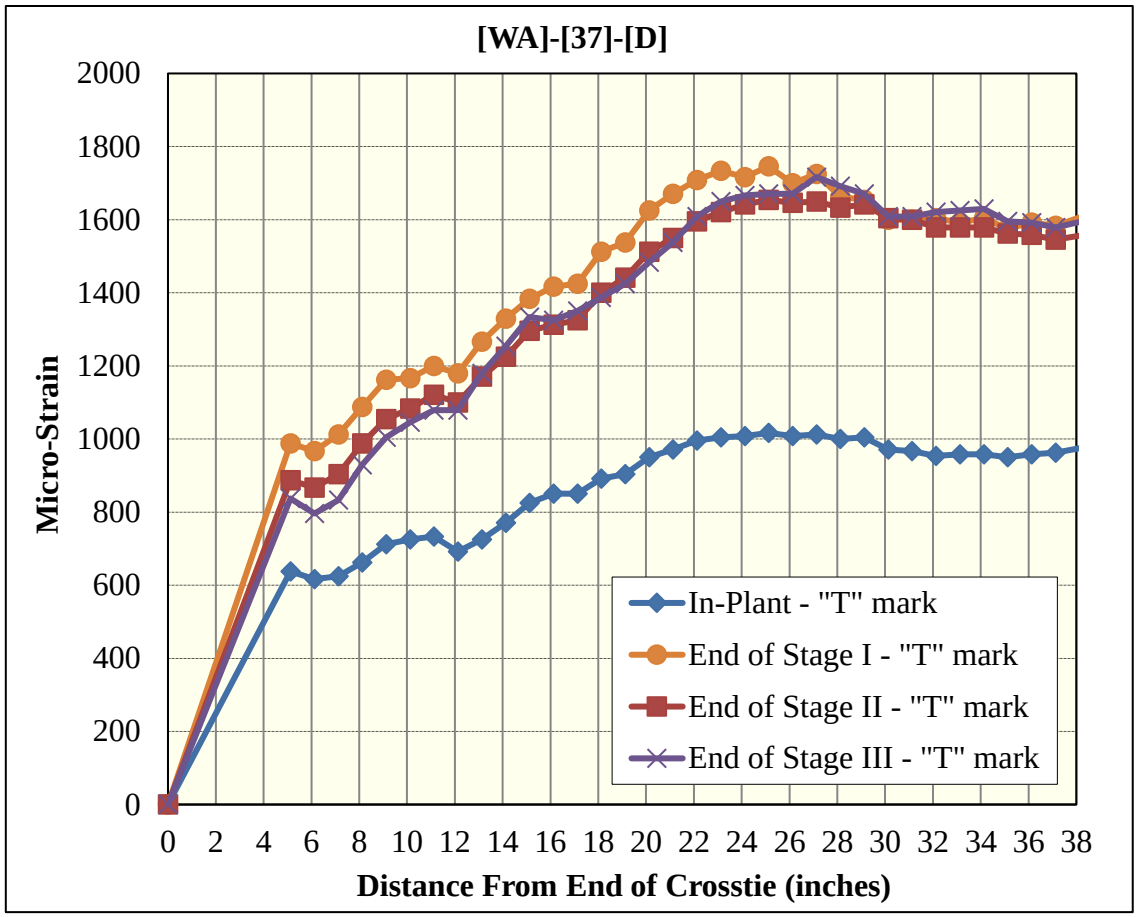

Figure 188 Surface-strain profiles for [WA]-[37]-[D] (Whittemore gage)

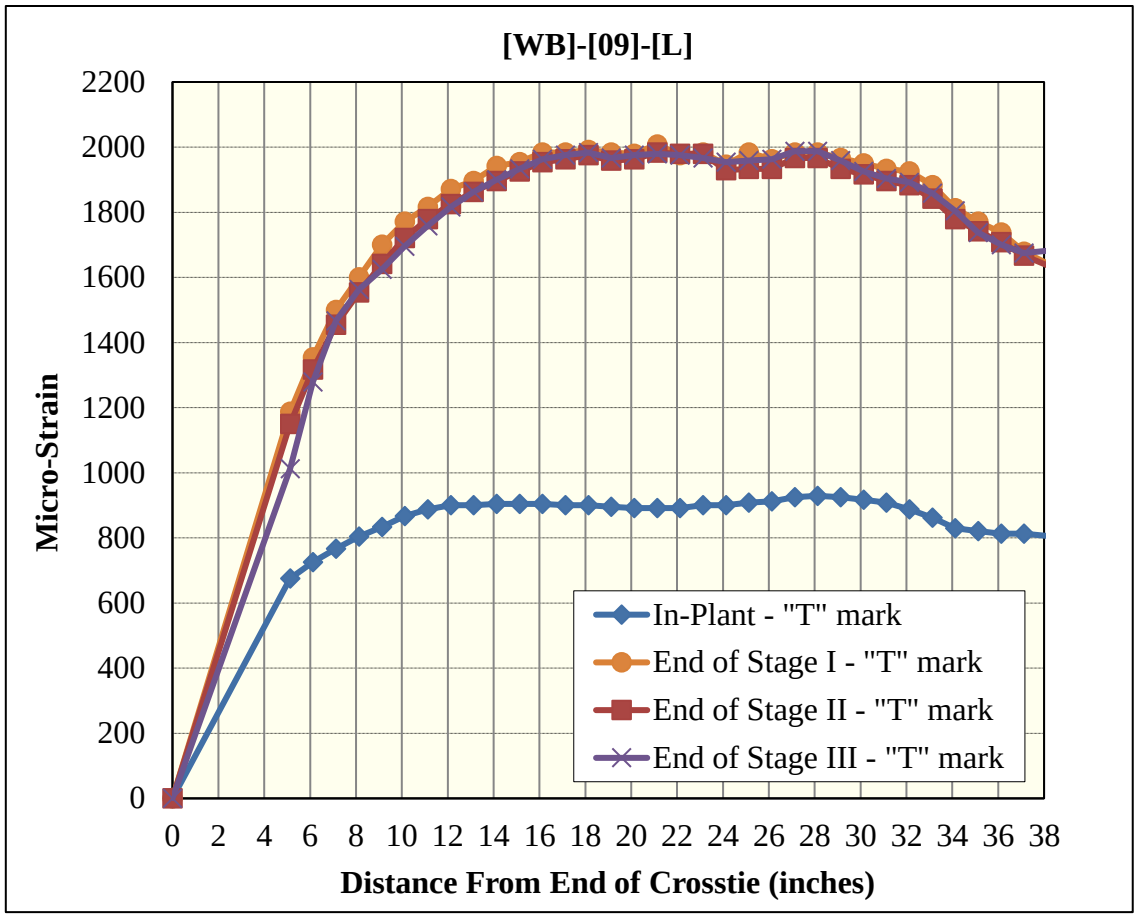

Figure 189 Surface-strain profiles for [WB]-[09]-[L] (Whittemore gage)

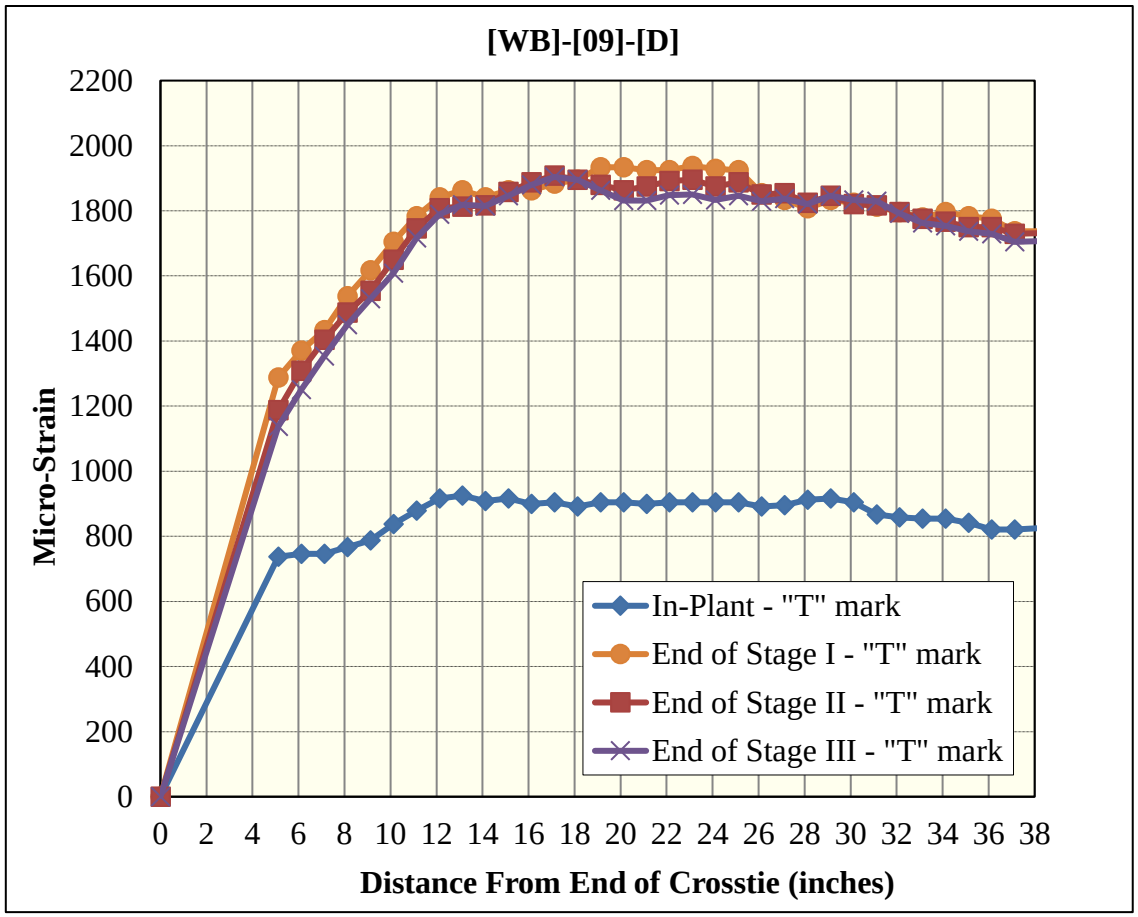

Figure 190 Surface-strain profiles for [WB]-[09]-[D] (Whittemore gage)

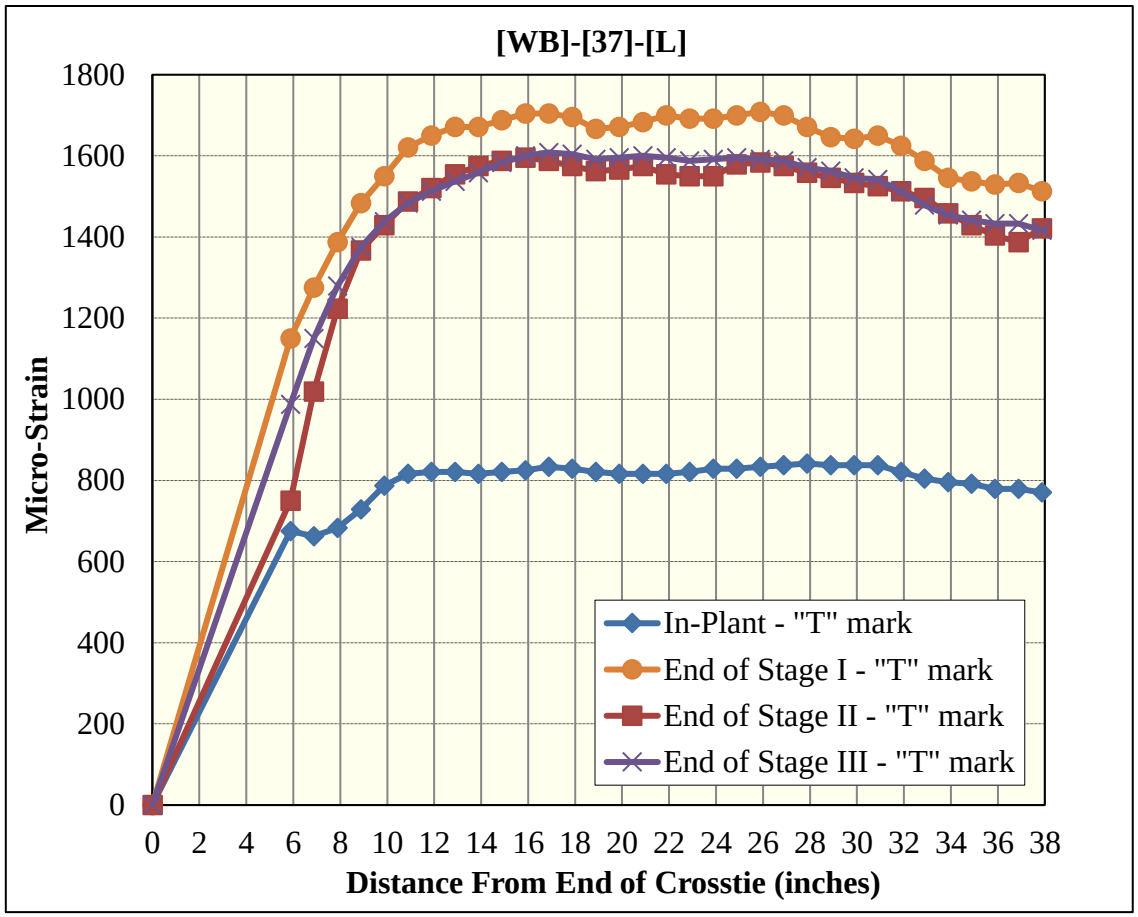

Figure 191 Surface-strain profiles for [WB]-[37]-[L] (Whittemore gage)

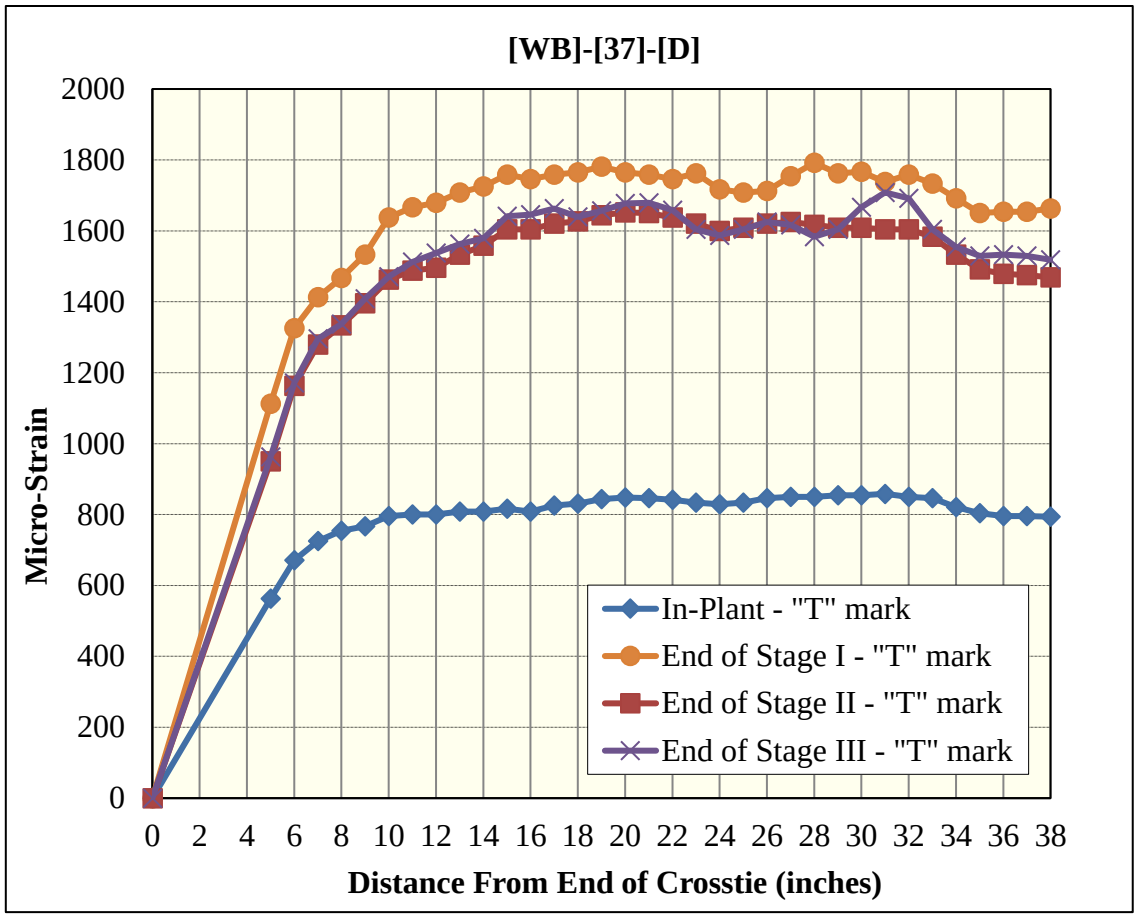

Figure 192 Surface-strain profiles for [WB]-[37]-[D] (Whittemore gage)

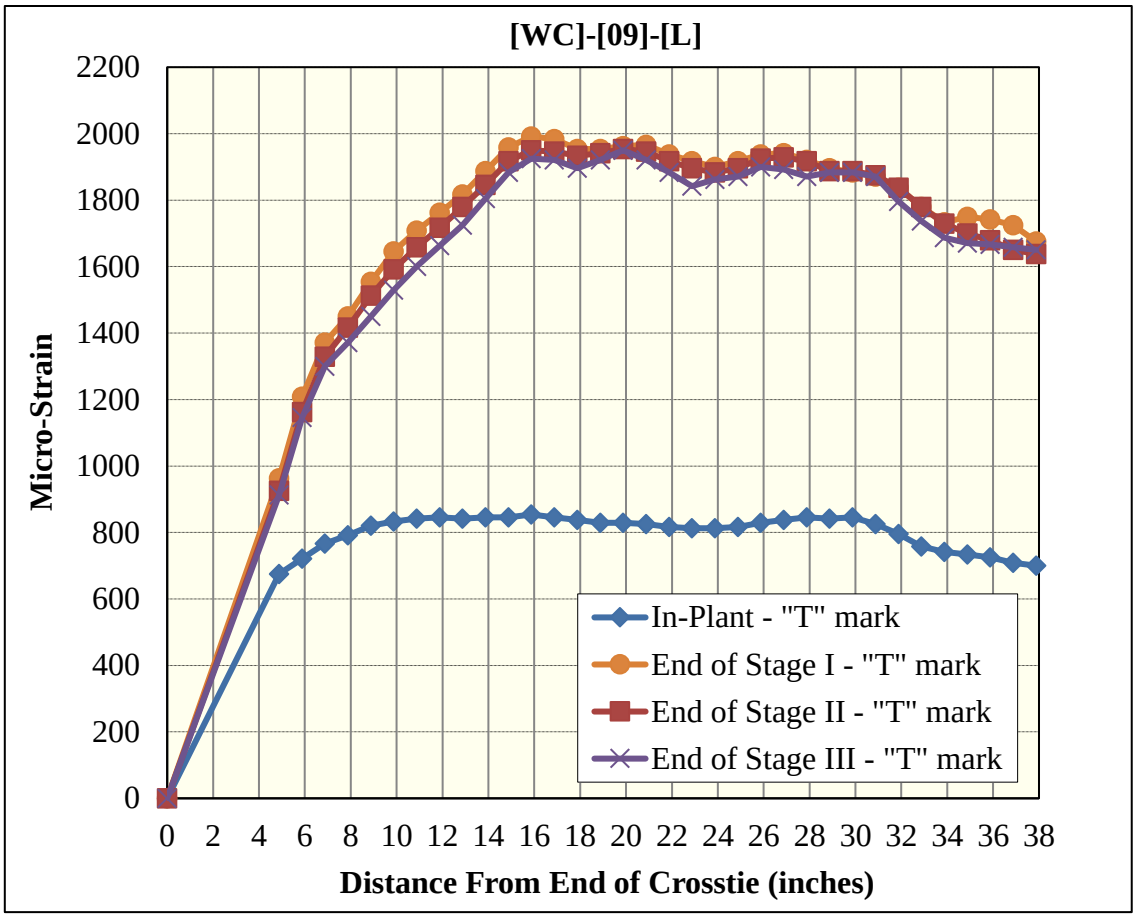

Figure 193 Surface-strain profiles for [WC]-[09]-[L] (Whittemore gage)

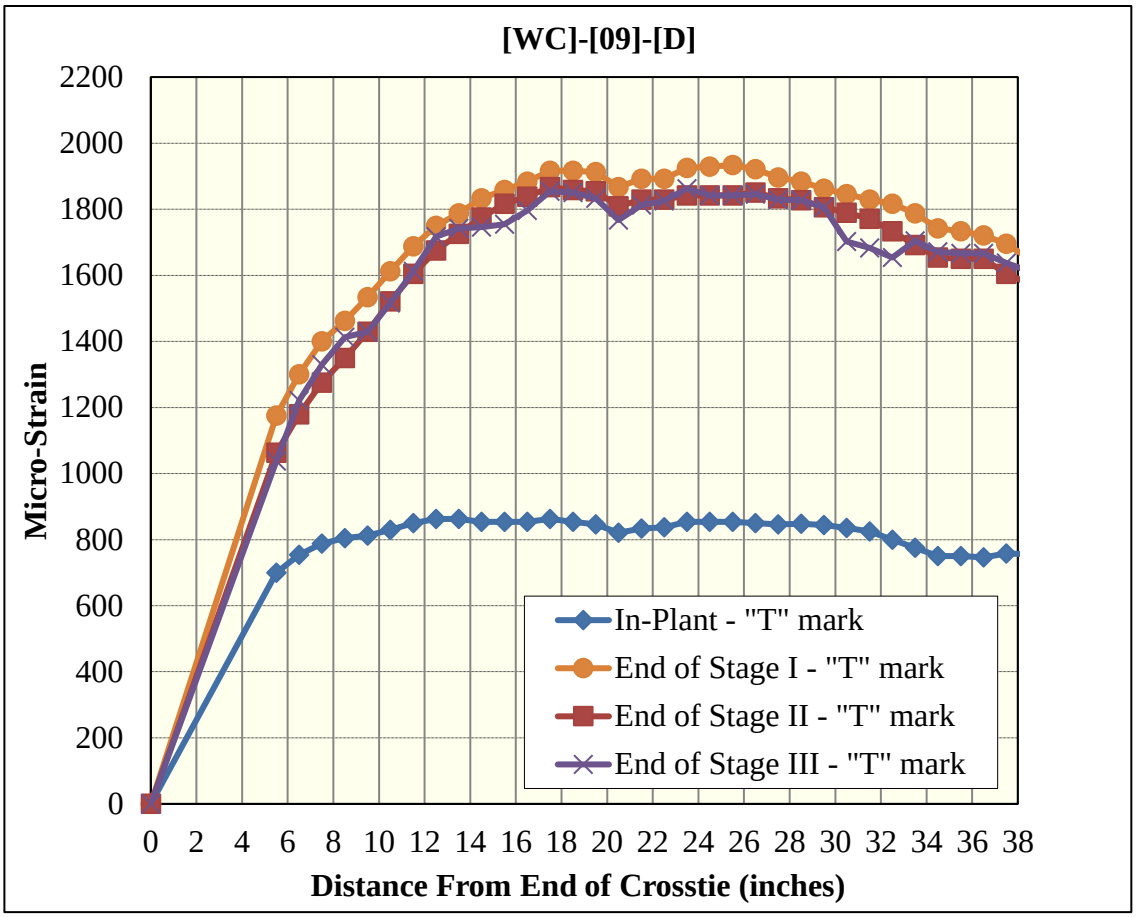

Figure 194 Surface-strain profiles for [WC]-[09]-[D] (Whittemore gage)

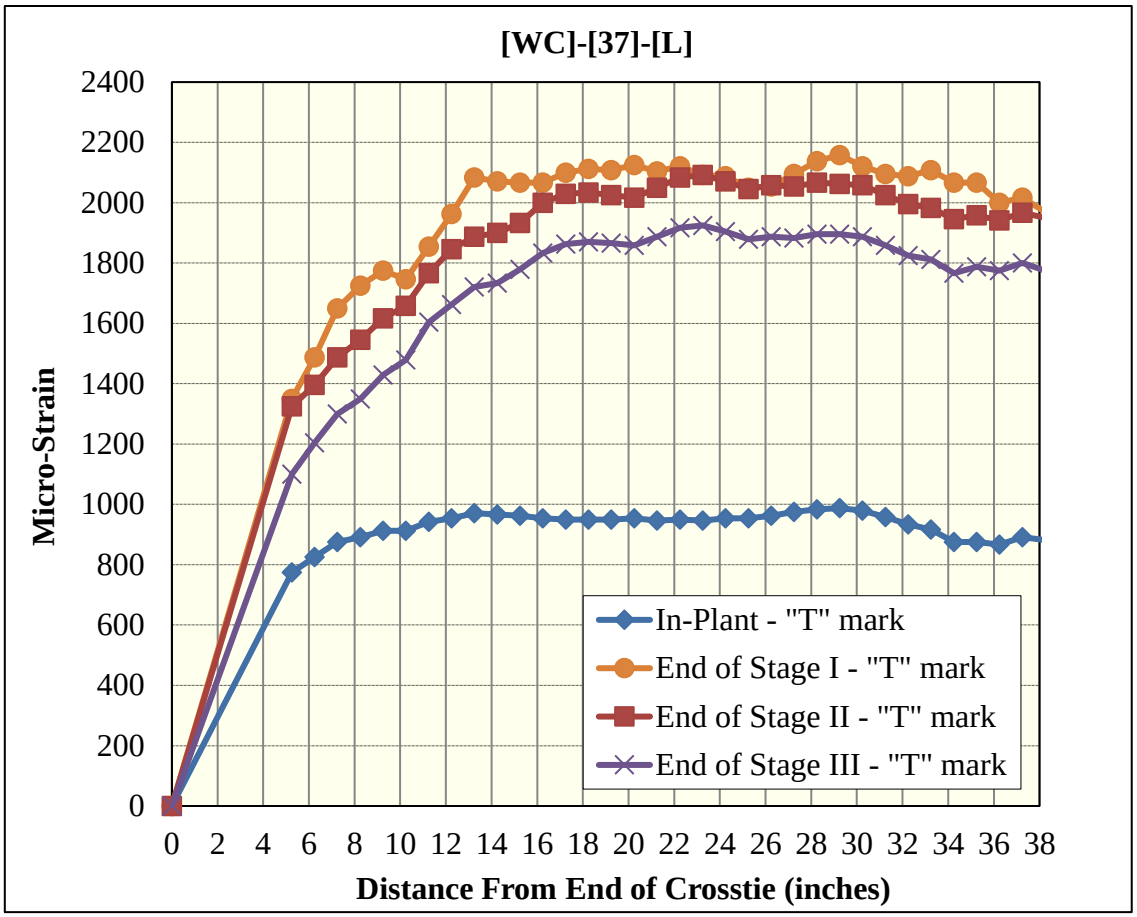

Figure 195 Surface-strain profiles for [WC]-[37]-[L] (Whittemore gage)

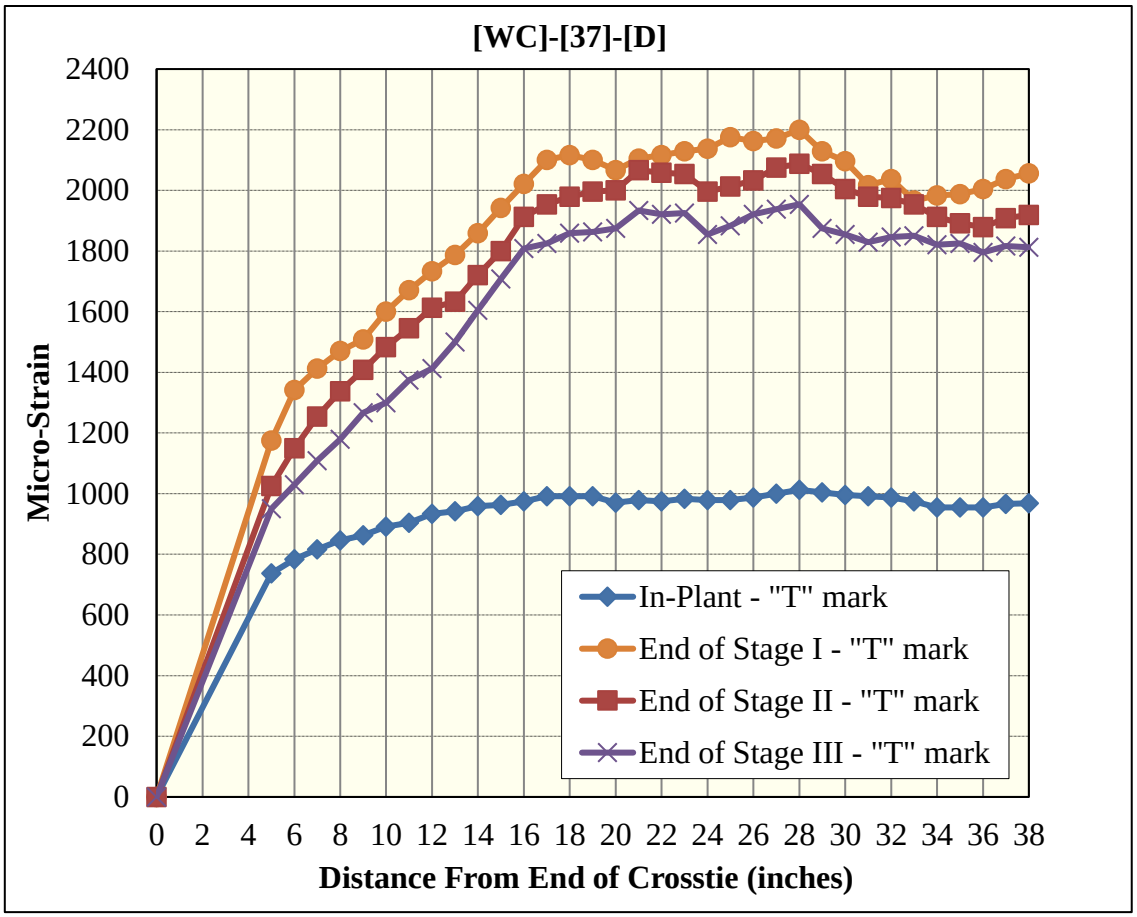

Figure 196 Surface-strain profiles for [WC]-[37]-[D] (Whittemore gage)

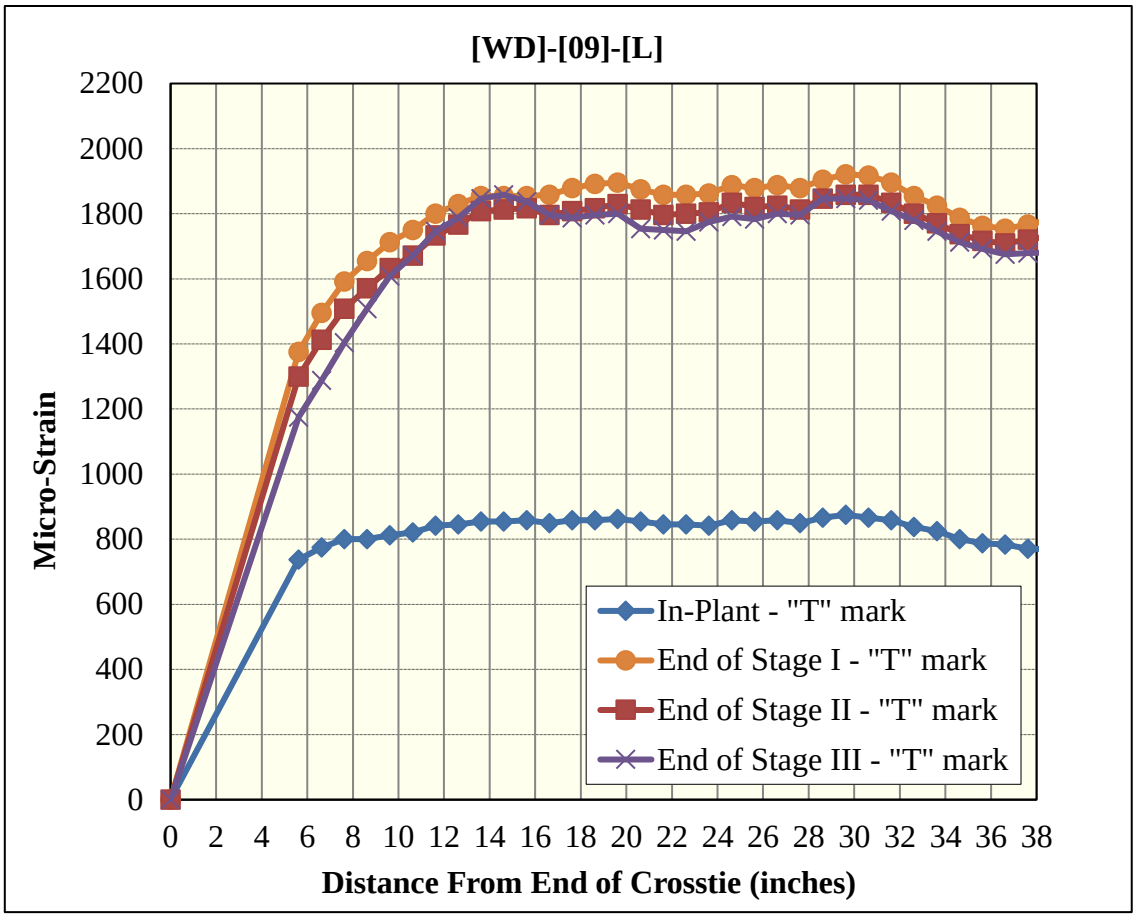

Figure 197 Surface-strain profiles for [WD]-[09]-[L] (Whittemore gage)

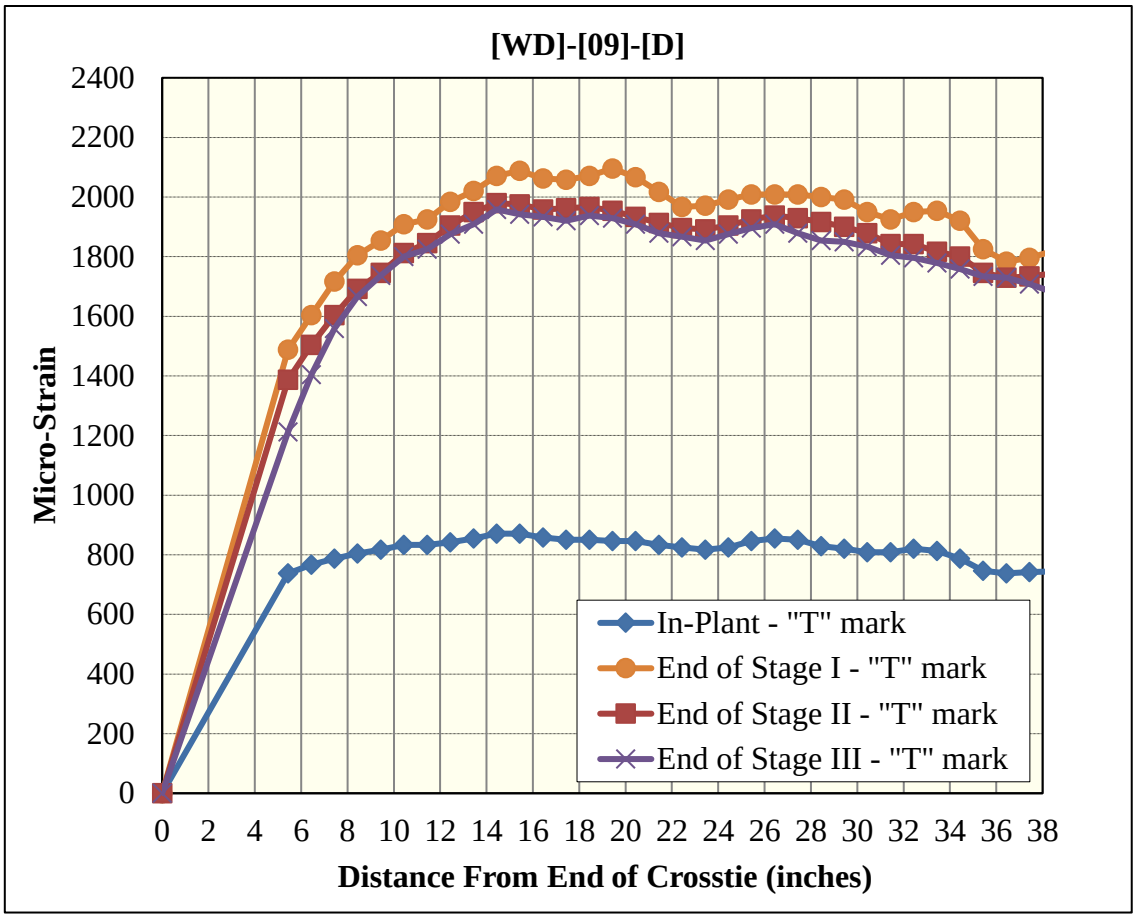

Figure 198 Surface-strain profiles for [WD]-[09]-[D] (Whittemore gage)

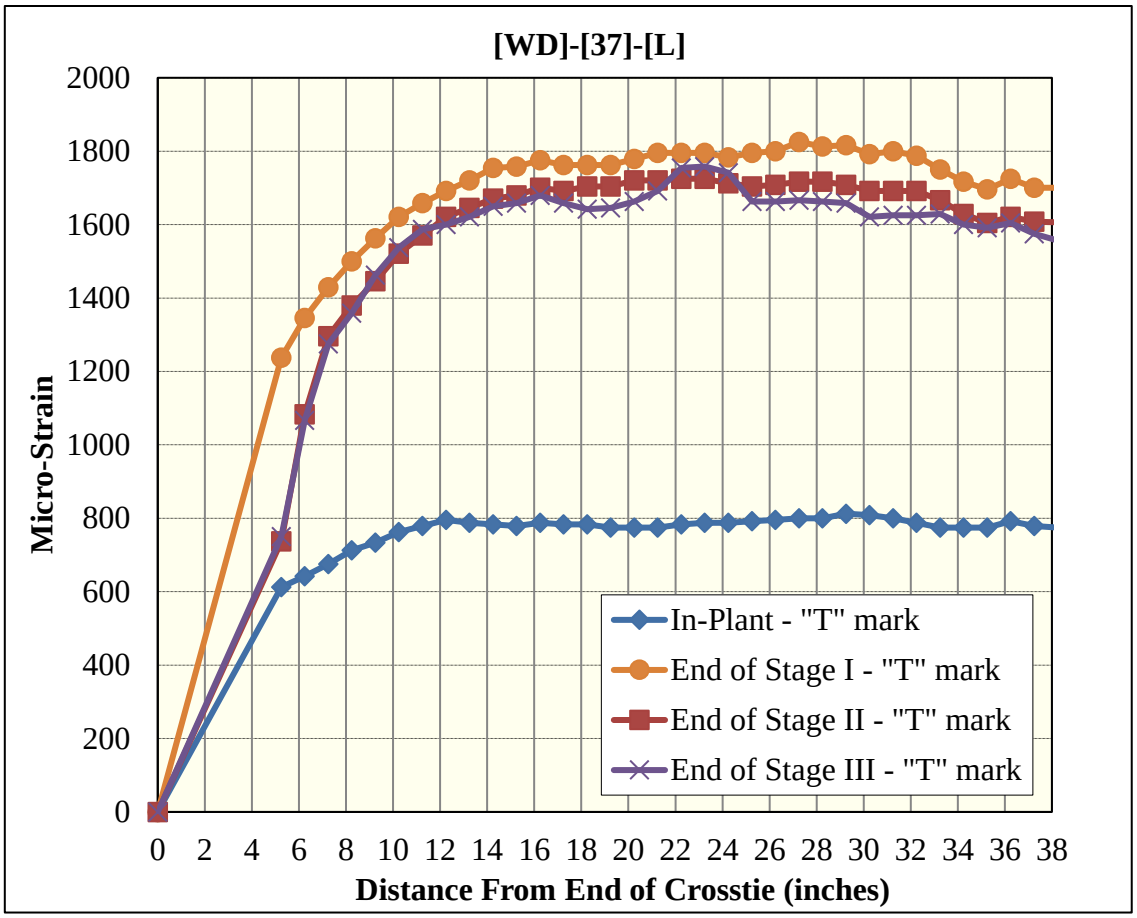

Figure 199 Surface-strain profiles for [WD]-[37]-[L] (Whittemore gage)

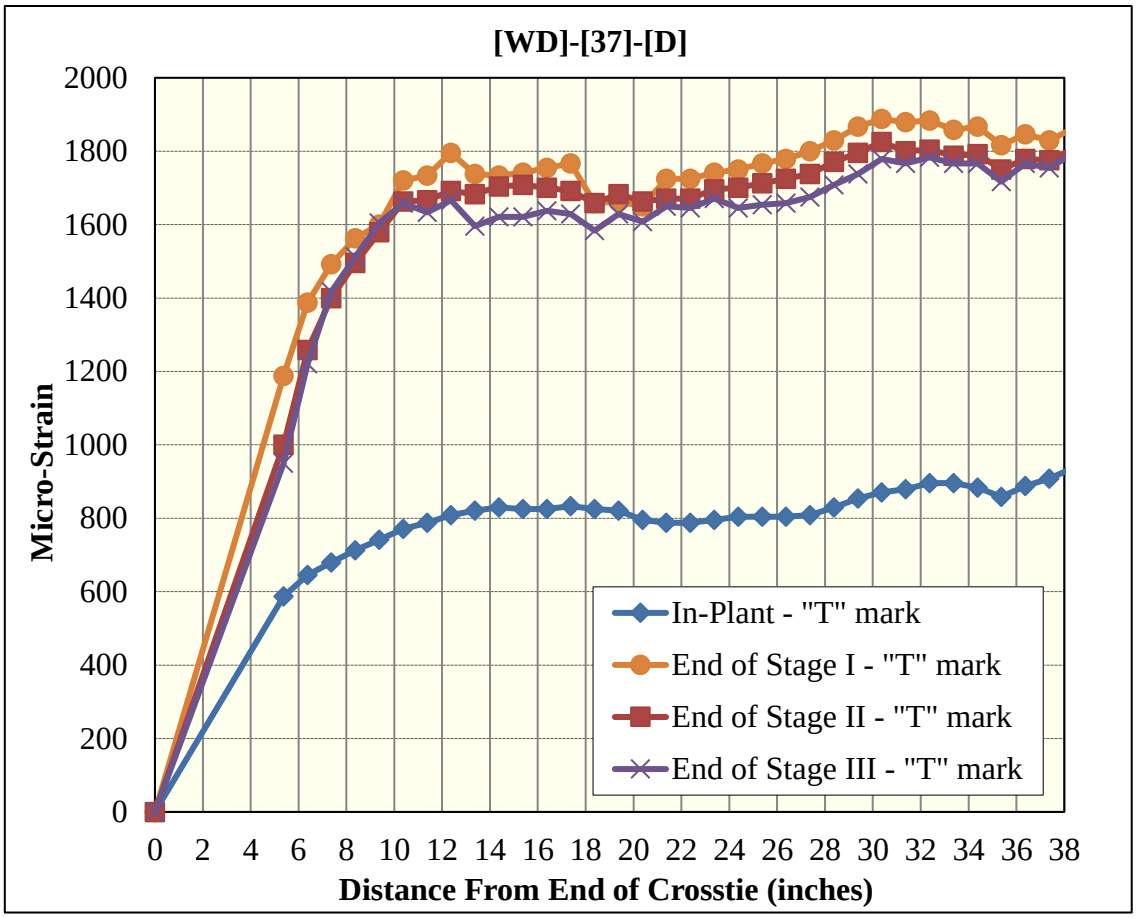

Figure 200 Surface-strain profiles for [WD]-[37]-[D] (Whittemore gage)

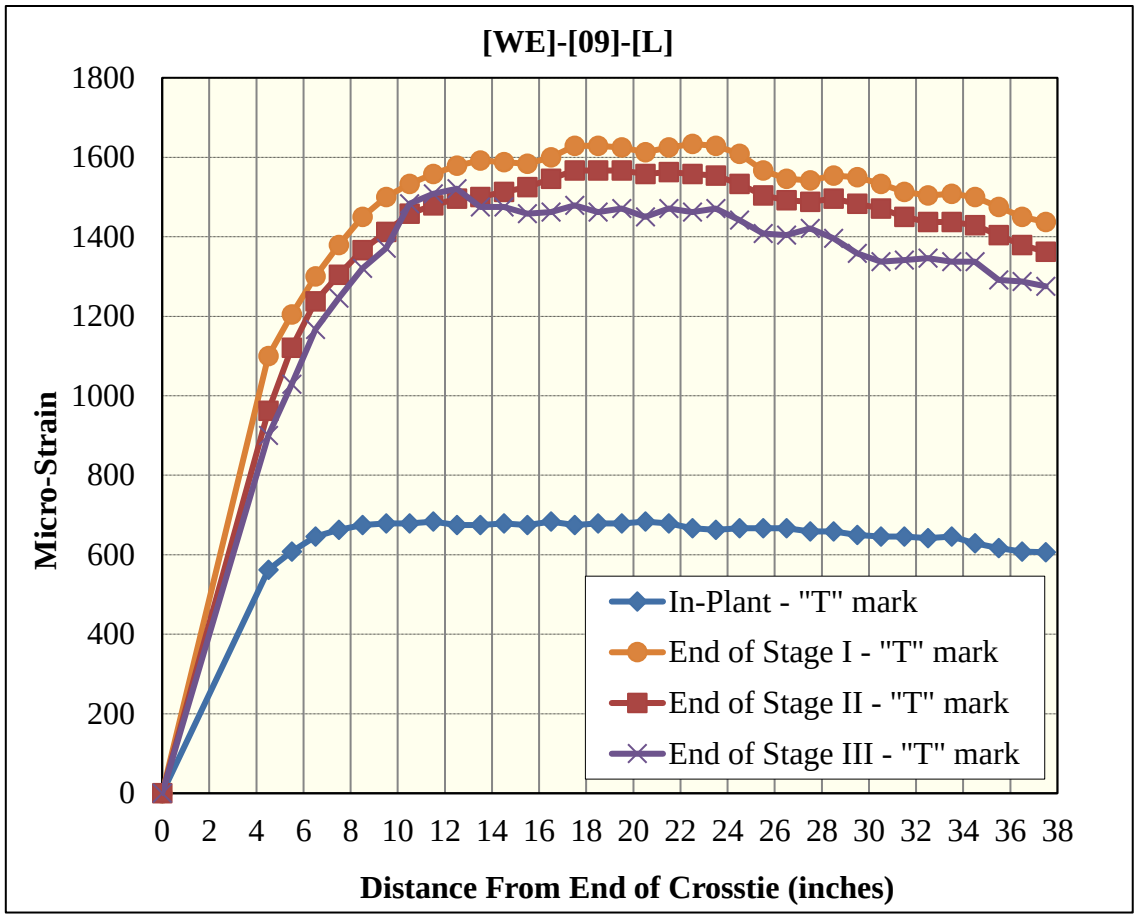

Figure 201 Surface-strain profiles for [WE]-[09]-[L] (Whittemore gage)

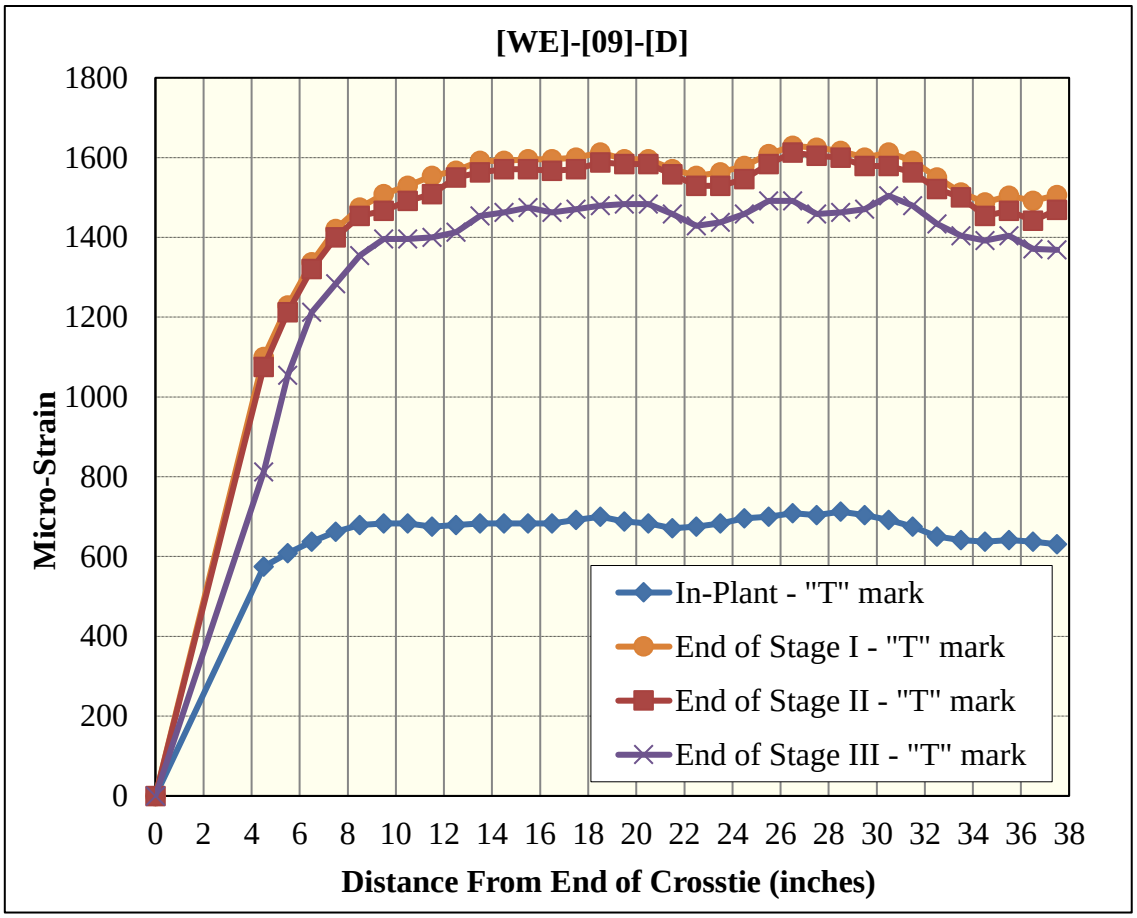

Figure 202 Surface-strain profiles for [WE]-[09]-[D] (Whittemore gage)

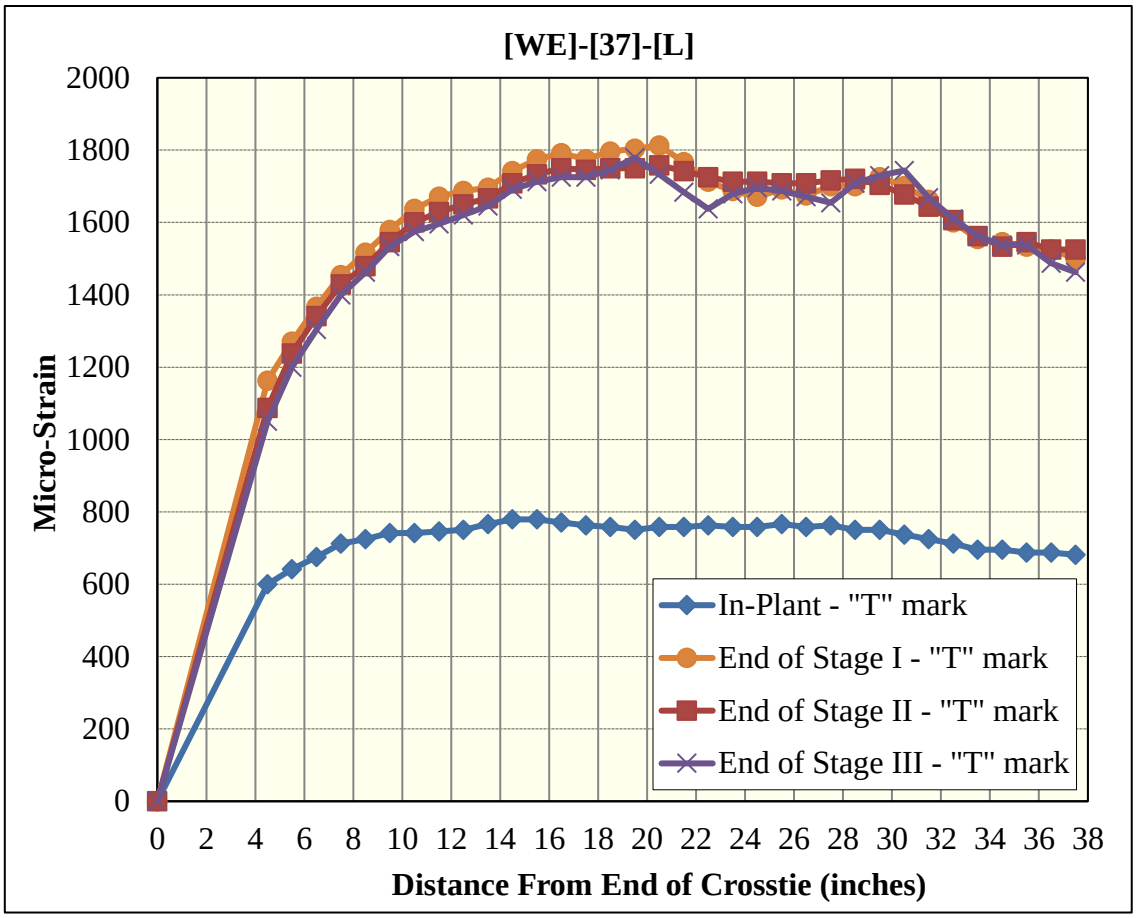

Figure 203 Surface-strain profiles for [WE]-[37]-[L] (Whittemore gage)

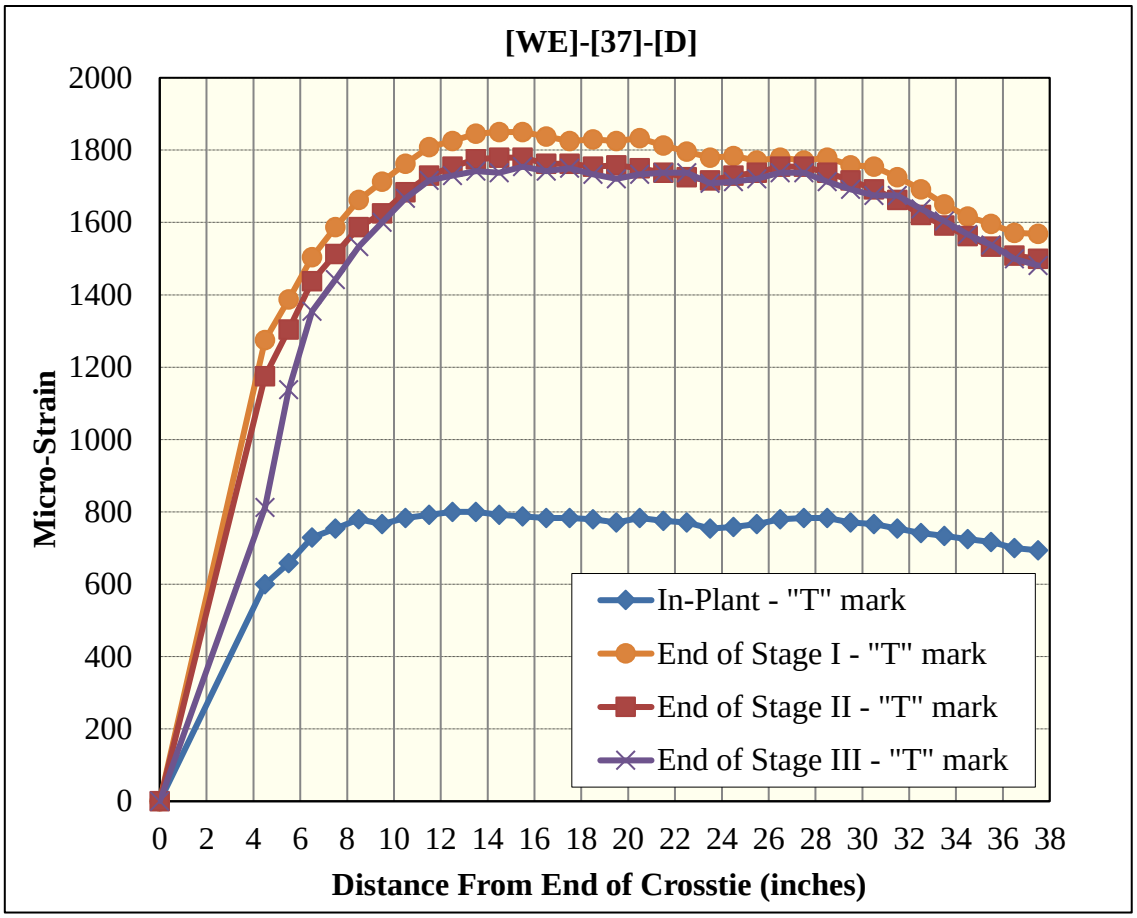

Figure 204 Surface-strain profiles for [WE]-[37]-[D] (Whittemore gage)

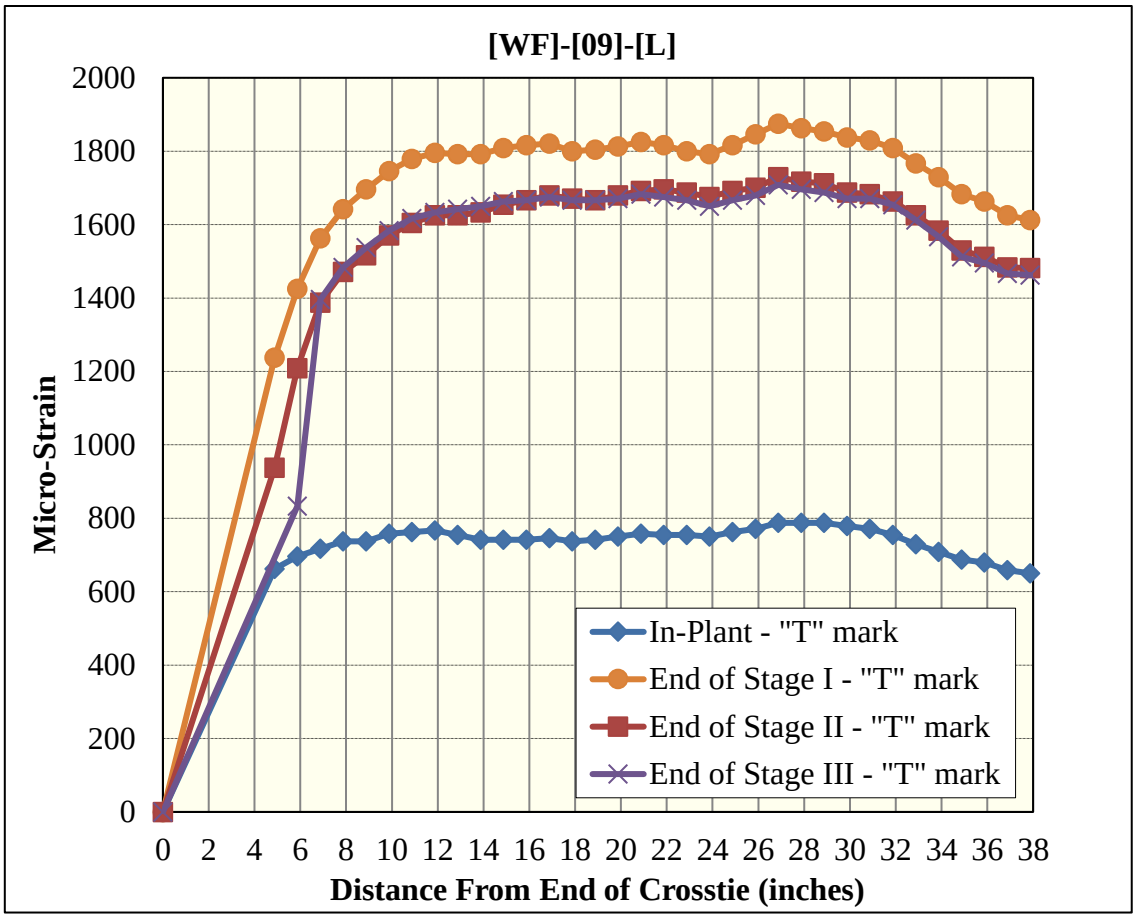

Figure 205 Surface-strain profiles for [WF]-[09]-[L] (Whittemore gage)

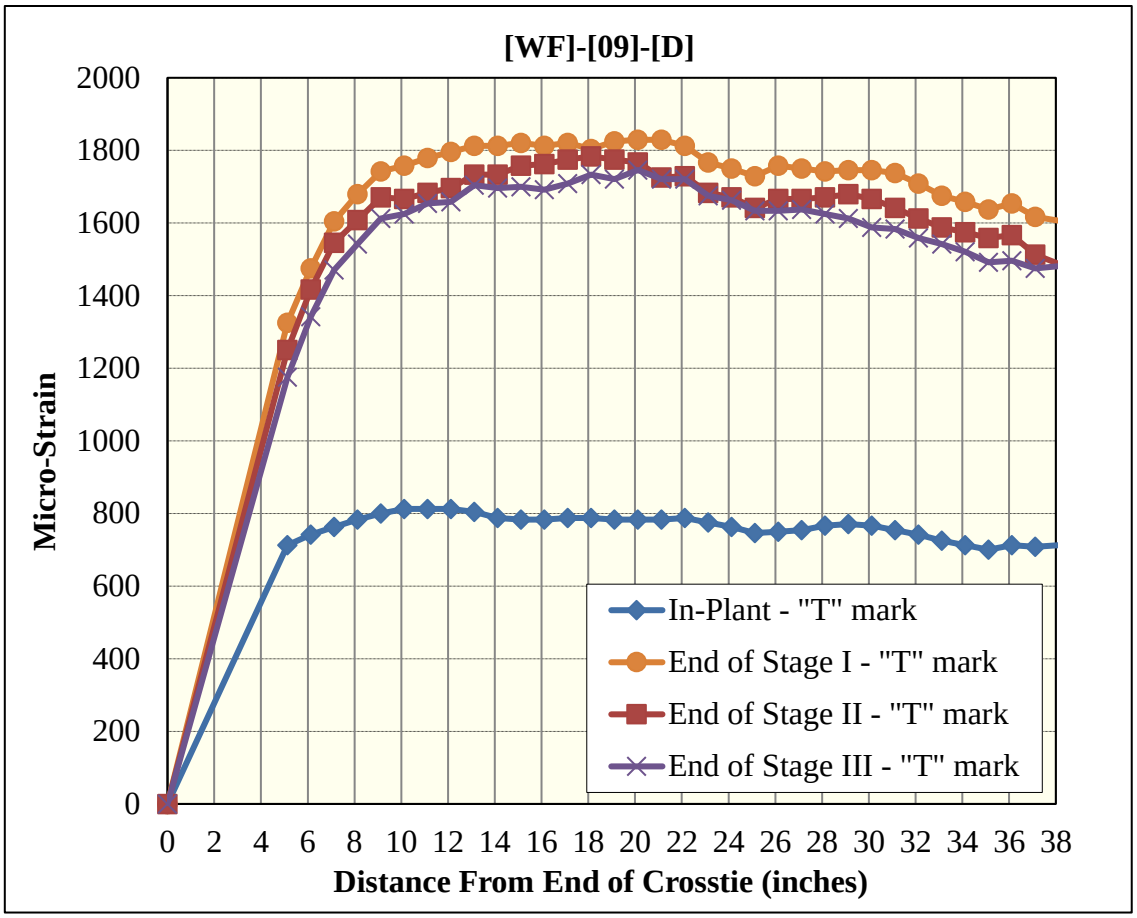

Figure 206 Surface-strain profiles for [WF]-[09]-[D] (Whittemore gage)

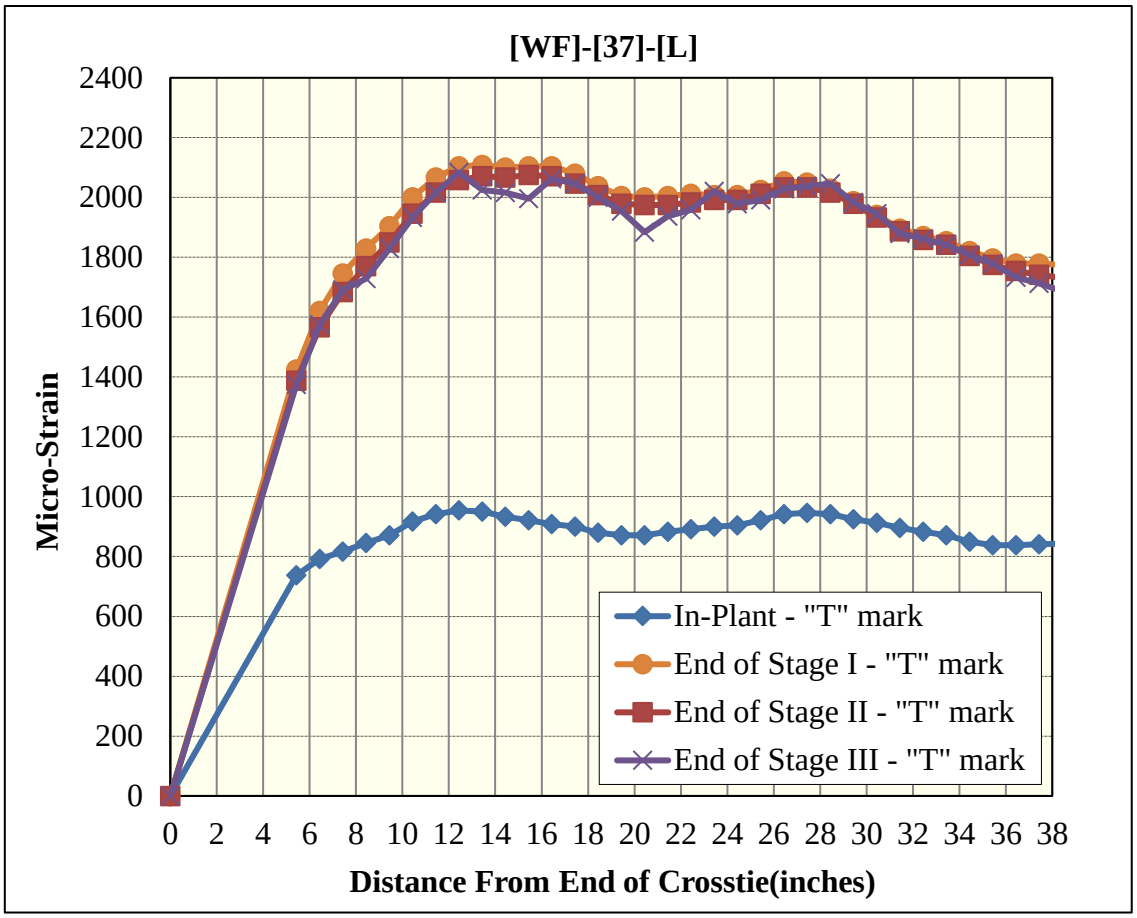

Figure 207 Surface-strain profiles for [WF]-[37]-[L] (Whittemore gage)

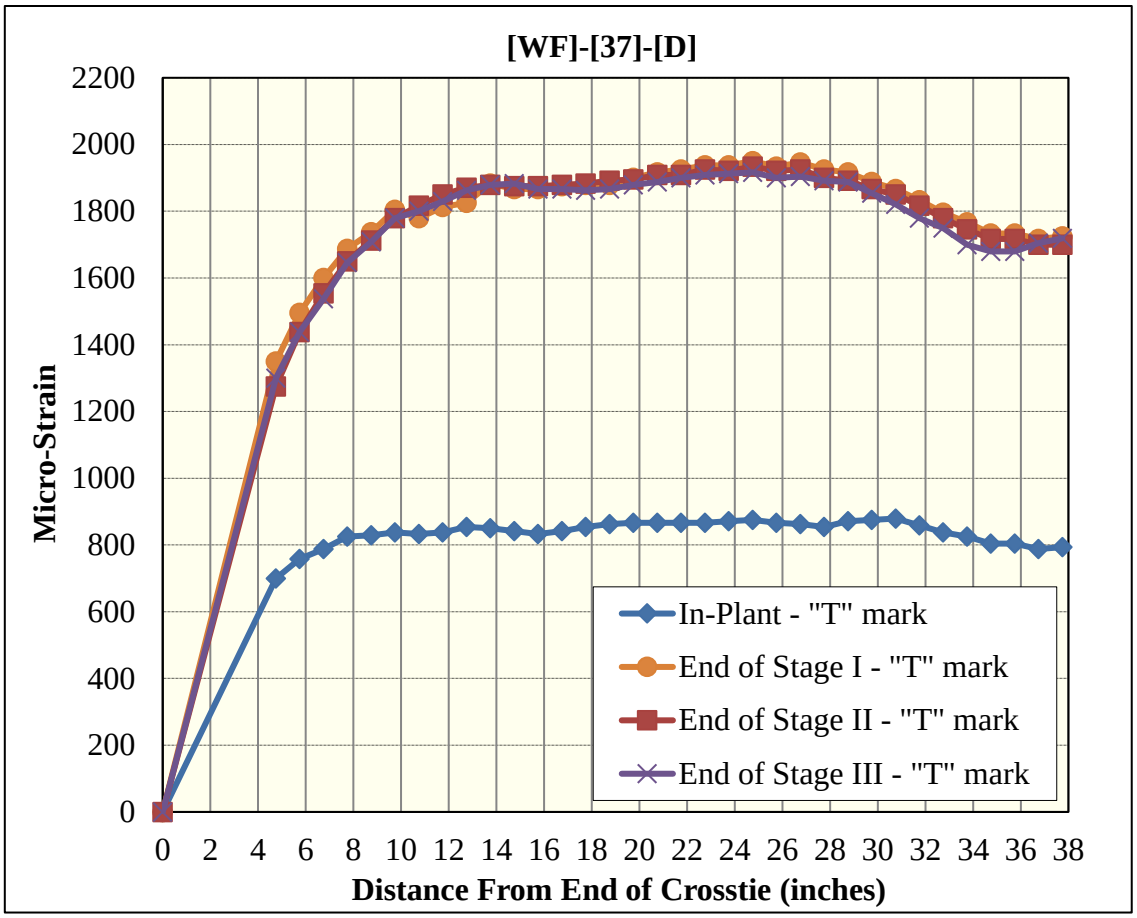

Figure 208 Surface-strain profiles for [WF]-[37]-[D] (Whittemore gage)

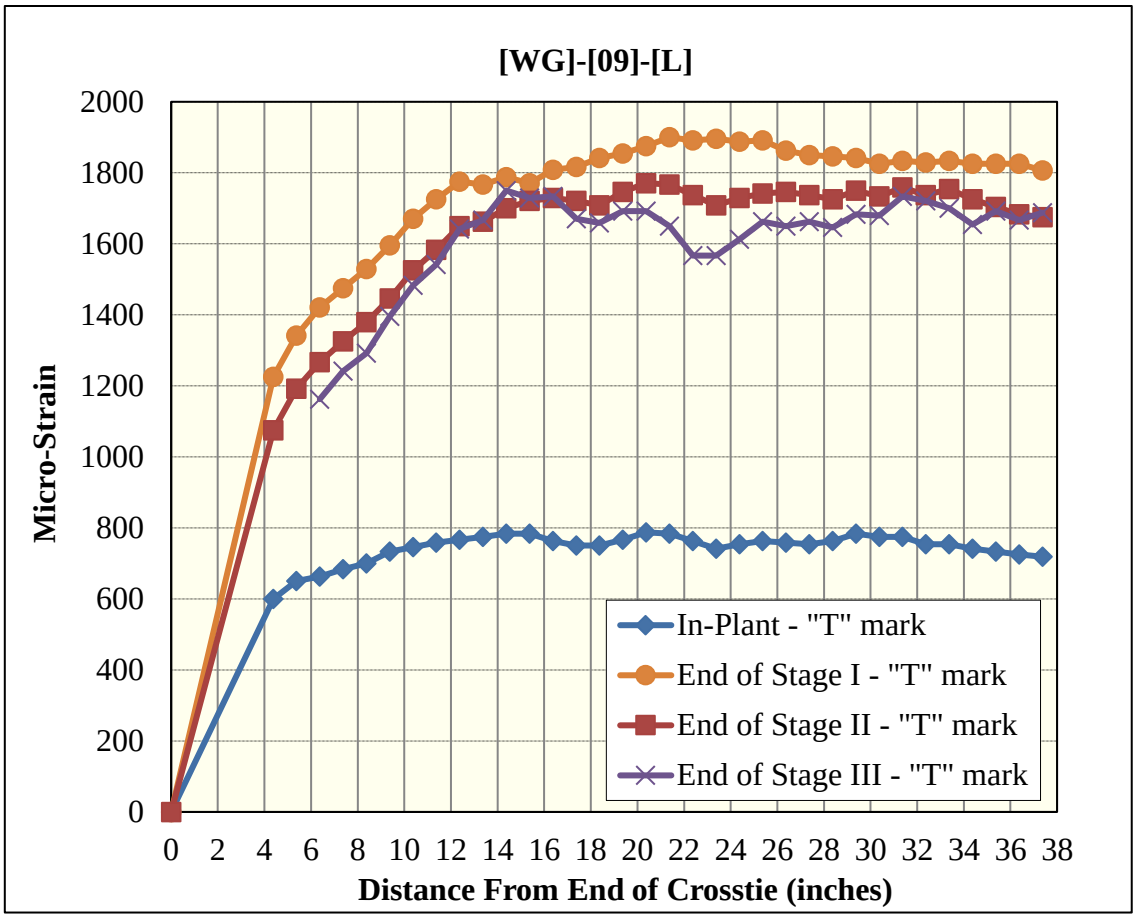

Figure 209 Surface-strain profiles for [WG]-[09]-[L] (Whittemore gage)

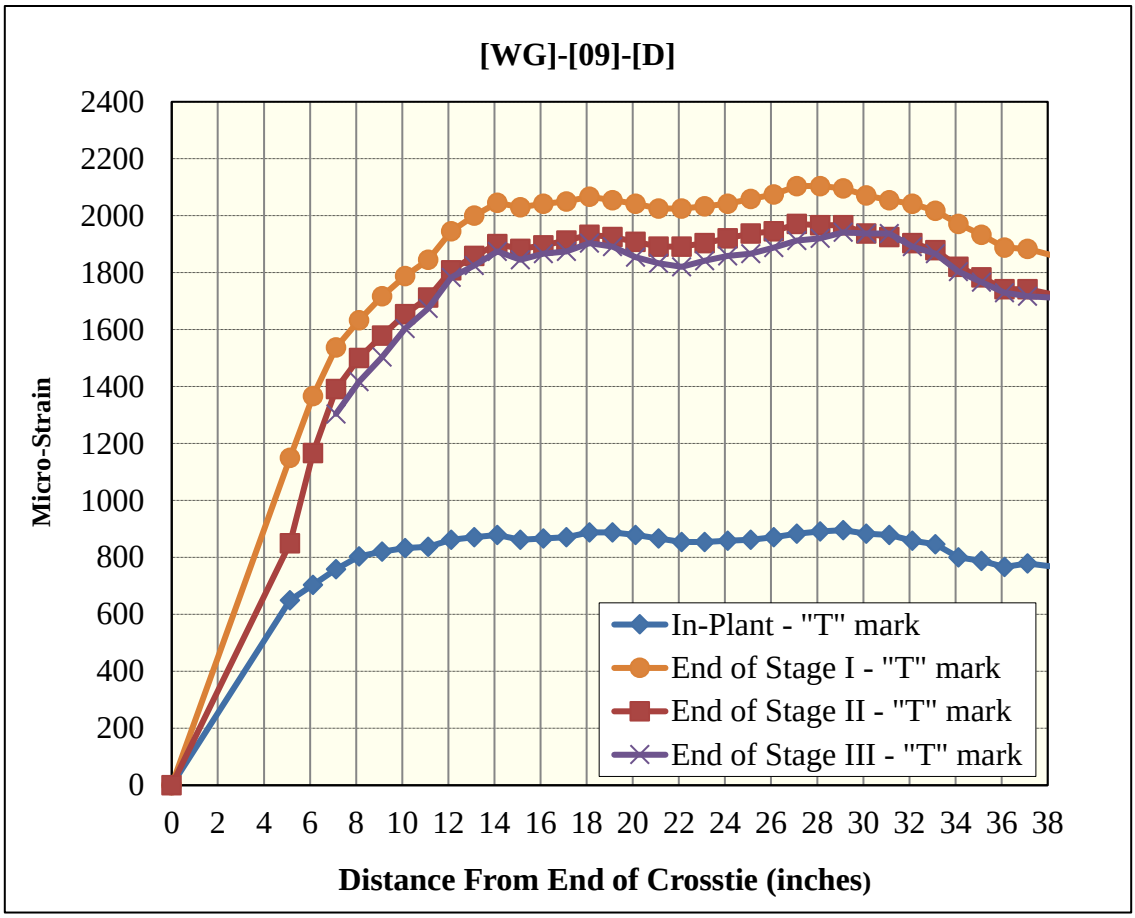

Figure 210 Surface-strain profiles for [WG]-[09]-[D] (Whittemore gage)

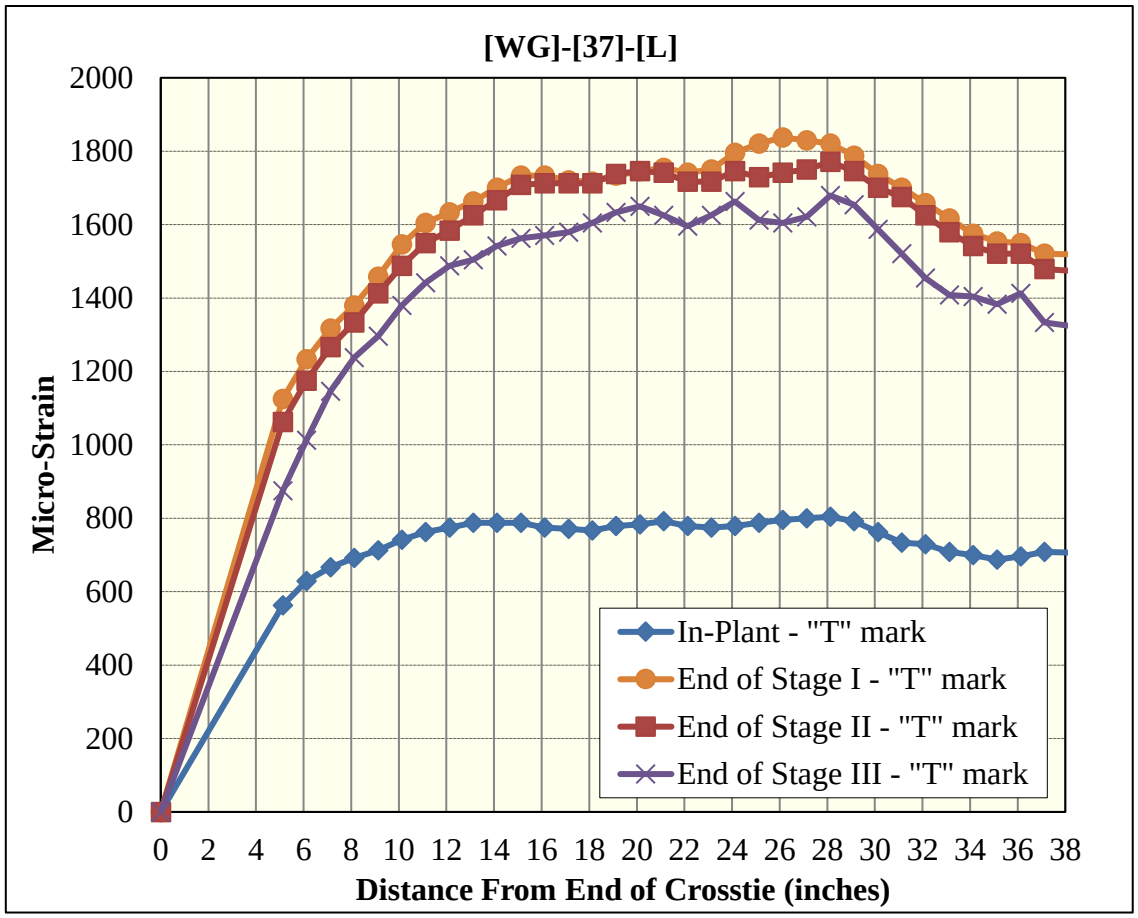

Figure 211 Surface-strain profiles for [WG]-[37]-[L] (Whittemore gage)

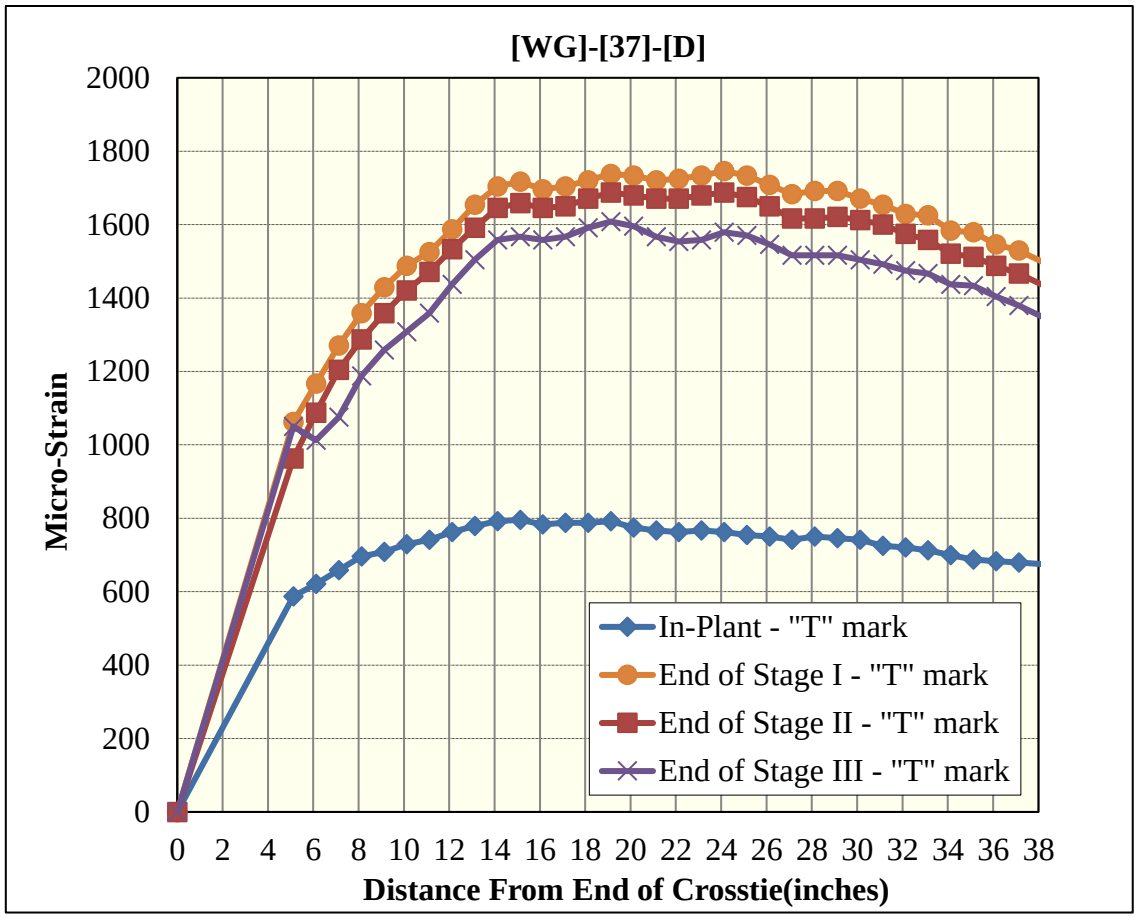

Figure 212 Surface-strain profiles for [WG]-[37]-[D] (Whittemore gage)

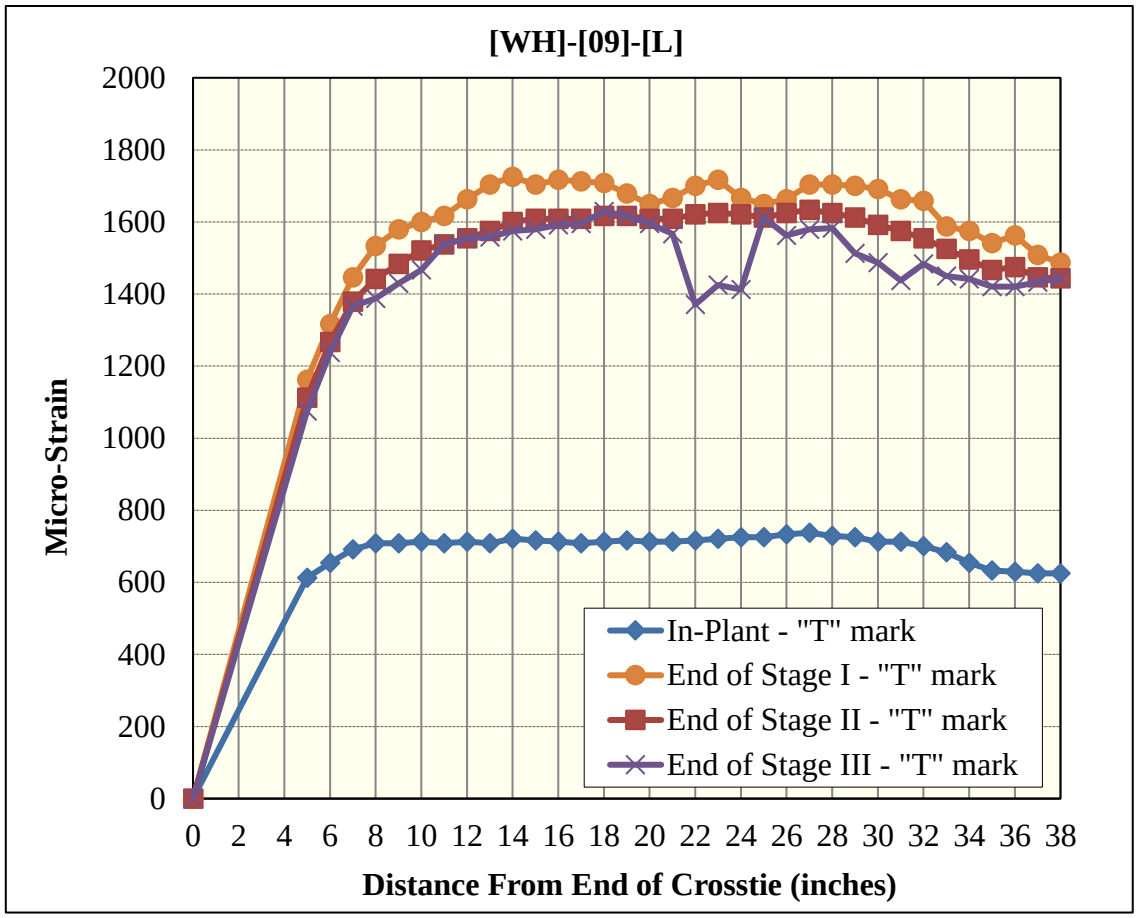

Figure 213 Surface-strain profiles for [WH]-[09]-[L] (Whittemore gage)

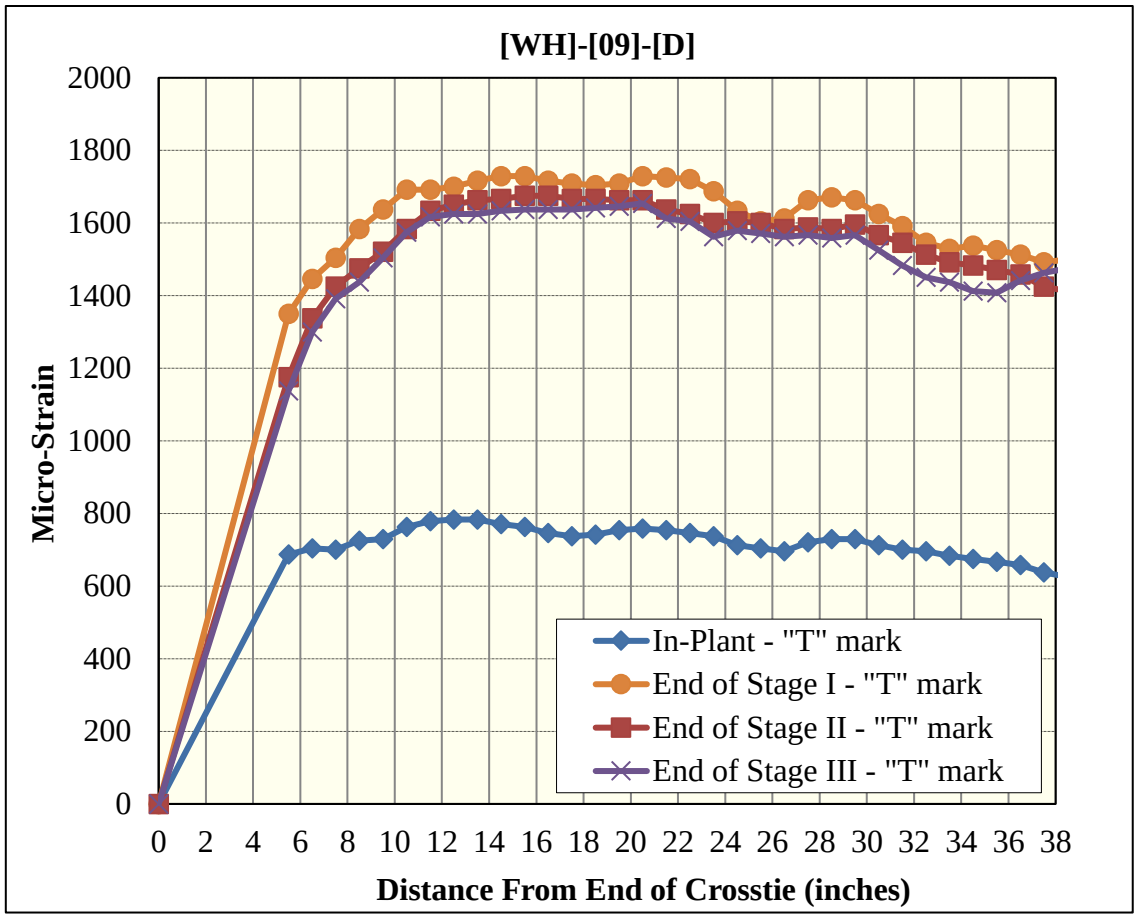

Figure 214 Surface-strain profiles for [WH]-[09]-[D] (Whittemore gage)

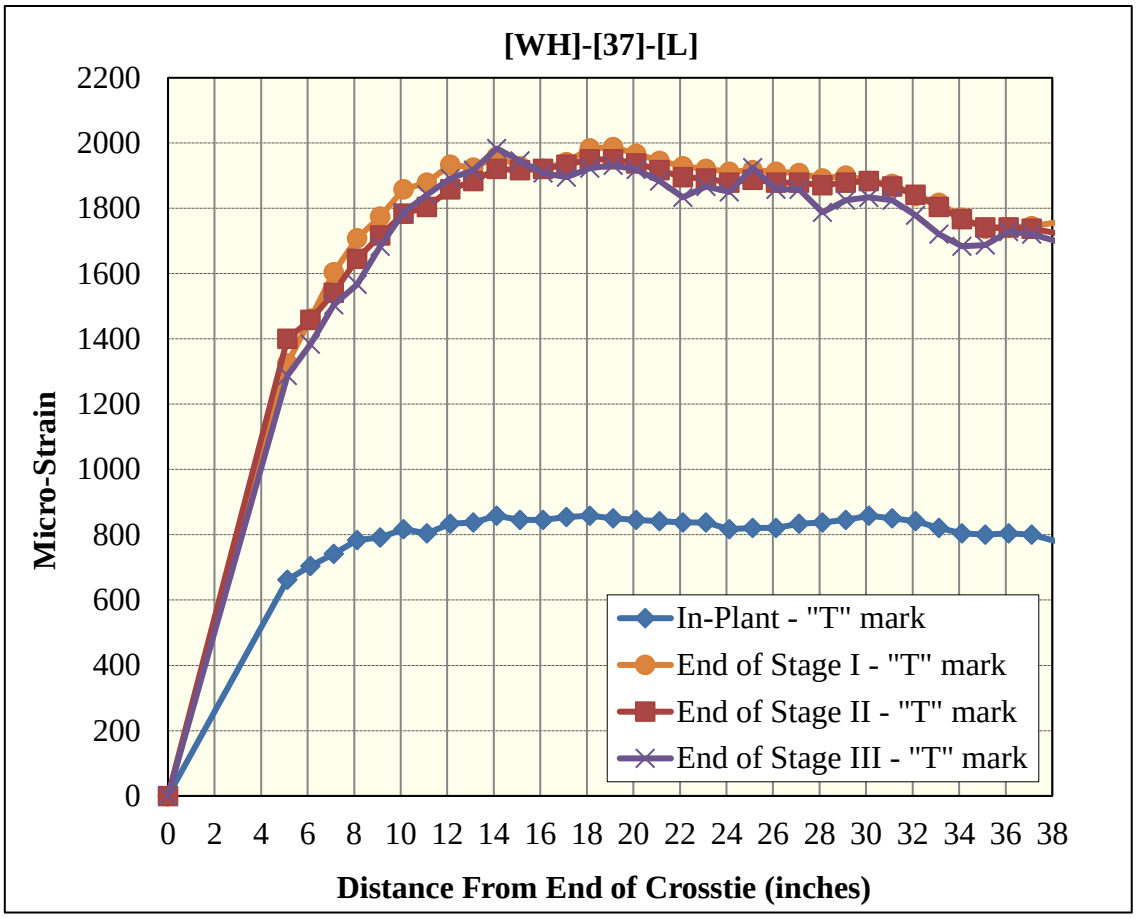

Figure 215 Surface-strain profiles for [WH]-[37]-[L] (Whittemore gage)

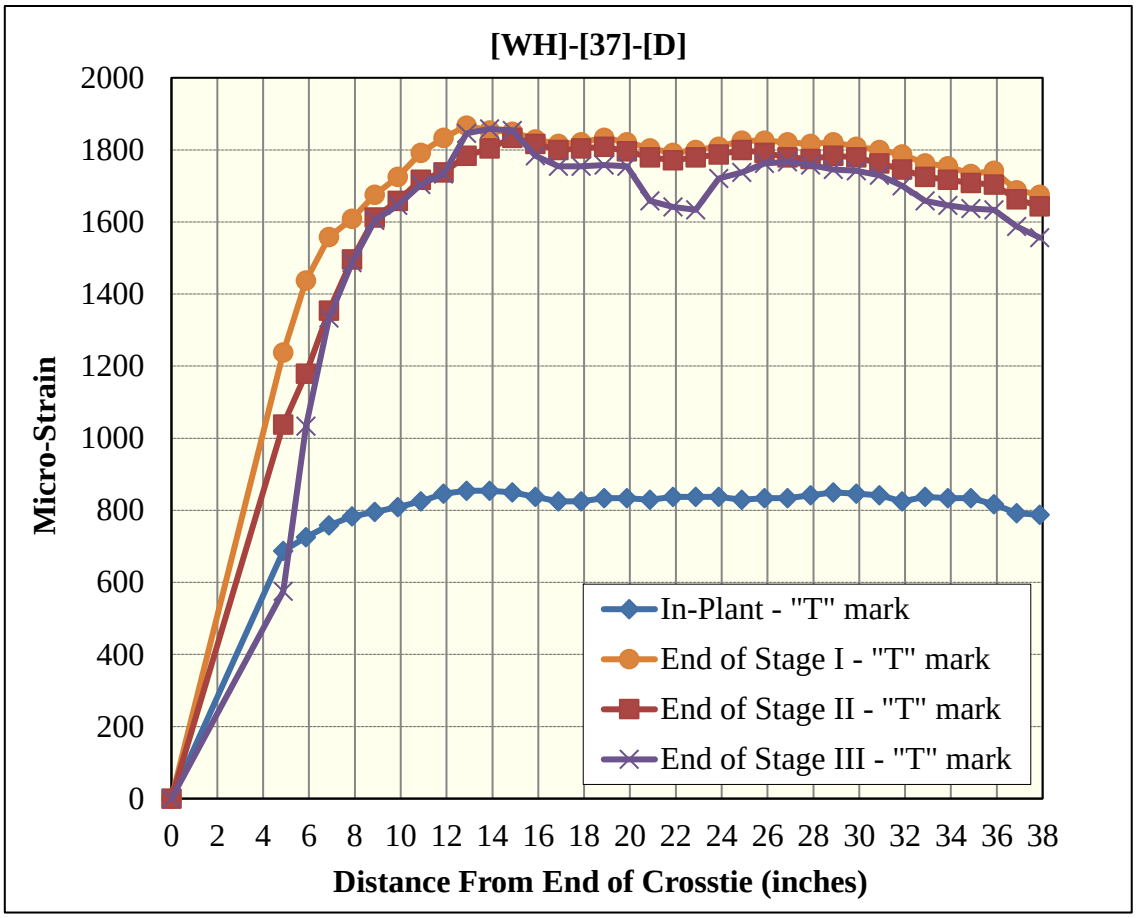

Figure 216 Surface-strain profiles for [WH]-[37]-[D] (Whittemore gage)

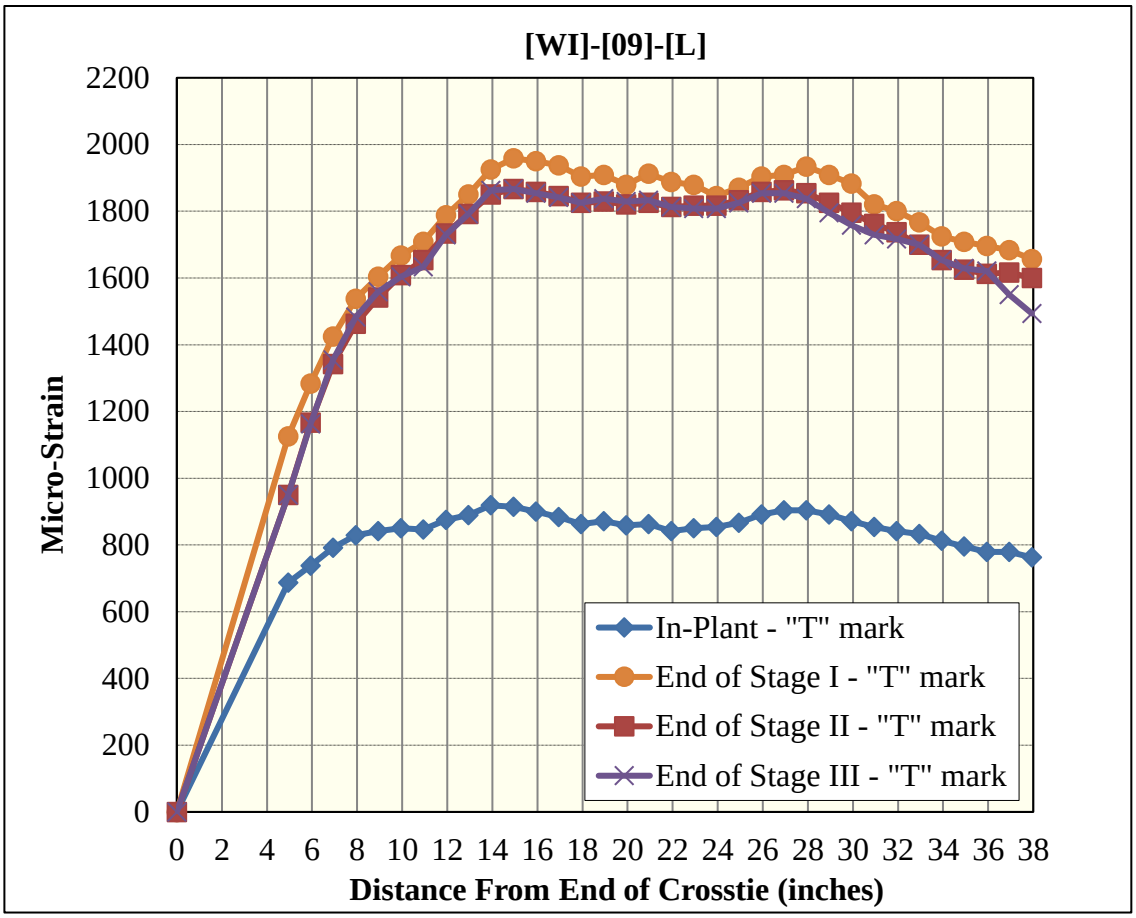

Figure 217 Surface-strain profiles for [WI]-[09]-[L] (Whittemore gage)

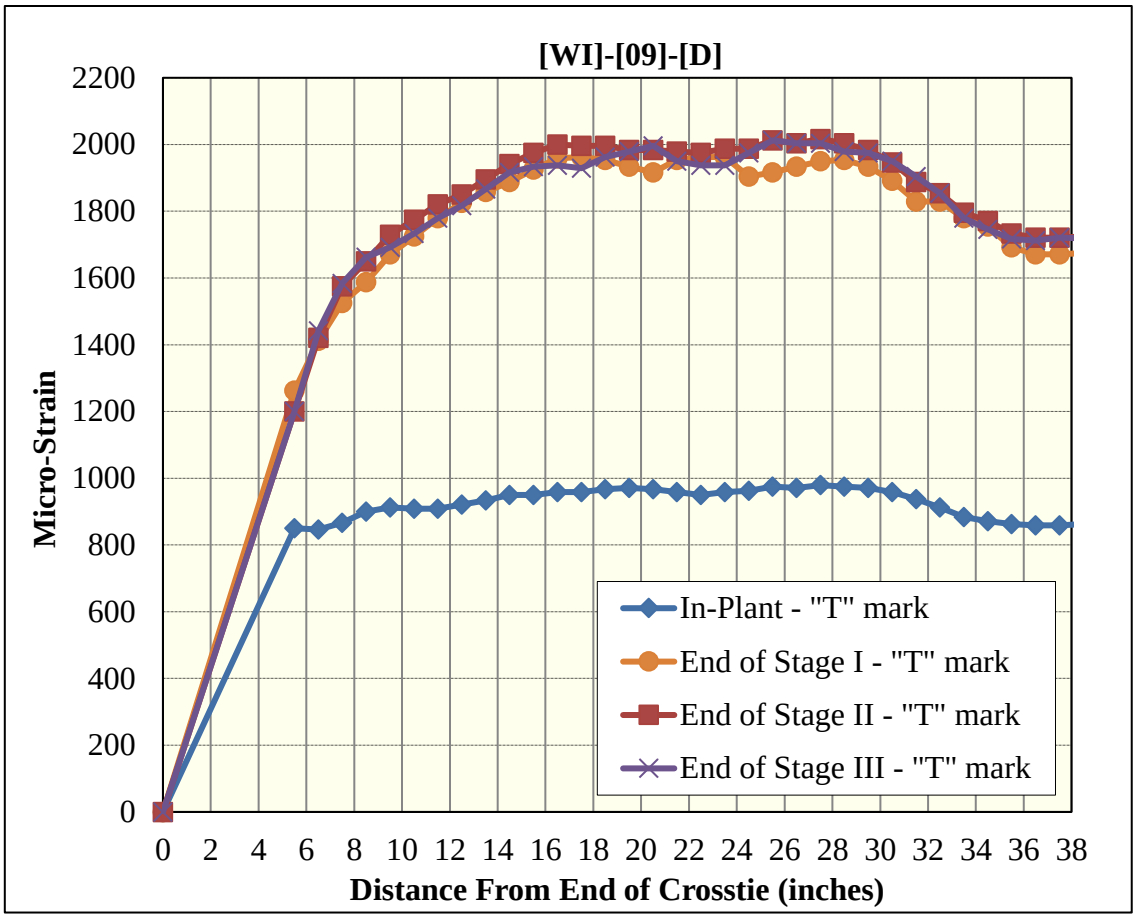

Figure 218 Surface-strain profiles for [WI]-[09]-[D] (Whittemore gage)

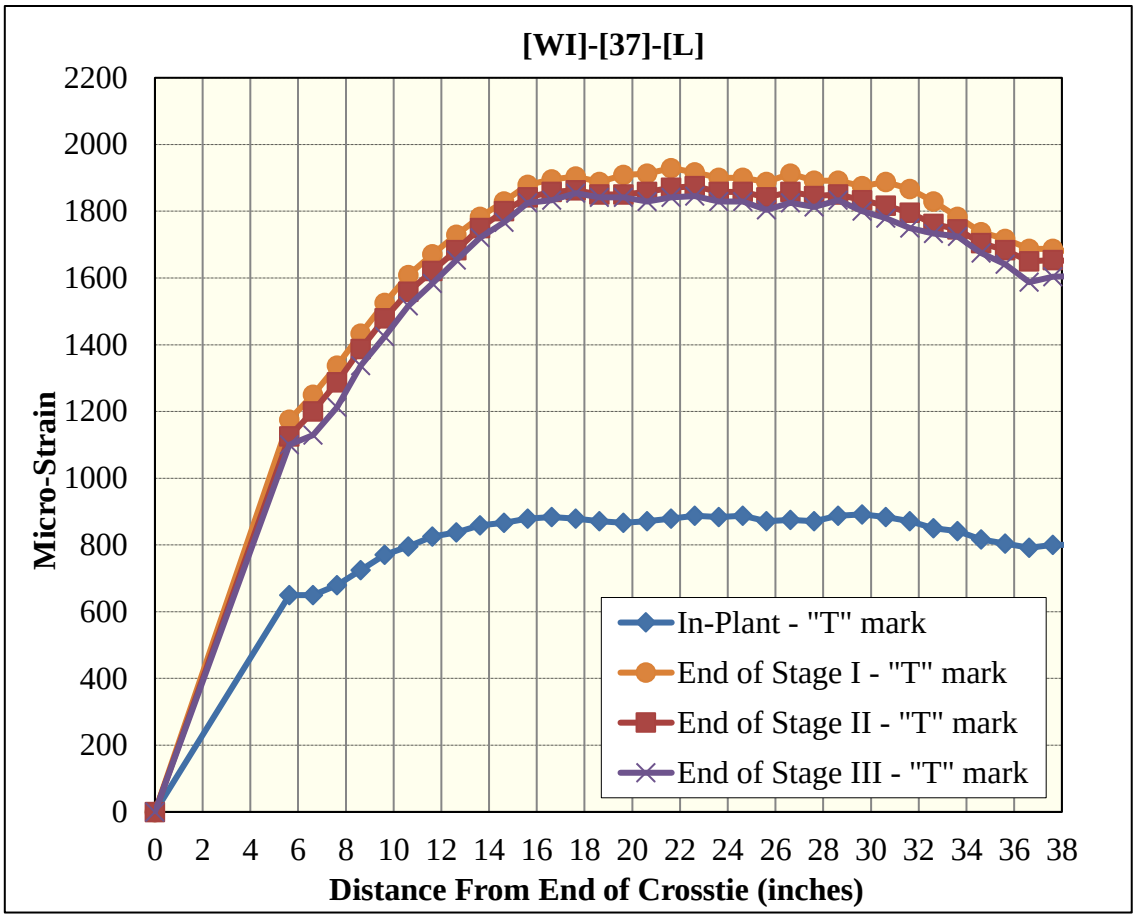

Figure 219 Surface-strain profiles for [WI]-[37]-[L] (Whittemore gage)

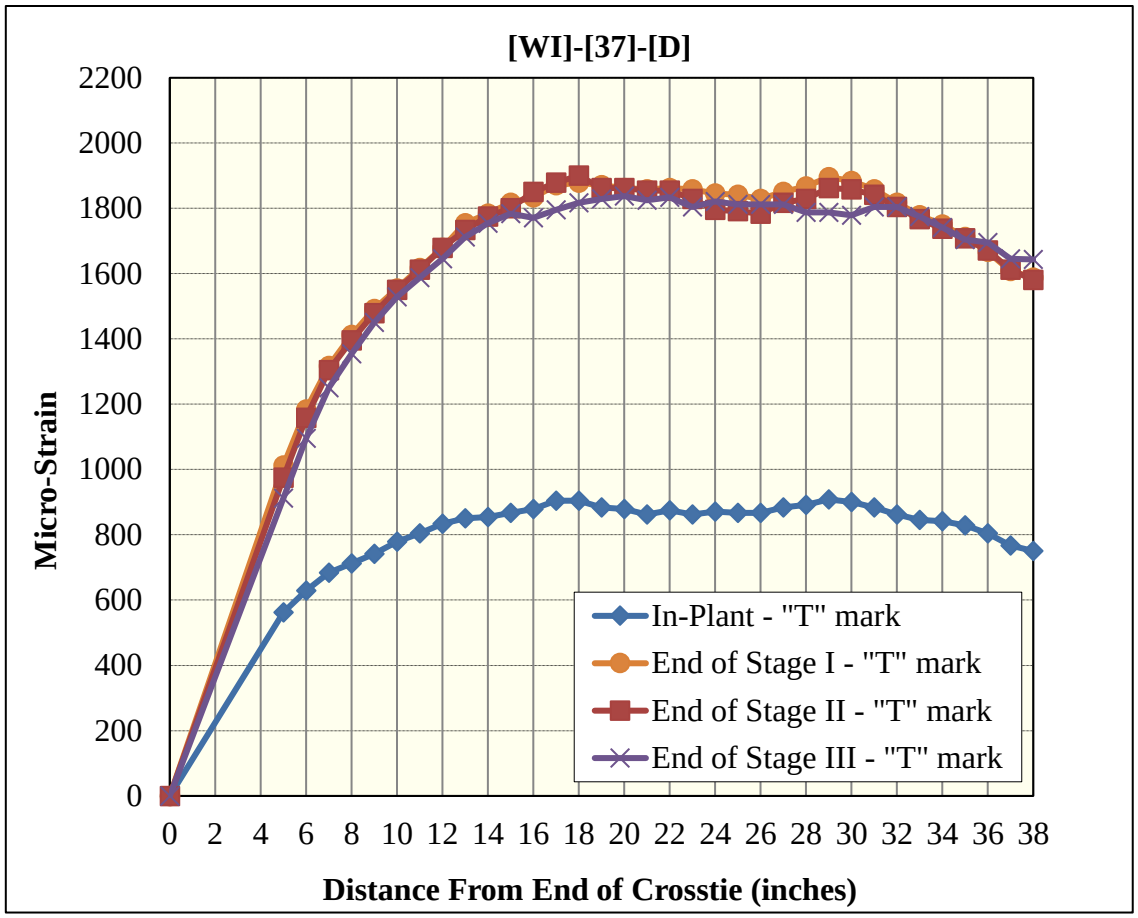

Figure 220 Surface-strain profiles for [WI]-[37]-[D] (Whittemore gage)

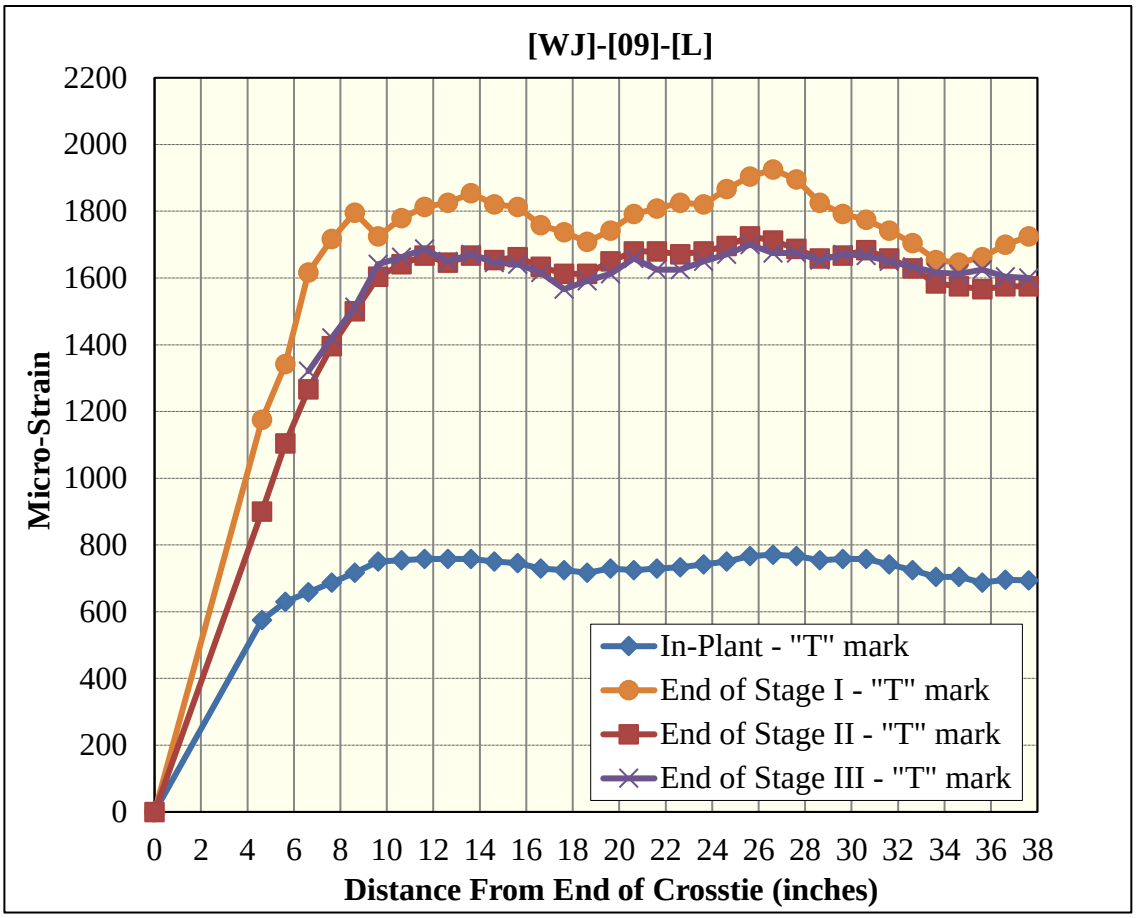

Figure 221 Surface-strain profiles for [WJ]-[09]-[L] (Whittemore gage)

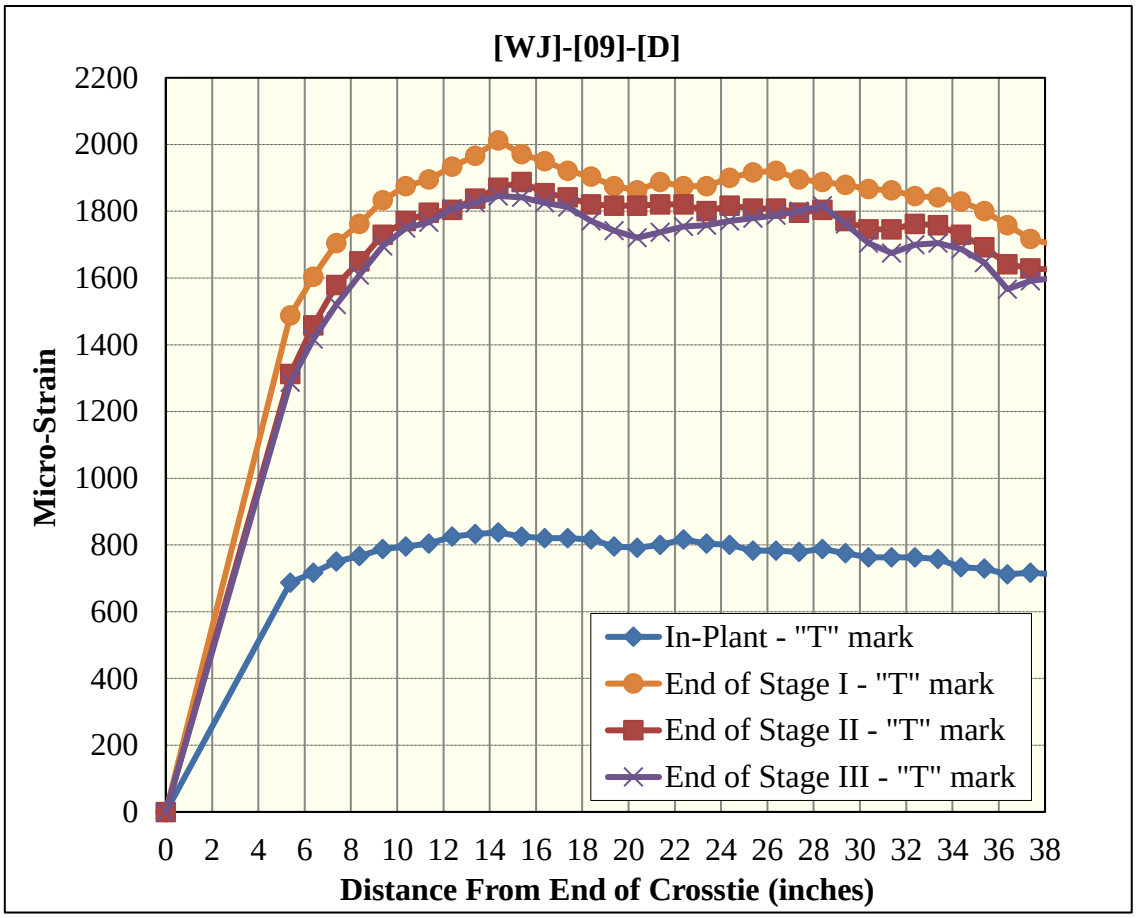

Figure 222 Surface-strain profiles for [WJ]-[09]-[D] (Whittemore gage)

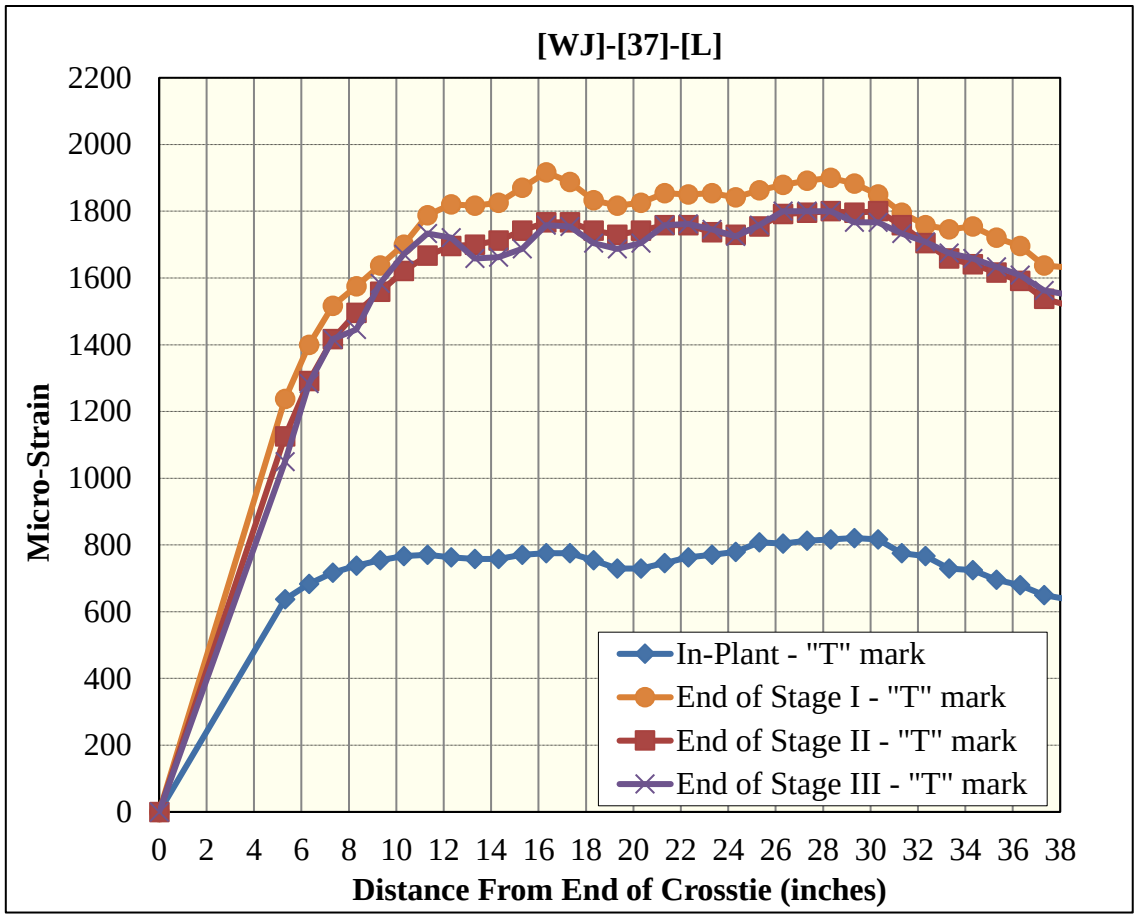

Figure 223 Surface-strain profiles for [WJ]-[37]-[L] (Whittemore gage)

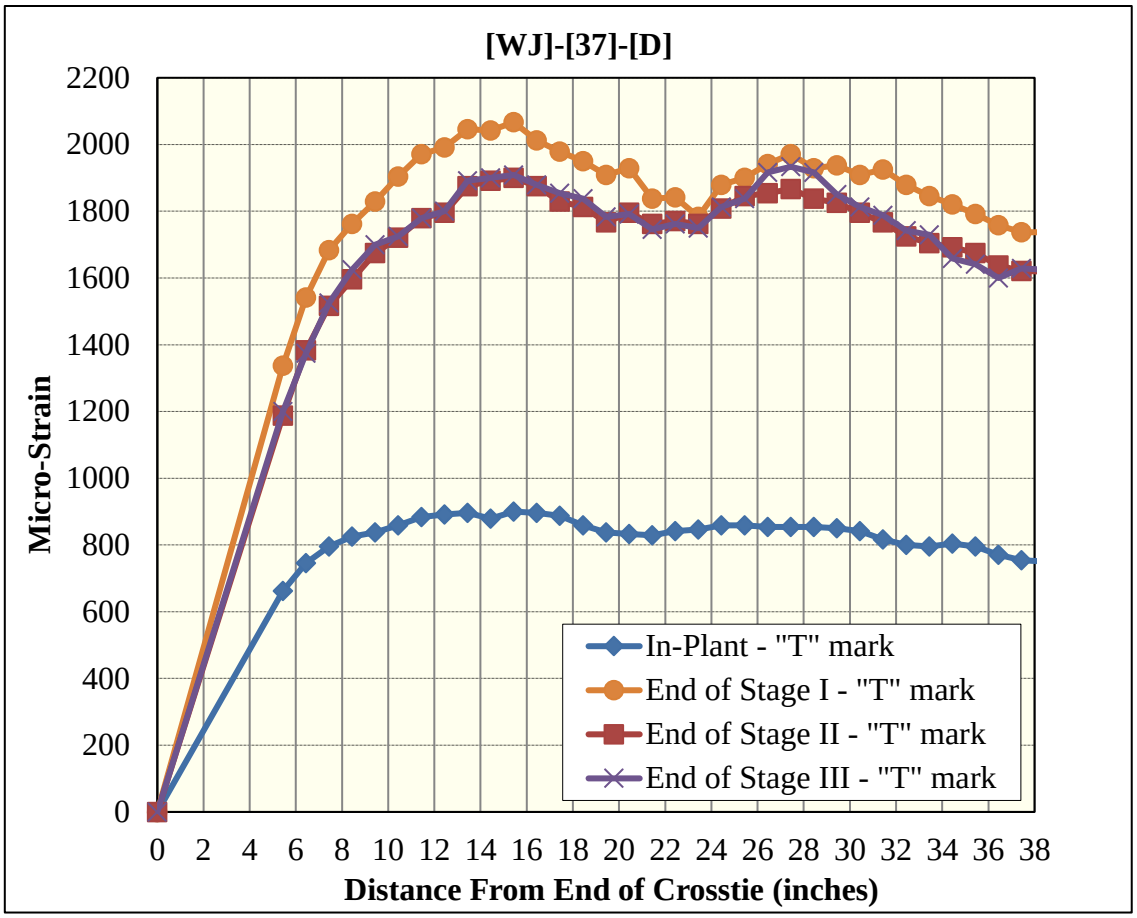

Figure 224 Surface-strain profiles for [WJ]-[37]-[D] (Whittemore gage)

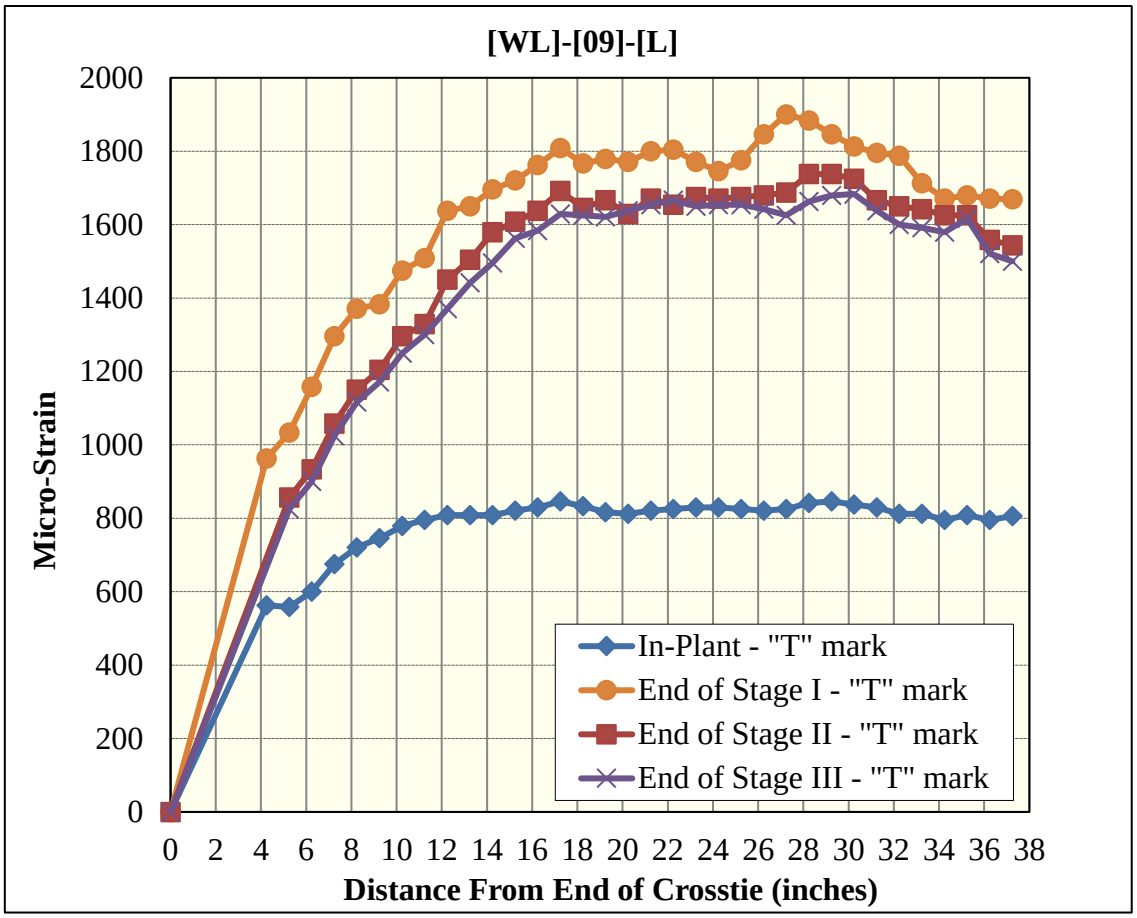

Figure 225 Surface-strain profiles for [WL]-[09]-[L] (Whittemore gage)

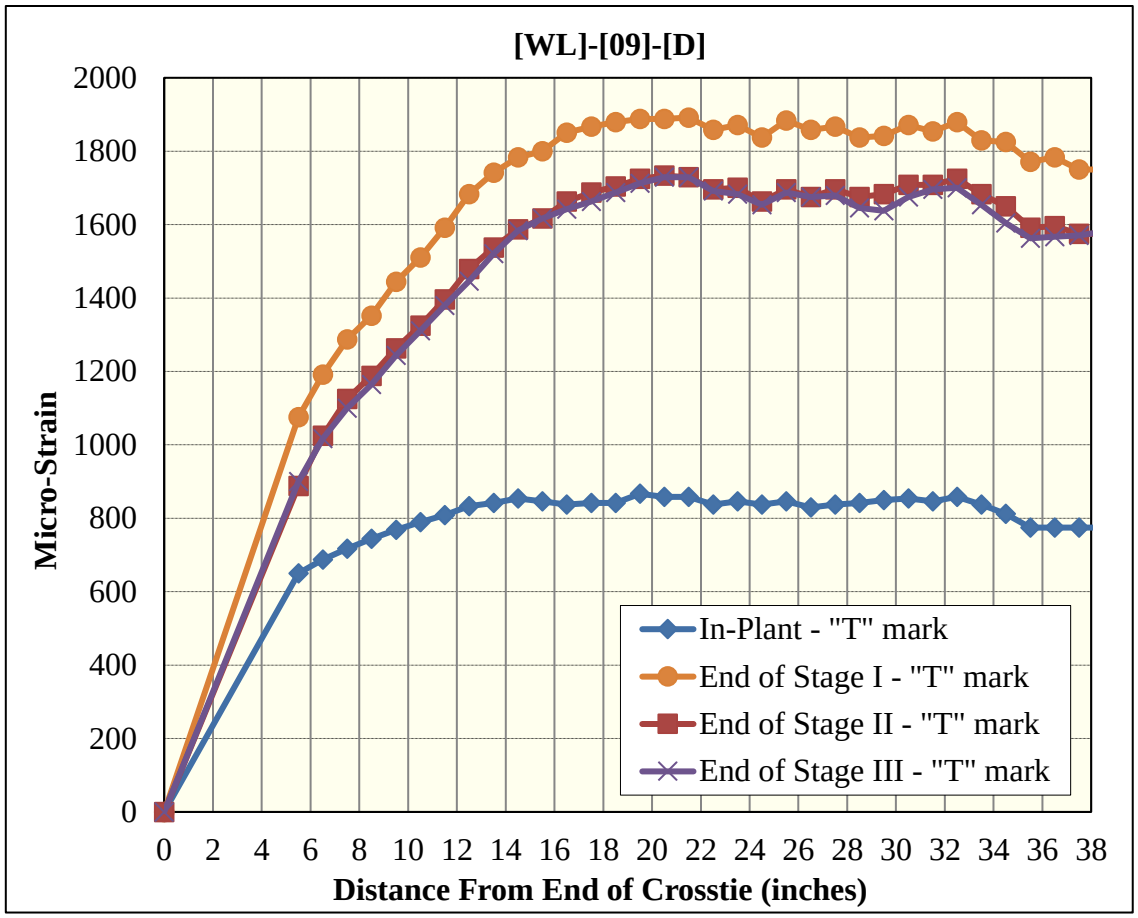

Figure 226 Surface-strain profiles for [WL]-[09]-[D] (Whittemore gage)

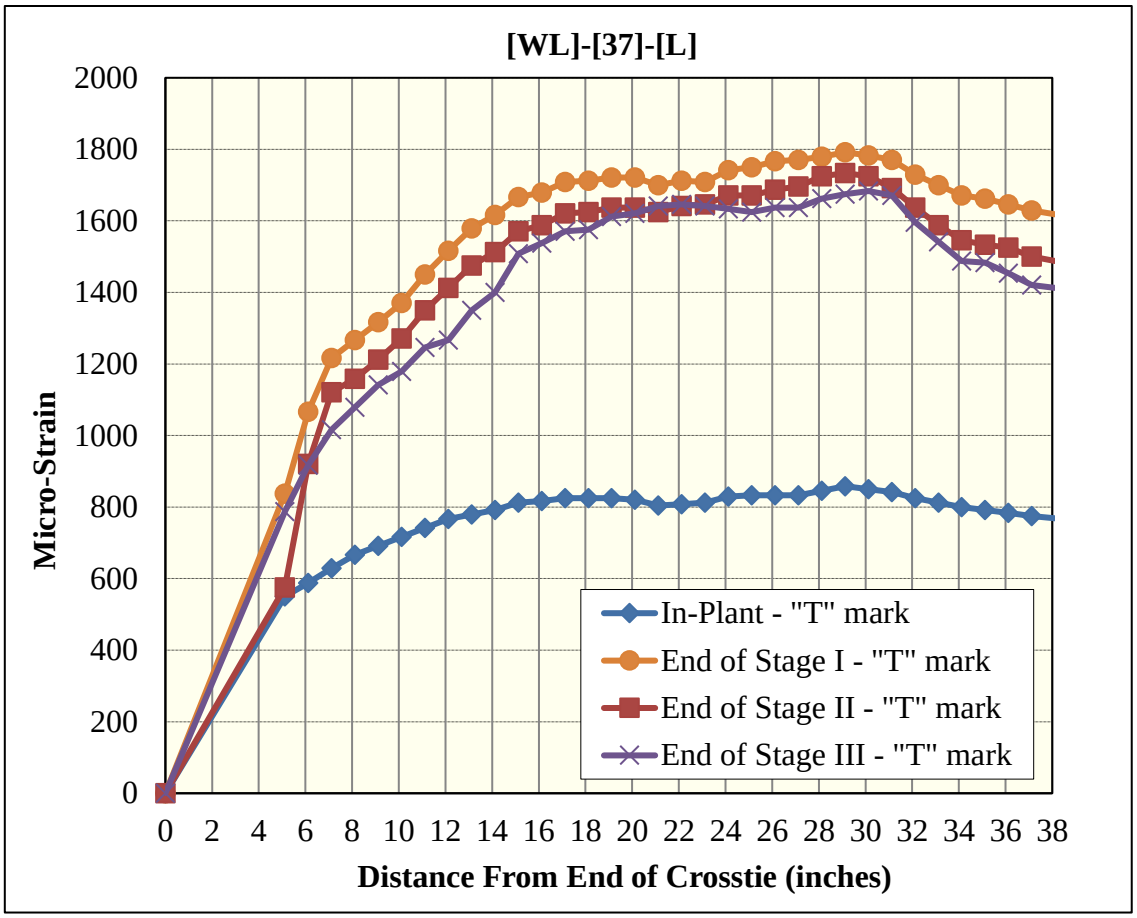

Figure 227 Surface-strain profiles for [WL]-[37]-[L] (Whittemore gage)

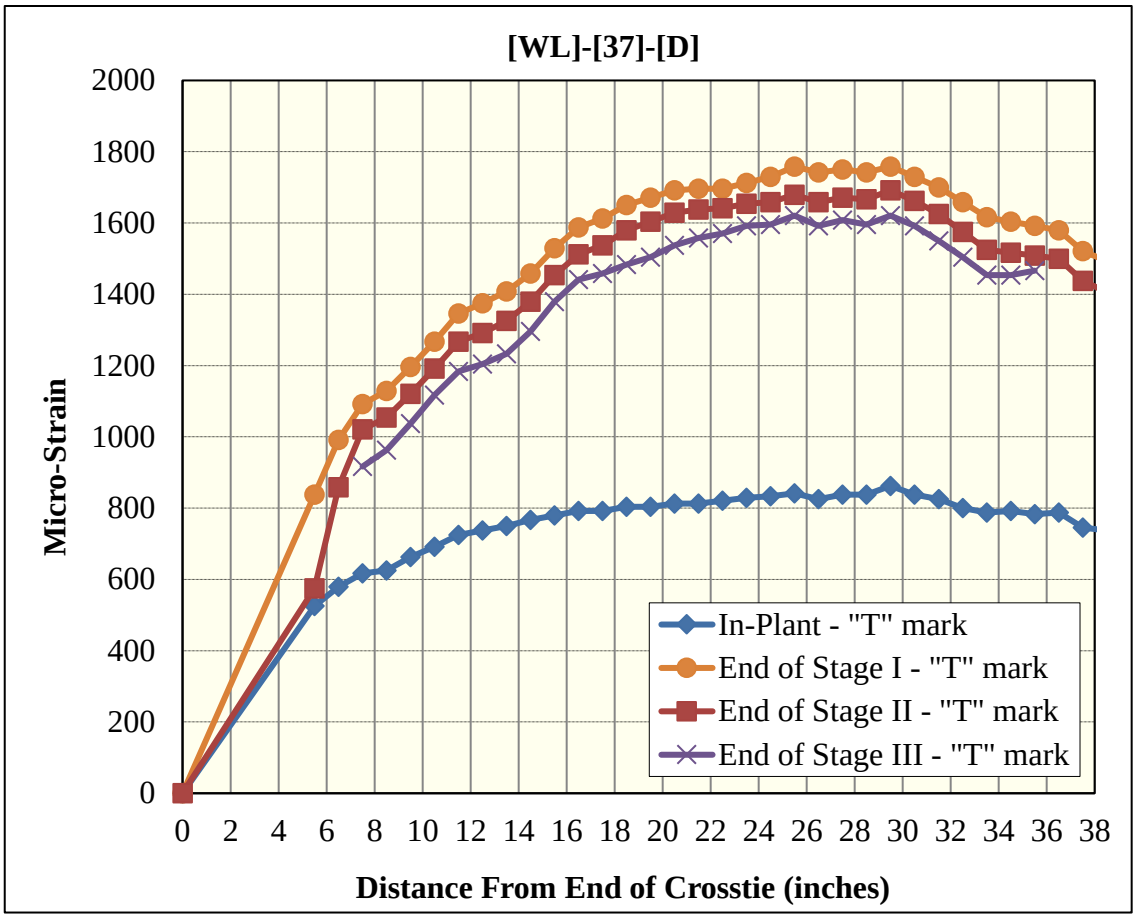

Figure 228 Surface-strain profiles for [WL]-[37]-[D] (Whittemore gage)

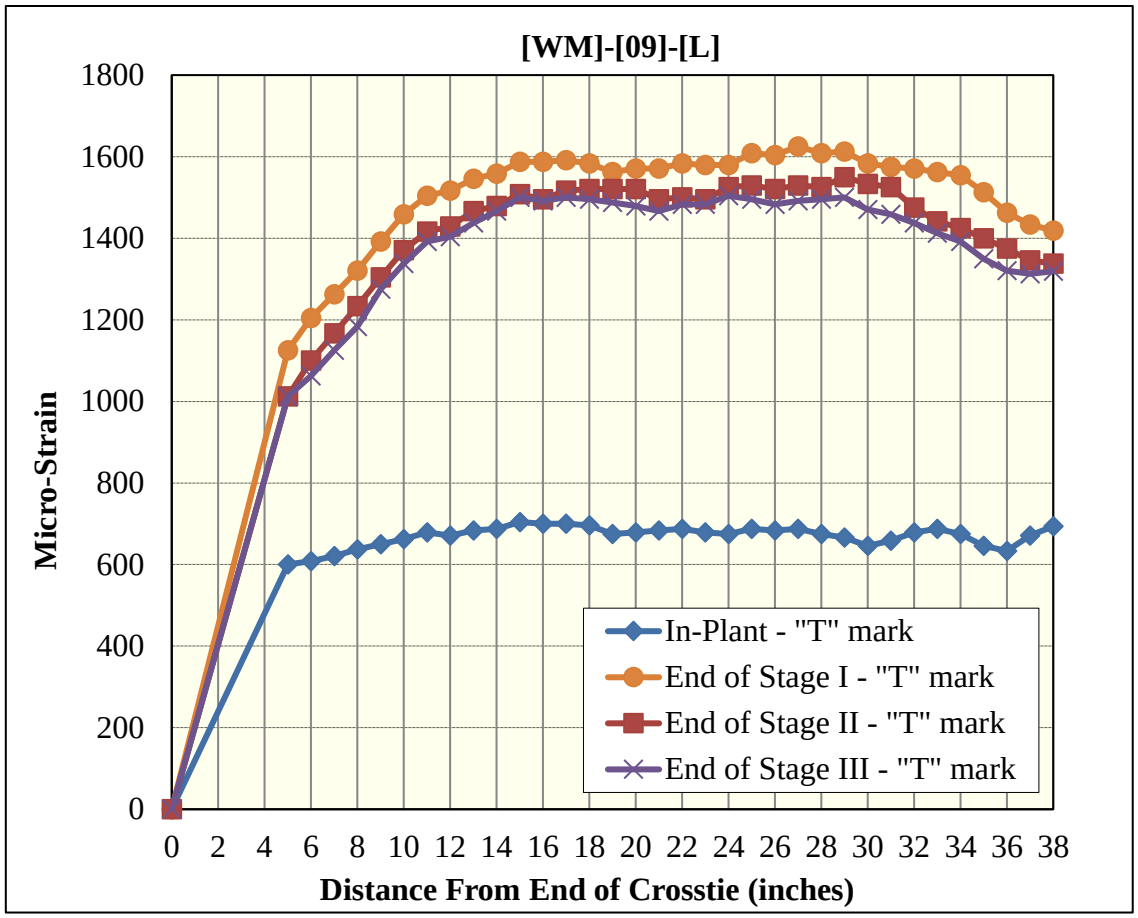

Figure 229 Surface-strain profiles for [WM]-[09]-[L] (Whittemore gage)

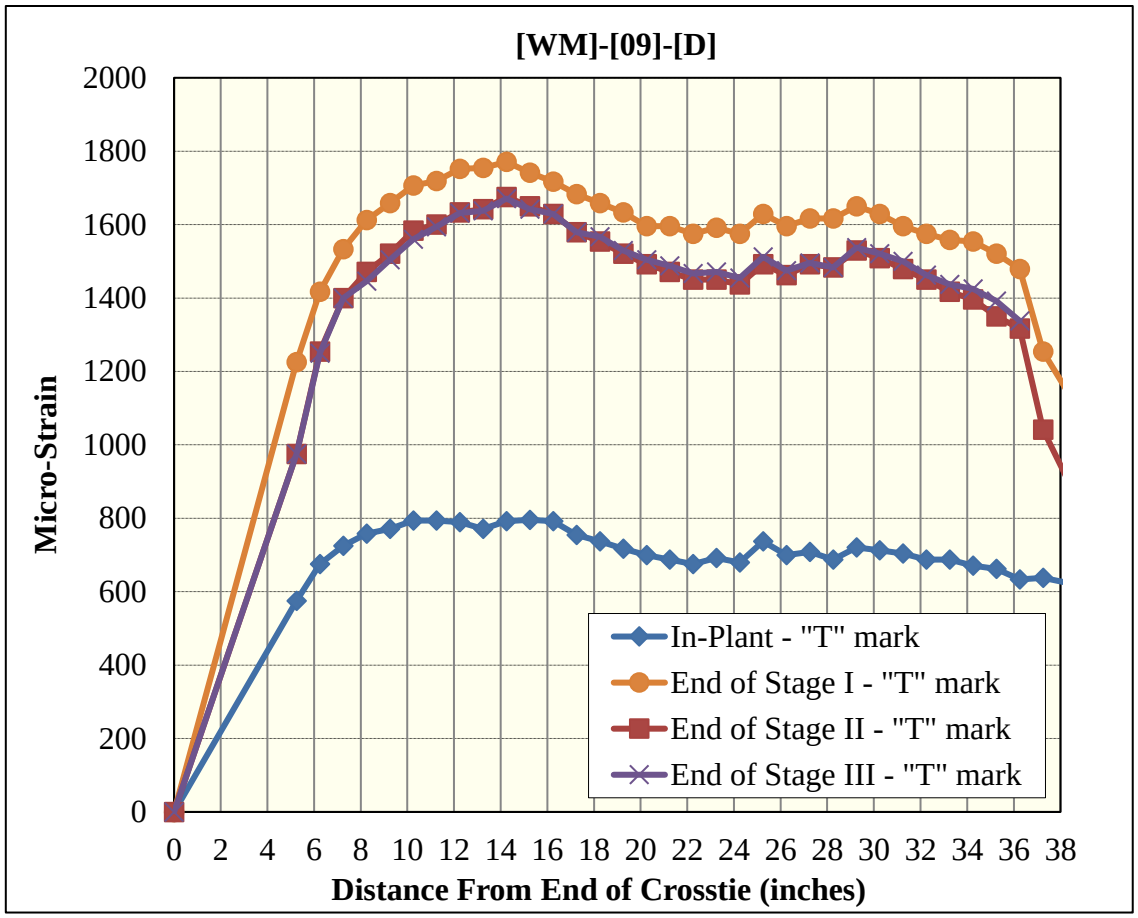

Figure 230 Surface-strain profiles for [WM]-[09]-[D] (Whittemore gage)

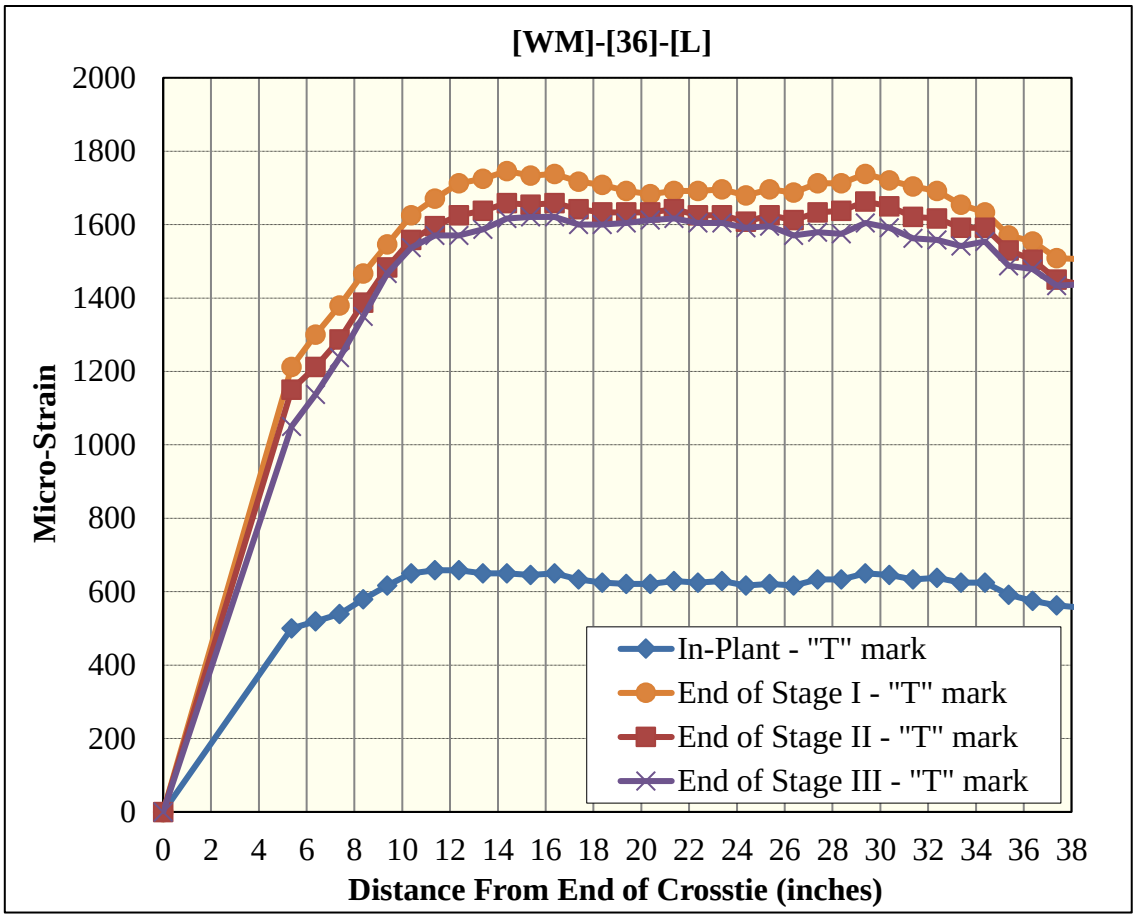

Figure 231 Surface-strain profiles for [WM]-[36]-[L] (Whittemore gage)

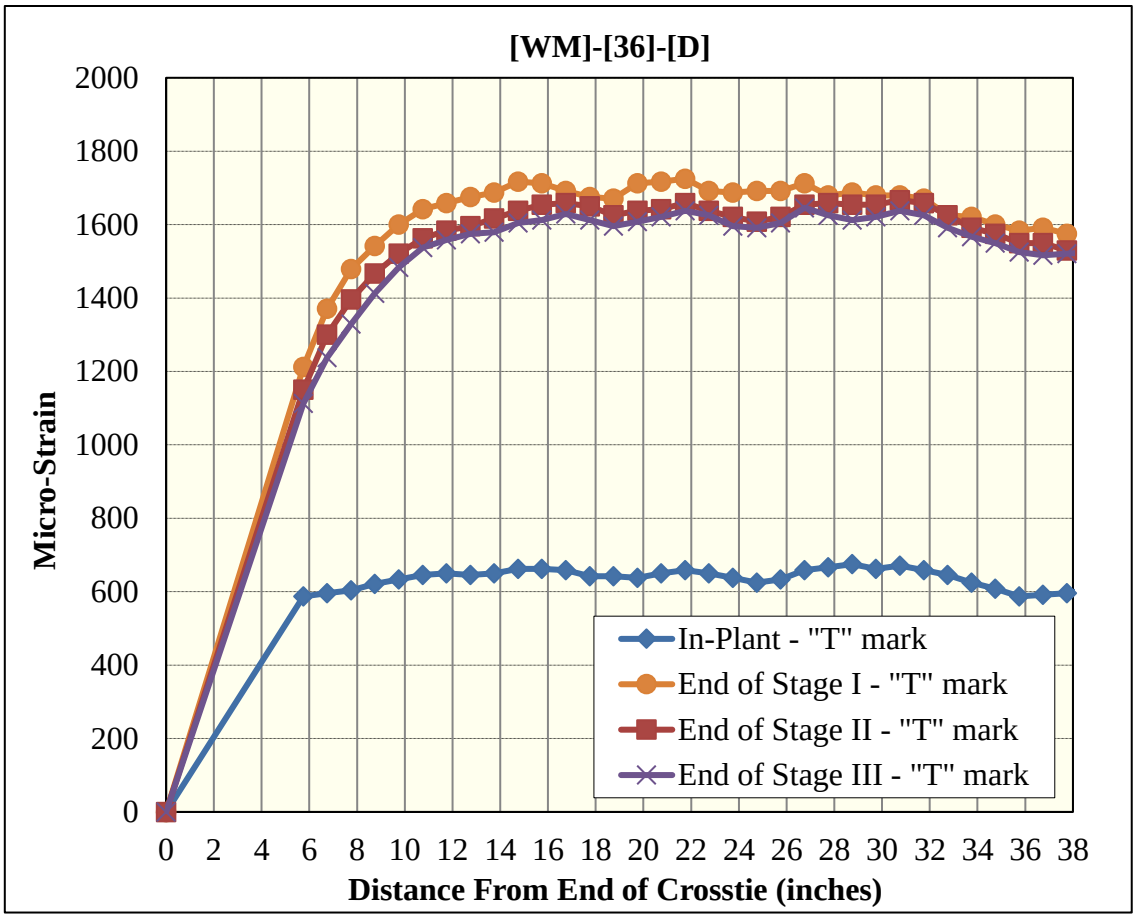

Figure 232 Surface-strain profiles for [WM]-[36]-[D] (Whittemore gage)

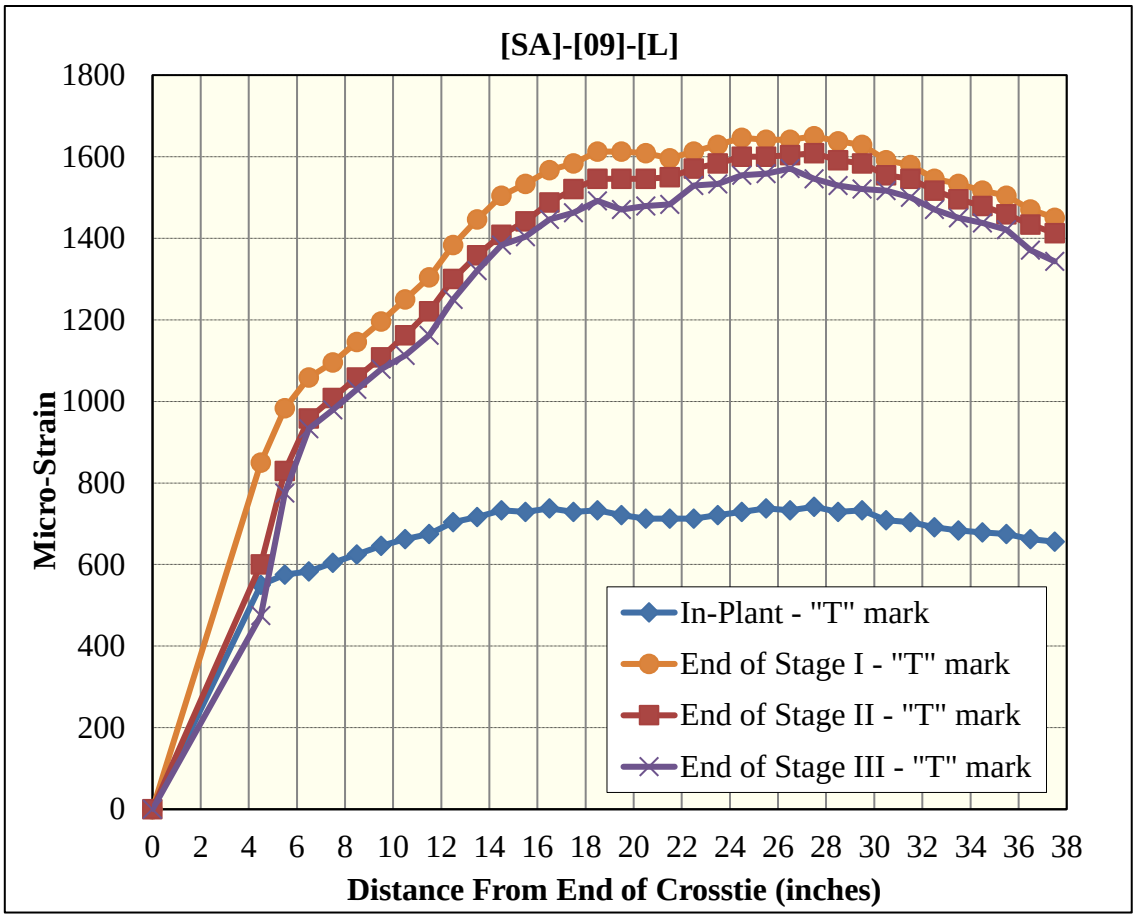

Figure 233 Surface-strain profiles for [SA]-[09]-[L] (Whittemore gage)

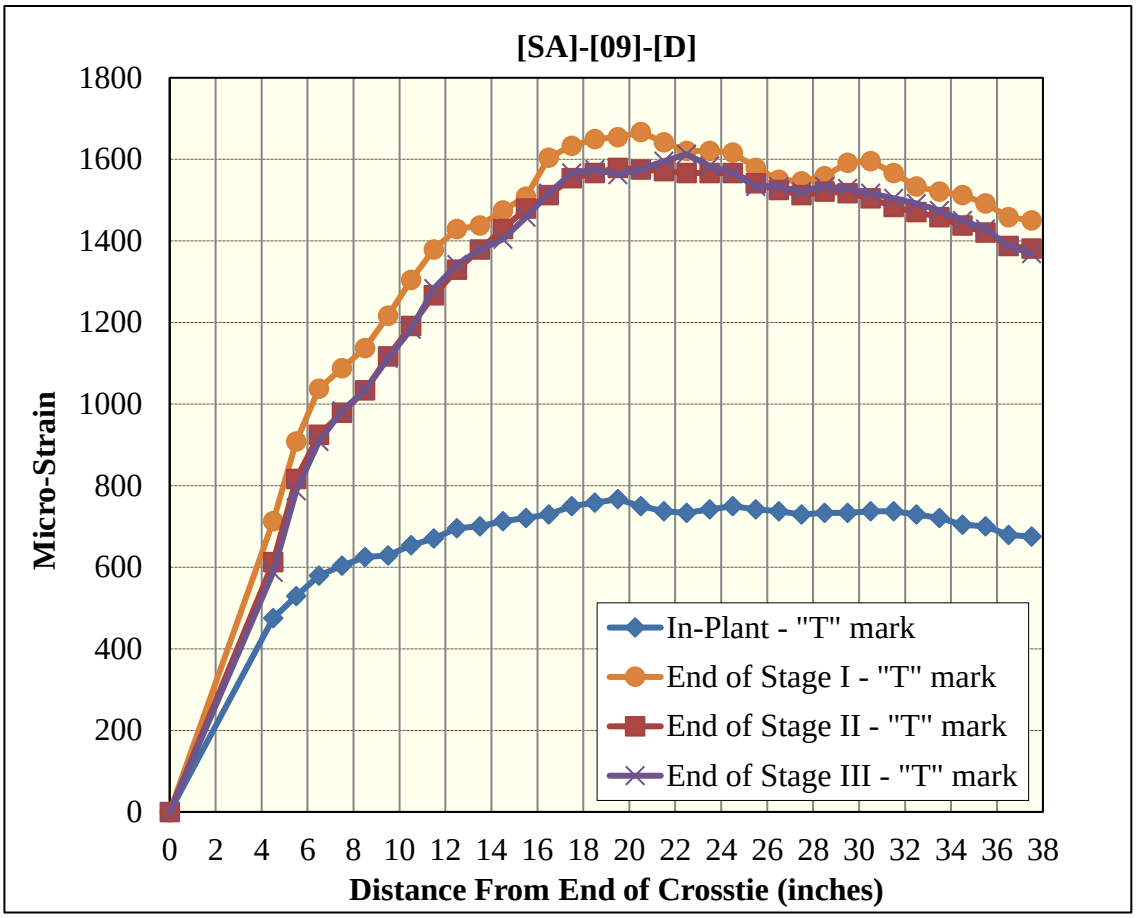

Figure 234 Surface-strain profiles for [SA]-[09]-[D] (Whittemore gage)

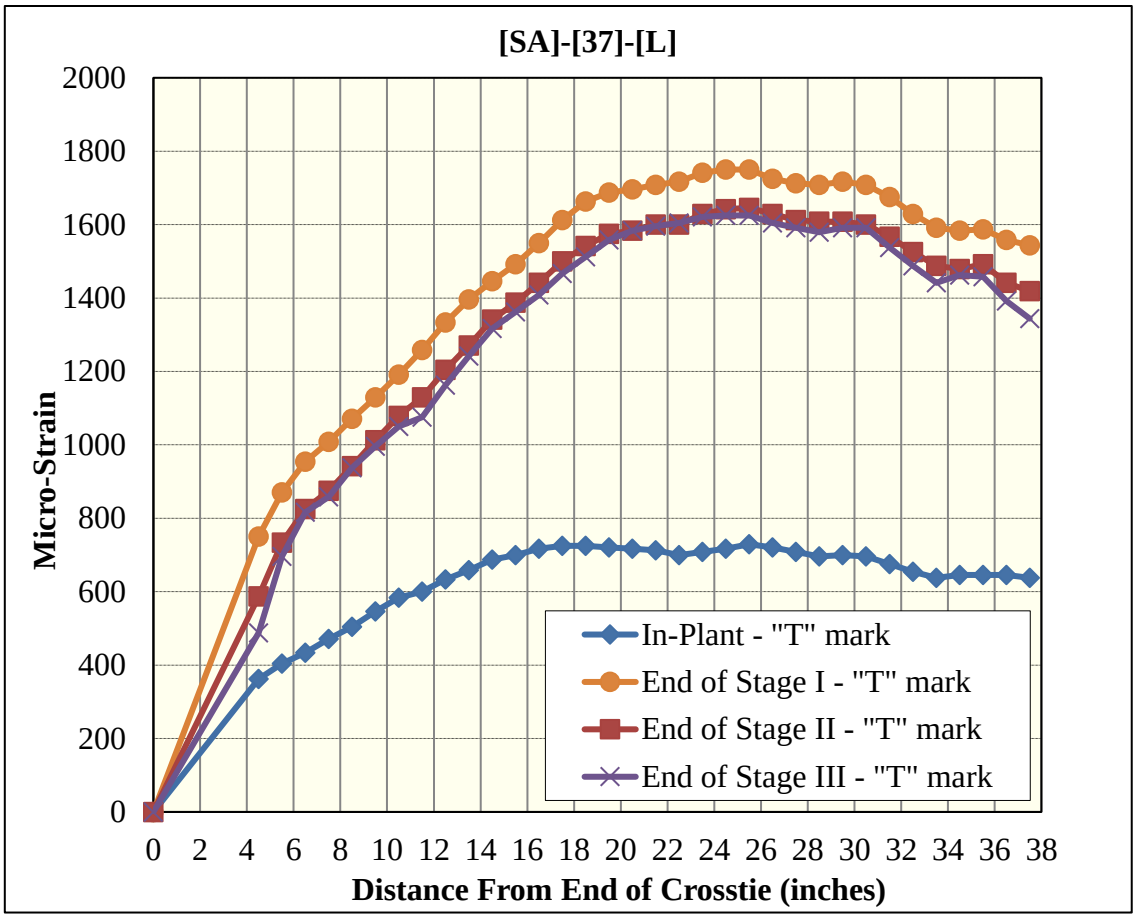

Figure 235 Surface-strain profiles for [SA]-[37]-[L] (Whittemore gage)

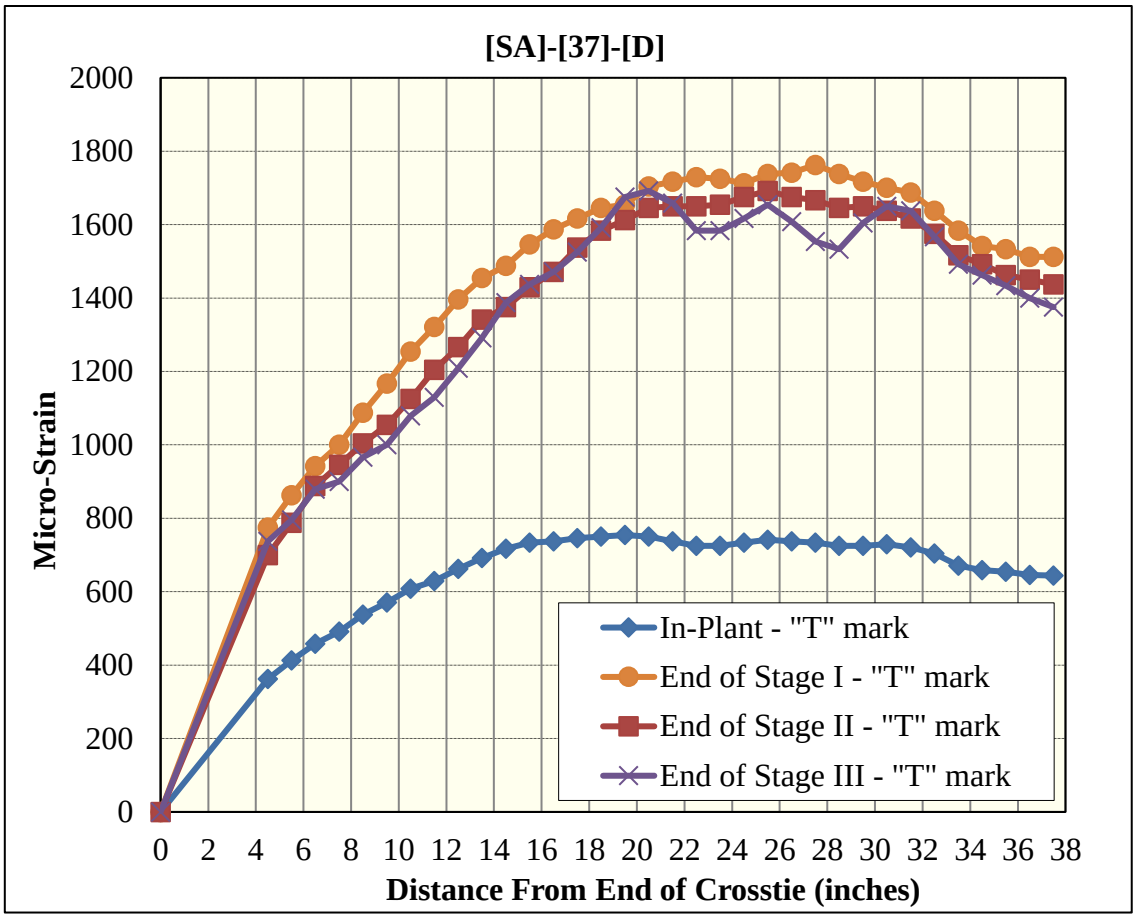

Figure 236 Surface-strain profiles for [SA]-[37]-[D] (Whittemore gage)

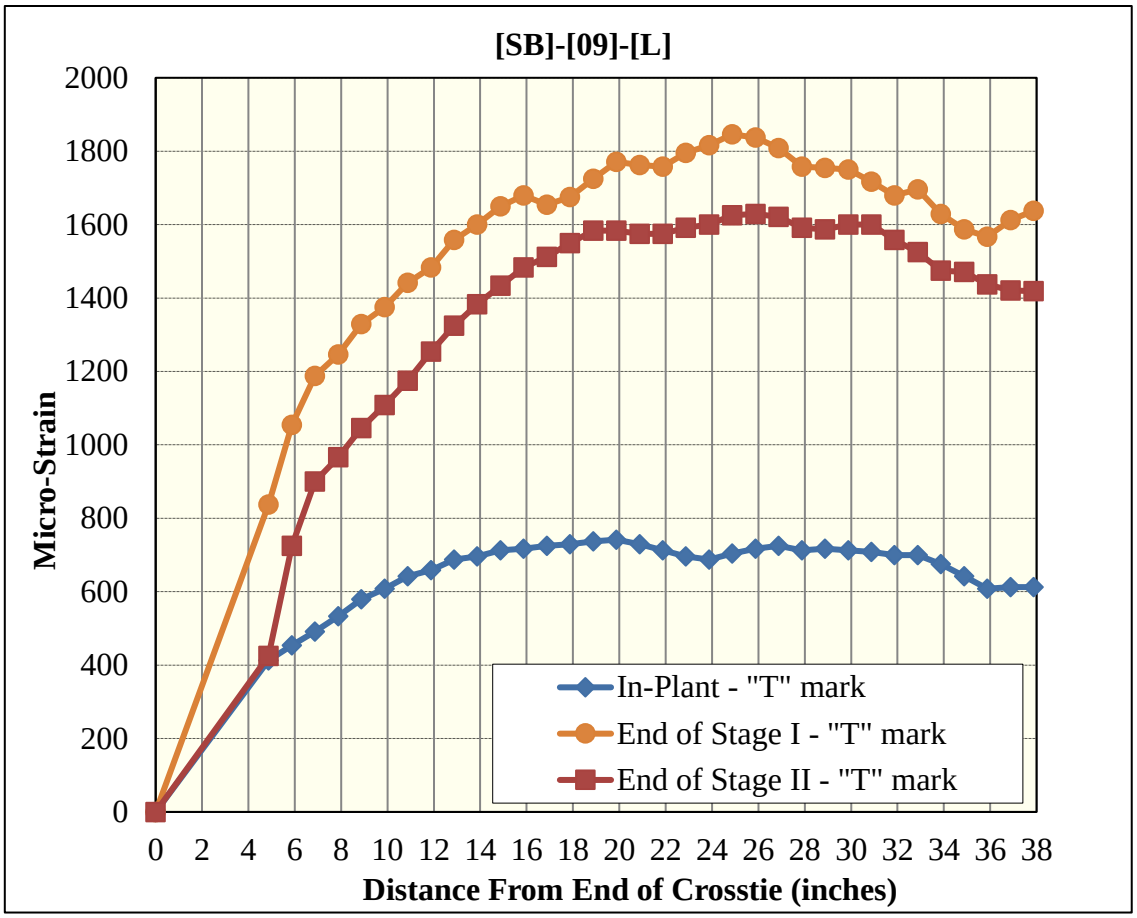

Figure 237 Surface-strain profiles for [SB]-[09]-[L] (Whittemore gage)

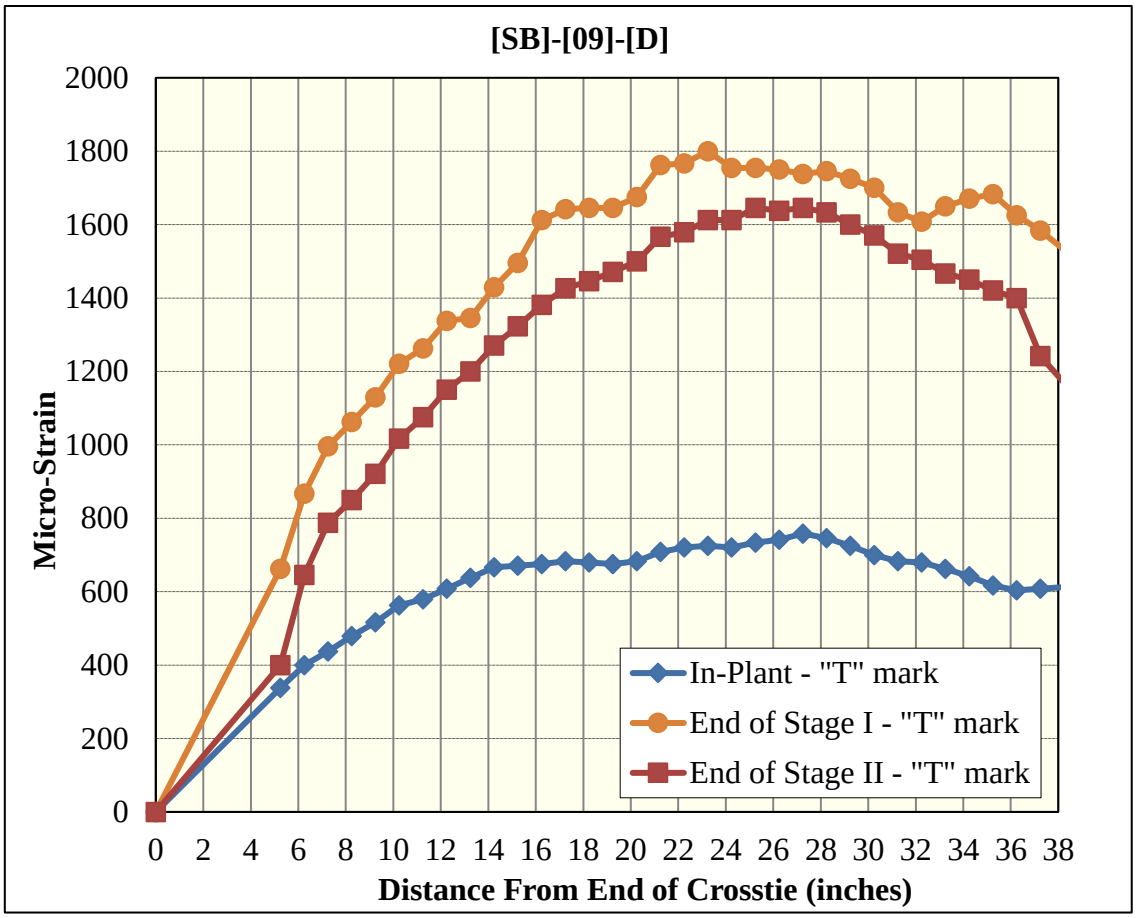

Figure 238 Surface-strain profiles for [SB]-[09]-[D] (Whittemore gage)

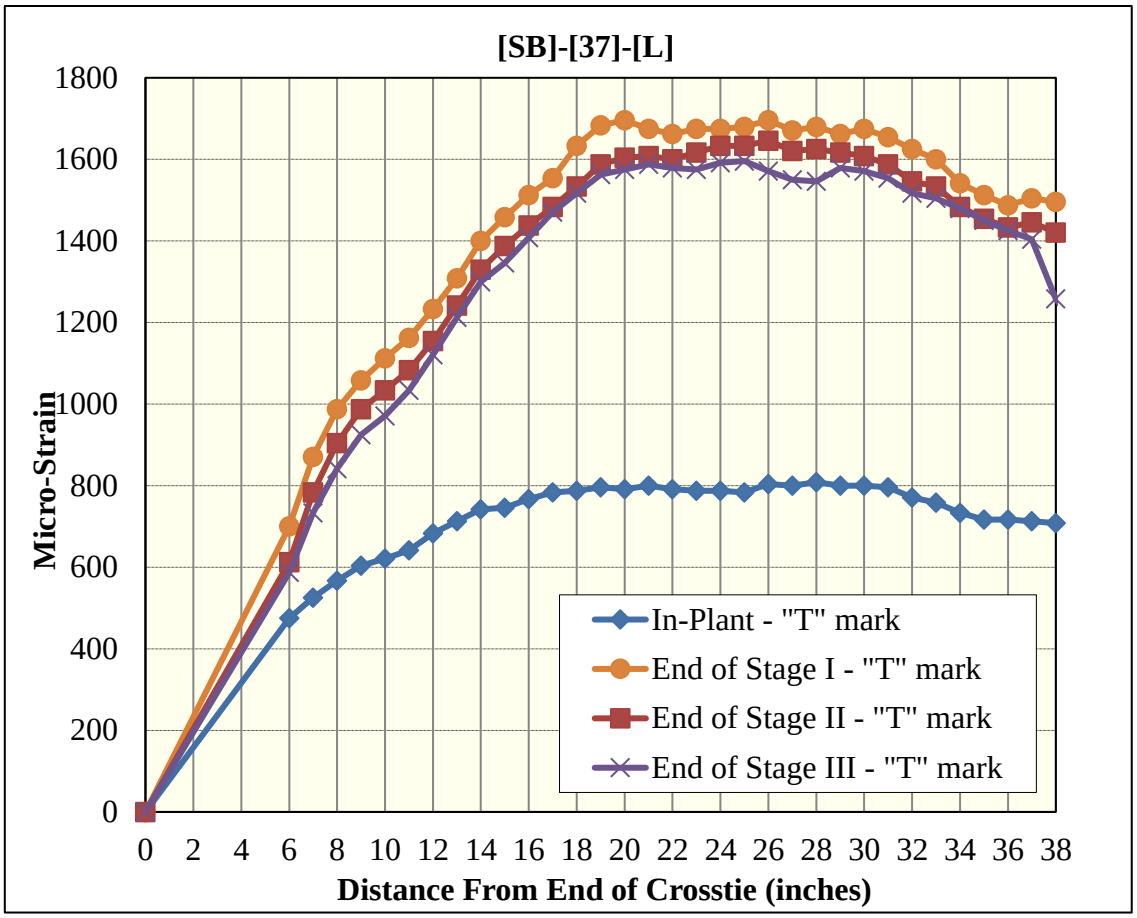

Figure 239 Surface-strain profiles for [SB]-[37]-[L] (Whittemore gage)

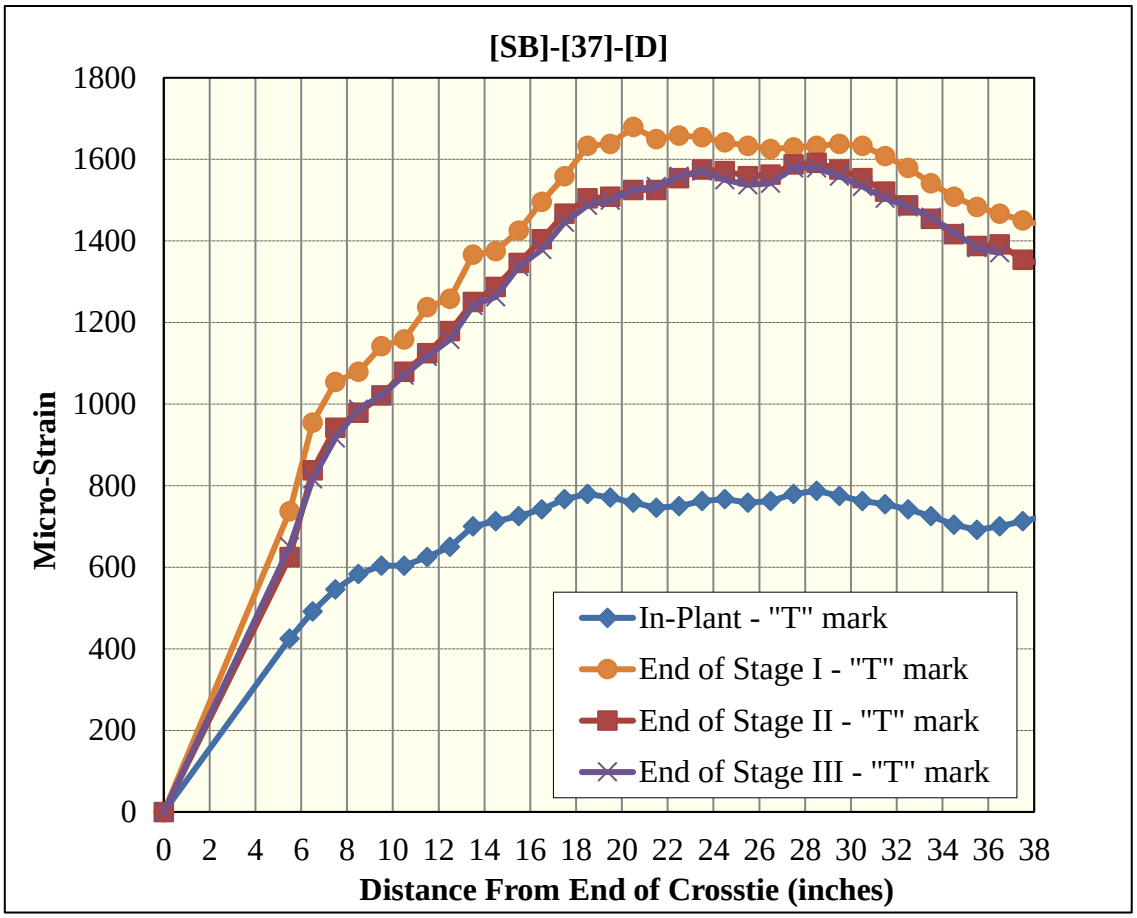

Figure 240 Surface-strain profiles for [SB]-[37]-[D] (Whittemore gage)

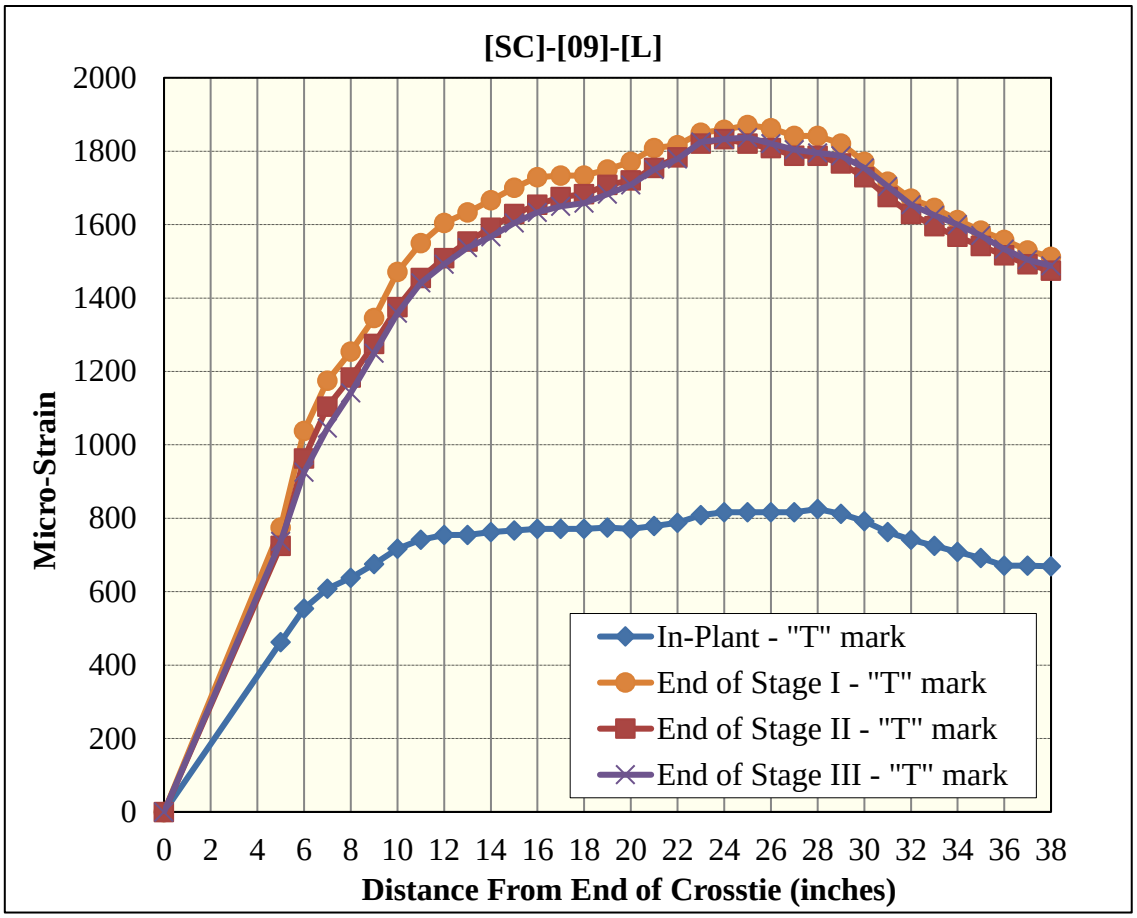

Figure 241 Surface-strain profiles for [SC]-[09]-[L] (Whittemore gage)

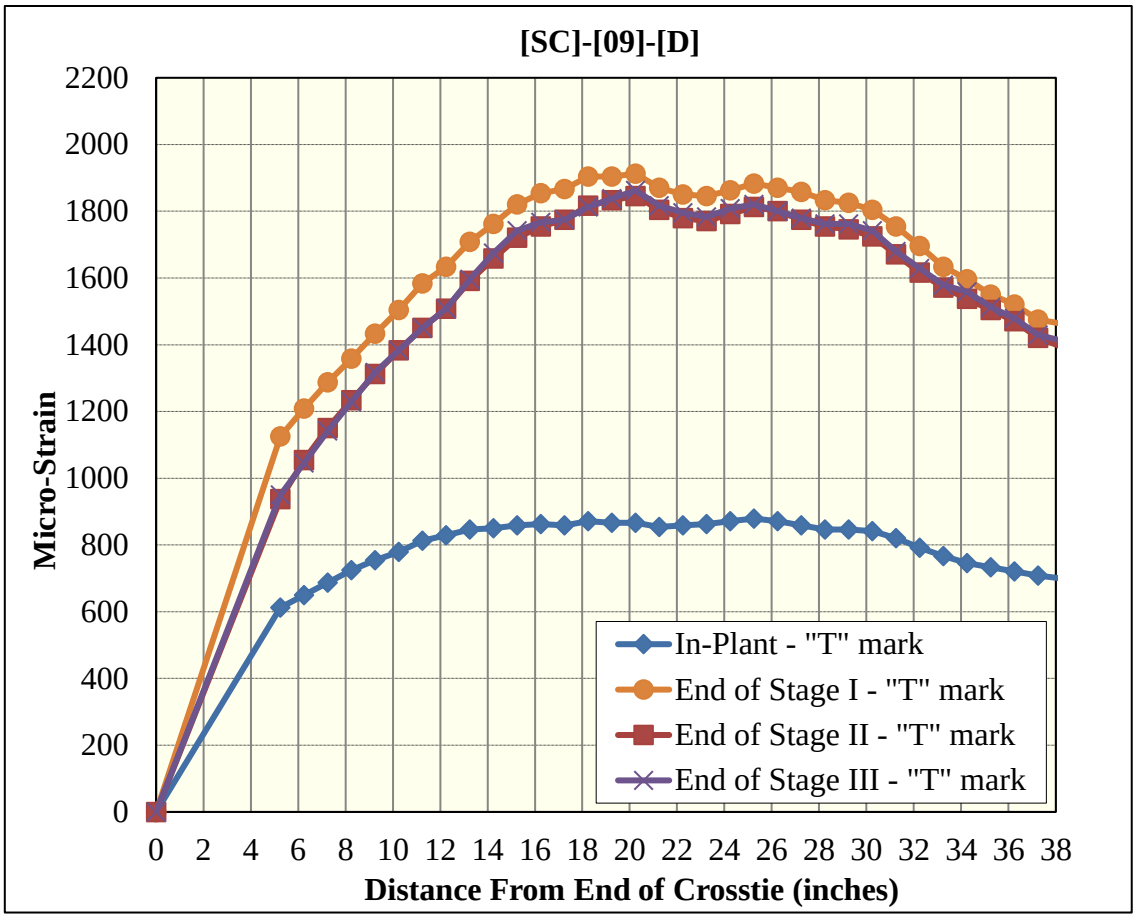

Figure 242 Surface-strain profiles for [SC]-[09]-[D] (Whittemore gage)

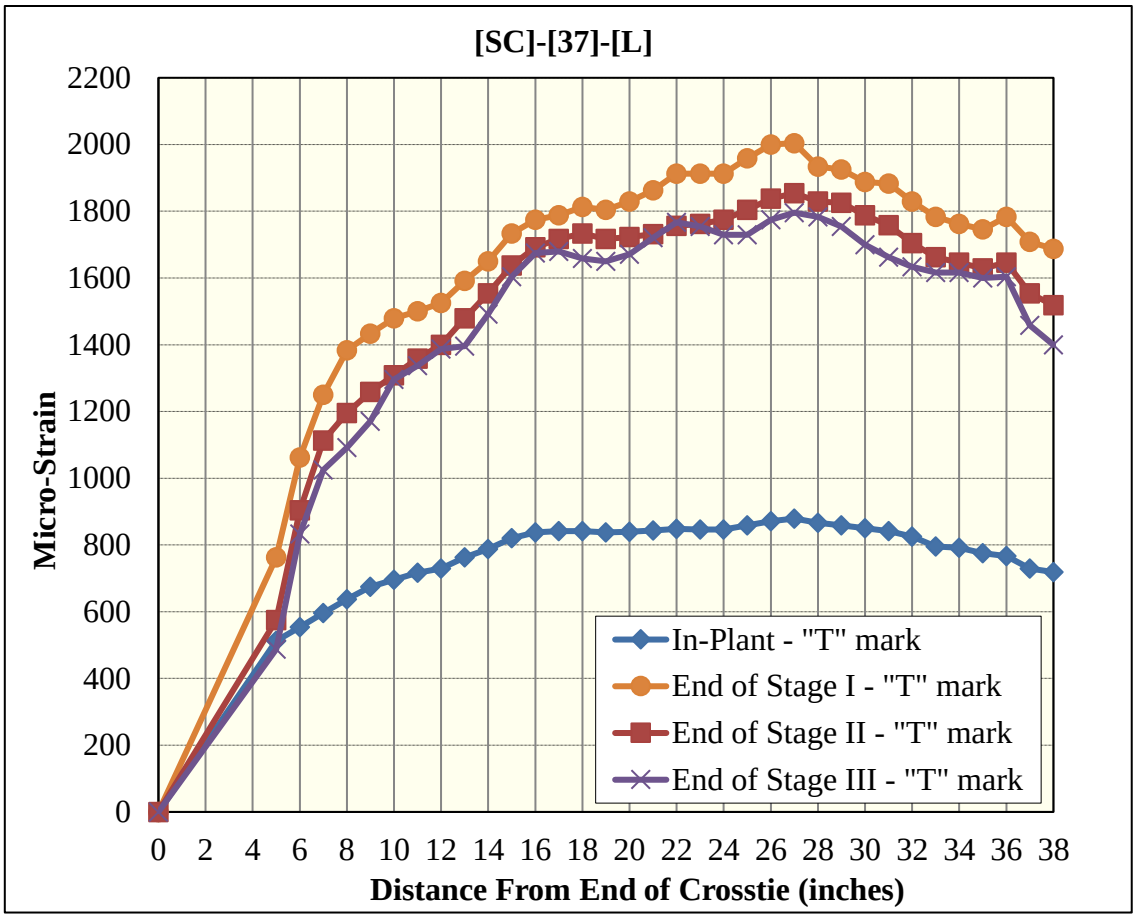

Figure 243 Surface-strain profiles for [SC]-[37]-[L] (Whittemore gage)

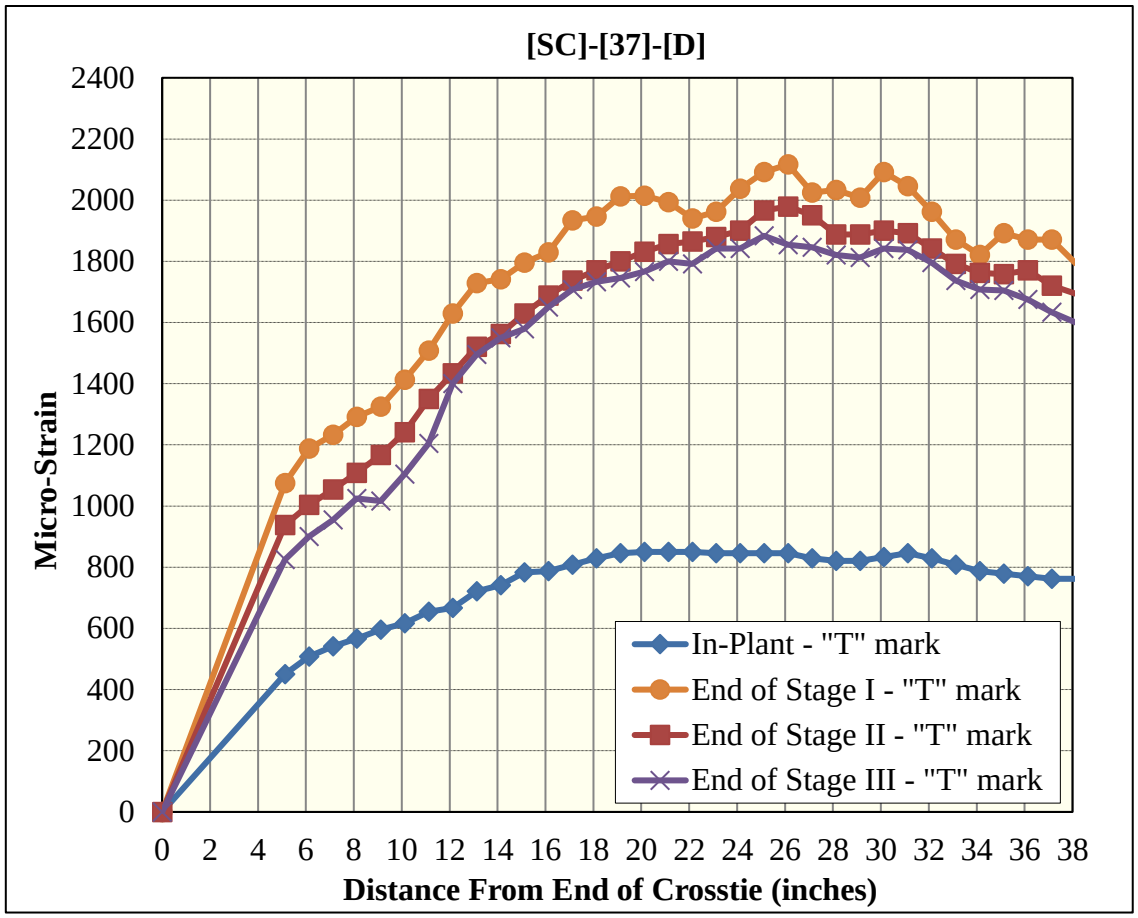

Figure 244 Surface-strain profiles for [SC]-[37]-[D] (Whittemore gage)

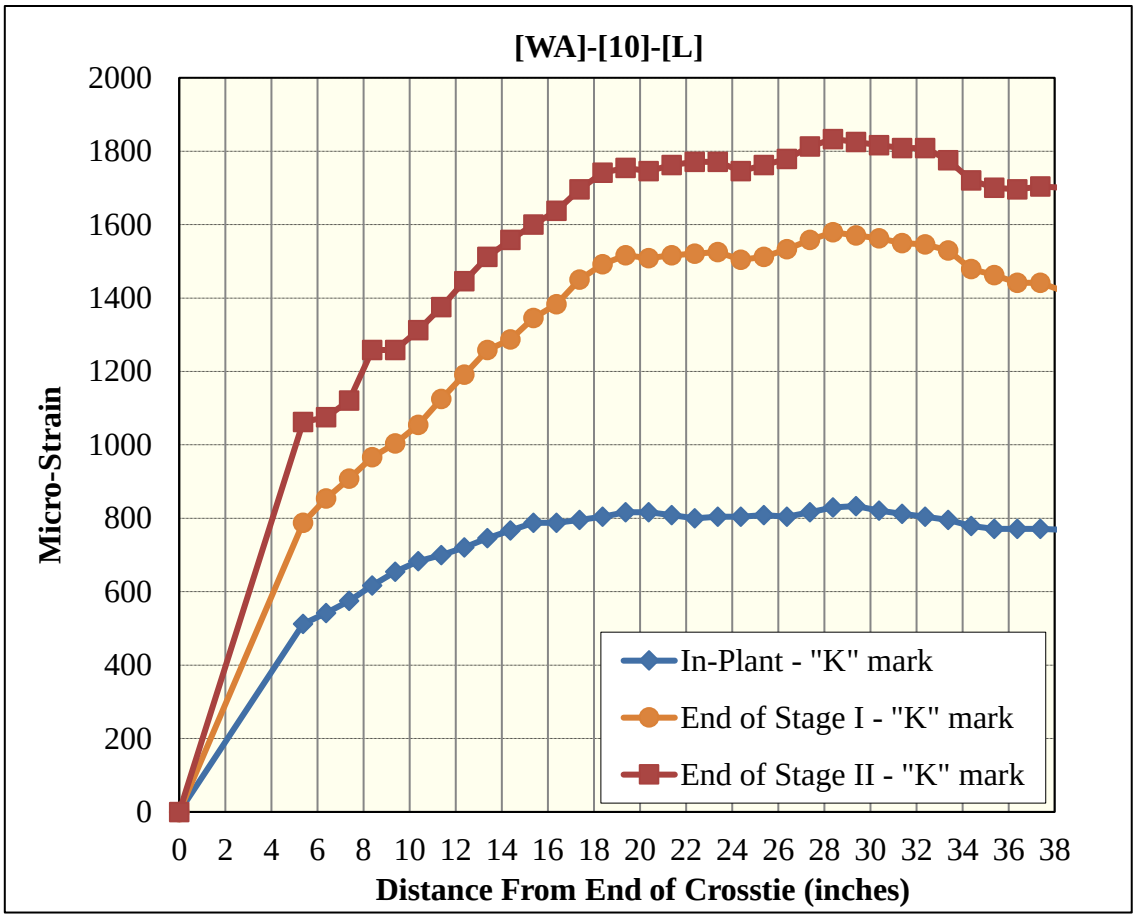

Figure 245 Surface-strain profiles for [WA]-[10]-[L] (Whittemore gage)

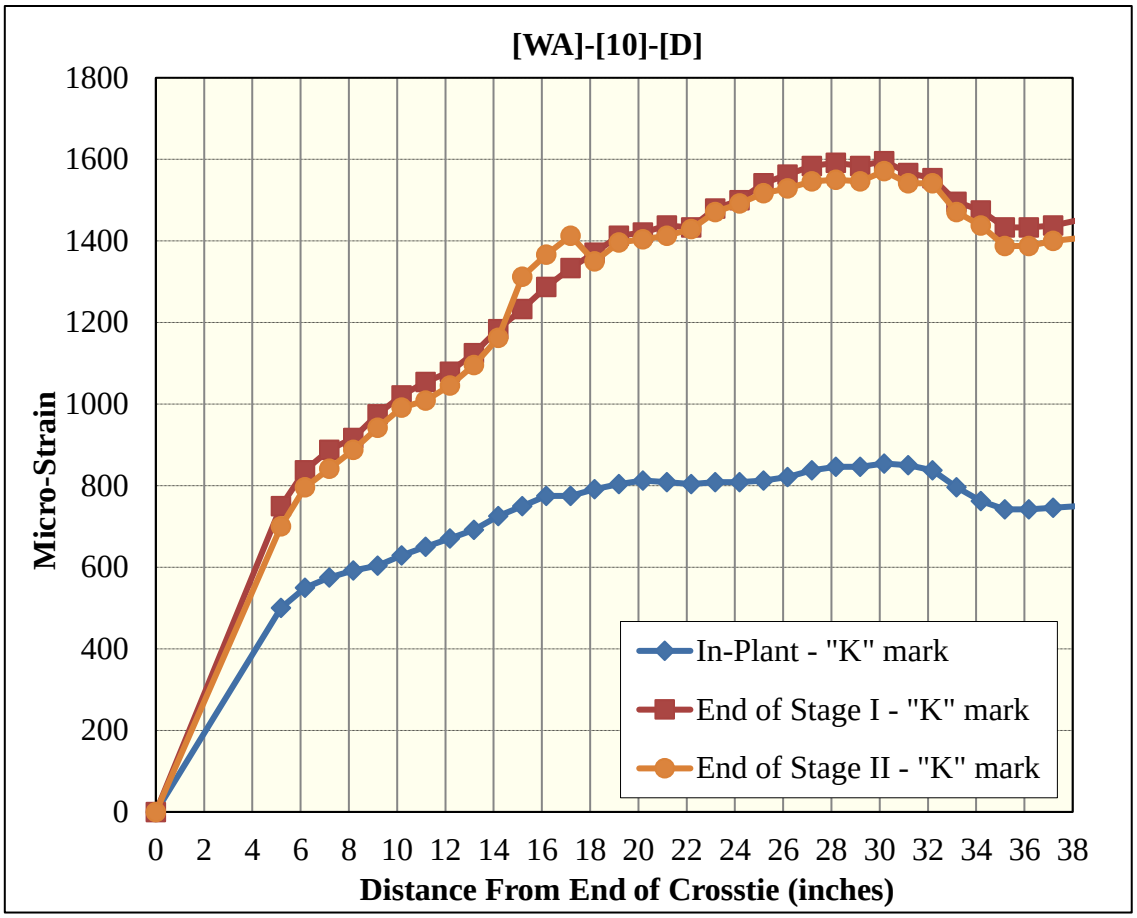

Figure 246 Surface-strain profiles for [WA]-[10]-[D] (Whittemore gage)

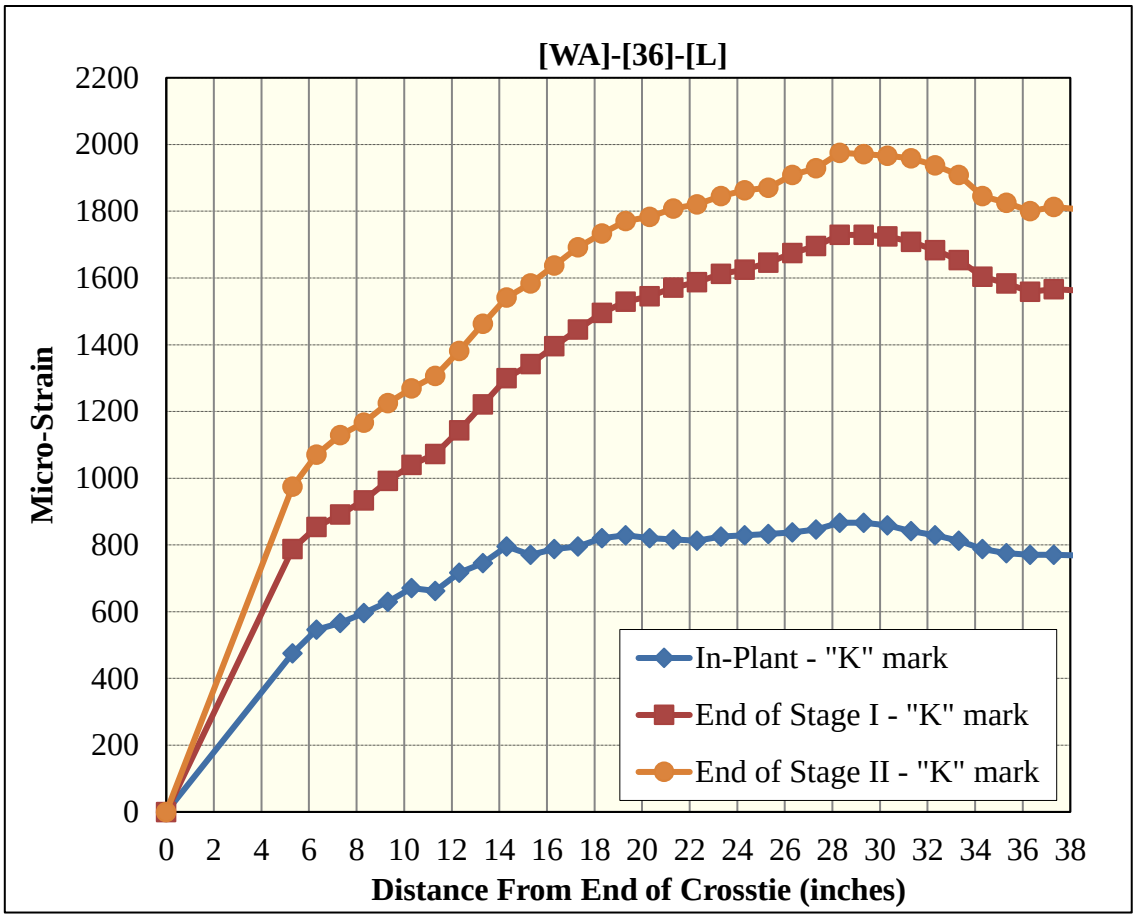

Figure 247 Surface-strain profiles for [WA]-[36]-[L] (Whittemore gage)

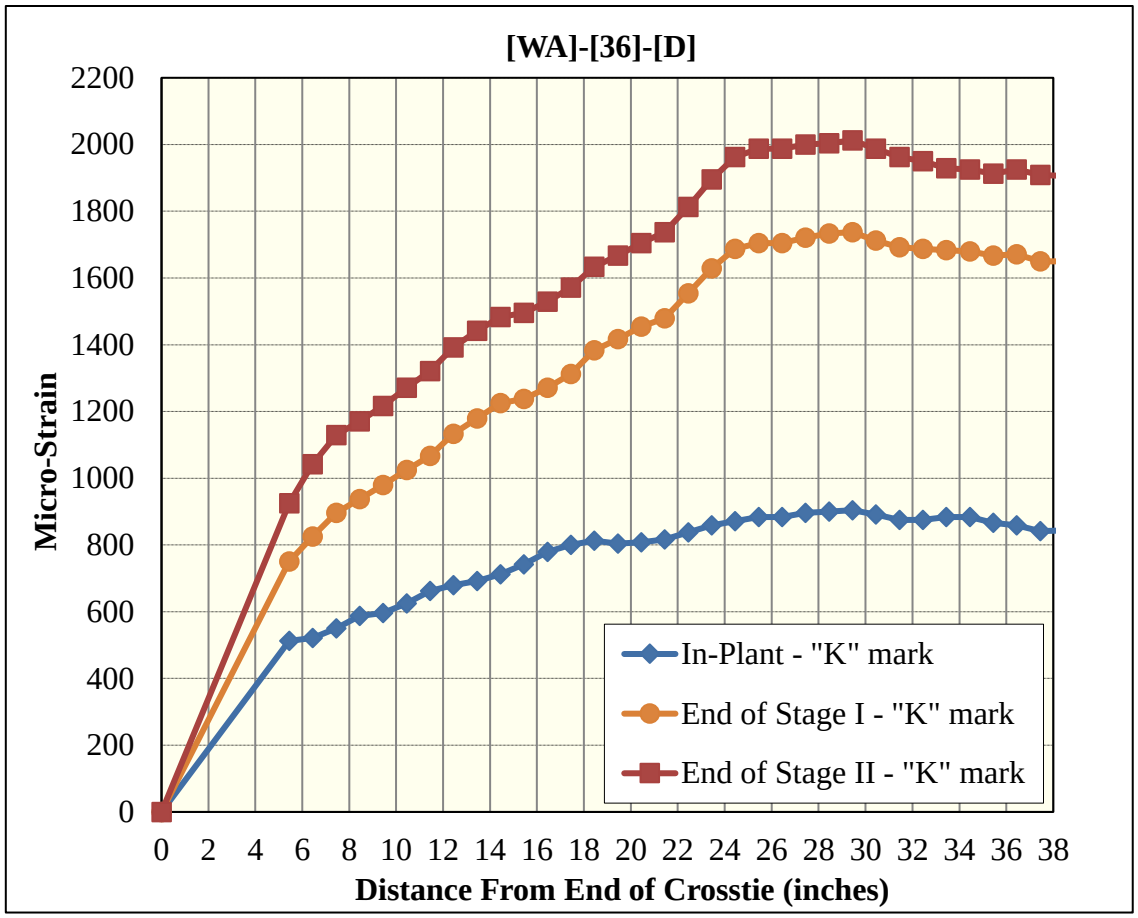

Figure 248 Surface-strain profiles for [WA]-[36]-[D] (Whittemore gage)

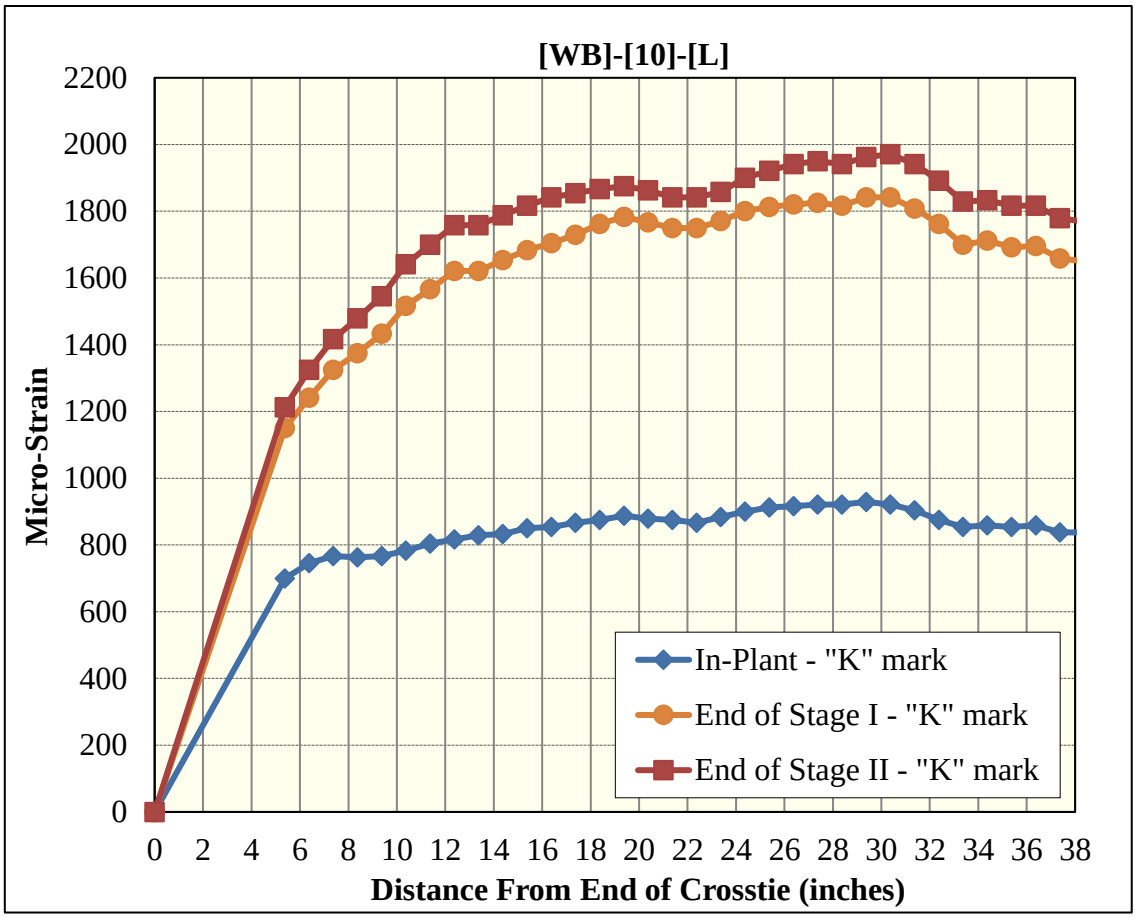

Figure 249 Surface-strain profiles for [WB]-[10]-[L] (Whittemore gage)

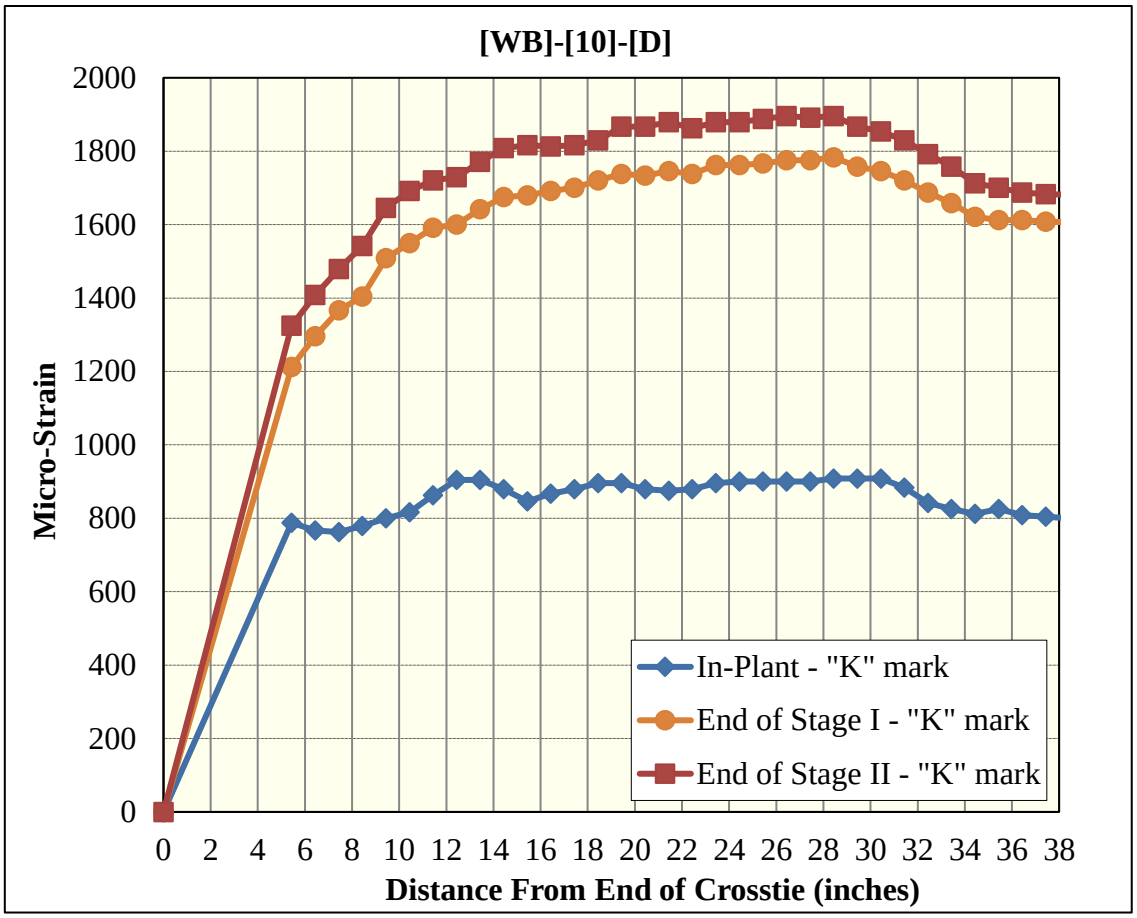

Figure 250 Surface-strain profiles for [WB]-[10]-[D] (Whittemore gage)

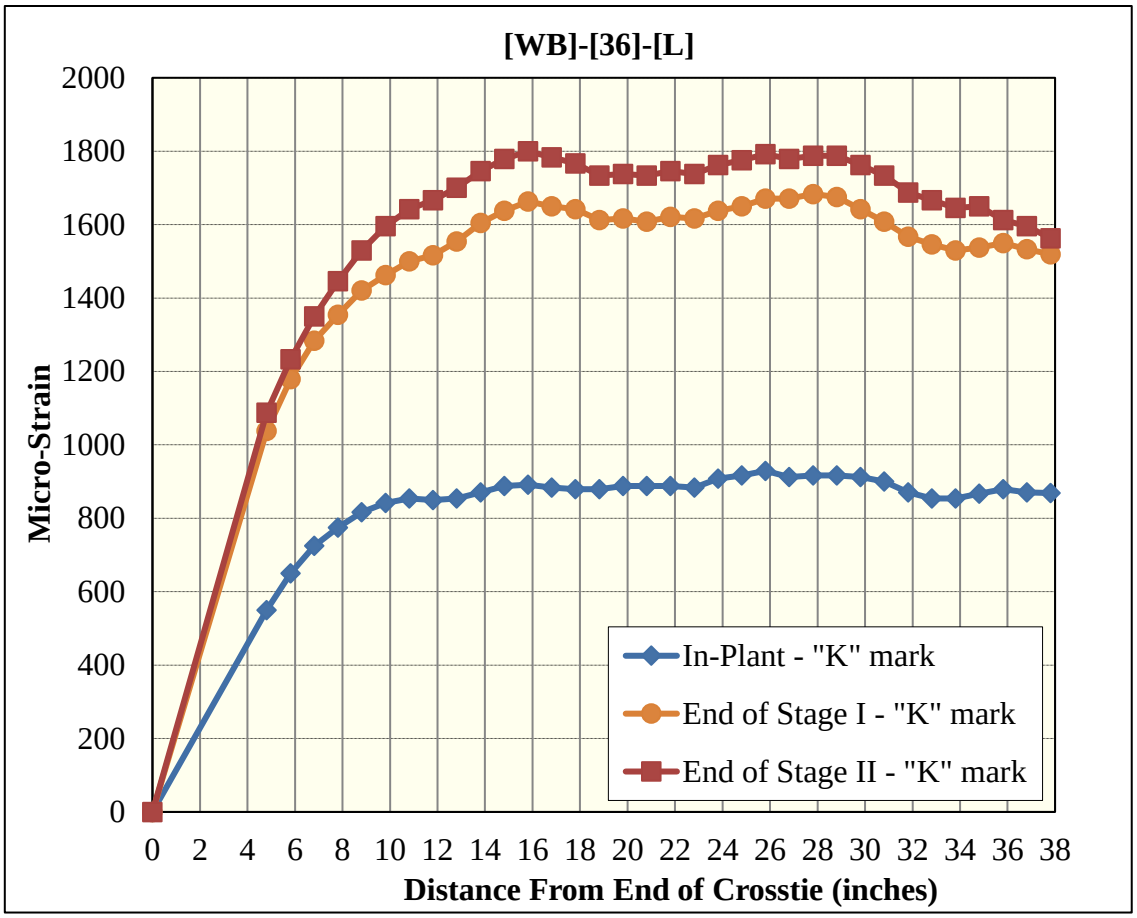

Figure 251 Surface-strain profiles for [WB]-[36]-[L] (Whittemore gage)

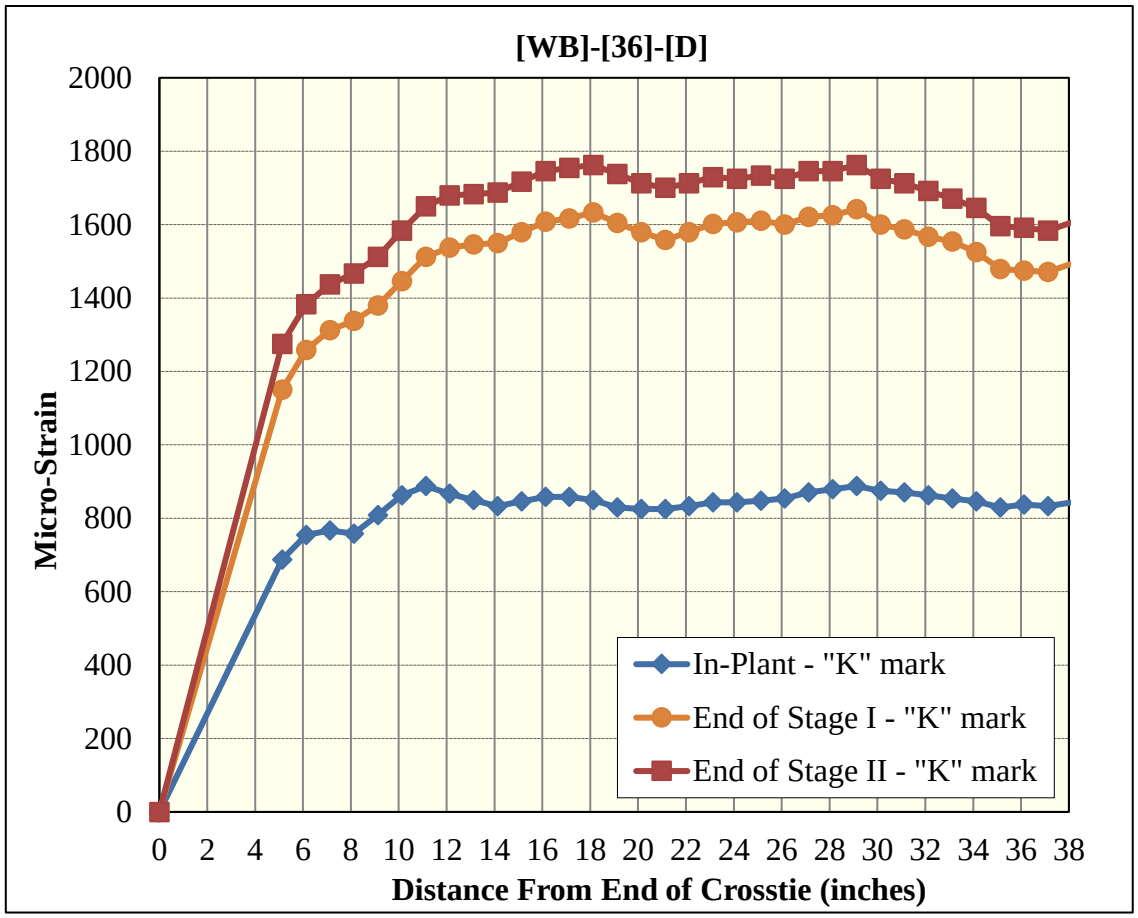

Figure 252 Surface-strain profiles for [WB]-[36]-[D] (Whittemore gage)

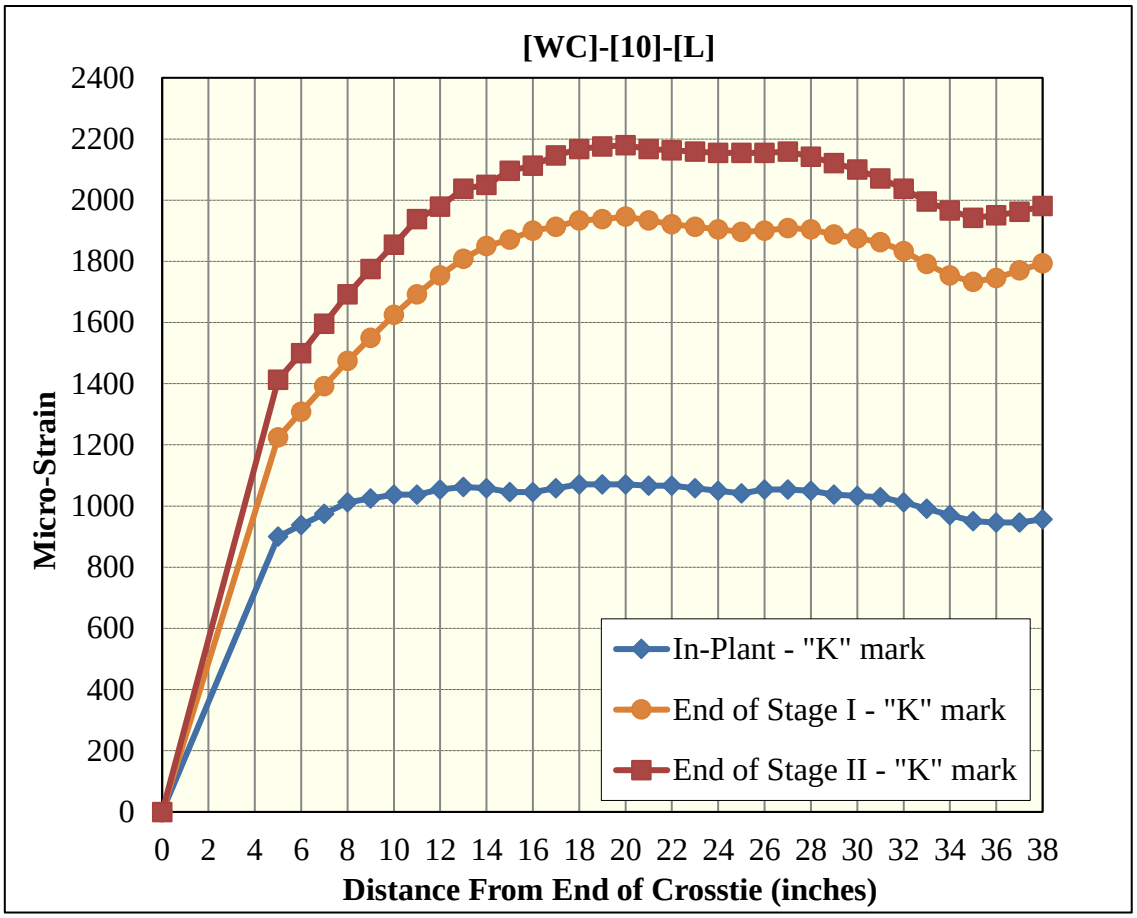

Figure 253 Surface-strain profiles for [WC]-[10]-[L] (Whittemore gage)

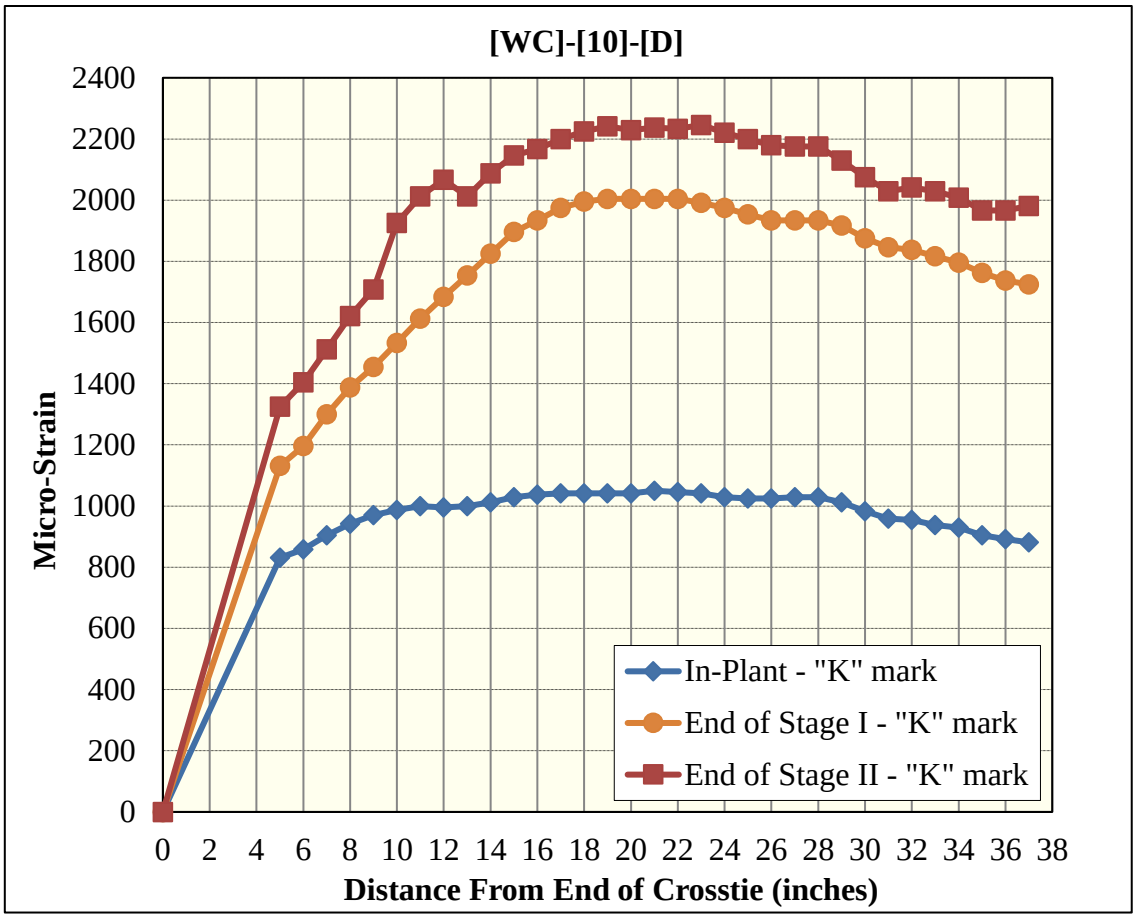

Figure 254 Surface-strain profiles for [WC]-[10]-[D] (Whittemore gage)

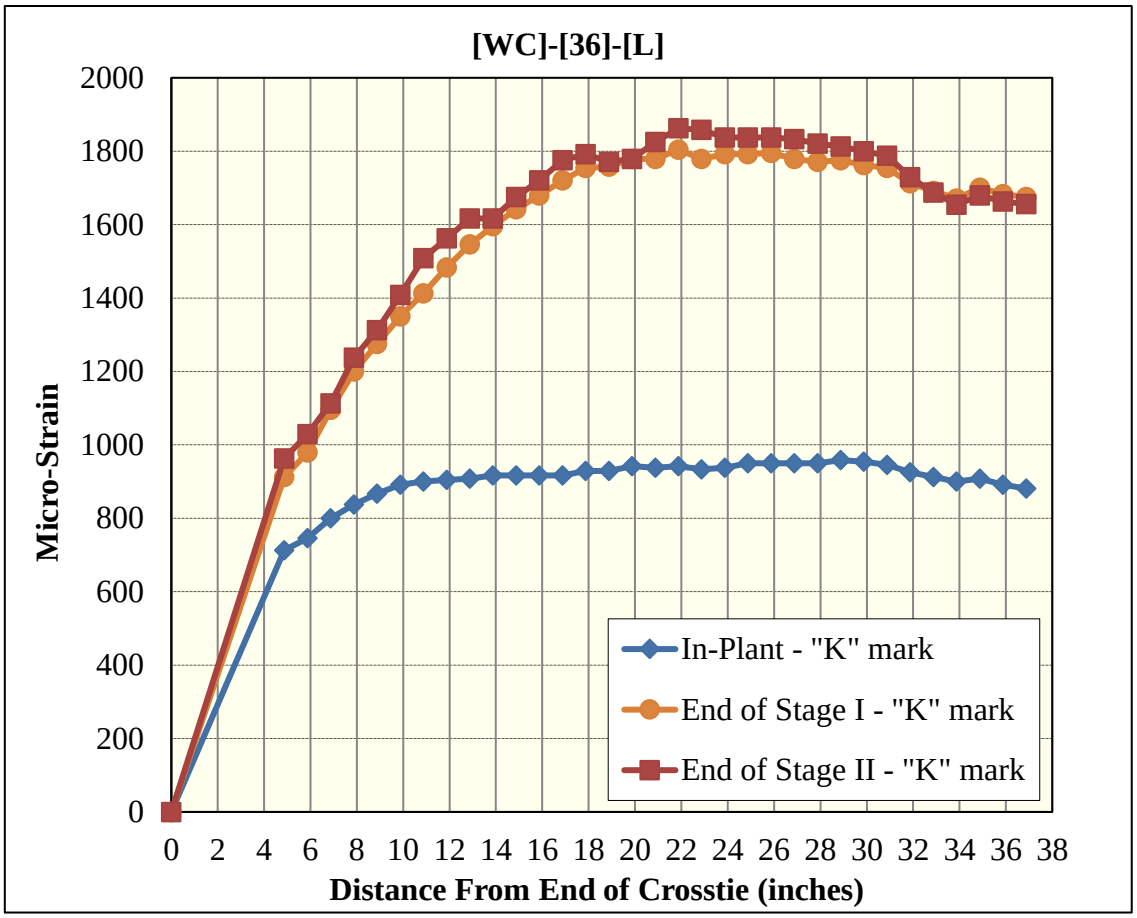

Figure 255 Surface-strain profiles for [WC]-[36]-[L] (Whittemore gage)

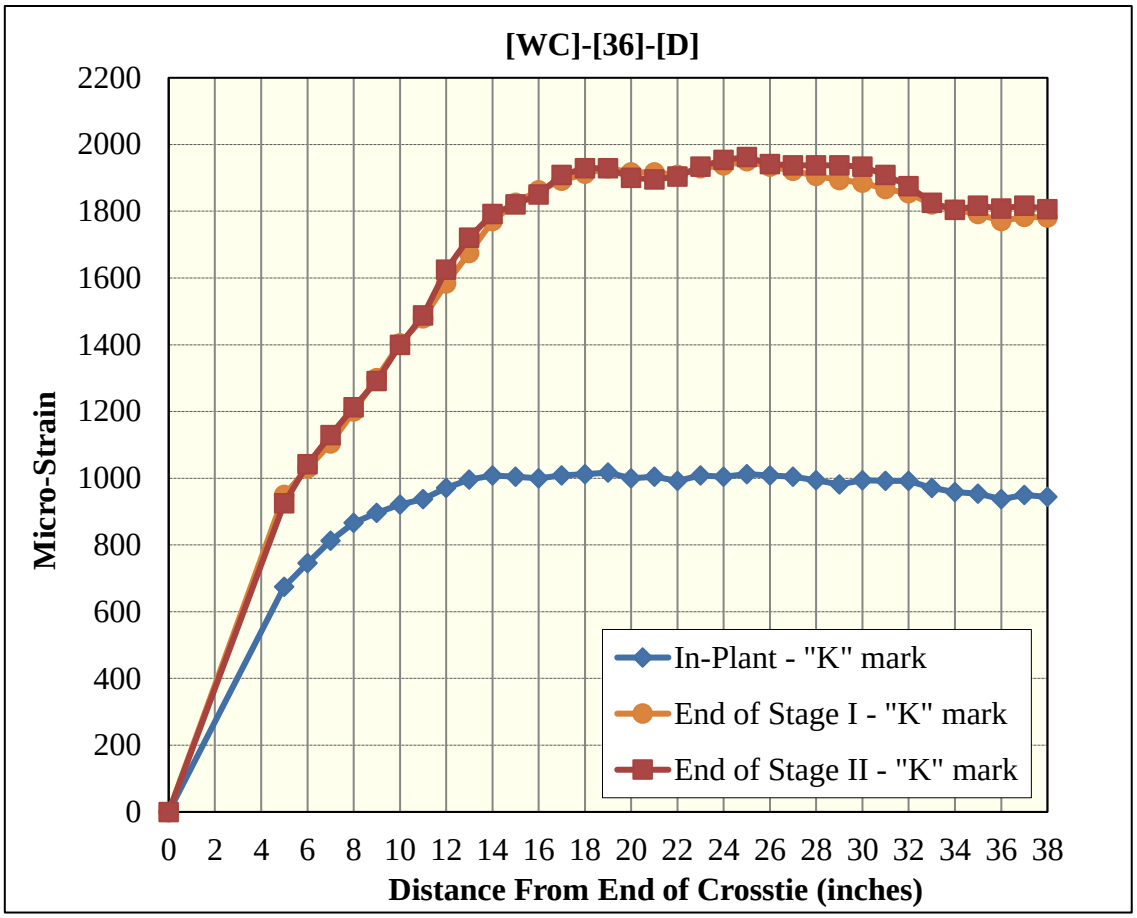

Figure 256 Surface-strain profiles for [WC]-[36]-[D] (Whittemore gage)

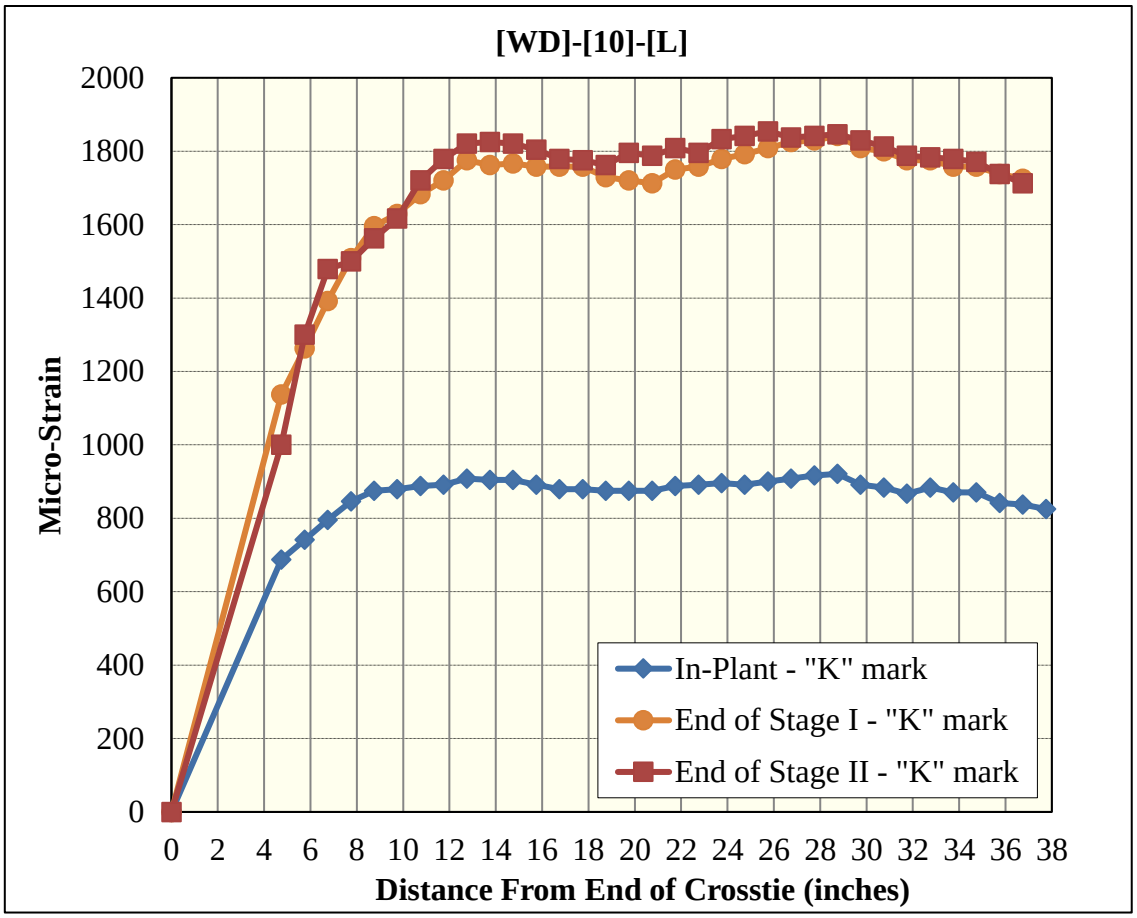

Figure 257 Surface-strain profiles for [WD]-[10]-[L] (Whittemore gage)

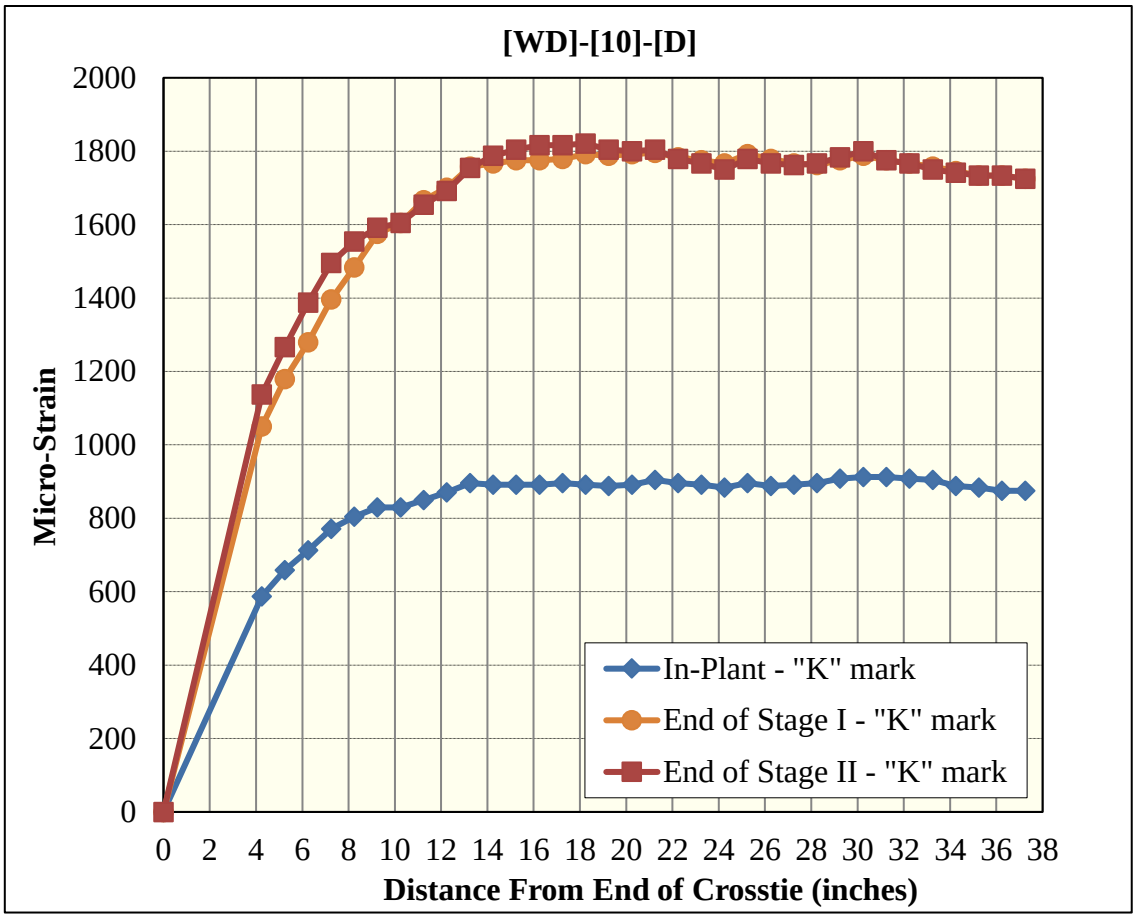

Figure 258 Surface-strain profiles for [WD]-[10]-[D] (Whittemore gage)

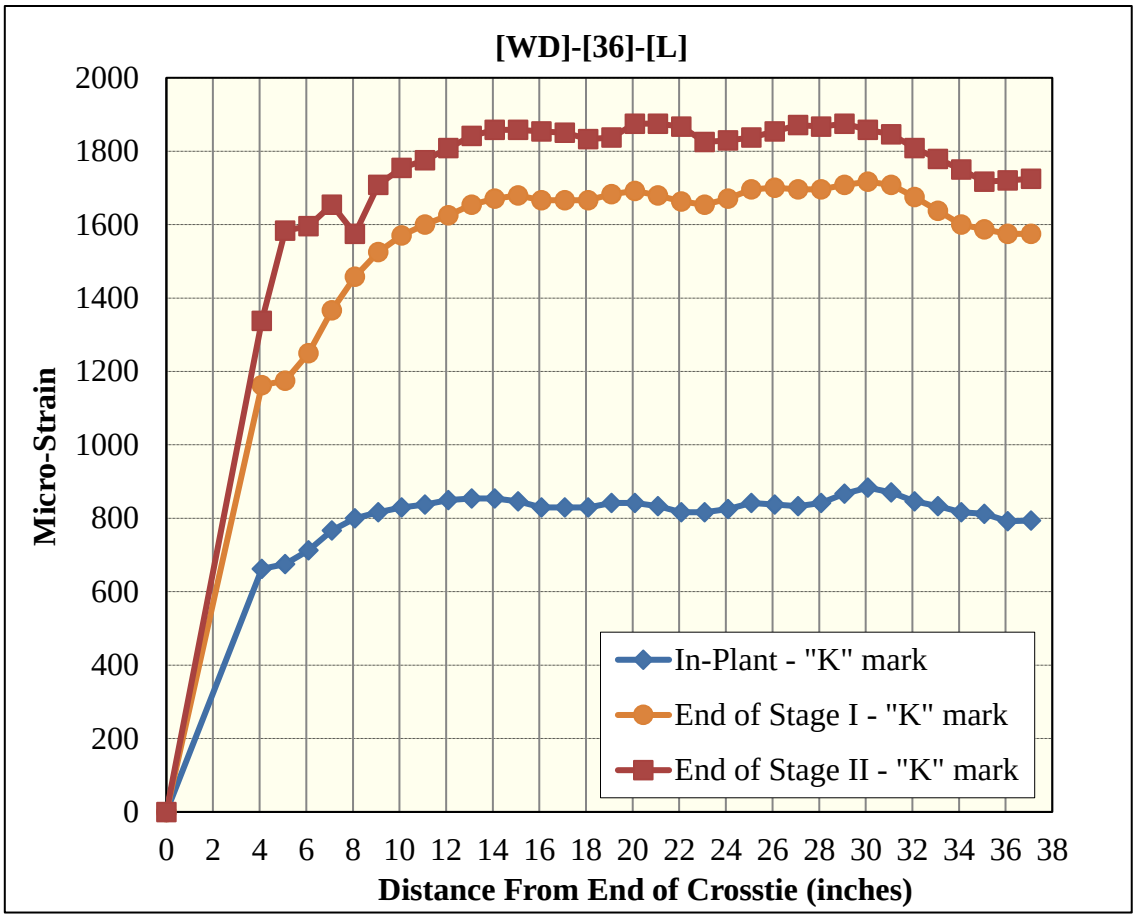

Figure 259 Surface-strain profiles for [WD]-[36]-[L] (Whittemore gage)

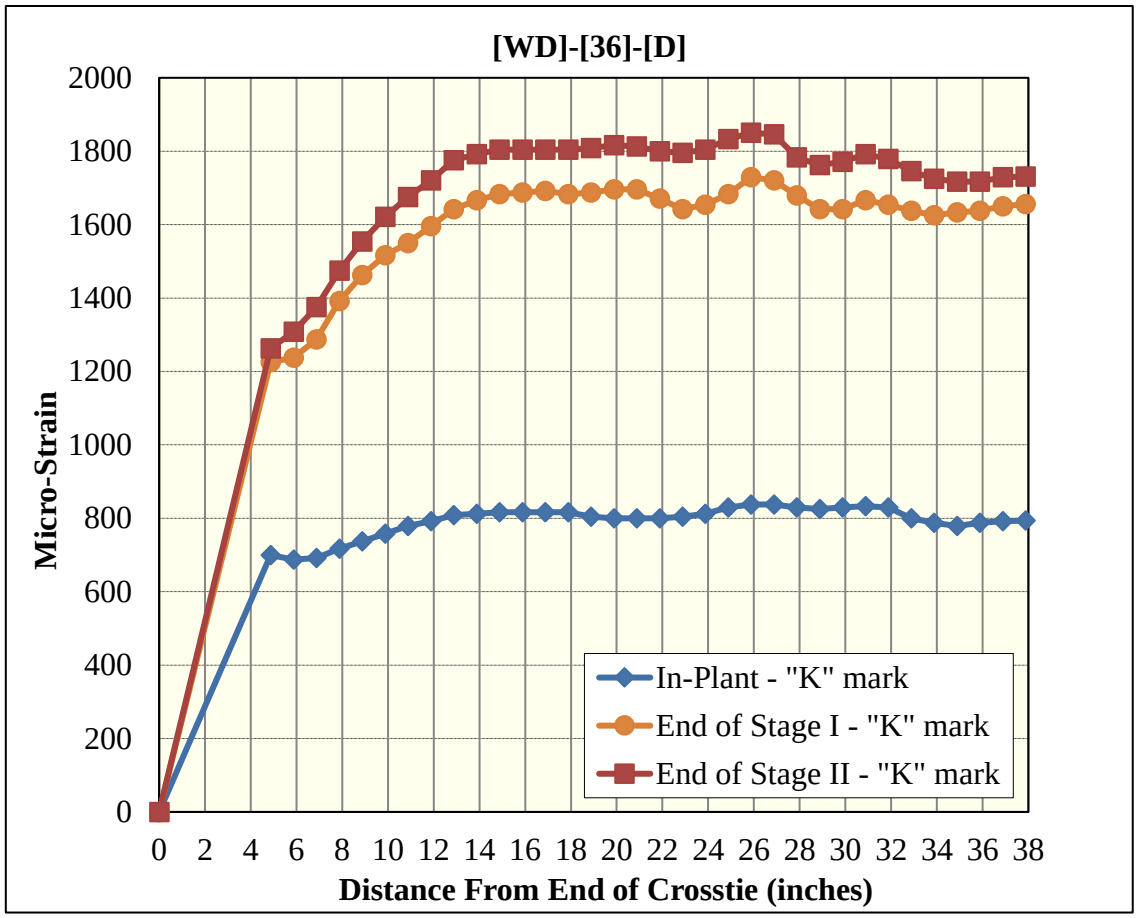

Figure 260 Surface-strain profiles for [WD]-[36]-[D] (Whittemore gage)

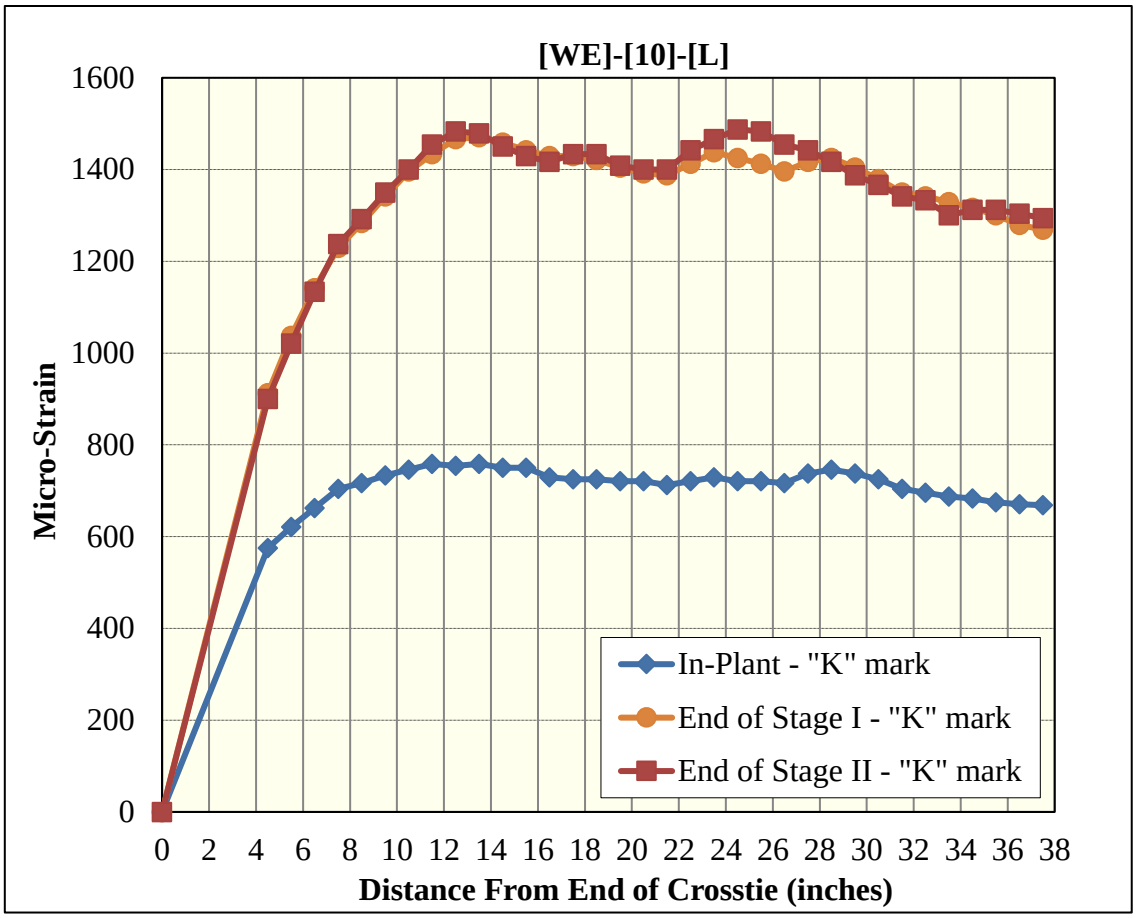

Figure 261 Surface-strain profiles for [WE]-[10]-[L] (Whittemore gage)

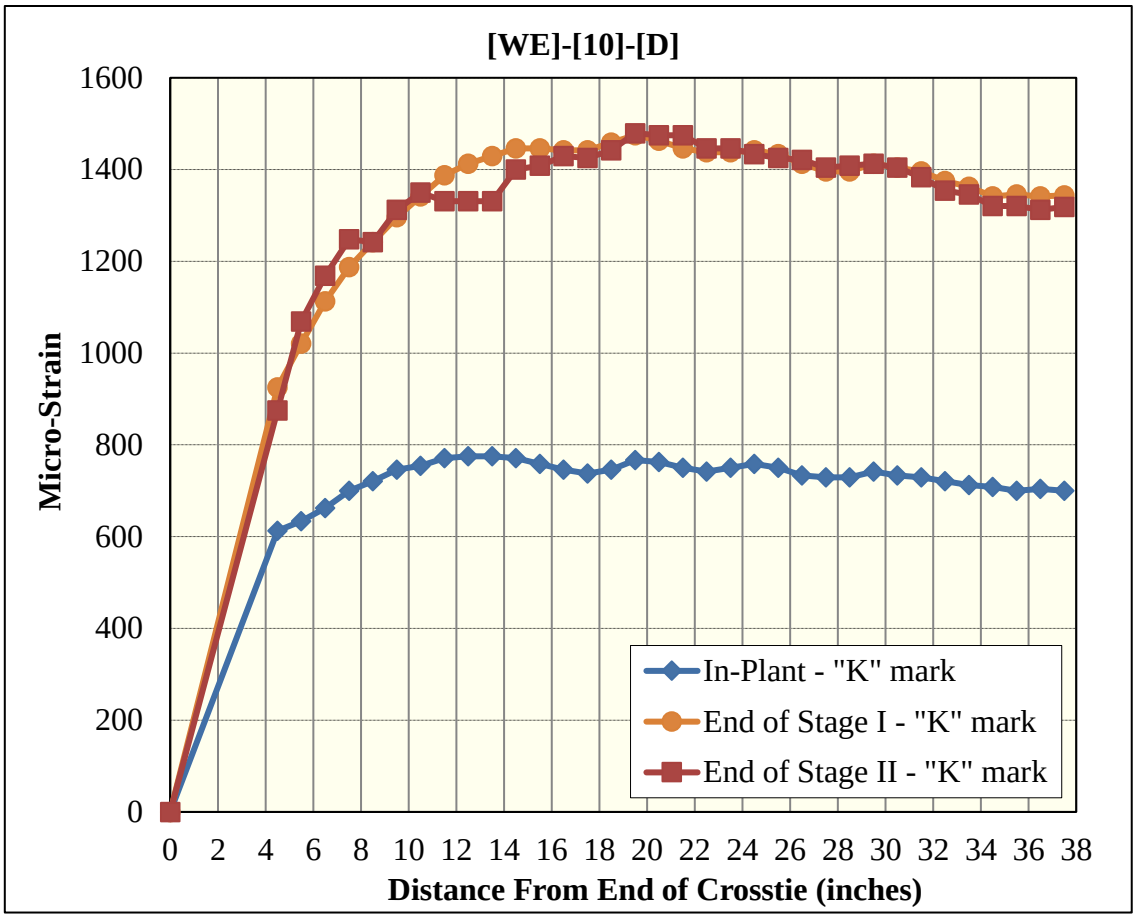

Figure 262 Surface-strain profiles for [WE]-[10]-[D] (Whittemore gage)

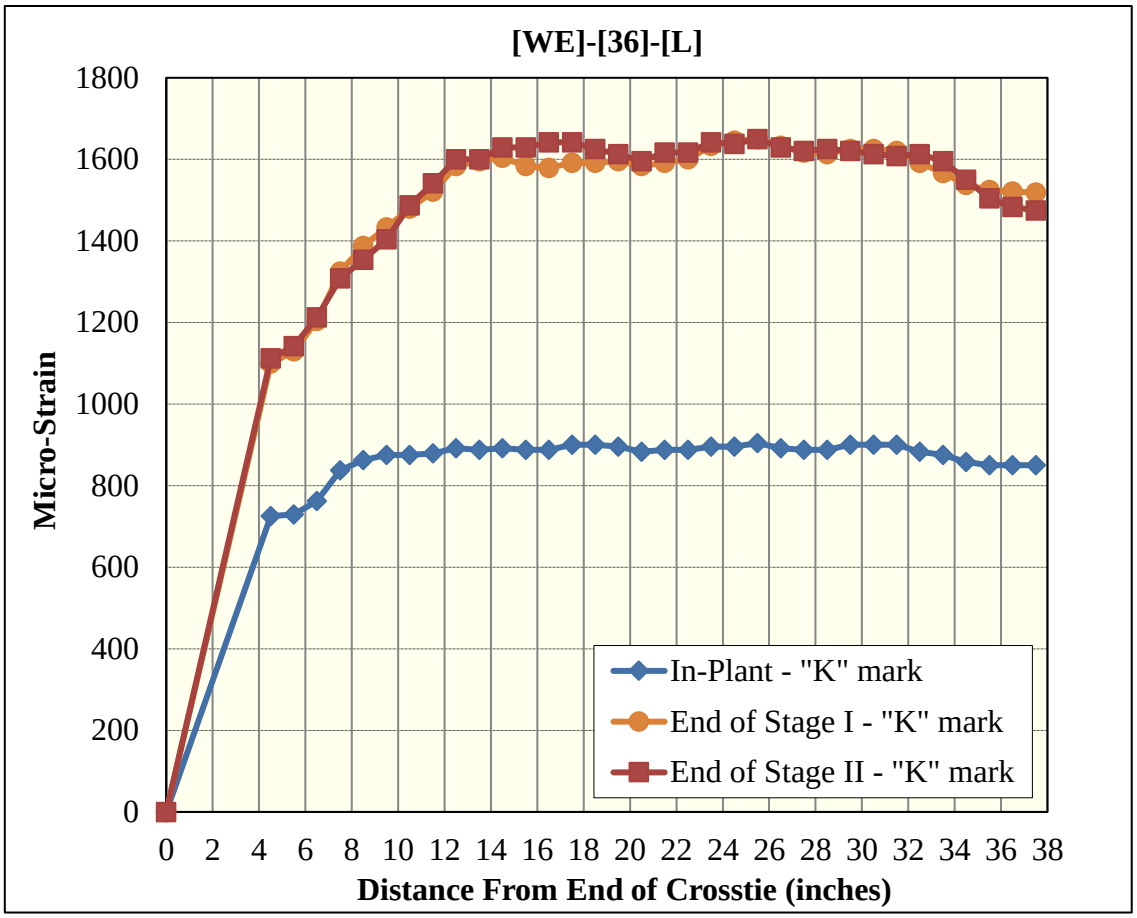

Figure 263 Surface-strain profiles for [WE]-[36]-[L] (Whittemore gage)

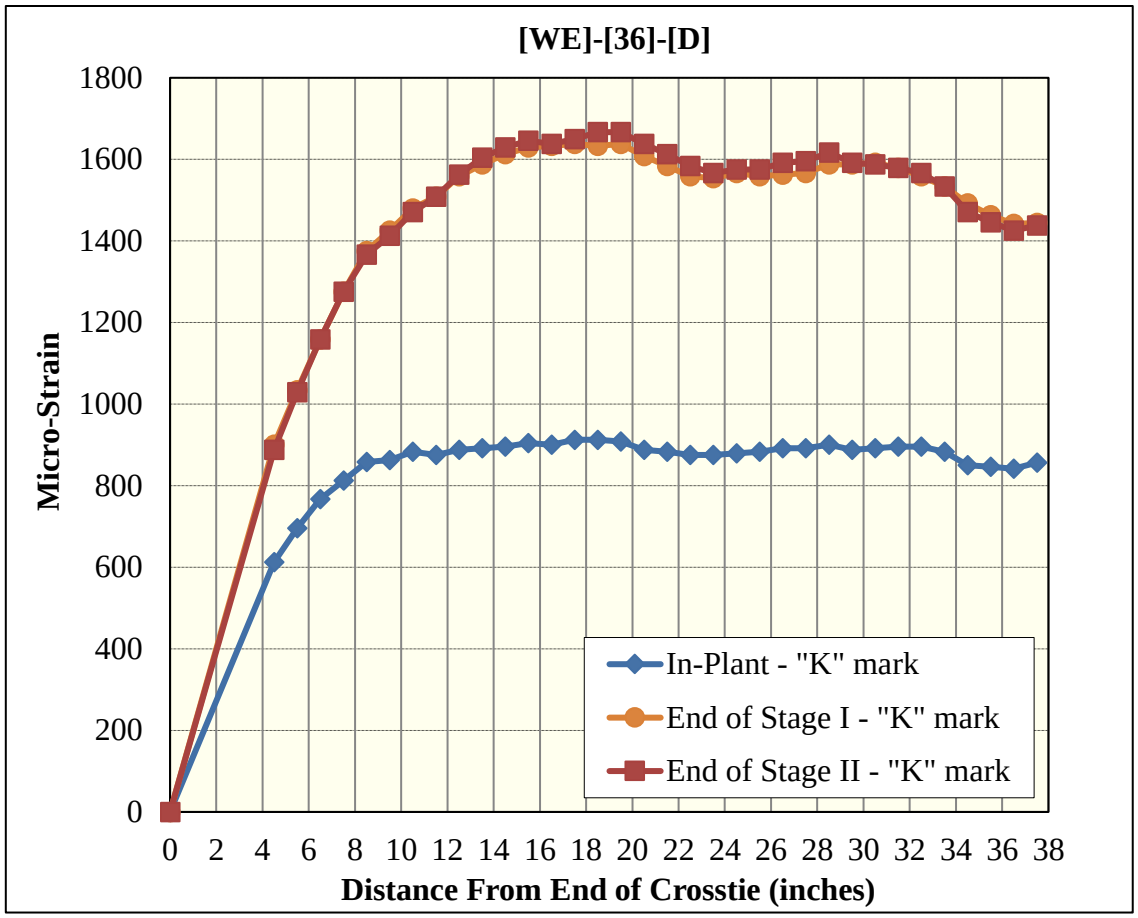

Figure 264 Surface-strain profiles for [WE]-[36]-[D] (Whittemore gage)

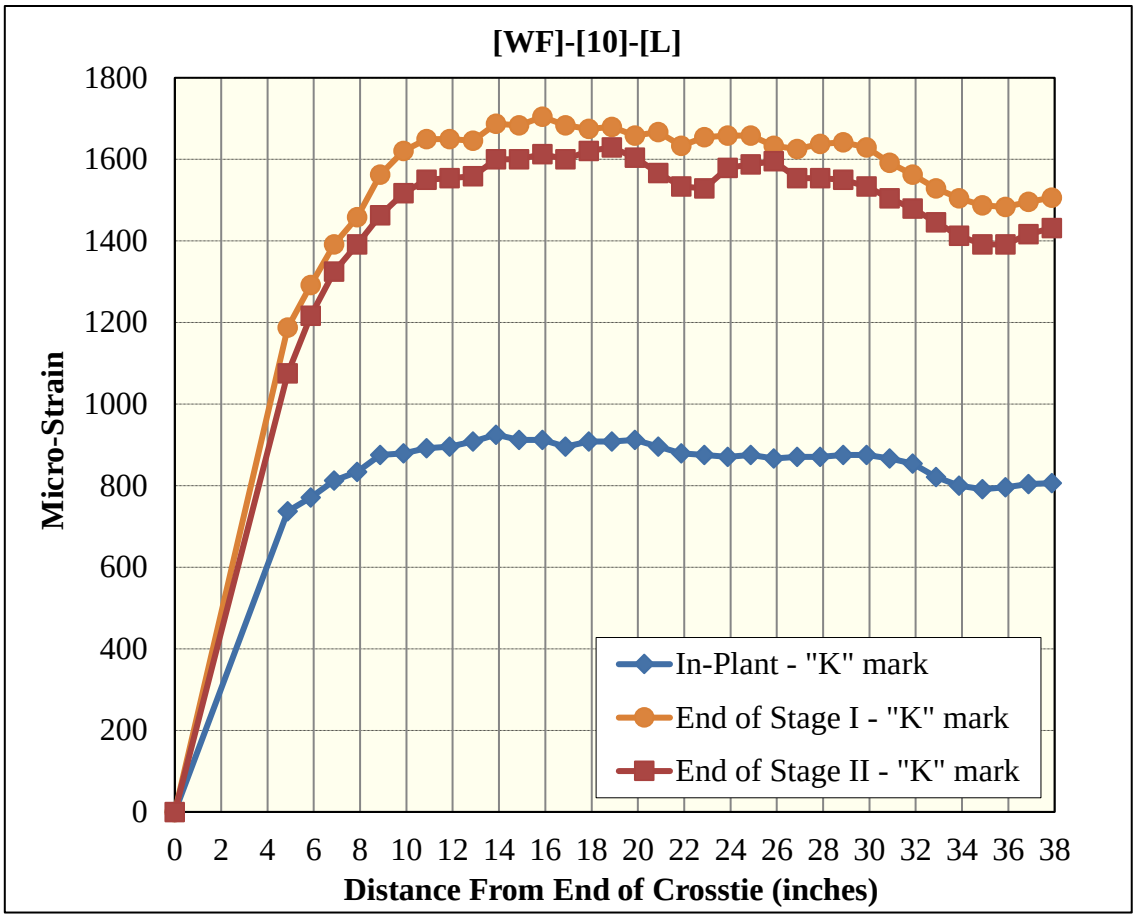

Figure 265 Surface-strain profiles for [WF]-[10]-[L] (Whittemore gage)

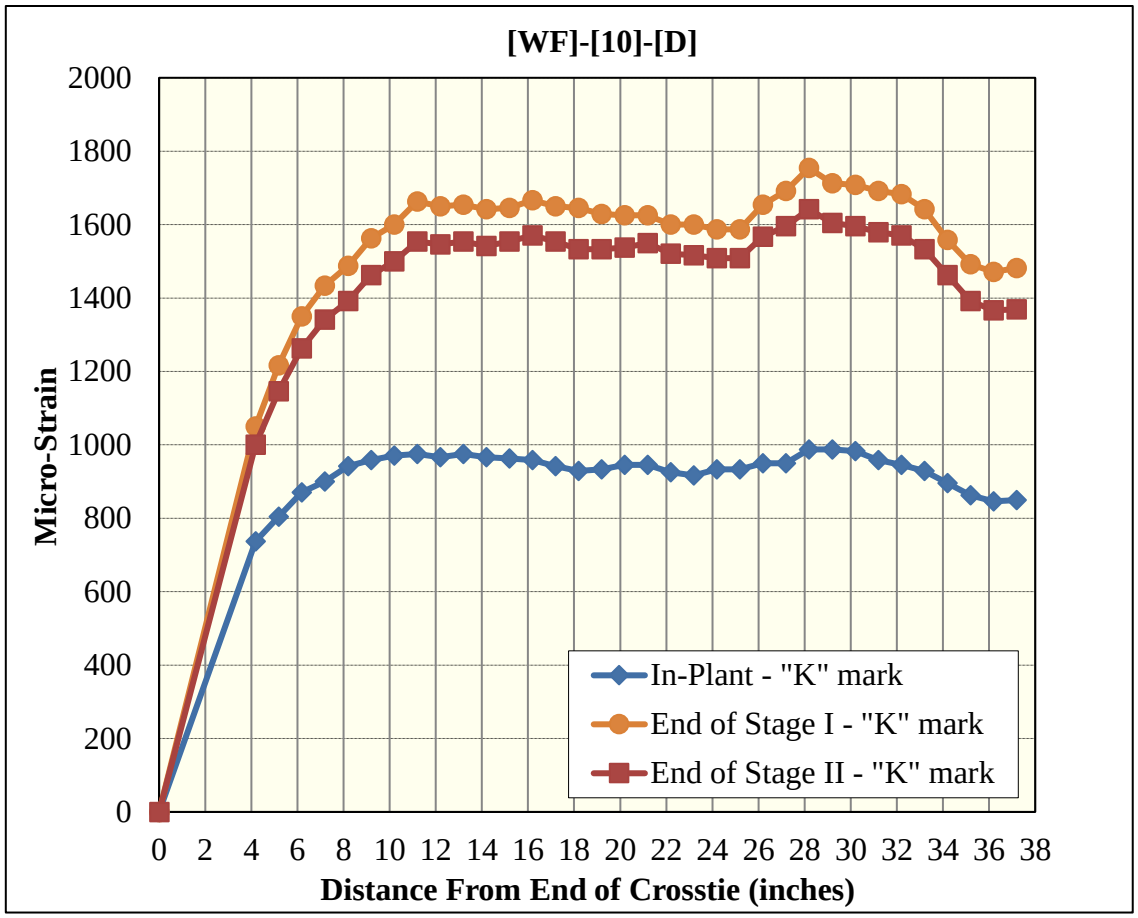

Figure 266 Surface-strain profiles for [WF]-[10]-[D] (Whittemore gage)

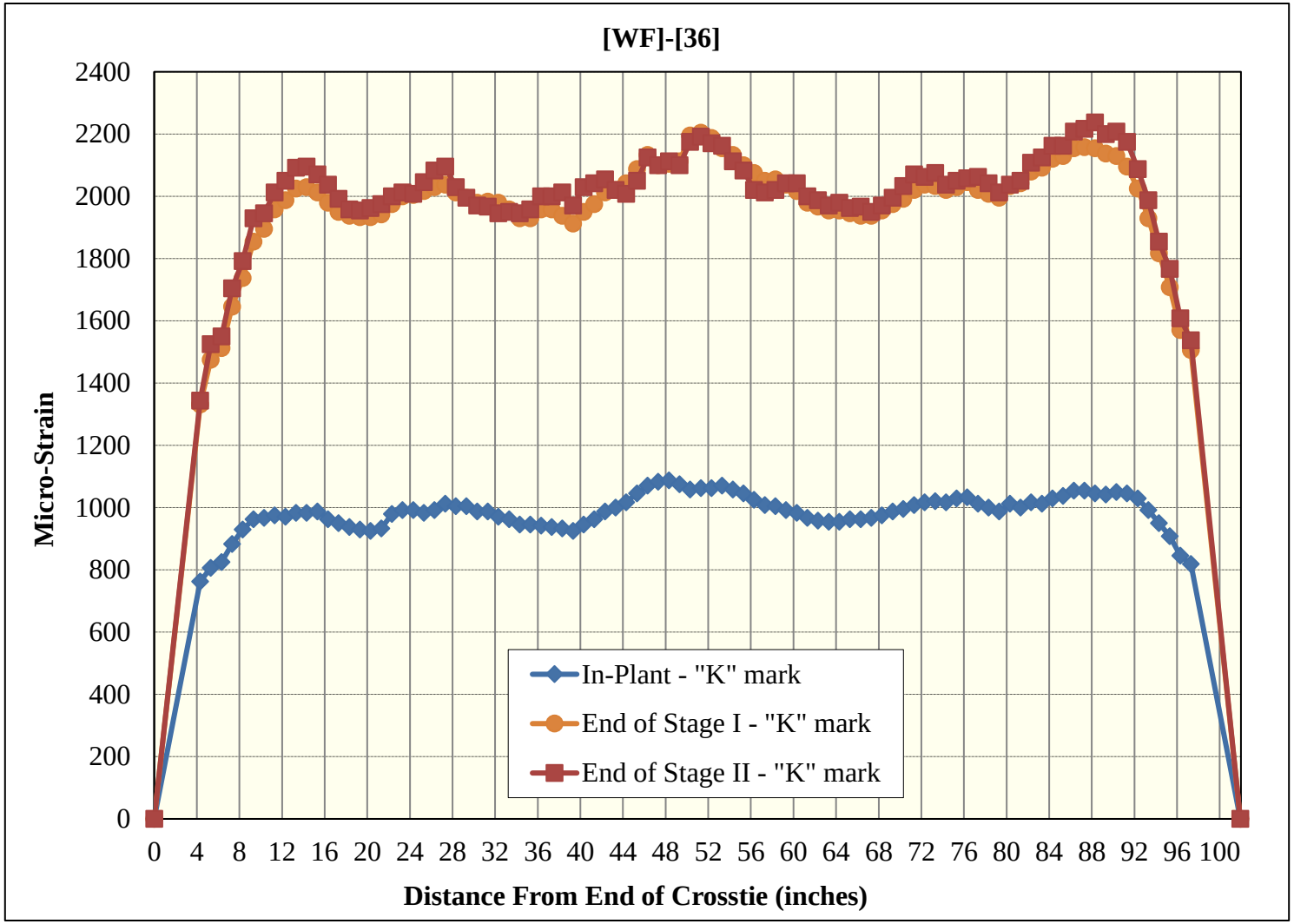

Figure 267 Surface-strain profiles for [WF]-[36] (Whittemore gage)

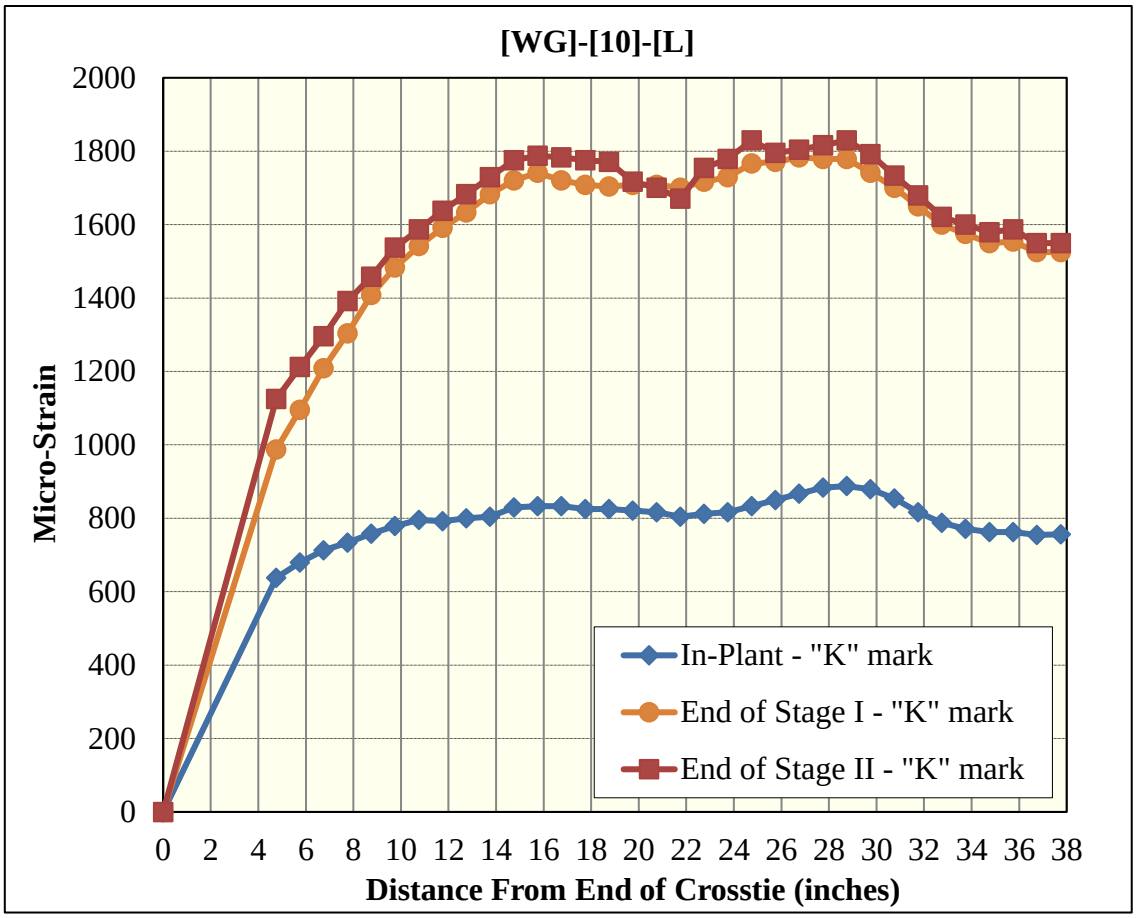

Figure 268 Surface-strain profiles for [WG]-[10]-[L] (Whittemore gage)

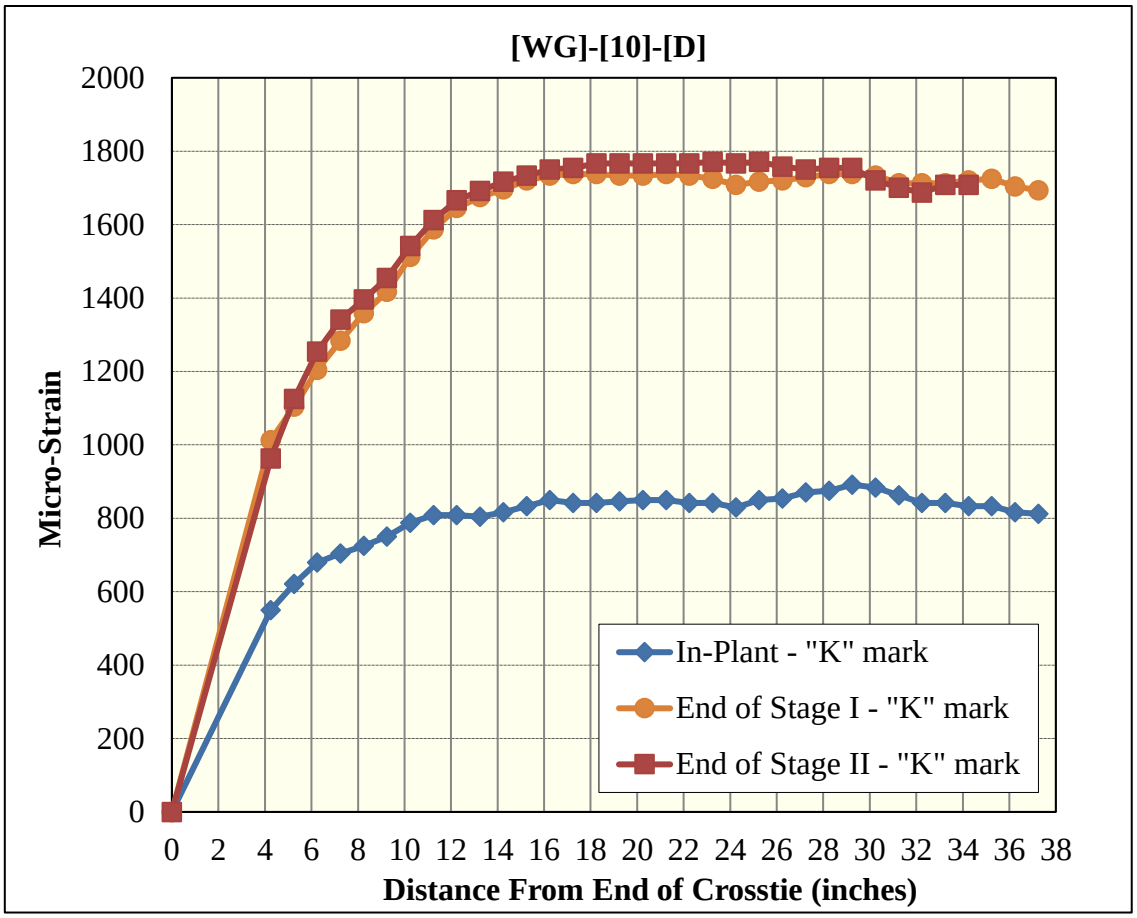

Figure 269 Surface-strain profiles for [WG]-[10]-[D] (Whittemore gage)

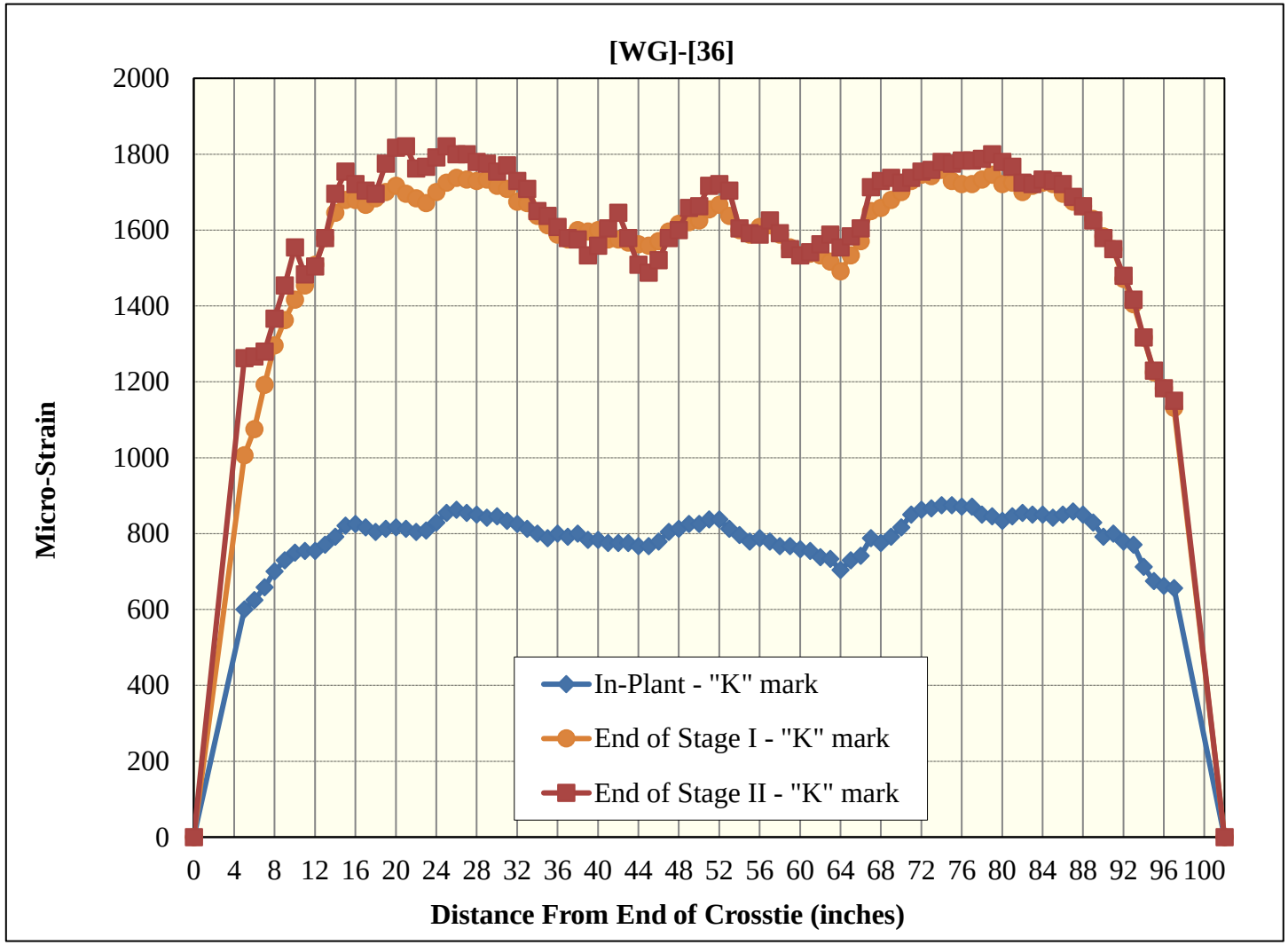

Figure 270 Surface-strain profiles for [WG]-[36] (Whittemore gage)

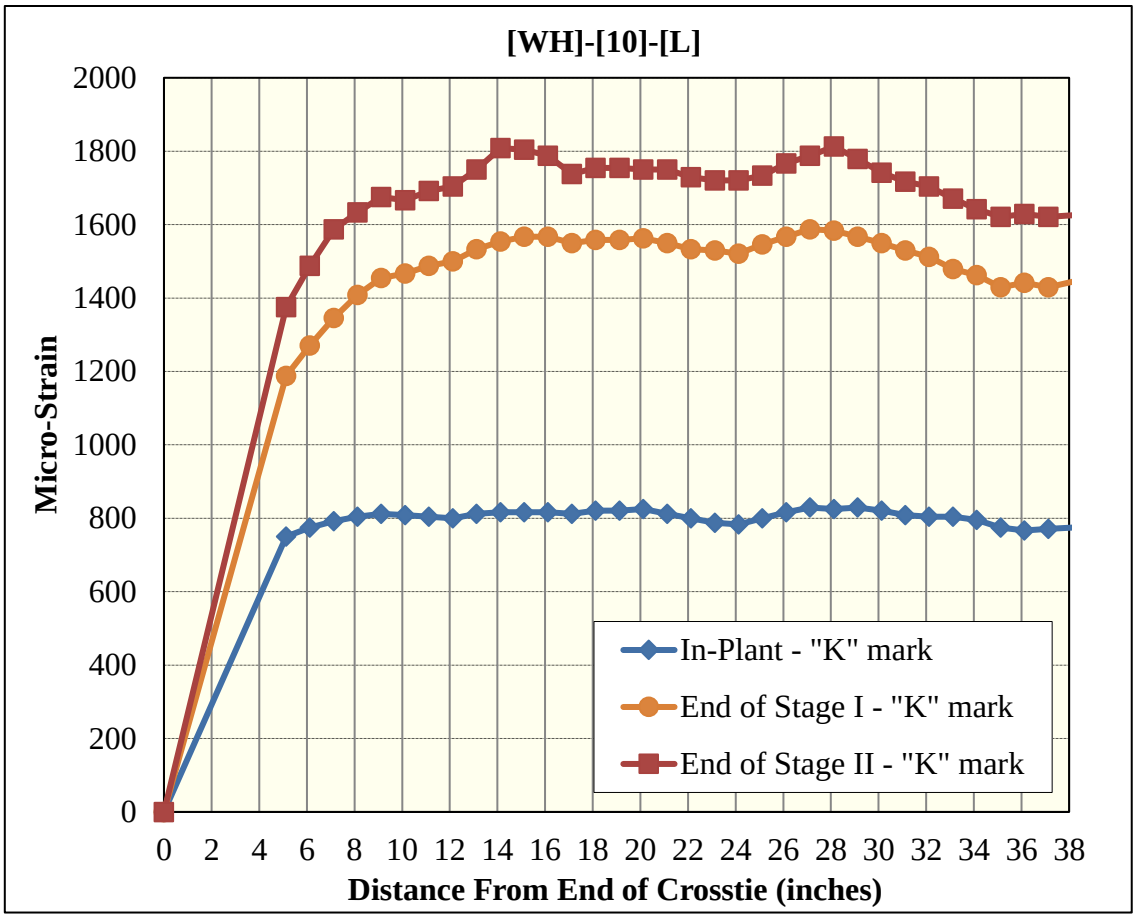

Figure 271 Surface-strain profiles for [WH]-[10]-[L] (Whittemore gage)

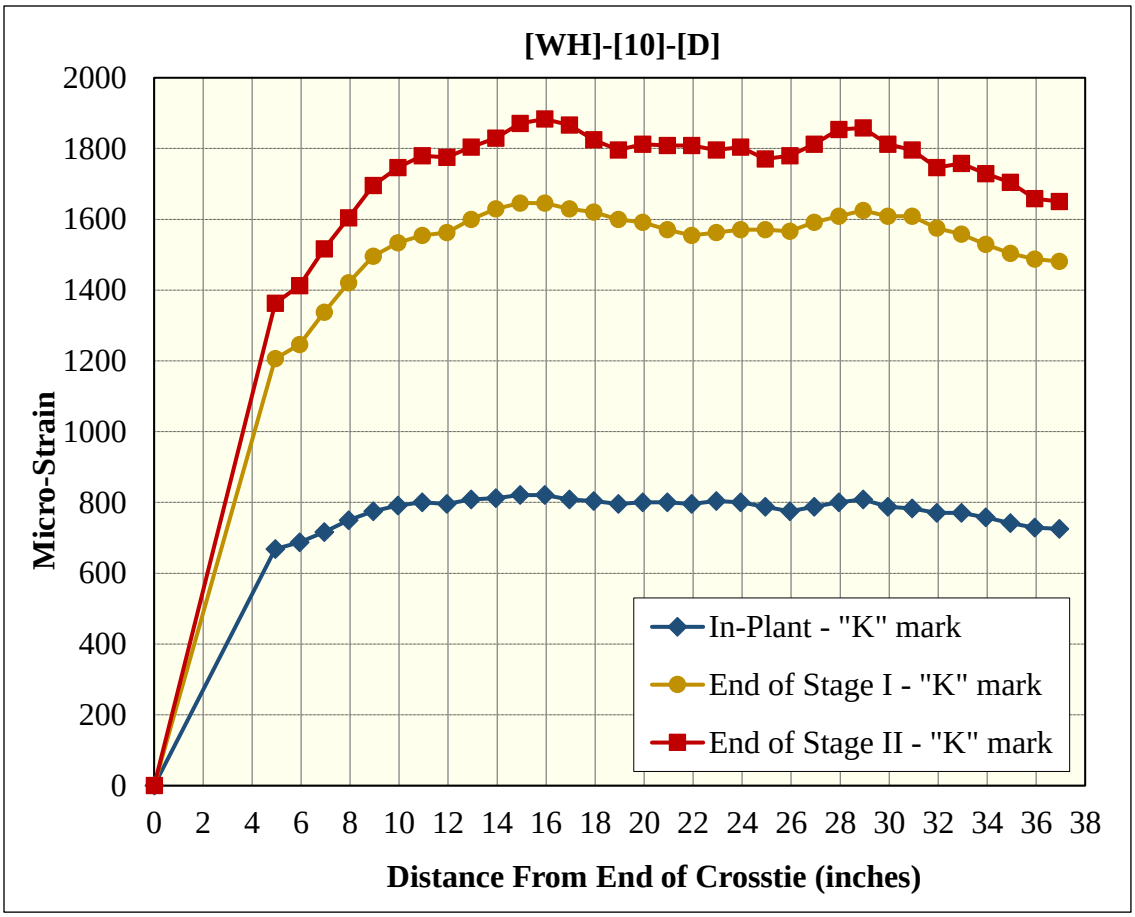

Figure 272 Surface-strain profiles for [WH]-[10]-[D] (Whittemore gage)

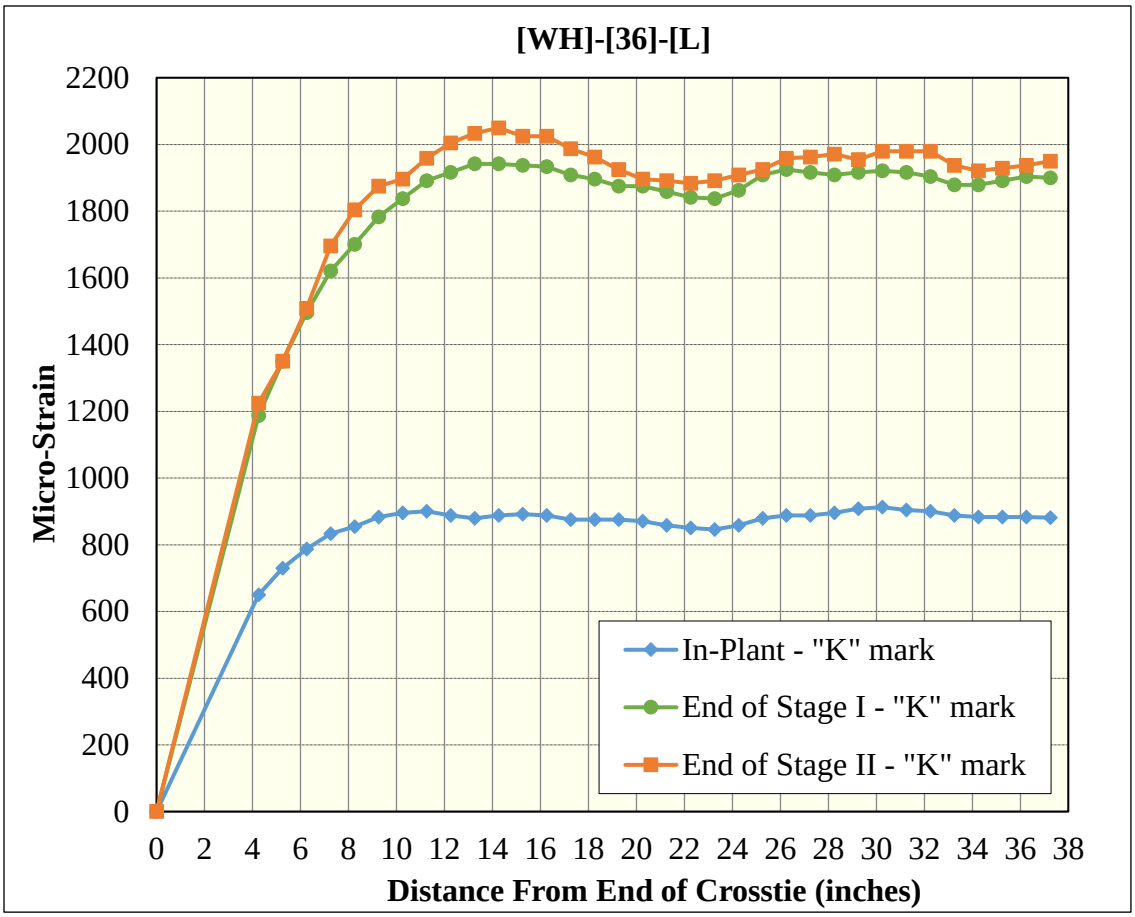

Figure 273 Surface-strain profiles for [WH]-[36]-[L] (Whittemore gage)

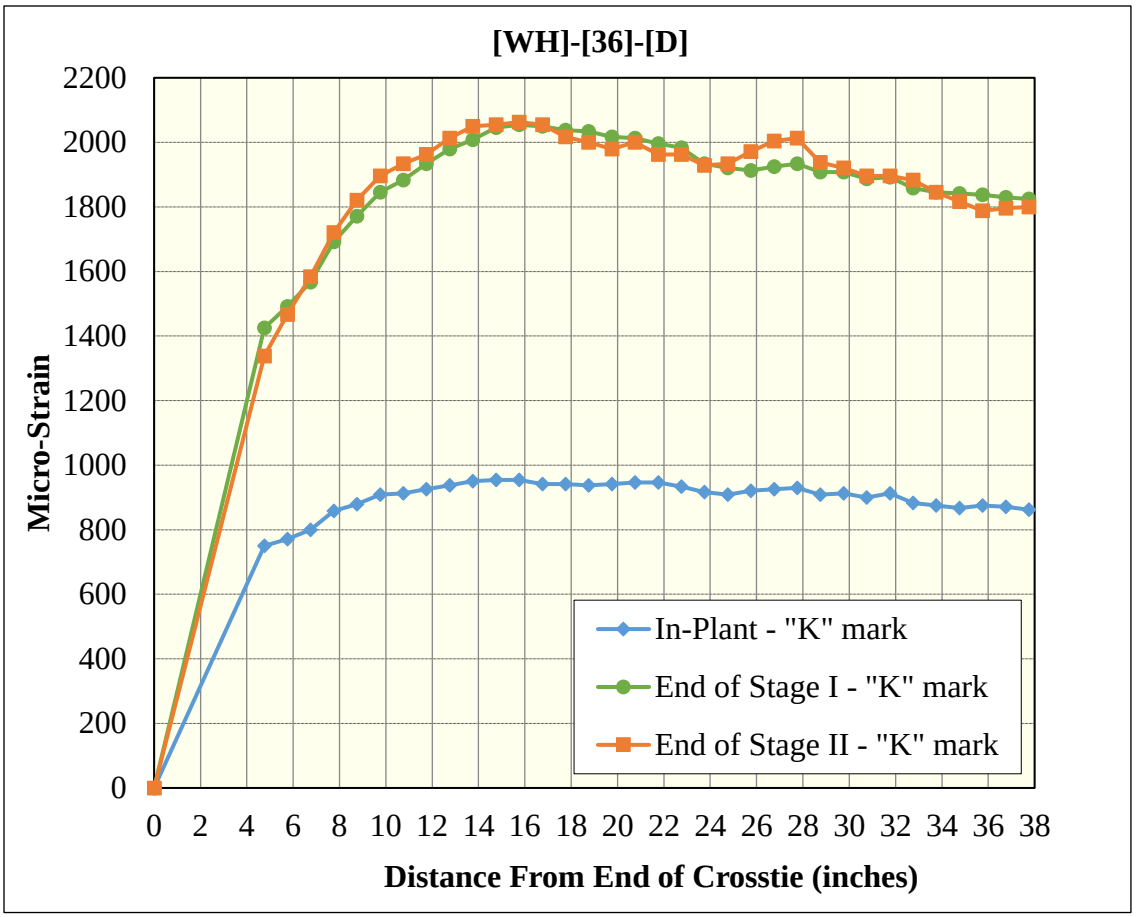

Figure 274 Surface-strain profiles for [WH]-[36]-[D] (Whittemore gage)

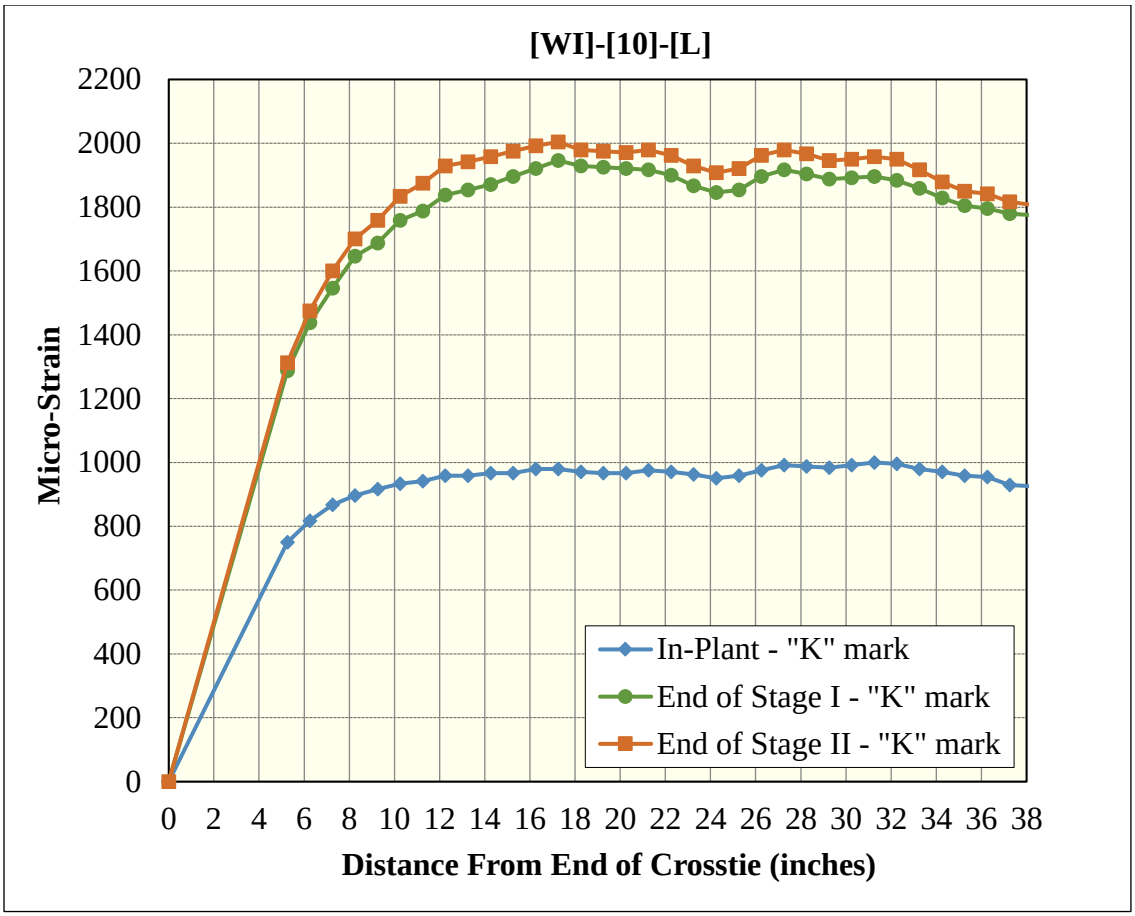

Figure 275 Surface-strain profiles for [WI]-[10]-[L] (Whittemore gage)

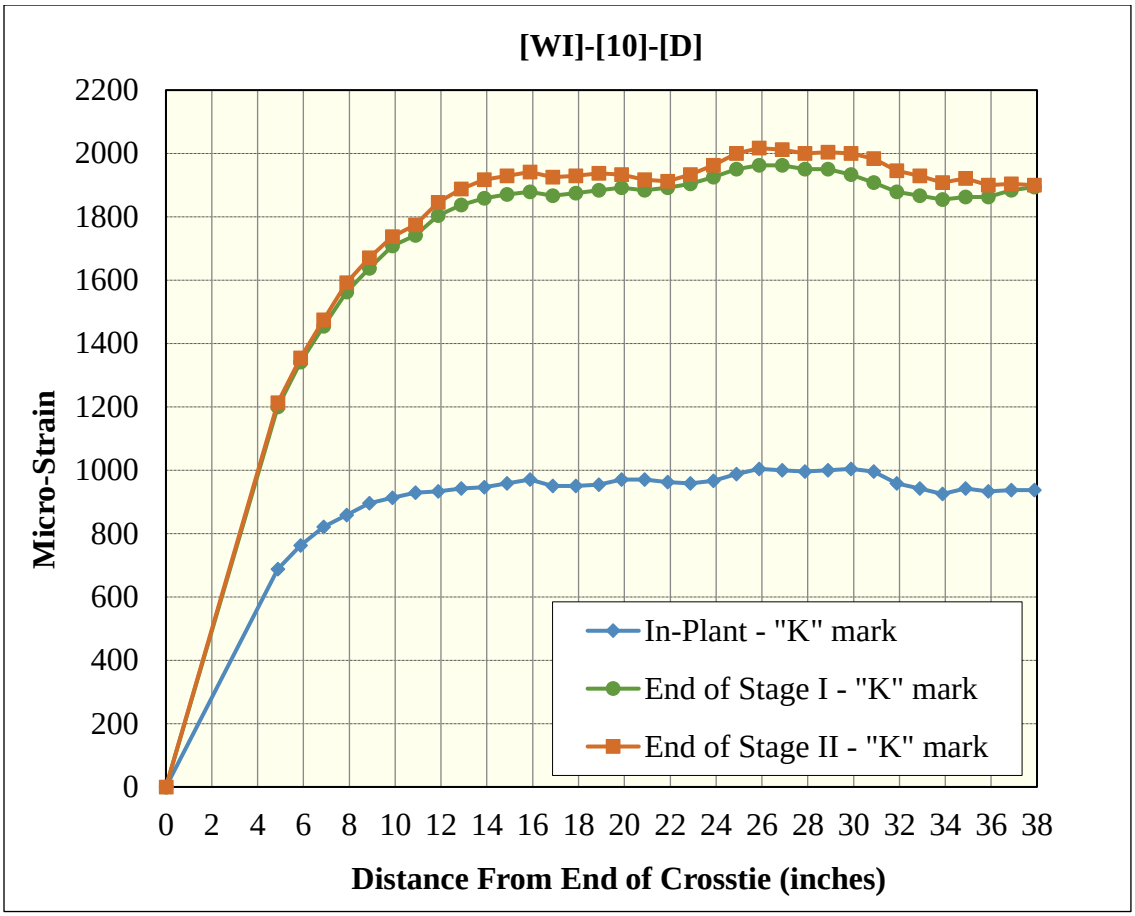

Figure 276 Surface-strain profiles for [WI]-[10]-[D] (Whittemore gage)

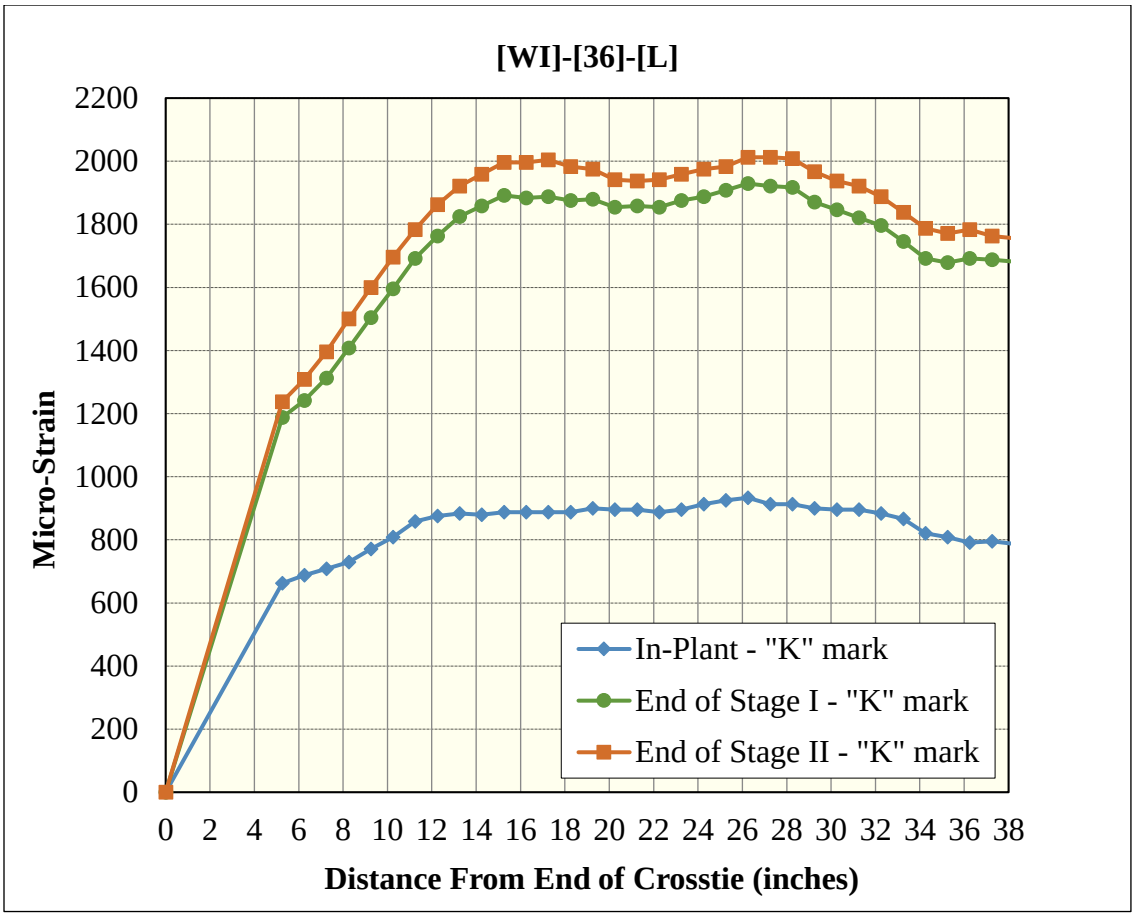

Figure 277 Surface-strain profiles for [WI]-[36]-[L] (Whittemore gage)

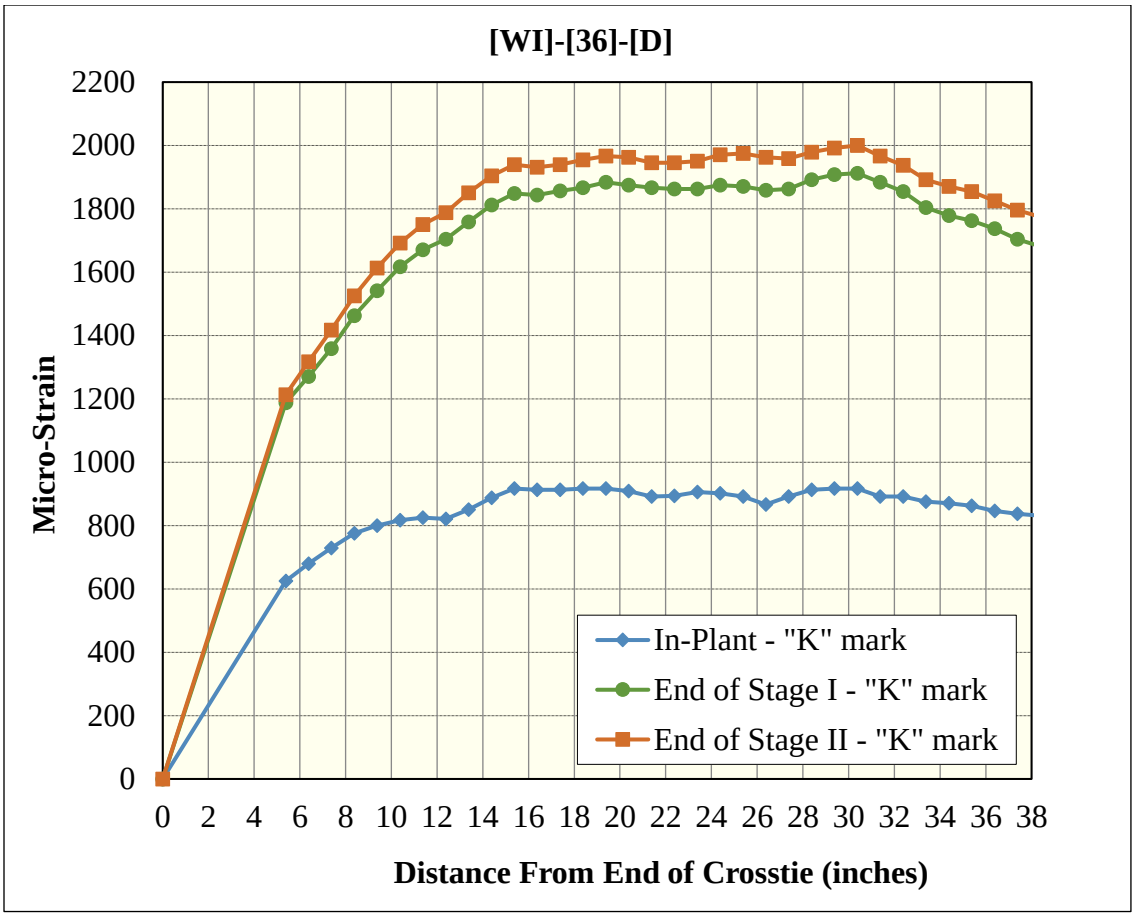

Figure 278 Surface-strain profiles for [WI]-[36]-[D] (Whittemore gage)

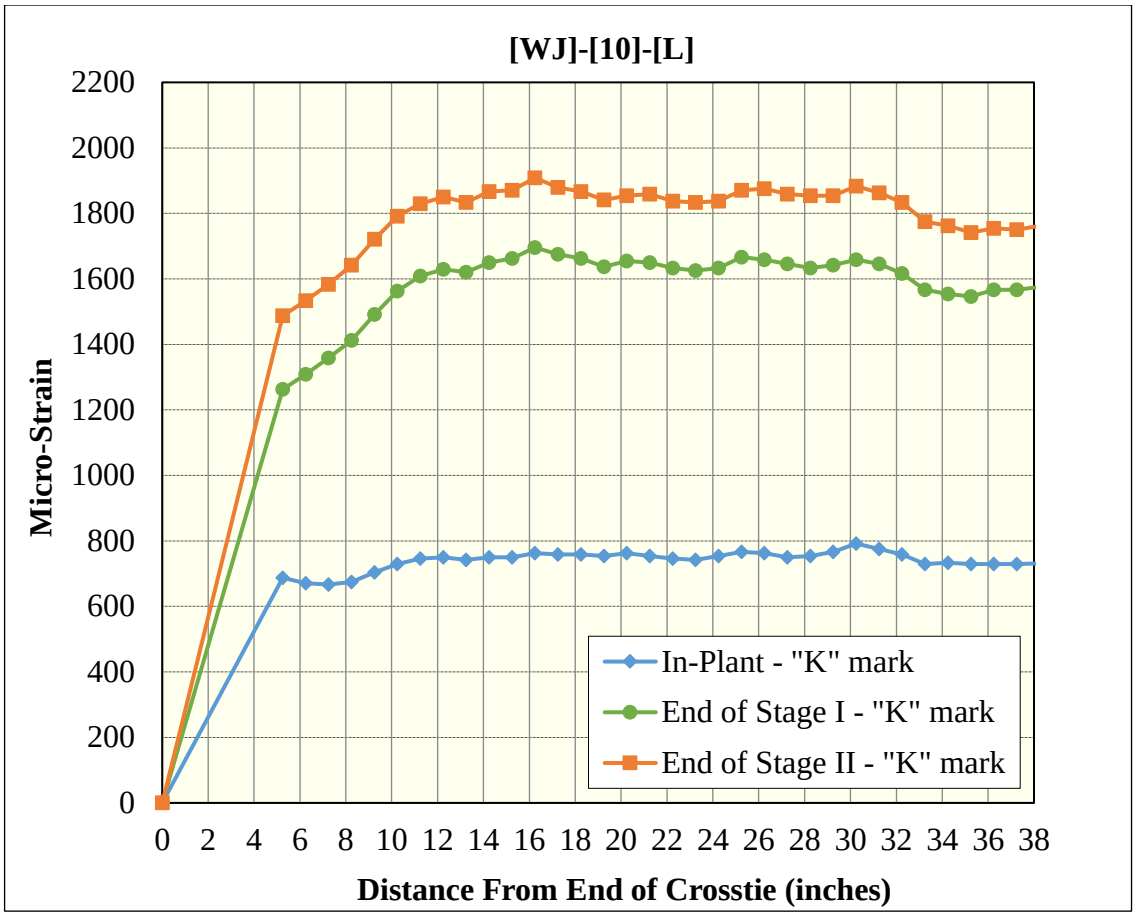

Figure 279 Surface-strain profiles for [WJ]-[10]-[L] (Whittemore gage)

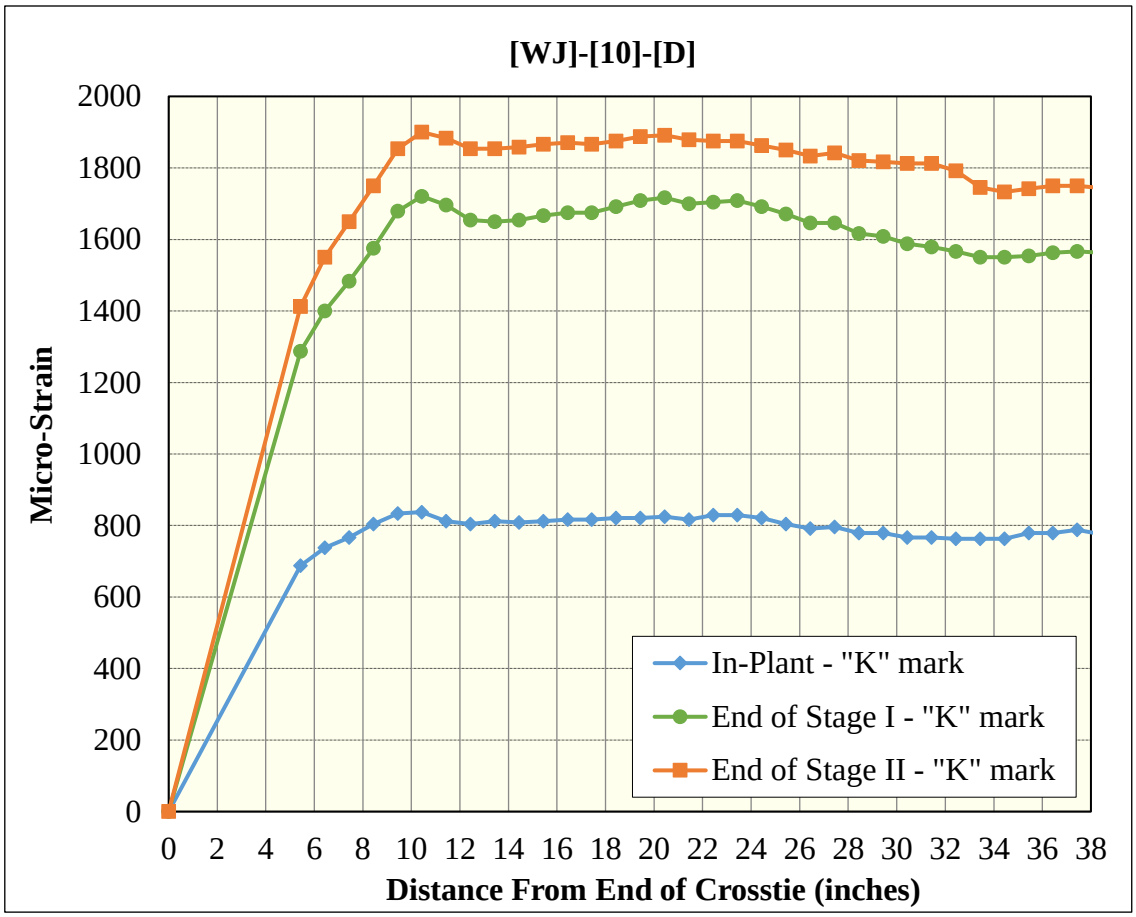

Figure 280 Surface-strain profiles for [WJ]-[10]-[D] (Whittemore gage)

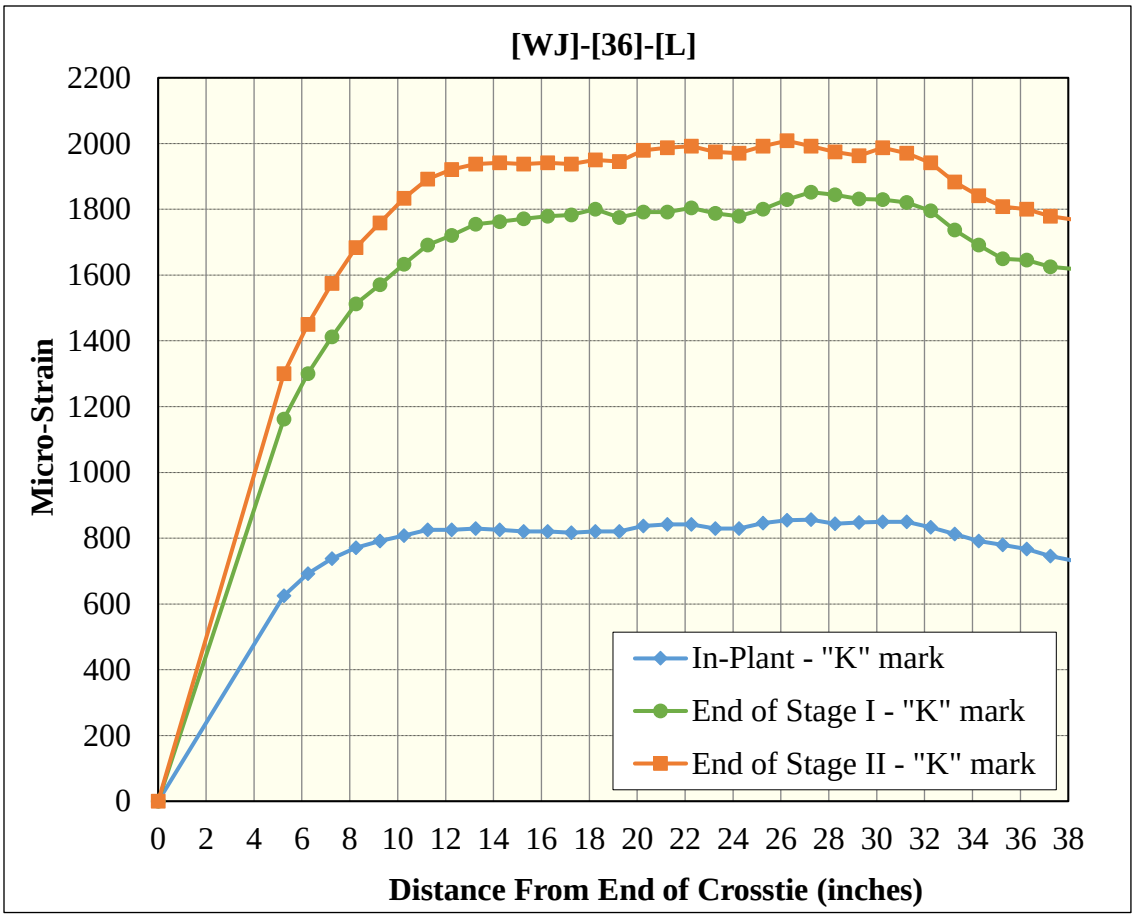

Figure 281 Surface-strain profiles for [WJ]-[36]-[L] (Whittemore gage)

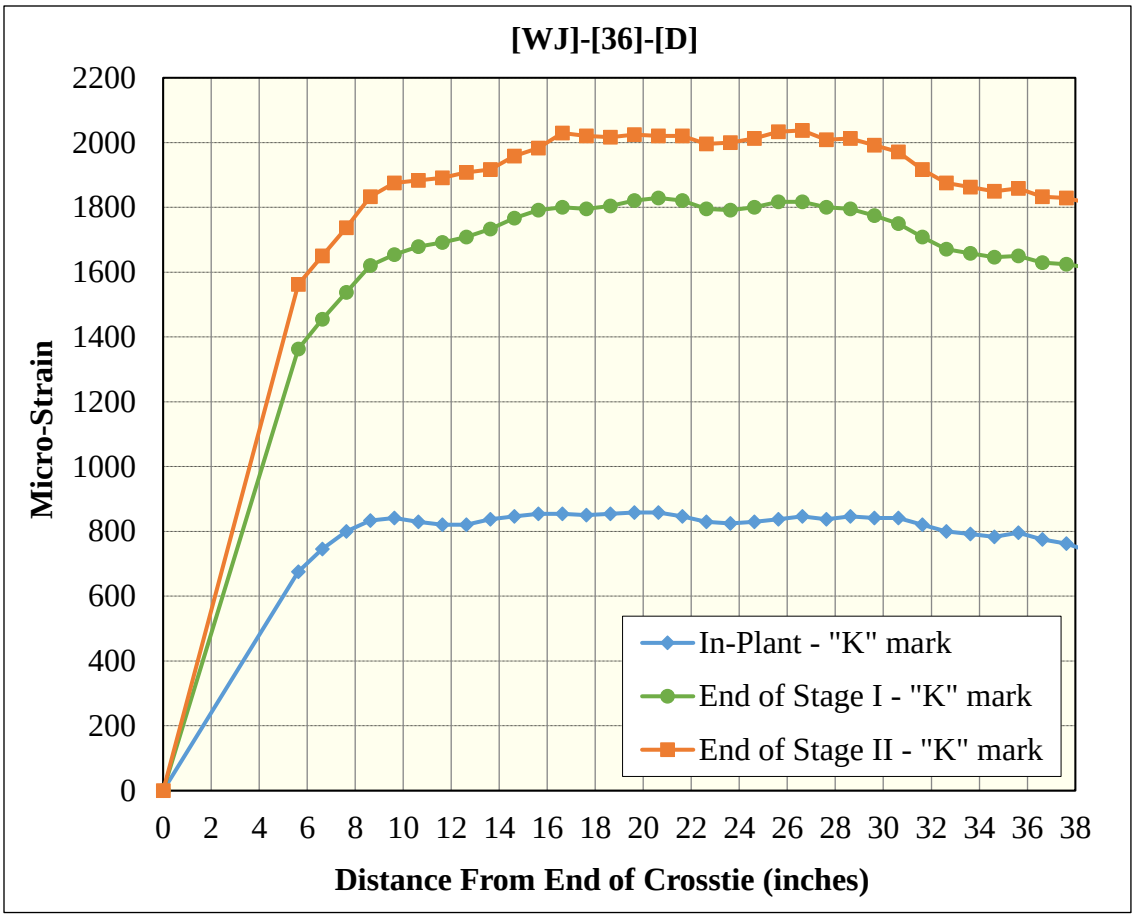

Figure 282 Surface-strain profiles for [WJ]-[36]-[D] (Whittemore gage)

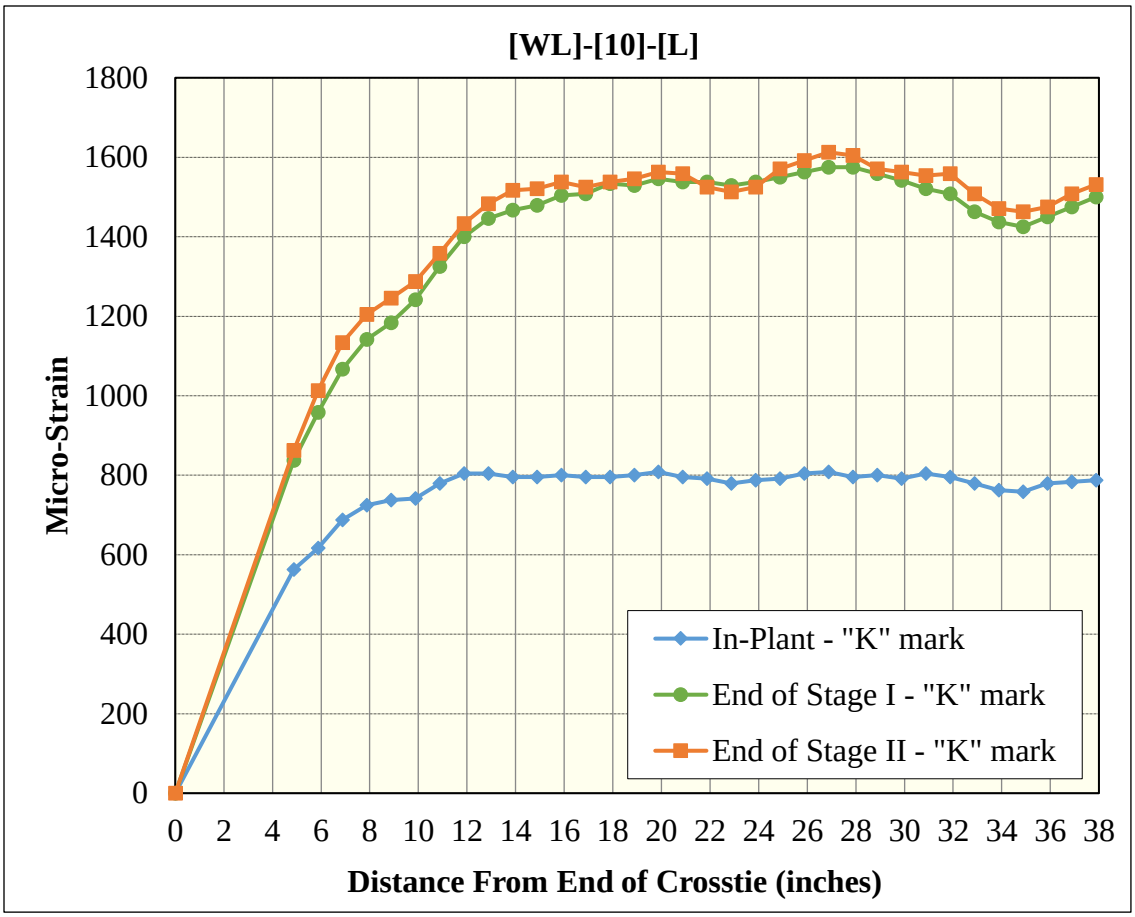

Figure 283 Surface-strain profiles for [WL]-[10]-[L] (Whittemore gage)

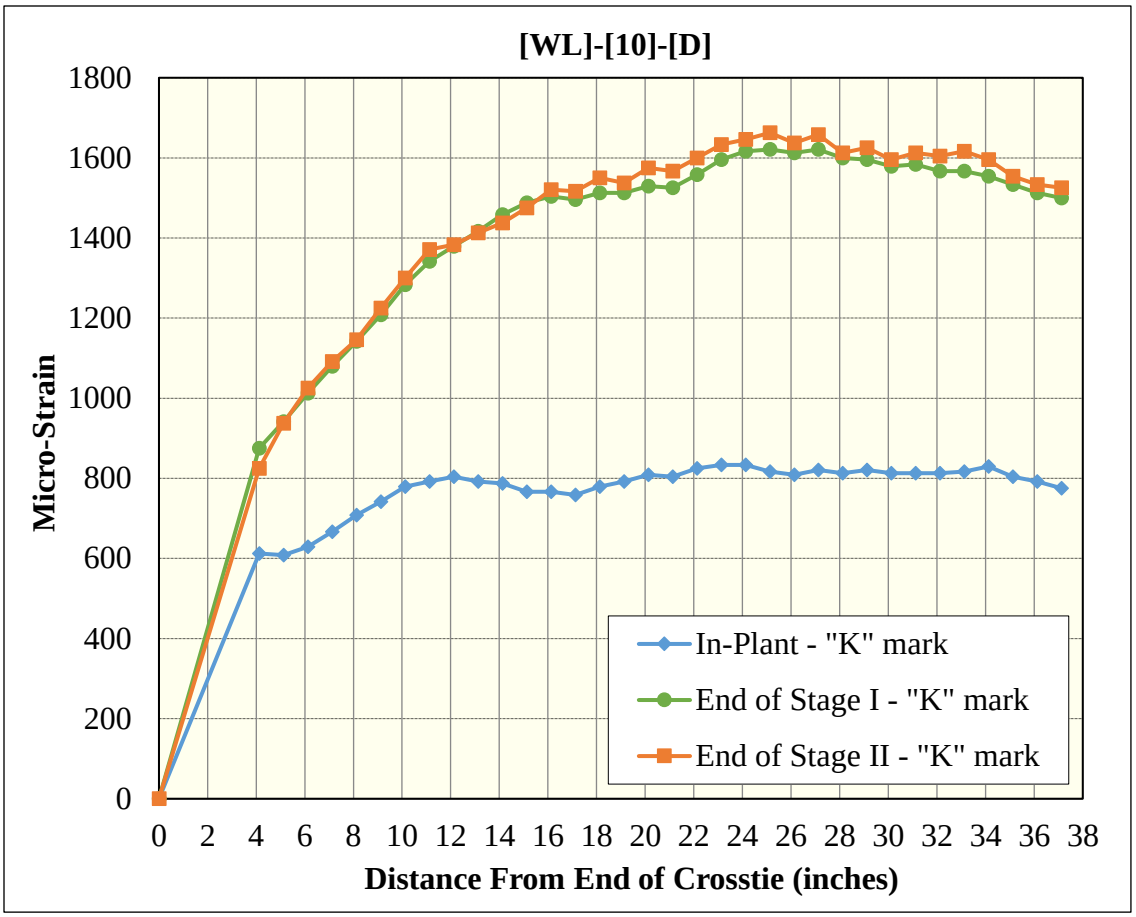

Figure 284 Surface-strain profiles for [WL]-[10]-[D] (Whittemore gage)

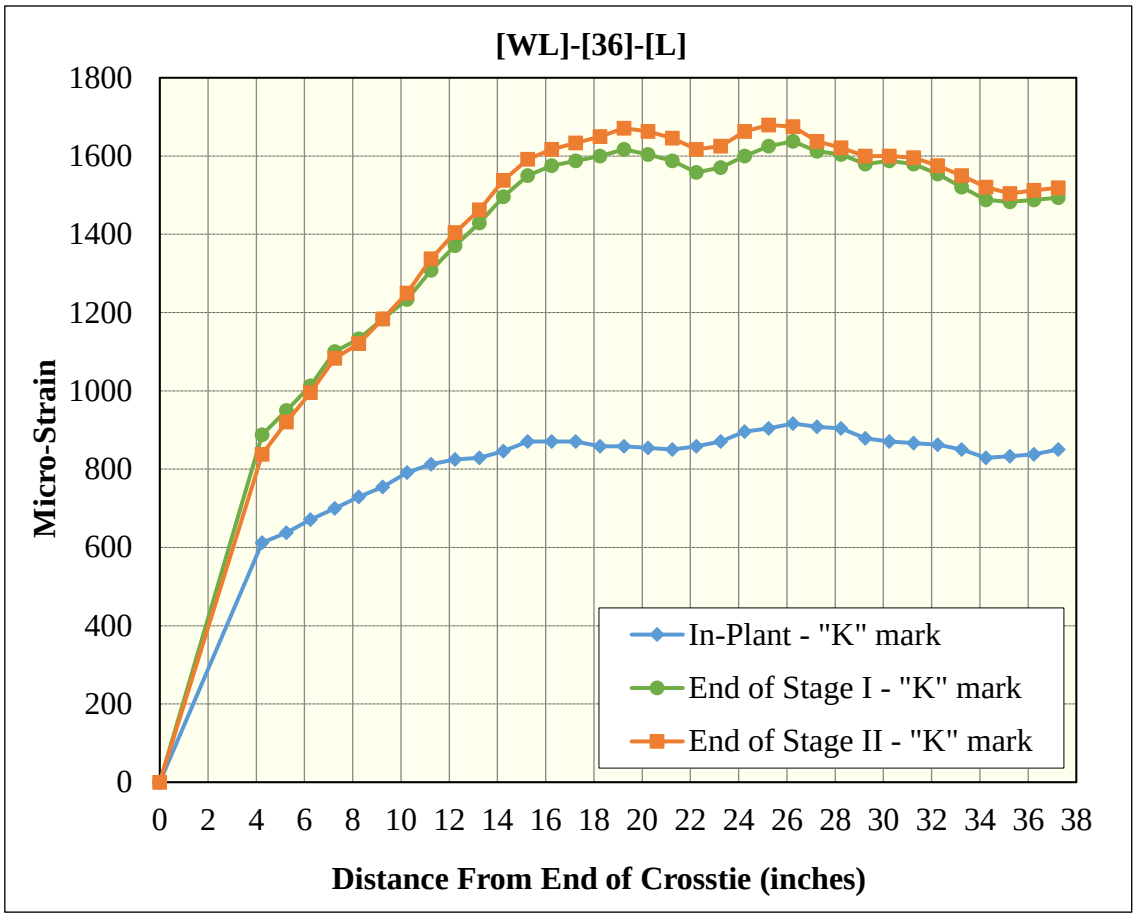

Figure 285 Surface-strain profiles for [WL]-[36]-[L] (Whittemore gage)

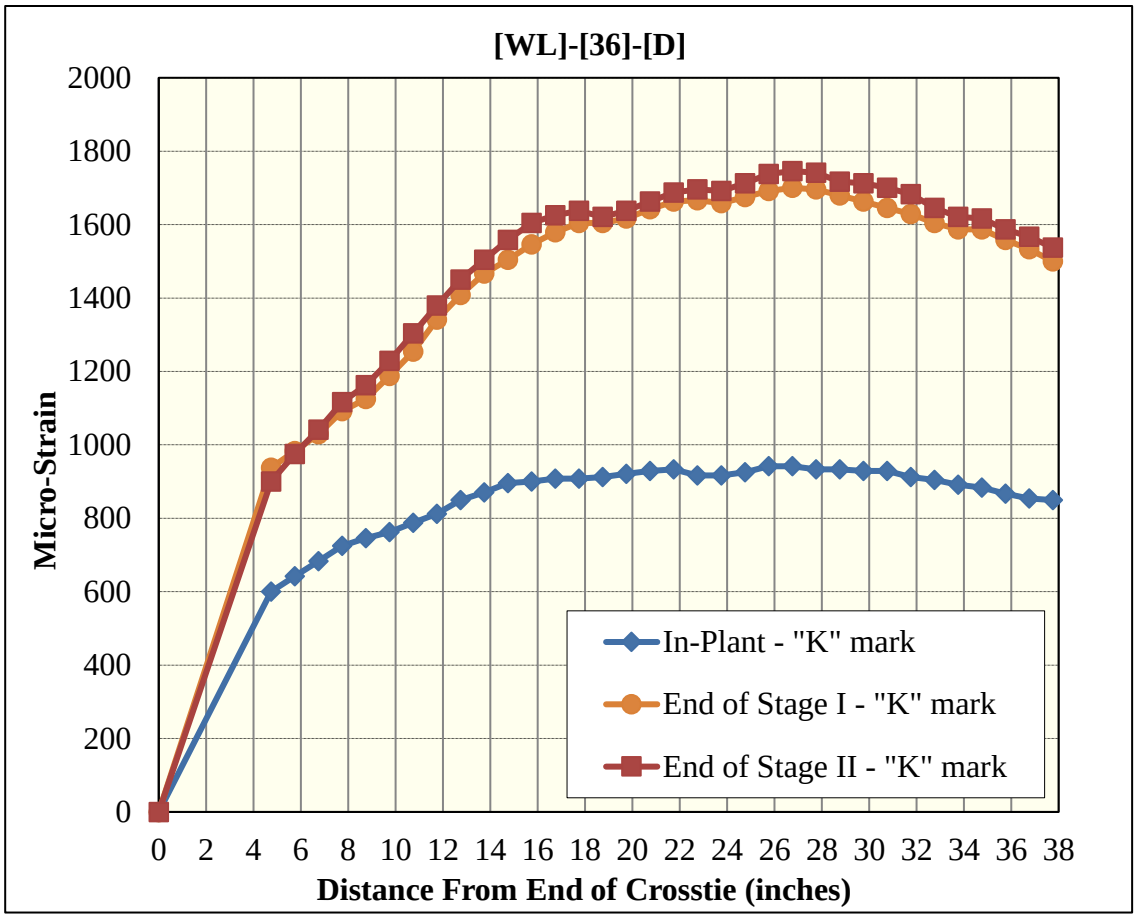

Figure 286 Surface-strain profiles for [WL]-[36]-[D] (Whittemore gage)

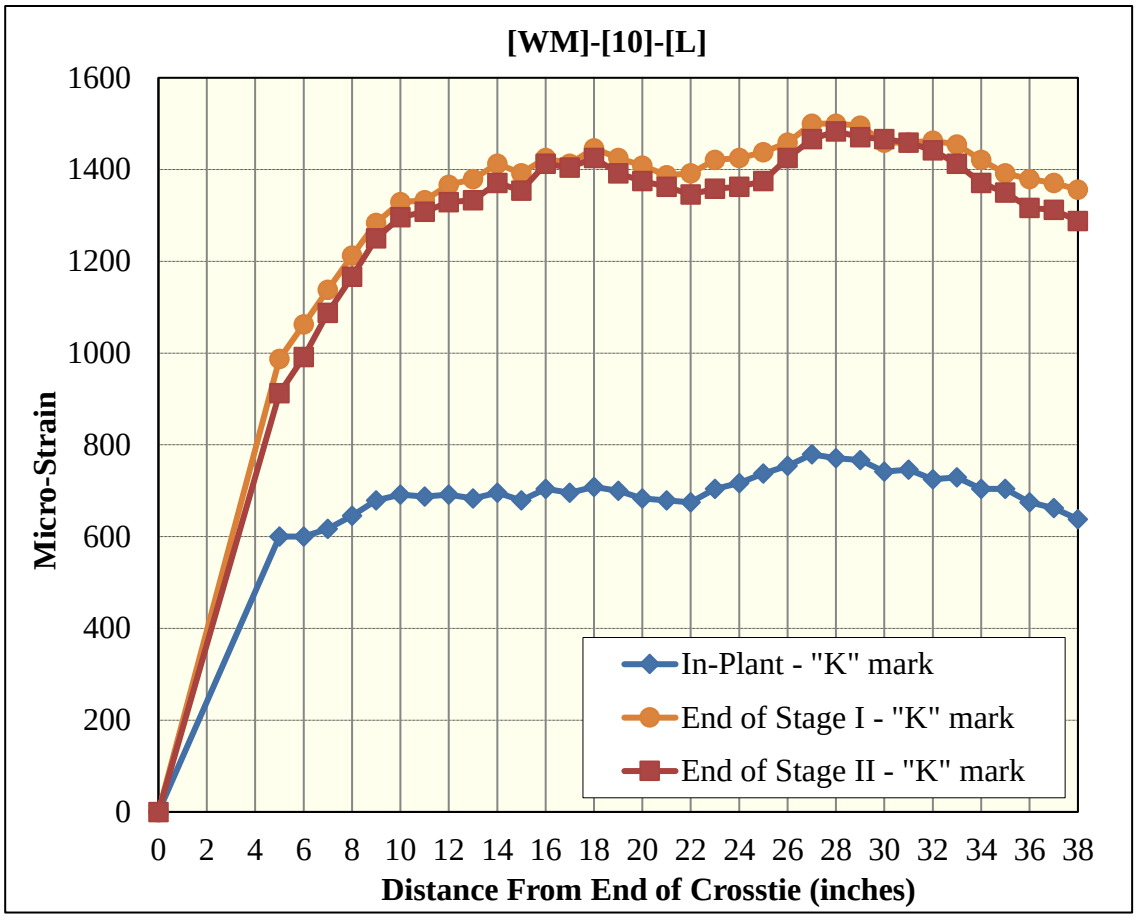

Figure 287 Surface-strain profiles for [WM]-[10]-[L] (Whittemore gage)

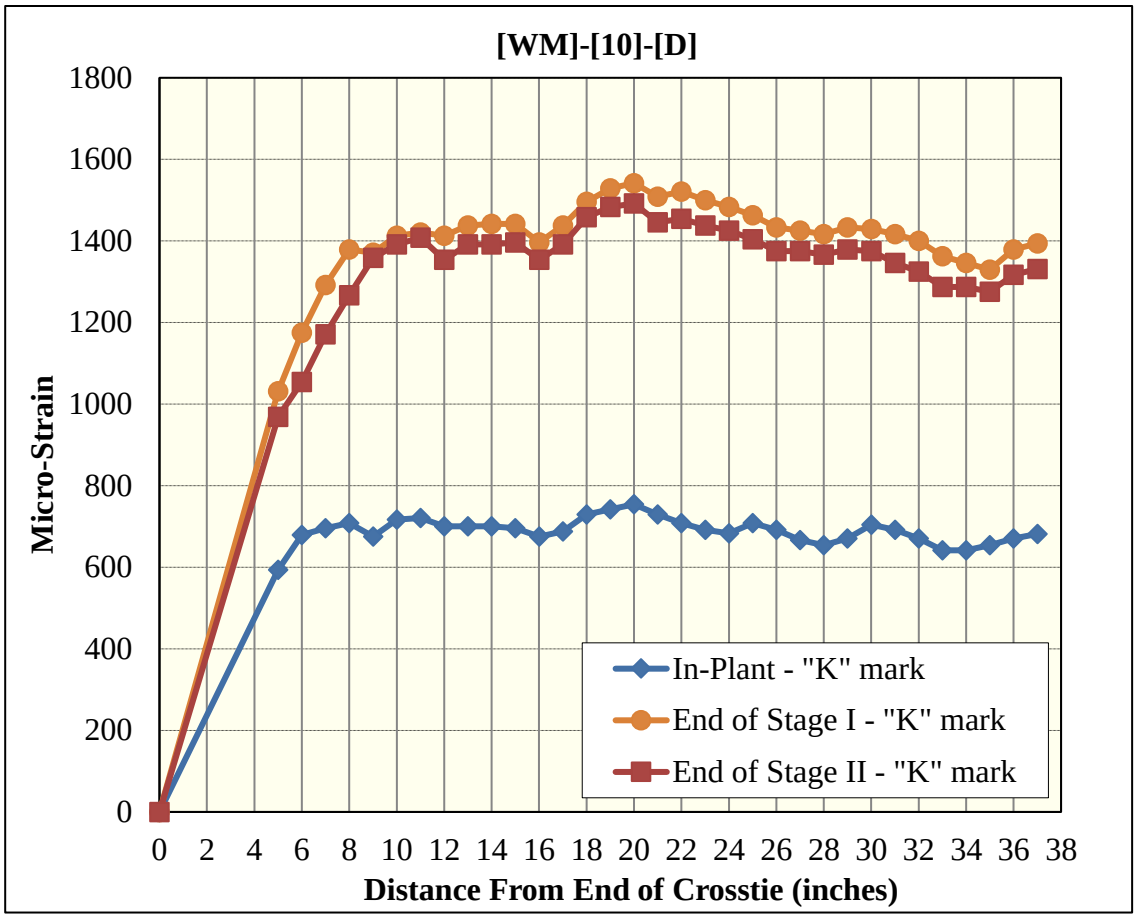

Figure 288 Surface-strain profiles for [WM]-[10]-[D] (Whittemore gage)

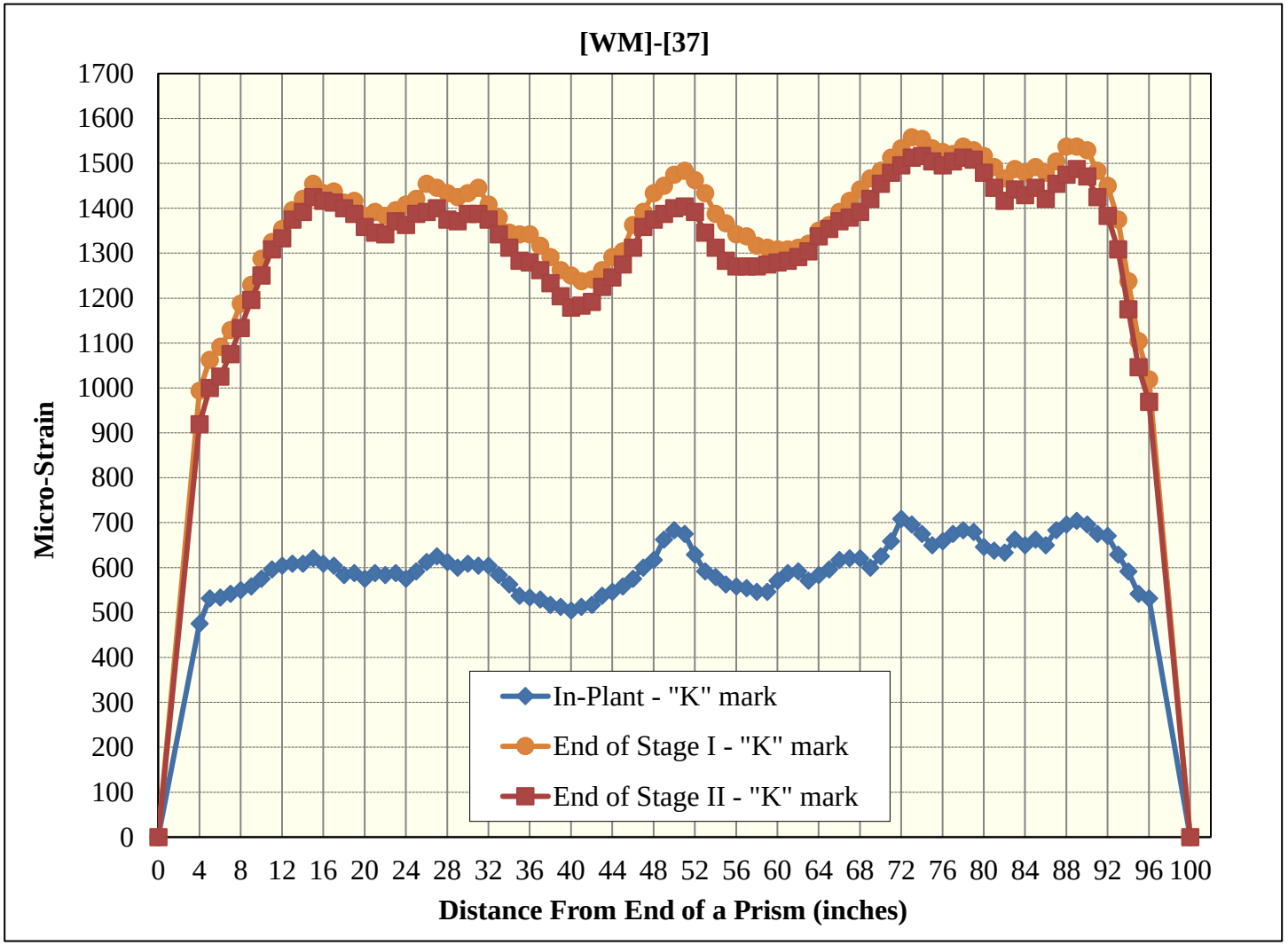

Figure 289 Surface-strain profiles for [WM]-[37] (Whittemore gage)

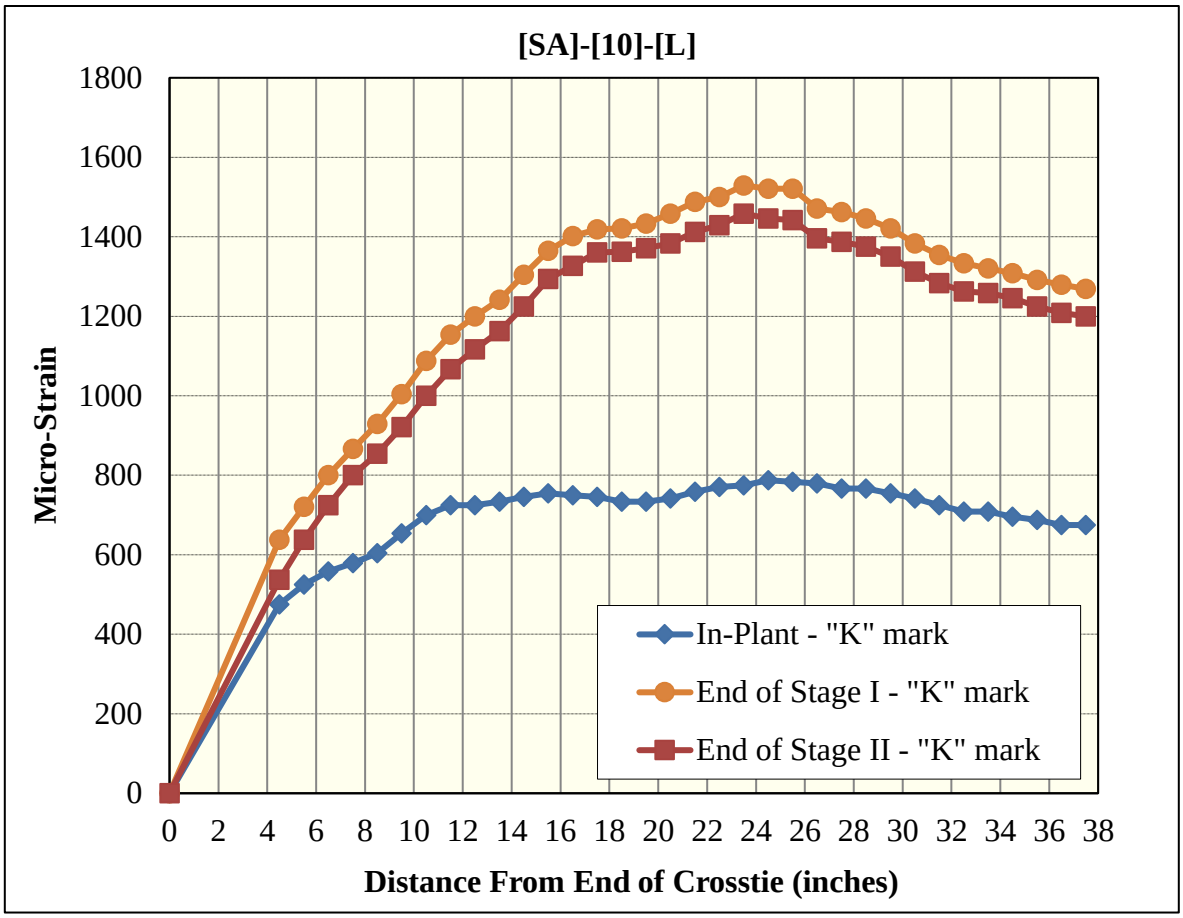

Figure 290 Surface-strain profiles for [SA]-[10]-[L] (Whittemore gage)

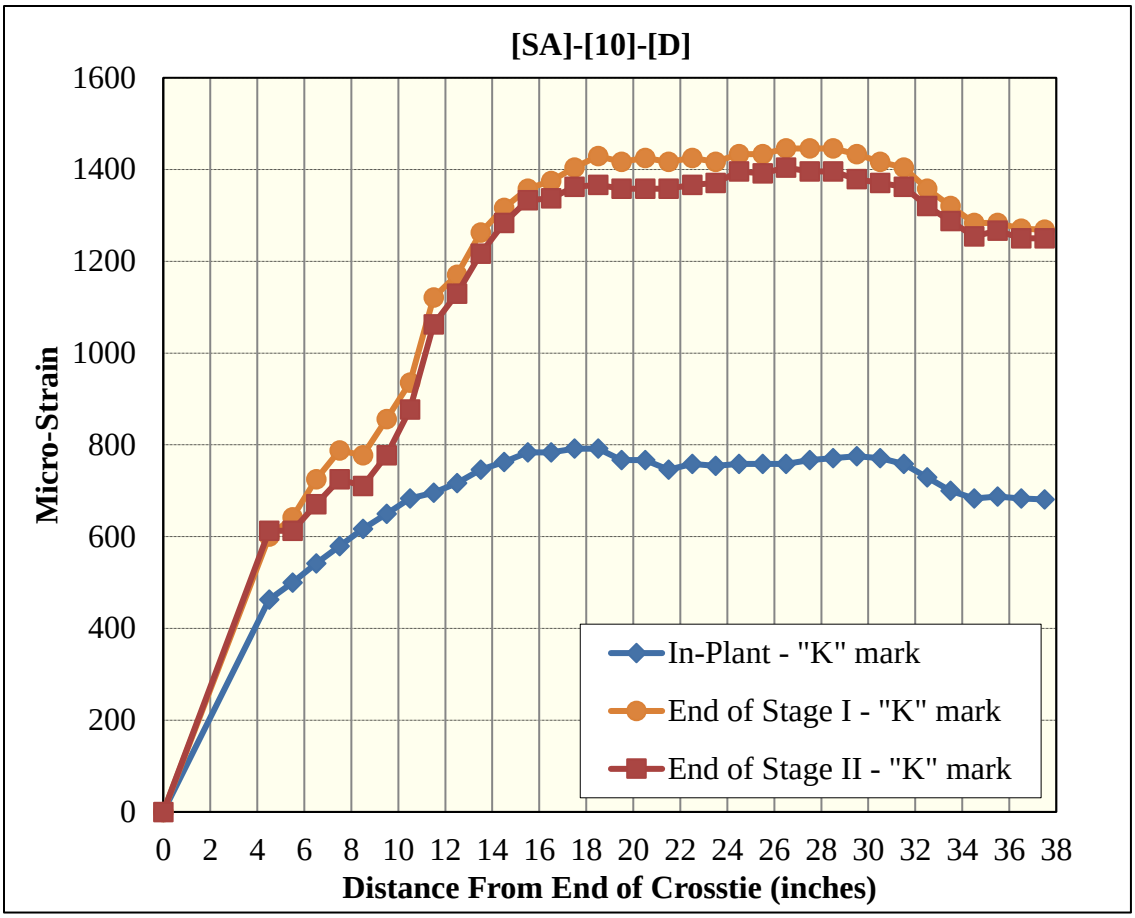

Figure 291 Surface-strain profiles for [SA]-[10]-[D] (Whittemore gage)

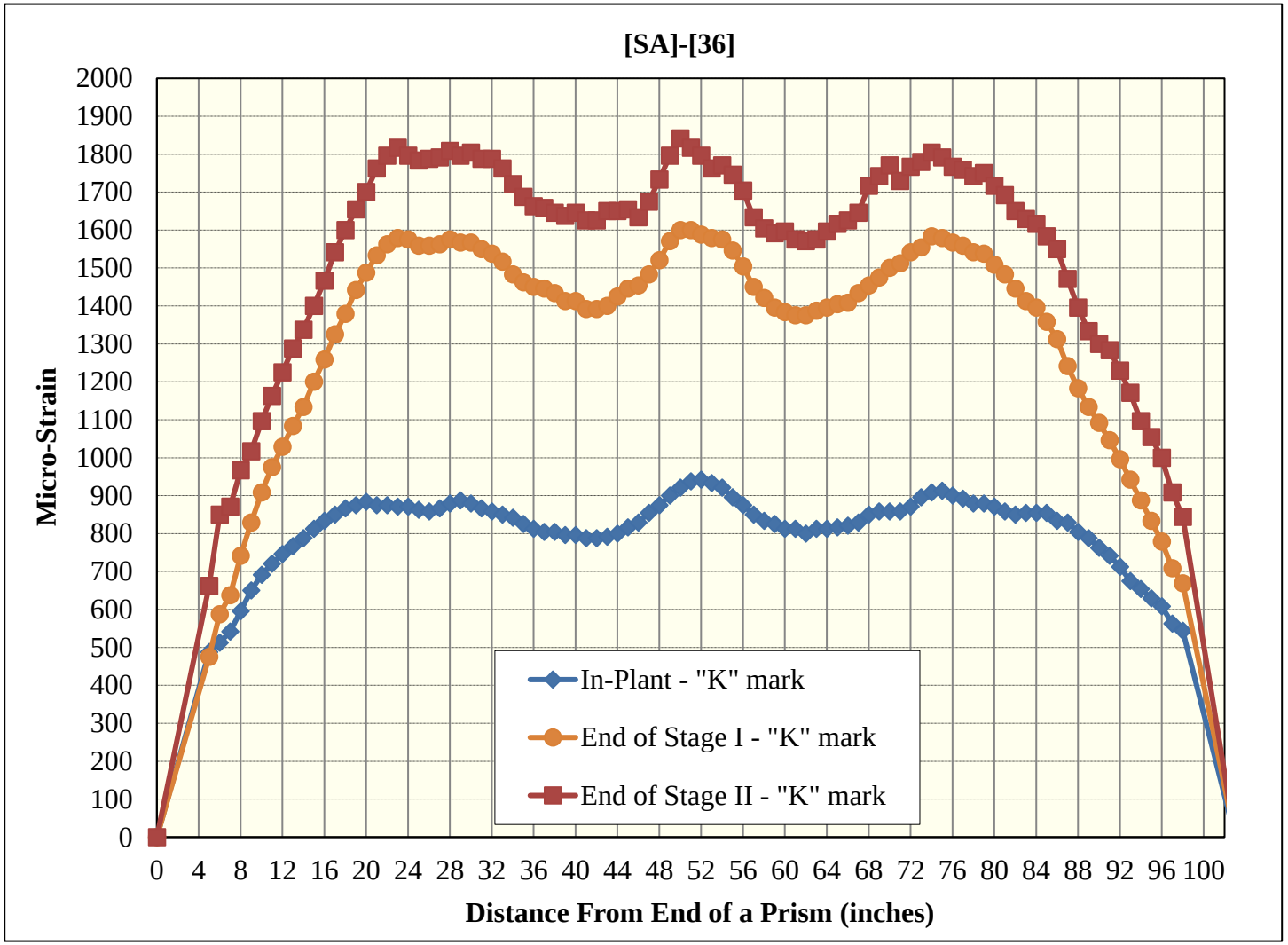

Figure 292 Surface-strain profiles for [SA]-[36] (Whittemore gage)

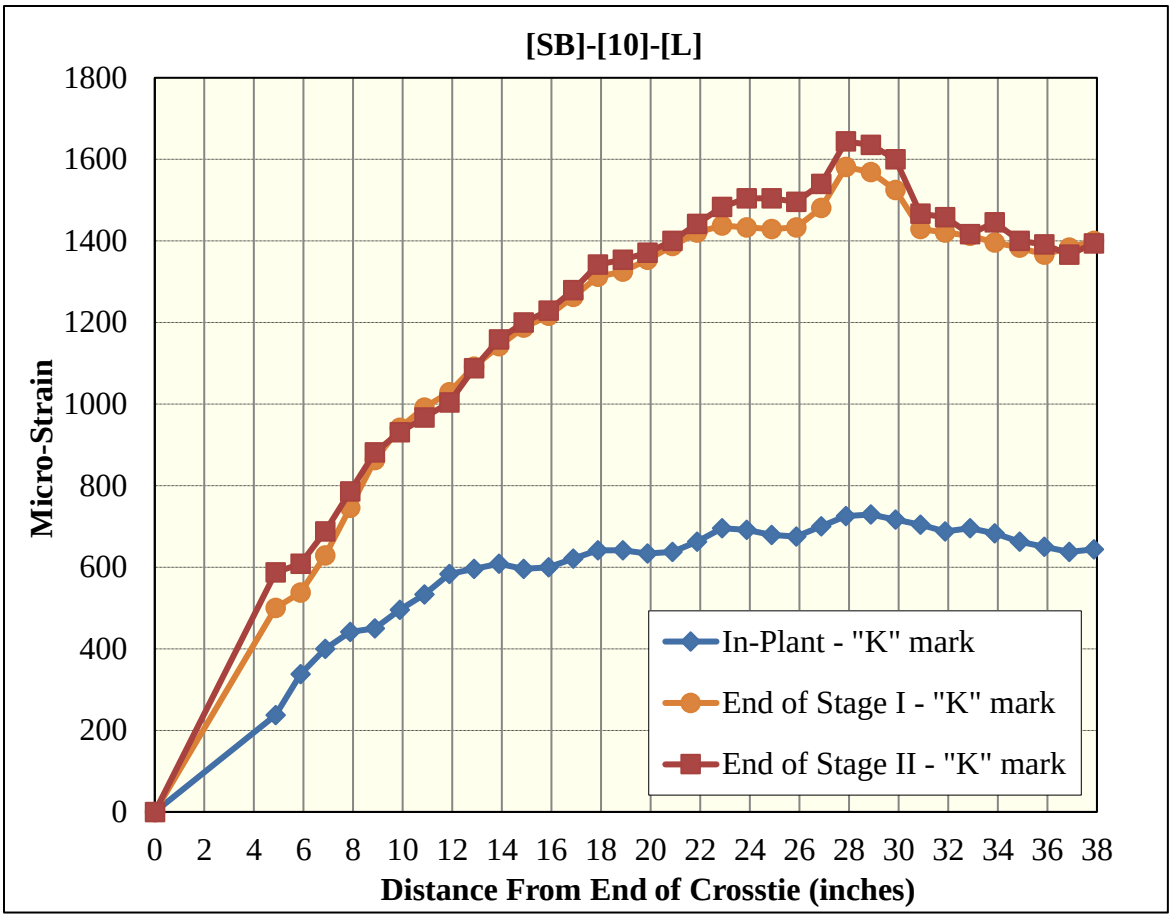

Figure 293 Surface-strain profiles for [SB]-[10]-[L] (Whittemore gage)

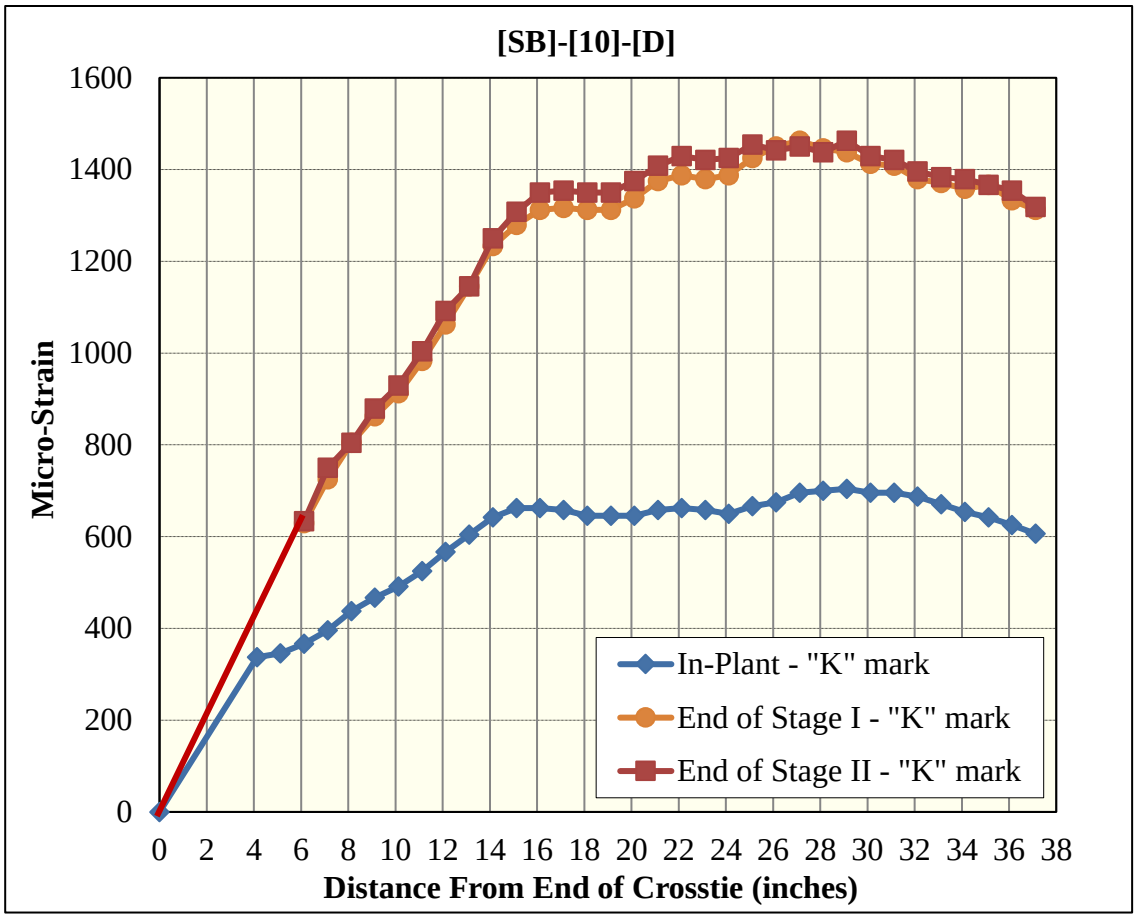

Figure 294 Surface-strain profiles for [SB]-[10]-[D] (Whittemore gage)

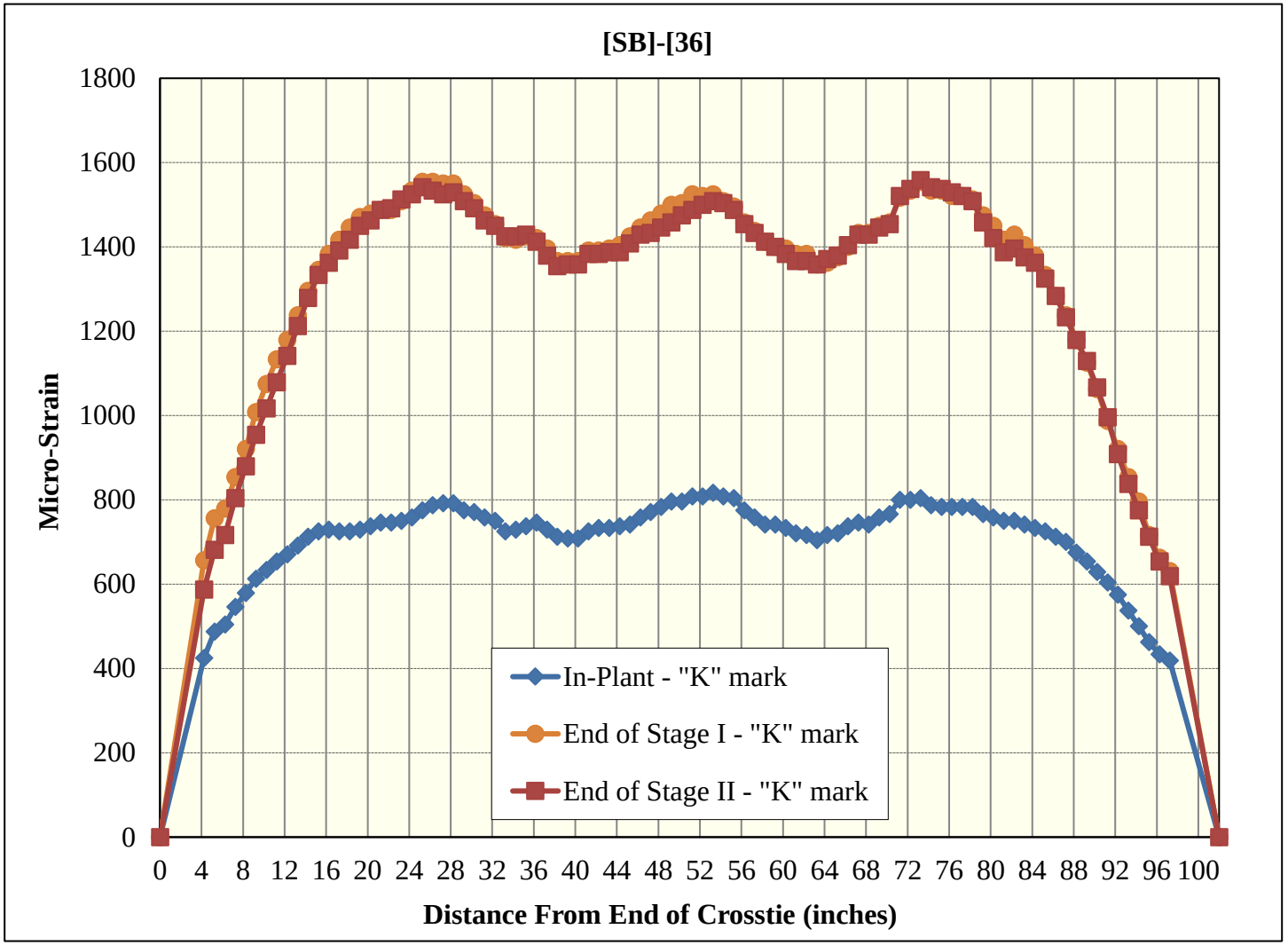

Figure 295 Surface-strain profiles for [SB]-[36] (Whittemore gage)

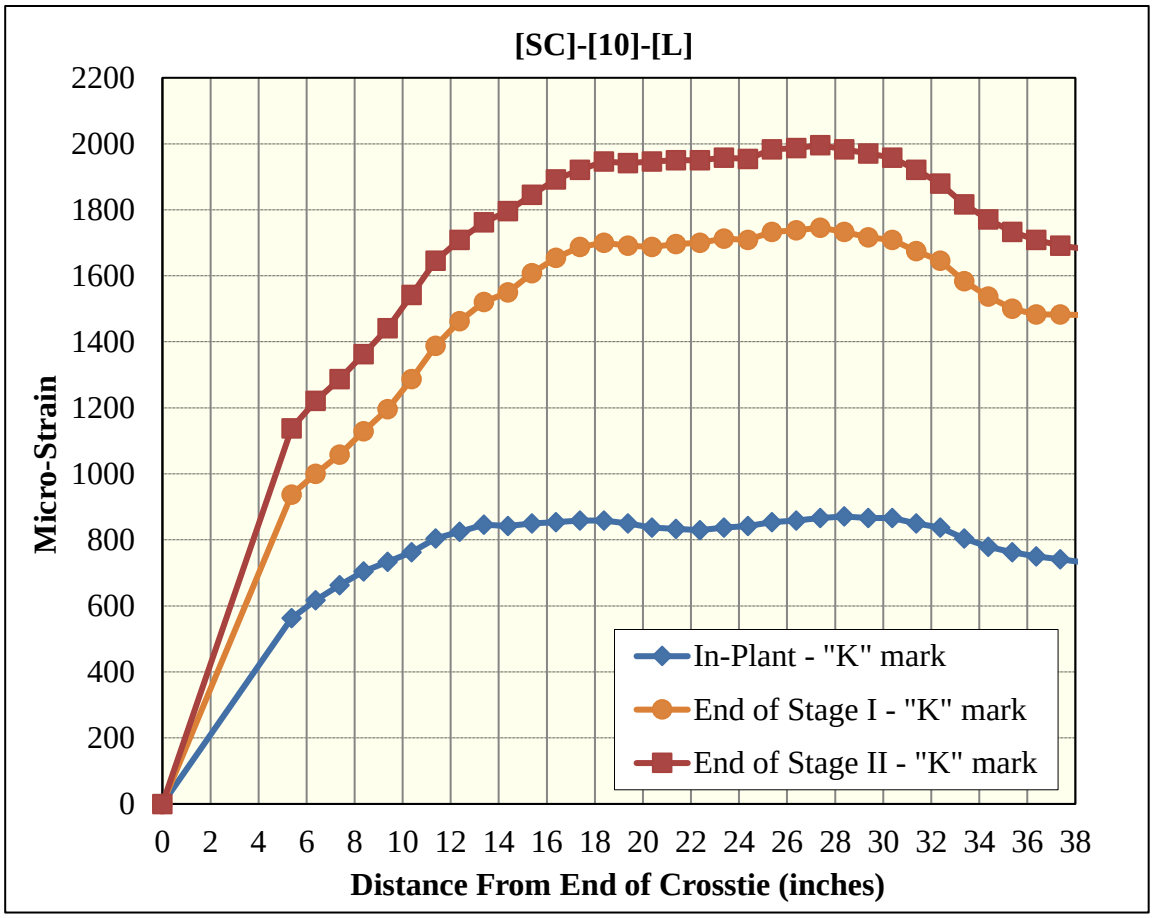

Figure 296 Surface-strain profiles for [SC]-[10]-[L] (Whittemore gage)

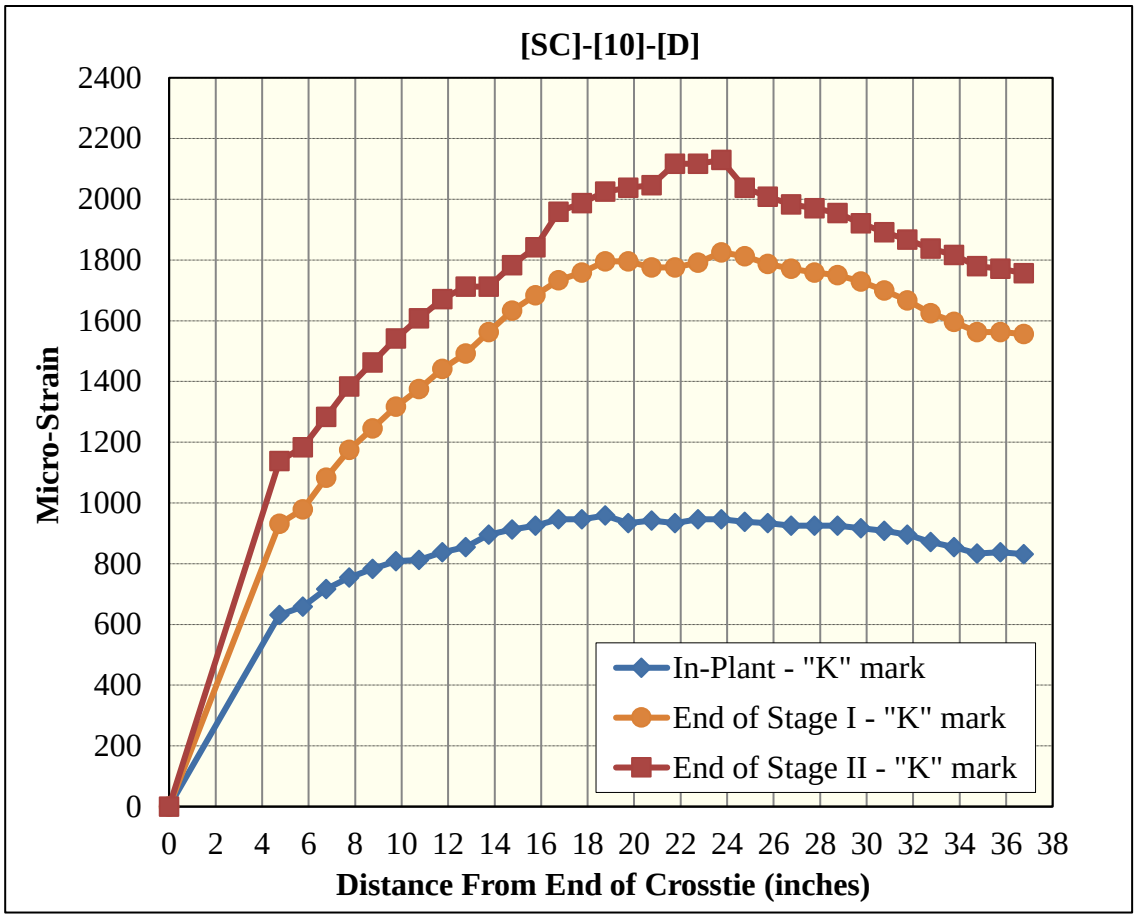

Figure 297 Surface-strain profiles for [SC]-[10]-[D] (Whittemore gage)

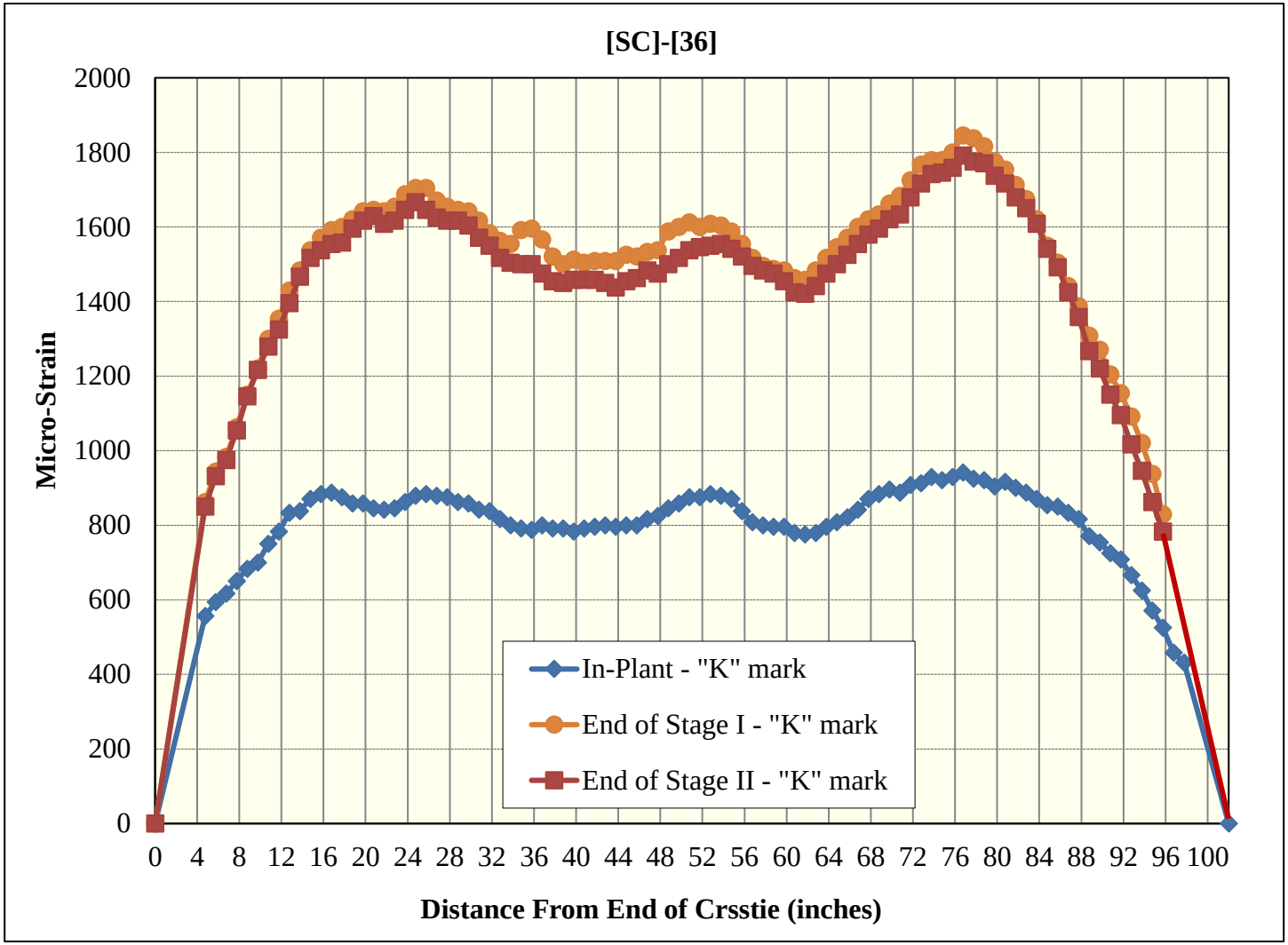

Figure 298 Surface-strain profiles for [SC]-[36] (Whittemore gage)